UNIVERSITAT DE
BARCELONA

P-Stereogenic ligands
with the *tert*-butylmethylphosphine fragment.
Coordination chemistry and catalysis
of their organometallic complexes

Albert Gallen Ortiz

Organic Chemistry PhD program

P-Stereogenic ligands with the *tert*-butylmethylphosphine fragment. Coordination chemistry and catalysis of their organometallic complexes

Albert Gallen Ortiz

Organic Chemistry PhD Program
Inorganic and Organic Chemistry Department
University of Barcelona

Thesis directors
Prof. Antoni Riera Escalé
Dr. Arnald Grabulosa Rodríguez
Inorganic and Organic Department
University of Barcelona
IRB Barcelona

Memòria presentada per **Albert Gallen Ortiz** per a optar al títol de DOCTOR en Química per la Universitat de Barcelona.

Albert Gallen Ortiz

Barcelona, desembre de 2018

El **Prof. Antoni Riera Escalé**, catedràtic del departament de Química Inorgànica i Orgànica, Secció de Química Orgànica, de la Facultat de Química de la Universitat de Barcelona, i el **Dr. Arnald Grabulosa Rodríguez**, professor titular del departament de Química Inorgànica i Orgànica, Secció de Química Inorgànica, de la Facultat de Química de la Universitat de Barcelona,

CERTIFIQUEN: que la present tesi doctoral titulada "*P-Stereogenic ligands with the tert-butylmethylphosphine fragment.*
Coordination chemistry and catalysis of their organometallic complexes" presentada per **Albert Gallen Ortiz** per optar al títol de doctor per la Universitat de Barcelona, ha estat realitzada sota la seva direcció en el Departament de Química Inorgànica i Orgànica de la Facultat de Química de la Universitat de Barcelona.

Barcelona, desembre de 2018

Prof. Antoni Riera Escalé   Dr. Arnald Grabulosa Rodríguez

Per als meus pares,
amb profunda admiració

<<*It's a dangerous business, Frodo, going out your door. You step onto the road, and if you don't keep your feet, there's no knowing where you might be swept off to.*>>

J.R.R. Tolkien, *The Lord of the Rings*

Acknowledgments

≪*You are here to learn the subtle science and exact art of potion-making* […] *I don't expect you will really understand the beauty of the softly simmering cauldron with its shimmering fumes, the delicate power of liquids that creep through human veins, bewitching the mind, ensnaring the senses.... I can teach you how to bottle fame, brew glory, even stopper death.*≫

J.K. Rowling, *Harry Potter and the Philosopher's Stone.*

I així va començar tot... Aquesta era, si fa no fa, la meva visió del que era la química cap als meus onze anys, i fins i tot ara, després de "sobreviure" la carrera, el màster i quatre anys de Tesi Doctoral, confesso que encara hi trobo quelcom "màgic" cada cop que el baló de reacció canvia de color o del fons del tub de RMN hi apareixen tot de cristalls (quan hi ha sort)...

Resulta una tasca difícil, arribats a aquest punt, d'agrair a totes aquelles persones que, al llarg d'aquests anys de Tesi, han contribuït a fer que allò que semblava tan llunyà arribi al seu final. Per on començar? En primer lloc, voldria donar les gràcies al Dr. Antoni Riera per haver-me permès realitzar aquesta Tesi Doctoral al seu grup de recerca tot i sabent que "els zànganos inorgànics no perdonem res" i al Dr. Xavier Verdaguer pel seu interès i el seu bon humor. Al Dr. Arnald Grabulosa: mil milions (factorial) de gràcies. Què podria dir als lectors de l'Arnald? Doncs que a ell no li agrada la química... l'entusiasma! És realment extraordinària la passió amb la que viu la seva feina i que transmet (us ho asseguro) a tots els seus estudiants. Ferm defensor de les pelis de terror, de la censura de tota forma de manifestació artística (especialment el teatre i els musicals), quan mani – diu ell–, maniàtic de la neteja (la netedat es mitja vida i l'altre mitja és brutícia) ha estat molt enriquidor haver compartit aquests anys amb ell. Vull agrair també, seguint l'ordre dels "capos", al Dr. Guillermo Muller per la seva dedicació en el seguiment d'aquesta Tesi exòtica; per tenir sempre la porta del despatx oberta per resoldre qualsevol dubte (per aquells qui no ho sapigueu té un coneixement enciclopèdic) i sobretot pels seus excel·lents consells en l'àmbit de la bibliografia ("el problema es que no se lee"*); en el mestratge en la manipulació d'hidrogen a alta pressió (*"un cuarto de vuelta y sin apretar"*) i pel seu sentit de l'humor quan és capaç d'arreglar un cromatògraf en menys d'un minut i et respon:* "os dejaré mi teléfono".

A la Dra. Montserrat Ferrer, per tot el recolzament que m'ha donat al llarg d'aquesta Tesi que ha sigut "dureza auténtica" *i per ser la primera en ensenyar-me* "la química de veritat", *a* "batallar amb els elements" *i a perseverar en els moments difícils quan els compostos es resisteixen. També, voldria agrair la Dra. Mercè Rocamora pels seus bons consells i el seu suport tant dins com fora del laboratori.*

A l'equip de Ressonància Magnètica Nuclear, en especial als doctors Anna Linares (sense ella no hi haurien ni la meitat d'espectres de fòsfor a la tesi...) i Francisco Cárdenas per trobar sempre una estona per a les meves mostres.

Molts agraïments també a la Dra. Laura Ortiz per ensenyar-me el món de l'espectrometria de masses i per les mostres "problemàtiques" que la feien anar de bòlit.

A Virginia Álvarez, por introducirme en el vasto mundo de la química por primera vez. Si estoy aquí Virginia es gracias a ti.

Als meus companys de laboratori de l'IRB: Anna (fatal!) per ser la millor dissenyadora de tesis de la història; Ernest (sempre amb la flor al cul); Craig (because you're always making me laugh)*; Albert (no t'estressis home!); Marta (no es nota no que ets de Girona... fua); Joan "en Matarín" (que compartim amistats jaja) i Pep (molta sort en el PhD!!).*

Al nostre grup dels matins; on algun dia s'hi descobrirà la sopa d'all: Imma (sort que ella posa un xic de sensatesa), Guti (toia!), en Miquel Seco (bé, però quan portava croissants... o llibres antics) moltes gràcies!

Als "antics doctorands" a qui dec molt bones estones: en Pau (correcto!) *per ensenyar-me a moure pel laboratori. Ho admeto mai seré capaç d'ocupar dues vitrines i fer quatre refluxos simultàniament... A la Marta (fresca!), per tot el temps que vam passar plegats "aguantant" en Manel: ella sí que m'entenia... i per tenir el mèrit de decorar un laboratori de mecanismes amb "boas" i micos de colors.*

Al grup de "basurisme" en particular a la Dra. Saskia Speed (mai la cregueu quan us digui "anem a fer una cervesa" en seran cinc com a mínim...); a la Laia (Laiups!) per treure'm un somriure cada dia (t'has convertit en "la xunga" del departament y lo sabes*); a en Javier pel seu bon humor mentre ens "gaseja" el laboratori amb les seves fosfines i a la Hellen perquè el DMSO congela, per una societat en ordre i bé pel "hellenisme"* (ayy mi bebé... ya sabes como sigue)*.*

A en Jordi i la Laia pels donuts del "dunkin" i darrere el cafè amb sacarina; pel gran viatge a Pamplona i els vespres de cine... quants records!

Als meus bons amics del "Divertigrupo" (siempre nos quedará Cerdeña...) *en particular a la secció* "del amoche"*:* Lucía, núcleo del equipo y decidida organizadora de eventos, porque incluso cuando se hace el silencio sabes salir adelante y decir "pues parece que se ha quedado buena tarde"; *Judit!!* (hierro!) *escaladora experta i* madame *del Molino... si si, jo se que dirigeixes el garito... Àlex pel seu gran sentit de l'humor i el seu "palique",* ayy aquellos viajes astrales a Bóveda... A Alejandro, Laura, Sara, Adri, Marta, Clara... madre mía cuanta gente... si ya lo digo yo que "en la variedad está el gusto".

A l'Eva i l'Asier per aguantar-me en les meves "sessions de teràpia de tesi" i per tot l'ajut que m'heu brindat aquests anys. Asier! A ti te debo una frase más. Por ser un buen amigo y estar ahí siempre: "Mila esker guztiagatik".

A tu Mel, per estar al meu costat en aquests mesos tan durs, per recordar-me que hi ha vida més enllà de la feina i per tot l'afecte que em brindes, gràcies bonica.

"At last but not at least", vull agrair a la meva família el seu suport incondicional. En especial als meus pares, per a mi, els millors exemples a seguir. Per la paciència que han tingut i per ensenyar-me que amb esforç i dedicació tot objectiu és possible d'aconseguir.

Barcelona, desembre de 2018

Table of contents

Chapter I. General introduction and objectives

1.   General introduction and objectives

One of the most important areas in Organometallic Chemistry is the synthesis, characterisation and study of the reactivity of compounds with potential application as catalytic precursors for homogenous catalysis.[1] Organic reactions catalysed by transition metal complexes have experienced an intense growth during the last decades. The main goals that spur this research are the optimisation, in terms of conversion and selectivity, of already known processes; the expansion of the scope of the reactions towards more challenging substrates and the discovery of new useful transformations for the preparation of highly valued products.[2]

The control of the enantioselectivity in those processes in which chiral compounds are formed demands the design of suitable chiral catalysts bearing stereogenic elements adjustable to the requirements of substrates.[3]

The need of optically pure substances is mainly driven because of the different behaviour of the two enantiomers of a compound when interacting with biological structures present in living beings. For instance, an optically pure enantiomer of a drug can be active while the other might be inactive or even cause severe side effects.[4]

As a consequence pharmaceutics, agrochemicals and cosmetic industry demand more efficient enantioselective processes. At present, for industry it is not enough to look for efficiency from an economical point of view, since the environmental impact must also be minimised to comply with the ever-increasing legal constraints regarding waste generation and management. All these requirements are among the so called Green Chemistry principles,[5] which constitute an approach to chemistry that aims to maximise efficiency and minimise hazardous effects on human health and the environment. While no reaction can be perfectly "green", the overall negative impact of the chemical industry can be reduced by means of waste prevention, atom economy and use of renewable feedstock, among others.

Asymmetric homogeneous catalysis is a powerful tool to deal with this challenge by means of design and preparation of suitable catalytic precursors for organic reactions in order to make them *chemo- regio-* and *enantio*especific, allowing a targeted synthesis towards the desired product under mild conditions and with a high atom economy.[6]

Since the origins of asymmetric homogeneous catalysis with transition metals, chiral phosphines and derivatives have been the preferred type of ligands.[6a,b,7] Nowadays, the synthesis of new phosphorus ligands is still an extremely active area,

fostered by a continuous need of new ligands that lead to faster and more selective processes, operating under milder conditions. This research is leading to new families of chiral phosphines exploiting all possible sources of diversity including stereogenic centres, axes and planes.[8] A particularly appealing family is that of *P*-stereogenic phosphines (*i.e.* those that contain phosphorus atoms bound to three different substituents), a ligand type that, despite being linked to the origins of asymmetric catalysis, was neglected for a long time[9] and now is experiencing an intense renaissance.[10]

There are many examples of organic reactions catalysed by transition metal systems containing *P*-stereogenic ligands such as hydrogenation, transfer hydrogenation, allylic substitution, hydrovinylation, hydroformylation and cycloaddition reactions. By far, the more studied is the Rh-catalysed asymmetric hydrogenation of olefins,[10b] which can be considered as the responsible of the research that was carried out in the development of libraries of *P*-stereogenic ligands.

Although it is not generally true, it seems reasonable that this kind of ligands provide very enantioselective catalysts because the stereogenic element (the phosphorus atom) is directly bounded to the metal centre.[8b,11]

What is more, an exciting possibility is to have catalytic precursors in which the metallic atom itself is a stereogenic centre, the so-called chiral-at-metal complexes.[12] In fact, nowadays, the combination of chiral ligands with *M*-stereogenic metallic centres represents an area of intense activity.[13]

At the *Unitat de Recerca en Síntesi Asimètrica* (URSA) research group at the University of Barcelona and the Institute for Research in Biomedicine (IRB Barcelona), we have been working during the last decade on the development of new methodologies for the synthesis of *P*-stereogenic ligands. Two of the most relevant advances have been the preparation with high yields of optically pure aminophosphine-boranes and phosphinous acid-boranes by means of asymmetric synthesis, using the *cis*-1-amino-2-indanol as chiral auxiliary (Scheme 1).[14]
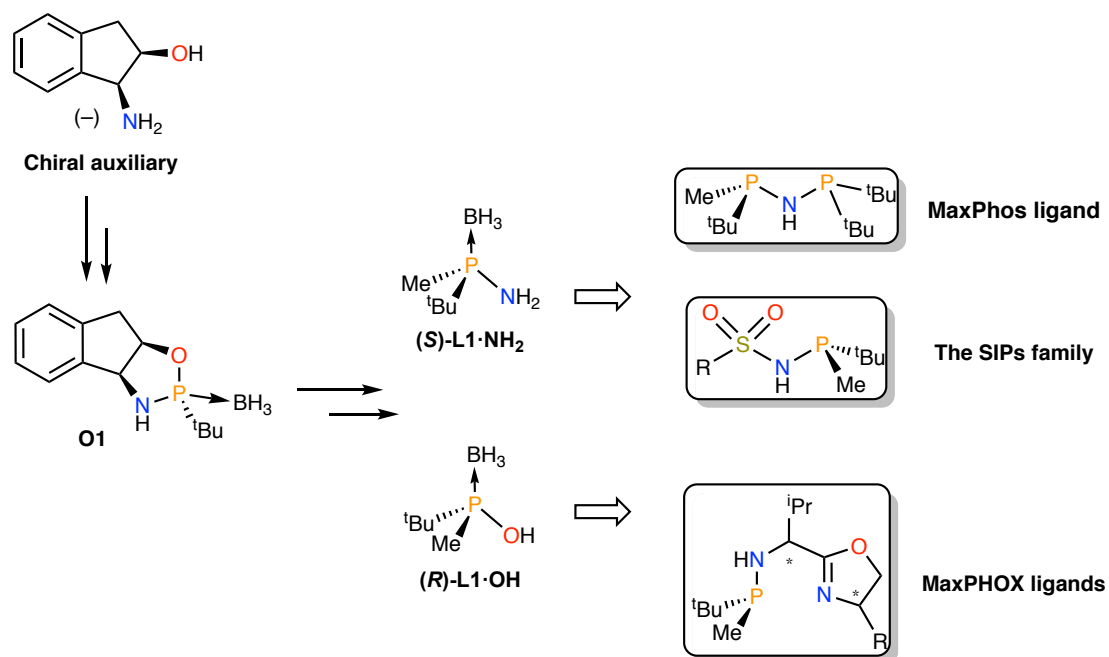
Scheme 1. Preparation of some relevant ligands by stereoselective synthesis using *cis*-1-amino-2-indanol as chiral auxiliary.

These *P*-stereogenic synthons have been found to be very adequate for the preparation of many relevant ligands such as MaxPhos,[15] which have proved to be an excellent ligand for Rh-catalysed enantioselective hydrogenations and Pauson-Khand reactions; the *P*-stereogenic iminophosphoranes (SIPs) family, useful in [2+2+2] Rh-catalysed cycloaddition of endyines[15a] and more recently, the small library of oxazoline-based *P,N*-ligands MaxPHOX,[16] allowing high enantioselectivities in the Ir-catalysed hydrogenation of aryl imines.

In the present THESIS these studies on the design and study of new *P*-stereogenic ligands, their complexes and performance in asymmetric catalysis have been continued.

The **first general objective (Chapter 3)** was the exploration of the coordination chemistry of a particular Secondary Phosphine Oxide (SPO), which presents a tautomeric equilibrium between the air-stable pentavalent form (the oxide) and the trivalent form (phosphinous acid), ready to coordinate a metallic centre (Scheme 2).[17]

P–H form   **O–H form**   *Pseudobidentate coordination*
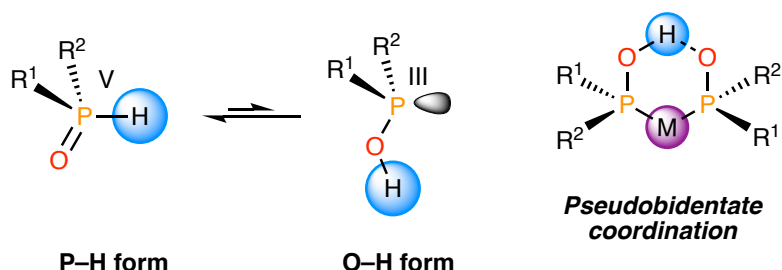
Scheme 2. Tautomeric equilibrium of Secondary Phosphine Oxides (SPOs) and assembly of two SPO units.

Although SPOs were described more than fifty years ago, their appealing air-stability in contrast to many phosphines and derivatives are placing them, nowadays, in the spotlight. Their unique properties have spurred the study of the applications of SPOs in catalysis, specially due to their ability to form pseudobidentate architectures having an intramolecular hydrogen bond.[18]

Interestingly, *P*-stereogenic SPOs are configurationally stable but, despite that, very few catalytic applications in asymmetric catalysis have been reported in the literature,[19] probably due to the lack of convenient preparative methods.

Our goal was the synthesis of enantiopure *t*-BuMe(O)PH (**L1**),[14d,20] which despite being very simple had not been prepared in an optically pure form. Indeed, **L1** was detected in previous studies in the group as a byproduct of the acidic hydrolysis of aminophosphines, such as (*R*)-**L1·NH₂**[14d] and using this methodology it was possible to obtain enantioenriched (*S*)-**L1**, albeit with low *ee* (Scheme 3).

In this THESIS, we planned to develop a reliable synthesis of optically pure (*S*)-**L1** by deprotection of *tert*-butyl(methyl)phosphinous acid-borane (*S*)-**L1·OH** since its synthesis in enantiomerically pure form had been described. (Scheme 3)[14b-e,20]

(*R*)-**L1·NH₂**   (*S*)-**L1**   (*S*)-**L1·OH**
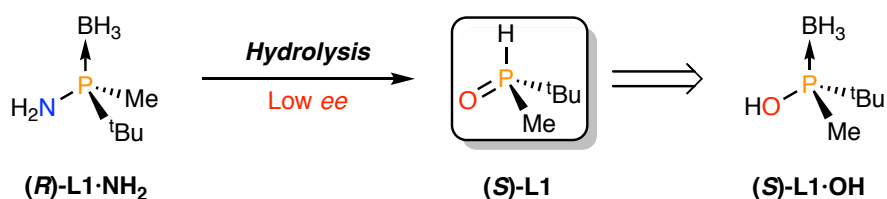
Scheme 3. Synthetic strategy for the preparation of optically pure (*R*)-**L1**.

4

This SPO is particularly interesting since contains the sterically dissymmetric *t*-Bu/Me combination, which has yielded extremely important phosphine ligands for asymmetric reactions.[21] Its coordination chemistry with several noble metals is discussed in Chapter 3, showing their rich variety of coordination modes and their catalytic applications.

The election of the location and absolute configurations of chiral elements in the catalysts play a crucial role in the stereoselective discrimination of the substrates.

A few years ago, our group reported the MaxPhos ligand (Scheme 4), which is a rare example of *P*-stereogenic, C_1-symmetric ligand with a short bridge between the phosphorus atoms.[15b]
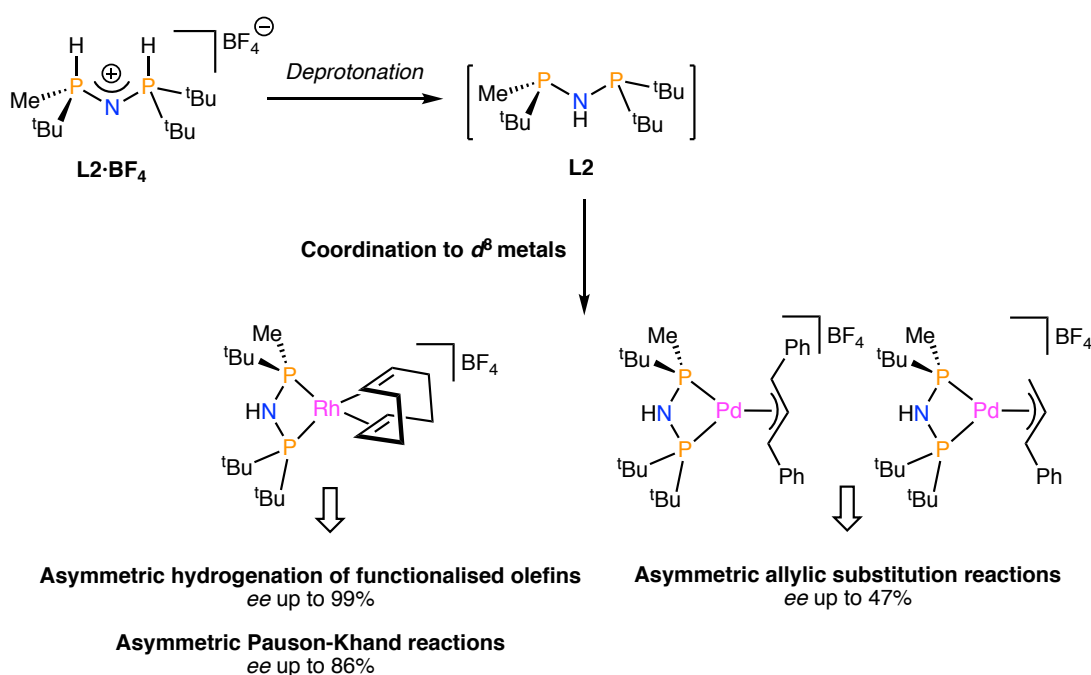
Scheme 4. Coordination chemistry of the MaxPhos ligand with several d^8 metals and its catalytic applications.

In addition, thanks to a tautomeric equilibrium involving the P atoms and the NH bridge, it was obtained as its bench-stable crystalline tetrafluoroborate salt, in contrast to many of the new generation highly basic and air-sensitive *P*-stereogenic ligands with alkyl substituents.[15b]

The coordination chemistry of this ligand was initially explored with Rh(I)-diene complexes,[15b,c] which were found to be excellent precursors for the asymmetric hydrogenation of functionalised olefins[15b,c] and later for intramolecular Pauson-Khand reactions.[15d] These studies were followed by the synthesis of several Ni(II) and Pd(II) complexes some of which were used in asymmetric allylic substitutions.[15c]

In all the reported cases, the MaxPhos ligand **L2** was coordinated to d^8 metals with square-planar geometry. With the aim of expanding the range of metals coordinated to MaxPhos, **the second general objective (Chapter 4)** was the preparation of some *M*-stereogenic Rh, Ir and Ru complexes with this C_1-symmetric ligand (Scheme 5). This research, presented in Chapter 4, was carried out in collaboration with Dr. Daniel Carmona from the *Consejo Superior de Investigaciones Científicas* (CSIC) institute in Zaragoza.
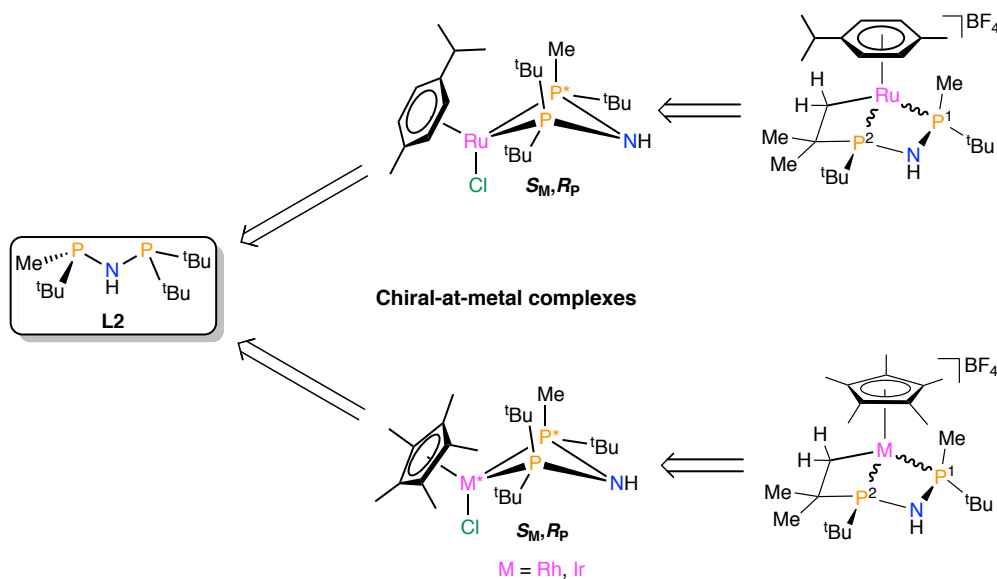
Scheme 5. Synthetic strategies for the preparation of chiral-at-metal MaxPhos complexes.

The MaxPhos ligand **L2** possesses a stereogenic phosphorus atom due to the presence of one Me and one *t*-Bu groups and the different electronic and steric requirements of the Me/*t*-Bu couple determine the stereochemistry of its coordination chemistry. We chose this type of complexes because the C_1-symmetric nature of MaxPhos results in a stereogenic metal atom upon coordination in pseudotetrahedral $(\eta^n\text{-ring})$M complexes. The C–H activation of the *tert*-butyl group of these complexes was studied and also some catalytic applications.

Finally, in our efforts to develop useful *P*-stereogenic ligands for asymmetric catalysis,[15b] our group recently reported a series of highly modular phosphinooxazoline ligands, named MaxPHOX. [Ir(MaxPHOX)COD]BArF complexes gave the highest stereoselectivity ever reported in the hydrogenation of cyclic enamides (Scheme 6).[16a]

MaxPHOX   Phosphinous acid   Amino acid   Amino alcohol

[Ir(MaxPHOX)COD]BArF

Asymmetric hydrogenation of β,α-enamides

β-enamides

α-enamides

[Ir(MaxPHOX)COD]BArF

H₂

Conversions and *ee* up to 99%
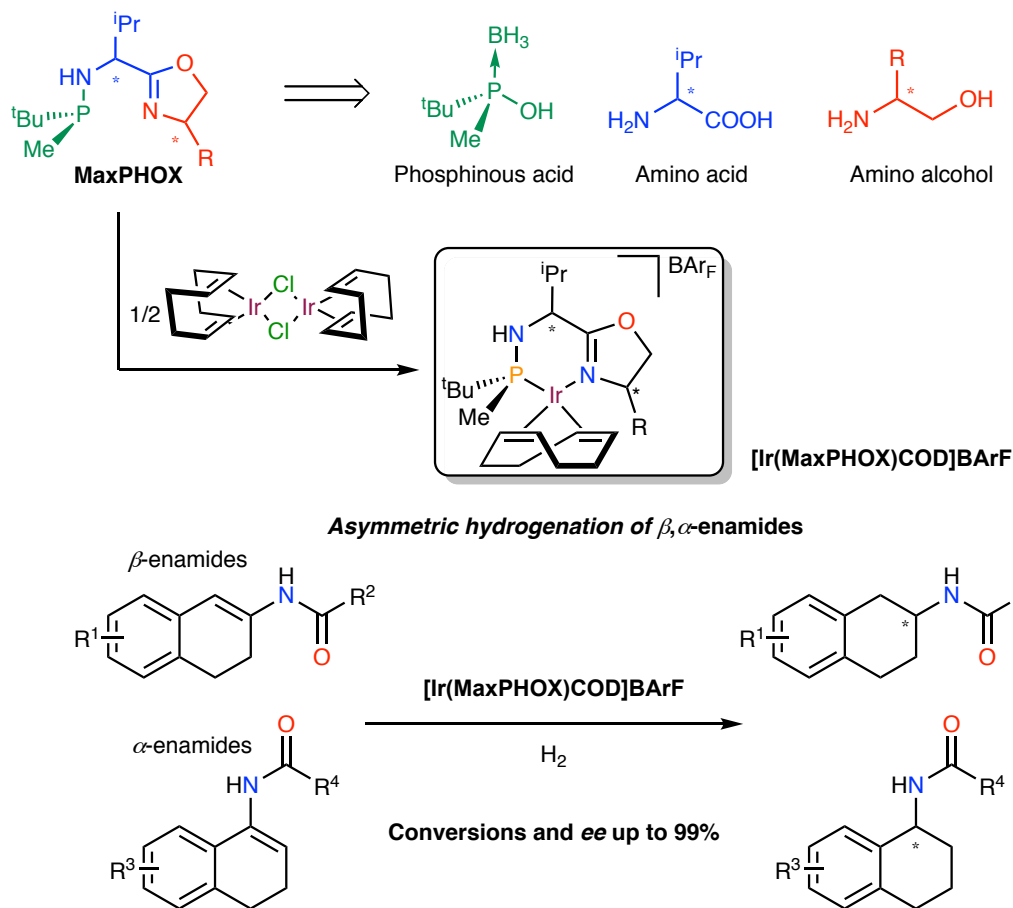
Scheme 6. Precedents on the Ir-catalysed hydrogenation of β,α-enamides.

Very recently, these studies have been extended to the hydrogenation of *N*-aryl imines affording excellent yields and enantioselectivities (Scheme 7).[16b] It was found that the actual catalysts were cyclometallated Ir(III) monohydrido complexes, analogous to those reported by Pfaltz and co-workers a few years ago.[22]
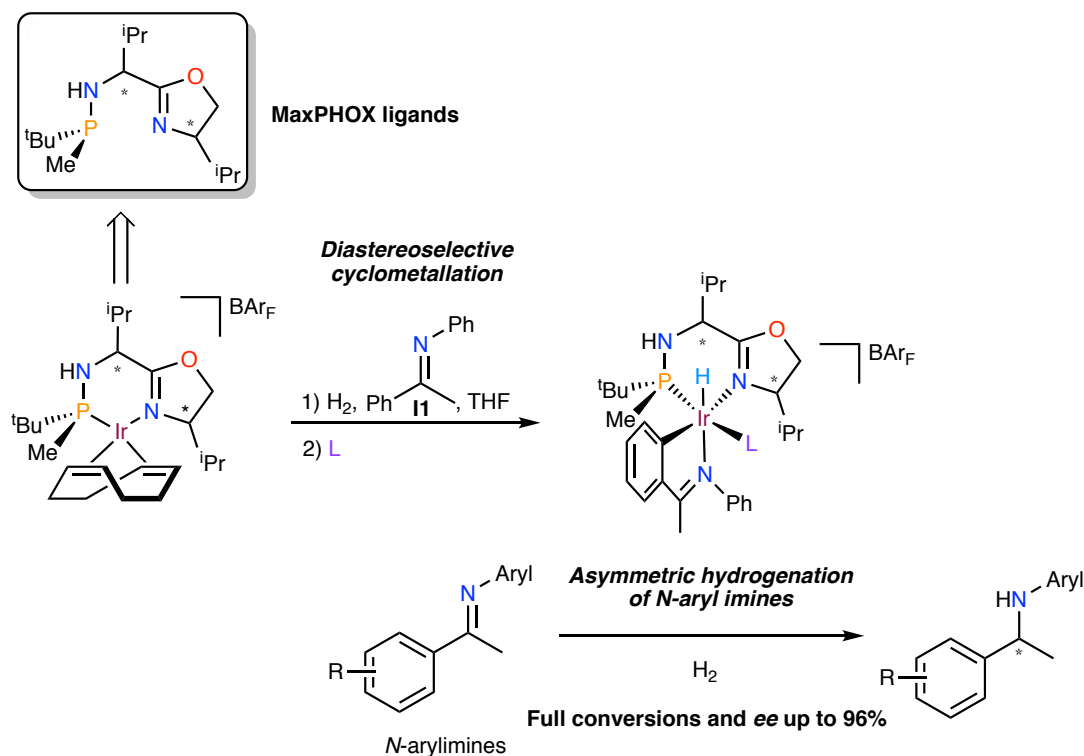
Scheme 7. Preparation of Ir-MaxPHOX complexes and its application in asymmetric hydrogenation of *N*-aryl imines.

The **third general objective (Chapter 5)** was to advance the characterisation studies of such cyclometallated Ir-MaxPHOX complexes in order to find a stable iridacycle that could be used as catalyst for asymmetric transformations. Upon the addition of monodentate ligands, several very stable iridium complexes have been isolated and fully characterised, two of them by X-ray diffraction studies. Interestingly, despite the many possible isomers, only one or two isomers were formed, depending on the incoming ligand and the absolute configuration of the substituents of the oxazoline. Some of the new complexes have proven to be excellent catalysts for the hydrogenation both *N*-aryl imines but also the more challenging *N*-alkyl imines, affording excellent levels of activity and enantioselectivity, never reported before for these systems, under mild conditions. Besides, these catalytic studies have been complemented with theoretical calculations, carried out in collaboration with prof. Agustí Lledós from the *Universitat Autònoma de Barcelona* (UAB) in order to highlight some mechanistic features of the asymmetric hydrogenation process: one of the least known hydrogenation mechanisms.

The **specific objectives** of this THESIS can be summarised as follows:

- Synthesis of the optically pure, *P*-stereogenic SPO *t*-BuMeP(O)H and the exploration of its coordination chemistry towards Ni(II), Ir(I), Rh(I), Au(I), Ru(II) and Pd(II).

- Study of the combination of a phosphinous acid and a phosphinite unit to form a C_2-symmetric pseudobidentate ligand with an intramolecular H-bridge.

- Exploration of the catalytic activity of the preformed phosphinous acid complexes bearing the SPO unit in several asymmetric transition metal catalysed reactions.

- Study of the coordination chemistry of the C_1-symmetric, *P*-stereogenic MaxPhos ligand with Ir(III)-, Rh(III)- and Ru(II)-η^n-ring moieties in order to prepare chiral-at-metal complexes with a definite stereochemistry.

- Study of the intramolecular aliphatic activation of one of the *t*-Bu groups of the MaxPhos ligand in the Ir(III), Rh(III) and Ru(II) *M*-stereogenic complexes.

- Evaluation of the catalytic activity of the *M*-stereogenic complexes in asymmetric hydrogen-transfer reactions.

- Preparation of a family of cyclometallated Ir-MaxPHOX complexes with different ancillary ligands and study of their catalytic activity in the asymmetric hydrogenation of *N*-alkyl imines.

- Study by means of both experimental and theoretical methods the mechanism of Ir-catalysed hydrogenation of *N*-alkyl imines with MaxPHOX ligands.

1.1. *References*

(1)   (a) Crabtree, R. H. *The organometallic chemistry of the transition metals*; 3 ed.; Wiley & Sons: New York, 2001 (b) Elschenbroich, C. *Organometallics*; 3 ed.; Wiley-VCH: Weinheim, 2006.

(2)   *Applied Homogeneous Catalysis with Organometallic Compounds*; 2nd ed.; Cornils, B.; Herrmann, W. A., Eds.; Wiley-VCH: New York, 2002.

(3)   Tucker, C. E.; de Vries, J. G. *Topics in Cat.* **2002**, *19*, 111-118.

(4)   Blaser, H.-U.; Federsel, H.-J.; Ed. *Asymmetric Catalysis on Industrial Scale: Challenges, Approaches and Solutions*; 2 ed.; Wiley, 2010.

(5)   Anastas, P. T.; Warner, J. C. *Green Chemistry: Theory and Practice*; Oxford University Press: Oxford, 1998.

(6)   (a) Noyori, R. *Asymmetric Catalysis in Organic Synthesis*; Wiley and Sons, Inc.: New York, 1994 (b) *Comprehensive asymmetric catalysis*; Jacobsen, E. N.; Pfaltz, A.; Yamamoto, A., Eds.; Springer: Berlin, 1999 (c) Andrushko, N.; Börner, A. In *Phosphorus Ligands in Asymmetric Catalysis: Synthesis and Applications*; Börner, A., Ed.; Wiley-VCH: Weinheim, 2008; Vol. 3.

(7)   Zhou, Q.-L.; Ed. *Privileged Chiral Ligands and Catalysts*; Wiley-VCH: Weinheim, 2011.

(8)   (a) Dodds, D. L.; Gillespie, J. A.; Grabulosa, A.; Kamer, P. C. J. *Appl. Organomet. Chem.* **2010**, *24*, 64-64 (b) Kamer, P. C. J.; van Leeuwen, P. W. N. M.; Ed. *Phosphorus(III) Ligands in Homogeneous Catalysis: Design and Synthesis*; Wiley, 2012.

(9)   Pietrusiewicz, K. M.; Zablocka, M. *Chem. Rev.* **1994**, *94*, 1375-1411.

(10)   (a) Grabulosa, A.; Granell, J.; Muller, G. *Coord. Chem. Rev.* **2007**, *251*, 25-90 (b) Grabulosa, A. *P-Stereogenic Ligands in Enantioselective Catalysis*; Royal Society of Chemistry: Cambridge, 2011 (c) Kolodiazhnyi, O. I. *Tetrahedron: Asymmetry* **2012**, *23*, 1-46 (d) Kolodiazhnyi, O. I.; Kukhar, V. P.; Kolodiazhna, A. O. *Tetrahedron: Asymmetry* **2014**, *25*, 865-922 (e) Dutartre, M.; Bayardon, J.; Jugé, S. *Chem. Soc. Rev.* **2016**, *45*, 5771-5794 (f) Kolodiazhnyi, O. I.; Kolodiazhna, A. *Tetrahedron: Asymmetry* **2017**, *28*, 1651-1674.

(11)   Lipkowitz, K. B.; Sakamoto, T.; Stack, J. *Chirality* **2003**, *15*, 759-765.

(12)   (a) Gong, L.; Chen, L. A.; Meggers, E. *Angew. Chem. Int. Ed.* **2014**, *53*, 10868-10874 (b) Huo, H.; Shen, X.; Wang, C.; Zhang, L.; Röse, P.; Chen, L.-A.; Harms, K.; Marsch, M.; Hilt, G.; Meggers, E. *Nature* **2014**, *515*, 100 (c) Huang, X.; Li, X.; Xie, X.; Harms, K.; Riedel, R.; Meggers, E. *Nat. Commun.* **2017**, *8*, 2245 (d) Ma, J.; Zhang, X.; Huang, X.; Luo, S.; Meggers, E. *Nat. Protoc.* **2018**, *13*, 605.

(13)   (a) Carmona, D.; Lamata, M. P.; Oro, L. A. *Eur. J. Inorg. Chem.* **2002**, 2239-2251 (b) Pardo, P.; Carmona, D.; Lamata, P.; Rodríguez, R.; Lahoz, F. J.; García-Orduña, P.; Oro, L. A. *Organometallics* **2014**, *33*, 6927-6936 (c) Carmona, M.; Rodríguez, R.; Passarelli, V.; Lahoz, F. J.; García-Orduña, P.; Carmona, D. *J. Am. Chem. Soc.* **2018**, *140*, 912-915.

(14)   (a) Revés, M.; Ferrer, C.; León, T.; Doran, S.; Etayo, P.; Vidal-Ferran, A.; Riera, A.; Verdaguer, X. *Angew. Chem. Int. Ed.* **2010**, *49*, 9452-9455 (b) León, T.; Riera, A.; Verdaguer, X. *J. Am. Chem. Soc.* **2011**, *133*, 5740-5743 (c) Zijlstra, H.; León, T.; de Cózar, A.; Guerra, C. F.; Byrom, D.; Riera, A.; Verdaguer, X.; Bickelhaupt, F. M. *J. Am. Chem. Soc.* **2013**, *135*, 4483-4491 (d) Orgué, S.; Flores-Gaspar, A.; Biosca, M.; Pàmies, O.; Diéguez, M.; Riera, A.; Verdaguer, X. *Chem. Commun.* **2015**, *51*, 17548-17551 (e) Salomó, E.; Orgué, S.; Riera, A.; Verdaguer, X. *Synthesis* **2016**, 2659-2663.

(15) (a) León, T.; Parera, M.; Roglans, A.; Riera, A.; Verdaguer, X. *Angew. Chem. Int. Ed.* **2012**, *51*, 6951-6955 (b) Cristóbal-Lecina, E.; Etayo, P.; Doran, S.; Revés, M.; Martín-Gago, P.; Grabulosa, A.; Constantino, A. R.; Vidal-Ferran, A.; Riera, A.; Verdaguer, X. *Adv. Synth. Catal.* **2014**, *356*, 795-804 (c) Grabulosa, A.; Doran, S.; Brandariz, G.; Muller, G.; Benet-Buchholz, J.; Riera, A.; Verdaguer, X. *Organometallics* **2014**, *33*, 692-701 (d) Cristóbal-Lecina, E.; Costantino, A. R.; Grabulosa, A.; Riera, A.; Verdaguer, X. *Organometallics* **2015**, *34*, 4989-4993.

(16) (a) Salomó, E.; Orgué, S.; Riera, A.; Verdaguer, X. *Angew. Chem. Int. Ed.* **2016**, *55*, 7988-7992 (b) Salomo, E.; Rojo, P.; Hernández-Lladó, P.; Riera, A.; Verdaguer, X. *J. Org. Chem.* **2018**, *83*, 4618-4627.

(17) Roundhill, D. M.; Sperline, R. P.; Beaulieu, W. B. *Coord. Chem. Rev.* **1978**, *26*, 263-279.

(18) Achard, T. *Chimia* **2016**, *70*, 8-19.

(19) Jiang, X.; Minnaard, A. J.; Hessen, B.; Feringa, B. L.; Duchateau, A. L. L.; Andrien, J. G. O.; Boogers, J. A. F.; de Vries, J. G. *Org. Lett.* **2003**, *5*, 1503-1506.

(20) Salomó, E.; Prades, A.; Riera, A.; Verdaguer, X. *J. Org. Chem.* **2017**, *82*, 7065-7069.

(21) Imamoto, T. *Chem. Rec.* **2016**, *16*, 2655-2669.

(22) Schramm, Y.; Barrios-Landeros, F.; Pfaltz, A. *Chem. Sci.* **2013**, *4*, 2760-2766.

Chapter II. Precedents on the preparation of P-stereogenic ligands

2. Precedents on the preparation of *P*-stereogenic ligands

This chapter offers a summary of the different synthetic strategies towards enantioenriched *P*-stereogenic phosphines reported up to now. As one of the aims of the present THESIS was the preparation of several *P*-stereogenic ligands with the sterically dissymmetric ^{t}Bu/Me combination at phosphorus, this Chapter is especially focused on this kind of ligands.

2.1. *Historical overview*

More than a century has passed since the discovery that compounds with tetrahedral sp^3 phosphorus atoms linked to different substituents, generally known as *P*-stereogenic compounds, are configurationally stable and can be separated into a pair of enantiomeric forms.[1]

Unlike amines, which have an energy barrier for pyramidal inversion[2] around 25 kJ·mol^{-1}, P(III) compounds, such as phosphines, do not racemise as easily at room temperature due to their higher energy inversion barriers[2a,3] of more than 150 kJ·mol^{-1}. Therefore, heating above 100 ºC is usually needed in order to racemise *P*-stereogenic phosphines through the well-known pyramidal, "umbrella", inversion (Scheme 1).
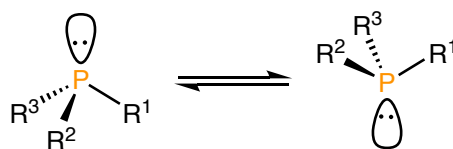
Scheme 1. Pyramidal inversion of a general P(III) compound.

The history of this class of compounds starts, indeed, in 1911 when Meisenheimer and Lichtenstadt[1] synthesised ethylmethylphenylphosphine oxide **1** as a racemic mixture and were able to separate each enantiomer (Figure 1).
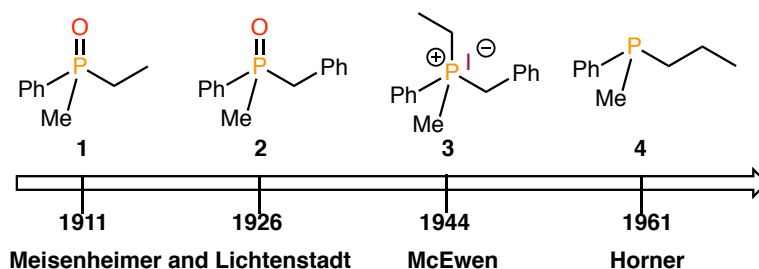
Figure 1. Early examples *P*-stereogenic compounds resolved between 1911 and 1961.

It took fifteen years for the same laboratory to repeat that feat and apply the same method to resolve benzylmethylphenylphosphine oxide **2**.[4] Soon afterwards, in 1944, McEwen and co-workers[5] were able to resolve the first acyclic phosphonium salt, **3**. However, it was not until 1961 when Horner and co-workers[6] isolated, for the first time, optically pure *trivalent* phosphines, proving that, unlike amines, they do not racemise at room temperature.[6-7] At that time there was no interest on applying these compounds in catalysis but to perform stereochemical studies.[8]

During the 1967–1968 period, two key breakthroughs had a huge impact in the field of homogeneous catalysis. The first one was the hydrogenation of certain olefins and acetylenes by a soluble rhodium complex [RhCl(PPh$_3$)$_3$], reported by Wilkinson and co-workers.[9] The second was the first asymmetric catalytic reaction ever performed, which took place in Noyori's laboratories.[10] Two years later, the research groups led by Knowles[11] and Horner[12] independently, replaced the achiral triphenylphosphine ligands in the Wilkinson catalyst by optically enriched *P*-stereogenic phosphines. The chiral precatalysts were tested in the hydrogenation of prochiral alkenes, and, even though the enantioselectivities achieved were low (Scheme 2), they proved for the first time, that enantioselective catalytic homogeneous hydrogenations were feasible.[11-12]

L* = (structure **4**)

R^1 = Ph, R^2 = COOH, 15% *ee*
R^1 = CH$_2$COOH, R^2 = COOH, 3% *ee*
R^1 = Ph, R^2 = Et, 8% *ee*
R^1 = Ph, R^2 = OMe, <5% *ee*
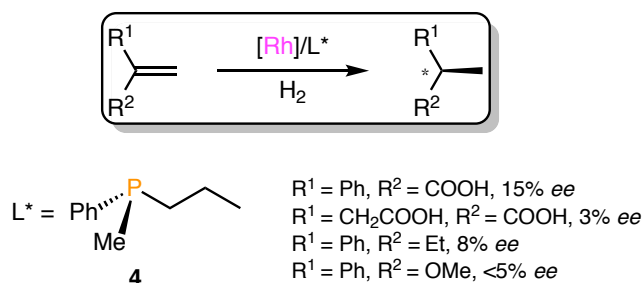
Scheme 2. First results in enantioselective hydrogenation.

Those findings awakened the interest to carry out research on the behaviour of *P*-stereogenic compounds in catalysis, and since then, the development of new synthetic

strategies for their preparation has run in parallel to their application in enantioselective transformations.

Also at the late 1960s, it was discovered that (*S*)-amino-3-(3,4-dihydroxyphenyl)propanoic acid (L-DOPA) was very efficient for the treatment of Parkinson's disease, thereby creating a sudden demand for this rare aminoacid. Knowles and co-workers,[13] at Montsanto, used vanillin as precursor for the preparation in large scale of L-DOPA. By that time, they decided to use the early-developed enantioselective hydrogenation for the efficient synthesis of that compound (Scheme 3).
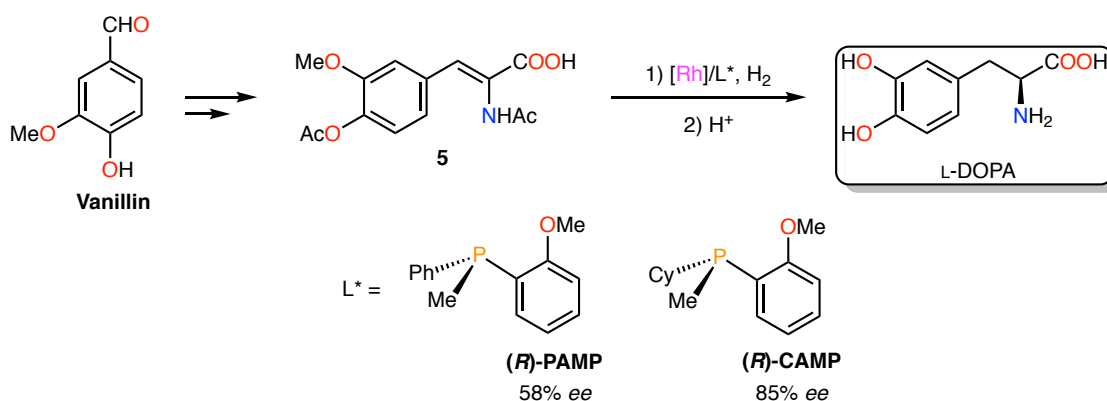
Scheme 3. Montsanto's L-DOPA synthesis.

After several experiments, it was found that PAMP and CAMP, bearing the *o*-anisyl group, were competent systems for the hydrogenation of **5** in useful levels of *ee*. Actually, that was the first time that enzyme-like selectivity was achieved with an artificial "man-made" catalyst.

Almost at the same time, Dang and Kagan[14] reported the chelating C_2-diphosphine DIOP, which displayed similar results in the hydrogenation of a derivative of precursor **5**, in spite of not having the chirality on the phosphorus atom (Figure 2).
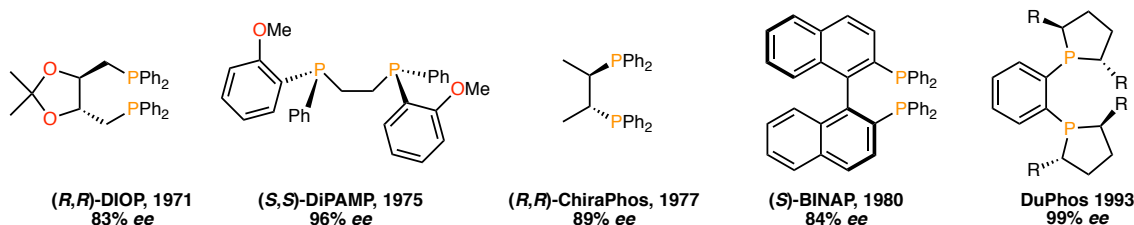
Figure 2. Chelating C_2-diphosphines, their *ee* values in Rh-catalysed hydrogenation of **5** are given below.

Soon afterwards, Knowles and co-workers[15] prepared the DiPAMP ligand obtaining an outstanding, at that time, 96% *ee* (Figure 2). Those results entailed the asymmetric hydrogenation of many other substrates such as enol esters, enamides, and related systems with similar levels of enantioselectivity.[16] That work was considered a milestone in the field of enantioselective homogeneous catalysis and allowed William S. Knowles to be awarded with the Nobel Prize in Chemistry in 2001, along with Ryoji Noyori and Barry Sharpless.[13b]

In spite of the success of DiPAMP, the good results with phosphorus ligands having the chirality on the backbone such as DIOP[14], as well as those of Bosnich[17] with ChiraPhos; Noyori[18] with BINAP; Burk[19] with DuPhos and many others (Figure 2) along with the intrinsic difficulties in the preparation of *P*-stereogenic phosphines, left them in the shadow for a long period. Indeed, a literature search reveals that, in spite of its versatility, applications of *P*-stereogenic compounds in catalysis are less abundant than those of phosphorus compounds with axial chirality, such as the BINAP, or bearing stereogenic carbon atoms on the backbone as DIOP.

However, with the use of boranes as protecting groups[20] instead of phosphine oxides there is a strong renewed interest in the development of new synthetic methods of optically pure *P*-stereogenic compounds.

In fact, both the methods of synthesis of *P*-stereogenic compounds and their application in asymmetric synthesis have been thoroughly reviewed. Pietrusiewicz and Zablocka[21] reported in 1994 a detailed review including resolution of racemic mixtures and stereoselective synthesis. In 2007 that report was completed with other excellent works such as the reported in the groups of Muller and co-workers[22] and Glueck.[23] A. Grabulosa[24] published in 2011 a fully comprehensive book covering the synthesis of *P*-stereogenic compounds and their application in homogeneous catalysis.[24] Börner[25] and Kolodiazhnyi[26] have also reviewed the more recent progress in this field.

2.2. *Preparation by resolution of racemic mixtures*

2.2.1. *Separation by resolution agents*

The first methods for the preparation of optically pure *P*-stereogenic compounds consisted of the separation of diastereomeric adducts of phosphine oxides and phosphonium salts with chiral auxiliaries.[21,24] The reaction of the chiral auxiliary with a racemate gives a diastereomeric mixture, which can be separated by physical methods, such as recrystallisation, due to the different physical properties of diastereomers.

Although the first resolving agents were non-metallic auxiliaries[24] in 1968 the use of a chiral platinum complex was reported.[27] After that, chiral palladacycles and other chiral complexes[21] were also proved useful to this purpose.[22,25] At present, resolution of racemic mixtures is becoming less used as more efficient synthetic procedures are appearing. However, it is still a useful procedure when there are no other ways to obtain a particular ligand.[28] In fact, at present, some optically pure Secondary Phosphine Oxides (SPOs), are still being prepared by diastereomeric resolution,[29] like $^{t}BuPhP(O)H$,[30] the most prominent one, as it will be explained in Chapter 3.

An example of the application of this methodology can be found in the preparation of the optically pure *tert*-butylphenylphosphinous acid borane **6** reported by Stankevic and Pietrusiewicz[31] (Scheme 4).
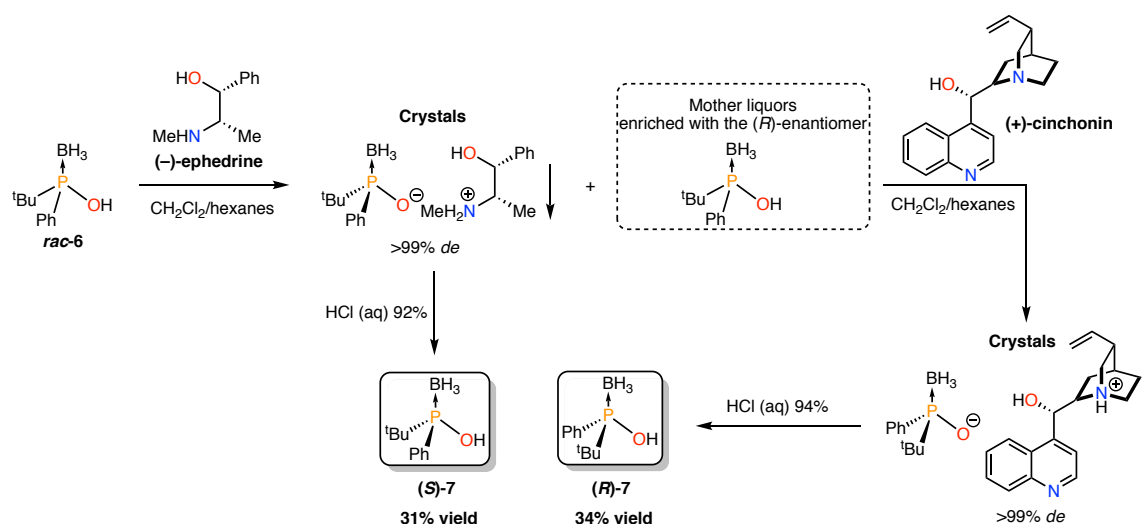
Scheme 4. Stankevic's and Pietrusiewicz's preparation of (*S*)- and (*R*)-**7**.

Two consecutive crystallisations using ephedrine and cinchonine as resolving agents allow the preparation of both enantiomers of **7**.[31]

2.2.2. *Separation by chromatographic methods*

HPLC with chiral stationary phases represent the most useful method for the analysis of the optical purity of *P*-stereogenic compounds. Nevertheless, it can be also used on a preparative scale to resolve racemic mixtures of conveniently protected phosphorus ligands. Hence, HPLC resolutions have been mostly performed over phosphine-boranes[32] and phosphine oxides.[33] Although this seems to be a very attractive methodology to obtain enantiomerically enriched *P*-stereogenic compounds, in practice, it requires special equipment, preparative columns and large volumes of high quality solvents, which are beyond the economic possibilities of many research laboratories. In spite of that, when there are no enantioselective synthetic routes to a particular phosphine and the chemical resolution methods fail, a chromatographic separation of the racemic mixture is worth considering, as may be the only way to obtain the enantiopure compound. Notwithstanding, in spite of the economic costs mentioned, there are examples of successful separations of alkyl-phosphine-boranes with the ᵗBu/Me combination, such as the TrichickenfootPhos borane reported by Hoge and co-workers.[32c] Indeed, in this paper they stated that "*despite the stigma associated with chiral preparatory HPLC separations, this type of separations is becoming increasingly important to the pharmaceutical industry.*"

Resolution of racemic mixtures has been partially displaced by more versatile methods based on stereoselective synthesis, since the overall yields in racemic resolutions can never top, by definition, 50%. These methods are described in the next Section.

2.3. *Preparation by asymmetric synthesis*

Stereoselective methodologies rely on the induction of chirality into phosphorus compounds through stereoselective reactions by means of the use of chiral auxiliaries, such as alcohols or amines, favouring the formation of one single enantiomer. *P*-stereogenic compounds can be isolated and stored in an optically pure form, and undergo substitution reactions that sometimes fully preserve or invert the P configuration, although the reaction must be performed carefully in order to avoid racemisation. In particular, it has been found that, in the presence of a nucleophile,

when the *P*-stereogenic reagent contains a substituent that can act as a leaving group, it undergoes a S$_N$2@P reaction (Scheme 5).[34]
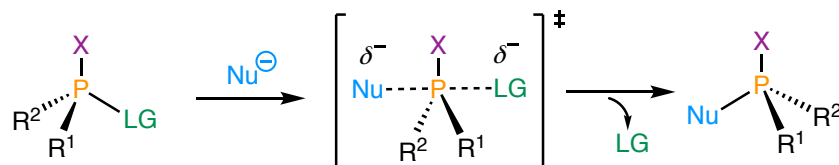
Scheme 5. Mechanism of the S$_N$2@P reaction. Nu = nucleophile, LG = leaving group, X = lone pair, BH$_3$, etc.

In contrast to carbon, the phosphorus has vacant *d*-orbitals and consequently the can form stable compounds with trigonal bipyramidal and even octahedral geometries.[35] When long-lived five-coordinated intermediates are formed, Berry pseudorotations can take place, influencing the stereochemistry, and racemisation or even full retention can occur.[35]

In a trigonal-bypiramidal species the five substituents are not equivalent: three of them are equatorial while nucleophile and the leaving group are apical.[36] This fact leads to a differentiation of the stereochemistry of the reaction products depending on the direction in which the nucleophile attacks the phosphorus centre. More precisely, S$_N$2@P proceeding via a *backside* attack usually results in inversion of the phosphorus configuration while S$_N$2@P *frontside* reactions lead to products with retention (Scheme 6).
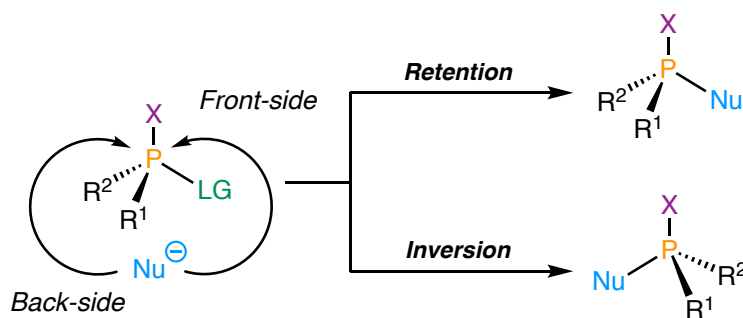
Scheme 6. *Frontside* and *backside* S$_N$2@P transformations.

In spite of the very different mechanisms, substitution reactions on phosphorus compounds are usually found to occur with inversion of configuration[35] as in the classic S$_N$2 process of organic chemistry. A notable exception is the substitutions in certain P-heterocycles, such as *N*-methyl-oxazaphospholidines,[37] which are important synthons in the preparation of *P*-stereogenic ligands.

2.3.1. *Resolution of diastereomeric mixtures*

2.3.1.1. *Alcohols as chiral auxiliaries*

Chiral alcohols (menthol, *endo*-borneol, glucofuranose derivatives, and others) serve as cheap and accessible chiral auxiliaries for the preparation of enantiopure *P*-stereogenic compounds.[38] In 1967, Cram,[39] Mislow and co-workers[38a] reported the synthesis of *P*-stereogenic phosphine oxides via resolution of diastereomeric menthylphosphinates and subsequent addition of Grignard reagents. The reduction of the phosphine oxide with trichlorosilane yielded the chiral phosphine (Scheme 7).
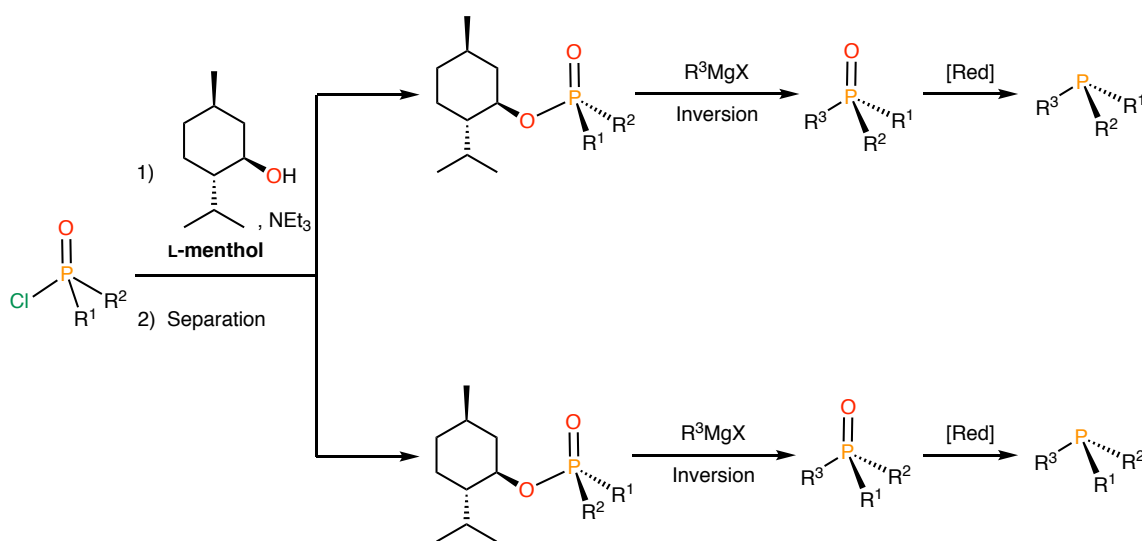
Scheme 7. Synthesis of *P*-stereogenic phosphines employing L-menthol.

After the works of Cram and Mislow, Horner[40] and other groups[16a,41] prepared unsymmetrically substituted menthylphosphinates and separated them into their diastereomers by crystallisation.

Since the reduction step for the obtention of the free *P*-stereogenic ligands is usually performed with silanes[42] or hydrides,[43] the harsh conditions required often produce a significant loss of optical purity[42c] or even racemisation.[43a]

Phosphine-boranes, like oxides, are also stable and easily-to-handle, with the important advantage that can be deboronated with retention of configuration preserving the optical purity of the phosphorus atom. In 1990, Imamoto and co-workers[20a] took benefit of this feature and overcame the drawback of racemisation associated with deprotection of oxides by adapting the use of L-menthol as chiral auxiliary to phosphine-boranes. They found that the stereospecific reductive cleavage of the P–O

bond of the menthylphosphinate forms the corresponding highly nucleophilic phosphide anion, which can undergo reactions with different electrophiles (Scheme 8).
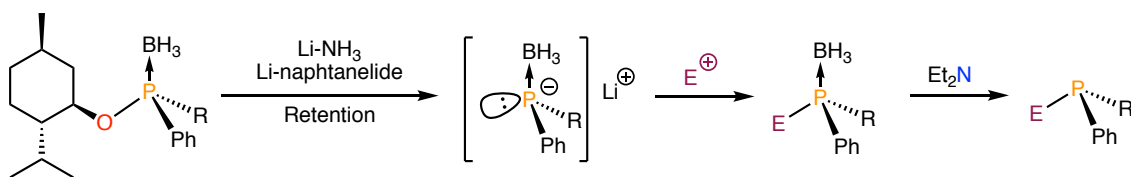
Scheme 8. Formation of the phosphide anion and reactivity towards electrophiles (E).

Both, Knowles and co-workers[15] and Imamoto and co-workers[20a] used these methods to prepare the DiPAMP ligand. Knowles based the synthesis on the $S_N2@P$ reaction of the menthylphosphinate with the Grignard reagent. Then, after dimerization by means of oxidative Cu-promoted coupling, the resulting diphosphine oxide was reduced with trichlorosilane (Scheme 9).
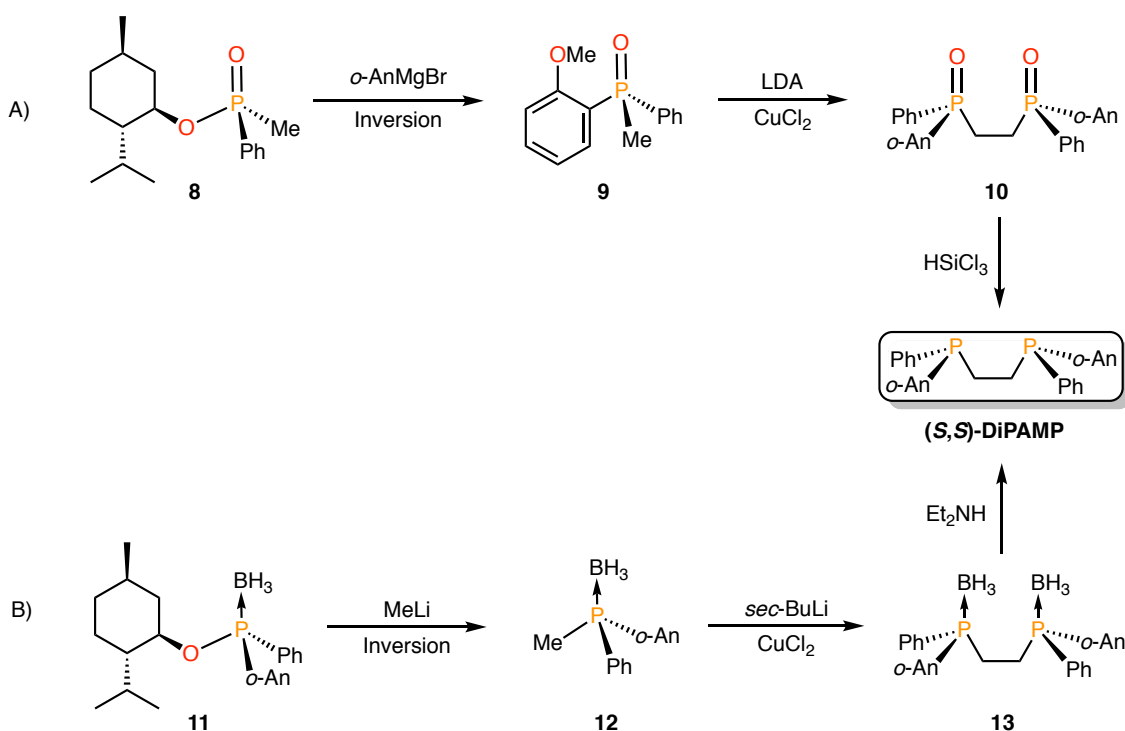
Scheme 9. Knowles' (a) and Imamoto's (b) procedures towards the DiPAMP ligand.

In contrast, Imamoto and coworkers[20a] applied its own methodology, cleaving the P–O bond of the boronated menthylphosphinate, which later undergoes a similar coupling, promoted by the $CuCl_2$ and *sec*-butyl lithium. Final deprotection of the diphosphine with diethylamine affords the desired DiPAMP ligand (Scheme 9).

More recently, Buono and co-workers[44] and Han and co-workers[45] have also used L-menthol in the preparation of optically pure Secondary Phosphine Oxides (SPOs) as it is detailed in Chapter 3.

Many phosphine oxides, phosphine-boranes and free phosphines have been obtained using these procedures.[21-22,24] One of the reasons that explain the success of the method is that the auxiliary is easily available and inexpensive. Also, it allows the possibility to modify the compound after performing the resolution step. However, this synthetic flexibility is limited by the steric hindrance of the substituents at phosphorus and by the Grignard reagent used.[38a] Other more basic and nucleophilic organolithium reagents can be also used,[46] but when it comes to work with oxides, the optical purities are usually much lower.[47]

2.3.1.2. *Amines as chiral auxiliaries*

With the same idea of the previous section, it has been reported the preparation and separation of diastereomeric mixtures using chiral amines as auxiliaries. The reaction between a racemic chlorophosphine and an optically pure amine yields a diastereomeric mixture of aminophosphines that in certain cases can be separated. Kolodiazhnyi and co-workers[48] described for the first time the reaction *N*-(1-methylbenzyl)amine and *tert*-butylchlorophenylphosphine in the presence of triethylamine allowing the formation of a mixture aminophosphines with some diastereoselectivity (Scheme 10).
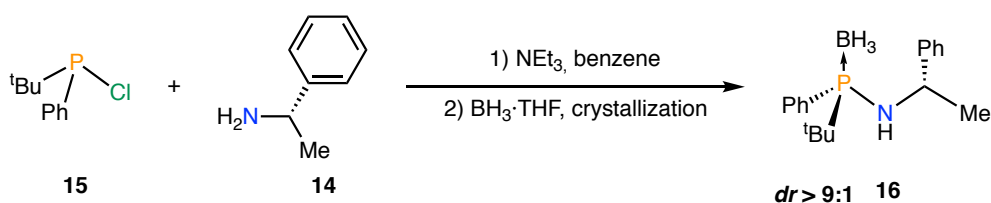
Scheme 10. Preparation of diastereomerically enriched aminophosphines.

They found that the diastereomeric ratio was strongly dependent on the reaction conditions, the base employed (generally a tertiary amine), the solvent and the temperature. They observed the best discrimination using benzene as solvent and an equimolar ratio of reagents. Protection with the borane group followed by crystallisation allowed the obtention of a single diastereomer.

Based on this method, Riera, Verdaguer and co-workers[49] developed their own methodology, reporting the preparation of a new family of *P*-stereogenic

aminophosphines. They studied the reaction of chiral amines with *rac*-^tBuMePCl and (*R*)-2-amino-2-phenylacetamide in the presence of an external base (Scheme 11).
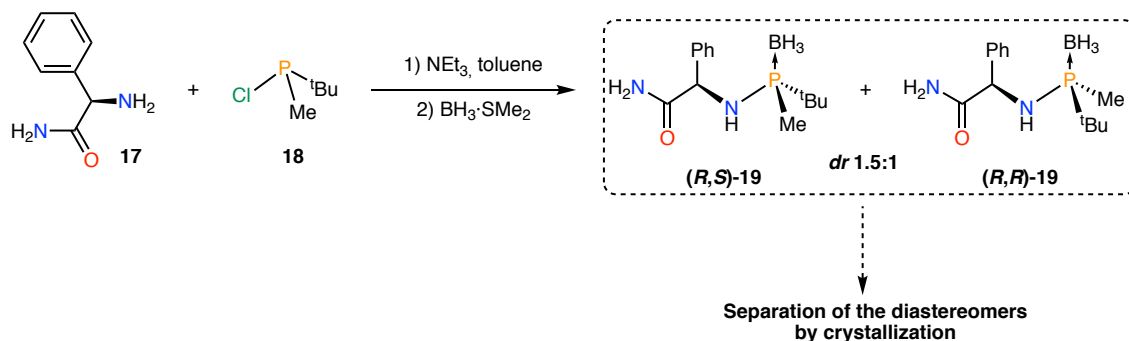
Scheme 11. Riera and Verdaguer methodology for the synthesis of stereogenic phosphines with chiral auxiliaries.

Although the diastereomeric ratio obtained was not particularly high, it provided a mixture of diastereomers that could be easily separated by crystallisation even at multigram scale. These optically pure aminophosphines were found to suffer a reductive cleavage of the C–N bond with lithium in liquid ammonia yielding optically pure aminophosphine-borane **L1·NH₂** (Scheme 12).[49]
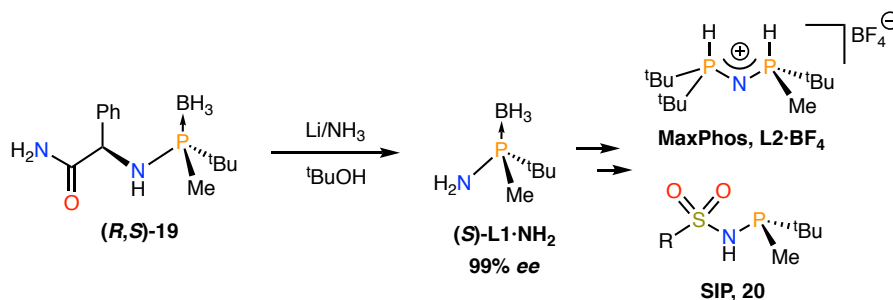
Scheme 12. Benzylic bond cleavage with Li/NH₃(l) to yield optically pure aminophopshine borane (*S*)-**L1·NH₂,** precursor of the ligands MaxPhos and SiP.

The chiral aminophosphine synthon **L1·NH₂** has been found to be essential for the preparation of many bidentate *N*-bridged, *P*-stereogenic ligands such as MaxPhos[50] that have displayed excellent results in Rh-catalysed asymmetric hydrogenations, or the phosphinosulphinamides (SIPs)[51], very useful on the intramolecular cycloaddition of terminal enediynes.

2.3.2. *Methods based on bifunctional auxiliaries*

In the 1990s several authors designed methods to prepare optically pure phosphines,[20b,52] based on an enantiopure *P*-stereogenic cyclic compound which suffered sequential substitution reactions at the phosphorus atom with a well-determined stereochemical course (Scheme 13).

A, B = N, O, S
X = BH$_3$, O, S

Sequential substitutions
i) R^{2}M
ii) R^{3}M
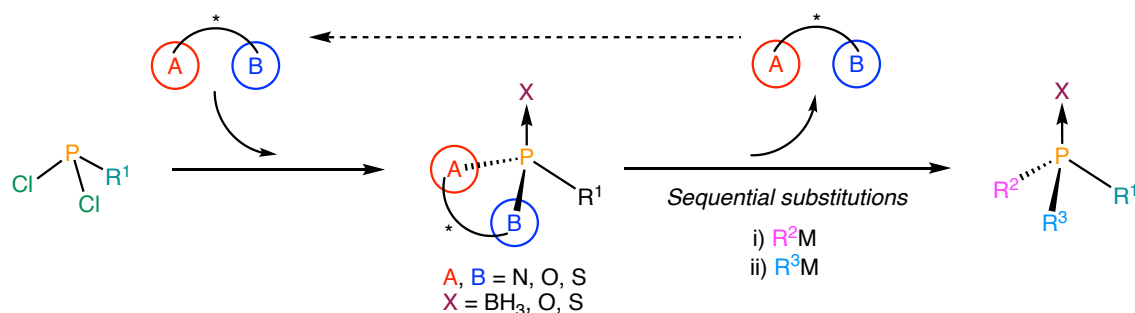
Scheme 13. Preparation of *P*-stereogenic compounds using bifunctional chiral auxiliaries.

It was found that the best manner to synthesise *P*-stereogenic ligands with high optical purity consisted on resolving the phosphorus atom with a diastereomerically pure bifunctional auxiliary, forming a *P*-stereogenic heterocycle. This heterocycle should have two leaving groups with different reactivity, in order to allow the later displacement of the auxiliary via stepwise substitutions.

The presence of a protecting group, such as a borane, apart from protecting the species from oxidation, it also keeps the stereochemical identity of all the intermediates generated during the process. Hence, this procedure implies working with precursors such as oxides,[53] sulfides,[52] or phosphine-boranes.[20b]

Regarding the auxiliary, a variety of species can form an enantiopure *P*-stereogenic heterocycle bearing two leaving groups with different reactivity (Figure 3).

(1*R*,2*S*)-(–)-ephedrine
Jugé 1990

Camphor derivative
Corey 1993

***cis*-1-amino-2-indanol**
Riera, Verdaguer 2011

p-chlorophenol derivative
Senanayake 2013
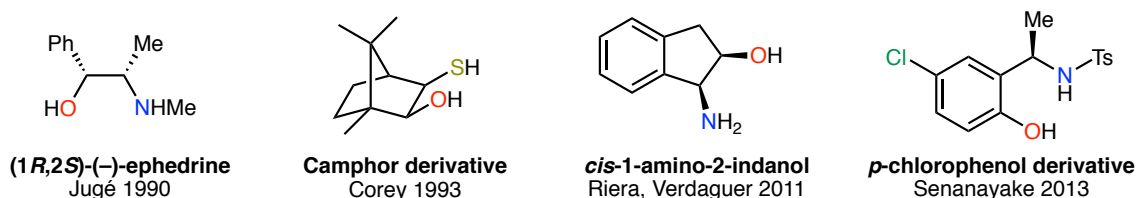
Figure 3. Selected optically pure bifunctional heterocycles.

Three of the auxiliaries depicted in Figure 3 have led to the development of independent and complementary methodologies that have allowed the obtention of

many *P*-stereogenic compounds with different steric and electronic properties. In the following sections the most important of these methodologies are presented.

2.3.2.1. *The Jugé-Stephan method*

Although different auxiliaries have been employed, the most widespread method, due to its versatility and relative simplicity, was developed in 1990 by Jugé and Stephan.[20b] It uses phosphine-boranes as precursors and the aminoalcohol ephedrine as chiral auxiliary, as it is depicted in Scheme 14.
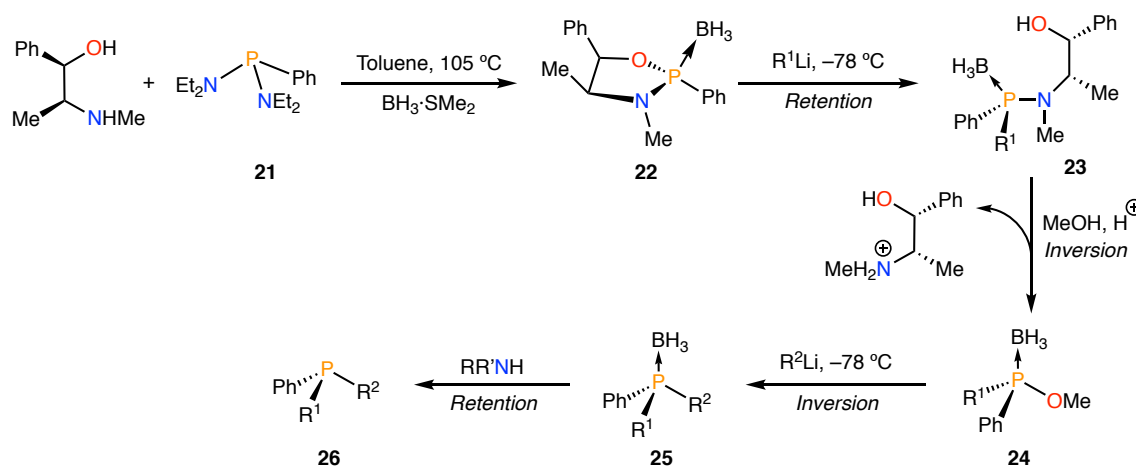
Scheme 14. Synthesis of *P*-stereogenic phosphines using the Jugé-Stephan method.

The Jugé-Stephan method consists on 5 steps that allow the obtention of tertiary phosphines with high optical purity. In general PhP(NEt$_2$)$_2$ (as it is depicted in Scheme 14) contains a phenyl group, even though there are reported examples with other aryl substituents attached in this position.[54]

1) Stereoselective cyclisation of the ephedrine

The first step is the formation of the diastereomerically pure oxazaphospholidine-borane **22** by condensation of *bis*(diethylamino)phenylphosphine (**21**) with (–)-ephedrine at 105 ºC in toluene, followed by protection with the borane group. It is important to remark that this cyclisation occurs in a highly stereoselective manner (*dr* > 90%) forming preferentially the R_P diastereomer. This behaviour has been attributed to steric effects, since the substituents on the carbon atoms of the ephedrine are *trans* to the phenyl group attached to the phosphorus atom.[55] More recent studies suggest that indeed the stereocontrol is mainly done by the carbon atom containing the phenyl substituent coming from the ephedrine.[56]

2) Selective ring-opening of the oxazaphospholidine borane

Reaction of **22** with organolithium reagents at –78 ºC in THF or Et$_2$O affords aminophosphine-boranes by selective cleavage of the P–O bond (Scheme 14).[55] This nucleophilic ring-opening occurs with retention of configuration at phosphorus atom with high diastereomeric excesses. Although Grignard reagents can be also used in this process, they require harsher conditions, which produces significant erosion on the stereoselectivity.[53]

In 2011, Riera, Verdaguer and co-workers[37] found that the stereochemical course of the aperture of oxazaphospholidine-boranes depends *directly* on the substituents attached to the nitrogen adjacent to the phosphorus atom. In contrast, the other substituents of the auxiliary or the groups attached to the phosphorus do not play any relevant role in the stereoselectivity of the reaction. Hence, they demonstrated both experimentally and computationally that if the nitrogen does not have any substituents, the reaction occurs with inversion of configuration at phosphorus atom whereas when the nitrogen is substituted, such as in ephedrine, the reaction takes place with retention of configuration at the P atom (Scheme 15).
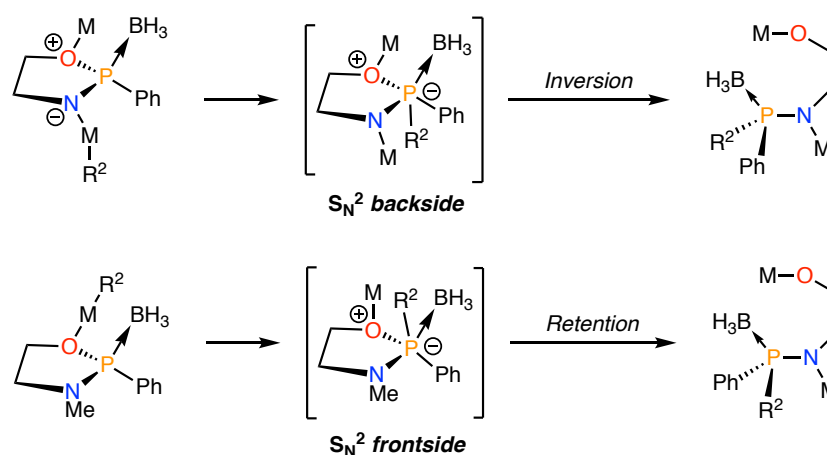
Scheme 15. Proposed mechanisms by Riera, Verdaguer and co-workers[37] for the ring-opening of oxazaphospholidine boranes.

As it is depicted in Scheme 15, when the oxazaphospholidine-borane does not contain a substituted nitrogen atom, a *backside* S$_N$2@P reaction occurs. In this case, two equivalents of the organolithium compound are required since one is used to deprotonate the secondary amine while the other undergoes the nucleophilic substitution, forming a P(V) intermediate, which evolves in the desired product with stereochemical inversion. On the other hand, in the case of *N*-substituted derivatives, a

frontside $S_N2@P$ type reaction takes place, where the organolithium coordinates the borane group (the nitrogen is now sterically hindered) furnishing the P(V) intermediate and leading to the aminophosphine-borane with retention of configuration.

3) Stereoselective acidic methanolysis of aminophosphine-boranes

In this step, the P–N bond is broken by acidic methanolysis in the presence of sulfuric acid, with the formation of the corresponding phosphinite-borane. The methanolysis reaction takes place with inversion at phosphorus following a "classic" $S_N2@P$ process (Scheme 16).
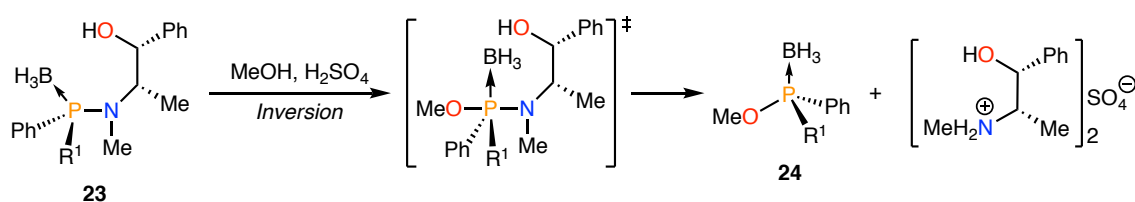
Scheme 16. Acidic methanolysis of aminophosphine-boranes.

In general, increasing the size and the basicity of the phosphorus substituents implies a clear decrease of the reaction yields.[54c,57] It is found that aminophosphine-boranes having *tert*-butyl[56] or adamantyl[54a] substituents are completely unreactive, which is an important limitation of the Jugé-Stephan method.

4) Formation of the phosphine-boranes by nucleophilic substitution

Another organolthium reagent can be used to substitute the methoxy group on **24**, furnishing optically pure tertiary *P*-stereogenic phosphines **25** (Scheme 17).
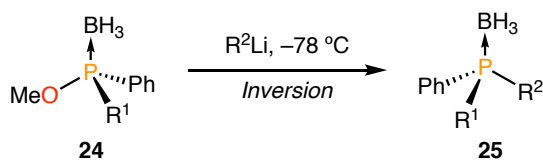
Scheme 17. Nucleophilic substitution of the OMe group.

The mechanism can be understood as a typical $S_N2@P$ giving therefore substituted products with stereochemical inversion of configuration.

In general, the reaction proceeds without problems with high yields and stereochemical control, both with aryl and alkyllithium reagents with the exception of

very bulky groups or *o,o'*-disubstituted arenes as it was demonstrated by Mezzeti and co-workers.[54c] Muller, Grabulosa and co-workers[58] studied this reaction step increasing the steric hindrance of the alkyllithium (where alkyl = Me, *i*-Pr, *t*-Bu) with phosphinite boranes bearing a bulky aryl substituent (2-biphenylyl, 1-naphthyl or 9-phenanthyrl) and they found that while the Me group worked smoothly, the isopropyl reacted with difficulties and the *tert*-butyl did not react at all.

5) Deprotection of the phosphine-boranes

Since nearly all the compounds obtained with this method are *P*-stereogenic boranes with one or more aryl substituents, they can be deprotected by reaction with amines, forming the corresponding amine-borane adducts and releasing the free phosphine. Several amines such as diethylamine,[20b,55,57,59] 1,4-diazabicyclo[2.2.2]octane (DABCO),[60] or morpholine[54c,57-58,61] have been used with good results.

Smoother deprotections with ethanol[60c] or cyclooctadiene[62] have also been reported for specially electron-poor phosphine-boranes, but they are not generally applicable.

Once the final deprotected phosphine is obtained, it is usually reacted immediately in order to prevent oxidation to P(V).

One of the strengths of the Jugé-Stephan methodology is the possibility of further functionalization of the *P*-stereogenic phosphine-borane.[21,24] For example, if the phosphine-borane **25** (see Scheme 17) bears a methyl group, it can be deprotonated by *sec*-BuLi and the resulting carbanion can be subjected to many reactions allowing the preparation of a variety of mono and bidentate *P*-stereogenic ligands.[21,24] For instance, C_2-diphosphine-boranes can be obtained by oxidative coupling in the presence of Cu(II)[20,54c,57,62-63] and by double nucleophilic substitutions over dichlorosilanes[61-63] or (*bis*)benzylic electrophiles.[59a,b]

Formylations,[64] carboxylations[65] and silylations[58,63a,66] of the carbanion were also described. Some aminophosphine-boranes have been employed as starting materials for the synthesis of aminophosphine-phosphinites[59d,60b,67] including polymer supported compounds.[68] Furthermore, Rossell, Muller and co-workers[66a] made possible the synthesis of carbosilane dendrimers functionalised with *P*-stereogenic phosphine-boranes using an α-carbanion. The same procedure was later applied by the same group to the synthesis of *P*-stereogenic silylated dendrons.[66b]

As it can be seen, a large number of *P*-stereogenic ligands, often arylphosphines, have been synthesised using ephedrine as chiral auxiliary.[22,24] In spite of this, the method has limitations when trying to obtain crowded or basic phosphines.[22,24,54d,59f] In particular, problems have been found when introducing voluminous substituents such as *o,o'*-disubstituted arenes[54c,58,63a] because they usually undergo elimination reaction at the ephedrine substituent.[54d]

2.3.2.2. *The Riera-Verdaguer method*

Sterically hindered phosphines are very interesting as they have provided excellent results in asymmetric transformations such as metal-catalysed hydrogenations[50,69] hydroborations,[70] aldol reactions[69c] and hydroacylations[71] among others.

This exceptional behaviour of the bulky phosphines, especially bearing the tBu/Me or tBu/Ph combinations spurred the interest of the development of new methodologies to efficiently prepare these types of *P*-stereogenic ligands. In this line, Riera, Verdaguer and co-workers[37,49-51,72] used *cis*-1-amino-2-indanol in the synthesis of hindered and basic ligands. The synthetic methodology relies on the formation of the oxazaphospholidine-borane compound shown in Scheme 18.
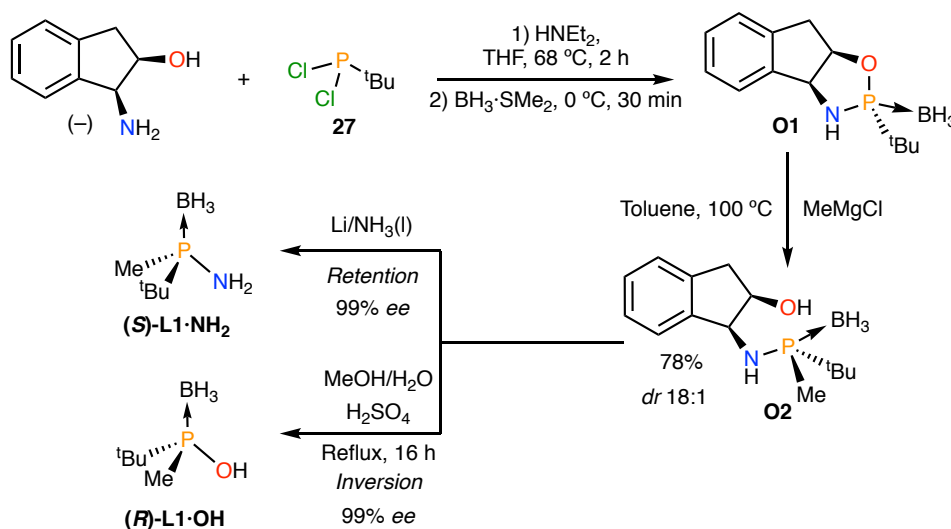
Scheme 18. Synthesis of chiral synthons aminophosphine-borane (*S*)-**L1·NH₂** and phopshinous acid-borane (*R*)-**L1·OH**.

Reaction between *cis*-1-amino-2-indanol and *tert*-butyldichlorophosphine in the presence of diethyl amine as base affords the heterocycle **O1**, after protection of the free phosphine with the borane group. At this point, **O1** can be reacted with different Grignard reagents such as MeMgBr or PhMgBr. It is interesting to note that the ring-opening reaction of the oxazaphospholidine-borane with nucleophiles takes place

always with inversion of configuration at phosphorus whereas in the well-known Jugé-Stephan method, the aperture step with an organolithium reagent occurs with retention of configuration.[72a]

Compound **O2** gives access to the aminophosphine **(*S*)-L1·NH₂** and phosphinous acid-borane **(*R*)-L1·OH** in both enantiomeric forms, respectively, which are key chiral synthons for the preparation of different *P*-stereogenic ligands as it is described in more detail in Chapter 3.

Aminophosphine-borane **(*S*)-L1·NH₂** can be prepared by reductive cleavage of the C–N benzylic bond with $Li/NH_3(l)$, which yields the desired product without *ee* erosion preserving the stereochemistry at phosphorus. In contrast, acidic methanolysis of **O2** furnishes the optically pure phosphinous acid-borane **(*R*)-L1·OH** with inversion of configuration. Both synthons have a complementary reactivity because while aminophosphine **(*S*)-L1·NH₂** acts as a nucleophile, phosphinous acid-borane **(*R*)-L1·OH** can be used as an electrophile.

The reactivity of **(*R*)-L1·OH** as an electrophile can be understood when the –OH group is converted to a good leaving group and hence activated in front of nucleophiles. This strategy, initially reported by Pietrusiewicz[31] and later expanded by Buono and co-workers[73] is based on the activation of optically pure phosphinous acid boranes with MsCl, followed by their reduction with sodium tetrahydroborate (see Scheme 19) to furnish the phosphine-boranes in a $S_N2@P$ reaction without optical purity loss. Buono and co-workers[73] expanded the scope of this reaction using other aryl groups as substituents and reducing the temperature of the first step (Scheme 19) achieving the reduced phosphine-boranes with high enantioselectivities.
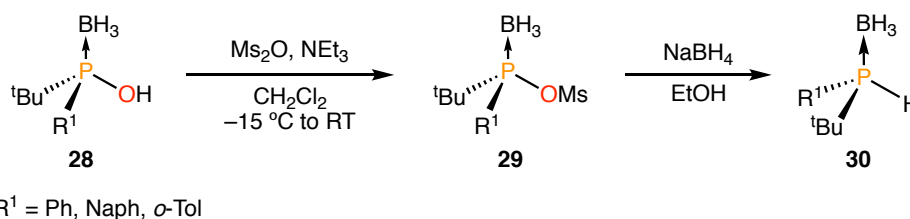
Scheme 19. Buono's methodology for the reduction of phosphinous acid-boranes.

However, none of these authors were able to prepare the key synthon **L1·OH** developed by Riera, Verdaguer and co-workers[37,49-51,72] and consequently they could not study its further activation or reduction. Although activation with MsCl of synthon **L1·OH** proved to be more difficult compared to its analogous compounds bearing the $^tBu/Ph$ combination, after some experimentation they found a set of conditions and

managed to successfully stabilize the phosphinyl-mesyl anhydride without racemisation. Its subsequent reactivity in front of different nucleophiles was later studied showing its versatility in the formation of a large family of aminophosphine-boranes (Scheme 20).
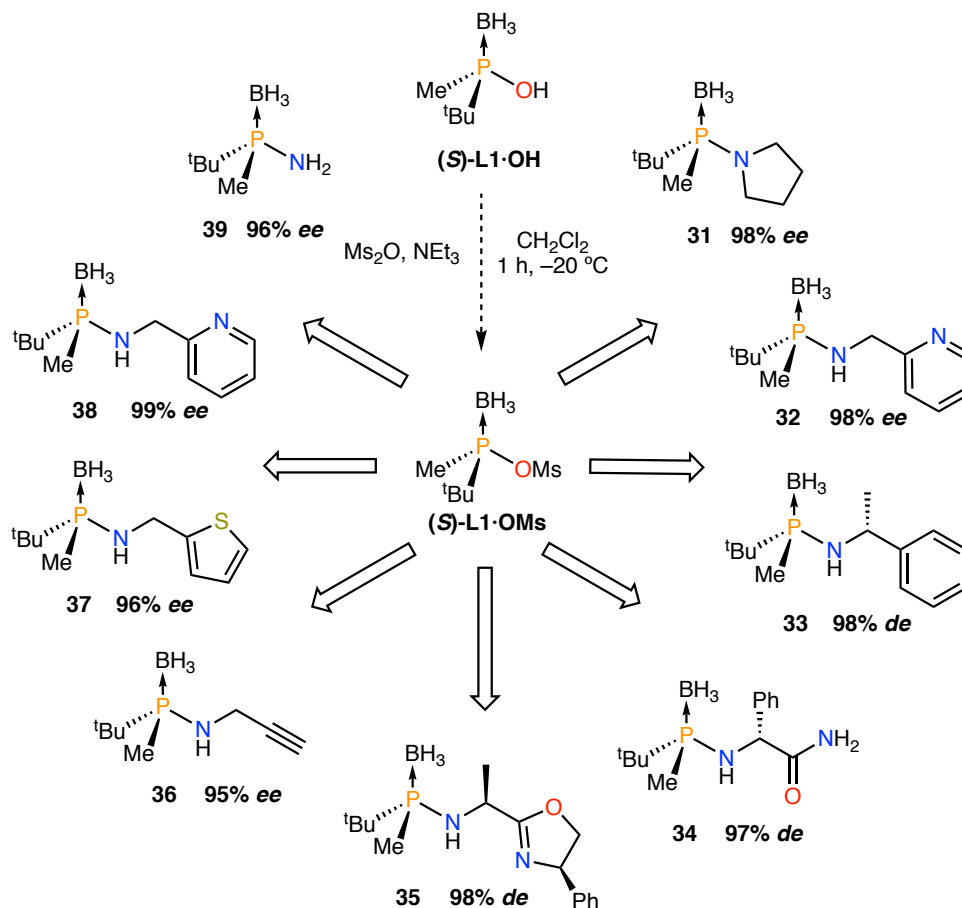
Scheme 20. Reactivity of **(*S*)-L1·OH** and S_N2@P with different nucleophiles.

As it is shown in Scheme 20 functionalisation of synthon **(*S*)-L1·OH** has assessed the preparation of a many aminophosphine-boranes with excellent enantioselectivities. Particularly remarkable is the synthesis of compound **35**, which is crucial for the obtention of MaxPHOX-type ligands, as it will be discussed in detail in Chapter 5.

The strategy developed by Riera and Verdaguer can be considered as a complementary route to the Jugé-Stephan method and it represents the only methodology that allows the access to sterically hindered alkyl phosphines with useful levels of *ee*.

2.3.2.3. *The Senanayake method*

Another strategy was developed in 2013 by Senanayake and co-workers,[69e] for the preparation of optically pure tertiary phosphine oxides. They designed a chiral auxiliary with an activated P–N bond that reacts with hindered Grignard reagents.

Firstly, in a similar way to the Jugé-Stephan method, their synthesis starts with the diastereoselective formation of an oxazaphosphinane **41** (Scheme 21) that undergoes a ring-opening reaction with organomagnesium reagents.
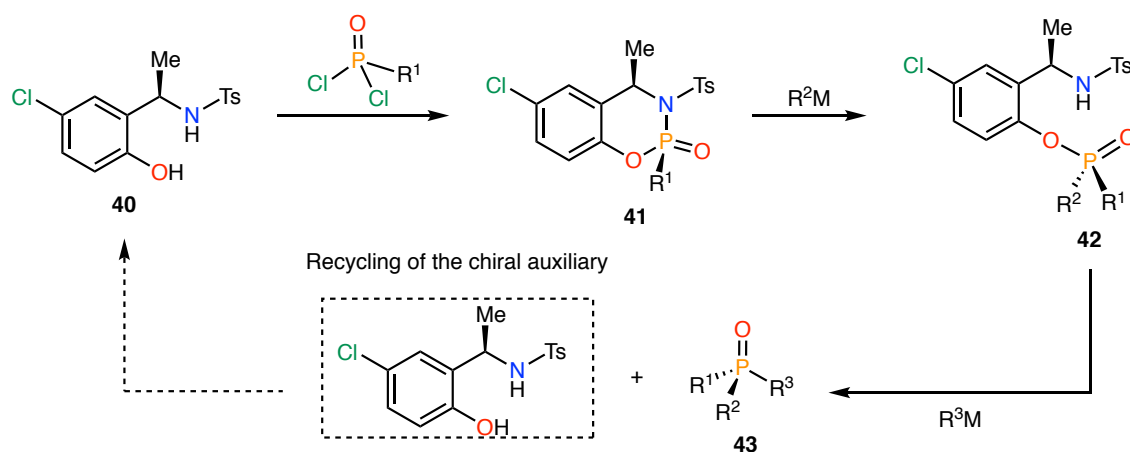
Scheme 21. Senanayake's method for the synthesis of chiral phosphine oxides.

Interestingly, the nucleophilic attack of the organometallic reagent regioselectively cleaves the P–N bond. The addition of the second organometallic compound releases the *N*-tosyl-2-(1-aminoethyl)-4-chlorophenol auxiliary and furnishes the corresponding phosphine oxide **43**.

One advantage of Senanayake's strategy is that it allows the introduction of bulky substituents on the phosphorus atom, allowing the formation of sterically hindered systems, most of them combining the *P*-stereogeneicity with axial chirality (Figure 4).

(*R*)-BI-DIME   **(*R*$_P$,*S*)-MeO-POP**   **MeO-BiPOP**   **(*R*)-BoQPHOS**
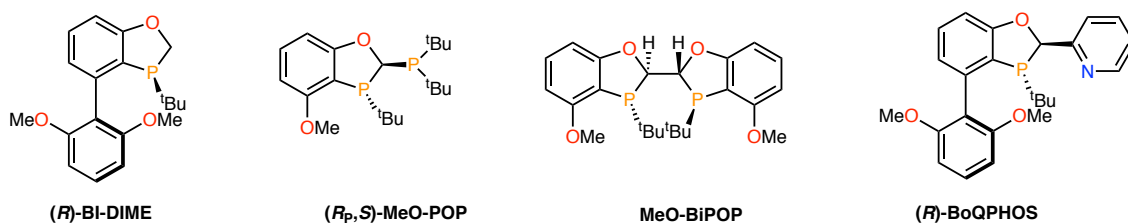
Figure 4. Selected *P*-stereogenic ligands prepared following Senanayake's methodology.

With such methodology, many relevant ligands have been developed (Figure 4) such as the Bi-DIME,[74] MeO-POP,[75] MeO-BiPOP,[76] or the BoQPHOS[77] that have proven to be suitable for many important asymmetric transformations.

It has to be noted, however, that the method yields a phosphine oxide that has to be reduced with silanes or hydrides to the free phosphine, a step that often results in some erosion of the enantiopurity of the final ligands.

2.3.3. *Methods based on enantioselective deprotonation*

A methyl group directly attached to a phosphorus atom can be deprotonated by strong bases. Under the appropriate conditions, in the presence of a chiral diamine, the asymmetric deprotonation of a prochiral compound provides the corresponding chiral α-carbanion, which can be used to access a rich variety of *P*-stereogenic compounds. White and co-workers[78] were the first to develop this idea in 1989, studying the metallation of dimethylphenylphosphine oxide (**44**) with *n*-BuLi in the presence of (–)-sparteine (Scheme 22).
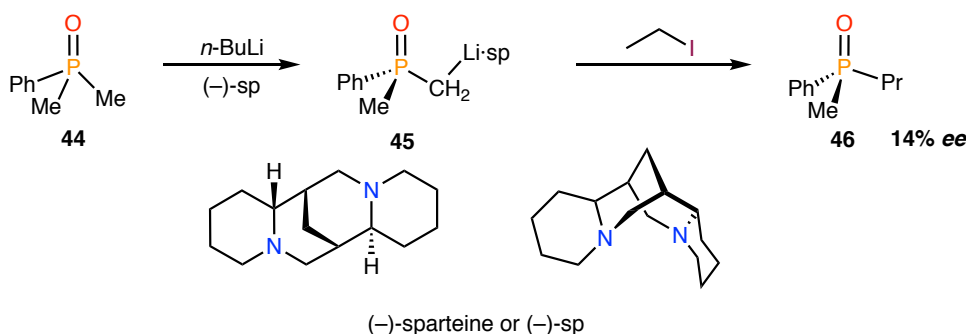
Scheme 22. Formation of carbanion **45** and reaction with iodoethane.

After quenching carbanion **45** with iodoethane, they obtained oxide **46** but with a disappointingly low *ee*. This discouraging result made the procedure to remain ignored until 1995, when Evans[79] and later Imamoto[80] described a method for the enantioselective synthesis of α-carbanions using prochiral dimethylphosphine-boranes by means of a deprotonation with organolithium reagents and sparteine as chiral auxiliary.

After that first breakthrough, the procedure has been successfully applied to the synthesis of many families of mono- and diphosphines with alkyl substituents, especially those bearing the ^{t}Bu/Me combination.[22,24,38b,81]

All these synthesis are based on the use of (–)-sparteine (Scheme 22), also known as (–)-lupinidine, which is an optically pure tertiary diamine naturally occurring that can be isolated from certain *papilonaceous plants* such as Scotch Brooms.[82]

The reaction can be divided in two steps. Firstly, the enantioselective deprotonation of one of the enantiotopic Me groups of the dimethylphosphine-borane with *sec*-butyllithium at low temperature in the presence of (–)-sparteine (Scheme 23).
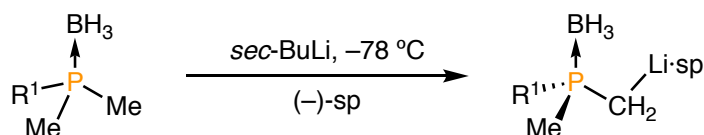
Scheme 23. Deprotonation step in the Evans-Imamoto method.

In this step, the chiral environment created by the chiral diamine allows the differentiation of the enantiotopic methyl substituents, where only one group is deprotonated, affording in a very stereoselective way a *P*-stereogenic α-carbanion. In the second step, the carbanion is reacted with a large variety of electrophiles as it is depicted in Scheme 24.
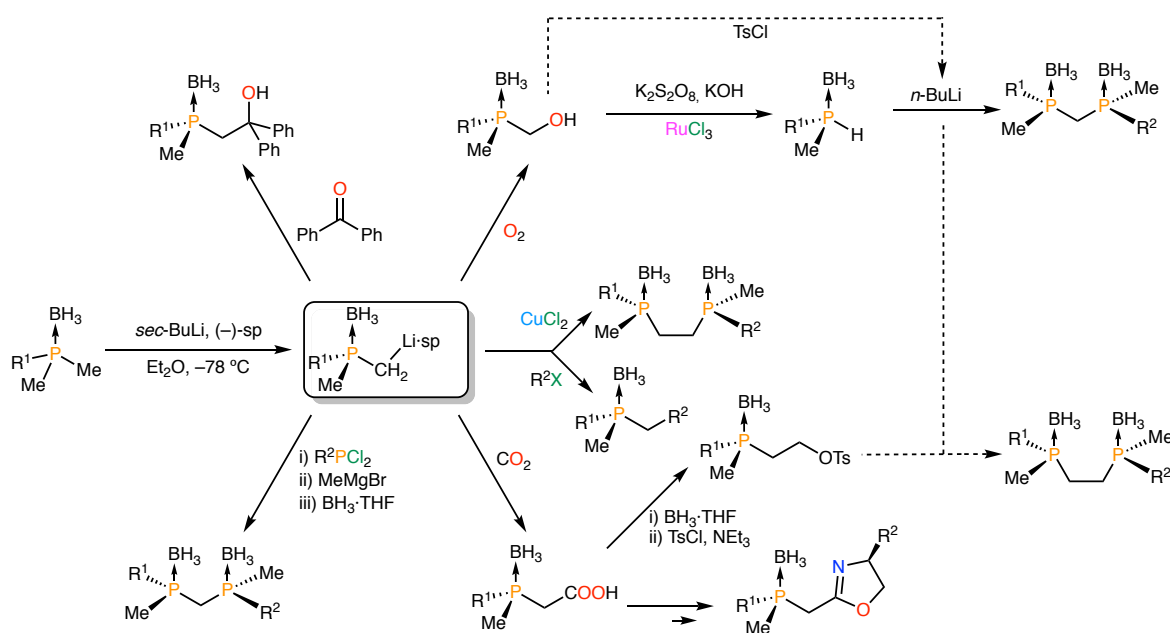
Scheme 24. Overview of procedures for the obtention of *P*-stereogenic compounds by enantioselective deprotonation of dimethylphosphine derivatives.

Dimethyl phosphine-boranes can be synthesised, in an efficient and inexpensive way, by successive treatments of PCl_3 with an alkyl Grignard reagent, methylmagnesium bromide and final boronation with $BH_3 \cdot THF$ complex (Scheme 25).[80]
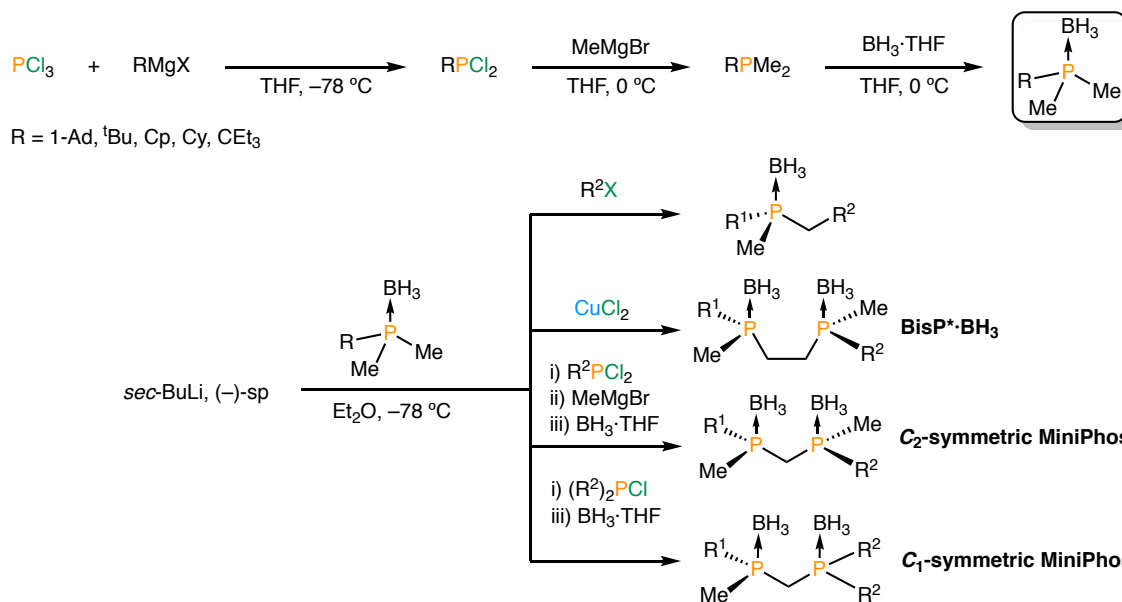
Scheme 25. Synthesis of alkyldimethylphosphine-boranes and derived compounds.

Although the synthetic methodology was originally developed for the preparation of boronated 1,2-bis(alkylmethylphosphino)ethanes (BisP*·BH$_3$)[80,83] and MiniPhos,[83a,84] the obtention of *P*-stereogenic monophosphines has also been explored in other laboratories.

Recently, Muller, Grabulosa and co-workers[85] expanded the scope of this reaction preparing a family of phosphine-boranes bearing the *tert*-butyl, methyl and phenylethyl substituted groups, treating the "*in situ*" formed carbanion with benzyl halides as electrophiles (Scheme 26).
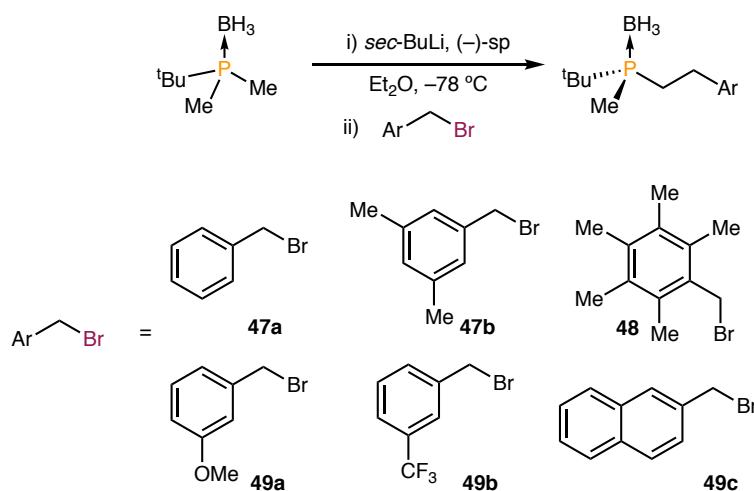
Scheme 26. Preparation of phenylphosphine-boranes.

In 2000, Imamoto and co-workers[86] prepared enantioenriched hydroxymethylphosphine-boranes (**50**, Scheme 27) by oxidation of carbanion.
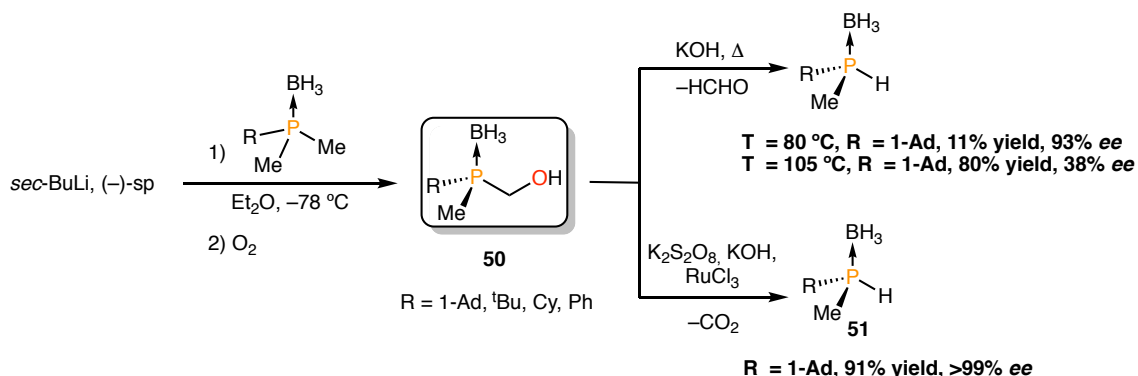
Scheme 27. Synthesis of hydroxymethylphosphine-boranes and secondary phosphine-boranes.

Interestingly, **50** can be further functionalised maintaining its optical purity.[86] Dehydroformilation of **50** yields secondary phosphine-boranes **51**, but proceeds with either low yields or low enantioselectivities. In contrast, oxidative degradation with potassium peroxodisulfate and ruthenium trichloride allows the synthesis of **51** with higher yields and optical purity.[86]

Furthermore, secondary phosphine-boranes can be easily deprotonated and transformed into extremely nucleophilic phosphide-borane anions, which are prone to react with electrophiles.[24] For instance, Imamoto and co-workers[87] made them react with aryl halides such as fluoroarene tricarbonylchromium complexes in order to obtain, after some transformations, diarylphosphine-boranes (Scheme 28).
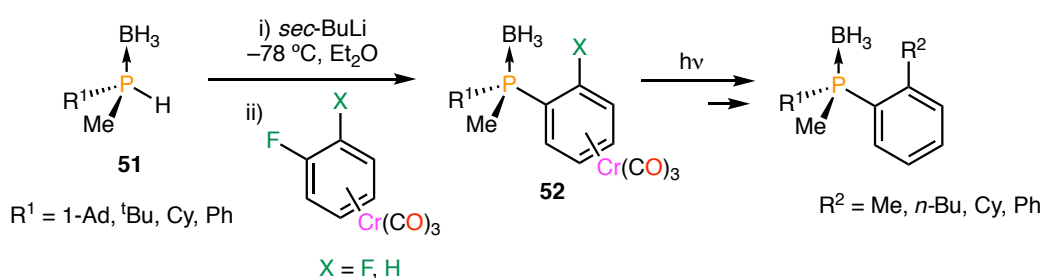
Scheme 28. Synthesis of *o*-substituted arylphosphine-boranes.

Imamoto and co-workers[88] also used *P*-stereogenic secondary phosphine-boranes as synthons for the preparation of C_1-symmetric **BisP*·BH₃**, (Scheme 29), which resulted effective ligands for Rh-catalysed asymmetric hydrogenations of functionalised olefins.
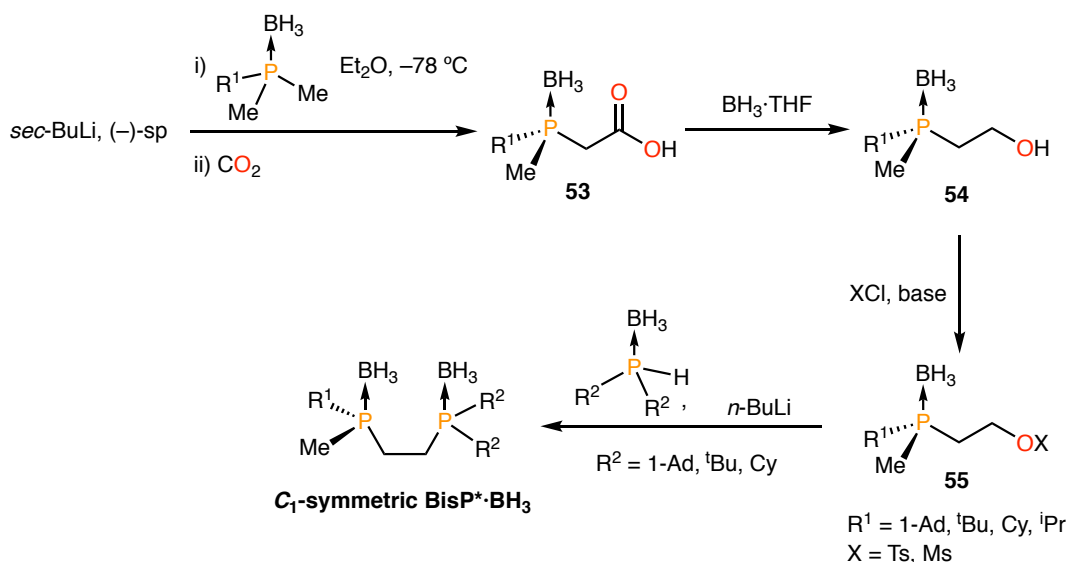
Scheme 29. Transformation of secondary phosphine-boranes into unsymmetrical **BisP*·BH₃**.

The *P*-stereogenic phosphide was reacted with a previously prepared tosylated or mesylated precursors **55** furnishing the desired products. In general, unsymmetrical **BisP*·BH₃**[88] were obtained in high optical purity, even though the yields are strongly dependent on the substituents. For instance, couplings with the *tert*-butyl phosphide usually take place with yields lower than 20%.

The same group also reported the conversion of secondary phosphine-boranes into derivatives with an halogen substituent on the phosphorus atom (**56**, Scheme 30).[89]
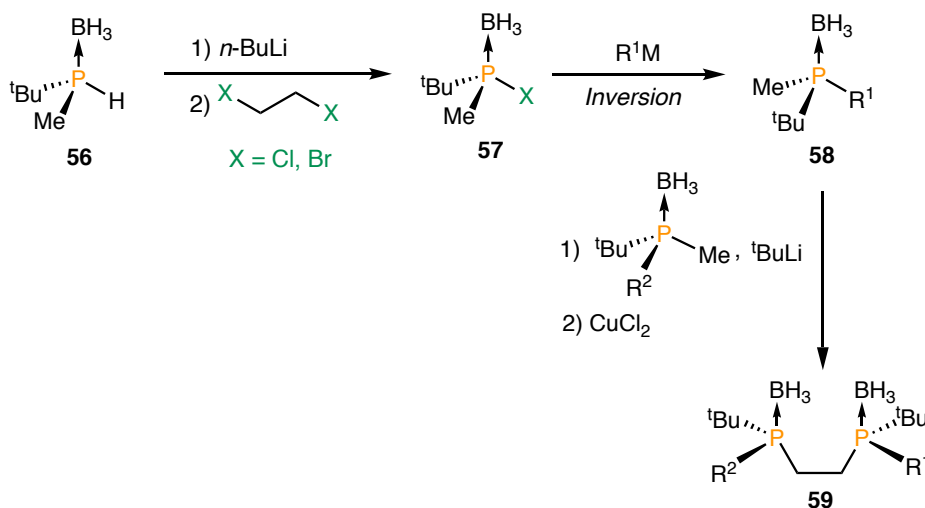
Scheme 30. Transformation of secondary phosphine-boranes into halophosphine-boranes and further reactivity.

The halogenated compounds were not isolated due to their easy racemisation. They were used "*in situ*" instead as starting materials to obtain a variety of tertiary phosphine-boranes. Such transformation into tertiary *P*-stereogenic compounds (**58**) always proceeds in a stereoselective manner, even though the stereochemical course of the reaction was found to be dependent on the nature of the nucleophile. Moreover, deprotonation of **58** with *sec*-BuLi or *tert*-BuLi and subsequent oxidative coupling produced unsymmetrical *P*-stereogenic diphosphines **59**.

Livinghouse and co-workers[90] developed an efficient route to prepare optically pure secondary phosphine-boranes by an asymmetric lithiation/trapping-reductive elimination procedure that can be seen as an overall "asymmetric demethylation" (Scheme 31).
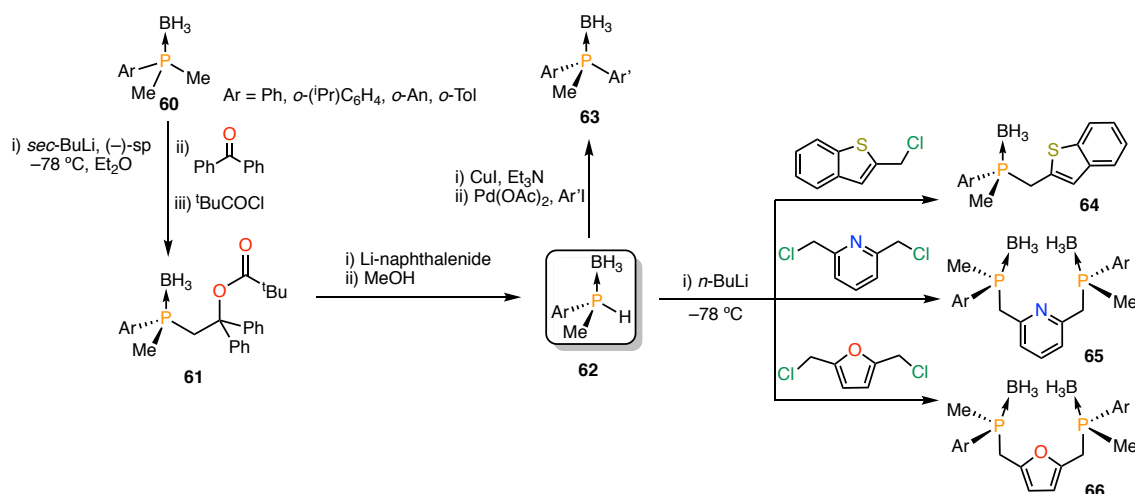
Scheme 31. Livinghouse's methodology for the obtention of secondary phosphine-boranes and their transformations.

Secondary phosphine-boranes **60** were deprotonated and further alkylated with 2-(chloromethyl)benzotiophene, furnishing **61** in good yields and keeping its optical purity.[90a] Reaction of deprotonated **62** with dihalides provided the corresponding enantiopure diphosphine-boranes (**64**, **65** and **66**) also with good yields and enantioselectivities.[90b] Additionally, the already known Cu(I)-Pd(0) co-catalysed cross coupling of **62** with aryl iodides[91] gives access to a large family of diarylphosphine-boranes **63** with excellent levels of stereocontrol.

It is important to note that, while the methodologies for the deprotection of aryl phosphine-boranes rely on the use of secondary amines such reagents do not work with trialkylphosphine-boranes due to its higher basicity. In this case, fluorinated acids, such as the tetrafluoroboric acid, are used. It seems that sequential substitutions on the

H atoms of the borane by F allows the easy deboronation of the phosphine-BF$_3$ adduct.[92]

Although the success of the Evans-Imamoto method is undisputed, during the last years there have been severe sparteine shortages, making the method often unusable. For this reason many research groups are looking for alternative surrogates of sparteine, but at present none of them has the adequate properties to substitute natural sparteine.[93]

2.4. *Preparation by asymmetric catalysis*

The synthetic procedures based on resolution of racemic mixtures or asymmetric catalysis, described in the preceding sections, constitute the main methods of preparation of enantiomerically pure *P*-stereogenic compounds and require stoichiometric amounts of chiral reagents or expensive HPLC equipment.

A much more desirable way would be the use of enantioselective catalysis starting from achiral or racemic reagents.[24] These procedures would ideally reduce the high cost usually associated with the preparation of *P*-stereogenic compounds.

Such an approach has scarcely been used in the preparation of *P*-stereogenic compounds until the last fifteen years,[94] when transition metal complexes were found to catalyse a variety of reactions leading to optically enriched phosphines and derivatives.[23,95]

The obtained phosphines are good ligands themselves and hence compete with the other phosphorus ligands present in the structure of the catalysts. Such competition does not necessarily mean a drawback because coordination of the obtained ligand to the metal can have the positive effect of "chirality breeding", for instance, when the obtained phosphine catalyses its own formation.[24]

In the following sections, the most remarkable metal-catalysed synthesis of *P*-stereogenic phosphines [95a,96] are described.

Primary and secondary phosphines can oxidatively add to low-valent transition metal complexes to form phosphide complexes.[97] In contrast to phosphines, metal phosphide complexes are known to undergo fast pyramidal inversion, which can be measured by NMR. As a representative example, typical energy values for the inversion of tertiary phosphines, PR$_3$, are around 155 kJ·mol^{-1}, whereas inversion barriers for some phosphide platinum complexes range from 42 to 67 kJ mol^{-1} according to NMR analyses.[97d]

As a consequence, phosphide complexes containing other chiral ligands usually generate mixtures of diastereoisomers, which in turn preferentially triggers the formation of one of the two phosphide-coordinated enantiomers.[97d]

These facts set the basis of the general method for the metal-catalysed asymmetric synthesis of *P*-stereogenic phosphines, which are formed by reaction of these complexes with electrophiles (Scheme 32).
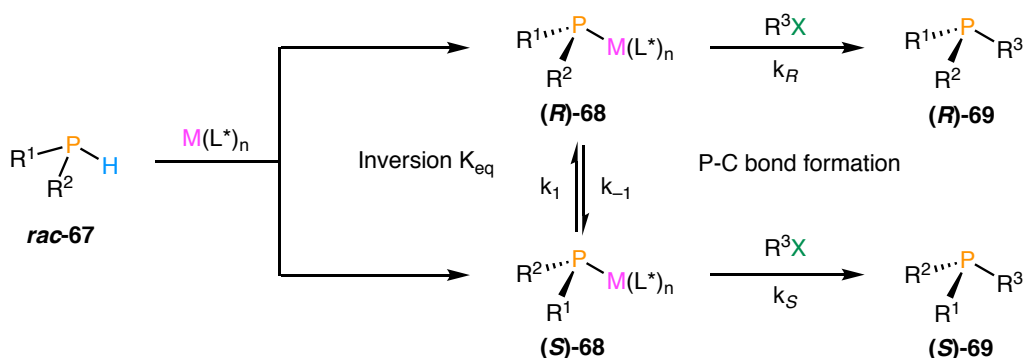
Scheme 32. Basis of metal-catalysed preparation of *P*-stereogenic phosphines.

The interplay between the rates of phosphorus inversion (which interconverts (*R*)-**68** and (*S*)-**68**) and the rates of electrophilic attack to each diastereomer of **68** will dictate the enantiomeric excess of **69**.

Different synthetic methods have been developed according to the above-mentioned principles for the preparation of *P*-stereogenic complexes by asymmetric catalysis (Scheme 33).
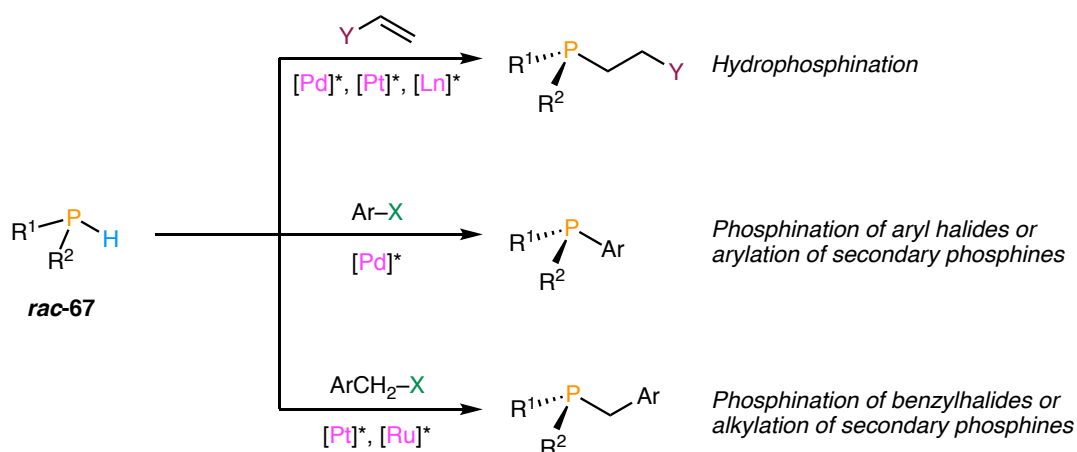
Scheme 33. General strategies for the metal-catalysed asymmetric synthesis of *P*-stereogenic phosphines.

All the reactions depicted in Scheme 33 are likely to proceed through phosphide complexes as intermediates. The first processes are the Pt-,[98] Pd-[99] and Ln-[100]catalysed hydrophosphination of activated alkenes, whereas the second represents a cross-coupling reaction between secondary phosphines and aryl halides catalysed by Pd complexes.[41,101] More recently, it has also been described the Pt[102] and Ru[103]-catalysed alkylation of secondary phosphines or phosphination of benzyl halides. It is interesting to mention that even though the most studied systems are based on metal-phosphide complexes, there are examples in the literature that occurs through other intermediates such as the Rh-catalysed desymmetrisation of prochiral dialkynylphosphine oxides[104] and Ru[105] or Mo-catalysed metathesis.[106]

2.4.1. *Hydrophosphination of alkenes and alkynes*

Transition metal-catalysed hydrophosphinations[107] are reactions based on the addition of a P–C bond across a multiple bond. For a given prochiral substrate (usually an activated alkene, see Scheme 34), a new stereogenic carbon and/or phosphorus atoms can be formed, whose absolute configurations are susceptible to enantiocontrol by the chiral catalyst.
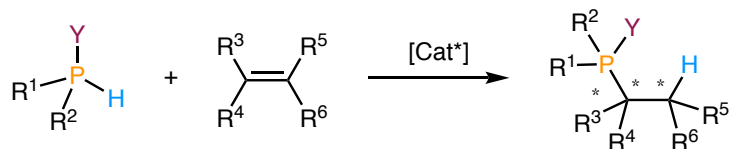
Scheme 34. Catalytic hydrophosphination of alkenes, where Y = BH_3, O or a lone pair.

Although some hydrophosphinations can proceed uncatalysed,[108] the process itself is challenging because it requires a tightly binding chiral ligand, which ideally should not be displaced by the substrates or products of the reaction.

The mechanism can be understood as an oxidative addition of the P–H bond to the low-valent metal centre, usually a Pd(0) complex, followed by olefin insertion and reductive elimination to yield the product. Since the alkene can insert into the M–P bond or into the M–H bond, two different pathways are proposed[98b,107] (Scheme 35).
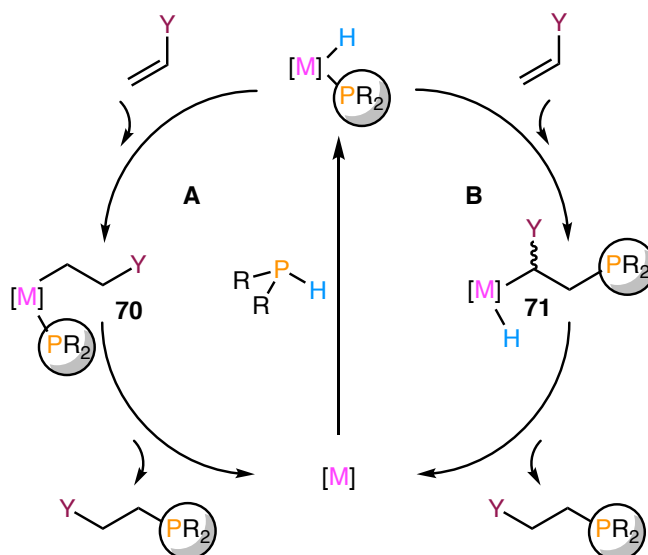
Scheme 35. Proposed pathways for the metal-catalysed hydrophosphination.

The first route A involves alkene insertion into the M–P bond to form complexes **70** followed by C–H reductive elimination. Alternatively, in route B the alkene inserts into the M–H bond to form complexes **71** followed by P–C reductive elimination.[98]

The first example of this type of reactions was reported by Pringle and co-workers[109] more than twenty years ago. They showed that hydrophosphination is a suitable reaction to prepare phosphine ligands for its application in homogeneous catalysis by using Pt(0) metal complexes.

More recently Glueck and co-workers[110] applied this reaction for the preparation of *P*-stereogenic phosphines and derivatives catalysed by Pt(Me-Duphos) complexes (Scheme 36).

Y = CN, COO(^{t}Bu)

up to 27% *ee*

R^1, R^2 = Me, Cy, Ph, *o*-An, ^{i}Bu, 2,4,6-tris-(^{i}Pr)phenyl
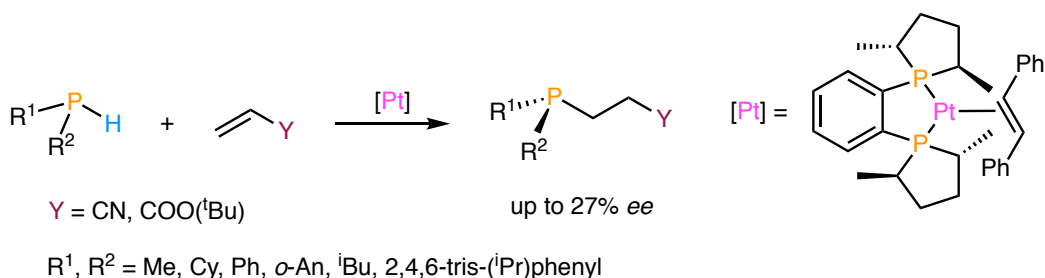
Scheme 36. Enantioselective Pt(0)-catalysed hydrophosphination.

Although the results obtained are still far away from the desired useful levels of enantioselectivity it represents the first example of preparation of *P*-stereogenic phosphines by asymmetric catalysis.[110-111].

Tanaka[99a], Gaumont[99b,c] and co-workers described examples of Pd(II)-catalysed hydrophosphinations of acetylenes with racemic secondary phosphine-boranes (Scheme 37).
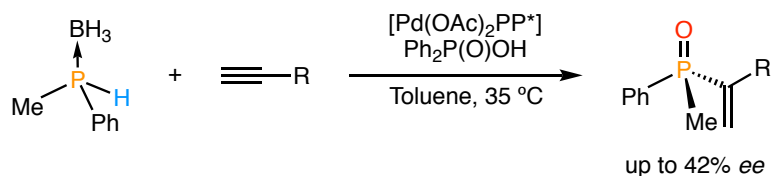
Scheme 37. Pd(II)-catalysed hydrophosphination of terminal alkynes.

The reaction was performed with several chiral bidentate ligands displaying some selectivity towards the Markovnikov addition product with up to 70% conversion and low stereoselectivity.

2.4.2. *Phosphination of aryl halides*

Phosphination consists in the cross-coupling reaction of a secondary phosphine -or derivatives- with an aryl halide or triflate. Actually, asymmetric Pd-catalysed phosphinations of aryl halides with secondary phosphines are among the most studied metal-catalysed reactions producing *P*-stereogenic phosphines (Scheme 38).
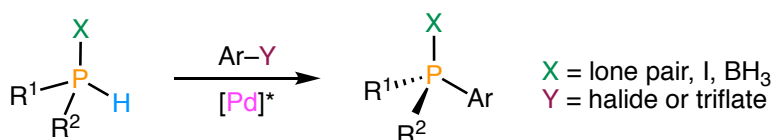
Scheme 38. Cross-coupling of an aryl halide or triflate with a secondary phosphine or derivative.

The first studies of this reaction were carried out using optically pure phosphines or derivatives and non-chiral palladium catalysts such as [Pd(PPh$_3$)$_4$]. Under these conditions, it was found that the stereochemistry of the P–C bond were strongly dependent on the protective group X and the reaction conditions. Xu and co-workers[112] reported the cross coupling of isopropylmethylphosphinates with aryl and vinyl halides with clean retention of configuration at phosphorus, whereas Imamoto and co-workers[41,113] discovered that employing secondary phosphine-boranes the stereochemistry of the P–C bond formation ranged from almost complete retention or inversion, depending on the solvent and base used. Later reports of Livinghouse and co-workers[114] stated that the presence of Cu(I) on the Pd-catalysed arylations of secondary phosphine-boranes was able to generate configurationally stable

metallophosphides yielding tertiary phosphine-boranes with inversion of configuration at phosphorus with excellent levels of stereocontrol.

More recently the studies have shifted towards the use racemic phosphines and chiral enantiopure metal catalysts. In this line Glueck and co-workers[101a,115] reported the first Pd-catalysed asymmetric phosphination by reaction of *rac*-**72** with different substituted benzene-derivatives (Scheme 39).
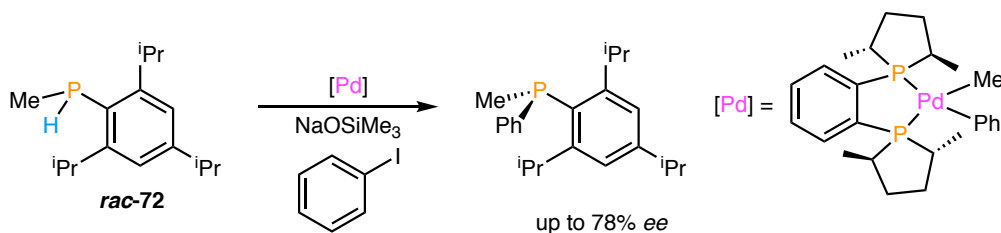
Scheme 39. Pd-catalysed cross-coupling of *rac*-**72** with phenyl iodide.

After screening different solvents and a set of aryl compounds, they found the best results using a Pd-Me-Duphos catalyst with phenyl iodide in toluene, displaying good conversions and interesting enantioselectivities.

Several other enantiopure Pd-diphosphine complexes were also employed as catalytic precursors, were yields and enantioselectivities of the products were strongly influenced by the structure of the diphosphine. In fact, it was found that series of DuPhos ligands such as Me/Et/*i*-Pr-DuPhos did not yield to major improvements. Furthermore, the same group developed an intramolecular version of Pd-catalysed phosphination to prepare *P*-stereogenic benzophospholanes.[116] Again the rate and selectivity appeared dependent on the precursor and the diphosphine used in the catalyst.

Different variations of the reaction have also been explored. Helmchen and co-workers[117] developed series of phosphine oxazoline ligands (PHOX) with a stereogenic phosphorus atom by either nucleophilic and electrophilic substitutions at the appropriate phosphorus precursors. Since their synthesis was limited by achiral substrates, they overcame those difficulties by developing the Pd-catalysed phosphination of *o*-substituted aryl iodides (Scheme 40).
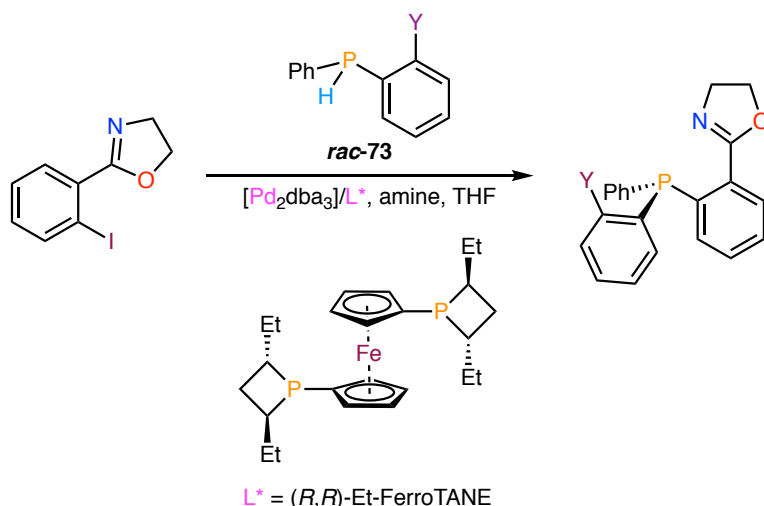
Scheme 40. Pd-catalysed phopshination of *o*-substituted aryl iodides.

They developed a system in which the catalyst is generated "*in situ*" from Pd(0) and a chiral diphosphine. After some experimentation screening different diphosphines they found that the best results were displayed by the **(*R,R*)-Et-FerroTANE** ligand achieving enantioselectivities of up to 93% ee.

In parallel, Glueck and co-workers[118] introduced the phosphination reaction of phosphine-boranes. Compared to free secondary phosphines, phosphine-boranes have the advantage that they cannot inhibit the catalyst by displacement of its phosphine ligands. Their air-stability is also an advantage when carrying out their catalytic syntheses and facilitating the purification of the products. In this line the group investigated the preparation of **PAMP·BH₃** by this method, consisting on the coupling of methylphenylphosphine-borane with *o*-iodoanisole (Scheme 41).
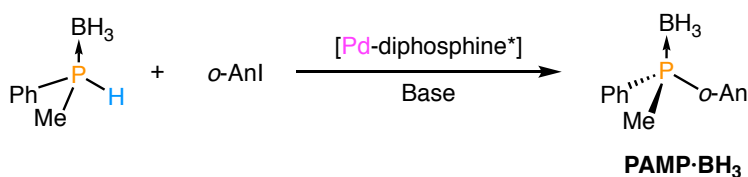
Scheme 41. Enantioselective arylation for the preparation of **PAMP·BH₃**.

A range of different chiral diphosphines such as **Chiraphos**, **Me-DuPhos**, **Tol-BINAP**, among others was tested in this reaction but only moderate enantioselectivities were found. Nevertheless, it represents the only attempt, at present, to prepare a well-known ligand like **PAMP·BH₃** by means of asymmetric catalysis.

2.4.3. *Alkylation of secondary phosphines*

In 2006 and 2009, two independent research groups reported the first examples of Pt-[102] and Ru[103]-catalysed alkylation of secondary phosphines. This reaction is particularly challenging since the achiral base-mediated alkylation competes with the catalytic transformation. In order to overcome this process, the metal catalyst should be the most nucleophilic species present in the media making the metal-catalysed reaction faster than its undesired achiral base-mediated alkylation.

Glueck and co-workers[102,119] studied the alkylation of substrate *rac*-**74** catalysed by Pt-Me-DuPhos-based catalysts obtaining low conversions but promising *ee* values up to 77% (Scheme 42).
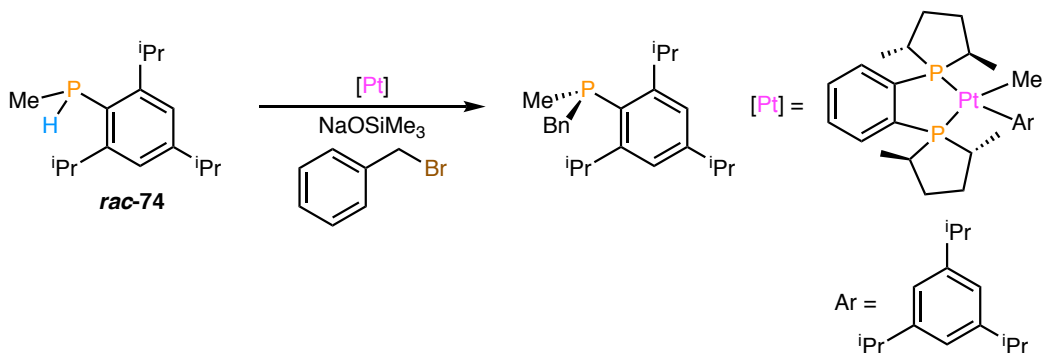
Scheme 42. Pt-catalysed asymmetric alkylation of secondary phosphines.

The reaction can be applied to a variety of secondary mono- and diphosphines and benzyl bromides. However, the substituents attached to the phosphorus have a strong influence on the stereochemical outcome.[119-120]

When the substrate is a secondary diphosphine (Scheme 43) the selectivity of the first alkylation can affect the outcome of the second one due to substrate control. This influence depends on the length of the link, $(CH_2)_n$, between the two P–H reactive sites.
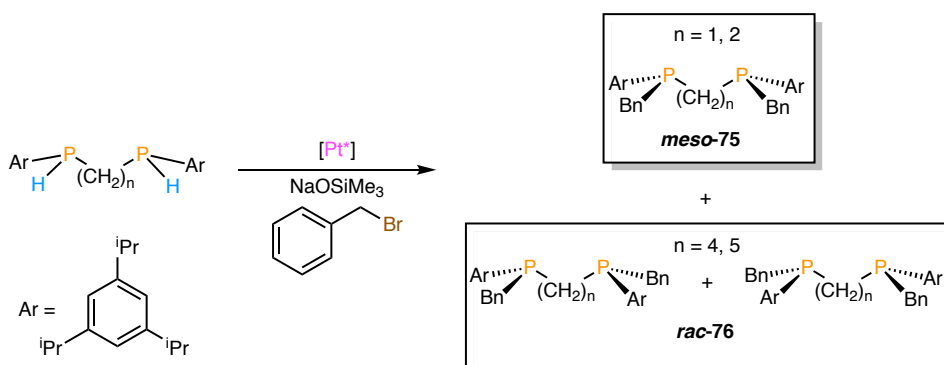
Scheme 43. Pt-catalysed asymmetric alkylation of secondary diphosphines.

In general, the use of substrates with short links (n = 1, 2) results in predominantly *meso*-compounds due to substrate control. In contrast, four or five methylene groups (n = 4, 5) provide a long enough linker to isolate the reactive sites, which results in prevalent *rac*-selective alkylation. Nevertheless, for n = 3 an intermediate behaviour is observed, where the catalyst control is only slightly affected by the substrate.

As a final example, Bergman and co-workers[103] developed the Ru-catalyst depicted in Scheme 44 for the alkylation of *rac*-77 with benzyl chloride.
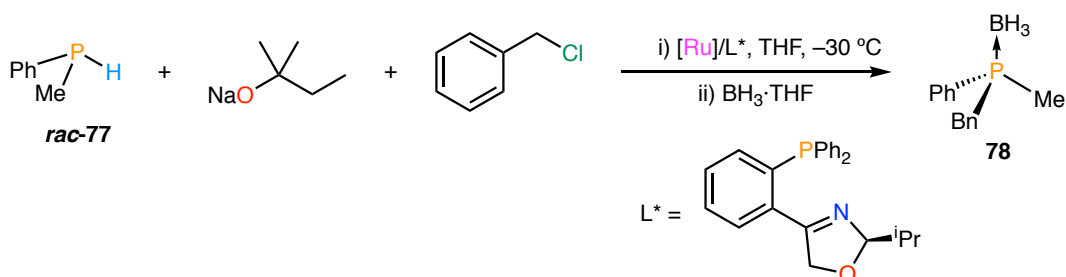
Scheme 44. Ru-catalysed enantioselective alkylation.

The high nucleophilicity of this type of ruthenium catalysts allows the preparation of several *P*-stereogenic derivatives even using benzylbromides and bis(benzylic) compounds as substrates with moderate yields but low enantioselectivities.

Despite all the efforts devoted to the catalytic, enantioselective preparation of *P*-stereogenic phosphines, the current methods are still very limited in scope and usually yield ligands with low enantioselectivity, making them, at present, unusable to prepare ligands for asymmetric catalysis.

2.5. *Conclusions*

This chapter has summarized the main available methods for the synthesis of *P*-stereogenic phosphines and some of their derivatives. The development of the different synthetic strategies, ranging from classical resolutions to asymmetric catalysis, is still an intensive area of research and much further progress can be expected in the near future.

Up to now, quite a large number of *P*-stereogenic ligands, with different structural types and different functionalities have been obtained and constitute a promising *pool* to be tested in asymmetric catalysis. Enantioselective transformations in which the chirality is transferred from phosphine ligands to the desired organic substrates have been developed with almost perfect stereoselectivity. Following these successful insights, it is reasonable to think that the *P*-stereogenic factor, alone or in conjunction with other chiral elements can still lead useful and even "privileged" ligands for asymmetric catalysis.

2.6. *References*

(1)   Meisenheimer, J.; Lichtenstadt, L. *Chem. Ber.* **1911**, *44*, 356-359.

(2)   (a) Rauk, A.; Allen, L. C.; Mislow, K. *Angew. Chem. Int. Ed.* **1970**, *9*, 400-414 (b) Baechler, R. D.; Andose, J. D.; Stackhouse, J.; Mislow, K. *J. Am. Chem. Soc.* **1972**, *94*, 8060-8065.

(3)   (a) Rauk, A.; Andose, J. D.; Frick, W. G.; Tang, R.; Mislow, K. *J. Am. Chem. Soc.* **1971**, *93*, 6507-6515 (b) Hoge, G. *J. Am. Chem. Soc.* **2004**, *126*, 9920-9921 (c) Reichl, K. D.; Ess, D. H.; Radosevich, A. T. *J. Am. Chem. Soc.* **2013**, *135*, 9354-9357.

(4)   Meisenheimer, J.; Casper, J.; Horing, M.; Lauter, W.; Lichtenstadt, L.; Samuel, W. *Liebigs Ann. Chem.* **1926**, 213-248.

(5)   Kumli, K. F.; McEwen, W. E.; VanderWerf, C. A. *J. Am. Chem. Soc.* **1959**, *81*, 248-249.

(6)   Horner, L.; Winkler, H.; Rapp, A.; Mentrup, A.; Hoffmann, H.; Beck, P. *Tetrahedron Lett.* **1961**, *2*, 161-166.

(7)   Horner, L. *Pure Appl. Chem.* **1964**, *9*, 225-244.

(8)   (a) Davies, W. C.; Mann, F. G. *J. Chem. Soc.* **1944**, 276-283 (b) McEwen, W. E.; Kumli, K. F.; Blade-Font, A.; Zanger, M.; VanderWerf, C. A. *J. Am. Chem. Soc.* **1964**, *86*, 2378-2384.

(9)   Osborn, J. A.; Jardine, F. H.; Young, J. F.; Wilkinson, G. J. *J. Chem. Soc. (A)* **1966**, 1711-1732.

(10)   Nozaki, H.; Moriuti, S.; Takaya, H.; Noyori, R. *Tetrahedron Lett.* **1966**, *7*, 5239-5244.

(11)   Knowles, W. S.; Sabacky, M. J. *Chem. Commun.* **1968**, 1445-1446.

(12)   Horner, L.; Siegel, H.; Büthe, H. *Angew. Chem. Int. Ed.* **1968**, *7*, 942-942.

(13)   (a) Knowles, W. S.; Sabacky, M. J.; Vineyard, B. D. *J. Chem. Soc., Chem. Commun.* **1972**, 10-11 (b) Knowles, W. S. *Adv. Synth. Catal.* **2003**, *345*, 3-13.

(14)   (a) Dang, T.; Kagan, H. B. *J. Chem. Soc., Chem. Commun.* **1971**, 481 (b) Kagan, H. B.; Dang, T. *J. Am. Chem. Soc.* **1972**, *94*, 6429-6433.

(15)   Knowles, W. S.; Sabacky, M. J.; Vineyard, B. D.; Weinkauff, D. J. *J. Am. Chem. Soc.* **1975**, *97*, 2567-2568.

(16)   (a) Vineyard, B. D.; Knowles, W. S.; Sabacky, M. J.; Bachman, G. L.; Weinkauff, D. J. *J. Am. Chem. Soc.* **1977**, *99*, 5946-5952 (b) Knowles, W. S. *Acc. Chem. Res.* **1983**, *16*, 106-112.

(17)   Fryzuk, M. D.; Bosnich, B. *J. Am. Chem. Soc.* **1977**, *99*, 6262-6267.

(18)   Miyashita, A.; Yasuda, A.; Takaya, H.; Toriumi, K.; Ito, T.; Souchi, T.; Noyori, R. *J. Am. Chem. Soc.* **1980**, *102*, 7932-7934.

(19)   Burk, M. J.; Feaster, J. E.; Nugent, W. A.; Harlow, R. L. *J. Am. Chem. Soc.* **1993**, *115*, 10125-10138.

(20)   (a) Imamoto, T.; Hoshiki, T.; Onozawa, T.; Kusumoto, T.; Sato, K. *J. Am. Chem. Soc.* **1990**, *112*, 5244-5252 (b) Jugé, S.; Stephan, M.; Laffitte, J. A.; Genêt, J. P. *Tetrahedron Lett.* **1990**, *31*, 6357-6360.

(21)   Pietrusiewicz, K. M.; Zablocka, M. *Chem. Rev.* **1994**, *94*, 1375-1411.

(22)   Grabulosa, A.; Granell, J.; Muller, G. *Coord. Chem. Rev.* **2007**, *251*, 25-90.

(23)   Glueck, D. S. *Synlett* **2007**, 2627-2634.

(24)   Grabulosa, A. *P-Stereogenic Ligands in Enantioselective Catalysis*; Royal Society of Chemistry: Cambridge, 2011.

(25)   Lühr, S.; Holz, J.; Börner, A. *ChemCatChem* **2011**, *3*, 1708-1730.

(26)   Kolodiazhnyi, O. I. *Tetrahedron: Asymmetry* **2012**, *23*, 1-46.

(27)   Chan, T. H. *Chem. Commun.* **1968**, 895-896.

(28)   Imamoto, T.; Oohara, N.; Takahashi, H. *Synthesis* **2004**, 1353-1358.

(29)   Ackermann, L. In *Phosphorus Ligands in Asymmetric Catalysis: Synthesis and Applications*; Börner, A., Ed.; Wiley-VCH: Weinheim, 2008; Vol. 2.

(30)   (a) Lam, W.; Haynes, R. K.; Yeung, L.; Chan, E. W. *Tetrahedron Lett.* **1996**, *37*, 4733-4736 (b) Haynes, R. K.; Au-Yeung, T.; Chan, W.; Lam, W.; Li, Z.; Yeung, L.; Chan, A. S. C.; Li, P.; Koen, M.; Mitchell, C. R.; Vonwiller, S. C. *Eur. J. Org. Chem.* **2000**, 3205-3216.

(31)   Stankevič, M.; Pietrusiewicz, K. M. *J. Org. Chem.* **2007**, *72*, 816-822.

(32)   (a) Tsuruta, H.; Imamoto, T. *Tetrahedron: Asymmetry* **1999**, *10*, 877-882 (b) Carmichael, D.; Doucet, H.; Brown, J. M. *Chem. Commun.* **1999**, 261-262 (c) Hoge, G.; Wu, H.; Kissel, W. S.; Pflum, D. A.; Greene, D. J.; Bao, J. *J. Am. Chem. Soc.* **2004**, *126*, 5966-5967 (d) MacKay, J. A.; Vedejs, E. *J. Org. Chem.* **2006**, *71*, 498-503.

(33)   (a) Pescher, P.; Caude, M.; Rosset, R.; Tambute, A. *J. Chromatography* **1986**, *371*, 159-175 (b) Brandi, A.; Cicchi, S.; Gasparrini, F.; Maggio, F.; Villani, C.; Koprowski, M.; Pietrusiewicz, K. M. *Tetrahedron: Asymmetry* **1995**, *6*, 2017-2022 (c) Jiang, X.; Minnaard, A. J.; Hessen, B.; Feringa, B. L.; Duchateau, A. L. L.; Andrien, J. G. O.; Boogers, J. A. F.; de Vries, J. G. *Org. Lett.* **2003**, *5*, 1503-1506 (d) Imamoto, T.; Crépy, K. V. L.; Katagiri, K. *Tetrahedron: Asymmetry* **2004**, *15*, 2213-2218 (e) Jiang, X.; van den Berg, M.; Minnaard, A. J.; Feringa, B. L.; de Vries, J. G. *Tetrahedron: Asymmetry* **2004**, *15*, 2223-2229 (f) Bigeault, J.; Giordano, L.; Buono, G. *Angew. Chem. Int. Ed.* **2005**, *44*, 4753-4757 (g) Widhalm, M.; Brecker, L.; Mereiter, K. *Tetrahedron: Asymmetry* **2006**, *17*, 1355-1369.

(34)   DeBruin, K. E.; Zon, G.; Naumann, K.; Mislow, K. *J. Am. Chem. Soc.* **1969**, *91*, 7027-7030.

(35)   Kolodiazhnyi, O. I.; Kolodiazhna, A. *Tetrahedron: Asymmetry* **2017**, *28*, 1651-1674.

(36)   (a) Kyba, E. P. *J. Am. Chem. Soc.* **1975**, *97*, 2554-2555 (b) Kyba, E. P. *J. Am. Chem. Soc.* **1976**, *98*, 4805-4809 (c) Tollefson, M. B.; Li, J. J.; Beak, P. *J. Am. Chem. Soc.* **1996**, *118*, 9052-9061 (d) Zhao, C.-Q.; Yao, L.; Liu, L.-J.; Xu, Z.-Y.; Nie, S.-Z.; Xiao, X.-Q. *Org. Biomol. Chem.* **2016**, *14*, 1702-1706 (e) Chen, L.; Fang, X.-Y.; Zou, Y.-X. *Org. Biomol. Chem.* **2018**, *16*, 951-956.

(37)   Zijlstra, H.; León, T.; de Cózar, A.; Guerra, C. F.; Byrom, D.; Riera, A.; Verdaguer, X.; Bickelhaupt, F. M. *J. Am. Chem. Soc.* **2013**, *135*, 4483-4491.

(38)   (a) Korpiun, O.; Lewis, R. A.; Chickos, J.; Mislow, K. *J. Am. Chem. Soc.* **1968**, *90*, 4842-4846 (b) Crépy, K. V. L.; Imamoto, T. *Top. Curr. Chem.* **2003**, *229*, 1-40.

(39)   Nudelman, A.; Cram, D. J. *J. Am. Chem. Soc.* **1968**, *90*, 3869-3870.

(40)   Horner, L.; Schlotthauer, B. *Phosphorus, Sulfur Relat. Elem.* **1978**, *4*, 155-165.

(41)   Oshiki, T.; Imamoto, T. *J. Am. Chem. Soc.* **1992**, *114*, 3975-3977.

(42)   (a) Naumann, K.; Zon, G.; Mislow, K. *J. Am. Chem. Soc.* **1969**, *91*, 7012-7023 (b) Marsi, K. L. *J. Org. Chem.* **1974**, *39*, 265-267 (c) Valentine, D.; Blount, J. F.; Toth, K. *J. Org. Chem.* **1980**, *45*, 3691-3698 (d) Imamoto, T.; Kikuchi, S.; Miura, T.; Wada, Y. *Org. Lett.* **2001**, *3*, 87-90 (e) Stankevič, M.; Pietrusiewicz, K. M. *Synlett* **2003**, 1012-1016 (f) Busacca, C. A.; Lorenz, J. C.; Grinberg, N.; Haddad, N.; Hrapchak, M.; Latli, B.; Lee, H.; Sabila, P.; Saha, A.; Sarvestani, M.; Shen, S.; Varsolona, R.; Wei, X.; Senanayake, C. H. *Org. Lett.* **2005**, *7*, 4277-4280 (g) Pehlivan, L.; Métay, E.; Delbrayelle, D.; Mignani, G.; Lemaire, M. *Tetrahedron* **2012**, *68*, 3151-3155 (h) Krenske, E. H. *J. Org. Chem.* **2012**, *77*, 1-4 (i) Herault, D.; Nguyen, D. H.; Nuel, D.; Buono, G. *Chem. Soc. Rev.* **2015**, *44*, 2508-2528 (j) Sowa, S.; Stankevič, M.; Szmigielska, A.; Małuszyńska, H.; Kozioł, A. E.; Pietrusiewicz, K. M. *J. Org. Chem.* **2015**, *80*, 1672-1688 (k)

Schirmer, M.-L.; Jopp, S.; Holz, J.; Spannenberg, A.; Werner, T. *Adv. Synth. Catal.* **2016**, *358*, 26-29 (l) Li, P.; Wischert, R.; Métivier, P. *Angew. Chem. Int. Ed.* **2017**, *56*, 15989-15992 (m) Emanuelsson, E.; Webster, R. L.; Provis-Evans, C. *Adv. Synth. Catal.* **2018A**, *360*, 3999-4004.

(43) (a) Henson, P. D.; Naumann, K.; Mislow, K. *J. Am. Chem. Soc.* **1969**, *91*, 5645-5646 (b) Wozniak, L. A.; Krzyzanowska, B.; Stec, W. J. *J. Org. Chem.* **1992**, *57*, 6057-6060 (c) Sprott, K. T.; Hanson, P. R. *J. Org. Chem.* **2000**, *65*, 4721-4728 (d) Dornhaus, F.; Bolte, M.; Lerner, H.; Wagner, M. *Eur. J. Inorg. Chem.* **2006**, 1777-1785 (e) Coetzee, J.; Eastham, G. R.; Slawin, A. M. Z.; Cole-Hamilton, D. J. *Org. Biomol. Chem.* **2012**, *10*, 3677-3688 (f) Bhattacharyya, K. X.; Dreyfuss, S.; Saffon, N.; Mezailles, N. *Chem. Commun.* **2016**, *52*, 5179-5182.

(44) Leyris, A.; Bigeault, J.; Nuel, D.; Giordano, L.; Buono, G. *Tetrahedron Lett.* **2007**, *48*, 5247-5250.

(45) Xu, Q.; Zhao, C.; Han, L. *J. Am. Chem. Soc.* **2008**, *130*, 12648-12655.

(46) Lewis, R. A.; Mislow, K. *J. Am. Chem. Soc.* **1969**, *91*, 7009-7012.

(47) (a) Lewis, R. A.; Naumann, K.; DeBruin, K. E.; Mislow, K. *Chem. Commun.* **1969**, 1010-1011 (b) Oshiki, T.; Imamoto, T. *Bull. Chem. Soc. Jpn.* **1990**, *63*, 3719-3721.

(48) Kolodiazhnyi, O. I.; Gryskun, E. V.; Andrushko, N. V.; Freytag, M.; Jones, P. G.; Schmutzler, R. *Tetrahedron: Asymmetry* **2003**, *14*, 181-183.

(49) Revés, M.; Ferrer, C.; León, T.; Doran, S.; Etayo, P.; Vidal-Ferran, A.; Riera, A.; Verdaguer, X. *Angew. Chem. Int. Ed.* **2010**, *49*, 9452-9455.

(50) Cristóbal-Lecina, E.; Etayo, P.; Doran, S.; Revés, M.; Martín-Gago, P.; Grabulosa, A.; Constantino, A. R.; Vidal-Ferran, A.; Riera, A.; Verdaguer, X. *Adv. Synth. Catal.* **2014**, *356*, 795-804.

(51) León, T.; Parera, M.; Roglans, A.; Riera, A.; Verdaguer, X. *Angew. Chem. Int. Ed.* **2012**, *51*, 6951-6955.

(52) Corey, E. J.; Chen, Z.; Tanoury, G. J. *J. Am. Chem. Soc.* **1993**, *115*, 11000-11001.

(53) Carey, J. V.; Barker, M. D.; Brown, J. M.; Russell, M. J. H. *J. Chem. Soc. Perkin Trans. 1* **1993**, 831-839.

(54) (a) Brown, J. M.; Laing, J. C. P. *J. Organomet. Chem.* **1997**, *529*, 435-444 (b) Nettekoven, U.; Widhalm, M.; Kamer, P. C. J.; van Leeuwen, P. W. N. M.; Mereiter, K.; Lutz, M.; Spek, A. L. *Organometallics* **2000**, *19*, 2299-2309 (c) Maienza, F.; Spindler, F.; Thommen, M.; Pugin, B.; Malan, C.; Mezzetti, A. *J. Org. Chem.* **2002**, *67*, 5239-5249 (d) Stephan, M.; Sterk, D.; Modec, B.; Mohar, B. *J. Org. Chem.* **2007**, *72*, 8010-8018.

(55) Jugé, S.; Stephan, M.; Merdès, R.; Genêt, J. P.; Halut-Desportes, S. *J. Chem. Soc., Chem. Commun.* **1993**, 531-533.

(56) Rippert, A. J.; Linden, A.; Hansen, H. *Helv. Chim. Acta* **2000**, *83*, 311-321.

(57) Zupancic, B.; Mohar, B.; Stephan, M. *Adv. Synth. Catal.* **2008**, *350*, 2024-2032.

(58) Grabulosa, A.; Muller, G.; Ordinas, J. I.; Mezzetti, A.; Maestro, M. A.; Font-Bardia, M.; Solans, X. *Organometallics* **2005**, *24*, 4961-4973.

(59) (a) Zhu, G.; Terry, M.; Zhang, X. *Tetrahedron Lett.* **1996**, *37*, 4475-4478 (b) Zhu, G.; Terry, M.; Zhang, X. *J. Organomet. Chem.* **1997**, *547*, 97-101 (c) Nettekoven, U.; Kamer, P. C. J.; van Leeuwen, P. W. N. M.; Widhalm, M.; Spek, A. L.; Lutz, M. *J. Org. Chem.* **1999**, *64*, 3996-4004 (d) Ewalds, R.; Eggeling, E. B.; Hewat, A. C.; Kamer, P. C. J.; van Leeuwen, P. W. N. M.; Vogt, D. *Chem. Eur. J.* **2000**, *6*, 1496-1504 (e) Nettekoven, U.; Kamer, P. C. J.; van Leeuwen, P. W. N. M. *Organometallics* **2000**, *19*, 4596-4607 (f) Nettekoven, U.; Widhalm, M.; Kalchhauser, H.; Kamer, P. C. J.; van Leeuwen, P. W. N. M.; Lutz, M.;

Spek, A. L. *J. Org. Chem.* **2001**, *66*, 759-770 (g) Colby, E. A.; Jamison, T. F. *J. Org. Chem.* **2003**, *68*, 156-166.

(60)   (a) Yang, H.; Lugan, N.; Mathieu, R. *Organometallics* **1997**, *16*, 2089-2095 (b) Moulin, D.; Darcel, C.; Jugé, S. *Tetrahedron: Asymmetry* **1999**, *10*, 4729-4743 (c) Moulin, D.; Bago, S.; Bauduin, C.; Darcel, C.; Jugé, S. *Tetrahedron: Asymmetry* **2000**, *11*, 3939-3956.

(61)   (a) Stoop, R. M.; Mezzetti, A.; Spindler, F. *Organometallics* **1998**, *17*, 668-675 (b) Maienza, F.; Santoro, F.; Spindler, F.; Malan, C.; Mezzetti, A. *Tetrahedron: Asymmetry* **2002**, *13*, 1817-1824 (c) Rodríguez, L. I.; Rossell, O.; Seco, M.; Muller, G. *J. Organomet. Chem.* **2009**, *694*, 1938.

(62)   Darcel, C.; Kaloun, E. B.; Merdès, R.; Moulin, D.; Riegel, N.; Thorimbert, S.; Genêt, J. P.; Jugé, S. *J. Organomet. Chem.* **2001**, *624*, 333-343.

(63)   (a) Grabulosa, A., Universitat de Barcelona, 2005 (b) Zupancic, B.; Mohar, B.; Stephan, M. *Tetrahedron Lett.* **2009**, *50*, 7382-7384.

(64)   Johansson, M. J.; Andersson, K. H. O.; Kann, N. *J. Org. Chem.* **2008**, *73*, 4458-4463.

(65)   (a) Lam, H.; Horton, P. N.; Hursthouse, M. B.; Aldous, D. J.; Hii, K. K. *Tetrahedron Lett.* **2005**, *46*, 8145-8148 (b) Vargas, S.; Rubio, M.; Suárez, A.; del Río, D.; Álvarez, E.; Pizzano, A. *Organometallics* **2006**, *25*, 961-973.

(66)   (a) Rodríguez, L.; Rossell, O.; Seco, M.; Grabulosa, A.; Muller, G.; Rocamora, M. *Organometallics* **2006**, *25*, 1368-1376 (b) Rodríguez, L.; Rossell, O.; Seco, M.; Muller, G. *Organometallics* **2008**, *27*, 1328-1333.

(67)   Agbossou-Niedecorn, F.; Suisse, I. *Coord. Chem. Rev.* **2003**, *242*, 145-158.

(68)   den Heeten, R.; Swennenhuis, B. H. G.; van Leeuwen, P. W. N. M.; de Vries, J. G.; Kamer, P. C. J. *Angew. Chem. Int. Ed.* **2008**, *47*, 6602-6605.

(69)   (a) Geng, H.; Zhang, W.; Chen, J.; Hou, G.; Zhou, L.; Zou, Y.; Wu, W.; Zhang, X. *Angew. Chem. Int. Ed.* **2009**, *48*, 6052-6054 (b) Benhaim, C.; Bouchard, L.; Pelletier, G.; Sellstedt, J.; Kristofova, L.; Daigneault, S. *Org. Lett.* **2010**, *12*, 2008-2011 (c) Yanagisawa, A.; Takeshita, S.; Izumi, Y.; Yoshida, K. *J. Am. Chem. Soc.* **2010**, *132*, 5328-5329 (d) Imamoto, T.; Tamura, K.; Zhang, Z.; Horiuchi, Y.; Sugiya, M.; Yoshida, K.; Yanagisawa, A.; Gridnev, I. D. *J. Am. Chem. Soc.* **2012**, *134*, 1754-1769 (e) Han, Z. S.; Goyal, N.; Herbage, M. A.; Sieber, J. D.; Qu, B.; Xu, Y.; Li, Z.; Reeves, J. T.; Desrosiers, J.-N.; Ma, S.; Grinberg, N.; Lee, H.; Mangunuru, H. P. R.; Zhang, Y.; Krishnamurthy, D.; Lu, B. Z.; Song, J. J.; Wang, G.; Senanayake, C. H. *J. Am. Chem. Soc.* **2013**, *135*, 2474-2477.

(70)   Noh, D.; Chea, H.; Ju, J.; Yun, J. *Angew. Chem. Int. Ed.* **2009**, *48*, 6062-6064.

(71)   Shibata, Y.; Tanaka, K. *J. Am. Chem. Soc.* **2009**, *131*, 12552-12553.

(72)   (a) León, T.; Riera, A.; Verdaguer, X. *J. Am. Chem. Soc.* **2011**, *133*, 5740-5743 (b) Doran, S.; Achard, T.; Riera, A.; Verdaguer, X. *J. Organomet. Chem.* **2012**, *717*, 135-140 (c) Orgué, S.; Flores-Gaspar, A.; Biosca, M.; Pàmies, O.; Diéguez, M.; Riera, A.; Verdaguer, X. *Chem. Commun.* **2015**, *51*, 17548-17551 (d) Salomó, E.; Orgué, S.; Riera, A.; Verdaguer, X. *Synthesis* **2016**, 2659-2663 (e) Salomó, E.; Prades, A.; Riera, A.; Verdaguer, X. *J. Org. Chem.* **2017**, *82*, 7065-7069.

(73)   Gatineau, D.; Giordano, L.; Buono, G. *J. Am. Chem. Soc.* **2011**, *133*, 10728-10731.

(74)   Tang, W.; Capacci, A. G.; Wei, X.; Li, W.; White, A.; Patel, N. D.; Savoie, J.; Gao, J. J.; Rodriguez, S.; Qu, B.; Haddad, N.; Lu, B. Z.; Krishnamurthy, D.; Yee, N. K.; Senanayake, C. H. *Angew. Chem. Int. Ed.* **2010**, *49*, 5879-5883.

(75)   Tang, W.; Capacci, A. G.; White, A.; Ma, S.; Rodriguez, S.; Qu, B.; Savoie, J.; Patel, N. D.; Wei, X.; Haddad, N.; Grinberg, N.; Yee, N. K.; Krishnamurthy, D.; Senanayake, C. H. *Org. Lett.* **2010**, *12*, 1104-1107.

52

(76)   Tang, W.; Qu, B.; Capacci, A. G.; Rodriguez, S.; Wei, X.; Haddad, N.; Narayanan, B.; Ma, S.; Grinberg, N.; Yee, N. K.; Krishnamurthy, D.; Senanayake, C. H. *Org. Lett.* **2010**, *12*, 176-179.

(77)   Qu, B.; Samankumara, L. P.; Savoie, J.; Fandrick, D. R.; Haddad, N.; Wei, X.; Ma, S.; Lee, H.; Rodriguez, S.; Busacca, C. A.; Yee, N. K.; Song, J. J.; Senanayake, C. H. *J. Org. Chem.* **2014**, *79*, 993-1000.

(78)   Byrne, L. T.; Engelbardt, L. M.; Jacobsen, G. E.; Leung, W.; Papasergio, R. I.; Raston, C. L.; Skelton, B. W.; Twiss, P.; White, A. H. *J. Chem. Soc. Dalton Trans.* **1989**, 105-113.

(79)   Muci, A. R.; Campos, K. R.; Evans, D. A. *J. Am. Chem. Soc.* **1995**, *117*, 9075-9076.

(80)   Imamoto, T.; Watanabe, J.; Wada, Y.; Masuda, H.; Yamada, H.; Tsuruta, H.; Matsukawa, S.; Yamaguchi, K. *J. Am. Chem. Soc.* **1998**, *120*, 1635-1636.

(81)   (a) Valentine, D. H.; Hillhouse, J. H. *Synthesis* **2003**, 2437-2460 (b) Imamoto, T. In *Phosphorus Ligands in Asymmetric Catalysis: Synthesis and Applications*; Börner, A., Ed.; Wiley-VCH: Weinheim, 2008; Vol. 3.

(82)   (a) Couch, J. F. *J. Am. Chem. Soc.* **1932**, *54*, 1691-1692 (b) Couch, J. F. *J. Am. Chem. Soc.* **1936**, *58*, 1296-1299.

(83)   (a) Gridnev, I. D.; Yamamoi, Y.; Higashi, N.; Tsuruta, H.; Yasutake, M.; Imamoto, T. *Adv. Synth. Catal.* **2001**, *343*, 118-136 (b) Oohara, N.; Katagiri, K.; Imamoto, T. *Tetrahedron: Asymmetry* **2003**, *14*, 2171-2175.

(84)   (a) Yamanoi, Y.; Imamoto, T. *J. Org. Chem.* **1999**, *64*, 2988-2989 (b) Imamoto, T. *Pure Appl. Chem.* **2001**, *73*, 373-376 (c) Imamoto, T.; Tamura, K.; Ogura, T.; Ikematsu, Y.; Mayama, D.; Sugiya, M. *Tetrahedron: Asymmetry* **2010**, *21*, 1522-1528.

(85)   Aznar, R.; Grabulosa, A.; Mannu, A.; Muller, G.; Sainz, D.; Moreno, V.; Font-Bardia, M.; Calvet, T.; Lorenzo, J. *Organometallics* **2013**, *32*, 2344-2362.

(86)   Nagata, K.; Matsukawa, S.; Imamoto, T. *J. Org. Chem.* **2000**, *65*, 4185-4188.

(87)   Katagiri, K.; Danjo, H.; Yamaguchi, K.; Imamoto, T. *Tetrahedron* **2005**, *61*, 4701-4707.

(88)   (a) Ohashi, A.; Imamoto, T. *Tetrahedron Lett.* **2001**, *42*, 1099-1101 (b) Ohashi, A.; Kikuchi, S.; Yasutake, M.; Imamoto, T. *Eur. J. Org. Chem.* **2002**, 2535-2546.

(89)   Imamoto, T.; Saitoh, Y.; Koide, A.; Ogura, T.; Yoshida, K. *Angew. Chem. Int. Ed.* **2007**, *46*, 8636-8639.

(90)   (a) Wolfe, B.; Livinghouse, T. *J. Org. Chem.* **2001**, *66*, 1514-1516 (b) Heath, H.; Wolfe, B.; Livinghouse, T.; Bae, S. K. *Synthesis* **2001**, 2341-2347.

(91)   Al-Masum, M.; Kumaraswamy, G.; Livinghouse, T. *J. Org. Chem.* **2000**, *65*, 4776-4778.

(92)   (a) McKinstry, L.; Livinghouse, T. *Tetrahedron Lett.* **1994**, *35*, 9319-9322 (b) McKinstry, L.; Overberg, J. J.; Soubra-Ghaoui, C.; Walsh, D. S.; Robins, K. A. *J. Org. Chem.* **2000**, *65*, 2261-2263.

(93)   (a) Dearden, M. J.; Firkin, C. R.; Hermet, J. R.; O'Brien, P. *J. Am. Chem. Soc.* **2002**, *124*, 11870-11871 (b) Strohmann, C.; Strohfeldt, K.; Schildbach, D.; McGrath, M. J.; O'Brien, P. *Organometallics* **2004**, *23*, 5389-5391 (c) Dixon, A. J.; McGrath, M. J.; O'Brien, P. *Org. Synth.* **2006**, *83*, 141-154 (d) O'Brien, P. *Chem. Commun.* **2008**, 655-667 (e) Stead, D.; O'Brien, P.; Sanderson, A. *Org. Lett.* **2008**, *10*, 1409-1412.

(94)   (a) Glueck, D. S. *Chem. Eur. J.* **2008**, *14*, 7108-7117 (b) Glueck, D. S. *Top. Organomet. Chem.* **2010**, *31*, 65-100 (c) Glueck, D. S. *Catal. Sci. Technol.* **2011**, *1*, 1099-1108.

(95)   (a) Schwan, A. L. *Chem. Soc. Rev.* **2004**, *33*, 218-224 (b) Glueck, D. S. *Dalton Trans.* **2008**, 5276-5286.

(96) Glueck, D. S. *Coord. Chem. Rev.* **2008**, *252*, 2171-2179.

(97) (a) Buhro, W. E.; Zwick, B. D.; Georgiou, S.; Hutchinson, J. P.; Gladysz, J. A. *J. Am. Chem. Soc.* **1988**, *110*, 2427-2439 (b) Crisp, G. T.; Salem, G.; Wild, S. B. *Organometallics* **1989**, *8*, 2360-2367 (c) Bohle, D. S.; Clark, G. R.; Rickard, C. E. F.; Roper, W. R. *J. Organomet. Chem.* **1990**, *393*, 243-285 (d) Zhuravel, M. A.; Glueck, D. S.; Zakharov, L. V.; Rheingold, A. L. *Organometallics* **2002**, *21*, 3208-3214.

(98) (a) Wicht, D. K.; Kourkine, I. V.; Lew, B. M.; Nthenge, J. M.; Glueck, D. S. *J. Am. Chem. Soc.* **1997**, *119*, 5039-5040 (b) Wicht, D. K.; Kourkine, I. V.; Kovacik, I.; Glueck, D. S.; Concolino, T. H.; Yap, G. P. A.; Incarvito, C.; Rheingold, A. L. *Organometallics* **1999**, *18*, 5381-5394.

(99) (a) Han, L.; Zhao, C.; Onozawa, S.; Goto, M.; Tanaka, M. *J. Am. Chem. Soc.* **2002**, *124*, 3842-3843 (b) Mimeau, D.; Gaumont, A. *J. Org. Chem.* **2003**, *68*, 7016-7022 (c) Join, B.; Mimeau, D.; Delacroix, O.; Gaumont, A. *Chem. Commun.* **2006**, 3249-3251.

(100) Douglass, M. R.; Marks, T. J. *J. Am. Chem. Soc.* **2000**, *122*, 1824-1825.

(101) (a) Moncarz, J. R.; Laritcheva, N. F.; Glueck, D. S. *J. Am. Chem. Soc.* **2002**, *124*, 13356-13357 (b) Huang, Y.; Li, Y.; Leung, P.-H.; Hayashi, T. *J. Am. Chem. Soc.* **2014**, *136*, 4865-4868 (c) Dub, P. A.; Gordon, J. C. *Dalton Trans.* **2016**, *45*, 6756-6781.

(102) Scriban, C.; Glueck, D. S. *J. Am. Chem. Soc.* **2006**, *128*, 2788-2789.

(103) (a) Chan, V. S.; Stewart, I. C.; Bergman, R. G.; Toste, F. D. *J. Am. Chem. Soc.* **2006**, *128*, 2786-2787 (b) Chan, V. S.; Chiu, M.; Bergman, R. G.; Toste, F. D. *J. Am. Chem. Soc.* **2009**, *131*, 6021-6032.

(104) Nishida, G.; Noguchi, K.; Hirano, M.; Tanaka, K. *Angew. Chem. Int. Ed.* **2008**, *47*, 3410-3413.

(105) Demchuk, O. M.; Pietrusiewicz, K. M.; Michrowska, A.; Grela, K. *Org. Lett.* **2003**, *5*, 3217-3220.

(106) Schrock, R. R.; Hoveyda, A. H. *Angew. Chem. Int. Ed.* **2003**, *42*, 4592-4633.

(107) *Catalytic Heterofunctionalization. From Hydroamination to Hydrozirconation*; Wiley-VCH: Weinheim, 2001.

(108) (a) Bourumeau, K.; Gaumont, A.; Denis, J. *Tetrahedron Lett.* **1997**, *38*, 1923-1926 (b) Mimeau, D.; Delacroix, O.; Gaumont, A. *Chem. Commun.* **2003**, 2928-2929 (c) Mimeau, D.; Delacroix, O.; Join, B.; Gaumont, A. *C. R. Chimie* **2004**, *7*, 845-854 (d) Join, B.; Delacroix, O.; Gaumont, A. *Synlett* **2005**, 1881-1884.

(109) *Aqueous Organometallic Chemistry and Catalysis*; Horvath, I. T.; Joo, F., Eds.; Kluwer: Dordrecht, The Netherlands, 1995; Vol. 5.

(110) Wicht, D. K.; Zhuravel, M. A.; Gregush, R. V.; Glueck, D. S. *Organometallics* **1998**, *17*, 1412-1419.

(111) (a) Wicht, D. K.; Glueck, D. S.; Liable-Sands, L. M.; Rheingold, A. L. *Organometallics* **1999**, *18*, 5130-5140 (b) Wicht, D. K.; Kovacik, I.; Glueck, D. S.; Liable-Sands, L. M.; Incarvito, C. D.; Rheingold, A. L. *Organometallics* **1999**, *18*, 5141-5151 (c) Kovacik, I.; Wicht, D. K.; Grewal, N. S.; Glueck, D. S.; Incarvito, C. D.; Guzei, I. A.; Rheingold, A. L. *Organometallics* **2000**, *19*, 950-953.

(112) (a) Xu, Y.; Zhang, J. *J. Chem. Soc. Chem. Commun.* **1986**, 1606 (b) Zhang, J.; Xu, Y.; Huang, G.; Guo, H. *Tetrahedron Lett.* **1988**, *29*, 1955-1958 (c) Xu, Y.; Wei, H.; Zhang, J.; Huang, G. *Tetrahedron Lett.* **1989**, *30*, 949-952.

(113) Imamoto, T.; Oshiki, T.; Onozawa, T.; Matsuo, M.; Hikosaka, T.; Yanagawa, M. *Heteroatom. Chem.* **1992**, *3*, 563-575.

(114) Al-Masum, M.; Livinghouse, T. *Tetrahedron Lett.* **1999**, *40*, 7731-7734.

(115)   Blank, N. F.; Moncarz, J. R.; Brunker, T. J.; Scriban, C.; Anderson, B. J.; Amir, O.; Glueck, D. S.; Zakharov, L. V.; Golen, J. A.; Incarvito, C. D.; Rheingold, A. L. *J. Am. Chem. Soc.* **2007**, *129*, 6847-6858.

(116)   Brunker, T. J.; Anderson, B. J.; Blank, N. F.; Glueck, D. S.; Rheingold, A. L. *Org. Lett.* **2007**, *9*, 1109-1112.

(117)   Langer, T.; Janssen, J.; Helmchen, G. *Tetrahedron: Asymmetry* **1996**, *7*, 1599-1602.

(118)   (a) Moncarz, J. R.; Brunker, T. J.; Glueck, D. S.; Sommer, R. D.; Rheingold, A. L. *J. Am. Chem. Soc.* **2003**, *125*, 1180-1181 (b) Moncarz, J. R.; Brunker, T. J.; Jewett, J. C.; Orchowski, M.; Glueck, D. S.; Sommer, R. D.; Lam, K.; Incarvito, C. D.; Concolino, T. H.; Ceccarelli, C.; Zakharov, L. V.; Rheingold, A. L. *Organometallics* **2003**, *22*, 3205-3221.

(119)   Scriban, C.; Glueck, D. S.; Golen, J. A.; Rheingold, A. L. *Organometallics* **2007**, *26*, 1788-1800.

(120)   (a) Anderson, B. J.; Guino-o, M. A.; Glueck, D. S.; Golen, J. A.; DiPasquale, A. G.; Liable-Sands, L. M.; Rheingold, A. L. *Org. Lett.* **2008**, *10*, 4425-4428 (b) Chapp, T. W.; Glueck, D. S.; Golen, J. A.; Moore, C. E.; Rheingold, A. L. *Organometallics* **2010**, *29*, 378-388.

Chapter III. Coordination chemistry and catalysis with Secondary Phosphine Oxides (SPOs)

3.   Coordination chemistry and catalysis with Secondary Phosphine Oxides (SPOs)

3.1. *Precedents on the synthesis of SPOs*

Tertiary phosphines have been used in the preparation of countless coordination and organometallic complexes since they efficiently bind a large number of metallic centres. However, it is well known that some of these organophosphorus compounds are especially prone to oxidation, due to the non-bonding pair on the phosphorus atom, which reacts with the oxygen of air leading the formation of the corresponding unreactive oxide. The design of the phosphine ligands becomes crucial for the catalytic applications of the metallic precursors.

Often, however, these phosphines or even their transition-metal complexes are difficult to handle, due to its air and moisture-sensitivity, and their preparation requires laborious methods. For these reasons the use of phosphines at industrial scale is still limited. Fortunately, a number of protection strategies for phosphines have been developed. Among these, the use of BH_3 adducts[1] or the corresponding protonated species (phosphonium salts)[2] proved valuable. Particularly, coordination with BH_3 groups is still one of the most widely used protecting methods, but the release of the free phosphine needs the presence of an amine; a process that has always to take place before any coordination to transition metals.[1] Other options rely on the controlled oxidation of the trivalent phosphorus atom. The phosphine oxide can be subsequently deprotected through reduction, normally using silanes. That was the classical approach before the use of boranes as protecting groups and it inherently has several drawbacks such as the harsh reaction conditions, which sometimes lead to racemisation of the *P*-stereogenic compounds.

The protection methodology, however, postpones the problem of handling air-sensitive phosphines, rather than solving it. An alternative makes use of Secondary Phosphine Oxides (SPOs), which despite being known for more than 50 years, they currently represent a new class ligands with a remarkable stability and potential.

3.1.1. *The tautomeric equilibrium of SPOs*

Tautomerisation can be defined as the interconversion between constitutional isomers, also called tautomers.[3] Any reaction that simply involves the intramolecular transfer of a proton, and nothing else, is considered as a tautomerism. Well-known examples of tautomerism can be found in the protonation/deprotonation of carboxylic acids and in the proton exchange between the two nitrogen atoms in the imidazole ring. In these cases the products and the reagents are exactly the same. However, this situation cannot be extended to other cases whose best-known example is the keto-enol tautomerism.

A tautomeric equilibrium can also found for some organophosphorus compounds. In this respect, Secondary Phosphine Oxides (SPOs) and Heteroatom-Substituted Secondary Phosphine Oxides (HASPOs), are of particular interest because even though they contain a pentavalent phosphorus atom, they can be considered as potential ligands in homogeneous catalysis due to a tautomeric equilibrium with the trivalent phosphorus species. (HA)SPOs are weak acids and therefore, they can tautomerise in solution to phosphinous acids, as it is depicted in Scheme 1.

SPO — Phosphinous acid

R^1, R^2 = Alkyl, Aryl

(HA)SPO

R^1, R^2 = Alkyl, Aryl

X = O, N
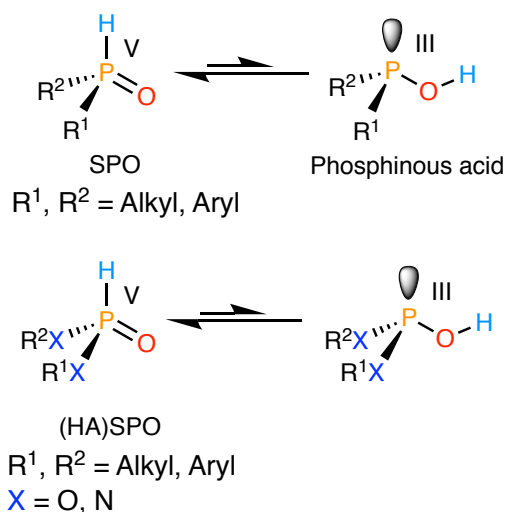
Scheme 1. Tautomerism of (HA)SPOs.

The trivalent tautomeric form, a phosphinous acid, is able to bind Lewis acids, and as a result, it has been recently suggested the term "preligands" for these compounds, which have been successfully used, in some cases, as ancillary ligands in homogenous catalysis.[4] However, little is still known about the chemical and physical properties of most of them, even though this information is crucial for an assessment of their coordination behaviour and lately their catalytic properties. In general, SPOs are

reputed to be stable towards oxygen, which has been explained by the dominance of the pentavalent tautomer in solution. It is assumed that this equilibrium is completely displaced towards the oxide form but the presence of transition metal cations or silylating agents[5] can shift the equilibrium to the trivalent form.

3.1.2. *Mechanistic insights*

As early as the 1960s, SPOs were studied by deuterium exchange experiments.[6] The results of these evidenced the clear predominance of the pentavalent tautomer in most instances, a fact that was supported by IR spectroscopic measurements confirming the formal P=O nature of alkyl- and aryl-substituted SPOs. In 2004, Pietrusiewicz, Duddeck and co-workers suggested,[7] from NMR studies, that the fast kinetics of the tautomeric equilibrium was due to the migration of an acidic proton. In this line, Hong and co-workers[8] proposed two reaction pathways (Scheme 2) for the transformation of secondary phosphine oxides to the corresponding phosphinous acids, based on DFT calculations.
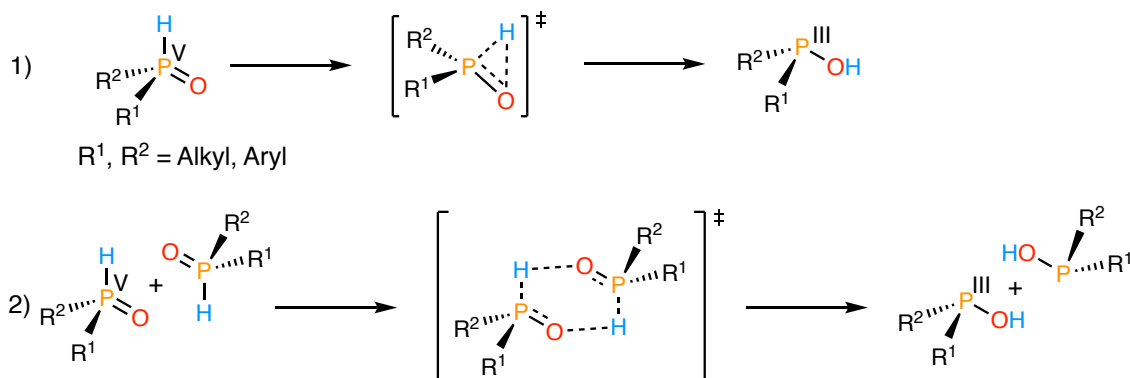
Scheme 2. Proposed routes for the conversion of secondary phosphine oxides to phosphinous acids. 1) Unimolecular pathway and 2) the bimolecular one.

In the first route, the unimolecular pathway, the tautomerism takes place due to the intramolecular migration of the hydroxyl proton, whereas in the bimolecular route the conversion can be rationalised by an intermolecular transfer of two hydrogen atoms in a synchronous exchange.

More recently Montchamp and Janesko[3] have shown that the reaction mechanism involves a simultaneous dissociation of a P–H bond and formation of an O–H bond and that the proton exchange which leads to the formal reduction of the P(V) species, can not take place in an intramolecular proton transfer. According to their DFT studies, the unimolecular pathway does not work for those SPO molecules containing very bulky substituents, since the distorted geometry of the tetrahedral species have very high-energy barriers.

3.1.3. *Factors that affect the tautomeric equilibrium*

Depending on the electronic character of the substituents at the P atom, the tautomeric equilibrium of SPOs shows some experimental tendencies. In 2010 Börner and co-workers[9] studied the tautomeric behaviour of five secondary phosphine oxides with different electronic properties (Figure 1).
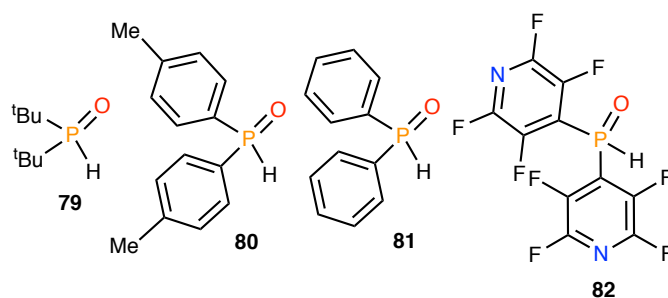
Figure 1. SPOs studied by Börner and co-workers.[9]

They concluded, according to NMR and IR spectroscopy, DFT calculations and X-ray structural analysis that only with strongly electron-withdrawing groups the phosphinous acid form can be observed in the equilibrium, whereas for all the other cases the phosphine oxide form completely dominates. This tendency has been clearly seen by ^{31}P NMR spectroscopy, whose chemical shifts and ^{31}P-^{1}H couplings revealed that with the exception of the perfluorinated phosphine in Figure 1, all other SPOs exist exclusively in the pentavalent tautomeric form. The unusual form of the free phosphinous acid can be found in the literature only in specific cases with, as it has been mentioned, extremely electron-withdrawing substituents.[10] Hence, since $(CF_3)_2P(OH)$ and $(C_2F_5)_2P(OH)$ and their analogues exist only in the trivalent form, less electron-withdrawing groups such as $2,4$-CF_3-C_6H_3 or C_5F_4N displays a solvent-dependent equilibrium where a representative fraction of the oxide tautomer can be also found.

Montchamp and Janesko[3] have suggested an explanation of this behaviour taking into account an additional resonance form in the prototropic tautomerism of SPOs (Scheme 3).

$$R^1, R^2 = Alkyl, Aryl$$
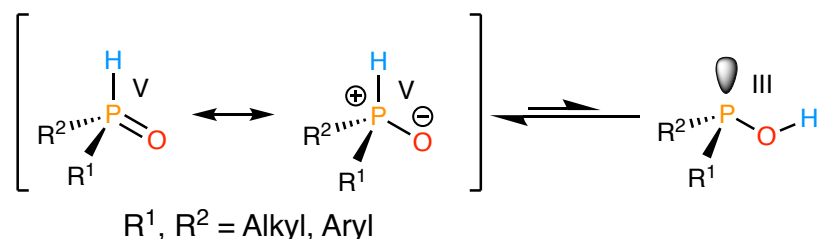
Scheme 3. Tautomerism and resonance forms of SPOs.

The phosphonium form depicted in Scheme 3 is destabilized by strong electron-withdrawing substituents such as the $-CF_3$ or the perfluorinated pyridines already mentioned. But this simple description allows the rationalization of other minor tendencies such as the influence of the solvent in the tautomerism. Interestingly, in more polar solvents like THF or CH_3OH, SPOs containing EWG groups have a large percentage of phosphinous acid in solution, being in some specific cases, such as the $(C_2F_5)_2P(OH)$, the only species detected. This remarkable solvent dependency is not observed for alkyl SPOs, which are always found as pentavalent oxides. Nevertheless, Börner and co-workers[9] have proved that the parameter that rules this effect is the hydrogen-bonding tendency of the solvent rather than the polarity.[9] To this end, they pursued NMR experiments in order to quantify the fraction of the trivalent tautomer in trifluoroethanol (more polar than methanol) and they observed a significant enhancement of the oxide form. Therefore, more than the polarity of the solvents, their hydrogen-bonding acceptor properties are the keystones that affect the state of the tautomeric equilibrium, because they are able to stabilize more effectively the zwitterionic resonance form depicted in Scheme 3.

Finally, it has to be mentioned that in the case of *P*-stereogenic secondary phosphine oxides, the tautomeric equilibrium does not affect the stereochemical integrity of the phosphorus atom[7,11] but, despite that, very few optically pure *P*-stereogenic SPOs have been prepared.

3.1.4. *Synthesis of achiral or racemic SPOs*

Traditionally, Secondary Phosphine Oxides have been easily prepared through hydrolysis of the corresponding phosphine halides.[12] Other widely used methodologies are based on the displacement of an alkoxide from a monosubstituted phosphinic ester by a Grignard reagent or by the reduction of a disubstituted phosphinic ester by treatment of lithium aluminium hydride (Scheme 4).[6,13]
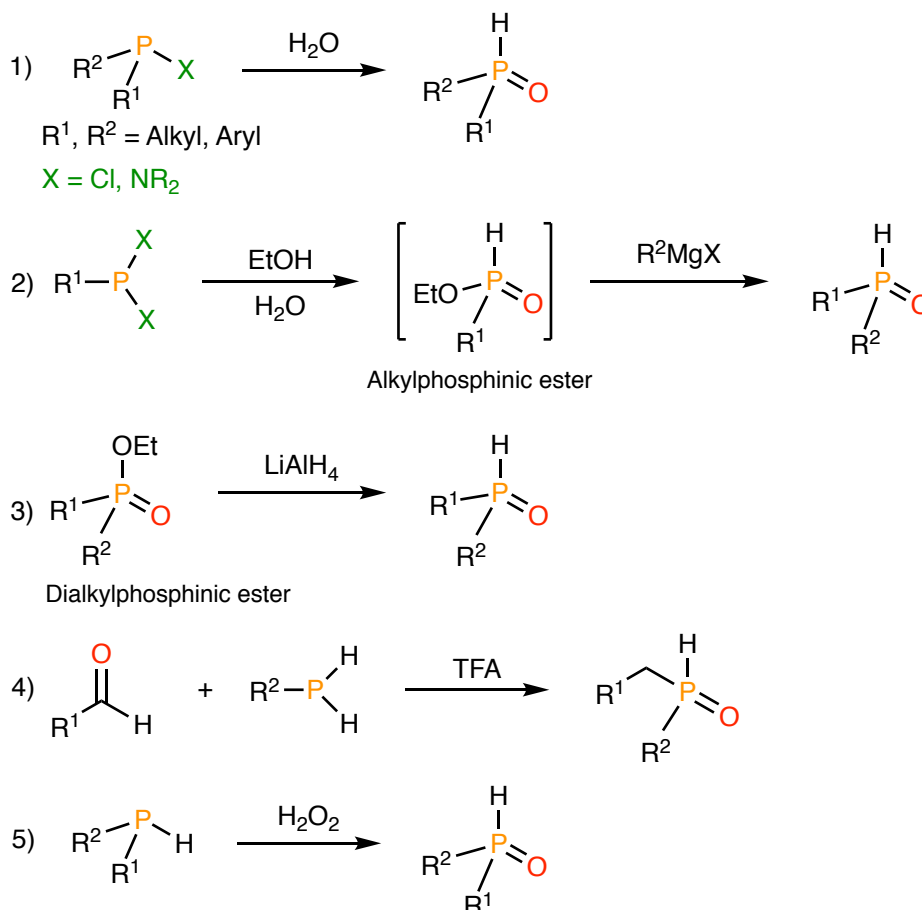
Scheme 4. Main synthetic strategies to prepare SPOs.

Condensation of aldehydes with primary phosphines also leads to the corresponding SPO in refluxing trifluoroacetic acid.[14] In addition, the obvious way to prepare SPOs through oxidation of secondary phosphines can be simply accomplished in the presence of hydrogen peroxide or molecular oxygen at 50–70 °C.[15] This method, however, requires further work-up of the obtained products since it usually produces undesired oxidised species and for this reason is rarely employed.

All these strategies allow the preparation of a variety of SPOs, especially containing aryl substituents.[16] In contrast, dialkyl-substituted secondary phosphine oxides are more difficult to prepare because due to their basicity they undergo non-desired secondary reactions involving the formation of P–O–P bonds. Li and co-workers[17] have reported a useful polymer-supported synthesis of dialkyl substituted SPOs,[17] depicted in Scheme 5.
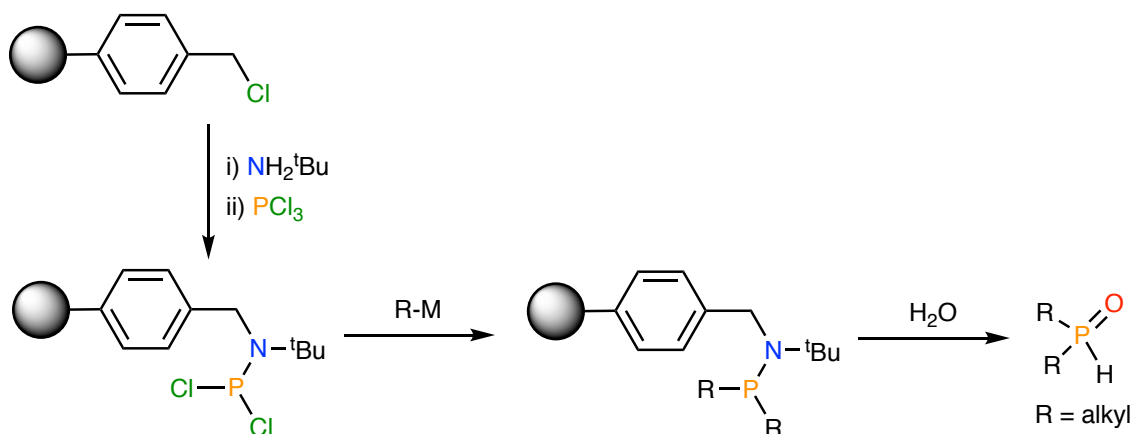
Scheme 5. Polymer-supported synthesis of dialkyl-substituted secondary phosphine oxides.

The polymer-supported aminophosphines can be straightforwardly prepared by treating Merrifield's resin with excess of *tert*-butylamine to form the polymer-supported secondary amine. This resin reacts with PCl_3 in the presence of triethylamine to give the polymer-supported clorophosphine precursor. Reaction of this precursor with a variety of organolithium and Grignard reagents in THF at room temperature leads to complete substitution of P–Cl bonds. Finally, the desired SPO can be easily obtained by direct cleavage with H_2O.[18]

This methodology has also allowed the preparation of bidentate systems by introducing 1,2-bis(dichlorophosphanyl)ethane instead of phosphorus trichloride. Once the diphosphine is attached to the resin, the chloride groups can be replaced by alkyl substituents or even alkoxides.[17]

In contrast, (HA)SPOs, *H*-phosphonates or their derivatives, can be directly obtained from the corresponding diamines, diols or aminoalcohols and PCl_3 in a one-pot or two-step procedure (Scheme 6).[19]
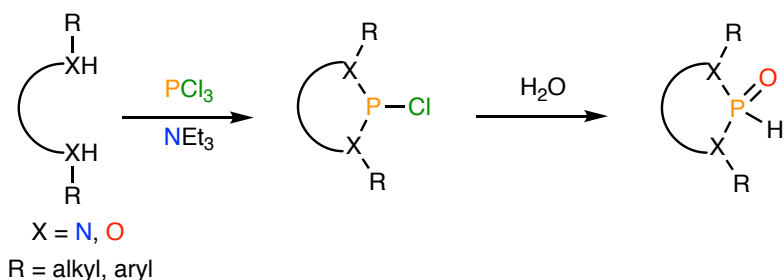
Scheme 6. General methodology for the preparation of (HA)SPOs.

Furthermore, other strategies have been developed in order to prepare HASPOs containing P–N bonds. A very recent methodology has been reported by Hong and co-workers[20] and it is based on the reaction of imines with organolithium and organomagnesium reagents followed by the condensation with a chlorophosphine (Scheme 7).
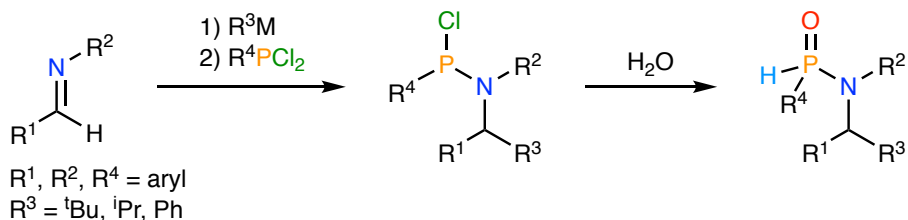
Scheme 7. Preparation of amino-substituted secondary phosphine oxides.

The subsequent aqueous work-up of the chloroaminophosphines leads to the corresponding amino-substituted secondary phosphine oxides.

Both procedures provide an attractive platform for the synthesis of enantiomerically enriched secondary phosphine oxides, since the backbone of the diamine or diol, along with the substituents of the imine, may contain stereogenic elements, as it is discussed in the next section.

3.1.5. *Synthesis of chiral SPOs*

Chiral SPOs can be classified into two broad categories: secondary phosphine oxides where the chirality of the molecule is due to stereogenic elements present in the scaffold and *P*-stereogenic SPOs where the phosphorus atom is responsible of the chirality of the molecule.

3.1.5.1. *SPOs bearing chiral backbones*

The first example of a secondary phosphine oxide with stereogenic centres in the scaffold was described in 1999 by Fiaud and co-workers[21] (Scheme 8). It must be noted, however, that the chirality of synthon **84** was introduced by diastereomeric resolution using quinine as resolving agent.
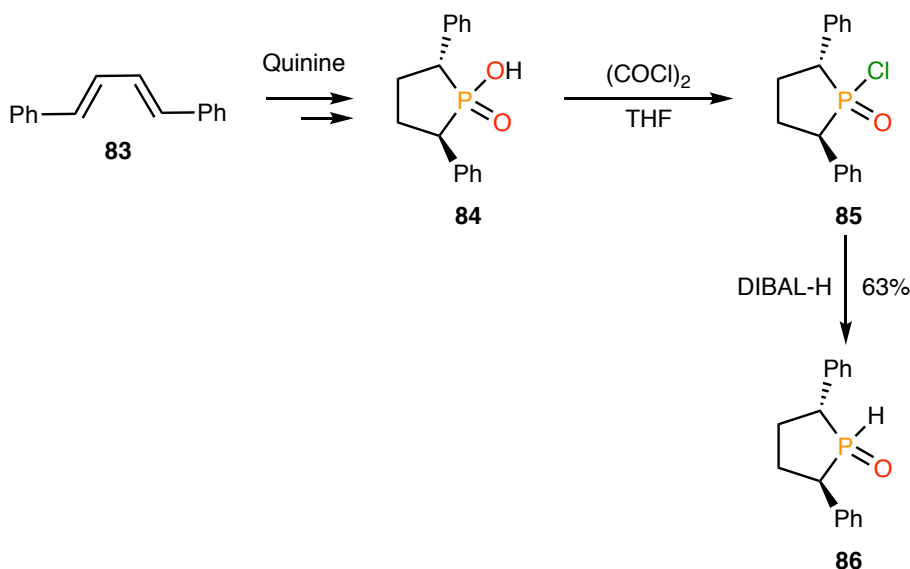
Scheme 8. Synthesis of the optically pure diphenylphospholane SPO.

A convenient method for the preparation of (HA)SPOs, described in the previous section, starts from, *e.g.* diamines or diols and inexpensive PX_3 precursors. An interesting system bearing chirality on the scaffold was reported in 2000 by Enders and co-workers,[22] making use of the enantiomerically enriched TADDOLs[22] (Scheme 9). Several (HA)SPOs have been prepared according to this general synthetic strategy and most of them have proved to be valuable ligands to nucleophilic catalysts.[23]
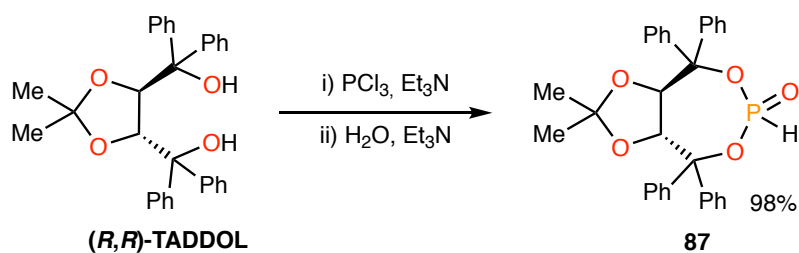
Scheme 9. Synthesis of the (*R*,*R*)–TADDOL-SPO derivative.

Some examples of enantiomerically enriched (HA)SPOs[24] have been obtained from the corresponding optically pure 1,2-diamines, as it is shown in Figure 2.
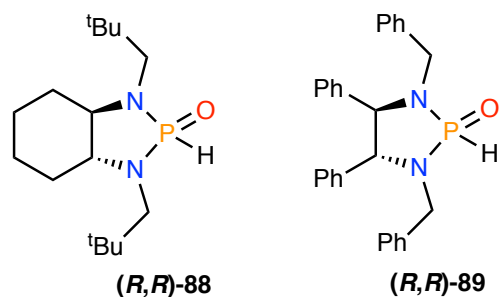
Figure 2. Selected chiral secondary diaminophosphine oxides.

As it can be seen, all the examples presented contain at least one stereogenic element in the backbone. An elegant synthesis of (HA)SPOs with an stereogenic phosphorus atom was reported by Hamada and co-workers.[25] In that synthesis, L-aspartic acid was converted in a few reaction steps into a chiral triamine. A diastereoselective formation of the corresponding triaminophosphine using PCl₃, followed by the subsequent hydrolysis yielded the desired diaminophosphine oxide (DIAPHOX).
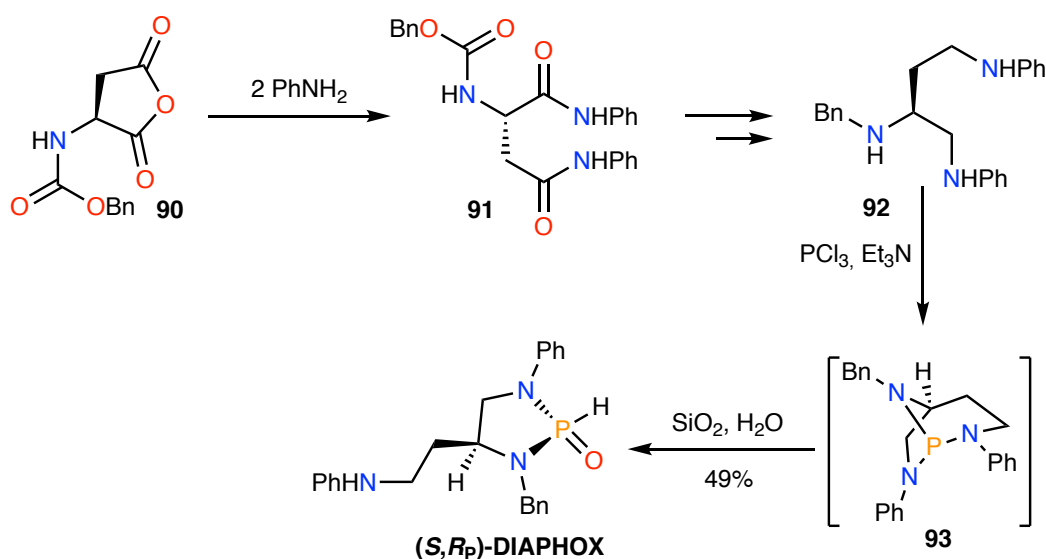
Scheme 10. Synthesis of the (*S*,*R*P)-**DIAPHOX** ligand.

The last step can be considered a S_N2 reaction, which can be easily achieved through column chromatography with wet silica. It is important to note that these special types of ligands have displayed excellent results in many palladium- and iridium-catalyzed asymmetric processes providing high enantiomeric excesses, especially in asymmetric allylic substitution reactions.[25a,26]

3.1.5.2. *P-stereogenic SPOs*

As it has been described, the preparation of secondary phosphine oxides with a chiral backbone constitutes a well-established process.[24] However, the synthesis of enantiomerically enriched, *P*-stereogenic SPOs have proved to be more difficult and only a few examples of optically pure SPOs have been reported so far.[27] Among the different methods for the preparation of *P*-stereogenic SPOs, the use of covalently attached chiral auxiliaries constitutes a well-established approach.

The use of menthol phosphinates as chiral auxiliaries in the preparation of *P*-stereogenic secondary phosphine oxides has broad scope. The first synthesis of a chiral, *P*-stereogenic SPO was reported in 1968,[6] when benzylphenylphosphine oxide was prepared by reduction of the corresponding menthol-precursor with lithium aluminium hydride (Scheme 11).

94 → **95**
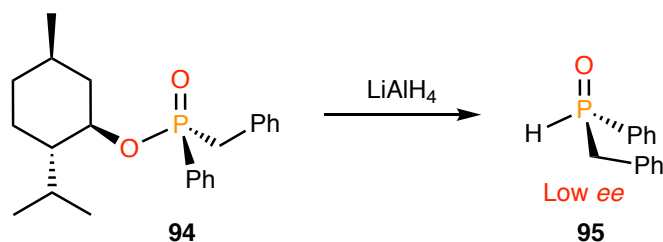
Scheme 11. Preparation of the first *P*-stereogenic SPO.

This method, however, as it was demonstrated by Mislow and co-workers[13] does not constitute a suitable strategy for the preparation of these secondary phosphine oxides, since it causes racemization, likely due to the presence of LiAlH$_4$.[13] The epimerization of the phosphorus can be rationalised by means of a hydride-addition-elimination mechanism involving a pentacoordinated dihydrido species (Scheme 12)
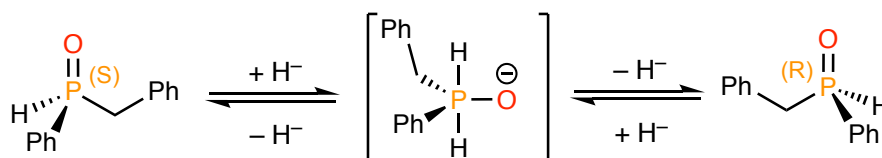
Scheme 12. Epimerization induced by LiAlH$_4$.

In order to overcome these difficulties Buono and co-workers[28] developed another synthetic route, which relies on the reaction of diastereomerically pure menthyl or adamantyl phosphinate precursors with different organolithium and Grignard reagents (Scheme 13). Replacement of the phosphinate moiety occurs with the expected inversion at the phosphorus atom.[29]
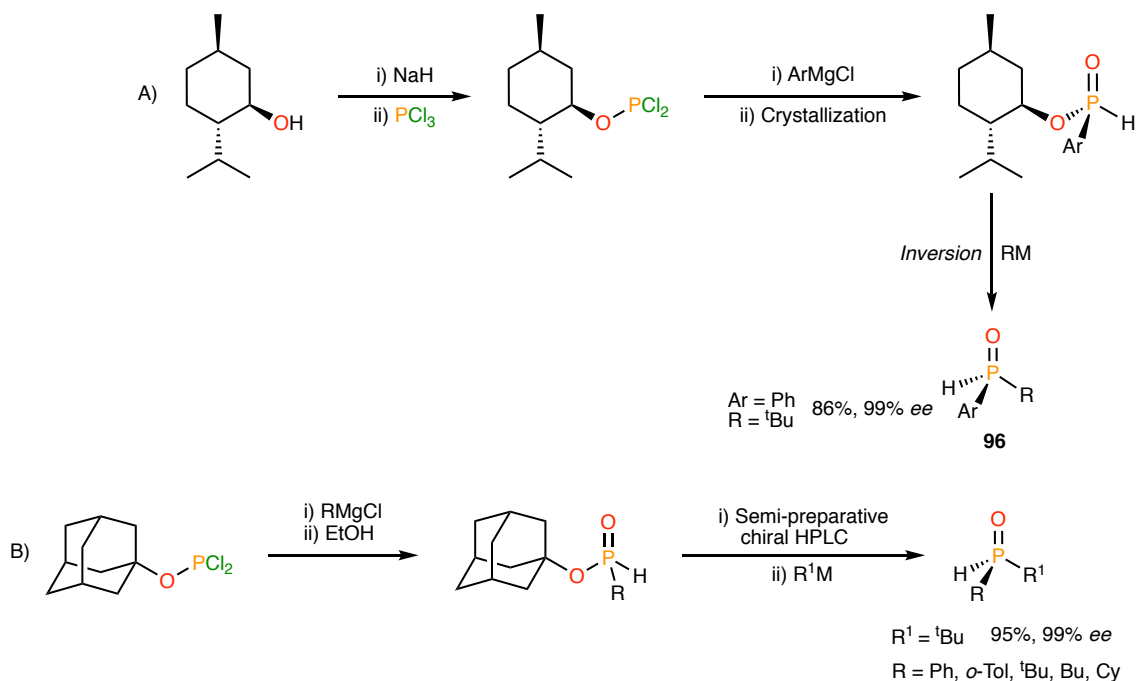
Scheme 13. Asymmetric synthesis of secondary phosphine oxides from organometallic precursors.

Although this reaction works with many organometallic reagents with useful levels of *ee*, the main drawbacks are the separation of the diastereomeric menthyl phosphinates used as starting materials, since its crystallization does not yield the optically pure products when the substituents attached to the phosphorus are different from the usual phenyl group. This problem can be overcome by means of semi-preparative HPLC,[30] even though it is an expensive technique. In addition, the steric hindrance of the organolithium and organomagnesium reagents and its excess in the reaction media, affect dramatically both the yield and the stereochemical purity of the obtained SPOs.

More recently, similar results have been obtained using α-D-glucosamine as a chiral precursor[31] with *ee* values comparable to those reported by Buono and co-workers.[30]

Optically pure *tert*-butylphenylphosphine oxide can be obtained using 1-phenylethylamine as resolving agent,[32] which starts from the conversion of the racemic SPO into the corresponding phosphanylthioic acid. Resolution of the phosphanylthioic acid with an enantiomerically enriched amine and subsequent desulfurization in the presence of Raney nickel[32a] provides the desired SPO (Scheme 14).
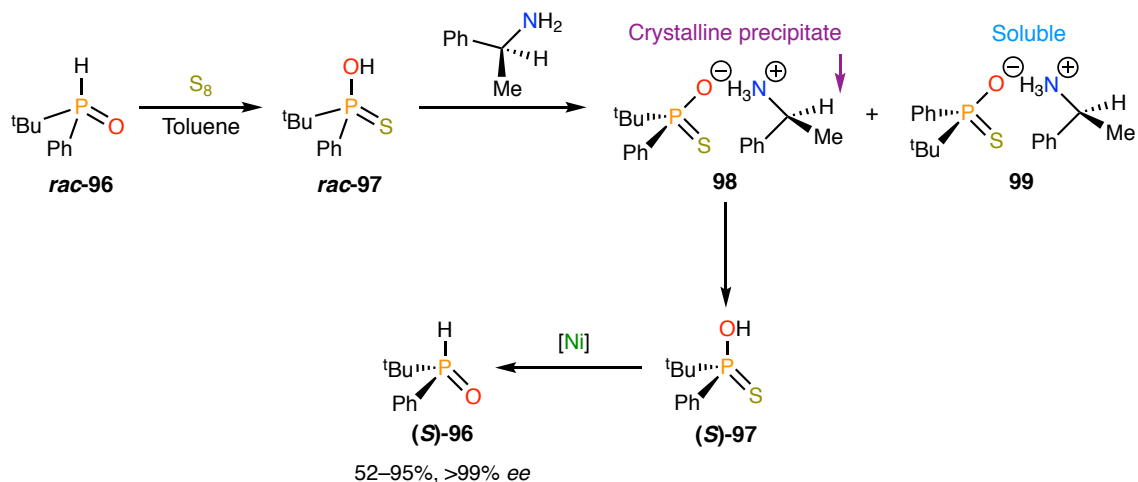
Scheme 14. Preparation of the optically pure *tert*-butylphenylphosphine oxide by means of diastereomeric resolution.

There are many examples of classical diastereomeric resolutions of racemic SPOs. Other efficient methods to separate **rac-96** have been described using (*S*)-mandelic acid or ephedrine as resolving agents.[33]

In parallel, Minnaard and co-workers[34] described an elegant dynamic resolution of ^{t}BuPhP(O)H by crystallisation with (–)-dibenzoyltartaric acid, achieving excellent *ee*'s.

Complementary to the above-mentioned methodologies, Feringa, de Vries and co-workers have successfully resolved various SPOs through preparative chiral HPLC.[21,35] This technique has mediated the isolation of general enantiomerically enriched SPOs (Figure 3).
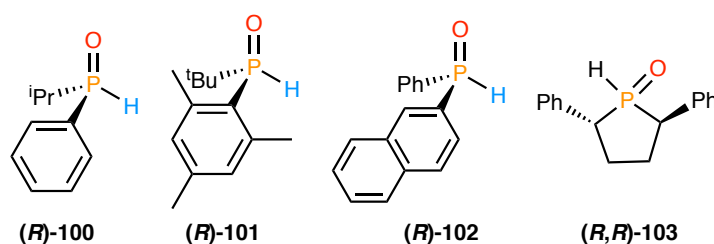
Figure 3. Enantiomerically enriched SPOs through preparative chiral HPLC.

Other strategies for the preparation of optically pure *tert*-butylphenylphosphine oxide via asymmetric synthesis were carried out in 2005 by Buono and co-workers.[29] In that work, they prepared, for the first time, the two enantiomers of the parent SPO using an oxazaphospholidine precursor derived from (*S*)-prolinol. The highly diastereoselective ring-opening of the oxazaphospholidine with *tert*-butyllitium in THF at low temperature (Scheme 15) constitutes the key step of the methodology.

70
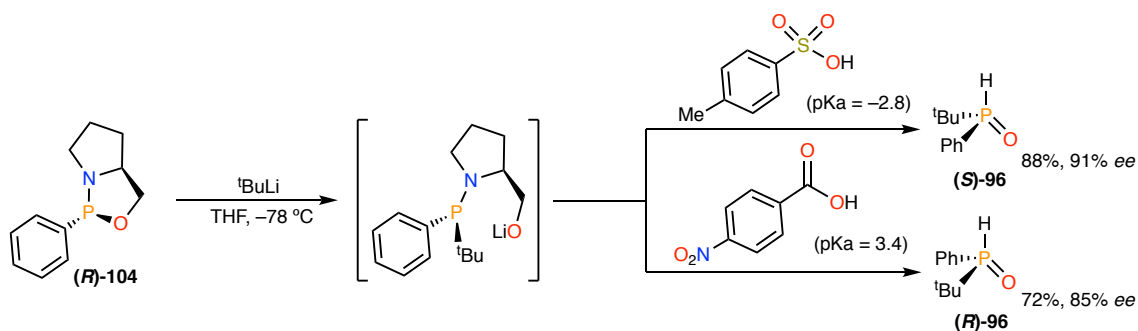
Scheme 15. Synthesis of both enantiomers of ^{t}BuPhP(O)H p-toluensulphonic or p-nitrobenzoic acids.

While this ring-opening reaction was shown to proceed with retention of the phosphorus configuration, the obtention of the two enantiomers of the SPO can be achieved by changing the Brønsted acid during work-up. Therefore strong Brønsted acids (pK$_a \leq 1$) lead to retention of configuration at phosphorus whereas weaker acids (pK$_a \approx$ 3–5) produce products with inversion. This strategy, however, cannot be extended to a wide variety of alkyl and aryl substituents on the phosphorus atom since less hindered nucleophiles lead to significant erosion on the ee.

Different approaches have been examined in order to introduce more than one stereogenic element in the structure of SPOs. To this end, Dubrovina, Börner and co-workers[36] prepared a mixture of diastereomeric dodecahydrodibenzophophole 5-oxides[36] employing as starting reagent one enantiomer of **105** (Scheme 16).
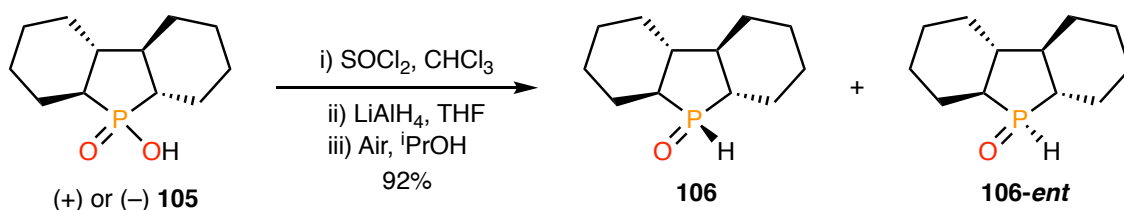
Scheme 16. Synthesis of chiral phospholanes.

Such reagent can be prepared in a few reaction steps from either 1,2-dibromobenzene or cyclohexanone.[13] However, formation of the corresponding chlorophospholane oxide and its subsequent reduction with LiAlH$_4$, leads to a mixture of diastereomeric secondary phosphine oxides after its final oxidation in the air.

In the search of a general method to prepare chiral SPOs from cheap precursors Han and co-workers[37] have described the use of aminoalcohols as chiral auxiliaries for these transformations, in particular for those SPOs containing naphthyl-derived

substituents in combination with bulky groups: *tert*-butyl, cyclohexyl, among others (Scheme 17).
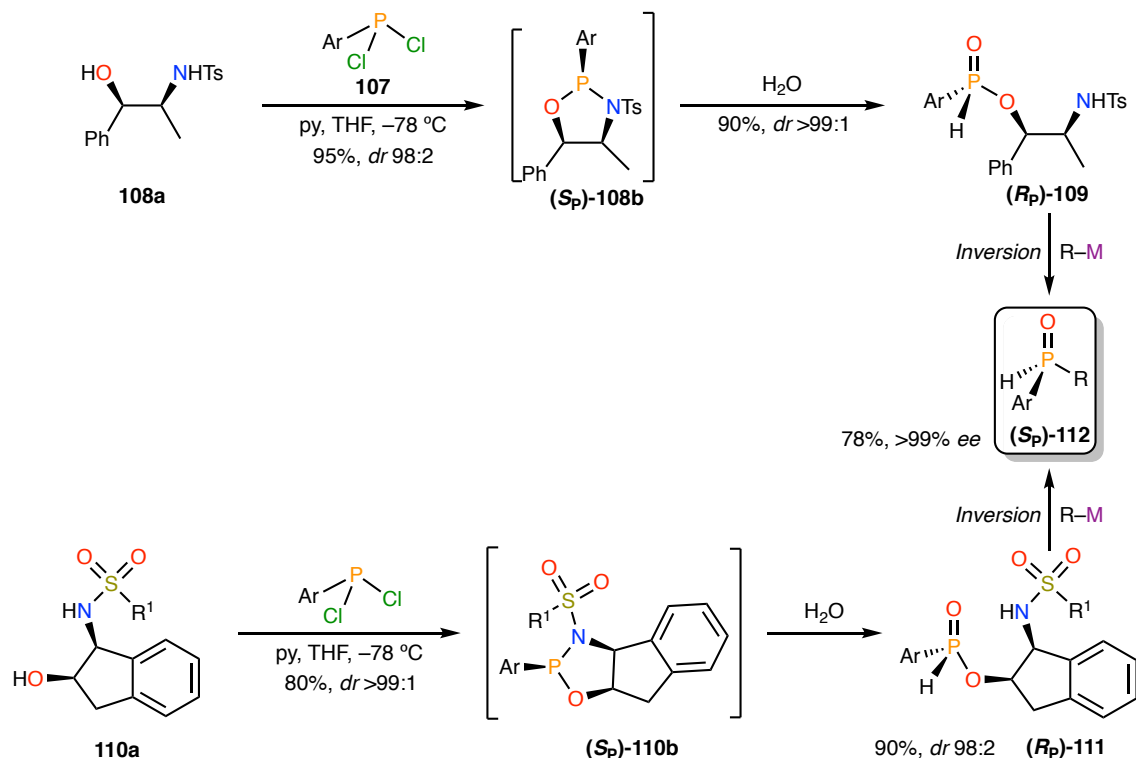
Scheme 17. Enantioselective synthesis of chiral SPOs employing aminoalcohols.

This last example emphasizes the potential use of aminoalcohols as chiral auxiliaries for the preparation of *P*-stereogenic SPOs, even though this methodology is, in fact, more general and can be extended to the synthesis of many *P*-stereogenic ligands so far.

3.2. *Synthesis of enantiopure t-BuMeP(O)H*

3.2.1. *Previous work*

In the previous section, some of the most important synthetic methods to prepare chiral SPOs have been discussed. Among them, enantioselective synthesis has proved to be the most challenging and less explored, especially in the use of optically pure aminoalcohols as chiral auxiliaries.

In this line, our group used *cis*-1-amino-2-indanol for the preparation of highly hindered *P*-stereogenic phosphines and derivatives, which had been also used as a chiral auxiliary for the preparation of optically pure sulfoxides.[38]

This methodology allows the preparation of oxazaphospholidines, which in turn are amenable for the synthesis of bulky *P*-stereogenic aminophoshines.[39] What is more, the strategy provides an alternative for the so called "Evans-Imamoto method" consisting on the deprotonation of dimethylphosphine boranes using (−)-sparteine as chiral auxiliary[40] and permits by using a single amino alcohol auxiliary, the synthesis of both enantiomers of key *P*-stereogenic intermediates.[41]

Our synthetic route, as it was explained in Chapter 2, starts with the condensation of *cis*-1-amino-2-indanol with *tert*-butyldichlorophosphine in the presence of diethyl amine affording the oxazaphospholidine ring **O1** after protection of the free phosphine with the borane group (Scheme 18).
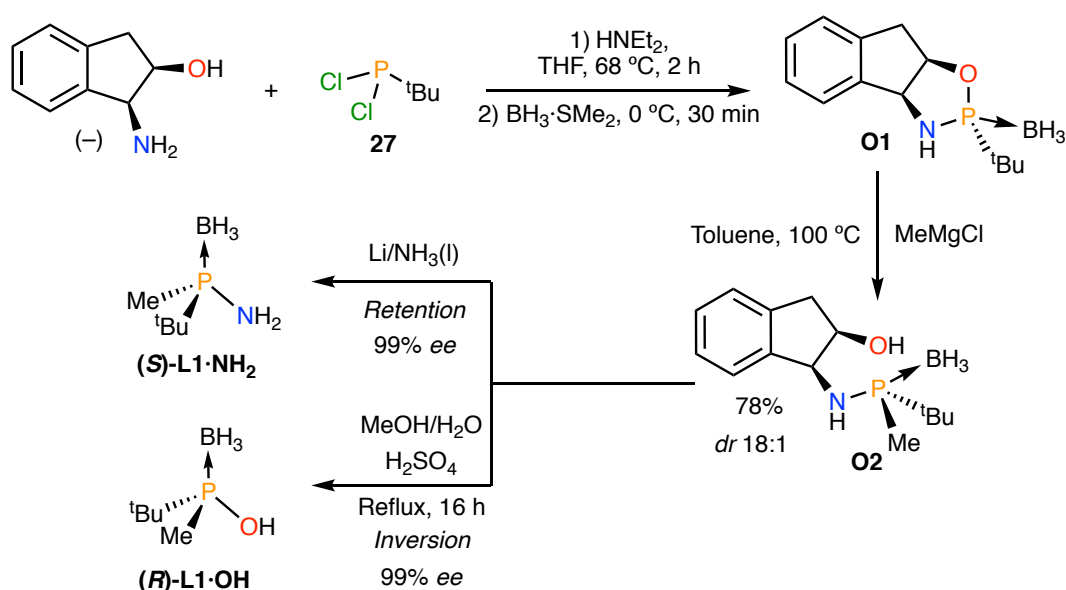
Scheme 18. Synthesis of the chiral synthons aminophopshine (*S*)-**L1·NH₂** and phosphinous acid borane (*R*)-**L1·OH**.

Then, the stereoselective ring-opening with Grignard reagents leads to the corresponding optically pure aminophosphines, a process that has also been studied with other organomagnesium reagents such as MeMgBr or PhMgBr. The **O2** synthon is a key intermediate, since it can access the preparation of aminophosphine (*S*)-**L1·NH₂** by means of a reductive cleavage of the benzylic C–N bond with lithium in liquid ammonia or phosphinous acid (*R*)-**L1·OH** via an acidic methanolysis using sulphuric acid. Interestingly, both reactions take place in a stereospecific manner, with stereochemical retention forming the aminophosphine, or inversion in the case of the phosphinous acid.

(*S*)-**L1·NH₂** and (*R*)-**L1·OH** are extremely useful synthons, since they have an opposite reactivity: while the aminophosphine (*S*)-**L1·NH₂** behaves as a nucleophile,

(*R*)-**L1·OH** phosphinous acid can be used as an electrophile. Indeed, previous studies[42] in the group showed that the conversion between the two species is possible without any optical purity loss, evidencing this complementary chemical nature, as it is depicted in Scheme 19.
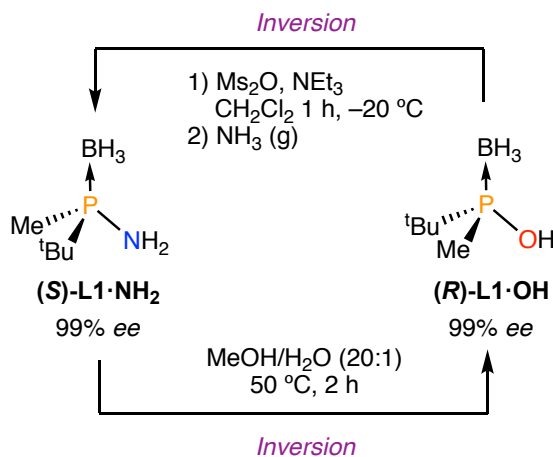
Scheme 19. Transformations between (*S*)-**L1·NH₂** and (*R*)-**L1·OH** without *ee* erosion.

Although synthon (*R*)-**L1·OH** is an invaluable intermediate for the preparation of the desired **L1** secondary phosphine oxide it is a difficult-to-handle gummy solid with a low melting point (54–56 ºC). On account of the nature of the compound, it contains an OH group which makes them more soluble in polar solvents, even in water, and as a result, the synthesis and the work-up steps are somewhat intricate, implying a sever decrease of the yield. Nevertheless, its main drawback is perhaps the limited stability of the compound, due to its decomposition to racemic secondary phosphine oxide and borane byproducts. In order to circumvent these problems, our group studied the transformation of this phosphinous acid borane in the corresponding dialkylammonium phosphonite salts.[42c]

Since (*R*)-**L1·OH** behaves as a weak Brønsted acid, having a measured pK_a of 4.76, it can be deprotonated by some amines, such as diisopropylamine, leading the formation of the dilakylammonium salt as a crystalline solid (Scheme 20).
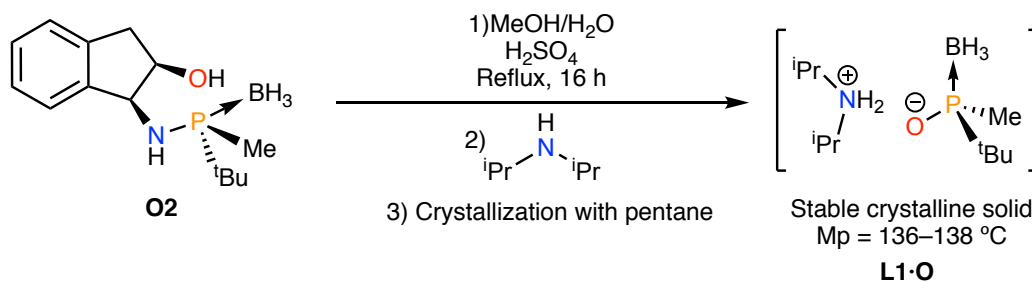
Scheme 20. Divergent synthesis for the phosphonite salt.

(*R*)-**L1·OH**, **L1·O** and (*S*)-**L1·NH₂** allowed the preparation of the desired Secondary Phosphine Oxide *t*-BuMe(O)PH **L1** which despite its simplicity, has only been mentioned in a few references in the literature. It was originally described in a racemic form a long time ago[43] and much more recently has been prepared by other groups, also as a racemate.[14,44]

In our previous studies, **L1** was detected as a subproduct of the acidic hydrolysis of aminophosphines[45] and using this methodology we were able to obtain enantioenriched (*R*)-**L1**, albeit with low *ee*. Having access to optically pure **L1** is particularly interesting since it contains the sterically dissymmetric *t*-Bu/Me combination, which has yielded extremely important phosphine ligands for asymmetric reactions.[42a,44b,46]

The desired oxide (*R*)-**L1** had been obtained in good yield by acidic hydrolysis of aminophosphine (*S*)-**L1·NH₂** using H_2SO_4 in a mixture of methanol/water at 40 ºC (Scheme 21).[45]
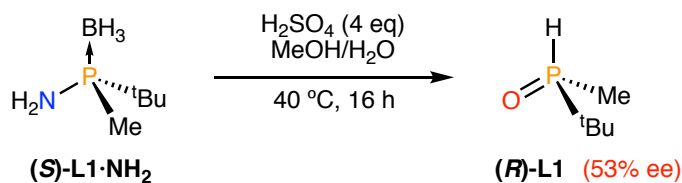
Scheme 21. Acidic hydrolysis of aminophosphine (*S*)-**L1·NH₂**.

However, this procedure afforded (*R*)-**L1** with a disappointingly low enantiomeric excess of 53%. Therefore, a more selective route was required.

3.2.2. *Optimisation of the synthesis*

In this THESIS, we envisaged the deprotection of *tert*-butyl(methyl)phosphinous acid borane **(*S*)-L1·OH** or its corresponding phosphinite salt, since its synthesis in enantiomerically pure form had been developed in our group (Scheme 22).[39,41,42b,c,45]
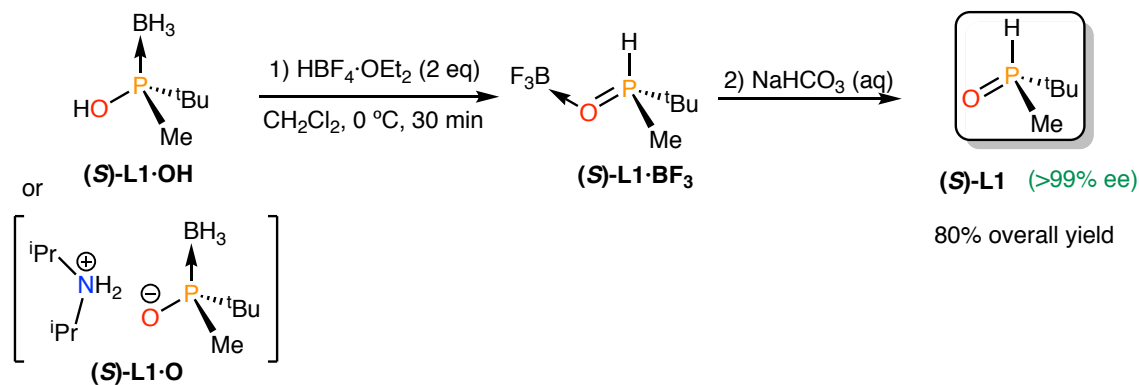
Scheme 22. Synthesis of **(*S*)-L1**. Its enantiomer has been prepared analogously.

Enantiopure **(*S*)-L1·OH** was prepared, as it has been mentioned, by direct hydrolysis of the corresponding *cis*-hydroxyindan-1-yl derivative.[39,45] Since the synthesis starts from *cis*-aminoindanol, both enantiomers are equally accessible.

Treatment of **(*S*)-L1·O** salt with HBF_4 in CH_2Cl_2 at 0 °C[33c,47] followed by an extractive work-up and addition of diethyl ether afforded a white solid in 29% yield that was identified as the boron trifluoride adduct of the desired compound. This species displays a quartet in the $^{31}P\{^1H\}$ NMR spectrum at 63 ppm with a coupling constant J_{PF} of 9.0 Hz. Fortunately, it was possible to obtain crystals suitable for X-ray diffraction studies of this compound whose molecular structure is depicted in Figure 4.
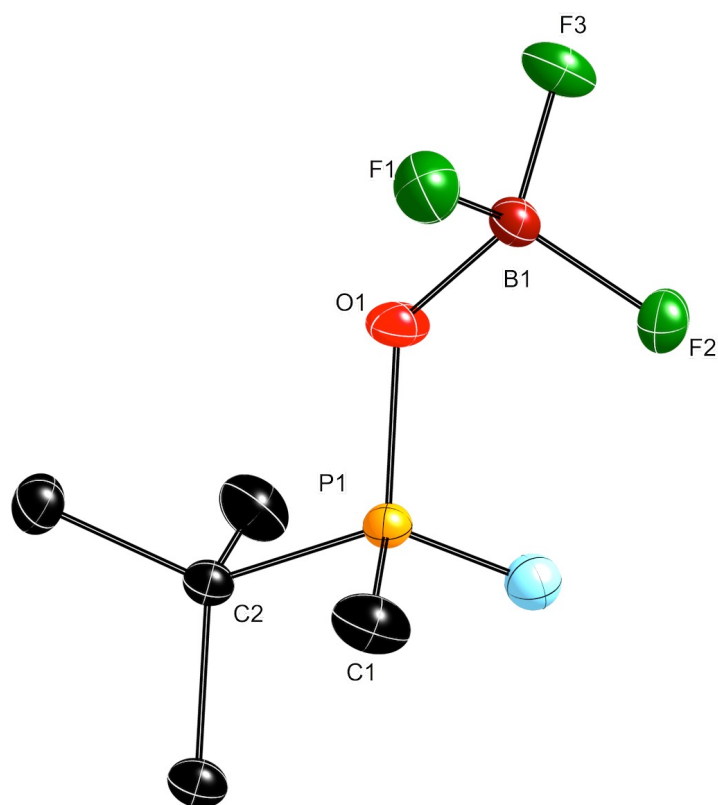
Figure 4 Molecular structure of (*S*)-**L1·BF₃**. Thermal ellipsoids are drawn at 50% probability level. Most of the H atoms have been omitted for clarity.

Table 1. Selected bond lengths (Å) and angles (°) of (*S*)-**L1·BF₃**.

Bond	Length (Å)
P1–O1	1.5489(16)
P1–C1	1.778(2)
P1–C2	1.815(2)
O1–B1	1.501(3)
B1–F1	1.379(3)
B1–F3	1.381(3)
B1–F2	1.398(3)
C2–C3	1.538(3)
C2–C4	1.540(3)
C2–C5	1.545(3)

Angle	(°)
O1–P1–C1	111.91(11)
O1–P1–C2	108.31(9)
C1–P1–C2	113.02(11)
B1–O1–P1	125.99(13)
F1–B1–F3	111.03(19)
F1–B1–F2	109.77(18)
F3–B1–F2	110.66(17)
F1–B1–O1	108.82(17)
F3–B1–O1	107.64(17)
F2–B1–O1	108.86(17)
C3–C2–C4	111.20(17)
C3–C2–C5	111.03(17)
C4–C2–C5	109.83(18)
C3–C2–P1	109.84(15)
C4–C2–P1	108.16(13)
C5–C2–P1	106.64(14)

(*S*)-L1·BF$_3$ constitutes the second reported crystal structure of a SPO–BF$_3$ adduct after a secondary phospholane oxide–BF$_3$ adduct reported by Toffano and co-workers[48] and crystallises in the monoclinic crystal system, an arrangement also found in related compounds of the literature.[49] The absolute configuration of the phosphorus atom, *S*, is the same as the employed phosphinous acid-borane (*S*)-L1·OH employed in this particular synthesis, proving that the reaction occurs with retention of configuration, as expected. The crystal structure supports that the mechanism of deboronation[50] takes place by substitution of the hydrogen atoms of the borane group by fluorine, as suggested by McKinstry and co-workers.[51]

When adduct (*S*)-L1·BF$_3$ was dissolved in CH$_2$Cl$_2$ and treated with NaHCO$_3$ saturated aqueous solution, the desired oxide (*S*)-L1 was obtained as a highly hygroscopic oil. The procedure could be performed with crude (*S*)-L1·BF$_3$ solution affording, after several extractions with small volumes of CH$_2$Cl$_2$ to maximise yield,[52] (*S*)-L1 in 80% yield. Gratifyingly, it was found that the compound had been obtained in optically pure form (>99% *ee*) after derivatisation for chromatographic analysis.[45]

It is important to note that the hydrolysis of adduct L1·BF$_3$ and therefore, of the whole process from (*S*)-L1·OH, takes place with retention of configuration at

phosphorus. The NMR data was consistent with the proposed structure of (*S*)-**L1** since a singlet is observed at δ = 45.5 ppm in the $^{31}P\{^1H\}$ NMR spectrum while in the ^1H spectrum the proton directly attached to the P appeared at δ = 6.60 ppm with a large $^1J_{PH}$ = 445 Hz.

Furthermore, we explored the chemistry of **L1** with sodium bis(trimethylsilyl)amide (NaHMDS) in order to detect the phosphinite anion as it was described by Tyler and co-workers.[52] In their work, they explain that deprotonation of ($^iPr)_2P(O)H$ **113** takes place only in the presence of NaHMDS or KHMDS, observing an important displacement of the signals in the $^{31}P\{^1H\}$ NMR spectrum from a chemical shift of δ = 55.8 ppm, belonging to the free oxide, to 121.6 ppm attributed to the phosphinite (Scheme 23).
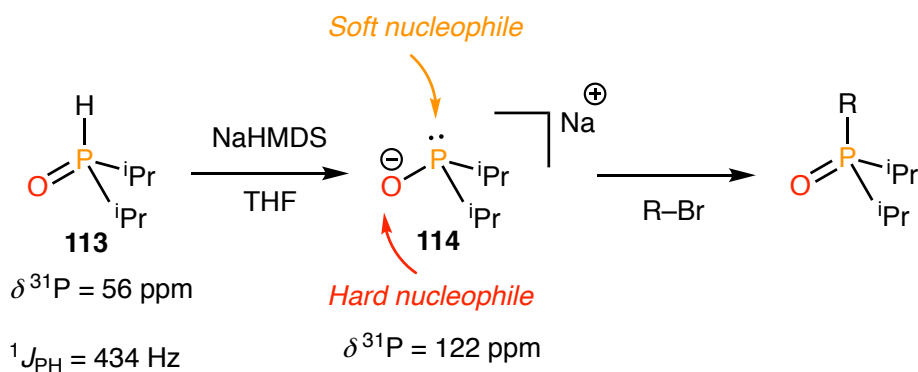
Scheme 23. Intermediate phosphinite anion studied by Tyler and co-workers.[52]

The parent reaction is particularly interesting since it offers an open door for a new reactivity of the **114** synthon as a nucleophile, preferring the P–C bond formation over O–C. Unfortunately, we found that our system was not compatible with such bases, since many subproducts were obtained instead, none of them in the region of 120 ppm in the $^{31}P\{^1H\}$ NMR spectrum.

In order to isolate the desired intermediate, we envisaged its coordination through the oxygen with bis(trimethylsilyl)acetamide or BSA.[53] The reaction was carried out in a solution of (*S*)-**L1** in dichloromethane adding 2 eq. of BSA under inert atmosphere. Surprisingly, the reaction did not work and the $^{31}P\{^1H\}$ NMR spectrum remained unchanged after the addition of BSA. In the light of these observations, it is possible that the BSA is not oxophilic enough to shift the tautomeric equilibrium towards the phosphinite, or if it does so, the hard oxygen nucleophile is cation passivated and only attacks strongly oxophilic substrates such as chlorosilanes.

On the other hand, it has to be mentioned that as both enantiomers of **L1·OH** are available, both enantiomers of **L1** are equally accessible and have been used in the complexation studies presented in this THESIS.

3.3. *Complexation of enantiopure t-BuMeP(O)H*

3.3.1. *Precedents on the complexation of SPOs*

In the field of organometallic chemistry and homogeneous catalysis, it is well known that P(III)-based ligands are the most important type of ligands due to their ability to stabilize transition metal centres.[54]

As it has been described in the previous sections, SPOs have proven to be appealing ligands, due to its air-stability, in contrast to many phosphines and derivatives. But what make them in the spotlight is their ability to coexist between two isomeric forms, with different oxidation states; therefore having distinct chemical properties. The tautomeric equilibrium between the pentavalent oxide form and the trivalent phosphinous acid form SPOs present a tautomeric equilibrium is completely shifted towards the oxide form except for phosphines with extremely electron-withdrawing groups[55] but the presence of a transition metal cation can shift the equilibrium to the trivalent form, forming a metallic complex with the phosphinous acid (Scheme 24).[56]
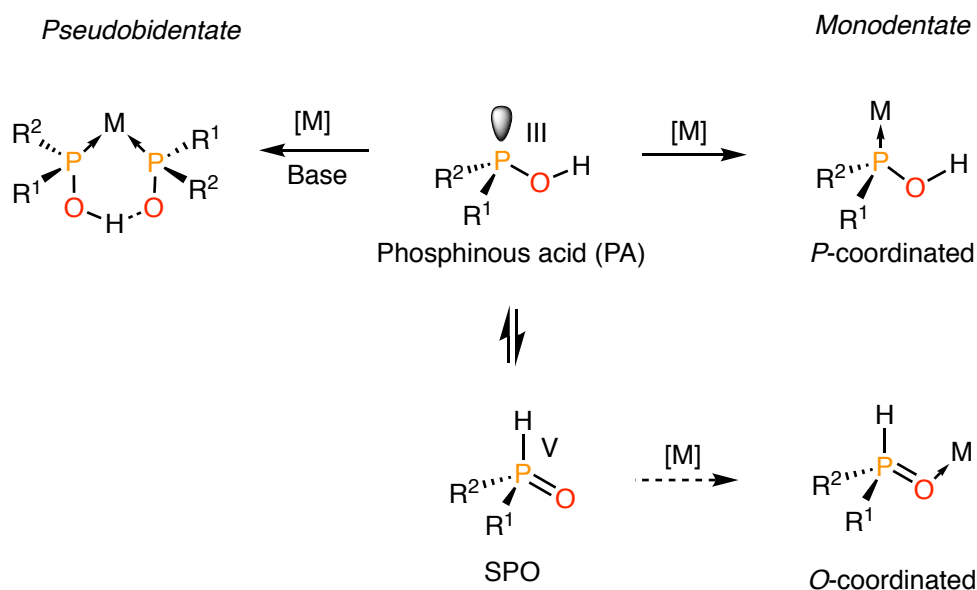
Scheme 24. Tautomeric equilibrium and coordination modes of secondary phosphine oxides.

80

As shown in Scheme 24, SPOs can act as ambidentate ligands by using the soft phosphorus atom in the phosphinous acid tautomer or the hard oxygen atom in the phosphine oxide tautomer. The coordinative behaviour depends on the affinity of the metal for one site or the other. Examples of *P*-coordinated complexes can be found for Fe, Pd, Ir, Au, Pt, Rh and Ru whereas the *O*-coordination has been described for example with Cr, Mo, W, Ru and Rh.[56-57]

Interestingly, two SPO units attached to a metal centre can form an intramolecular hydrogen bond, acting as a pseudobidentate ligand (Scheme 24) with a negative formal charge. This moiety can be formally considered as formed by combination of a neutral phosphinous acid and an anionic phosphinito unit. This process often requires an external base and leads to a stable six-membered ring. Although the formation of such species is both thermodynamically and kinetically favoured, the required *cis* geometry can not always be achieved and sometimes the *trans* isomers with two monodentate SPOs are obtained instead.[58]

Nevertheless, this pseudobidentate coordination mode has spurred interest into the study of the applications of SPOs in catalysis[11b,57b] and it has been found, for example, that dialkyl SPOs are excellent ligands for cross-coupling reactions.[59]

Interestingly, in the case of enantiopure *P*-stereogenic SPOs, the tautomeric equilibrium does not affect the stereochemical stability of the phosphorus atom[11b] but, despite that, very few catalytic applications of *P*-stereogenic SPOs in asymmetric catalysis have been reported in the literature,[35b,36a,60] probably due to the lack of methods for their preparation. It is interesting to note that sometimes the phosphinous acid ligand can be modified during the catalysis, such as in the allylic alkylation,[60a] in which the OH group is silylated by the BSA and therefore it is no longer a "true" phosphinous acid.

3.3.2. *Complexation of enantiopure t-BuMeP(O)H with several noble metals*

In the present THESIS it has been described the preparation of both enantiomers of the optically pure *t*-BuMeP(O)H **L1**. With this in hand, we studied its complexation to several metals, which revealed a rich variety in the coordination modes of this phosphine oxide.

3.3.2.1. *Ni complexes*

When considering catalyst design and access to well-defined species, the most used *d*-block metals tend to be noble metals such as iridium, rhodium, or palladium, among others. In contrast, examples with first-row and low-cost transition metals, such as nickel, remain more than sporadic, especially bearing SPOs as stabilizing ligands. In fact, the first Ni(II) complex with a pseudobidentate bridge was described in 1977[61] with a few reports on related structures a few years later.[62]

In 2005, Han and co-workers[63] disclosed the nickel-catalysed hydrophosphinylation of terminal alkynes with a mixture of [Ni(PPh$_2$Me)$_4$] and Ph$_2$P(O)H.[63] They were able to generate *in situ* a five-coordinated hydrido phosphinito nickel complex, by means of an oxidative addition of diphenylphosphine oxide and [Ni(PEt$_3$)$_4$], which was characterised by ^{1}H NMR spectroscopy but not isolated (Figure 5).

Furthermore, some years later, Fang and co-workers[64] reported another catalytic application for "*in situ*" Ni-SPO complexes, in this case, having diaminophosphine oxides as ligands which were reacted with Ni(II) sources for the Kumada coupling of deactivated aryl chlorides.[64]

Werner 1977	Han 2005	Fang 2012
115	**116**	**117**
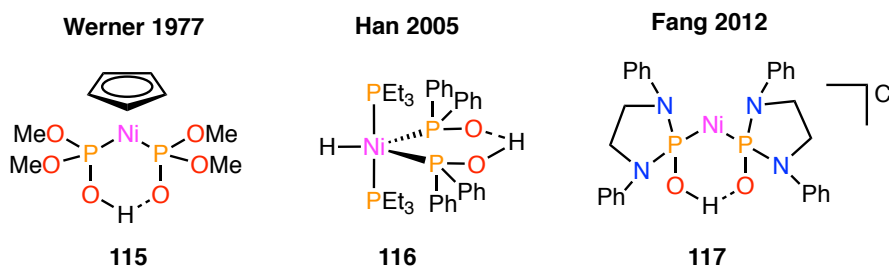
Figure 5. Reported Ni(II) complexes with SPOs.[63-64]

Although prone to promote hydrophosphinylation reactions, those structures having cationic Ni(II) species with metal-hydride or metal-carbon bonds could be of interest for migratory insertion of olefins to produce polymers.[62a,65] However, due to their high reactivity and their instability, these organonickel compounds are usually generated "*in situ*" from a nickel(II) halide precursor.[66]

More recently, Breuil and co-workers[67] reported that bis(cyclooctadiene)nickel(0), [Ni(COD)$_2$] reacts with sulfonamido-phosphines in the presence of a second phosphine ligand, leading to a self-assembled supramolecular organometallic species. Interestingly, very recently the same research group disclosed, for the first time, the

preparation of several diamagnetic π-allylic nickel complexes bearing a phosphinito-phosphinous acid system as stable solids (Figure 6).[68]
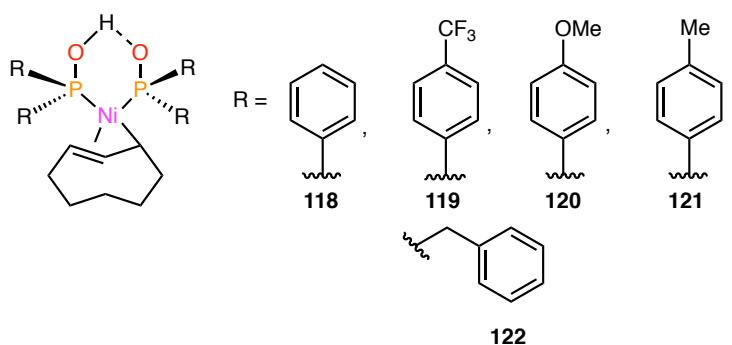
Figure 6. Ni-SPO allylic complexes prepared by Breuil and co-workers.[68]

In this study, Breuil and co-workers[67] pointed out that when [Ni(COD)$_2$] reacts with the SPO ligand in toluene and an excess of COD, to prevent the formation of metallic nickel, the process yields the corresponding pseudobidentate π-allylic nickel(II) complexes.

We envisaged the reaction of **L1** with [Ni(COD)$_2$] under the same conditions reported by Breuil and co-workers.[68] To do so, freshly prepared [Ni(COD)$_2$] was immediately dissolved with 2 eq. of (*R*)-**L1** in a 5:1 toluene/COD solution (Scheme 25).
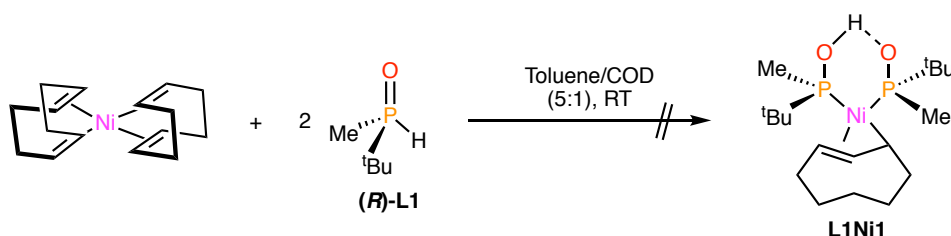
Scheme 25. Reaction of (*R*)-**L1** with [Ni(COD)$_2$].

The solution became darker and a brown solid was obtained. Unfortunately, when that solid was analysed by ^{1}H NMR (Figure 7) we obtained very broad signals and the characterisation of the complex still remains elusive. Nevertheless, the signals are consistent with the presence of two set of different protons, belonging to the Me and ^{t}Bu groups of the SPO ligand.
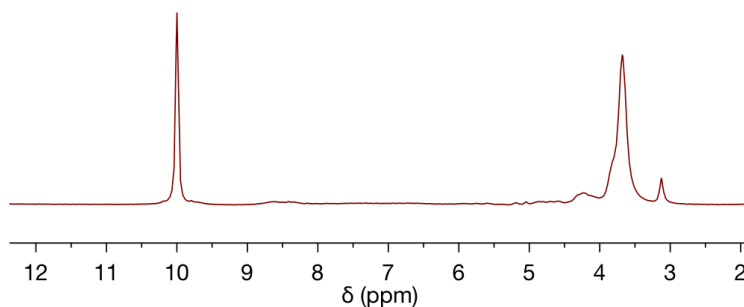
Figure 7. ^{1}H NMR(400 MHz, benzene-d_6, 25 °C) for the reaction crude **L1Ni1**.

In the view of this result we concluded that the paramagnetic species formed must have a tetrahedral coordination geometry (instead of the expected square-planar arrangement).

These unsuccessful attempts are in agreement with some results obtained by Breuil and co-workers[67] who noticed that basic and bulky aliphatic SPOs appeared to be less reactive with [Ni(COD)$_2$]. Indeed, when they used the bulkier mesityl or iso-propyl SPO analogues only degradation to metallic nickel was observed.[68]

3.3.2.2. *Ir complexes*

Complexation studies with Ir and SPO ligands are rare in the literature, despite it has been found that *in situ* prepared Ir precursors with SPO ligands are competent systems for asymmetric hydrogenation of ketimines[35b] and functionalized olefins.[69] Indeed, the only preformed Ir complexes described were reported in 2011 by Buono and co-workers[58a] using the non chiral (^{t}Bu)$_2$POH (Figure 8).
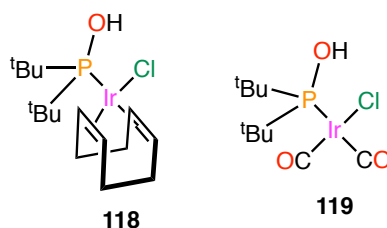
Figure 8. Reported Ir-SPO complexes with (^{t}Bu)$_2$POH.

Our first objective was the synthesis of the monocoordinated complex [IrCl(COD)(κ*P*-(*R*)-**L1**)] (**L1Ir1**) by reaction of [Ir(COD)Cl]$_2$ with (*R*)-**L1**, following the conditions reported by Buono and co-workers (Scheme 26).[58a]
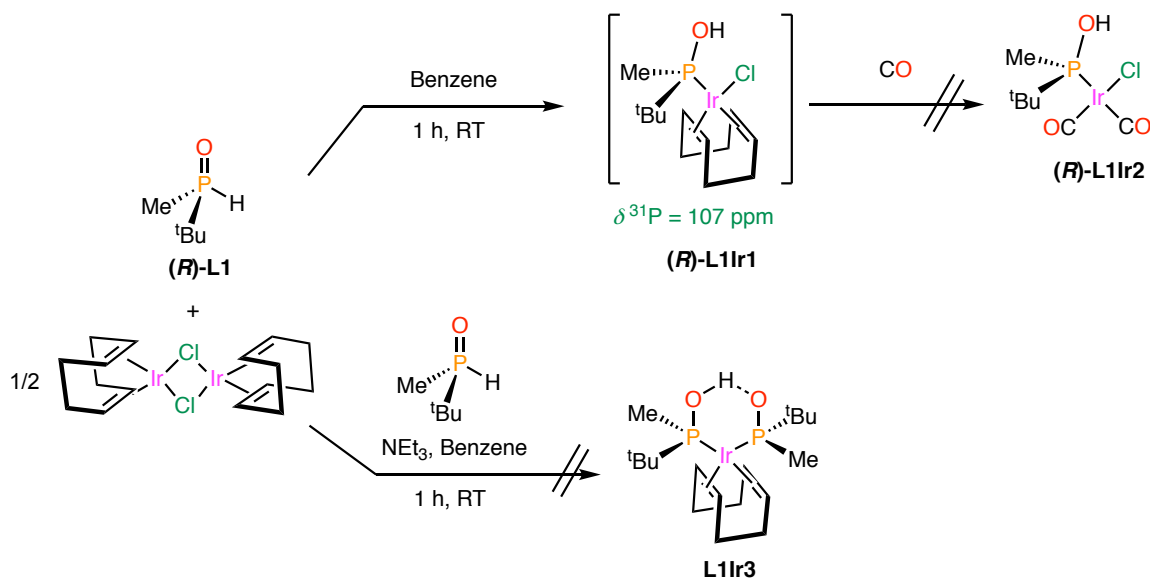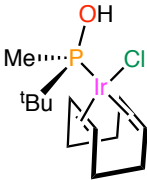
Scheme 26. Attempts to obtain Ir-SPO complexes.

The reaction was not successful in either THF of CH₂Cl₂ because multiple products were obtained according to $^{31}P\{^1H\}$ NMR spectroscopy.

In contrast, in benzene a singlet was detected at δ = 105 ppm that can probably be assigned to (**R**)-**L1Ir1**,[58a] a fact also supported by mass spectrometry. This complex, however, could not be isolated since it rapidly decomposed during precipitation.

In spite of the instability of (**R**)-**L1Ir1**, characterisation in solution was performed by ^1H and $^{31}P\{^1H\}$ NMR under inert atmosphere. The most representative spectroscopic data are depicted in Table 2.

Table 2. Selected NMR data for (**R**)-**L1Ir1**, δ is expressed in ppm, multiplicities and J (in Hz) are given in brackets.

	^1H NMR (C₆D₆)	$^{31}P\{^1H\}$ NMR (C₆D₆)
[IrCl(COD)(κP-(**R**)-**L1**)], (**R**)-**L1Ir1**	5.38 (m, 1H COD)	+105.7 (s)
	5.31 (m, 1H COD)	
	3.11 (m, 1H COD)	
	2.88 (m, 1H COD)	
	2.22-1.82 (m, 4H COD)	
	1.64-1.29 (m, 4H COD)	
	1.08 (d, $^3J_{HP}$ = 14.4, 9H ^tBu)	
	1.01 (d, $^2J_{HP}$ = 7.6, 3H Me)	

In addition, the molecular formula of **(*R*)-L1Ir1** was determined by mass spectrometry where the adduct $([M] + NH_4)^+$ was detected as molecular peak.

Several attempts were carried out in order to isolate the monocoordinated Ir complexes. A summary of the experiments is depicted in Table 3.

Table 3. Unsuccessful attempts to obtain **(*R*)-L1Ir1** and **(*R*)-L1Ir1'**.

Conditions	Outcome
CH$_2$Cl$_2$, RT, 1 h	Mixture of *P*- and *O*- coordinated species
THF, RT, 1 h	**(*R*)-L1Ir1** and **(*R*)-L1Ir1'** are detected in solution but decomposed upon precipitation with *n*-hexane
THF, 75 ºC reflux, 1 h	Mixture of *P*- and *O*- coordinated species
Hexane, 75 ºC reflux, 1 h	Mixture of *P*- and *O*- coordinated species

Interestingly, whereas the ^{31}P{^{1}H} NMR of the crude of the reaction showed remarkable differences when the reaction takes place at room temperature in benzene or in other solvents, the same NMR pattern was observed when the reaction mixture was heated to reflux. As it can be seen in Figure 9 multiple species appear both at down fields (*P*-coordinated region) and higher fields (*O*-coordinated region). The shape and the broadness of the signals might be indicative of a dynamic exchange between *P*- and *O*-coordination species.

86
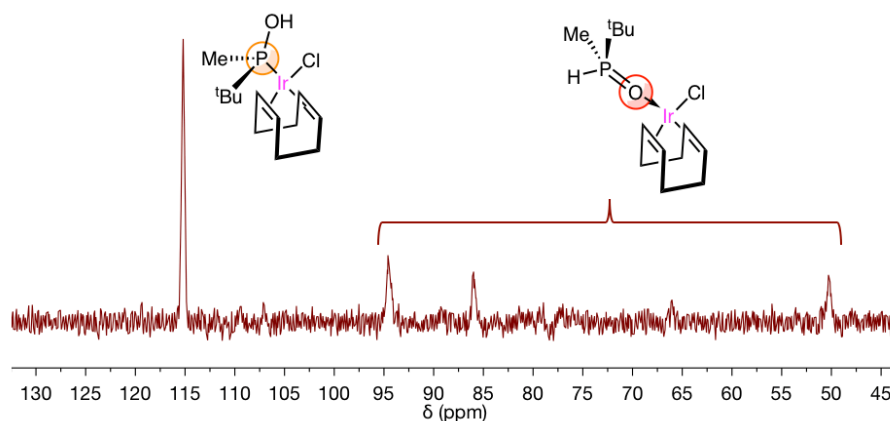
Figure 9. $^{31}P\{^1H\}$ NMR (162 MHz, benzene-d_6, 25 ºC) spectrum of the reaction of (**R**)-**L1Ir1** and (**R**)-**L1Ir1'** at 75 ºC in THF.

In order to stabilise the Ir centre, CO was bubbled through the solution to substitute the COD ligand[58a] but the formation of black iridium was immediately observed in all of the cases.

Finally, a few attempts to obtain the complex [Ir(COD)(κP-(**R**)-**L1**)$_2$] (**L1Ir3**) were carried out by the reaction of 0.5 eq. [Ir(COD)Cl]$_2$ with 2 eq. of (**R**)-**L1** in presence of a base (NEt$_3$, DBU) sometimes in the presence of halide abstractor (AgPF$_6$ or TlPF$_6$) but none of the experiments yielded any definite product.

These unsuccessful results are in agreement with the experiments reported by Buono and co-workers[58a] since the deprotonation with NEt$_3$ of the analogous complex containing (${}^tBu$)$_2$POH **120** (Scheme 27) yield a solid that did not displayed any phosphorus signal in the NMR. This solid was identified as the triethylammonium salt and the supernatant solution showed numerous peaks.
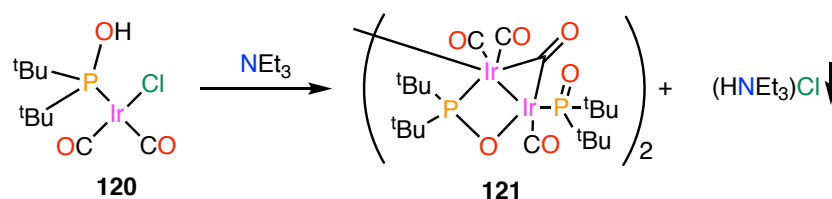
Scheme 27. Deprotonation of phopshinous acid complex **120** reported by Buono and co-workers.[58a]

They were able to grow some suitable crystals for X-ray analysis revealing the structure of a tetrameric Ir cluster **121**. Although this procedure is clearly not a preparative synthesis, it strongly suggests that the presence of a base triggers the formation of polymetallic species, containing Ir–Ir bonds.

Further experiments were performed in order to obtain Ir-monocoordinated complexes with **L1**, using another dimeric precursor, in this case, having coordinated cyclooctene ligands (Scheme 28).
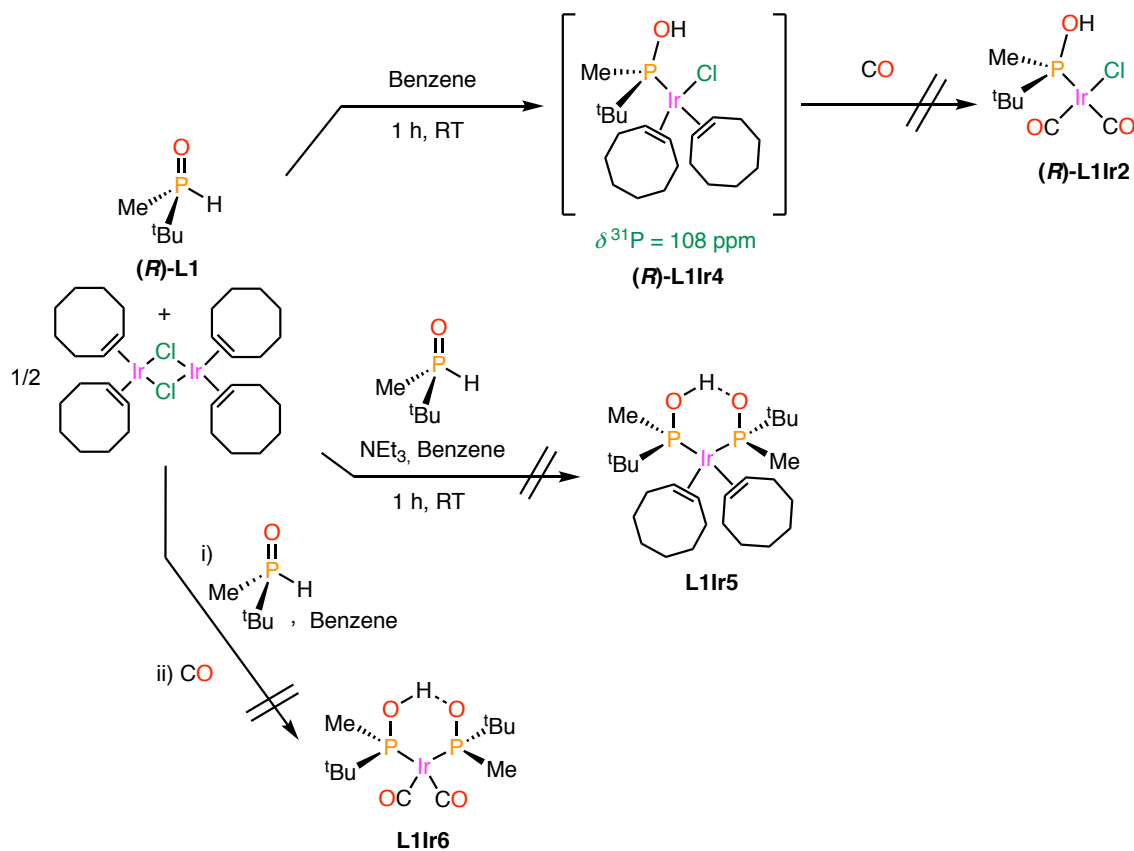
Scheme 28. Attempts to obtain mono and dicoordinated Ir complexes **L1Ir2**, **L1Ir4**, **L1Ir5** and **L1Ir6**.

A similar behaviour was observed in comparison to the analogous reactions with COD. Once more, it was only possible to detect the monocoordinated complex **L1Ir4** in benzene, showing a very close chemical shift $\delta = 108$ ppm compared to **L1Ir1**. Substitution of the olefins by CO did not yield any definite product, even though no precipitation of Ir(0) was observed in this case (Scheme 28).
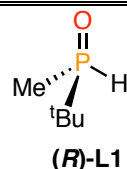
Attempts to isolate the pseudobidentate complex **L1Ir5** were unsuccessful even in the presence of bases such as NEt$_3$ or DBU with and without halide extractors: AgBF$_4$ and TlPF$_6$. Interestingly, a pair of multiplets at $\delta = 65$ ppm can be seen as a major product in the ^{31}P{^{1}H} NMR when the dimeric precursor is treated with a solution of 2 eq. of **L1** and then is bubbled with CO, for a couple of minutes, before the precipitation of black iridium (Scheme 28).

Unexpectedly, a very similar ^{31}P{^{1}H} NMR pattern is observed when the reaction is carried out using [Ir(COD)(CH$_3$CN)$_2$]BF$_4$ with 2 eq. of **L1** in THF at room

temperature. We have not been able to elucidate the structure of these species due to their instability in solution, but the chemical shifts could suggest a dicoordinated complex linked through the oxygen atoms, a fact supported by mass spectrometry, where the molecular peak contains two units of **L1**.

Finally, in order to conclude all these experiments, we studied the reaction of $IrCl_3$ with 3 eq. of (**R**)-**L1** in different alcohols as solvents (Table 4).

Table 4. Experiments with $IrCl_3 \cdot xH_2O$ as metallic source.

Solvent	Comments
^{i}PrOH	Decomposition
EtOH	Decomposition
MeOH	Unknown pure product

In all these reactions, Ir(III) was used instead of Ir(I) as a metallic precursor in the presence of reducing solvents, unfortunately the reaction did not lead any stable product when isopropanol or ethanol were employed as solvents. Unexpectedly, when the reaction was carried out in methanol a white solid was obtained after evaporation to dryness. NMR data (Figure 10) suggested that the structure of this product did not contain coordinated neither P–Ir nor P–O–Ir bonds since the chemical shifts in the $^{31}P\{^1H\}$ NMR were closer to those of the free ligand.
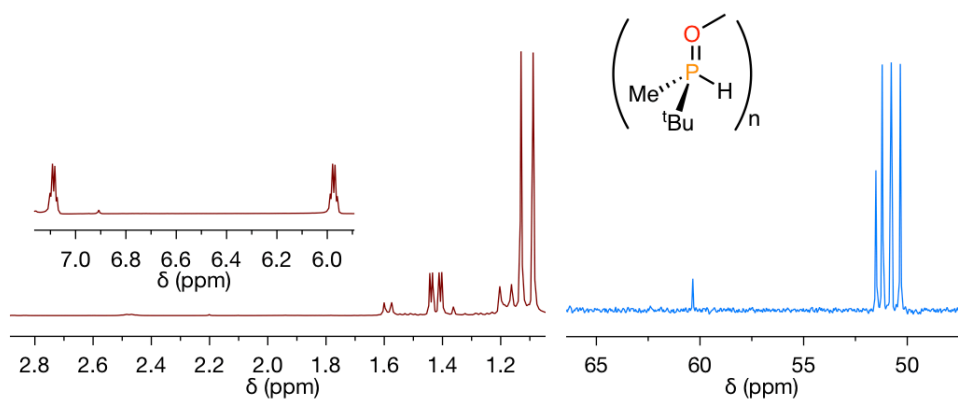
Figure 10. $^{31}P\{^1H\}$ NMR (162 MHz, methanol-d_4, 25 °C) (right) and ^{1}H NMR (400 MHz, methanol-d_4, 25 °C)(left) spectra of the unknown product obtained.

Additionally, the ^{1}H NMR displayed a very simple spectrum where we could only find the peaks belonging to the ^{t}Bu and Me groups. Taking into account all this information and according to mass spectrometry results, we suggest that the obtained structure might be a highly symmetric oligomer of the ligand containing, at least, 4 units of **L1**.

3.3.2.3. *Rh complexes*

Although the first application of Rh complexes with SPOs was disclosed in the early 1980s for the hydroformylation of linear olefins,[70] a more intense catalytic interest appeared when SPOs were successfully applied to asymmetric hydrogenation reactions of imines[69] and more recently of functionalised olefins.[60c] Despite these excellent catalytic results, little research about the nature of the Rh species involved in the catalysis has been performed so far.[69,71]

In particular, there are only a few examples of isolated pseudobidentate Rh complexes in the literature and all of them contain SPOs with EWG substituents (Figure 11).[71-72] It is interesting to recall that aryl SPOs tend to react faster with metallic centres, affording more stable complexes.
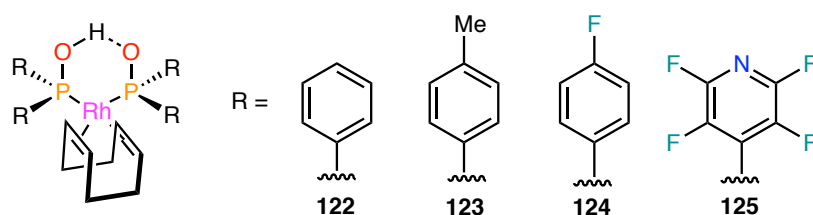
Figure 11. Pseudobidentate Rh complexes reported in the literature.

A clear example of this behaviour was discussed by Börner and co-workers.[72] They observed that while the SPO containing the perfluorinated ligand **125** reacted at −78 °C immediately to Rh, electron-richer di-*tert*-buthylphosphine oxide had given only traces of the expected complex, even at elevated temperatures.
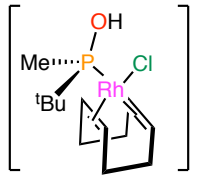
The studies of the coordination of **L1** to Rh moieties were started by reaction of dimer [Rh(COD)(μ-Cl)]$_2$ and two equivalents of **(R)-L1** in THF or dichloromethane but the expected complex [RhCl(COD)(κP-**(R)-L1**)] (**L1Rh2**) did not form, although it could be characterised by ^{31}P{^{1}H} NMR and ^{1}H NMR when the reaction was carried out in benzene−d_6 (Scheme 29).
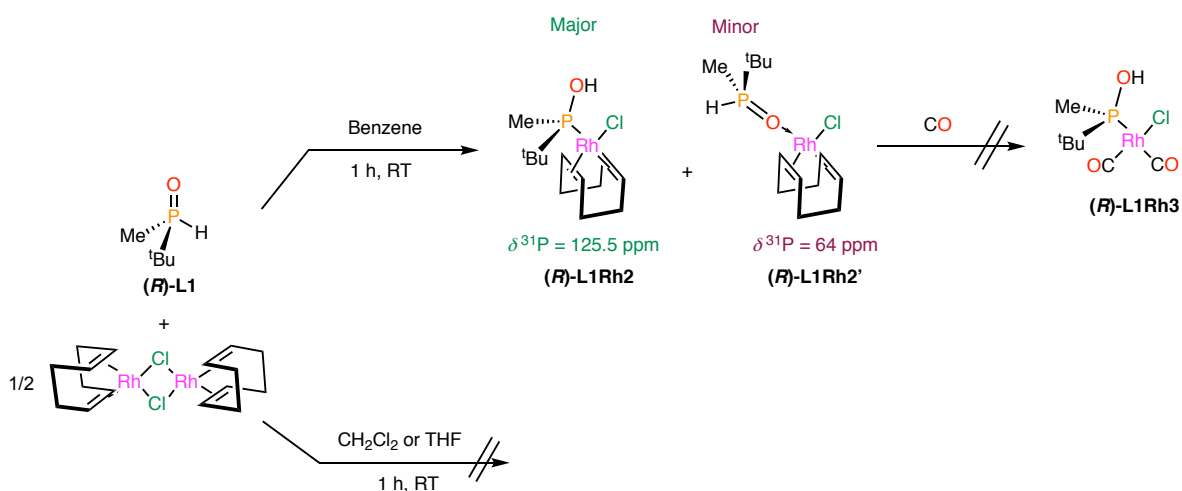
Scheme 29. Complexation studies with Rh.

This is in agreement with previous studies of Börner and co-workers,[72] who showed that dialkyl SPOs do not afford stable Rh complexes of this type. In contrast, the formation of (**R**)-**L1Rh2** could be detected when the reaction was carried out in benzene−d_6 under the same conditions described above for the analogous Ir complex. As expected, a doublet was observed in the ^{31}P{^{1}H} NMR spectrum at the *P*-coordinated region (δ = 125.5 ppm, $^1J_{PRh}$ = 158.5 Hz) that can be assigned to the desired complex. The minor *O*-coordinated complex can also be seen in the ^{31}P{^{1}H} NMR spectrum, displaying a singlet at 64 ppm. The most relevant spectroscopic data is depicted in Table 5.

Table 5. Selected NMR data of complex (**R**)-**L1Rh2** δ is expressed in ppm, multiplicities and *J* (in Hz) are given in brackets.

[RhCl(COD)(κP-(**R**)-**L1**)], (**R**)-**L1Rh2**	^{1}H NMR (C$_6$D$_6$)	^{31}P{^{1}H} NMR (C$_6$D$_6$)
	5.70 (m, 1H COD)	
	5.57 (m, 1H COD)	
	3.56 (m, 1H COD)	
	3.32 (m, 1H COD)	+125.5 (d, $^1J_{RhP}$ = 158.5)
	2.20–1.93 (m, 4H COD)	
	1.71 (m, 4H COD)	
	1.14 (d, $^3J_{HP}$ = 14.0, 9H ^{t}Bu)	
	1.33 (d, $^2J_{HP}$ = 7.4, 3H Me)	

Complex (**R**)-**L1Rh2** was also characterised by mass spectrometry with [M − Cl]$^+$ being the most abundant adduct found in solution.

91

Further experiments were designed in order to bind two **L1** ligands in pseudobidentate coordination fashion. To this end the precursors [Rh(acac)(COD)], [Rh(acac)(NBD)] and [Rh(acac)(C$_2$H$_4$)$_2$] were initially used because it was reasoned that the acac ligand could be replaced by two bridging **L1** assisted by the basic character of acetylacetonate (Scheme 30).[72-73]
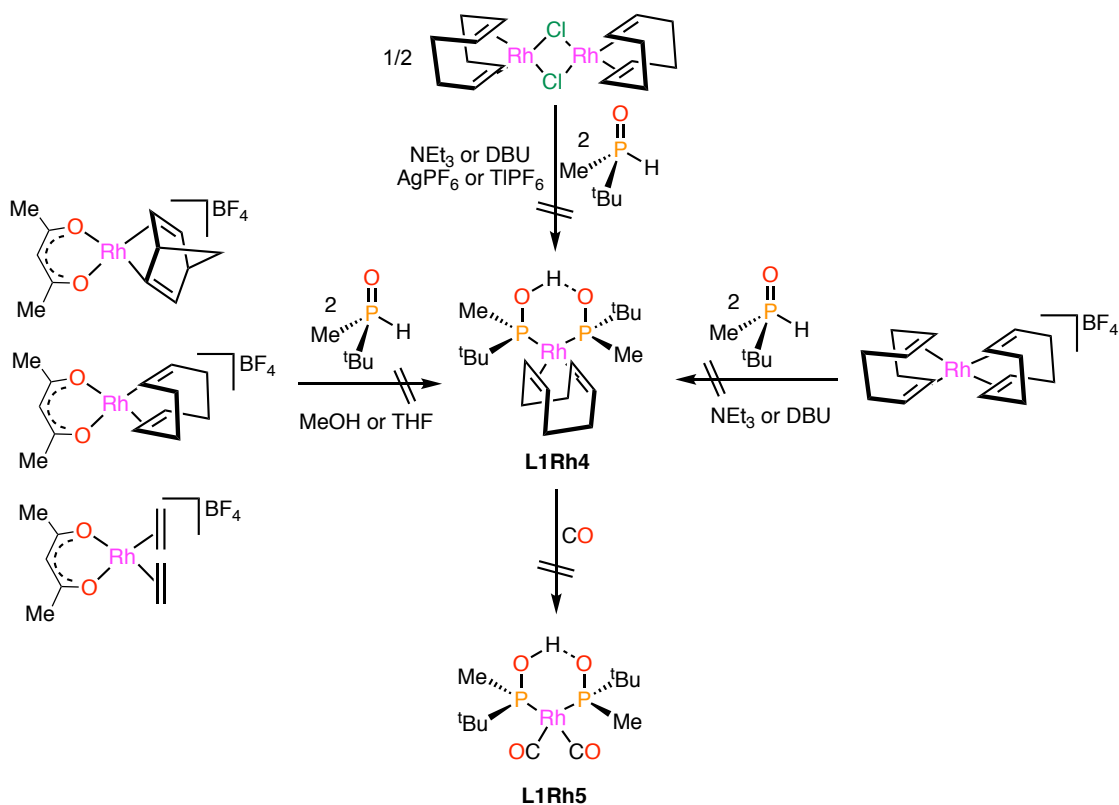
Scheme 30. Unsuccessful attempts to prepare the pseudobidentate complexes **L1Rh4** and **L1Rh5**.

The reactions were monitored by ^{31}P{^{1}H} NMR spectroscopy, which showed the appearance of pair of doublets ($^1J_{RhP}$ = 163.0 Hz) at the *P*-coordination region but the species resulted to be too unstable to allow its isolation. Finally, a few attempts to obtain the neutral complex [Rh(COD)(κ*P*-(*R*)-**L1**)$_2$] (**L1Rh4**) were carried out following the report of Buono and co-workers,[58a] by using [Rh(COD)$_2$]BF$_4$ and [Rh(COD)(μ-Cl)]$_2$ metallic precursors. However, none of our efforts to isolate the desired complex was successful, and the same happened when CO was bubbled in the presence of an excess of ligand **L1** to substitute the COD ligand and stabilise the system[58a] or when a base was added in the presence of an halide extractor (see Scheme 30).

After these unsuccessful experiments, the use of [Rh(CO)$_2$(μ-Cl)]$_2$, a precursor already containing the CO ligand, was finally explored. The reaction of this precursor

with 2 equivalents of (*S*)-**L1** in dichloromethane produced a stable solid that resulted to be *trans*-[RhClCO((*S*)-**L1**)₂] (**L1Rh1**) (Scheme 31).
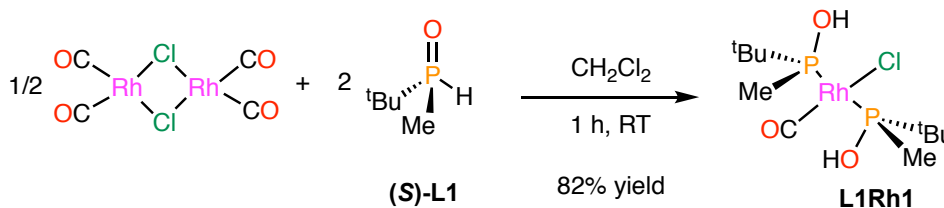
Scheme 31. Preparation of complex **L1Rh1**.

The *trans* arrangement of the phosphinous acid ligands was evidenced by the appearance of a single doublet in the $^{31}P\{^1H\}$ NMR spectrum at 129.9 ppm ($^1J_{RhP}$ = 117 Hz), while the *cis* complex should feature two different doublets. The expected multiplicity can be also found in the ^1H NMR spectrum; displaying only one set of ^tBu and Me signals (Figure 12).
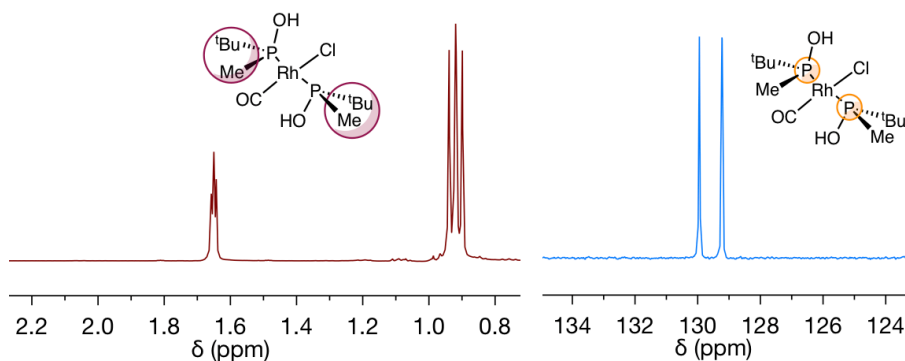
Figure 12. $^{31}P\{^1H\}$ NMR (162 MHz, CDCl₃, 25 ºC) (right) and ^1H NMR (400 MHz, CDCl₃, 25 ºC) (left) spectra of complex **L1Rh1**.

The synthesis was repeated adding different bases (NEt₃, DBU, Na₂CO₃…) in order to obtain the *cis* complex but the *trans* complex was formed for all cases. Indeed, there is a literature precedent[72] that Rh(I) precursors with bulky electron-rich SPOs react to form exclusively *trans*-complexes as happened in the present case.

Although for Rh-carbonyl complexes of this type no catalytic application has been found to date, they might be useful for the evaluation of the electronic properties of SPOs. In this sense, these electronic properties have only been investigated by Martin and co-workers[72] by the measurement and calculation of the IR frequencies of CO in different Rh carbonyl SPO complexes. It appears that generally the phosphinous acid form is less donating than most trisubstituted phosphine ligands. However, abstraction of the hydrogen makes the generated phosphinito an extremely strong donating ligand

93

(Tolman's electronic parameter ranging from 2006 to 2018 cm^{-1}). According to this, pseudobidentate anionic ligands display the strongest net-donation, close to phosphonium ylides, outclassing the *N*-heterocyclic carbenes. This kind of measurements are mainly recorded for aryl SPOs, and we think that it could be interesting to extend these studies with more electron-rich systems such as the one presented in this THESIS.

3.3.2.4. *Au complexes*

The coordination chemistry of gold(I) with SPO ligands has been scarcely explored. The first examples were reported by Schmidbaur and co-workers[74] with arylphosphinous acid ligands. More recently, van Leeuwen and co-workers[75] used the complex [^{t}Bu(1-naphthyl)P(OH)AuCl]$_2$ as a precursor for gold nanoparticles that proved to be active for the hydrogenation of substituted aldehydes. At the same time Schröder and co-workers[76] described the first use of molecular systems in enyne cycloisomerization and hydroxy- and methoxycyclisation reactions. It has to be noted that, to the best of our knowledge, there were no described Au complexes with optically pure *P*-stereogenic SPOs.

In our hands, phosphine oxide (*S*)-**L1** easily substituted the tht ligand when reacted with [Au(tht)Cl][77] in CH$_2$Cl$_2$ providing complex **L1Au1** as a pale grey solid in good yield (Scheme 32).
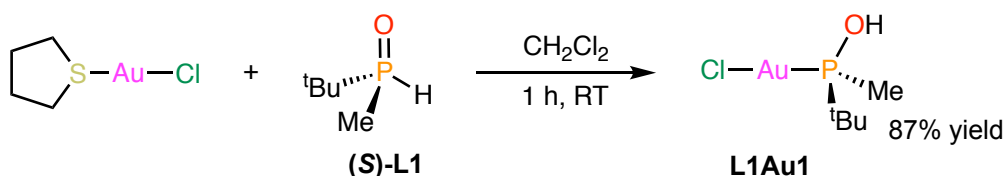
Scheme 32. Synthesis of complex **L1Au1**.

Although the prepared complex is air stable, the reduction to Au(0) occurred rapidly when the solution of **L1Au1** was exposed to light. The spectroscopic data was consistent with the proposed structure of **L1Au1**. The ^{31}P{^{1}H} NMR spectrum showed a singlet at δ = 113.6 ppm, a chemical shift comparable with that of similar compounds with other SPOs containing aryl substituents[76] while the ^{1}H NMR spectrum showed the expected doublets for the Me and ^{t}Bu substituents.

It was possible to grow crystals suitable for the determination of the crystal structure of **L1Au1** by X-ray analysis. The structure found is shown in Figure 13.
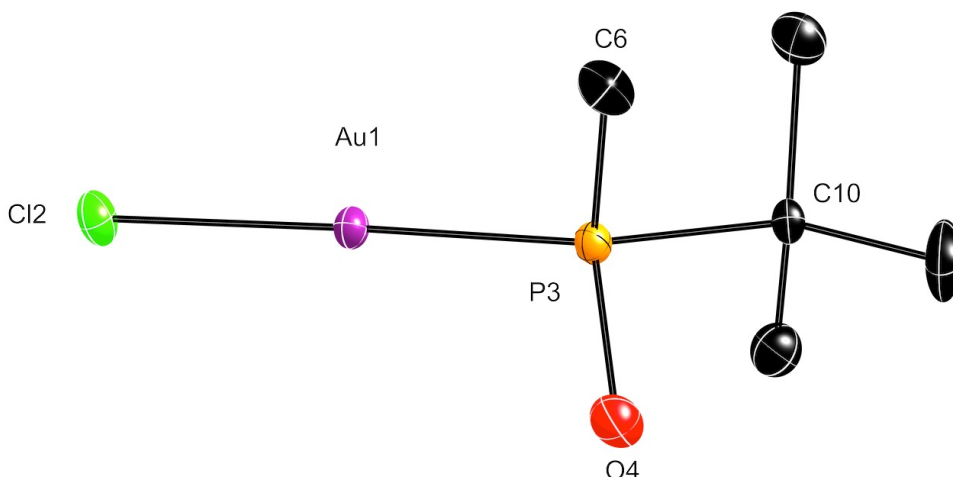
Figure 13. Molecular structure of **L1Au1** (thermal ellipsoids drawn at 50% probability level). The H atoms have been omitted for clarity.

Table 6. Selected bond lengths (Å) and angles (º) of **L1Au1**.

Bond	Length (Å)	Angle	(º)
Au1–Cl2	2.320(4)	C6–P3–O4	103.12(08)
Au1–P3	2.236(1)	C10–P3–C6	107.31(56)
P3–C6	1.789(9)	C10–P3–O4	103.71(91)
P3–C10	1.834(5)	Cl2–Au1–P3	178.98(03)
P3–O4	1.608(0)		

Crystals of **L1Au1** contained three molecules in the asymmetric unit with very similar distances and angles. The absolute configuration of the phosphorus atom was *S*, as expected.

In the literature Au-SPO complexes present symmetric dimeric structures with the gold centres stabilised by aurophilic interactions and interconnected by two terminal O-H···Cl hydrogen bonds.[76] In contrast in the crystal structure of **L1Au1** the O-H···Cl length and the P-Au-Cl angle are different for each of the three molecules. The Au–Cl (2.326 Å), Au–P (2.235 Å) and Au–O (3.234 Å) distances are in the typical range of bond lengths for this kind of gold complexes.[74b-d] Interestingly, the P-Au-Cl angle has a value of 178º, slightly deviated from the expected linearity of a Au(I) system. Similar values have been previously found in related complexes with very bulky biarylphosphines.[74b-d,76]

The packing of the molecules generates an interesting 3D structure in which the intermolecular aurophilic interactions between the gold centres occur only between the crystallographically identical molecules (Figure 14).
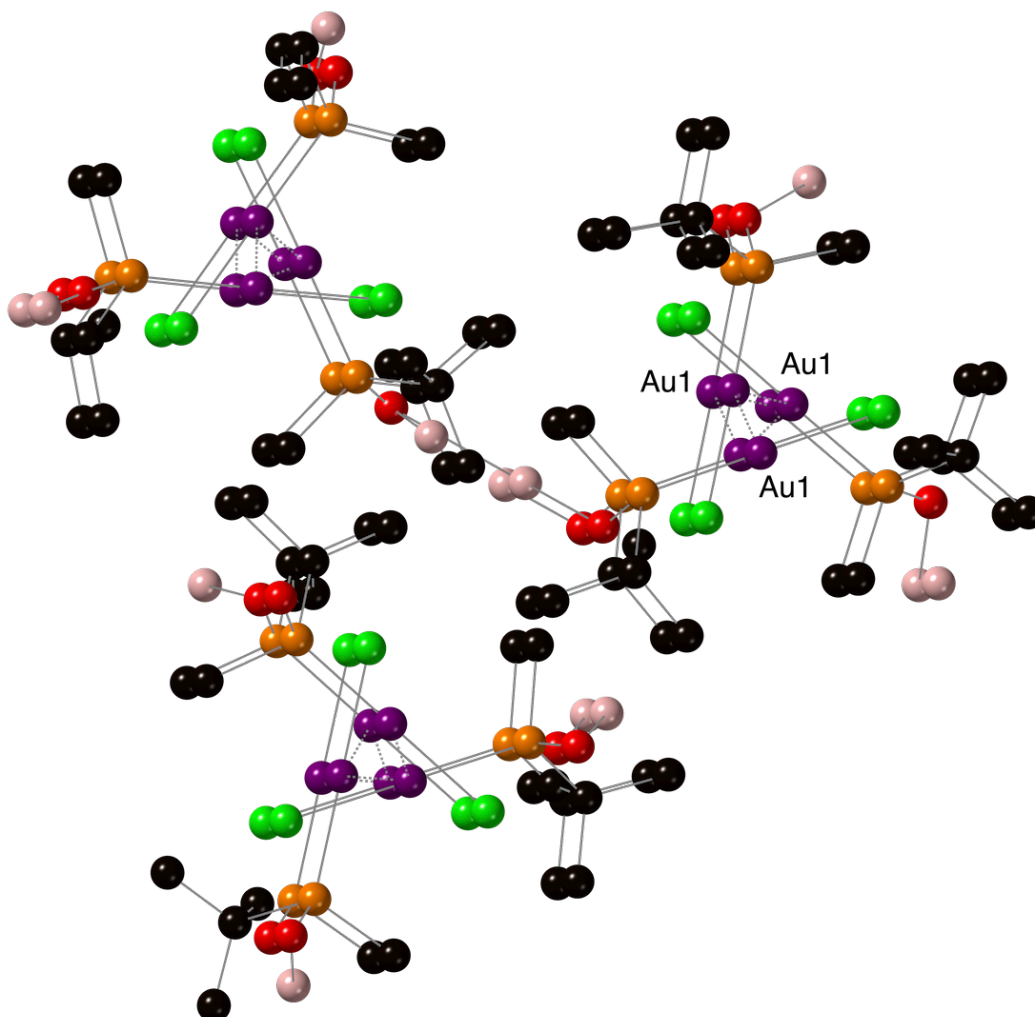
Figure 14. View of the molecular packing of compound **L1Au1** along the crystallographic c* axis. Most of the H atoms have been omitted for clarity. Selected bond length (Å) and angles (º): Au1–Au1 3.431(8); Au1–Au1–Au1 145.37(07).

The Au–Au distance is 3.43 Å and therefore these interactions can be considered rather weak because they range between 2.75 and 3.60 Å for a gold van der Waals radius of 3.60 Å.[78] Due to these aurophilic interactions, the three different molecules in the asymmetric unit generate non parallel chains.

3.3.2.5. *Ru complexes*

Although the first examples of Ru systems bearing PO–H···PO bridges were initially published during the 1980's,[79] it was not until 1999 when these studies were extended to SPOs.[80] Almost at the same time ruthenium complexes with atropoisomeric biaryl-SPOs were also described.[81]

In spite of this, the first reported Ru-SPO structure bearing a pseudobidentate ligation was described with P(OMe) substituents[82] and no catalytic applications were found for these complexes until the work of Ackermann[83] in 2005. They used electron-rich SPOs in ruthenium-catalyzed arylation reactions between pyridines or imines and aryl chlorides through a C-H bond activation mechanism.

The importance of this type of catalysts has been revisited more recently when applied to other reactions such as nitrile hydration by Tyler and co-workers[84] and Cadierno and co-workers (Figure 15).[85]
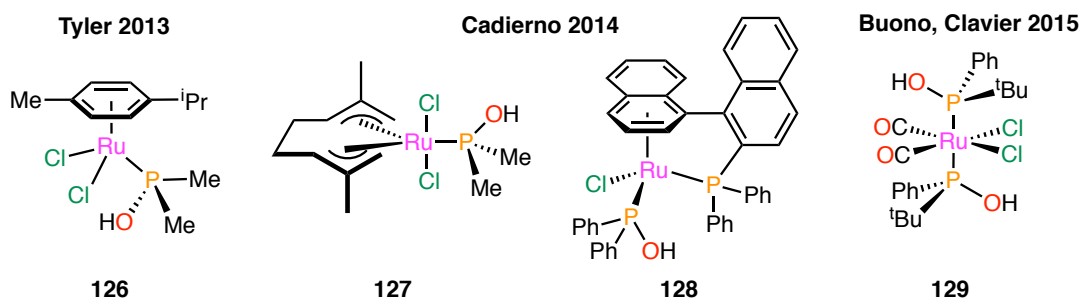
Figure 15. Selected phosphinous acid-Ru complexes.

In these studies, the intramolecular hydrogen bonds of SPOs moieties increased the reaction rate by activating water molecules. Other applications include the hydrogenation of aromatic compounds using Ru nanoparticles stabilised by a network of hydrogen bonds mediated by the SPOs at the surface.[86]

Ru complexes are competent catalysts for many challenging organic transformations[87] but there is still a lot of work to do in order to find efficient enantioselective processes, which have been studying intensively over the last decade in many applications such as transfer hydrogenation, cyclopropanation, olefin metathesis among others.[88]

One of the most important families of these compounds are the [RuCl$_2$(η^6-arene)P] complexes where P is a monophosphorus ligand. From a structural point of view, they can be considered as d^6 octahedral complexes or pseudotetrahedral if we consider that the arene ligand is coordinated through the centre. The η^6-arene occupies

three coordination positions, while the others are filled with ancillary Lewis bases. Due to this particular disposition of the ligands around the metal, these complexes have been commonly named "three-ledged piano stool" complexes. The metal-ligand bond is strongly influenced by the arene, which has a predominantly π-acceptor behaviour, therefore, arene-type ligands provide an extra stability to the complexes when the metal is electron-rich, or in other words, when it has a low oxidation state.

Mononuclear Ru-arene complexes are typically obtained by means of their dinuclear precursors. Due to the large number of interesting Ru(II)-based catalytic systems prepared using the dimer $[RuCl_2(p\text{-cymene})]_2$, which is more soluble in organic solvents than other dimers such as $[RuCl_2(benzene)]_2$, we started the study of the coordination chemistry of **L1** with this precursor following the procedures described by Ackermann and co-workers[89] and by Buono and co-workers[90] as it is depicted in Scheme 33.
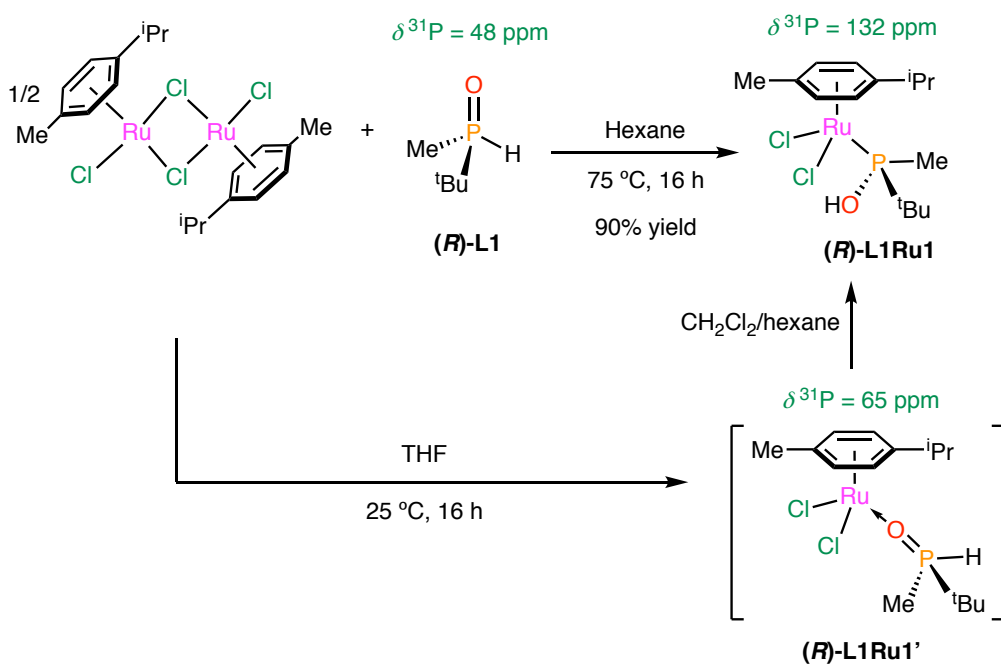
Scheme 33. Preparation of complexes (**R**)-**L1Ru1**' and (**R**)-**L1Ru1**.

The Ru dimer was reacted with a solution of (**R**)-**L1** in THF at 25 ºC and after 3 h appeared a singlet in the $^{31}P\{^1H\}$ spectrum at $\delta = 65$ ppm that was assigned to the *O*-coordinated complex (**R**)-**L1Ru1**'.[90] Interestingly, when we tried to isolate this species by precipitation with hexane, only the *P*-coordinated complex (**R**)-**L1Ru1** was obtained in 60% yield, which displayed a resonance at $\delta = 132$ ppm, typical of this kind of compounds.[85c,89-90] Additionally, the *P*-coordination of the ligand was also confirmed by the absence of $^1J_{HP}$ coupling constant in the ^1H NMR spectrum (Figure 16).
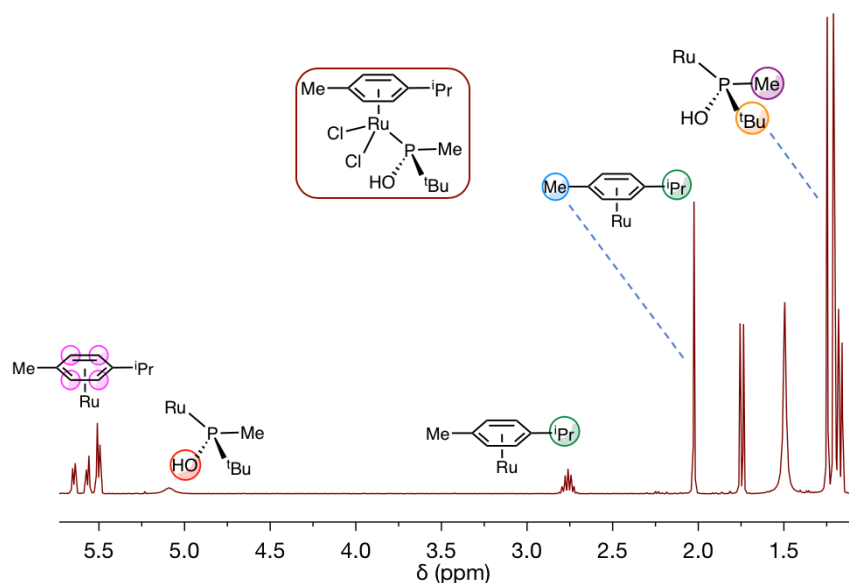
Figure 16. ^{1}H NMR (400 MHz, CDCl$_3$, 25 ºC) spectrum of complex (*R*)-**L1Ru1**.

In order to improve the yield, another synthetic procedure, consisting in running the reaction in refluxing hexane,[89] was carried out. It turned out that with this procedure (*R*)-**L1Ru1** was obtained quantitatively despite the fact that the starting Ru dimer is scarcely soluble in hexane.

Complex (*R*)-**L1Ru1** has been fully characterised by NMR spectroscopy, IR, elemental analysis and mass spectrometry. The structure of (*R*)-**L1Ru1** was unambiguously established by single-crystal X-ray diffraction studies (Figure 17).
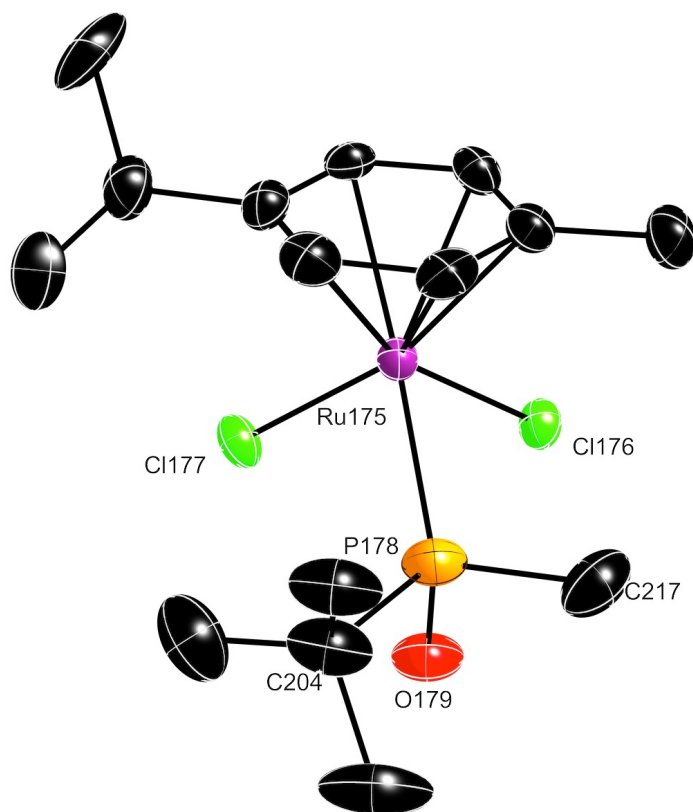
Figure 17. Molecular structure of one of the molecules of (*R*)-**L1Ru1** (thermal ellipsoids drawn at 50% probability level) in the unit cell. The other three molecules show some disorder, due to the rotation of the *p*-cymene ring. The H atoms have been omitted for clarity.

Table 7. Selected bond length (Å) and angles (º) of (*R*)-**L1Ru1.**

Bond	Length (Å)	Angle	(°)
P178–O179	1.620(4)	C217–P178–C204	105.14(17)
P178–C217	1.819(9)	C217–P178–O179	103.60(07)
P178–C204	1.845(1)	C204–P178–O179	100.09(35)
P178–Ru175	2.321(6)	P178–Ru175–Cl176	81.01(11)
Ru175–Cl176	2.423(0)	P178–Ru175–Cl177	87.94(70)
Ru175–Cl177	2.405(1)	Cl176–Ru175–Cl177	87.63(92)
C$_{arene}$*–Ru175	2.212(1)		

*Averaged value of the six η^6–Ph Ru–C distances.

The complex adopts a distorted octahedral structure with the expected three-legged "piano-stool" geometry around the Ru atom and the η^6-coordination of the p-cymene ring. Two chloride ligands and the phosphinous acid occupy the other three positions. Bond lengths and angles are similar to those reported in literature for analogous complexes.[85c,89-90] The structure contains an intramolecular hydrogen bond between the OH and one of the Cl atoms.

At this point, we decided to change the relatively electron-rich η^6-coordinated p-cymene fragment for an electron-poor arene. Complexes of this type are very interesting, since the aromatic ring can be displaced by a more electron-donor arene, for instance, coming from the ligand, affording what is commonly named a tethered complex, a strategy that has indeed widely explored by Muller, Grabulosa and co-workers.[91]

To this end, [RuCl$_2$(methyl benzoate)]$_2$ was heated with (*R*)-L1 in hexane, under the same conditions described for the analogous p-cymene Ru complex (*R*)-L1Ru1 (Scheme 34).
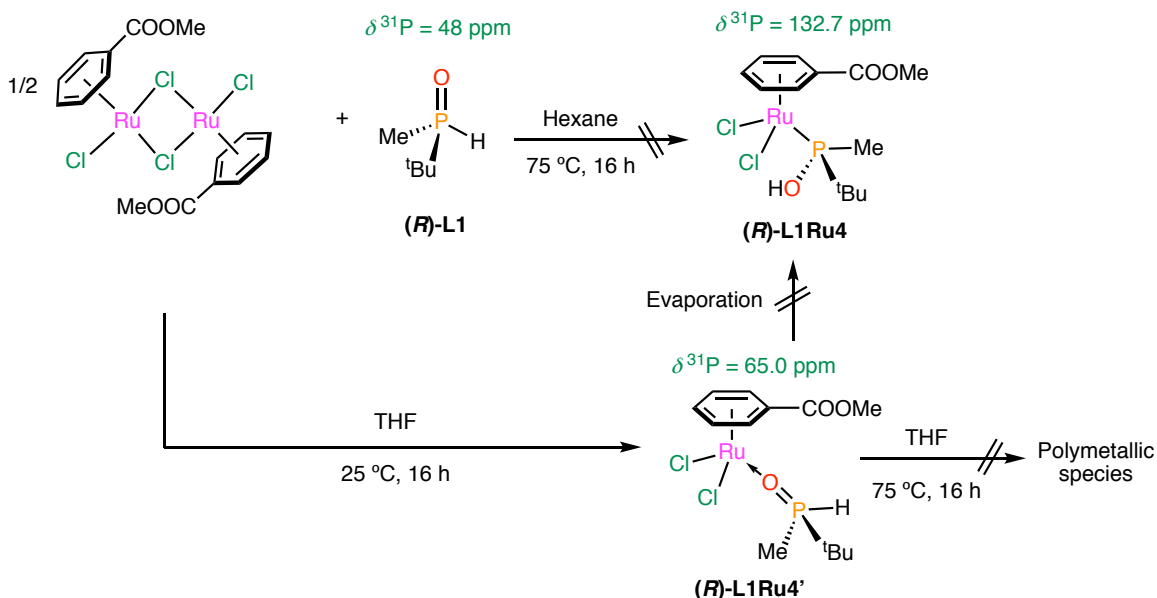
Scheme 34. Reactions of (*R*)-L1 with [RuCl$_2$(methyl benzoate)]$_2$ dimer.

Unfortunately, the reaction did not work, probably due to the extreme insolubility of the [RuCl$_2$(methyl benzoate)]$_2$. However, when the reaction was run in THF instead of n-hexane, the formation of the *O*-coordinated complex (*R*)-L1Ru4' could be followed monitoring the reaction by ^{31}P{^{1}H} NMR (Figure 18).
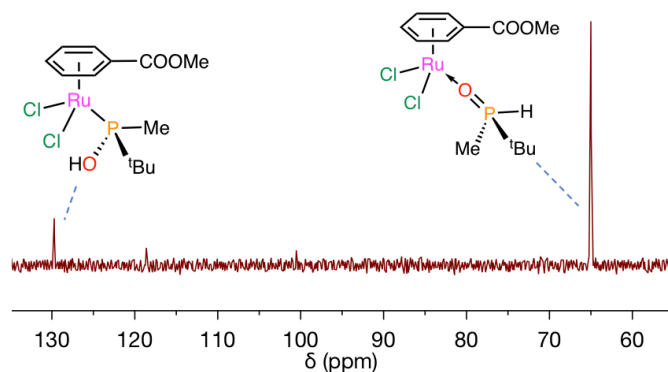
Figure 18. ^{31}P{^{1}H} NMR (162 MHz, P(OMe)$_3$)–INSERT of the reaction of (**R**)-**L1** with [RuCl$_2$(methyl benzoate)]$_2$ in THF.

While the major product was the *O*-coordinated complex (**R**)-**L1Ru4'** appearing at δ = 65 ppm in the ^{31}P{^{1}H} NMR, traces of the desired *P*-coordinated compound (**R**)-**L1Ru4** were also present (δ = 133 ppm), a fact also supported by mass spectrometry. The presence of an important amount of the remaining free ligand suggests that an equilibrium between the different species in solution is present.

Furthermore, when the reaction was heated to reflux in THF, a complex mixture was formed according to the myriad of peaks was found in the ^{31}P{^{1}H} NMR, probably due to the decoordination of the arene which was easily released thermally.

Attempts to substitute a chloride ligand by another (**R**)-**L1** moiety were unsuccessful (Scheme 35) even in the presence of halide extractors such as AgPF$_6$ or TlPF$_6$ with and without the presence of base.
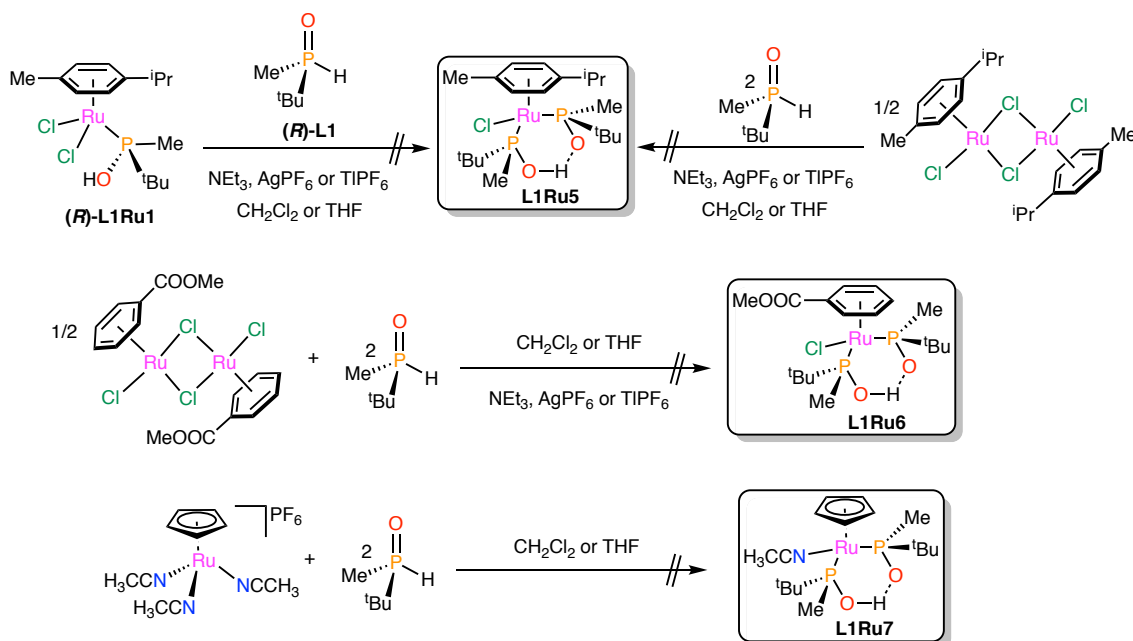
Scheme 35. Attempts to prepare the pseudobidentate complexes **L1Ru5** and **L1Ru6** and **L1Ru7**.

In all cases multiple signals appeared in the ^{31}P{^{1}H} NMR and we attribute this lack of reactivity due to the steric hindrance of the ^{t}Bu groups, since no examples of piano-stool Ru(II) complexes with two coordinated SPOs have been reported so far.

Anionic η^5-Cp-Ru complexes are known to be less reactive than their analogous η^6-arene counterparts, since they do not release the anionic arene so easily. We studied, in parallel, the complexation of (*R*)-**L1** in CH$_2$Cl$_2$ or THF to tris(acetonitrile)cyclopentadienylruthenium(II) hexafluorophosphate (Scheme 35) but no trace of dicoordinated product was observed, even heating the solution at 50 °C, where only free ligand could be detected. The lack of substitution of **L1** with the more labile acetonitrile ligands is in agreement with the behaviour of the related *p*-cymene/methyl benzoate systems and supports the hypothesis that sterically hindered SPOs cannot be linked in a pseudobidentate fashion in pseudotetrahedral Ru (II) compounds.

Reaction of RuCl$_3$ with 6 eq. of **L1** was also tested in different alcohols as solvents (MeOH, EtOH and ^{i}PrOH) but once again no reaction or decomposition was found depending on the conditions used.

As it was described for Rh, the coordination of bulky and basic phosphinous acids has been found to be difficult because of the lack of stability of the complexes formed. It is known, however, that electron-withdrawing ligands such as arylphosphines or carbonyl groups tend to facilitate the introduction of more than one SPO in the coordination sphere. This behaviour has been also observed for Ru by Buono and co-

workers,[58b] who reported recently the synthesis of ruthenium carbonyl complexes bearing SPOs which have been successfully applied in the cycloisomerisation of arenynes.

The treatment of $[RuCl_2(CO)_3]_2$ with **(S)-L1** in THF at room temperature allowed the obtention of the *O*-coordinated product (**L1Ru2**), isolated by precipitation with pentane in good yield (Scheme 36).
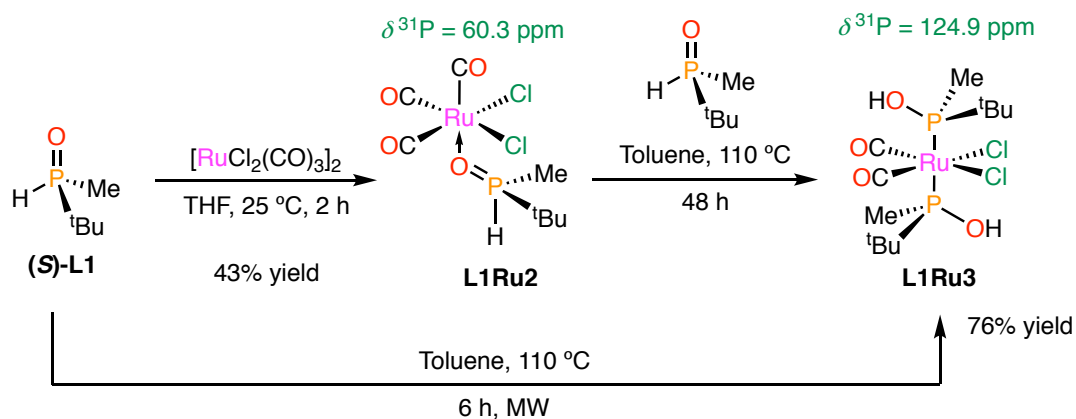
Scheme 36. Synthesis of complexes **L1Ru2** and **L1Ru3**.

Compound **L1Ru2** displays a singlet in the $^{31}P\{^1H\}$ NMR spectrum at the *O*-coordinated region (δ = 65 ppm) whereas the ^1H NMR spectrum further supports the identity of the compound with the observation of a doublet of quadruplets at δ = 7.01 ppm with a J_{HP} of 495 Hz, similar to other complexes with *O*-coordinated SPO ligands.[58b]

When we treated **L1Ru2** with another equivalent of **(S)-L1** in toluene at 110 ºC for two days, a new chemical shift in the $^{31}P\{^1H\}$ NMR spectrum was observed at δ = 126 ppm, which could be assigned to the *trans* complex containing two phosphinous acid ligands **L1Ru3** (see Scheme 36). In order to find a more convenient method, the reaction was carried out under microwave conditions, which led to a higher yield in much shorter time. **L1Ru3** has been fully characterised by spectroscopic means, and the *trans* geometry was confirmed by ^1H NMR and $^{13}C\{^1H\}$ NMR spectroscopy, both showing virtual coupling (Figure 19).
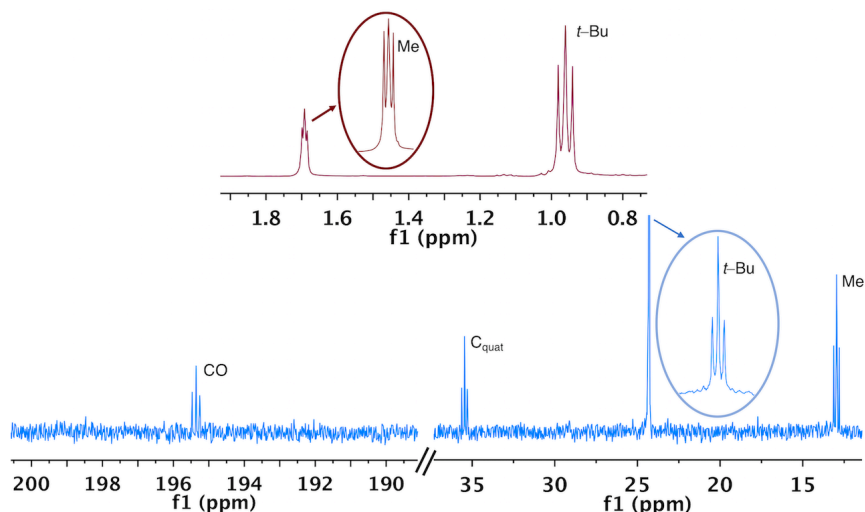
Figure 19. Expansions of the ^{1}H (top) and ^{13}C{^{1}H} (bottom) NMR spectra of **L1Ru3**.

Two IR v_{CO} stretching bands were observed at 2048 cm^{-1} and 2000 cm^{-1} a fact that agrees with the *cis* arrangement of the carbonyl ligands, as previously described by Buono and co-workers.[58b]

The reaction was repeated in the presence of different bases, but in all of the cases the same **L1Ru3** product was formed, without any trace of the *cis* isomer.

Taking into account that Ru-carbonyl complexes of this type are known to be competent systems for the cycloisomerisation of arenynes,[58b] it might be interesting to develop an asymmetric version of such reactions in order to evaluate the potential catalytic activity of Ru complexes with coordinated *P*-stereogenic SPOs.

3.3.2.6. *Pd complexes*

The application of Pd-SPO complexes received a boost in 2001 when Li and co-workers[18a] used dialkylphosphinous acids in catalytic cross-coupling reactions.[92] In addition, the same type of compounds were successfully applied in the Suzuki-Miyaura couplings of aryl chlorides[93] and in Heck reactions of 4-chloroquinolines.[94]

Particularly interesting are the Pd systems containing imidazole-based secondary phosphine oxides, which has promoted excellent results in Heck reactions, as it has been described by Hong, Shaikh and co-workers.[59,95] Hong and co-workers also reported the preparation of quinolyl-substituted secondary phosphine oxides in which the N of the heterocycle acts as an hemilabile ligand (Figure 20).[96]
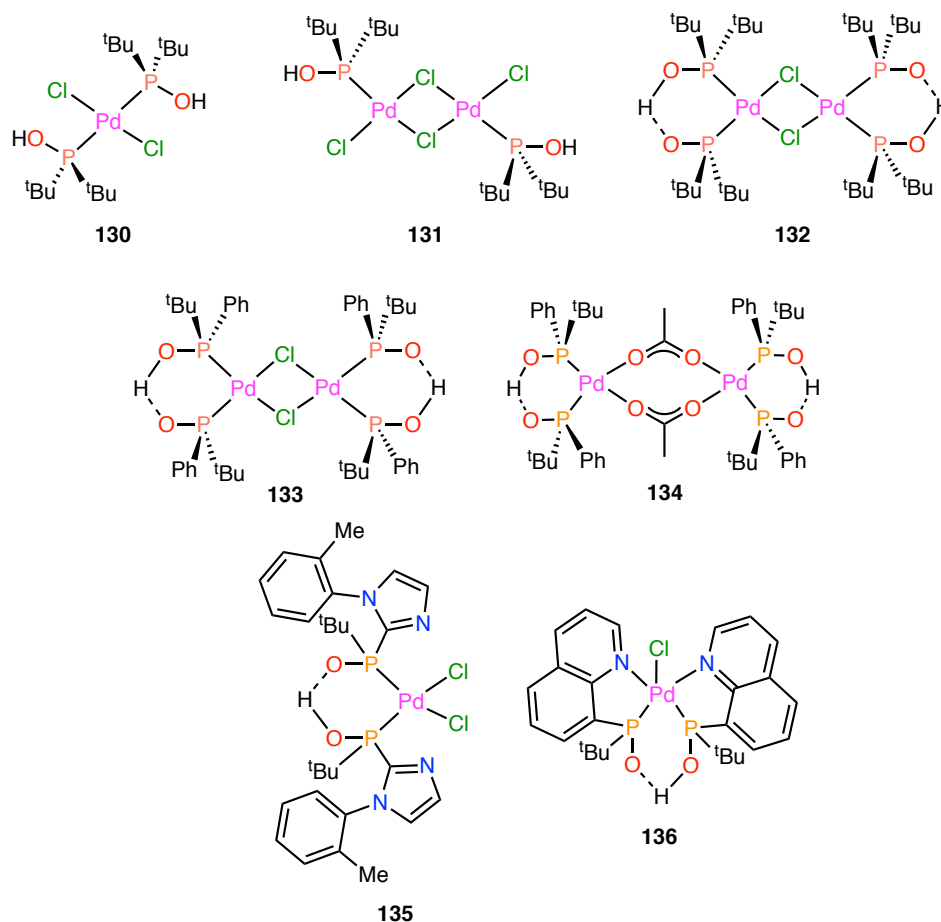
Figure 20. Selected phosphinous acid-coordinated palladium complexes from the literature. [59,94-96]

Furthermore, Buono and co-workers[97] described in 2008 an unprecedented application for dimeric acetate-Pd complexes, having the $^tBu/Cy$ combination in the SPO ligands, in the [2+1] cycloaddition reaction/ring expansion of alkynes with norbornadiene derivatives. The reaction afforded only the vinylidene cyclopropanes rather than the expected alkynyl products. An account by Clavier and Buono on the Pd- and Pt-phosphinous acids and their applications in this type of reactions has recently appeared.[98]

In spite of the extensive research carried out in this field, only few studies have been reported on the use of optically pure SPOs in the asymmetric version of these reactions, as it will be discussed in the last section of this chapter.

Having the literature precedents in mind, we started our studies with the complexation of **L1** with some Pd precursors, following the methods developed by Li and co-workers[18a] and by Buono and co-workers[60b] for related Pt compounds. Therefore, (*S*)-**L1** was treated with [PdCl₂(COD)] to afford a mixture of *cis* and *trans* isomers, *cis*-**L1Pd1** and *trans*-**L1Pd1** (Scheme 37).
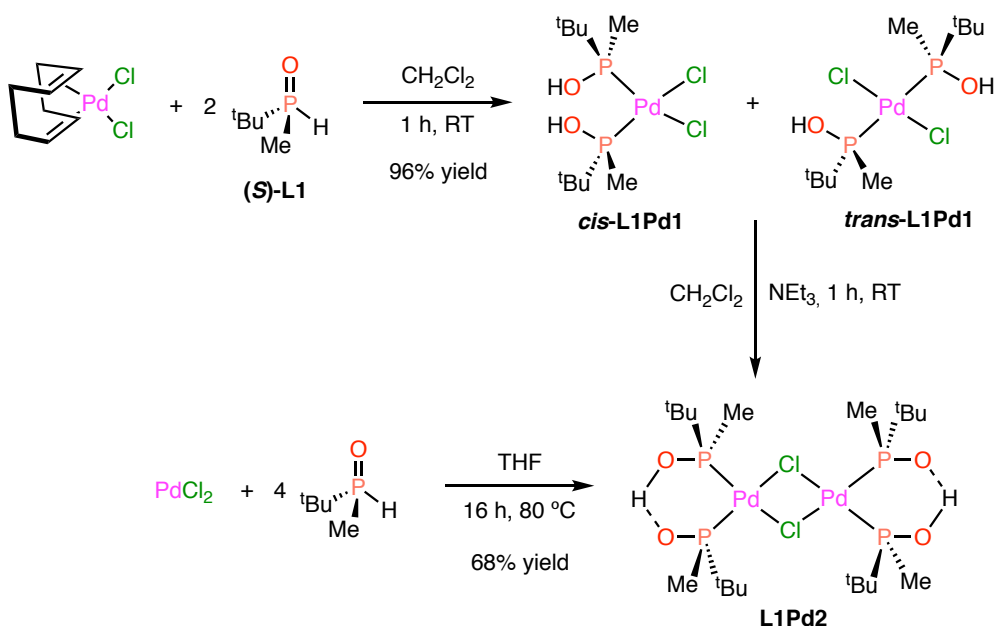
Scheme 37. Preparation of Pd complexes *cis*- and *trans*-**L1Pd1** and **L1Pd2**.

In the $^{31}P\{^{1}H\}$ NMR this mixture appeared as two singlets at δ = 130.0 and δ = 117.0 ppm for the *cis* and *trans* isomers respectively, in an approximate 1:2 ratio. Interestingly, when the mixture was concentrated *in vacuo* only the *trans* isomer was obtained. The proposed structure is supported by the ^{1}H NMR spectrum, in which the Me and *t*-Bu groups appear as pseudotriplets due to virtual coupling. However, when the isolated complex *trans*-**L1Pd1** was dissolved again, some *cis*-**L1Pd1** could be observed by NMR after a few hours.

Following the report of Li[93] the mixture of *cis*- and *trans*-**L1Pd1** was treated with NEt$_3$ to afford a single species at δ = 108.9 ppm in the $^{31}P\{^{1}H\}$ NMR spectrum, suggesting the formation of a dimeric phosphinito-phosphinous acid palladium complex (Scheme 37).[18b,60a] Complex **L1Pd2** appears to be extremely stable since after some experimentation it was found that it can be prepared by simply refluxing PdCl$_2$ in THF in air, in the absence of base. The product was fully characterised and the pseudobidentate coordination mode was unambiguously confirmed with X-ray diffraction (Figure 21).
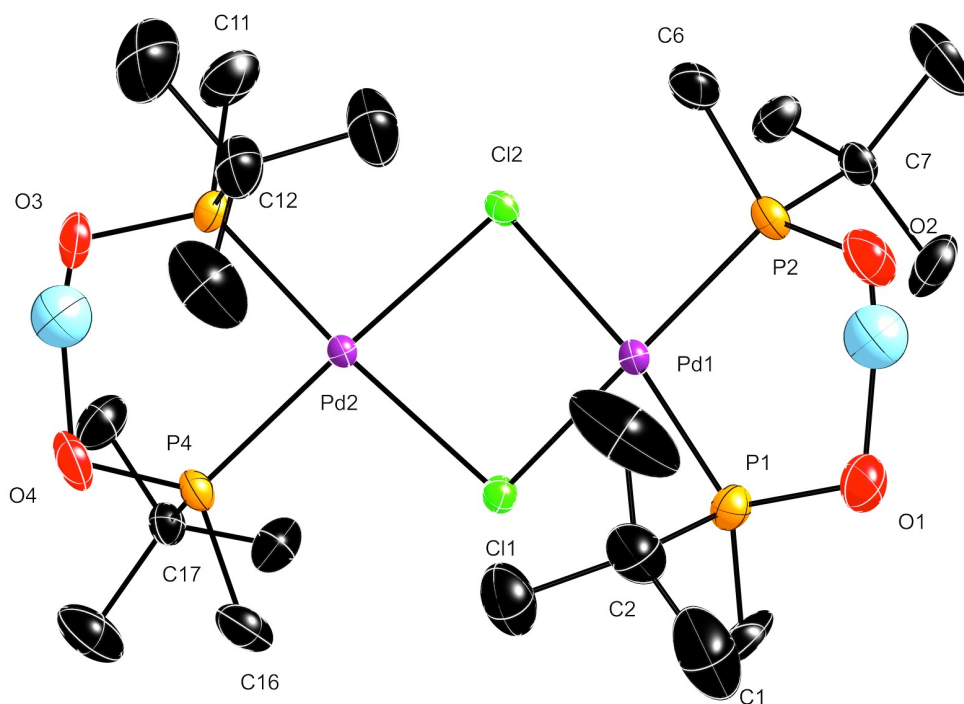
Figure 21. Molecular structure of complex **L1Pd2** (thermal ellipsoids drawn at 50% probability level). Most of the H atoms have been omitted for clarity.

Table 8. Selected bond length (Å) and angles (º) of **L1Pd2**.

Bond	Length (Å)	Angle	(º)
Pd1–Cl1	2.433(3)	Pd1–Cl1–Pd2	85.63(37)
Pd1–Cl2	2.440(5)	Pd1–Cl2–Pd2	85.72(21)
Pd2–Cl1	2.449(6)	Cl1–Pd1–Cl2	83.16(03)
Pd2–Cl2	2.438(4)	Cl1–Pd2–Cl2	82.86(54)
Pd1–P1	2.251(9)	P1–Pd1–P2	90.45(62)
Pd1–P2	2.251(9)	P3–Pd2–P4	90.78(18)
Pd2–P3	2.244(0)	C1–P1–O1	105.14(44)
Pd2–P4	2.256(6)	C2–P1–C1	106.91(24)
P1–C1	1.806(4)	C2–P1–O1	107.20(08)
P1–C2	1.853(3)	C6–P2–O2	104.83(53)
P1–O1	1.528(2)	C7–P2–C6	107.26(69)
P2–C6	1.795(4)	C7–P2–O2	105.35(15)
P2–C7	1.848(0)	C11–P3–O3	104.79(49)
P2–O2	1.555(3)	C12–P3–C11	107.29(95)
P3–C11	1.815(6)	C12–P3–O3	105.61(86)
P3–C12	1.824(9)	C16–P4–O4	105.00(35)

P3–O3	1.539(0)	C17–P4–C16	107.46(58)
P4–C16	1.788(6)	C17–P4–O4	106.20(30)
P4–C17	1.844(4)		
P4–O4	1.549(7)		

This complex shows a square-planar geometry with two palladium(II) centres coordinated with two phosphinous acid moieties and two bridging chlorides, with three C_2 axes passing through the centre of the molecule, as found for similar complexes.[82] The structure reveals that the core of the molecule has a diamond-shaped moiety consisting of four atoms (Pd(1), Pd(2), Cl(1) and Cl(2)) that are almost coplanar. A hydrogen bond links O(1) with O(2), and O(3) with O(4), forming a dimeric complex with a *bis*(pseudobidentate) ligand.

In parallel, some experimentation was carried out in order to exchange the bridging Cl ligand by Br and F. To this end, [PdCl$_2$(COD)] was reacted with 2 eq. of (*S*)-**L1** in the presence of LiBr or KF respectively (Scheme 38).
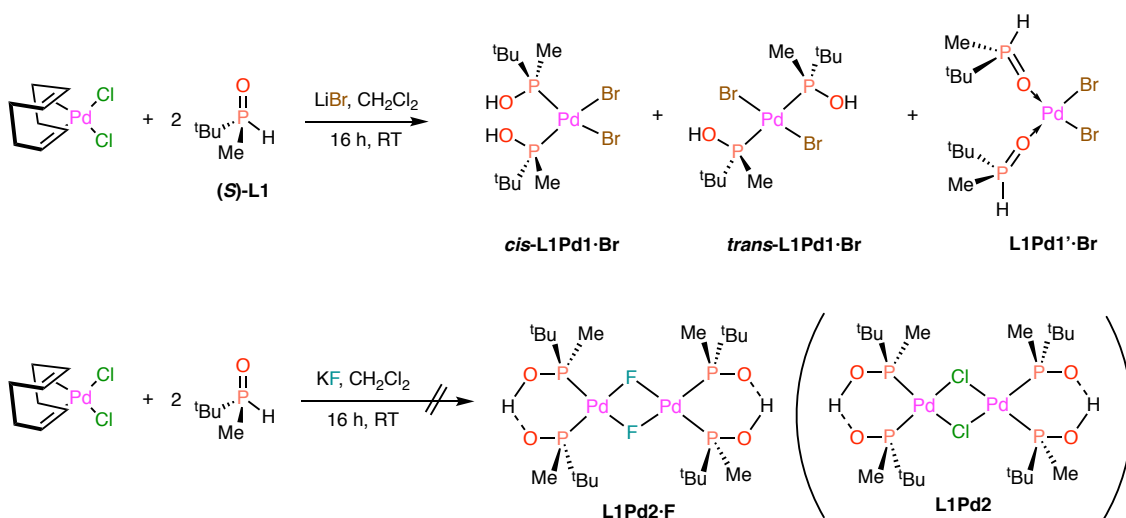
Scheme 38. Unsuccessful attempts to prepare bromide and fluoride Pd-SPO complexes.

Unfortunately, none of the experiments yielded any definite product since mixtures of *P*- and *O*-coordinated species were obtained when the reaction was performed with LiBr (Figure 22), while in the case of KF no reaction was observed in any of the cases.
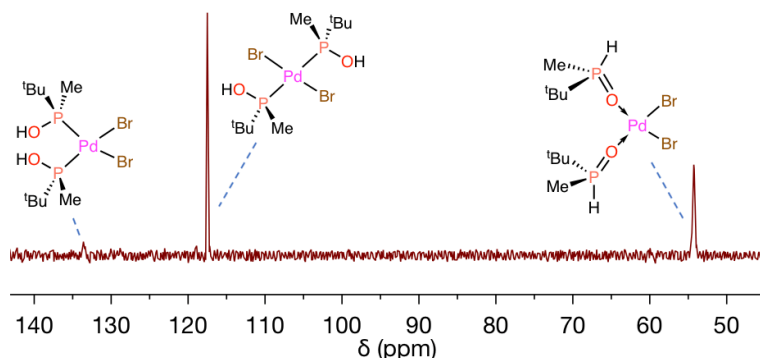
Figure 22. $^{31}P\{^1H\}$ NMR (162 MHz, CDCl$_3$, 25 °C) of the reaction between **(*S*)-L1** and [PdCl$_2$(COD)] in the presence of LiBr.

Arguably, it could be thought that the coordination of a bromide anion should be more favourable, due to its *softer* character. However, $^{31}P\{^1H\}$ NMR analyses of the reaction's crude showed a mixture of three different species: the *cis-/trans-* isomers and the *O*-coordinated bisphosphine derivative (Figure 22). Mass spectrometry results indicated no loss of Cl in any of the formed adducts, proving that the Cl/Br exchange was complete. In spite of that, only monomeric complexes having two bromide ligands were detected and no isotopic distribution of two palladium centres was found, indicating that no dimeric species were formed.

On the other hand, in principle, the *harder* character of the fluoride anion should stabilise the dimer due to antisymbiotic effect.[99] However, we unexpectedly detected the formation of **L1Pd2** instead, a fact that can be explained by the more favourable kinetics formation of this complex.

The lability of the ligands has important effects on catalytic activity. In this sense, as it has mentioned before, Pd acetate complexes with chiral SPOs have been successfully applied in [2+1] cycloadditions between norbornene derivatives and terminal alkynes, a reaction that is likely to proceed via palladium vinylidene species.[100] Therefore, **(*S*)-L1** was treated with Pd(OAc)$_2$ in refluxing toluene according to previous methodologies.[60b,100-101] $^{31}P\{^1H\}$ NMR spectrum displayed two singlets at δ = 110.6 ppm and δ = 106.9 ppm, which belong to the monomeric (**L1Pd3**) and dimeric (**L1Pd4**) species (Scheme 39) that coexist in equilibrium in 1:1 ratio.
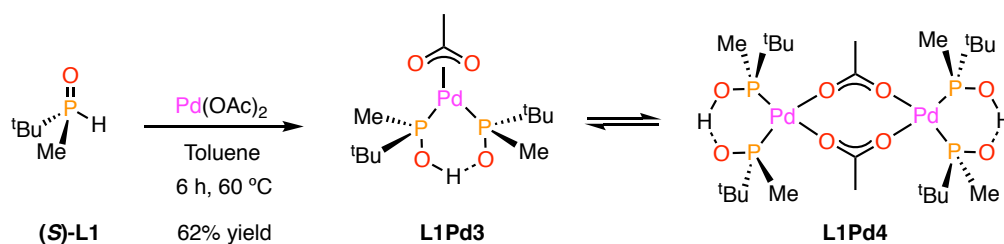
Scheme 39. Synthesis of **L1Pd3** and **L1Pd4** and their equilibrium in solution.

This equilibrium was also observed in the ^{1}H NMR spectrum, which shows duplication of signals for the methyl groups of the acetates and the ligands and for the *t*-Bu of the ligands (Figure 23).
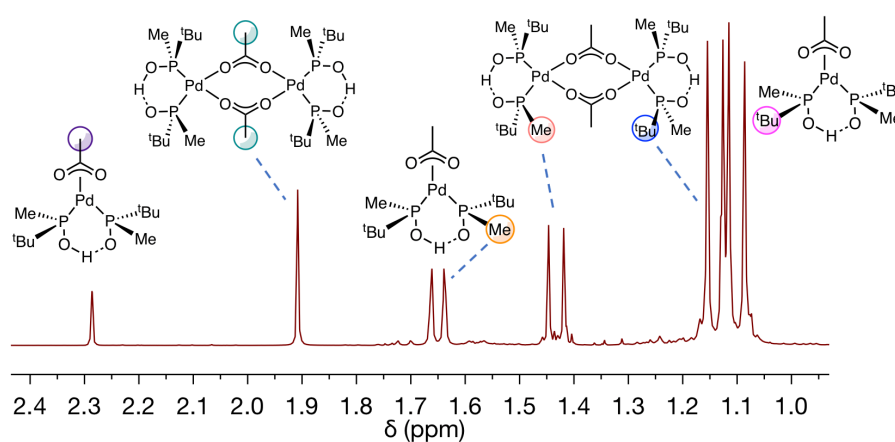
Figure 23. ^{1}H NMR (400 MHz, CDCl$_3$) spectrum of complexes **L1Pd3** and **L1Pd4**.

The unambiguous assignation was carried out by ^{1}H–^{13}C-HSQC experiments which showed correlation between the signals of the monomer and the dimer respectively.

111

Among all the Pd systems, π-allyl complexes are one of the most used families of catalytic precursors, since they are very useful in many organic reactions involving the formation of C–C and C–heteroatom bonds.[102]

Apart from that, these complexes have some advantages in comparison to other Pd compounds since most of them are stable in the air, they are soluble in almost all organic solvents and their preparation and characterisation can be carried out by the usual techniques. Pd(II) systems are mostly d^8 complexes with a square-planar geometry, in which two coordination positions are occupied by the η^3-allyl ligand, whereas the other two are filled typically by a chloride ligand and a monophosphine or by two phosphine units.

It is interesting to note that X-ray diffraction studies have proven that the η^3-allyl fragment is not, in fact, completely perpendicular to the plane formed by the Pd centre and the other two coordinative atoms. There is a distortion around 5 and 10º, which means that the plane of the allyl is canted with respect to the *xy* plane.[103]

In terms of catalytic applications, Pd-catalyzed asymmetric allylic substitution reactions with SPOs have been scarcely explored. Only Dai, and co-workers[60a] studied the asymmetric allylic alkylation of *rac*-acetoxy-1,3-diphenylpropene with dimethylmalonate under *in situ* conditions using the enantiomerically enriched *t*-BuPhP(O)H, with up to 80% *ee*. We envisaged the synthesis of allyl Pd complexes with **L1**, which are, to the best of our knowledge, the first monometallic[60a] allylpalladium SPO complexes ever reported.

At this point, it is convenient to define a proper nomenclature for the allylic hydrogen atoms, depicted in Figure 24.
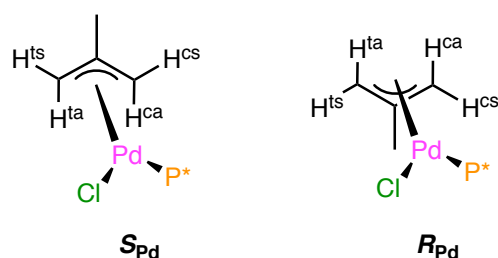
Figure 24. Nomenclature for the two diastereoisomers of complexes [PdCl(η^3-2-Me-allyl)P*].

For those complexes having a coordinated Cl and a monophosphorus ligand, the terminal carbons of the allyl group can be named as *cis* (c) or *trans* (t) with respect to the phosphorous atom, but at the same time they are *anti* (a) or *syn* (s) with respect to

the substituents of the central carbon of the allyl fragment. Therefore the four terminal hydrogen atoms can be defined as: H^{ts}, H^{ta}, H^{cs} and H^{ta}.

Furthermore, allyl complexes with a modentate chiral ligand have two distinguishable isomeric forms (Figure 24) due to the different spatial orientation of the allylic fragment with respect to the substituents of the *P*-stereogenic phosphorus. One of the most widely used nomenclatures to distinguish both diastereomers is based on the stereochemical descriptors S_{Pd} and R_{Pd}, which are assigned considering the allyl group as a single atom and the non-coplanar Cl–Pd–P fragment; having the priority according to the Cahn–Ingold–Prelog rules.[104]

Interestingly, these isomers present dynamic exchange in solution, whose mechanism have been extensively studied by several authors.[105]

There are, basically, two accepted mechanisms for the dynamic exchange between the two isomers, namely the *pseudorotacion* and π–σ–π *mechanisms*.

Pseudorotation of the allyl group can be understood as a simple twist of the allyl itself with respect of the axis along the bisector of the Cl–Pd–P angle (Scheme 40).
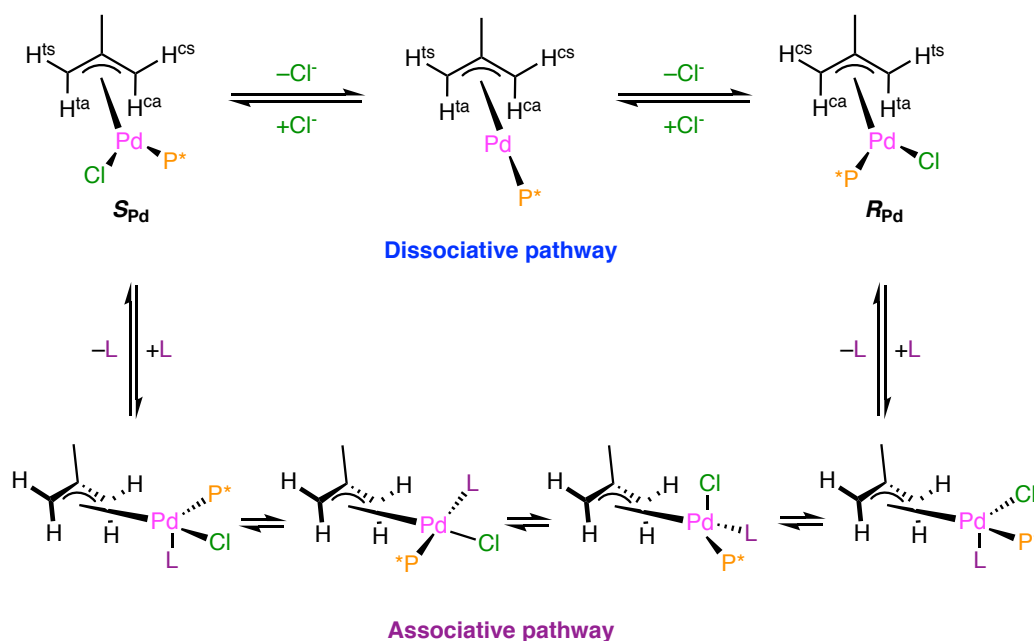
Scheme 40. Dissociative and associative pathways for the pseudorotation mechanism of the allyl fragment.

This twist cannot take place directly, since the geometrical distortions required are energetically forbidden. Hence, in order to explain the apparent rotation of the allyl fragment, two mechanisms are proposed. First, the so called, *dissociative*[106] where dissociation of the chloride ligand leads to a 14-electron tricoordinated intermediate. Then, recoordination of the ligand can trigger the formation of any of both isomers.

Secondly, the *associative* mechanism[106a] in which is postulated a pentacoordinated 18-electron intermediate. The *dissociative* mechanism is supported by NMR studies based on the NOE effect, while the other was initially proposed due to the experimental fact that traces of halides in solution or coordinative solvent molecules, accelerates the pseudorotation process.[107] In addition, pentacoordinated species have low energy barriers than the tricoordinated ones according to theoretical models.[108]

It is important to remark that *pseudorotation* implies the interconversion of the terminal carbons implying *syn-syn* and *anti-anti* exchanges of the allylic hydrogen atoms.

On the other hand, the $\pi-\sigma-\pi$ mechanism relies on the hapticity change of the allyl group.[105f,109] It consists on the formation of an η^1-allyl intermediate containing a σ(Pd–C) bond. The new single C–C bond of the allyl can rotate freely and form a new η^3-allyl complex by re-coordination of the double bond (Scheme 41).
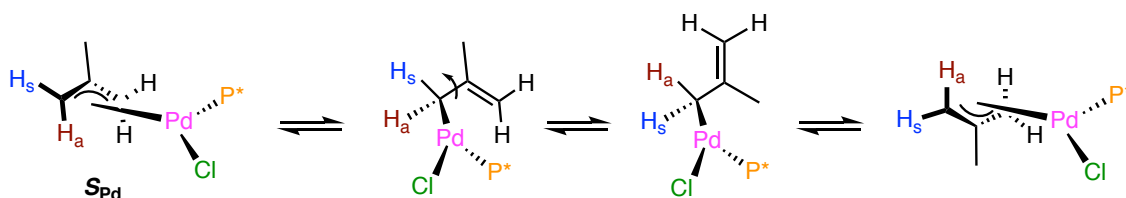
Scheme 41. $\pi-\sigma-\pi$ dynamic exchange of the allyl fragment.

According to this, the $\eta^3-\eta^1-\eta^3$ exchange allows the interconversion of the *syn* and *anti* allylic hydrogen atoms of the terminal carbon that does not decoordinate. In general, the carbon atom *trans* to P usually decoordinates faster due to the trans labilising effect in comparison to Cl.

In this THESIS we studied the coordination chemistry of (*S*)-**L1** with the allyl Pd dimers [Pd(η^3-2-Me-allyl)Cl]$_2$, [Pd(η^3-1-Ph-allyl)Cl]$_2$ and [Pd(η^3-1,2-Ph$_2$-allyl)Cl]$_2$ (Scheme 42).
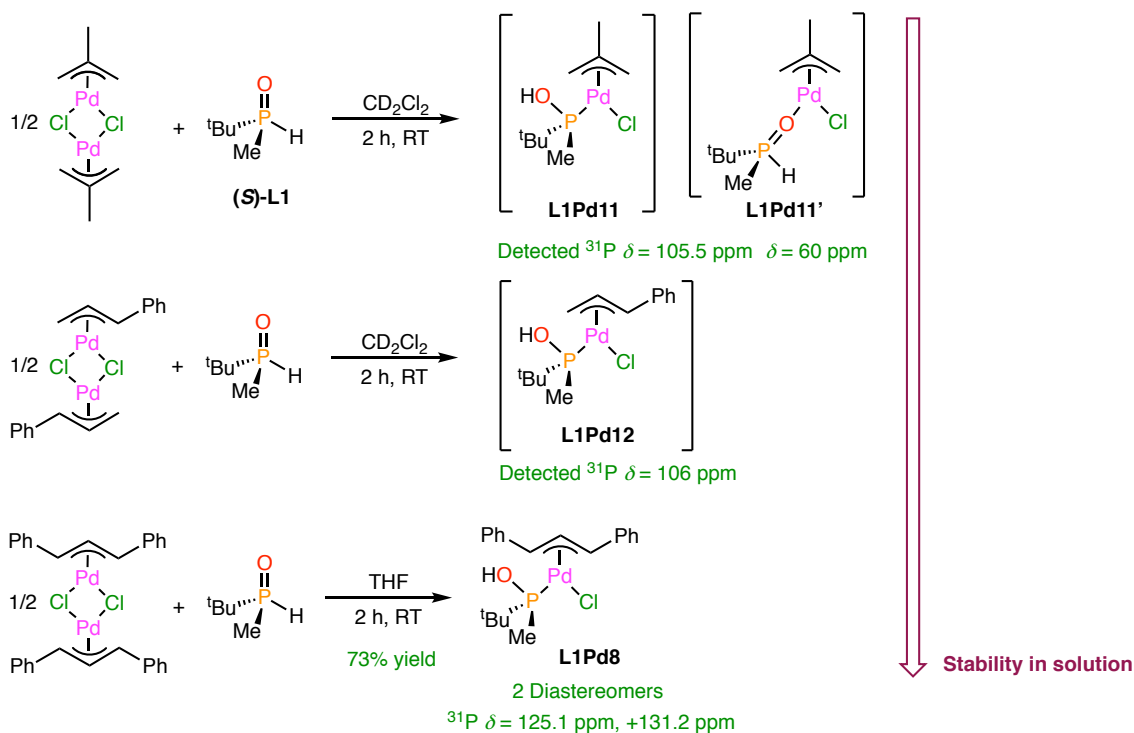
Scheme 42. Complexation of (*S*)-L1 with several allyl-Pd dimeric precursors.
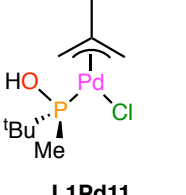
Treatment of (*S*)-L1 with 0.5 equivalents of [Pd(η^3-2-Me-allyl)Cl]$_2$ led to a mixture of *P*- and *O*- coordinated species of **L1Pd11** according to ^{31}P{^{1}H} NMR (Figure 25).
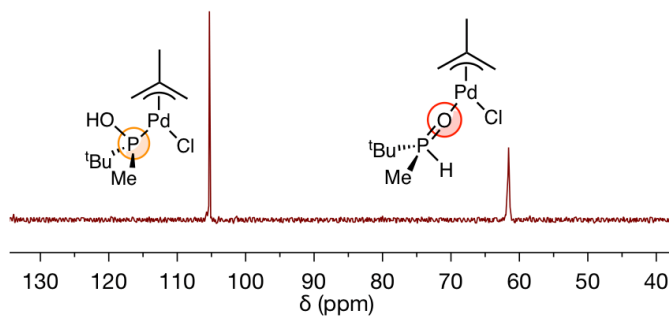
Figure 25. ^{31}P{^{1}H} NMR (162 MHz, CD$_2$Cl$_2$, 25 °C) of the crude showing **L1Pd11** and **L1Pd11'.**

The presence of one signal at $\delta = 105.5$ ppm suggests the formation of only one diastereomer of the methyl-allyl complex, discussed at the beginning of the section. However, there were also present *O*-coordinated species at $\delta = 60$ ppm, showing a broad peak due to dynamic exchange processes. These observations are in agreement with ^{1}H NMR data, which shows a duplication of the *syn, anti* protons and the methyl groups of the allyl fragment. Unfortunately, these complexes appeared to be extremely

unstable, even as solids, forming Pd(0) upon exposure to air. Although these difficulties, we were able to characterise them in solution running the reaction in CD_2Cl_2 (Table 9).

Table 9. Selected ^{1}H NMR(400 MHz, CD_2Cl_2, 25 ºC) data of complex **L1Pd11** δ is expressed in ppm, multiplicities and J (in Hz) are given in brackets.

	^{1}H NMR						
	Me	**Hst**	**H^{at}**	**H^{sc}**	**H^{ac}**	**P−Me**	**P−t-Bu**
	1.89	4.34	3.30	3.19	2.40	1.31	1.15
	(s)	(d, J = 2)	(d, J = 11)	(br s)	(s)	(d, J = 9)	(d, J = 15)

L1Pd11

As it has been discussed, η^3-2-Me-allyl complexes often give in solution mixtures of two diastereomers. However, when we have the η^3-1-Ph-allyl group, the situation becomes more complex, since the asymmetry of the allylic fragment allows the formation of more isomers. This complexity is mainly made by three factors: firstly, the Ph group substituted in one terminal carbon of the allyl group can be placed in *syn* or *anti* with respect of the central allylic proton. Secondly, the same Ph group can be located in *cis* (*Z*) or *trans* (*E*) with respect of the phosphorus atom coordinated to Pd. Finally, as it happened for the η^3-2-Me-allyl complexes, due to the chirality of the ligand, it is not the same when the Pd centre is coordinated to one face or another of the allyl which generates the pair of diastereomers, namely: S_{Pd} and R_{Pd}. That would mean, that there are 8 possible isomers for this system (Figure 26).
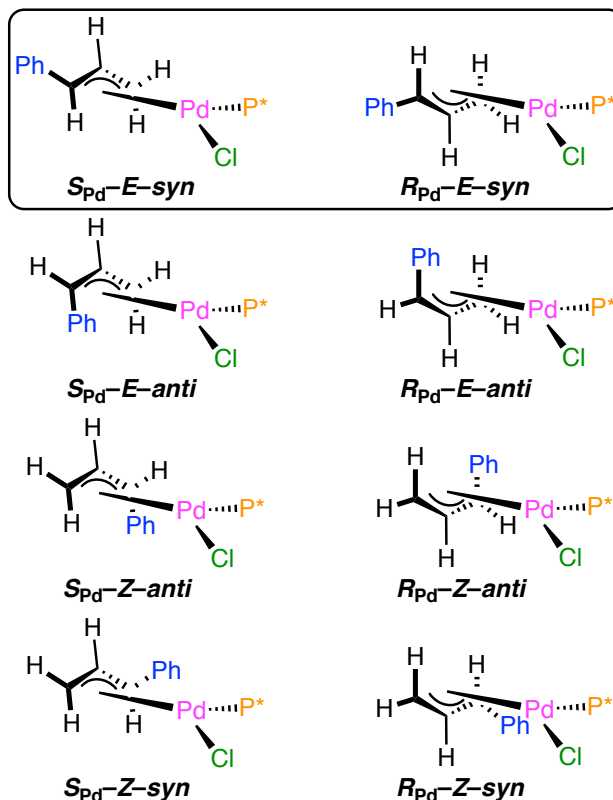
Figure 26. Eight possible isomers for the [PdCl(η^3-1-Ph-allyl)P*] system.

We can expect S_{Pd}-**E-syn** and R_{Pd}-**E-syn** to be the most abundant isomers because both contain the Ph in a *syn* position, which in turn is also *trans* to the phosphine.

While the use of [Pd(η^3-2-Me-allyl)Cl]$_2$, afforded mixtures of *P*- and *O*-coordinated species, [Pd(η^3-1-Ph-allyl)Cl]$_2$ lead only *P*-coordinated species, as confirmed by NMR studies.

^{31}P{^{1}H} NMR displayed a multiplet centred at $\delta = 106$ ppm, (Figure 27) which can be assigned to the mixture of isomers of **L1Pd12**. The bad resolution of the spectrum would require low temperature NMR experiments for the complete elucidation of the spectra. Unfortunately, at present it was not possible to carry out these experiments at the University of Barcelona.

117
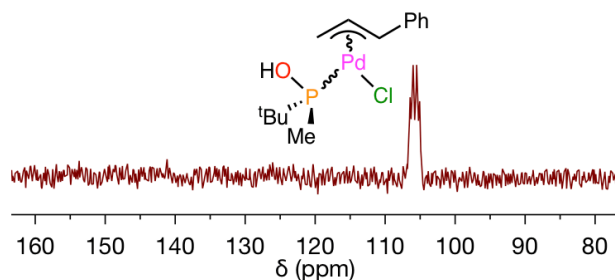
Figure 27. $^{31}P\{^1H\}$ NMR (162 MHz, CD$_2$Cl$_2$, 25 °C) of **L1Pd12**.

Once again, the stability of **L1Pd12** is also quite limited and signals of decomposition products could be seen in the $^{31}P\{^1H\}$ NMR after several hours in solution.

Finally, (**S**)-**L1** was reacted with 0.5 equivalents of the bulkier [Pd(η^3-1,2-Ph$_2$-allyl)Cl]$_2$ (see Scheme 42).

Gratifyingly, the introduction of another phenyl group in the allyl framework allowed the isolation of **L1Pd8** as a mixture of two diastereomeric species, which were present in unequal amounts in solution, as commonly found for allylpalladium complexes with chiral monophosphine ligands.[110] Therefore, in the ^1H NMR spectrum two sets of three allylic peaks were found, as expected (Figure 28).

Figure 28. ^1H NMR(400 MHz, CDCl$_3$, 25 °C) Selected allylic region of **L1Pd8**. Circled minor peaks belong to the other diastereomer of **L1Pd8**.

The $^{31}P\{^1H\}$ NMR data is consistent with the presence of two diastereomers, where two singlets at +131.2 ppm and +125.1 ppm, respectively, can be clearly seen.

All this results were also supported by mass spectrometry, showing the monoisotopic [M–Cl]$^+$ adduct as major fragmentation.

Discussion of the possible diastereoisomers for **L1Pd8** is identical to the one exposed for the η^3-2-Me-allyl complexes if we assume that the phenyl groups are

always located in *syn*, due to steric hindrance, as it is found for related complexes of this type.[110]

Allyl-Pd(II) systems bearing two phosphine ligands are mainly cationic[111] and can be prepared by reaction of the corresponding dimer with 4 eq. of the ligand and an inorganic salt with halide-abstractor properties, typically NH_4PF_6 or NH_4BF_4.[111b] In our case, however, the formation of the anionic pseudobidentate bridge triggered neutral complexes, the driving force being of the reaction the formation of the intramolecular six-membered ring.

We studied the reaction of (*S*)-L1 with $[Pd(\eta^3\text{-}2\text{-Me-allyl})Cl]_2$, $[Pd(\eta^3\text{-}1\text{-Ph-allyl})Cl]_2$ and $[Pd(\eta^3\text{-}1,2\text{-Ph}_2\text{-allyl})Cl]_2$ dimers in the presence of NEt_3 as base (Scheme 43).
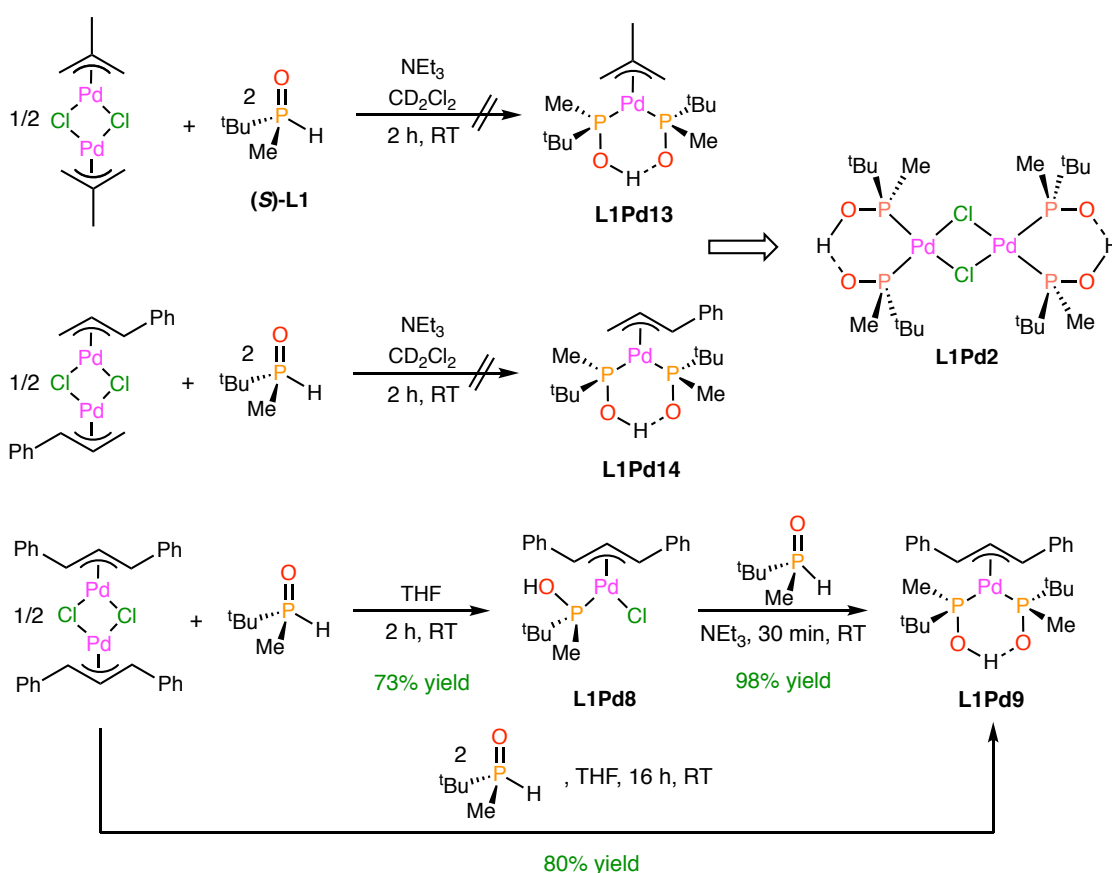
Scheme 43. Unsuccessful attempts to synthesise psudobidentate complexes **L1Pd13**, **L1Pd14** and preparation of **L1Pd9**.

In the cases of $[Pd(\eta^3\text{-}2\text{-Me-allyl})Cl]_2$ and $[Pd(\eta^3\text{-}1\text{-Ph-allyl})Cl]_2$ we were not able to obtain any of the corresponding dicoordinated allyl Pd complexes. However, even though the isolation of **L1Pd13** and **L1Pd14** complexes was not possible, we found that, interestingly, the addition of NEt_3, did not allow the obtention of the desired allylic compounds, but surprisingly **L1Pd2** was obtained instead.

The formation of the pseudobidentate bridge in solution could be achieved with the synthesis of **L1Pd9**, obtained by treatment of **L1Pd8** with one equivalent of **(S)-L1** in the presence of NEt$_3$ or directly reacting [Pd(η^3-1,2-Ph$_2$-allyl)Cl]$_2$ with 4 eq. of **(S)-L1.** The spectroscopic characterisation of the product showed two pairs of doublets in the ^{31}P{^{1}H} spectrum at δ = 109.4 and 106.6 ppm attributed to two isomers, due to the different spatial orientation of the allyl group (Figure 29).
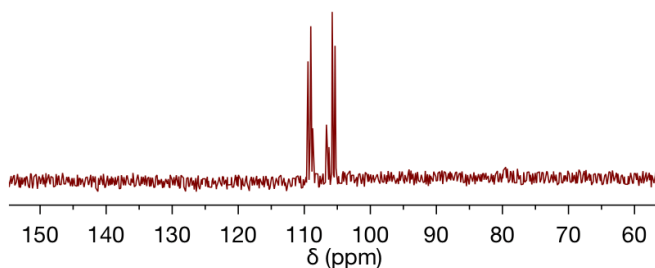
Figure 29. ^{31}P{^{1}H} NMR(162 MHz, CD$_2$Cl$_2$, 25 ºC) spectrum of **L1Pd9**.

The experiment was repeated without triethylamine but in the presence of excess of NH$_4$PF$_6$ in order to form the cationic bis(phosphinous acid) complex[112] but after aqueous work-up only **L1Pd9** could be isolated, highlighting the stability of the anionic bridge.

Although all the considerations about the geometry and the fluxional processes already described for the monocoordinated complexes are also present for allyl Pd systems with two ligands, very sharp and well-defined signals were obtained in all the NMR measurements. A clear example is depicted in the ^{1}H NMR, which also agrees with the proposed structure of **L1Pd9** where the three peaks, central, and terminal of the allyl fragment are present (Figure 30).
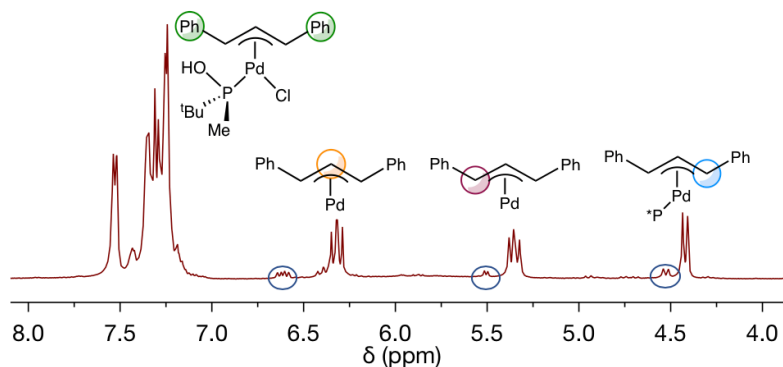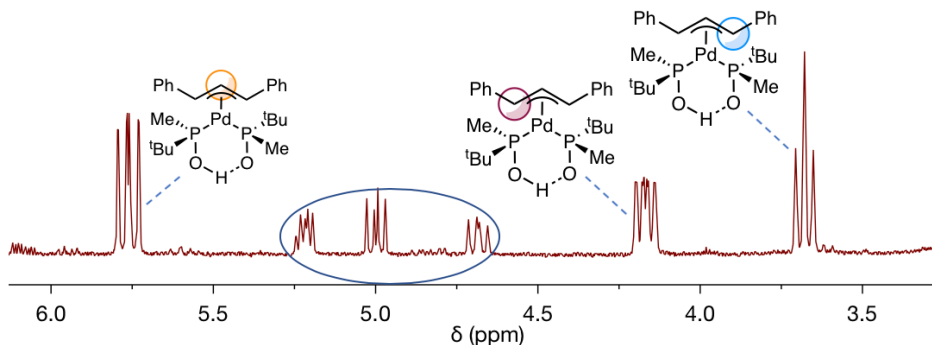

Figure 30. ^{1}H NMR(400 MHz, CDCl$_3$) Selected allylic region of **L1Pd9**. Circled peaks belong to the minor diastereomer of **L1Pd9**.

The duplication of the signals is due to the formation of the other diastereomer in an unequal amount.

Finally, for those complexes bearing the pseudobidentate architecture, a treatment with $HBF_4 \cdot OEt_2$ was carried out in order to form a BF_2 bridge, leading to the corresponding bidentate ligands (Scheme 44).
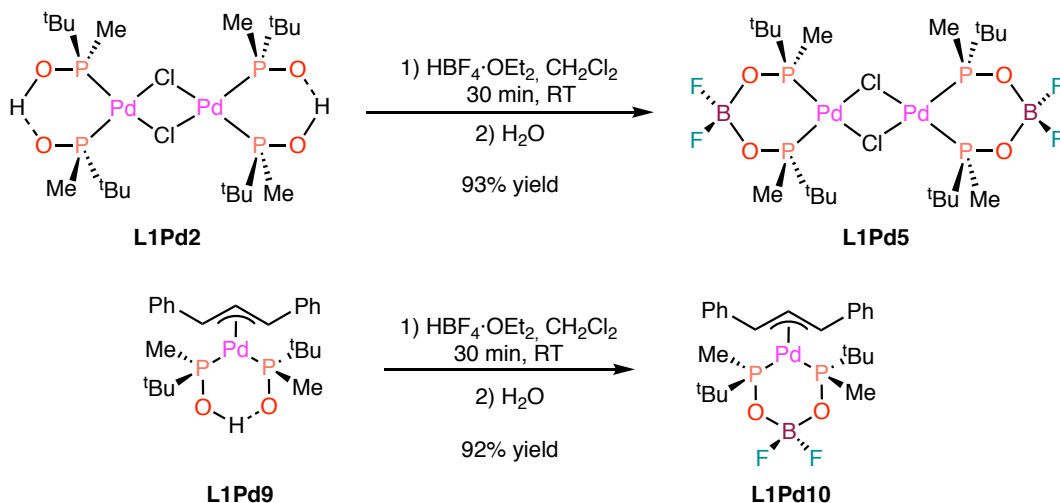
Scheme 44. Substitution of the OH bridge by the BF_2 unit in **L1Pd2** and **L1Pd9**.

The reaction worked smoothly for **L1Pd2**, giving dinuclear complex **L1Pd5**, which showed a triplet at δ = 138.9 ppm with a $^3J_{FP}$ = 6.6 Hz in the ^{19}F NMR due to the coupling of the fluorine atoms with the two equivalent phosphorus atoms. The presence of another adjacent triplet is due to the minor isotopologue of boron (^{10}B), as expected (Figure 31).
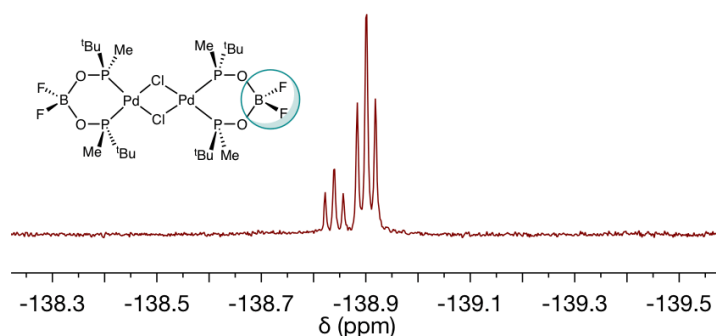
Figure 31. ^{19}F NMR (376 MHz, $CDCl_3$, 25 °C) of complex **L1Pd5**.

The same procedure was followed with **L1Pd4** and the same pattern was observed in the ^{19}F NMR but the presence of acetates could no be inferred from the ^{1}H NMR spectrum when the reaction was carried out with $HBF_4 \cdot OEt_2$.
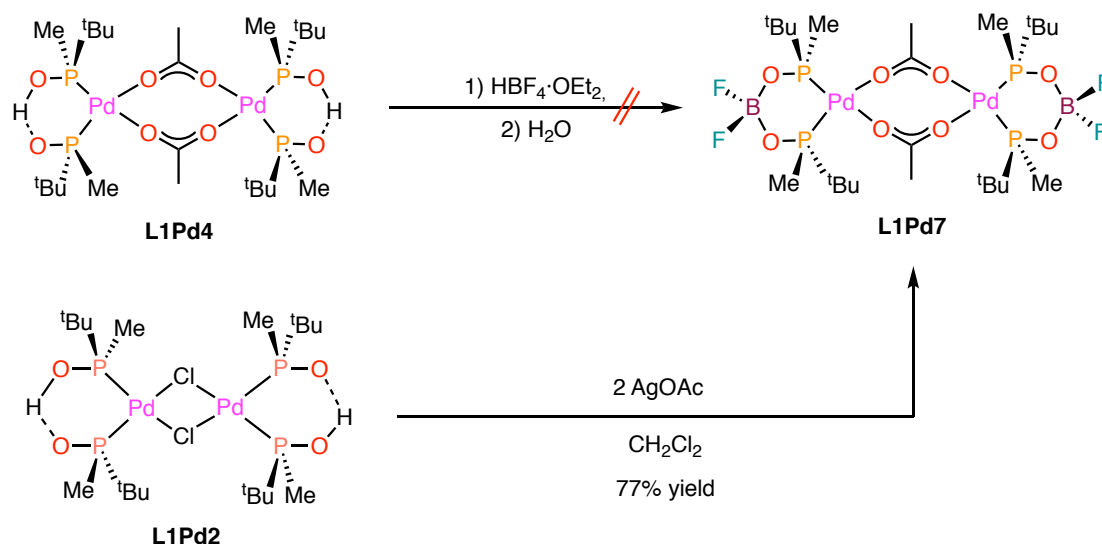
Scheme 45. Preparation of dinuclear complex **L1Pd7**.

However, we were able to obtain **L1Pd7** in moderate yield by treatment of the preformed complex **L1Pd2** with AgOAc. In this case, the signals of the methyl group of the acetato bridging ligand can be seen in the ^{1}H NMR (Figure 32). As it is shown in the spectrum, all the signals (Me, Me–P and ^{t}Bu–P) appeared duplicated in an unequal amount. These peaks are assigned to the minor mononuclear BF$_2$-bridged complex. Since we found, as it has been discussed, that without the addition of the silver salt, both species (monomer and dimer) coexist in equilibrium.
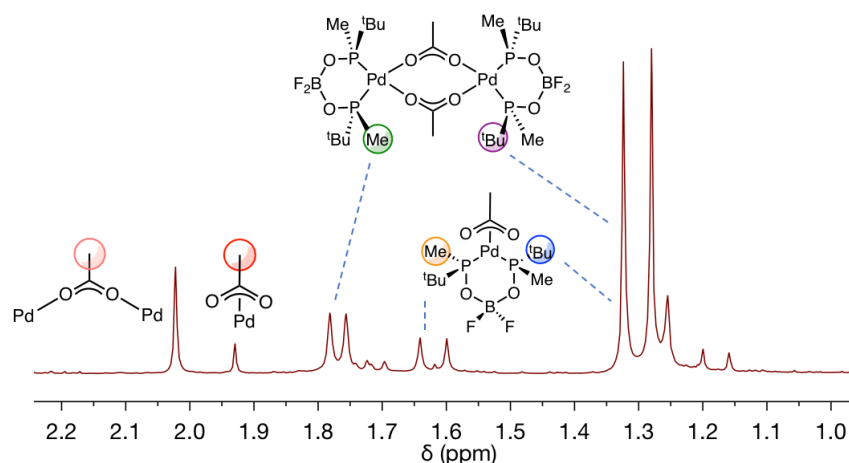
Figure 32. ^{1}H NMR(400 MHz, CDCl$_3$) Alkyl region of **L1Pd7**.

Furthermore, the ν_{CO} bands at 1610 cm^{-1} in the infrared spectrum also confirm the presence of the coordinated acetates of **L1Pd7**.

In the case of the allylpalladium complex **L1Pd9**, the BF$_2$-bridged complex **L1Pd10** could be straightforwardly obtained and was found to be very stable even in

the presence of water. In this case, a multiplet is observed in the ^{19}F NMR centred at δ = 138.9 ppm due to the non-equivalence of the P atoms, as a consequence of the allyl moiety. This can be clearly seen in the ^{31}P{^{1}H} NMR spectrum, which shows a pair of doublets at +125.9 and 118.3 ppm with a $^2J_{PP}$ of 81.0 Hz.

The X-ray crystal structure of *ent*-L1Pd10, could be obtained and a molecular representation of the complex is depicted in Figure 33.
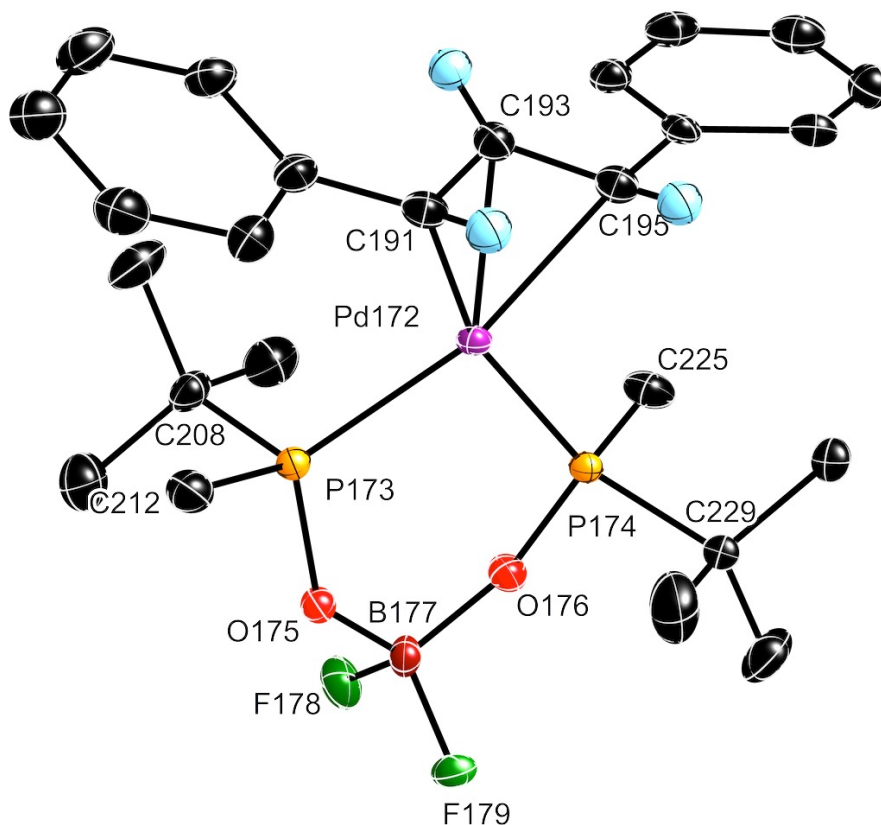
Figure 33. Molecular structure of complex *ent*-L1Pd10 (thermal ellipsoids drawn at 50% probability level). Most of the H atoms have been omitted for clarity.

Table 10. Selected bond length (Å) and angles (º) of *ent*-**L1Pd10**.

Bond	Length (Å)	Angle	(º)
Pd172–P173	2.291(7)	P173–Pd172–P174	91.68(12)
Pd172–P174	2.300(9)	C195–C193–C191	120.15(02)
Pd172–C191	2.246(7)	C208–P173–O175	100.31(43)
Pd172–C193	2.222(3)	C212–P173–O208	105.41(57)
Pd172–C195	2.271(2)	C212–P173–O175	104.63(15)
C191–C193	1.410(9)	C225–P174–O176	100.97(63)
C193–C195	1.398(2)	C229–P174–C225	104.27(32)
P173–C208	1.826(9)	C229–P174–O176	104.47(96)
P173–C212	1.854(2)	F178–B177–F179	109.54(06)
P174–C225	1.794(5)	O175–B177–O176	111.38(58)
P174–C229	1.847(4)	F178–B177–O176	105.81(55)
P174–O176	1.593(4)	F179–B177–O175	109.89(79)
B177–O175	1.462(8)	F178–B177–O175	109.75(02)
B177–O176	1.511(3)	F179–B177–O176	110.36(54)
B177–F178	1.360(5)		
B177–F179	1.375(5)		

Compound ***ent*-L1Pd10** represents the first described example of an allylpalladium complex with an optically pure SPO ligand. The Pd centre has a square-planar geometry and the absence of a counterion proves the anionic nature of the BF_2 bridge. The average Pd-Callyl distance is around 2.24 Å, the bridge O–B–O has an angle of 112.4º and the local geometry of boron atom is approximately tetrahedral. This bridge however is not symmetrically disposed a fact that makes that only one of the oxygen atoms, O(176), is in P–Pd–P plane. This is in line with the observation of the non-equivalence of the F atoms in solution observed by NMR.

3.4. *Catalysis with enantiopure t-BuMeP(O)H*

The potential application of *P*-stereogenic phosphines and derivatives in asymmetric catalysis has been widely explored in many organic transformations.[113] In terms of chiral induction, the use of bidentate phosphines over monodentate systems have derived in superior enantioselectivities, especially in asymmetric hydrogenation reactions.[114]

In this line, it is noteworthy to mention the family of *P*-stereogenic diphosphines reported by Imamoto and co-workers[46c,115] bearing the sterically dissymmetric tBu/Me combination. Ligands such as BisP*,[115l,116] MiniPhos,[115h,116-117] TrichickenfootPhos,[118] QuinoxP*,[119] BenzP*,[120] MaxPhos, developed in our group,[46b,121] or PCP pincer diphosphines[115n,122] (Figure 34) have yielded outstanding enantioselectivities in the asymmetric hydrogenation of functionalised prochiral alkenes.

BisP*
1998

MiniPHOS
1999

TrichickenfootPhos
2004

QuinoxP*
2005

BenzP*
2006

MaxPhos
2010

PCP-pincer diphosphines
2013
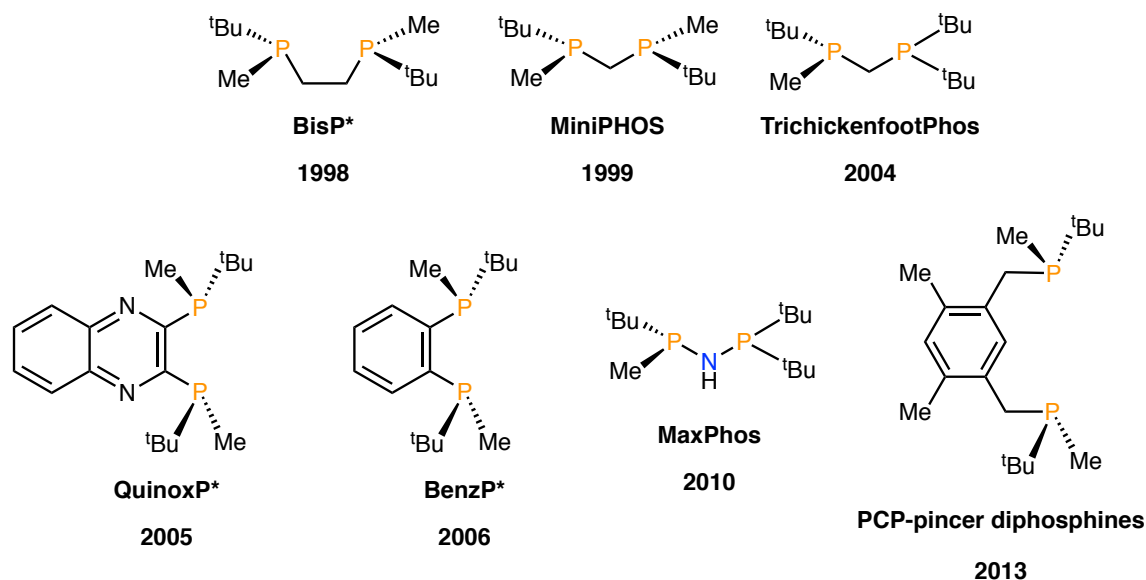
Figure 34. Selected diphosphine ligands with the tBu/Me groups at P.

Unfortunately, this kind of diphosphines is not exempt of drawbacks. The most serious is their air-sensitivity caused by the highly basic nature, which complicates their preparation and use, especially at large scale.

To overcome these difficulties, we designed our enantiopure secondary phosphine oxide **L1**, whose coordination chemistry towards several noble metals has been described in the previous sections. tBuMeP(O)H contains the dissymmetric tBu/Me combination,[46c,115] but also has the advantage of being completely air-stable. In

addition, is able to form, in some cases, a pseudobidentate bridge upon coordination to several metals (see Section 3.3.2).

The idea of forming supramolecular assemblies for its potential use in catalysis is an area of intensive research that have met success in some important catalytic transformations.[67,123]

Whereas the traditional ligand concept is based on the covalent attachment of donor atoms to a general backbone, such as in the "classic" diphosphines prepared by Imamoto's group, other strategies make use of dynamic self-assembly processes for the formation of *pseudobidentate* ligands, as it is the case in the SPO system presented in this thesis (Figure 35).

Bidentate ligand   *Pseudobidentate* **ligand**
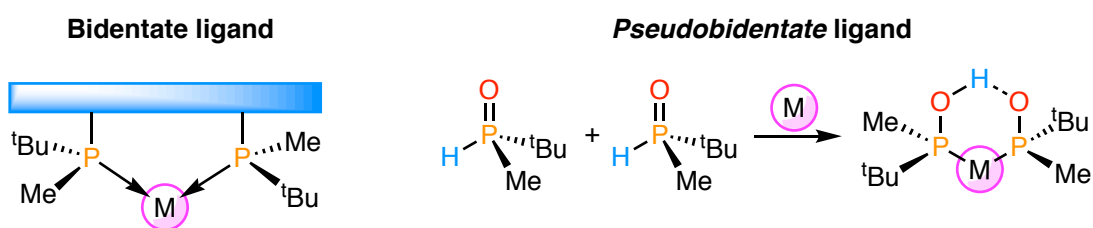
Figure 35. Bidentate ligand through a covalent attachment (left) and a self-assembly process of two monodentate ligands (right).

This approach represents a breakthrough in the design of new ligands, since it is *par essence* a modular route to envisage new and useful bidentate ligands. Among all the non-covalent interactions, hydrogen bonds play a prominent role in self-assembly processes for the generation of such bidentate architectures.

Since 1986 when Van Leeuween and co-workers reported the first application of SPOs on the Pt-catalysed hydroformylation of olefins,[124] the use of these systems have gained great interest. However, at present, there is still little research about the potential use of such catalysts in asymmetric catalytic reactions.

Hence, with all this in mind, the use of **L1** as a potential catalytic system for some model asymmetric reactions is presented through the following sections.

3.4.1. *Ir-catalysed enantioselective hydrogenation of N-aryl imines*

Although the field of enantioselective homogeneous hydrogenation is clearly dominated by Rh(I) and Ru(II) systems, it is closely followed by Ir(I) complexes, whose potential is being intensively explored at present. In particular, excellent results have been achieved for unfunctionalised alkenes and imines using Ir-based systems.

Imines are privileged substrates for the preparation of chiral amines, which are useful building blocks for final chemical, agrochemical and pharmaceutical industries. Among the variety of methods to prepare these substrates hydrogenation have proven to be one of the most efficient and clean methodologies.

The hydrogenation of imines is challenging because is difficult to find catalysts providing high enantioselectivity, broad applicability and acceptable rates at moderate hydrogen pressures.[125], Additional complications are the exchange between *E* and *Z* isomers in the case of acyclic substrates, the tendency to racemisation of the secondary amines obtained after the reaction and the inhibition of the catalyst by amine coordination. Iridium complexes are finding increased application in this reaction, where the most common substrates are (*E*)-*N*-aryl imines derived from acetophenone (Scheme 46).
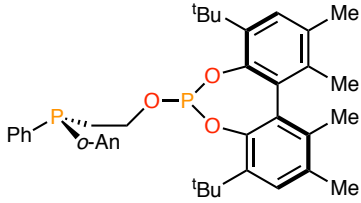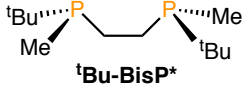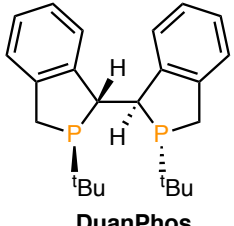
With these substrates, very good results have been obtained with several *P*-stereogenic ligands.[113c] Some of them are listed in Table 11.
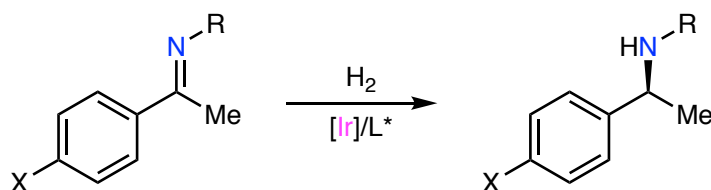
Scheme 46. Ir-catalysed hydrogenation of (*E*) imines derived from acetophenone.

Table 11. Results in the enantioselective hydrogenation of some (*E*) imines derived from acetophenone.

Entry	X	R	Ligand	*ee* (%)	References
1	H	Bn		82 (*S*)	
2	OMe	Bn		83	35b
3	H	Ph		0	
4	H	Ph	C₂-BIPNOR	57 (*R*)	126
5	H	Ph	TangPhos	73 (*R*)	127

6	H	Ph		84 (*R*)	128
7	H	Ph		86 (*R*)	129
8	H	*p*-CF$_3$C$_6$H$_4$		99	
9	H	Ph		93 (*R*)	127

Although the best results have been achieved with bidentate systems (entries 4 to 9) it is interesting to note that the secondary phosphine oxide *tert*-butylphenylphosphine oxide (entries 1 and 2) has lead to moderate *ee* for the hydrogenation of these substrates. Interestingly, the parent case represents the only reported example of a *P*-stereogenic SPO that has been successfully employed in this kind of transformations. Other secondary phosphine oxides did not lead to any improvement, and the scope of the reaction was very limited. Proof of this can be found in entry 3 where *N*-phenyl imine gave a racemic with this SPO and other secondary phosphine oxides.

With all this in mind, we prepared some *N*-aryl imines in order to study the potential catalytic application of our optically pure **L1** SPO.

3.4.1.1. *Synthesis of N-aryl imines*

Among the different methods to prepare imines, the most straightforward method is by condensation between a primary amine and a ketone or and aldehyde.[130]
We successfully prepared five *N*-aryl imines via condensation with the corresponding acetophenone derivative in a diethyl ether solution at 0 ºC using TiCl$_4$ as desiccant (Scheme 47).[130a]

X = H, R = Ph **I1 (70%)**
X = OMe, R = Ph **I2 (60%)**
X = H, R = 4-OMe-C$_6$H$_4$ **I3 (65%)**
X = H, R = Bn **I4 (80%)**
X = H, R = CH(Ph)$_2$ **I5 (75%)**
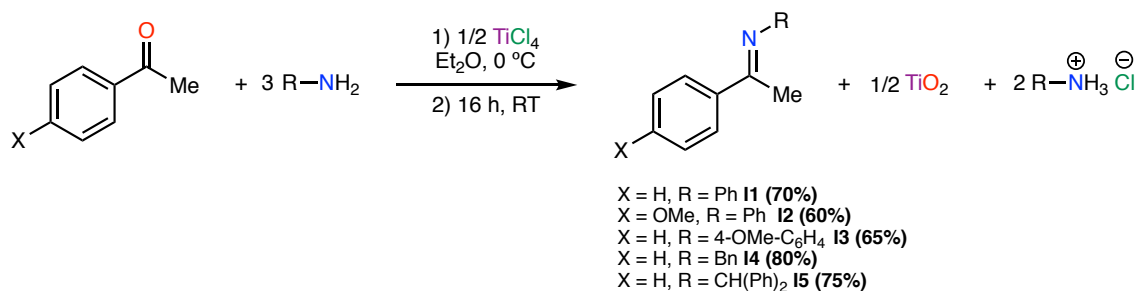
Scheme 47. Preparation of *N*-aryl imines **I1**, **I2**, **I3**, **I4**, and **I5**.

In those cases where a later purification was required, crystallization or vacuum distillation were the methods of choice, since SiO$_2$ often decomposes this kind of substrates.

3.4.1.2. *Ir-catalysed asymmetric hydrogenations with (R)-L1*

Due to the extremely instability of the Ir species formed with our optically pure (*R*)-**L1** (Section 3.3.2.2) we performed the catalytic essays "*in situ*" using 2 eq. of the ligand in order to ensure the enough amount of **L1** in solution as it was described for the ^{t}BuPhP(O)H by Feringa, de Vries and co-workers (Scheme 48).[35b]

X = H, R = Ph **I1**
X = OMe, R = Ph **I2**
X = H, R = 4-OMe-C$_6$H$_4$ **I3**
X = H, R = Bn **I4**
X = H, R = CH(Ph)$_2$ **I5**
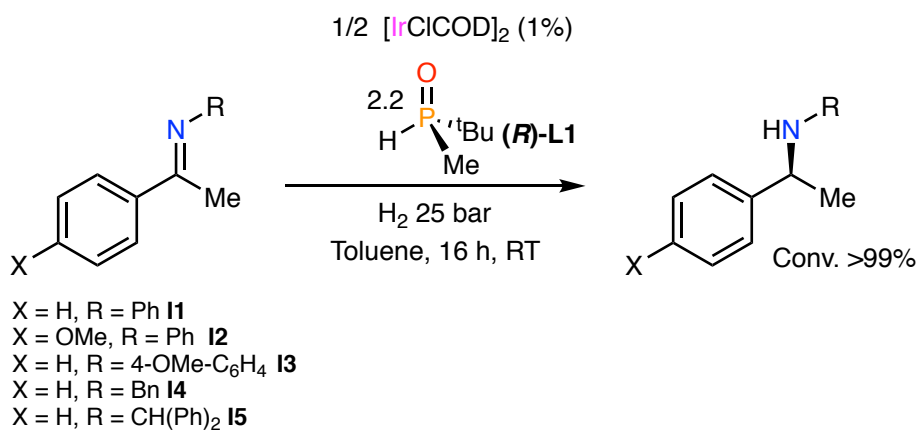
Scheme 48. "*In situ*" Ir-catalysed hydrogenations with (*R*)-**L1**. Conversions were expressed as consumption of the corresponding substrates determined by ^{1}H NMR and HPLC. Enantioselectivities were determined by HPLC.

All the substrates tested led to a 100% conversion under 25 bar of hydrogen, after 16 h at room temperature, employing [IrCl(COD)]$_2$ dimer as metallic precursor. The hydrogenated products were easily characterised by ^{1}H NMR due to the appearance of a quadruplet around 4–5 ppm (*J* ≈ 7 Hz) indicated the presence of a new proton in the iminium carbon. These high activities found for the present Ir system agree with the fast reactivity and instability observed for the Ir complexes studied.

129

Unfortunately, HPLC analysis showed that the amines were racemic, which indicates that the ligand, even in the case of forming a *pseudobidentate* architecture, does not create an efficient chiral environment around the Ir centre.

Finally, in spite of the very low *ee* obtained, it is noteworthy to mention that even though P-P "real" bidentate ligands have led to good results in the Ir-catalysed hydrogenation of *N*-aryl imines as it has been shown in Table 11, the best enantioselectivities are found in P-N systems, which perform better this kind of transformations.[131] Examples of useful P-N ligands and our contribution to the field will be developed in detail in Chapter 5.

3.4.2. *Rh-catalysed enantioselective hydrogenation of functionalised olefins*

Asymmetric hydrogenation constitutes the most important reaction in enantioselective homogeneous catalysis and it is the responsible of the development of the whole field.[113c] Since the discovery of the Wilkinson catalyst, [RhCl(PPh$_3$)$_3$], most of the work on hydrogenation has been carried out with functionalised alkenes as substrates and Rh(I) complexes as catalytic precursors.

Among the typical substrates to test the efficiency of new Rh(I) catalysts in these reactions, α-dehydroamino acids are the most routinely used, since it is one of the principal routes to obtain optically pure α-amino acids (Figure 36).

<div align="center">

α-Dehydroamino acid derivatives

</div>

(*Z*)-α-acetamidocinnamic acid (**ACA**)   Methyl (*Z*)-α-acetamidocinnamate (**MAC**)

α-acetamidoacrylic acid (**AAA**)   Methyl α-acetamidoacrylate (**MAA**)
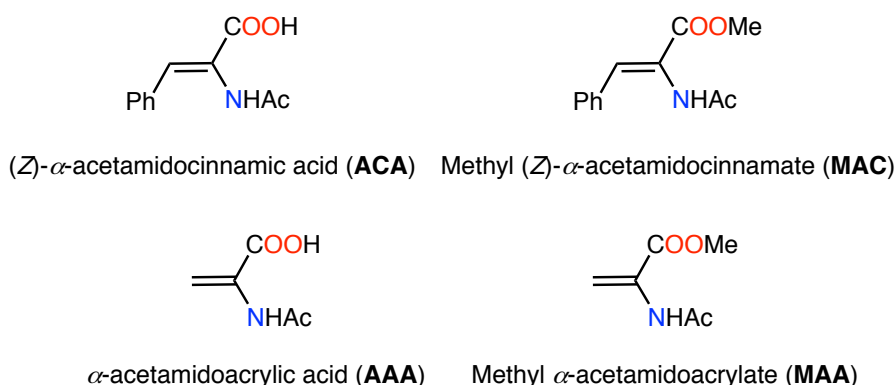
Figure 36. Typical substrates for Rh-catalysed asymmetric hydrogenation.

The most commonly employed substrates are (*Z*)-α-acetamidocinnamic acid (ACA), its methyl ester (MAC), acetamidoacrylic acid (AAA) and its methyl ester (MAA). Quantitative yields at mild hydrogen pressure (1–3 bar) are usually employed for this

kind of substrates, displaying *ee* equal or higher than 99% with many ligands[125], especially with *P*-stereogenic phosphines.

Basic diphosphines, having the dissymmetric ᵗBu/Me are among the best ligands for Rh-catalysed hydrogenation reaction of α-dehydroamino acids. Examples of such ligands for the enantioselective hydrogenation of MAA are depicted in Table 12.
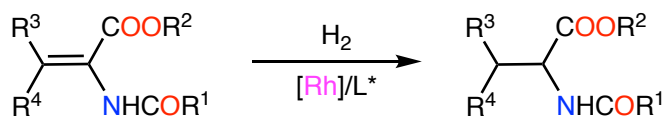
Scheme 49. Rh-catalysed asymmetric hydrogenation of α-dehydroamino acid derivatives.

Table 12. Selected ligands for the Rh-catalysed hydrogenation reaction of MAA.

Entry	R^1	R^2	R^3	R^4	Ligand	*ee* (%)	References
1	Me	H	H	H	R-MiniPhos	R = ᵗBu >99.9 (*R*)	132
2	Me	H	H	H	R-MiniPhos	R = Cy 99.1 (*R*)	132
3	Me	H	H	H	R-MiniPhos	R = ⁱPr 98 (*R*)	115h
4	Me	H	H	H	TrichickenfootPhos	>99 (*R*)	118a,133
5	Me	H	H	H	R-BisP*	R = ᵗBu 98.1 (*R*)	115b
6	Me	H	H	H	R-BisP*	R = Ad >99.9 (*R*)	115k
7	Me	H	H	H	MaxPhos	>99.9 (*S*)	46b

These functionalised alkenes are the most suitable and successful substrates for this kind of transformations due to the mechanism of the reaction, since they are able to chelate the rhodium atom during the catalytic cycle through the alkene and an additional donor atom, usually the carbonylic oxygen of an amide or an ester.

The mechanism of asymmetric olefin hydrogenation is the most extensively studied mechanism in homogeneous catalysis, therefore the associate literature is so

vast[134] that it would be impossible to give a detailed account in a few paragraphs. Especially, because new details and subtleties are continuously being reported.[135]. Despite all this activity, we are still far from a complete mechanistic understanding.[136]

Broadly speaking, there are two general mechanisms commonly known as *unsaturated* and *dihydride* (Scheme 50).
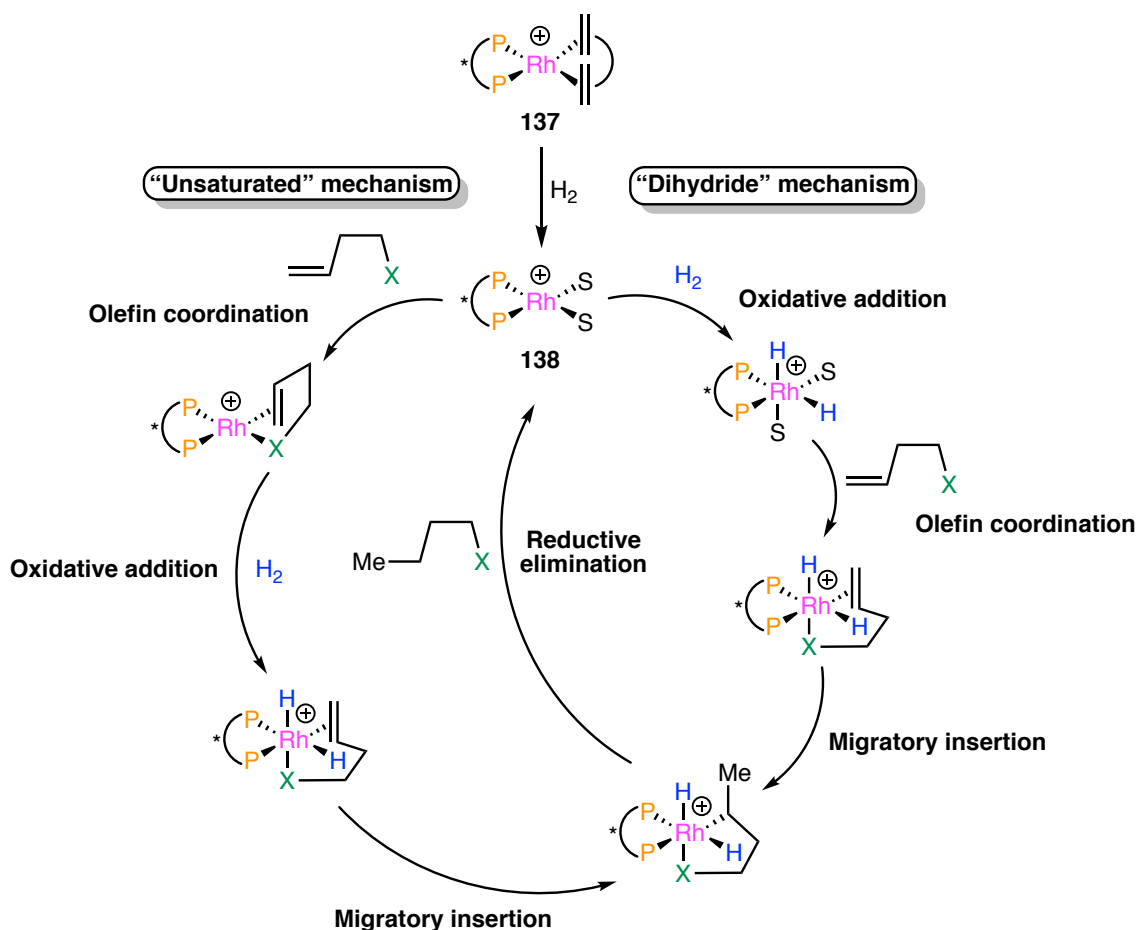
Scheme 50. The two accepted mechanisms of hydrogenation of functionalised olefins with Rh(I) systems.

As it is shown, both mechanisms take place through the same elementary steps involving similar Rh(I)/Rh(III) species, where the main difference is the order of substrate coordination/oxidative addition of dihydrogen at catalyst **138**. The usual precursors for **138** are cationic Rh(I)/diphosphine complexes **137** with dialkenes, such as COD, with weakly coordinating anions such as PF_6, BF_4, or BAr_F. Under hydrogen atmosphere, the coordinated alkene is easily hydrogenated and released to form the bis(solvato) complexes **138**.[137] These species show high affinity for dehydroamino acids, due to the bidentate complexation of the substrate to form a *bis*(chelated) complex.[138] Oxidative addition of hydrogen is thought to render Rh(III) dihydride

complexes, which suffer migratory insertion of the alkene into the Rh–H bond to afford alkyl-hydride complexes[137b,139] that collapse by reductive elimination to afford the hydrogenated substrate and regenerate the catalyst.

When it comes to the use of SPOs as ligands for Rh(I)-catalysed hydrogenation reactions only a very few studies have been carried out. Feringa, de Vries and co-workers[69] used the optically pure ^{t}BuPhP(O)H, which was successfully applied in the hydrogenation of imines, for the "*in situ*" asymmetric hydrogenation of *N*-acyl dehydroamino acids and esters. However, the reaction gave low enantiomeric excesses employing the cationic [Rh(COD)$_2$]BF$_4$ precursor, even though they found that switching the solvent in some dehydroamino acids from EtOAc to CH$_2$Cl$_2$ led to the opposite enantiomer.

Better results were published in 2014 by Han and co-workers,[71] who described the "*in situ*" Rh-catalysed hydrogenation of α-acetamidocinnamates using optically pure menthylphenylphosphinates, achieving enantioselectivities up to 99.6%. They were able to grow suitable crystals for X-ray determination of a solution with [Rh(COD)$_2$]OTf and the ligand ^{t}BuPhP(O)H and they found that the complexes formed did not contain the expected pseudobidenate bridge, but a OTf$^-$ moiety instead (Figure 37).[71]
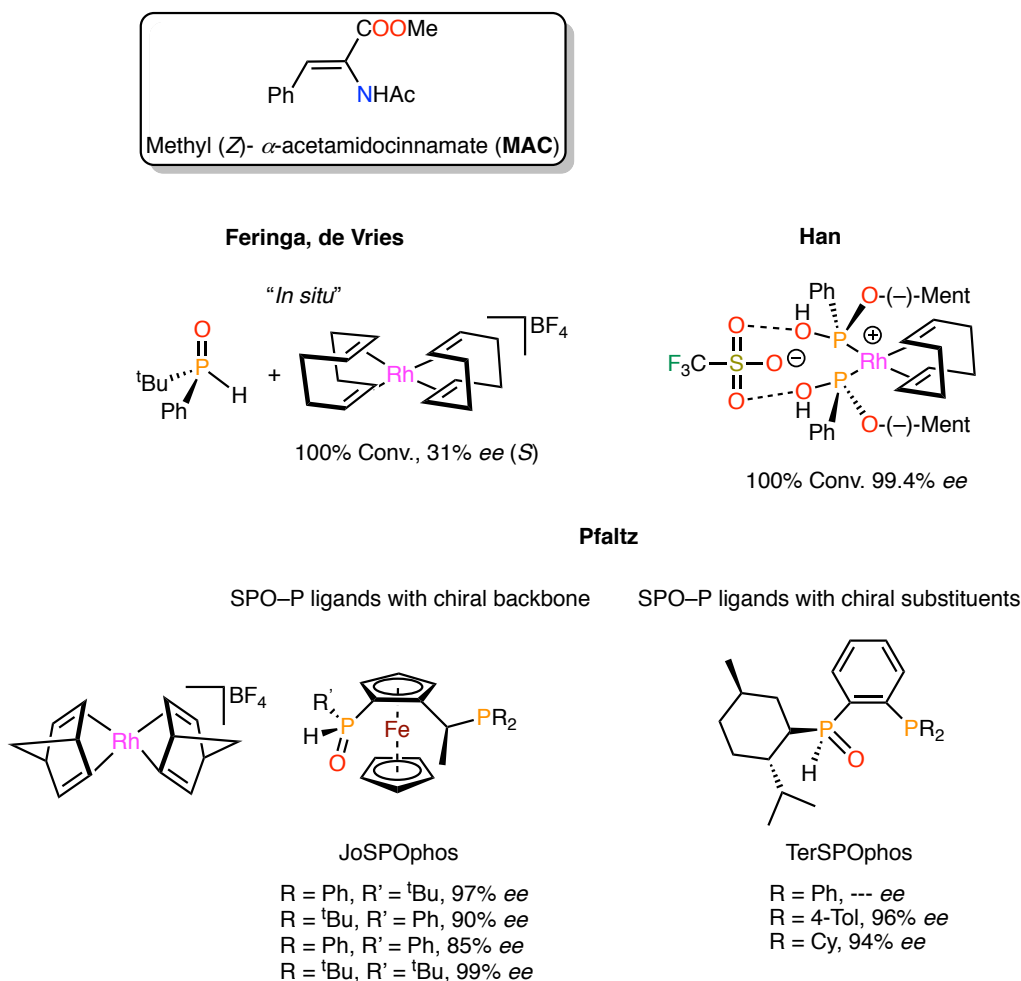
Figure 37. Rh(I)-catalysed asymmetric hydrogenation of MAC with chiral SPOs.

The best results in the field, however, were reported by Pfaltz and co-workers[60c] who thought that the scarce research done were due to the insufficient affinity of the SPO for Rh. With this in mind, they successfully combined an SPO with PR_2 moiety, which should not only lead to a stronger coordination to the metal but also should give better-defined complexes. Indeed they successfully prepared two SPO–P ligands with the chirality on the backbone but also with a chiral SPO (Figure 37).

The first SPO–P family was based on a chiral ferrocenyl backbone, which leads to ligands similar to the well-known Josiphos[140] while the second gives menthyl derivatives. Both families were tested in the hydrogenation of α-acetocinnamates achieving the best results reported for these SPO systems, displaying enantioselectivities up to 99% *ee*.

With this background in hand, we envisaged the asymmetric hydrogenation of several α-dehydroamino acids (MAA and MAC), the α,β-unsaturated carboxylic ester dimethyl itaconate (DMI), and the allylic alcohol *trans*-3,7-dimethyl-2,6-octadien-1-ol or

geraniol with our optically pure ligand **(*R*)-L1** (2 eq.) with [Rh(COD)$_2$]BF$_4$ as metallic precursor at 3 bar of H$_2$ for 16 h (Scheme 51).

R^3 = R^4 = H, R^1 = CH$_2$COOMe, (**DMI**), 90% conv.
R^3 = R^4 = H, R^1 = NHAc, (**MAA**), 100% conv.   <5% *ee*
R^3 = H, R^4 = Ph, R^1 = NHAc, (**MAC**), 100% conv.
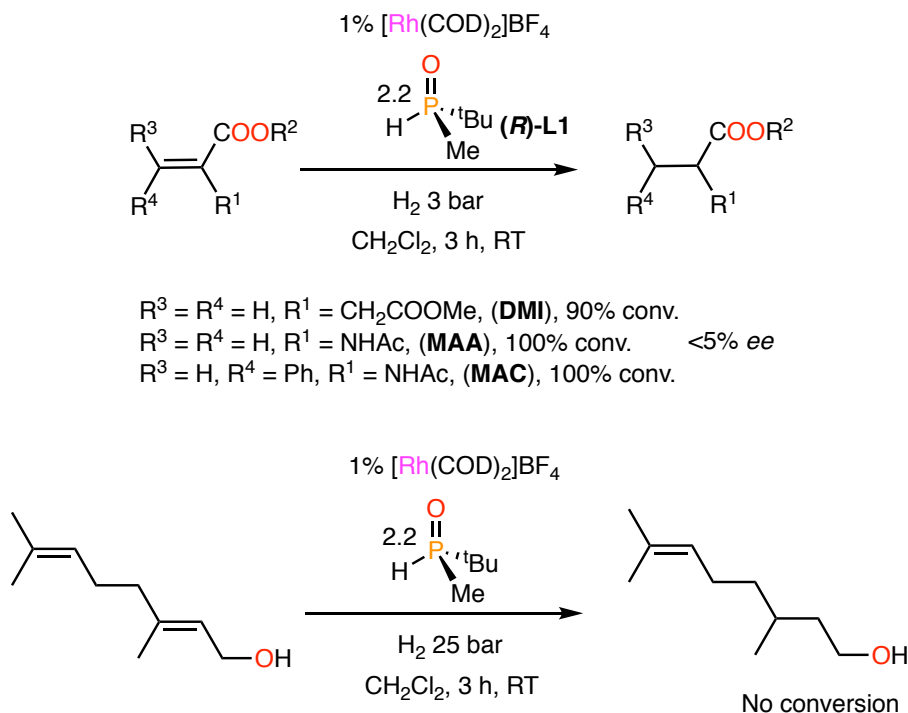
Scheme 51. Catalytic results for the hydrogenation of different substrates with **(*R*)-L1**. Conversions are expressed as consumption of the corresponding substrates and were determined by GC.

Interestingly, MAC, MAA were fully hydrogenated after 3 h of reaction, whereas a 90% of conversion was achieved for DMI as it was determined by GC but with a disappointingly low *ee* of around 5%. Reaction with geraniol as substrate was completely unsuccessful even increasing the pressure of hydrogen until 25 bar.

In spite of the low *ee* obtained, the systems studied are very active in the hydrogenation of this kind of substrates. Particularly interesting to note is that, in the literature, the only Rh-based systems with SPOs that have achieved very high enantioselectivities are those bearing a "true" bidentate ligand, due to coordination of an anion[71] in the bridge, or simply having a backbone between the two phosphine units.[60c] It seems, therefore, that pseudobidentate ligands formed by association of two SPOs are not appropriate in Rh-catalysed olefin hydrogenation.

3.4.3. *Ru-catalysed enantioselective hydrogen transfer of acetophenone*

Hydrogen transfer reactions consist of a formal transfer of two hydrogen atoms from a hydrogen donor to a prochiral substrate, typically ketones, catalysed by ruthenium(II) complexes under basic conditions.[141]

The model substrate, used to test the efficiency of Ru(II) complexes, for hydrogen transfer of ketones is acetophenone with isopropanol as hydrogen source and potassium *tert*-butoxide or KOH as base (Scheme 52).
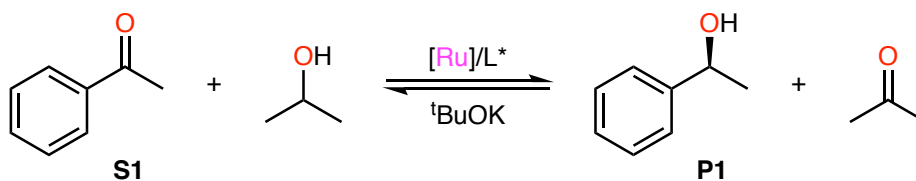
Scheme 52. Ru(II)-catalysed enantioselective hydrogen transfer of acetophenone.

The reaction has the important advantage of not involving hydrogen gas but on the downside, in some cases, the reaction is reversible and does not lead to complete conversions. It has been observed that sometimes produces racemisation of the final chiral alcohol. These problems can be minimised by performing the reaction in isopropanol as solvent.

Some results of the parent reaction with *P*-stereogenic ligands are depicted in Figure 38.
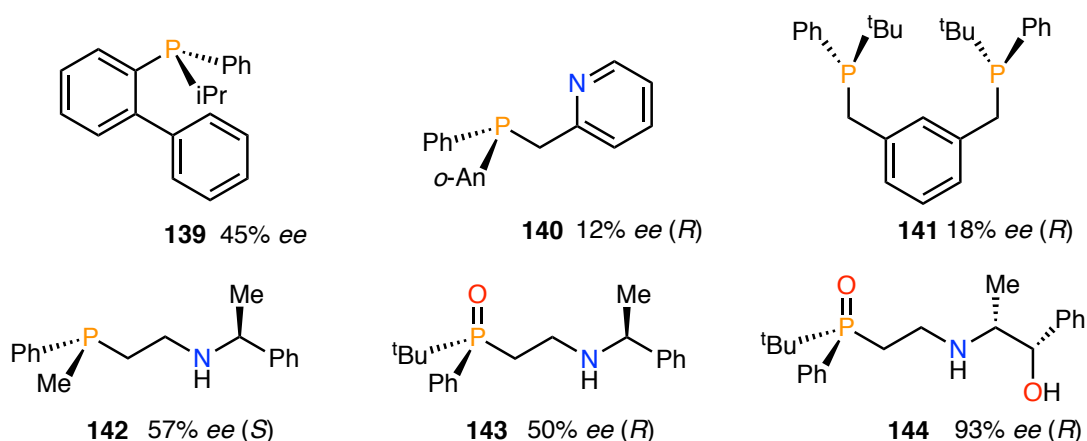
Figure 38. Results of enantioselective hydrogen transfer of acetophenone for some *P*-stereogenic ligands.

As it can be seen, moderate enantioselectivities are obtained with the monophosphine with the 2-biphenylyl group[142] low with the *P,N* ligand[143] or with a pincer ligand.[144] The best results are displayed by the β-aminophosphines and their oxides.[145] Although it has been found that phosphine oxides provide better activities and similar enantioselectivities than trivalent phosphines.[145], no experiments have been reported for this reaction with SPO ligands so far.

In terms of the mechanism of this reaction, there are numerous studies both theoretical[141g,146] and experimental[147] and even though the "true" mechanism remains unclear there are mainly two proposed pathways when a *d*-block metal is involved: the *inner sphere hydridic route*[141g] and the *outer sphere hydridic route*.[141c]

The inner sphere mechanism (Scheme 53) consists on several elementary steps being the first one the formation of the active catalytic species, in this case, the metallic hydride, formed by a Ru(II) precursor, the hydride source (in the present case isopropanol) and a strong base. This first step implies a β-elimination affording the Ru-H species and acetone. Then, the substrate is coordinated through the oxygen of the carbonyl group, which suffers a hydride insertion yielding the alkoxyde derivative. This complexation of the prochiral substrate is the key step to obtain good selectivities in the process.
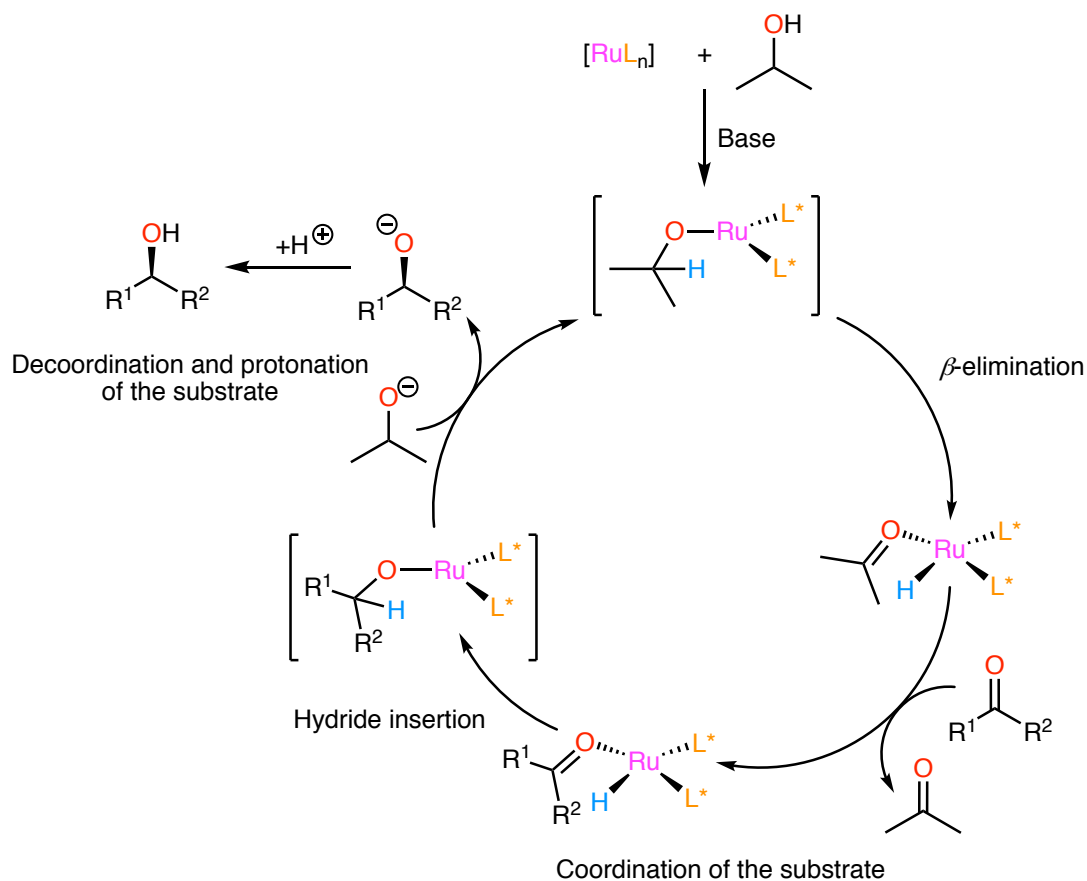
Scheme 53. *Inner sphere hydridic route* for the Ru(II)-catalysed asymmetric transfer hydrogenation of acetophenone.

The vacant coordination site is filled with an isopropoxide ligand coming from the reaction media. The presence of the coordinated isopropoxide promotes the release of the alkoxyde of the substrate, which, once protonated, affords the reaction product.

On the other hand, Noyori and co-workers[148] proposed in 1997 another mechanism based in an outer sphere approach where the substrate does not coordinate with the metallic centre. The formation of a transition state (Figure 39) allows the concerted hydrogen-transfer of two hydrogen atoms to the substrate, one coming from the metal while the other comes from the ligand.
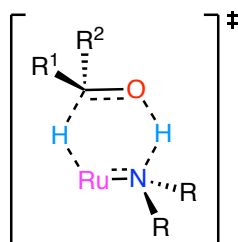
Figure 39. Transition state proposed by Noyori[148] for the hydrogen-transfer reaction of ketones.

This H-transfer can only take place if there is a M–NH fragment where NH is enough acidic to activate the ketone.

As it has been discussed there are no precedents in the literature of SPOs as potential ligands for the enantioselective hydrogen-transfer of ketones. In our case we were able to prepare and isolate three new Ru(II) complexes, **L1Ru1**, **L1Ru2** and **L1Ru3** with the secondary phosphine oxide unit, **L1**. All of them were tested in the asymmetric reduction of acetophenone, in the presence of ^{t}BuOK as base, in refluxing iPrOH. Aliquots were extracted each hour in all the three experiments respectively and the conversion was analysed by GC. The dependence of the concentration *vs* time is depicted in Figure 40.
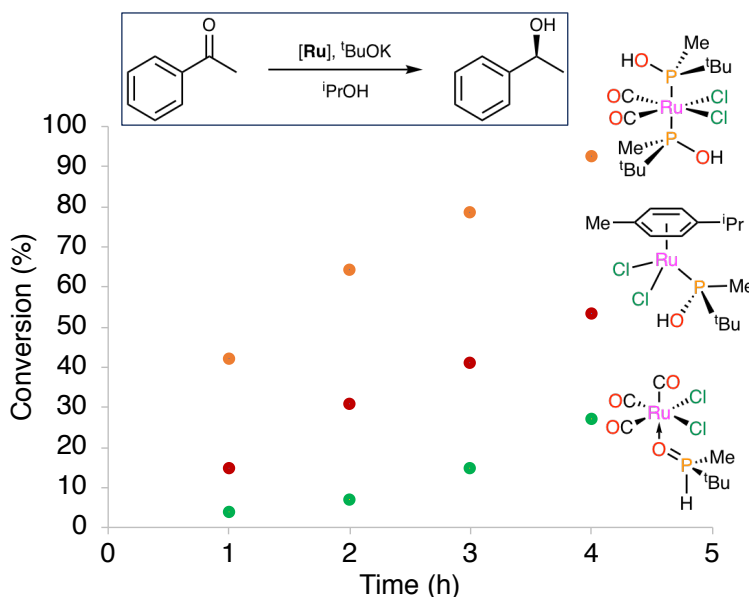
Figure 40. Conversion (%) *vs* time (h) for the Ru(II)-catalysed asymmetric hydrogen transfer of acetophenone with **L1Ru1**, **L1Ru2** and **L1Ru3**, expressed as consumption of acetophenone and determined by GC.

As it can be seen, all the complexes tested are active for the hydrogen transfer reduction of acetophenone, with bisphosphine complex **L1Ru3** being the most active one. Although all the compounds led to almost complete conversions before 5 hours, all of them did not produce any noticeable enantioselectivity. It seems that in all cases the *P*-stereogenic ligand dos not create an efficient chiral environment around the Ru atom. However, the formation of a *pseudobidentate* bridge appears difficult to occur, since the protonic solvent ^{i}PrOH, would probably inhibit the formation of such supramolecular architectures.

3.4.4. *Pd-catalysed enantioselective Mizoroki-Heck reactions*

The Mizoroki-Heck (M–H) reaction can be defined as a Pd-catalysed coupling between aryl halides, tosylates or triflates with alkenes in the presence of a base, and is one of the most important C–C bond-forming reactions (Scheme 54).

X = I, OTf, etc
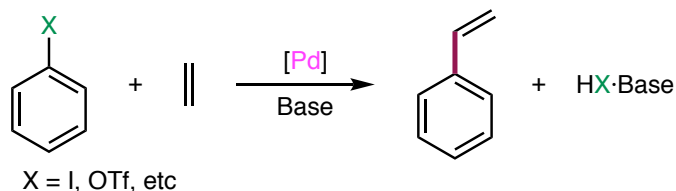
Scheme 54. General scheme of the Pd-catalysed M–H reaction.

Since its discovery in the 1970s by Mizoroki and Heck,[149] many studies have been carried out in order to improve the reaction conditions and the efficiency of the catalysts, most of them containing Pd centres.[150]

The mechanism of the reaction involves Pd(0) and Pd(II) species (Scheme 55) and its similar to other cross-coupling reactions such as the Suzuki-Miyaura, Stille or Sonogashira transformations, even though, strictly speaking, it cannot be included in this group.
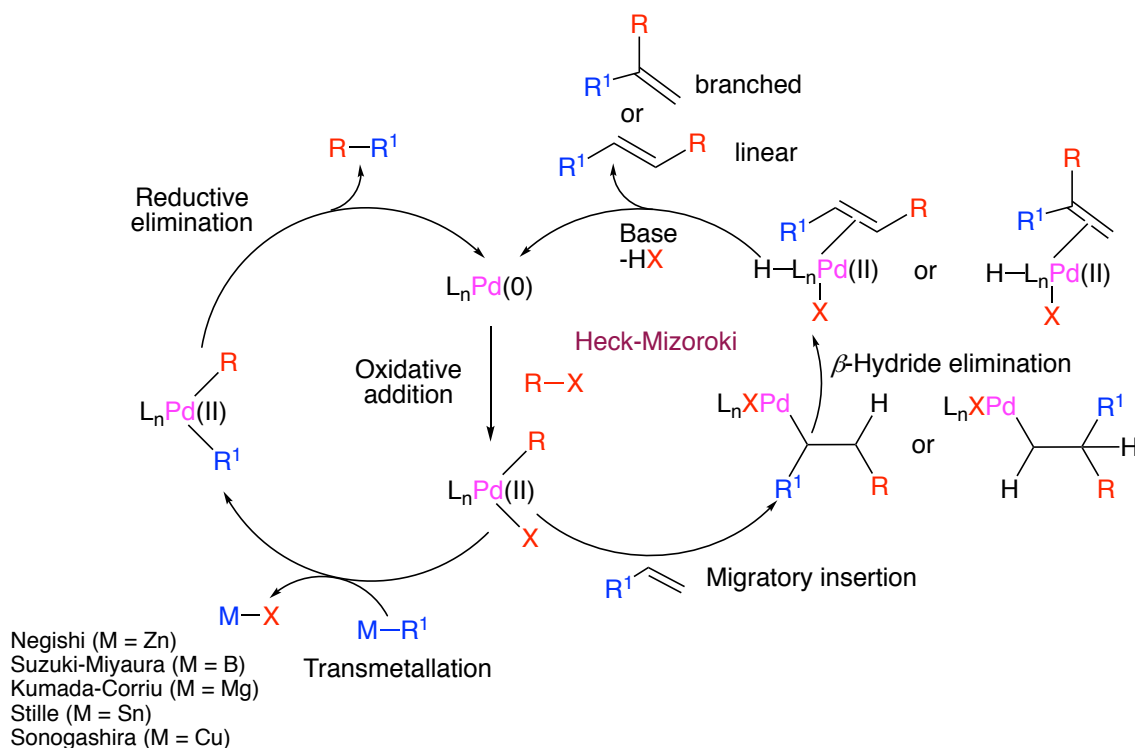
Scheme 55. General mechanism for the M–H and other cross-coupling reactions.

Nevertheless, the "true" catalyst is thought to be a Pd(0) species, which suffers oxidative addition of the aryl halide, insertion of the olefin, β-hydride elimination and a final reductive elimination to release the coupling product and regenerate the catalyst.

In principle, it would seem that the M–H reaction cannot be performed in an enantioselective fashion because it involves a Csp^2–Csp^2 coupling. However, as it has already mentioned, the mechanism of the reaction proceeds through a β-hydride elimination step. This makes that for certain substrates, the elimination creates a Csp^3 centre more easily than the usual Csp^2 centre. This behaviour has been observed for small cyclic substrates, such as dihydrofuran or cyclopentene, whose α-β-C–C bonds cannot rotate freely before the proton elimination step.

Although in the original version no stereocentres were formed, the enantioselective variant was developed and has received much attention for the last two decades.[151] Actually, in the literature, the asymmetric M–H reaction has been described intra- and intermolecularly for cyclic substrates (Scheme 56).
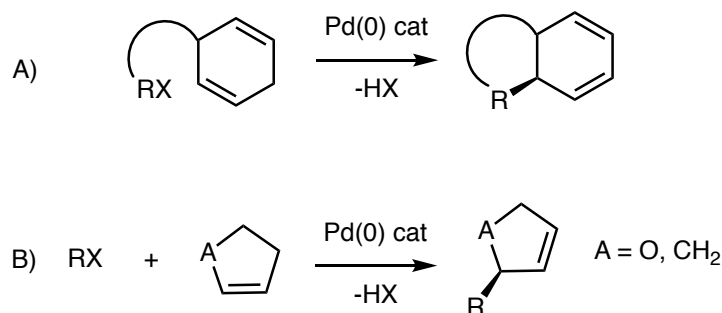
Scheme 56. General schemes of the intramolecular (A) and intermolecular (B) M–H reactions.

Nowadays, the asymmetric intramolecular Heck reaction constitutes a reliable method to build tertiary and quaternary stereocentres in complex molecules and is an important tool in natural product synthesis.[151a]

In contrast, the intermolecular version is much less developed, since it is more difficult to achieve good regio- and enantioselectivities.[151b] The model reactions consist of the coupling between aryl halides and triflates with 2,3-dihydrofuran or cyclopentene, the two most typical substrates in this reaction (Scheme 57).
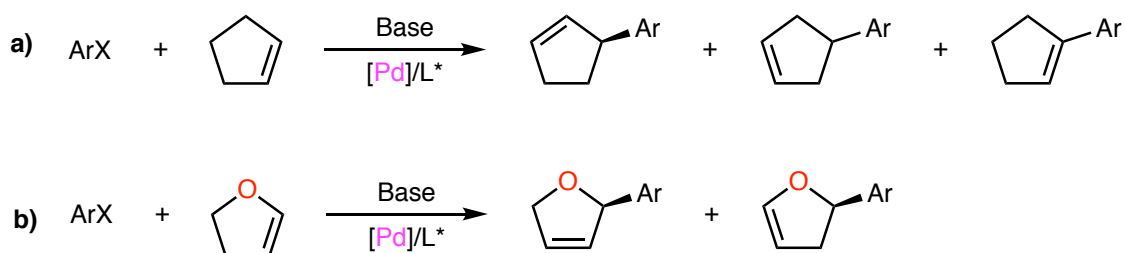
Scheme 57. Pd-catalysed asymmetric intermolecular M–H reaction of cyclopentene (a) and 2,3-dihydrofuran (b).

Some reports with chiral diphosphines and phosphinooxazoline ligands are summarized in Figure 41 just to show that the good yields and enantioselectivites obtained, may indicate that *P*-stereogenic ligands are good candidates as potential catalysts for these transformations.
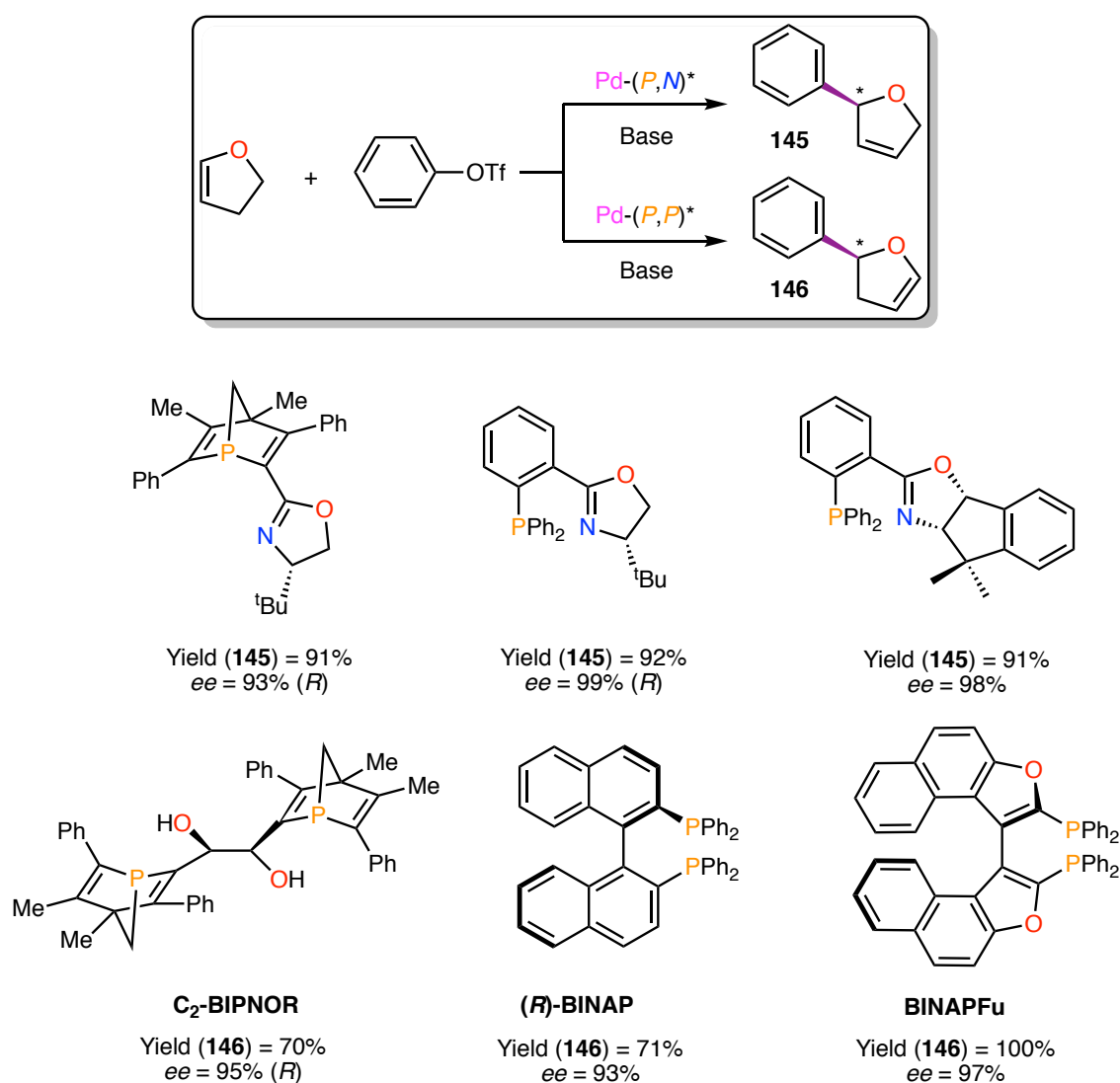
Figure 41. Examples of Pd-catalysed enantioselective M–H reactions with aryl triflates.

Interestingly, it has been found that in general *P,N*-based ligands[152] tend to produce the substituted 2,5-dihydrofuran whereas *P,P* systems[126,153] lead to the 2,3-dihydrofurans instead. This behaviour, however, cannot be extended to all cases because it is strongly dependent on the structure of the ligand. Besides, the reaction still requires heating up to at least 60 ºC, a fact that decreases enantioselectivity. It would desirable to develop chiral and highly active catalysts capable of performing these transformations at room temperature to hopefully improve the stereoselection.

Surprisingly, although the M–H reaction has been widely explored with SPO ligands, especially in the C–C bond forming of aryl chlorides[93-94,101b,154] no examples have been reported in the enantioselective version of this process.

Therefore, our idea was to develop new pseudobidentate Pd complexes having the *P*-stereogenic **L1** moiety with the aim of studying the enantioselective M–H reaction at low temperature (Figure 42).
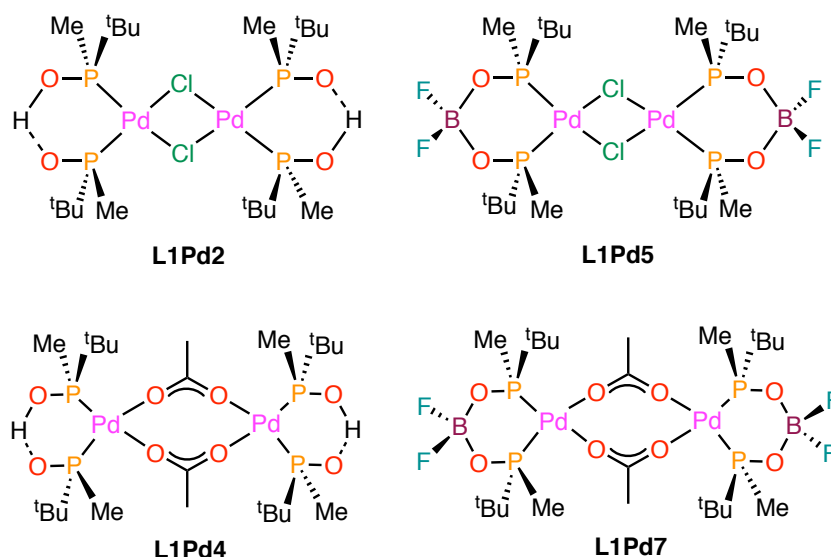
Figure 42. Pd complexes used as preformed catalysts for the asymmetric M–H reactions.

We studied both the pseudobidentate and the BF_2-bridged compounds, as catalysts for the enantioselective M–H reaction of cyclopentene and 2,3-dihydrofuran (Scheme 58).
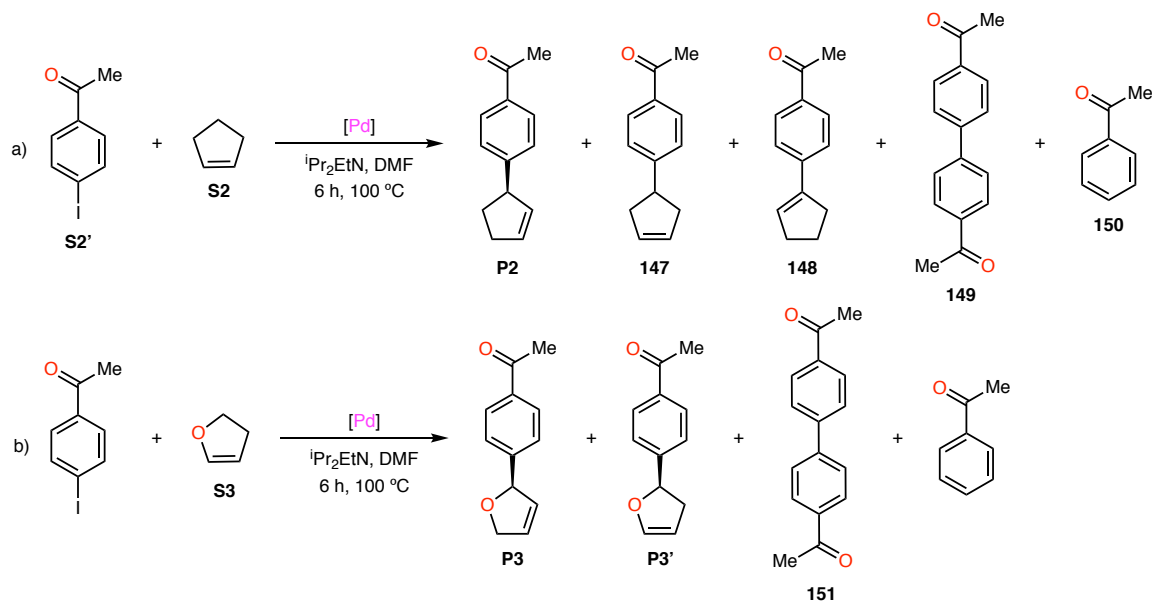
Scheme 58. Studied intermolecular asymmetric M–H reactions using cyclopentene (a) or 2,3-dihydrofuran (b) as substrates.

Thus, 4-iodoacetophenone and cyclopentene or 2,3-dihydrofuran were reacted using 5% of **L1Pd2**, **L1Pd4**, **L1Pd5** or **L1Pd7**, respectively, in the presence of diisopropylethylamine at 100 ºC for 6 hours in a microwave oven. In these preliminary studies 4-iodoacetophenone was chosen because it is known that aryl iodides are known to be good substrates in the M–H transformations compared to other aryl halides.[155]

Since it was the first time that the asymmetric M–H reaction was studied using 2,3-dihydrofuran as substrate in the group, it was necessary to develop the analytical method to determine conversion, product distribution and enantioselectivity. Due to the volatility of the reaction products, these parameters were conveniently evaluated using gas chromatography (GC) with both achiral and chiral columns coupled to a mass spectrometry detector.

Consequently all four complexes were tested under the above shown conditions and the obtained results are given in Table 13 and Table 14.

Table 13. M–H reaction of cyclopentene catalysed by Pd(SPO) complexes.

Precursor[a]	Conversion[b] (%)	Selectivity[c] (%)
PdCl$_2$/4 eq. (**R**)-**L1** ("*in situ*")	>99	40
Pd(OAc)$_2$/4 eq. (**R**)-**L1** ("*in situ*")	>99	70
L1Pd2	90	86
L1Pd4	94	75
L1Pd5	>99	90
L1Pd7	>99	74

a) Catalytic conditions: Pd complex (0.02 mmol), cyclopentene (1.2 mmol), 4-iodoacetophenone (0.4 mmol), ^{i}Pr$_2$EtN (1.2 mmol) and dodecane (0.4 mmol) dissolved in 6 mL of DMF. b) Conversion values are expressed as consumption of starting 4-iodoacetophenone, determined by GC. c) Selectivity values are expressed as the ratio of M–H products **P2**, **147** and **148** relative to the total conversion, determined by GC.

Table 14. M–H reaction of 2,3-dihydrofuran catalysed by Pd(SPO) complexes.

Precursor[a]	Conversion[b] (%)	Rel. isomers[c] (**P3**:**P3'**)
PdCl$_2$/ 4 eq. (**R**)-**L1** ("*in situ*")	>99	1:2
Pd(OAc)$_2$/ 4 eq. (**R**)-**L1** ("*in situ*")	>99	1:3
L1Pd2	>99	1:8
L1Pd4	>99	1:7
L1Pd5	95	1:8
L1Pd7	98	1:9

a) Catalytic conditions: Pd complex (0.02 mmol), 2,3-dihydrofuran (1.2 mmol), 4-iodoacetophenone (0.4 mmol), ^{i}Pr$_2$EtN (1.2 mmol) and dodecane (0.4 mmol) dissolved in 6 mL of DMF. b) Conversion values are expressed as consumption of starting 4-iodoacetophenone, determined by GC. c) Ratio of isomers determined by ^{1}H NMR and GC.

As it can be seen, all the complexes were very active for the M–H reaction of cyclopentene and 2,3-dihydrofuran as substrates, leading to complete conversions after 6 h. Homocoupling **149** or **151** and dehalogenated product **150** were not observed in any of the reactions. "*In situ*" experiments were carried out in order to compare the catalytic activity of the system with the preformed complexes. As it is shown, in all cases the "*in situ*" complexes led to superior conversions compared to the corresponding preformed complexes. Interestingly, in the coupling reaction of cyclopentene, better selectivities were found with the preformed complexes compared to the "*in situ*" experiments. This enhancement of the regioselectivity can be also seen in the reaction of 2,3-dihydrofuran, where modest differences in the isomeric ratio appeared again with the preformed complexes. However, there are not huge differences in terms of activity and selectivity between the *pseudobidentate* complexes and the BF$_2$-bridged analogues, being the latest slightly more active in both reactions. Interestingly, all these systems appeared to be very active even when the experiments were run at 3 h, displaying conversions around 85 to 90% in all cases for both "*in situ*" systems.

Unfortunately, in spite of the high activity and moderate selectivity of these reactions, no enantiomeric excess was found in any of the catalytic runs.

3.4.5. *Pd-catalysed allylic substitution reactions*

The substitution of a leaving group, located at an allylic position by a nucleophile and catalysed by a transition metal complex, is known as allylic substitution. Unlike most of the transition metal-catalysed reactions, allylic substitution involves reaction at sp^3 rather than sp^2 centres (Scheme 59).
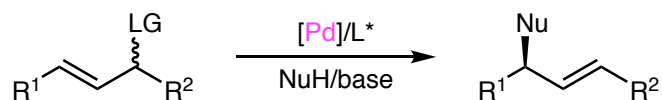
Scheme 59. General scheme for the Pd-catalysed asymmetric allylic substitution reaction. LG = leaving group; Nu = nucleophile.

Although, many transition metals catalysed the reaction,[156] palladium systems are the most widely used.[157]

Allylic substitution implies the formation of C–C as well as C–X (X = heteroatom) bonds under very mild conditions, which are compatible with many functional groups.[102a,158] When the reaction is performed with carbon nucleophiles, such as

malonates,[159] is named allylic alkylation, whereas in presence of nitrogen nucleophiles, usually primary and secondary amines,[159] is known as allylic amination.

Although the reaction was discovered more than 40 years ago,[157b] since then a huge number of publications on allylic substitution have appeared, some of them dealing with *P*-stereogenic ligands.

The catalytic cycle for stabilised '*soft*' nucleophiles *i.e.*, the conjugate bases of acids whose pKa value is lower than 25,[157b] involves the direct attack of the nucleophile on the coordinated allyl fragment (Scheme 60).[157b]
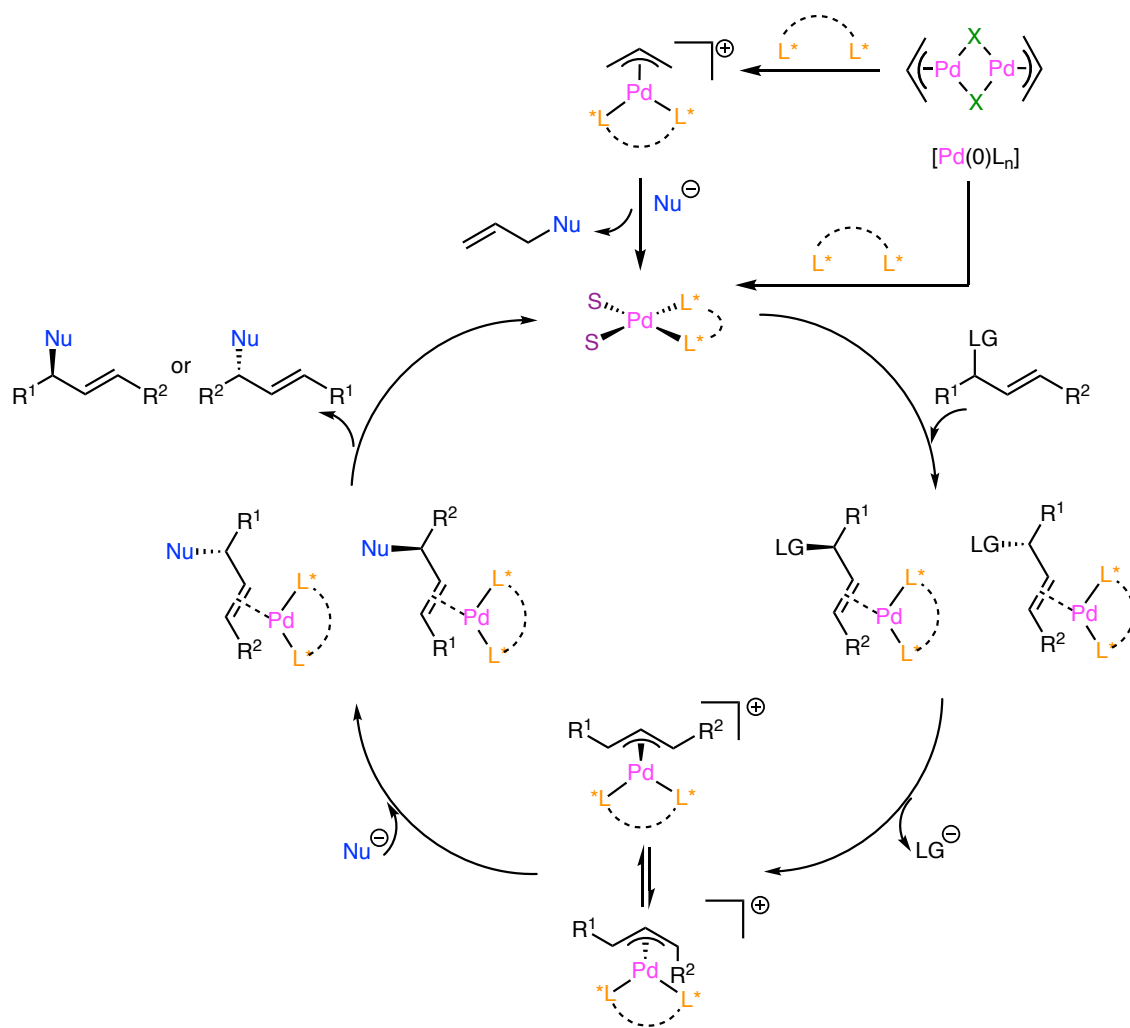
Scheme 60. Reaction mechanism for the Pd-catalysed allylic substitution reaction with "*soft*" nucleophiles. Where LG = leaving group, L*–L* = bidentate ligand or two monodentate ligands, Nu = nucleophile and S = solvent.

The catalytically active species are Pd(0) complexes in which two coordination vacant positions are occupied by solvent molecules. This very reactive species can be formed either by a allyl-Pd(II) precatalysts where nucleophilic attack on the allyl fragment leads to reduction of Pd(II) to Pd(0) or directly by a Pd(0) source such as

$[Pd_2(dba)_3]$. The initial step of the mechanism is the coordination of the substrate by one of the enantiotopic faces of the alkene. Oxidative addition generates the Pd(II) π-allylic intermediate with subsequent release of the leaving group. This complex, which suffers different dynamic exchanges due to the allyl group, undergoes nucleophilic attack at either terminal carbon, electrophilically activated by coordination to Pd(II). In special cases, the nucleophile can attack the central allylic position, leading to substituted cyclopropanes.[160] Decoordination of the substituted final product regenerates the catalytically active species again.

As it can be seen, the determining step for the regioselectivity of the process is the nucleophilic attack on the terminal carbons. If the R groups were different, the final product would be a mixture of two regioisomers, each of which could present a mixture of enantiomers. However, the correct chose of the most suitable ligands can drive the reaction towards one of the products.

Allylic substitutions with stabilised carbon nucleophiles, known as allylic alkylations, are the most important type of allylic substitutions. The benchmark reaction of enantioselective allylic substitution is the reaction of *rac*-3-acetoxy-1,3-diphenyl-1-propene with the stabilised carbanion derived from dimethylmalonate (DMM) in the presence of *N,O*-bis (trimethylsilyl)acetamide (BSA) and a palladium catalyst, what it has been called Trost conditions (Scheme 61).[161]
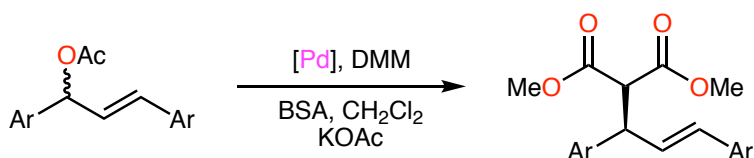
Scheme 61. Pd-catalysed allylic alkylation reaction under Trost conditions, where Ar is typically a phenyl group.

One of the reasons for the popularity of *rac*-3-acetoxy-1,3-diphenyl-1-propene as a model substrate for allylic alkylations is that many ligands give particularly good enantioselectivity with this substrate.[162] Changing the phenyl groups for smaller alkyl groups leads to much poorer results and constitute a challenge in this kind of transformations.

This reaction has been screened with a tremendous quantity of chiral catalysts and indeed is routinely used to test the performance of new ligands. In spite of its limited synthetic usefulness and the better or worse results obtained with this system, which are not necessarily extensible to other substrates.[158]

148

Earlier reports with BINAP[163], DIOP[164], CHIRAPHOS[165] and the *P*-stereogenic DIPAMP[165] yielded a racemic alkylated product but since then many mono- and bidentate *P*-stereogenic ligands have been used in the benchmark reaction for allylic substitution with very good results in some cases. Figure 43 lists some the systems giving rise to good conversions and enantioselectivities and illustrates the diversity of scaffolds of the ligands applied to enantioselective allylic substitution.[166]
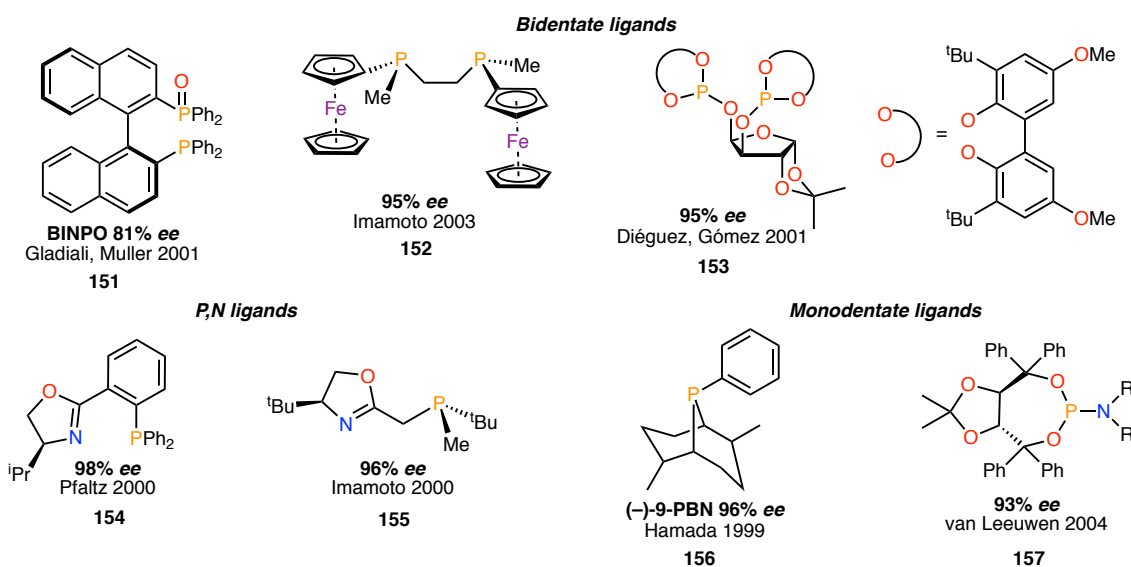
Figure 43. Examples of bidentate, *P,N* and monodentate ligands, some of them *P*-stereogenic, successfully applied in the Pd-catalysed allylic substitution reaction of *rac*-3-acetoxy-1,3-diphenyl-1-propene as model substrate.

As it can be seen, the best results have been achieved with phosphinooxazoline-based systems[167] or with monodentate phosphines[168] rather than bidentate ones. This experimental fact, might suggest that a longer distance between the chiral element and the η^3-allylic fragment can cause the *ee* erosion. Actually, when *rac*-3-acetoxy-1,3-diphenyl-1-propene is used as substrate the chiral discrimination produced by C_2-symmetric ligands is manly due to steric factors, because the two phosphorus atoms have the same electronic properties and hence, its contribution is by all means identical in both terminal carbons of the allyl fragment.

However, the best results in the field were obtained by Hamada and co-workers[26a,53a,169] with the development of a special type of HASPO ligands, the DIAPHOX family (Scheme 62) (see also Section 3.1.5.1).

R[1] = H, OMe, CF$_3$, ^{t}Bu
R[2] = H, OMe
R[3] = Ph, ^{t}Bu, 1-naph, 2-naph, 3-biph, 4-biph
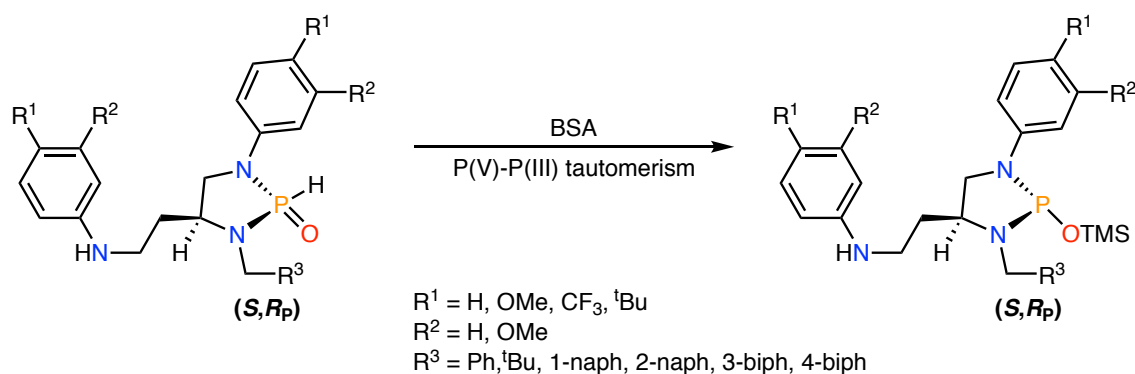
Scheme 62. DIAPHOX-HASPO ligands and their tautomerization induced by BSA.

In a similar manner to SPOs, DIAPHOX ligands are formally P(V) oxides that in the presence of BSA, tautomerize in P(III) species, that efficiently coordinate the Pd(0) centre. These excellent ligands have been tested in many allylic substitution reactions with more challenging substrates and nucleophiles with outstanding results.[26a,53a,169] For instance, alkylation and amination of *rac*-3-acetoxy-1,3-diphenyl-1-propene have yielded enantiomeric excesses up to 99% which have been extended also to other substrates[53b,170] It is interesting to note that the authors found that the addition of Zn(II) salts such as Zn(OAc)$_2$ in catalytic amount improved the *ee*.[169a] probably due to the coordination of the nucleophile to Zn(II) and hence creating a more efficient chiral discrimination.

In spite of these impressive results, allylic substitution reactions have been scarcely explored with SPO ligands. To the best of our knowledge, with the exception of the studies carried out by Hamada and co-workers with the HASPO-DIAPHOX ligand, which cannot be strictly considered as a Secondary Phosphine Oxide. Only Dai, Haynes and co-workers[60a] explored the catalytic activity of the enantiomerically enriched (*R*)-96 preligand in the asymmetric allylic alkylation of dimethylmalonate with *rac*-3-acetoxy-1,3-diphenyl-1-propene (Scheme 63).
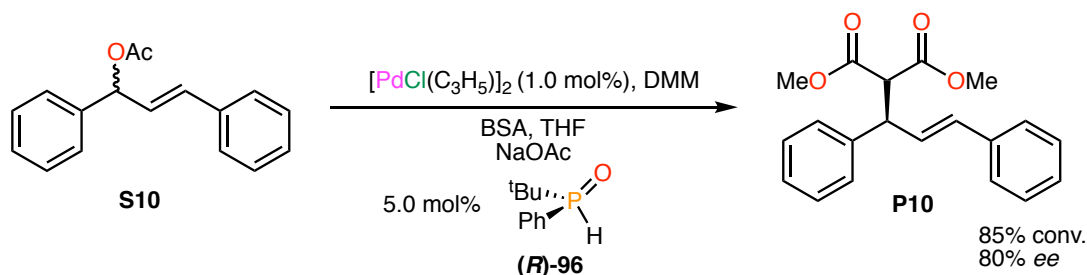
Scheme 63. Palladium-catalysed asymmetric allylic alkylation with (*R*)-96.

Interestingly, the highest enantioselectivities of up to 80% ee were accomplished using an "*in situ*" generated palladium complex with a metal to ligand ratio of 2.5.

With all this in hand, we carried out the catalytic studies of our preformed allyl-Pd complexes **L1Pd9** and **L1Pd10** in the allylic alkylation reaction of dimethylmalonate with cinnamyl acetate (Scheme 64) and with *rac*-3-acetoxy-1,3-diphenyl-1-propene (Scheme 65) as model substrates under the Trost conditions.[171] Furthermore, the same catalysts were tested in the allylic amination reaction of benzylamine with **S10** following the conditions previously described by our research group (Scheme 65).[112,172]

Depending on the nucleophile used, as it has been mentioned, we can distinguish between allylic alkylation when we form the dimethyl malonate "*in situ*" or allylic amination when benzylamine is employed instead. All the experiments were conducted at 24 h at room temperature in the presence of dichloromethane as solvent.

First, in order to evaluate the potential catalytic activity of **L1Pd9** and **L1Pd10**, they were previously tested employing cinnamyl actetate as substrate; the results are summarized in Table 15.
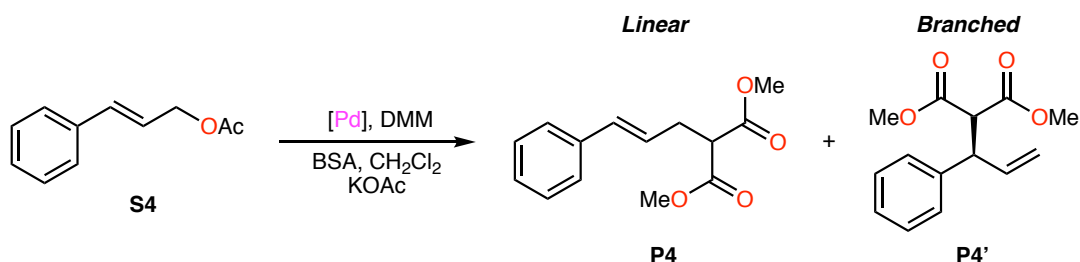
Scheme 64. Pd-catalysed allylic alkylation of cinnamyl acetate, **S4**.

Table 15. Results of the Pd-catalysed allylic substitution reaction of **S4** with precursors **L1Pd9** and **L1Pd10**.

Entry[a]	Precursor	Conv[b].(%)	branched/linear ratio[c]
1	**L1Pd9**	>99	1:45
2	**L1Pd10**	>99	All linear

a) Catalytic conditions for the allylic alkylations: [Pd] 0.01 mmol, **S4** 1 mmol, DMM 3 mmol, BSA 3 mmol, KOAc 1 mg and 5 mL of CH_2Cl_2. b) Conversion relative to the consumed substrate **S4**, determined by ^{1}H NMR and GC. c) Branched/linear ratio determined by GC.

Both catalysts were very active after 16 h of reaction at room temperature, giving full conversions. The branched/linear ratio was similar for both complexes being the linear product the predominant in all cases, even though the reaction appears to be

slightly more selective towards the linear product in the presence of the BF_2-bridged complex.

Once the potential activity of these complexes was evaluated, they were tested employing *rac*-3-acetoxy-1,3-diphenyl-1-propene as model substrate; the results are depicted in Table 16.
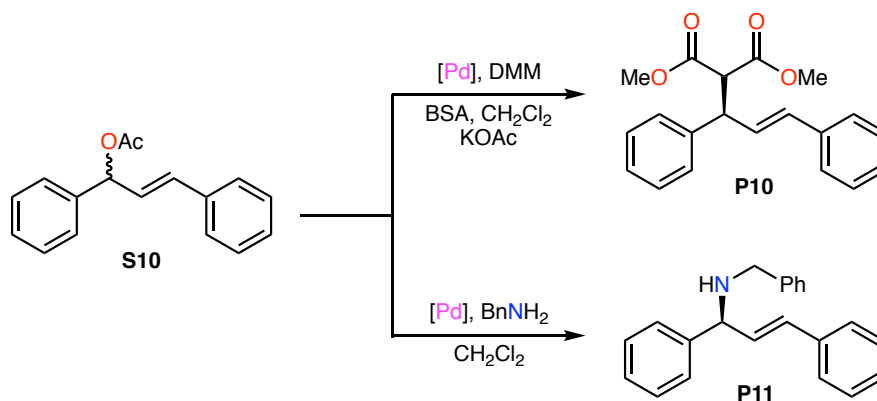
Scheme 65. Pd-catalysed allylic alkylation and amination reactions of *rac*-3-acetoxy-1,3-diphenyl-1-propene, **S10**.

Table 16. Results of the Pd-catalysed allylic substitution reaction of **S10** with precursors **L1Pd9** and **L1Pd10**.

Entry[a,b]	Precursor	Nucleophile	Conv[c].(%)	ee[d] (%)
1		DMM	>99	22 (*R*)
	L1Pd9			
2		$BnNH_2$	>99	13.3 (*S*)
3		DMM	>99	63 (*R*)
	L1Pd10			
4		$BnNH_2$	>99	32.5 (*S*)

a) Catalytic conditions for the allylic alkylations: [Pd] 0.01 mmol, **S10** 1 mmol, DMM 3 mmol, BSA 3 mmol, KOAc 1 mg and 5 mL of CH_2Cl_2. b) Catalytic conditions for the allylic aminations: [Pd] 0.01 mmol, **S10** 1 mmol, $BnNH_2$ 3 mmol and 5 mL of CH_2Cl_2. c) Conversion relative to the consumed substrate **S10**, determined by ^{1}H NMR and HPLC. d) Enantiomeric excess determined by HPLC.

Gratifyingly, all complexes displayed full conversions both using DMM or benzylamine as nucleophiles. However, a modest *ee* value was observed for the *pseudobidentate* complexes, proving that the supramolecular assembly can induce some discrimination on the substrate. Experiments with the BF_2-bridged complexes showed that increasing the rigidity of the bridge and hence, creating a "true" bidentate

ligand, has an important effect on the enantioselection of the reaction, affording *ee* up to 63% in the allylic alkylation reaction. Interestingly, this effect appears to be less important in the amination process, probably because the *harder* nucleophile not only attacks the allyl fragment, but also coordinates the metallic centre, decreasing the *ee*.

These preliminary results, even though modest, show that supramolecular catalysis by means of hydrogen-bridged assemblies of monodentate ligands can induce chirality in those systems, where no coordinative solvents or thermal effects are present. Hopefully, this would be the first step for further studies in the field, and open a door to more catalytically powerful architectures, perhaps increasing the number of hydrogen interactions within the *pseudobidentate* moieties and therefore making more robust systems with a broader field of application.

3.5. *Conclusions*

This Chapter has described the first asymmetric synthesis of optically pure, *P*-stereogenic SPO *t*-BuMeP(O)H (**L1**) and the exploration of its coordination chemistry towards Ir(I), Rh(I), Au(I), Ru(II), Pd(II) and Ni(II).

A rich variety of coordination modes, including the *O*-coordination of the pentavalent phosphine oxide and the *P*-coordination of the trivalent phosphinous acid tautomer has been found.

A new chiral Au(I) complex has been synthesised and crystallographically characterised, displaying aurophilic interactions between gold centres.

For Pd(II), the combination of a phosphinous acid and a phosphinite unit produced a C_2-pseudobidentate *P*-coordination mode bearing an intramolecular H-bridge. This bridge has been successfully substituted by a BF_2 moiety by treatment with tetrafluoroboric acid, increasing the rigidity of the system by forming a real bidentate ligand. This includes **L1Pd2**, an allyl complex with the anionic PO–H···OP bridge, whose BF_2 derivative (**L1Pd5**) has been successfully crystallised.

The catalytic results for all this systems have shown that, even though all of them are very active in different catalytic reactions, the poor rigidity and the lability of the pseudobidentate bridge does not create an efficient enough chiral environment for the chiral discrimination of the substrates tested.

BF_2-bridged complexes have proven to be more stereoselective catalysts in the allylic substitution reactions of **S10**, probably due to the presence of a well-defined bidentate, displaying *ee* values up to 63%.

The excellent enantioselectivies reported in Rh-catalysed asymmetric hydrogenations of functionalised olefins with diphosphines having the ^{t}Bu/Me combination at P could not be found for the systems described in this Chapter. The absence of a "truly bidentate" character of the catalytically active species and the type of reactions explored are probably to blame for the low enantioselection observed.

The results obtained in the present chapter have been recently published as a full paper: Gallen, A.; Orgue, S.; Muller, G.; Escudero, E. C.; Riera, A.; Verdaguer, X.; Grabulosa, A. *Dalton Trans.* **2018**, *47*, 5366-5379.

3.6. *References*

(1)   Ohff, M.; Holz, J.; Quirmbach, M.; Börner, A. *Synthesis* **1998**, 1391-1415.
(2)   Netherton, M. R.; Fu, G. C. *Org. Lett.* **2001**, *3*, 4295-4298.
(3)   Janesko, B. G.; Fisher, H. C.; Bridle, M. J.; Montchamp, J.-L. *J. Org. Chem.* **2015**, *80*, 10025-10032.
(4)   Ackermann, L. *Synlett* **2007**, 507-526.
(5)   Moraleda, D.; Gatineau, D.; Martin, D.; Giordano, L.; Buono, G. *Chem. Commun.* **2008**, 3031-3033.
(6)   Emmick, T. L.; Letsinger, R. L. *J. Am. Chem. Soc.* **1968**, *90*, 3459-3465.
(7)   Magiera, D.; Szmigielska, A.; Pietrusiewicz, K. M.; Duddeck, H. *Chirality* **2004**, *16*, 57-64.
(8)   Wei, C.-H.; Wu, C.-E.; Huang, Y.-L.; Kultyshev, R. G.; Hong, F.-E. *Chem. Eur. J.* **2007**, *13*, 1583-1593.
(9)   Christiansen, A.; Li, C.; Garland, M.; Selent, D.; Ludwig, R.; Spannenberg, A.; Baumann, W.; Franke, R.; Börner, A. *Eur. J. Org. Chem.* **2010**, 2733-2741.
(10)   (a) Kurscheid, B.; Wiebe, W.; Neumann, B.; Stammler, H.-G.; Hoge, B. *Eur. J. Inorg. Chem.* **2011**, 5523-5329 (b) Allefeld, N.; Grasse, M.; Ignat'ev, N.; Hoge, B. *Chem. Eur. J.* **2014**, *20*, 8615-8620.
(11)   (a) Magiera, D.; Baumann, W.; Podkorytov, Ivan S.; Omelanczuk, J.; Duddeck, H. *Eur. J. Inorg. Chem.* **2002**, 3253-3257 (b) Ackermann, L. *Synthesis* **2006**, 1557-1571.
(12)   Busacca, C. A.; Lorenz, J. C.; Grinberg, N.; Haddad, N.; Hrapchak, M.; Latli, B.; Lee, H.; Sabila, P.; Saha, A.; Sarvestani, M.; Shen, S.; Varsolona, R.; Wei, X.; Senanayake, C. H. *Org. Lett.* **2005**, *7*, 4277-4280.
(13)   Farnham, W. B.; Lewis, R. A.; Murray, R. K.; Mislow, K. *J. Am. Chem. Soc.* **1970**, *92*, 5808-5809.
(14)   Bloomfield, A. J.; Quian, J. M.; Herzon, S. B. *Organometallics* **2010**, *29*, 4193-4195.
(15)   Rauhut, M. M.; Currier, H. A. *J. Org. Chem.* **1961**, *26*, 4626-4628.
(16)   Quin, L. D.; Montgomery, R. E. *J. Org. Chem.* **1963**, *28*, 3315-3320.
(17)   Li, G. Y.; Fagan, P. J.; Watson, P. L. *Angew. Chem. Int. Ed.* **2001**, *40*, 1106-1109.
(18)   (a) Li, G. Y. *Angew. Chem. Int. Ed.* **2001**, *40*, 1513-1516 (b) Li, G. Y. *J. Organomet. Chem.* **2002**, *653*, 63-68.
(19)   (a) Ackermann, L.; Born, R. *Angew. Chem. Int. Ed.* **2005**, *44*, 2444-2447 (b) Christiansen, A.; Selent, D.; Spannenberg, A.; Köckerling, M.; Reinke, H.; Baumann, W.; Jiao, H.; Franke, R.; Börner, A. *Chem. Eur. J.* **2011**, *17*, 2120-2129.
(20)   Hu, C.-Y.; Chen, Y.-Q.; Lin, G.-Y.; Huang, M.-K.; Chang, Y.-C.; Hong, F.-E. *Eur. J. Inorg. Chem.* **2016**, 3131-3142.
(21)   Guillen, F.; Fiaud, J.-C. *Tetrahedron Lett.* **1999**, *40*, 2939-2942.
(22)   Enders, D.; Tedeschi, L.; Bats, J. W. *Angew. Chem. Int. Ed.* **2000**, *39*, 4605-4607.
(23)   (a) Nahm, M. R.; Linghu, X.; Potnick, J. R.; Yates, C. M.; White, P. S.; Johnson, J. S. *Angew. Chem. Int. Ed.* **2005**, *44*, 2377-2379 (b) Nahm, M. R.; Potnick, J. R.; White, P. S.; Johnson, J. S. *J. Am. Chem. Soc.* **2006**, *128*, 2751-2756.
(24)   De la Cruz, A.; Koeller, K. J.; Rath, N. P.; Spilling, C. D.; Vasconcelos, I. C. F. *Tetrahedron* **1998**, *54*, 10513-10524.

(25)   (a) Nemoto, T.; Jin, L.; Nakamura, H.; Hamada, Y. *Tetrahedron Lett.* **2006**, *47*, 6577-6581 (b) Nemoto, T.; Harada, T.; Matsumoto, T.; Hamada, Y. *Tetrahedron Lett.* **2007**, *48*, 6304-6307.

(26)   (a) Nemoto, T.; Matsumoto, T.; Masuda, T.; Hitomi, T.; Hatano, K.; Hamada, Y. *J. Am. Chem. Soc.* **2004**, *126*, 3690-3691 (b) Nemoto, T.; Fukuda, T.; Matsumoto, T.; Hitomi, T.; Hamada, Y. *Adv. Synth. Catal.* **2005**, *347*, 1504-1506 (c) Nemoto, T.; Masuda, T.; Matsumoto, T.; Hamada, Y. *J. Org. Chem.* **2005**, *70*, 7172-7178.

(27)   Pietrusiewicz, K. M.; Zablocka, M. *Chem. Rev.* **1994**, *94*, 1375-1411.

(28)   (a) Leyris, A.; Bigeault, J.; Nuel, D.; Giordano, L.; Buono, G. *Tetrahedron Lett.* **2007**, *48*, 5247-5250 (b) Gatineau, D.; Giordano, L.; Buono, G. *J. Am. Chem. Soc.* **2011**, *133*, 10728-10731.

(29)   Leyris, A.; Nuel, D.; Giordano, L.; Achard, M.; Buono, G. *Tetrahedron Lett.* **2005**, *46*, 8677-8680.

(30)   Gatineau, D.; Nguyen, D. H.; Hérault, D.; Vanthuyne, N.; Leclaire, J.; Giordano, L.; Buono, G. *J. Org. Chem.* **2015**, *80*, 4132-4141.

(31)   Copey, L.; Jean-Gérard, L.; Andrioletti, B.; Framery, E. *Tetrahedron Lett.* **2016**, *57*, 543-545.

(32)   (a) Michalski, J.; Skrzypczynski, Z. *J. Organomet. Chem.* **1975**, *97*, C31-C32 (b) Haynes, R. K.; Au-Yeung, T.; Chan, W.; Lam, W.; Li, Z.; Yeung, L.; Chan, A. S. C.; Li, P.; Koen, M.; Mitchell, C. R.; Vonwiller, S. C. *Eur. J. Org. Chem.* **2000**, 3205-3216.

(33)   (a) Drabowicz, J.; Lyzwa, P.; Omelanczuk, J.; Pietrusiewicz, K. M.; Mikolajczyk, M. *Tetrahedron: Asymmetry* **1999**, *10*, 2757-2763 (b) Wang, F.; Polavarapu, P. L.; Drabowicz, J.; Mikolajczyk, M. *J. Org. Chem.* **2000**, *65*, 7561-7565 (c) Stankevič, M.; Pietrusiewicz, K. M. *J. Org. Chem.* **2007**, *72*, 816-822.

(34)   (a) Holt, J.; Maj, A. M.; Schudde, E. P.; Pietrusiewicz, K. M.; Sieron, L.; Wieczorek, W.; Jerphagnon, T.; Arends, I. W. C. E.; Hanefeld, U.; Minnaard, A. J. *Synthesis* **2009**, 2061-2065 (b) Kortmann, F. A.; Chang, M.-C.; Otten, E.; Couzijn, E. P. A.; Lutz, M.; Minnaard, A. J. *Chem. Sci.* **2014**, *5*, 1322-1327.

(35)   (a) Cervinka, O.; Belovsky, O.; Hepnerova, M. *Chem. Commun.* **1970**, 562 (b) Jiang, X.; Minnaard, A. J.; Hessen, B.; Feringa, B. L.; Duchateau, A. L. L.; Andrien, J. G. O.; Boogers, J. A. F.; de Vries, J. G. *Org. Lett.* **2003**, *5*, 1503-1506.

(36)   (a) Dubrovina, N. V.; Börner, A. *Angew. Chem. Int. Ed.* **2004**, *43*, 5883-5886 (b) Dubrovina, N. V.; Jiao, H.; Tararov Vitali, I.; Spannenberg, A.; Kadyrov, R.; Monsees, A.; Christiansen, A.; Börner, A. *Eur. J. Org. Chem.* **2006**, 3412-3420.

(37)   Han, Z. S.; Wu, H.; Xu, Y.; Zhang, Y.; Qu, B.; Li, Z.; Caldwell, D. R.; Fandrick, K. R.; Zhang, L.; Roschangar, F.; Song, J. J.; Senanayake, C. H. *Org. Lett.* **2017**, *19*, 1796-1799.

(38)   (a) Han, Z.; Krishnamurthy, D.; Grover, P.; Fang, Q. K.; Senanayake, C. H. *J. Am. Chem. Soc.* **2002**, *124*, 7880-7881 (b) Han, Z.; Krishnamurthy, D.; Grover, P.; Wilkinson, H. S.; Fang, Q. K.; Su, X.; Lu, Z.-H.; Magiera, D.; Senanayake Chris, H. *Angew. Chem. Int. Ed.* **2003**, *42*, 2032-2035.

(39)   León, T.; Riera, A.; Verdaguer, X. *J. Am. Chem. Soc.* **2011**, *133*, 5740-5743.

(40)   Muci, A. R.; Campos, K. R.; Evans, D. A. *J. Am. Chem. Soc.* **1995**, *117*, 9075-9076.

(41)   Zijlstra, H.; León, T.; de Cózar, A.; Guerra, C. F.; Byrom, D.; Riera, A.; Verdaguer, X.; Bickelhaupt, F. M. *J. Am. Chem. Soc.* **2013**, *135*, 4483-4491.

(42)   (a) Salomó, E.; Orgué, S.; Riera, A.; Verdaguer, X. *Angew. Chem. Int. Ed.* **2016**, *55*, 7988-7992 (b) Salomó, E.; Orgué, S.; Riera, A.; Verdaguer, X. *Synthesis* **2016**, 2659-2663 (c) Salomó, E.; Prades, A.; Riera, A.; Verdaguer, X.

J. Org. Chem. **2017**, *82*, 7065-7069 (d) Salomo, E.; Rojo, P.; Hernández-Lladó, P.; Riera, A.; Verdaguer, X. *J. Org. Chem.* **2018**, *83*, 4618-4627.

(43)   (a) Brown, A. D.; Kosolapoff, G. M. *J. Chem. Soc. C* **1968**, 839-842 (b) Cooper, J. W.; Roberts, B. P. *J. Chem. Soc. Perkin Trans. 2* **1976**, 808-813.

(44)   (a) Bloomfield, A. J.; Herzon, S. B. *Org. Lett.* **2012**, *14*, 4370-4373 (b) Liu, Y.; Ding, B.; Liu, D.; Zhang, Z.; Liu, Y.; Zhang, W. *Res. Chem. Intermed.* **2017**, *43*, 4959-4966.

(45)   Orgué, S.; Flores-Gaspar, A.; Biosca, M.; Pàmies, O.; Diéguez, M.; Riera, A.; Verdaguer, X. *Chem. Commun.* **2015**, *51*, 17548-17551.

(46)   (a) Revés, M.; Ferrer, C.; León, T.; Doran, S.; Etayo, P.; Vidal-Ferran, A.; Riera, A.; Verdaguer, X. *Angew. Chem. Int. Ed.* **2010**, *49*, 9452-9455 (b) Cristóbal-Lecina, E.; Etayo, P.; Doran, S.; Revés, M.; Martín-Gago, P.; Grabulosa, A.; Constantino, A. R.; Vidal-Ferran, A.; Riera, A.; Verdaguer, X. *Adv. Synth. Catal.* **2014**, *356*, 795-804 (c) Imamoto, T. *Chem. Rec.* **2016**, *16*, 2655-2669.

(47)   McKinstry, L.; Livinghouse, T. *Tetrahedron Lett.* **1994**, *35*, 9319-9322.

(48)   Galland, A.; Paris, J. M.; Schlama, T.; Guillot, R.; Fiaud, J.-C.; Toffano, M. *Eur. J. Org. Chem.* **2007**, 863-873.

(49)   (a) Köster, R.; Tsay, Y.-H.; Synoradzki, L. *Chem. Ber.* **1987**, *120*, 1117-1123 (b) Neu, R. C.; Ouyang, E. Y.; Geier, S. J.; Zhao, X.; Ramos, A.; Stephan, D. W. *Dalton Trans.* **2010**, *39*, 4285-4294 (c) Sänger, I.; Schödel, F.; Bolte, M.; Lerner, H.-W. *J. Chem. Crystallogr.* **2012**, *42*, 472-474.

(50)   Imamoto, T.; Oshiki, T. *Tetrahedron Lett.* **1989**, *30*, 383-384.

(51)   McKinstry, L.; Overberg, J. J.; Soubra-Ghaoui, C.; Walsh, D. S.; Robins, K. A. *J. Org. Chem.* **2000**, *65*, 2261-2263.

(52)   Kendall, A. J.; Seidenkranz, D. T.; Tyler, D. R. *Organometallics* **2017**, *36*, 2412-2417.

(53)   (a) Nemoto, T.; Sakamoto, T.; Fukuyama, T.; Hamada, Y. *Tetrahedron Lett.* **2007**, *48*, 4977-4981 (b) Nemoto, T.; Hamada, T. *Chem. Rec.* **2007**, *7*, 150-158 (c) Nemoto, T.; Hamada, Y. *Tetrahedron* **2011**, *67*, 667-687.

(54)   (a) Andrushko, N.; Börner, A. In *Phosphorus Ligands in Asymmetric Catalysis: Synthesis and Applications*; Börner, A., Ed.; Wiley-VCH: Weinheim, 2008; Vol. 3 (b) Kamer, P. C. J.; van Leeuwen, P. W. N. M.; Ed. *Phosphorus(III) Ligands in Homogeneous Catalysis: Design and Synthesis*; Wiley, 2012.

(55)   (a) Griffiths, J. E.; Burg, A. B. *J. Chem. Soc.* **1960**, 1507-1508 (b) Hoge, B.; Neufeind, S.; Hettel, S.; Wiebe, W.; Thosen, C. *J. Organomet. Chem.* **2005**, *690*, 2382-2387 (c) Hoge, B.; Garcia, P.; Willner, H.; Oberhammer, H. *Chem. Eur. J.* **2006**, *12*, 3567-3574.

(56)   Roundhill, D. M.; Sperline, R. P.; Beaulieu, W. B. *Coord. Chem. Rev.* **1978**, *26*, 263-279.

(57)   (a) Walther, B. *Coord. Chem. Rev.* **1984**, *60*, 67-105 (b) Achard, T. *Chimia* **2016**, *70*, 8-19.

(58)   (a) Martin, D.; Moraleda, D.; Achard, T.; Giordano, L.; Buono, G. *Chem. Eur. J.* **2011**, *17*, 12729-12740 (b) Graux, L. V.; Giorgi, M.; Buono, G.; Clavier, H. *Organometallics* **2015**, *34*, 1864-1871.

(59)   Shaikh, T. M.; Weng, C.-M.; Hong, F.-E. *Coord. Chem. Rev.* **2012**, *256*, 771-803.

(60)   (a) Dai, W.; Yeung, K. K. Y.; Leung, W. H.; Haynes, R. K. *Tetrahedron: Asymmetry* **2003**, *14*, 2821-2826 (b) Gatineau, D.; Moraleda, D.; Naubron, J.-V.; Bürgi, T.; Giordano, L.; Buono, G. *Tetrahedron: Asymmetry* **2009**, *20*, 1912-1917 (c) Landert, H.; Spindler, F.; Wyss, A.; Blaser, H.; Pugin, B.; Ribourduoille, Y.; Gschwend, B.; Ramalingamm, B.; Pfaltz, A. *Angew. Chem. Int. Ed.* **2010**, *49*, 6873-6876 (d) Donets, P. A.; Cramer, N. *J. Am. Chem. Soc.* **2013**, *135*, 11772-11775.

(61)   Werner, H.; Khac, T. N. *Angew. Chem. Int. Ed. Engl.* **1977**, *16*, 324-325.
(62)   (a) Kläui, W.; Eberspach, W.; Schwarz, R. *J. Organomet. Chem.* **1983**, *252*, 347-357 (b) Walther, B.; Hartung, H.; Maschmeier, M.; Baumeister, U.; Messbauer, B. *Z. Anorg. Allg. Chem.* **1988**, *566*, 121-130.
(63)   (a) Han, L.-B.; Zhang, C.; Yazawa, H.; Shimada, S. *J. Am. Chem. Soc.* **2004**, *126*, 5080-5081 (b) Han, L.-B.; Ono, Y.; Yazawa, H. *Org. Lett.* **2005**, *7*, 2909-2911.
(64)   (a) Ackermann, L.; Althammer, A. *Chem. Unserer Zeit* **2009**, *43*, 74-83 (b) Jin, Z.; Li, Y.-J.; Ma, Y.-Q.; Qiu, L.-L.; Fang, J.-X. *Chem. Eur. J.* **2011**, *18*, 446-450.
(65)   (a) Bogdanovic, B.; Henc, B.; Meister, B.; Pauling, H.; Wilke, G. *Angew. Chem. Int. Ed. Engl.* **1972**, *11*, 1023-1024 (b) Bogdanovic, B.; Henc, B.; Löser, A.; Meister, B.; Pauling, H.; Wilke, G. *Angew. Chem. Int. Ed. Engl.* **1973**, *12*, 954-964 (c) Wilke, G. *Angew. Chem. Int. Ed. Engl.* **1988**, *27*, 185-206.
(66)   Speiser, F.; Braunstein, P.; Saussine, L. *Acc. Chem. Res.* **2005**, *38*, 784-793.
(67)   Boulens, P.; Pellier, E.; Jeanneau, E.; Reek, J. N. H.; Olivier-Bourbigou, H.; Breuil, P.-A. R. *Organometallics* **2015**, *34*, 1139-1142.
(68)   Lhermet, R.; Moser, E.; Jeanneau, E.; Olivier-Bourbigou, H.; Breuil, P.-A. R. *Chem. Eur. J.* **2017**, *23*, 7433-7437.
(69)   Jiang, X.; van den Berg, M.; Minnaard, A. J.; Feringa, B. L.; de Vries, J. G. *Tetrahedron: Asymmetry* **2004**, *15*, 2223-2229.
(70)   Matsumoto, M.; Tamura, M. *J. Mol. Catal.* **1983**, *19*, 365-376.
(71)   Wang, X.-B.; Goto, M.; Han, L.-B. *Chem. Eur. J.* **2014**, *20*, 3631-3635.
(72)   Christiansen, A.; Selent, D.; Spannenberg, A.; Baumann, W.; Franke, R.; Börner, A. *Organometallics* **2010**, *29*, 3139-3145.
(73)   Vicente, J.; Chicote, M. a. T. *Coord. Chem. Rev.* **1999**, *193–195*, 1143-1161.
(74)   (a) Schmidbaur, H.; Aly, A. A. M. *Angew. Chem. Int. Ed. Engl.* **1980**, *19*, 71-72 (b) Hollatz, C.; Schier, A.; Schmidbaur, H. *J. Am. Chem. Soc.* **1997**, *119*, 8115-8116 (c) Hollatz, C.; Schier, A.; Riede, J.; Schmidbaur, H. *J. Chem. Soc. Dalton Trans.* **1999**, 111-114 (d) Hollatz, C.; Schier, A.; Schmidbaur, H. *Inorg. Chim. Acta* **2000**, *300–302*, 191-199.
(75)   (a) Cano, I.; Chapman, A. M.; Urakawa, A.; van Leeuwen, P. W. N. M. *J. Am. Chem. Soc.* **2014**, *136*, 2520-2528 (b) Cano, I.; Huertos, M. A.; Chapman, A. M.; Buntkowsky, G.; Gutmann, T.; Groszewicz, P. B.; van Leeuwen, P. W. N. M. *J. Am. Chem. Soc.* **2015**, *137*, 7718-7727.
(76)   Schröder, F.; Tugny, C.; Salanouve, E.; Clavier, H.; Giordano, L.; Moraleda, D.; Gimbert, Y.; Mouriès-Mansuy, V.; Goddard, J.-P.; Fensterbank, L. *Organometallics* **2014**, *33*, 4051-4056.
(77)   Uson, R.; Laguna, A.; Laguna, M. *Inorg. Synth.* **1989**, *26*, 85-86.
(78)   Scherbaum, F.; Grohmann, A.; Huber, B.; Krüger, C.; Schmidbaur, H. *Angew. Chem. Int. Ed. Engl.* **1988**, *27*, 1544-1546.
(79)   (a) Robertson, I. W.; Stephenson, T. A. *Inorg. Chim. Acta* **1980**, *45*, L215-L216 (b) Kläui, W.; Buchholz, E. *Inorg. Chem.* **1988**, *27*, 3500-3506 (c) Rüther, T.; Englert, U.; Koelle, U. *Inorg. Chem.* **1998**, *37*, 4265-4271.
(80)   Torres-Lubián, R.; Rosales-Hoz, M. J.; Arif, A. M.; Ernst, R. D.; Paz-Sandoval, M. A. *J. Organomet. Chem.* **1999**, *585*, 68-82.
(81)   den Reijer, C. J.; Wörle, M.; Pregosin, P. S. *Organometallics* **2000**, *19*, 309-316.
(82)   Chan, E. Y. Y.; Zhang, Q.; Sau, Y.; Lo, S. M. F.; Sung, H. Y.; Williams, I. D.; Haynes, R. K.; Leung, W. *Inorg. Chem.* **2004**, *43*, 4921-4926.
(83)   Ackermann, L. *Org. Lett.* **2005**, *7*, 3123-3125.
(84)   Knapp, S. M. M.; Sherbow, T. J.; Yelle, R. B.; Juliette, J. J.; Tyler, D. R. *Organometallics* **2013**, *32*, 3744-3752.

(85)   (a) Tomas-Mendivil, E.; Suarez, F. J.; Diez, J.; Cadierno, V. *Chem. Commun.* **2014**, *50*, 9661-9664 (b) Tomas-Mendivil, E.; Menendez-Rodriguez, L.; Francos, J.; Crochet, P.; Cadierno, V. *RSC Adv.* **2014**, *4*, 63466-63474 (c) Gonzalez-Fernandez, R.; Gonzalez-Liste, P. J.; Borge, J.; Crochet, P.; Cadierno, V. *Catal. Sci. Technol.* **2016**, *6*, 4398-4409.

(86)   Rafter, E.; Gutmann, T.; Low, F.; Buntkowsky, G.; Philippot, K.; Chaudret, B.; van Leeuwen, P. W. N. M. *Catal. Sci. Technol.* **2013**, *3*, 595-599.

(87)   (a) Silverthorn, W. E. *Adv. Organomet. Chem.* **1975**, *13*, 48-137 (b) Le Bozec, H.; Touchard, D.; Dixneuf, P. H. *Adv. Organomet. Chem.* **1989**, *29*, 163-247 (c) Crabtree, R. H. *The organometallic chemistry of the transition metals*; 3 ed.; Wiley & Sons: New York, 2001.

(88)   (a) Consiglio, G.; Morandini, F. *Chem. Rev.* **1987**, *87*, 761-778 (b) Naota, T.; Takaya, H.; Murahashi, S. *Chem. Rev.* **1998**, *98*, 2599-2660.

(89)   Zell, D.; Warratz, S.; Gelman, D.; Garden, S. J.; Ackermann, L. *Chem. Eur. J.* **2016**, *22*, 1248-1252.

(90)   Graux, L. V.; Giorgi, M.; Buono, G.; Clavier, H. *Dalton Trans.* **2016**, *45*, 6491-6502.

(91)   (a) Aznar, R.; Muller, G.; Sainz, D.; Font-Bardia, M.; Solans, X. *Organometallics* **2008**, *27*, 1967-1969 (b) Navarro, M.; Vidal, D.; Clavero, P.; Grabulosa, A.; Muller, G. *Organometallics* **2015**, *34*, 973-994.

(92)   Miura, M. *Angew. Chem. Int. Ed.* **2004**, *43*, 2201-2203.

(93)   Li, G. Y. *J. Org. Chem.* **2002**, *67*, 3643-3650.

(94)   (a) Li, G. Y.; Zheng, G.; Noonan, A. F. *J. Org. Chem.* **2001**, *66*, 8677-8681 (b) Wolf, C.; Lerebours, R. *J. Org. Chem.* **2003**, *68*, 7077-7084.

(95)   Hu, D.-F.; Weng, C.-M.; Hong, F.-E. *Organometallics* **2011**, *30*, 1139-1147.

(96)   Chang, Y.-C.; Chang, W.-C.; Hu, C.-Y.; Hong, F.-E. *Organometallics* **2014**, *33*, 3523-3534.

(97)   Bigeault, J.; de Riggi, I.; Gimbert, Y.; Giordano, L.; Buono, G. *Synlett* **2008**, 1071-1075.

(98)   Clavier, H.; Buono, G. *Chem. Rec.* **2017**, *17*, 399-414.

(99)   Pearson, R. G. *Inorg. Chem.* **1973**, *12*, 712-713.

(100)   Bigeault, J.; Giordano, L.; Buono, G. *Angew. Chem. Int. Ed.* **2005**, *44*, 4753-4757.

(101)   (a) Jung, L.-Y.; Tsai, S.-H.; Hong, F.-E. *Organometallics* **2009**, *28*, 6044-6053 (b) Ackermann, L.; Potukuchi, H. K.; Kapdi, A. R.; Schulzke, C. *Chem. Eur. J.* **2010**, *16*, 3300-3303.

(102)   (a) Trost, B. M.; Verhoeven, T. R. In *Comprehensive Organometallic Chemistry*; Wilkinson, G., Stone, F. G. A., Abel, E. W., Eds.; Pergamon: Oxford, 1982; Vol. 8 (b) Godleski, S. A. In *Comprehensive Organic Synthesis*; Trost, B. M., Fleming, I., Semmelhack, M. F., Eds.; Pergamon: Oxford, 1991; Vol. 4.

(103)   Oberhansli, W. E.; Dahl, L. F. *J. Organomet. Chem.* **1965**, *3*, 43-54.

(104)   (a) Hayashi, T.; Kawatsura, M.; Uozumi, Y. *J. Am. Chem. Soc.* **1998**, *120*, 1681-1687 (b) Fairlamb, I. J. S.; Lloyd-Jones, G. C.; Vyskocil, S.; Kocovsky, P. *Chem. Eur. J.* **2002**, *8*, 4443-4453 (c) Faller, J. W.; Sarantopoulos, N. *Organometallics* **2004**, *23*, 2008-2014 (d) Achard, T.; Benet-Buchholz, J.; Escudero-Adán, E. C.; Riera, A.; Verdaguer, X. *Organometallics* **2011**, *30*, 3119-3130.

(105)   (a) Corrandini, P.; Maglio, G.; Musco, A.; Paiaro, G. *Chem. Commun.* **1966**, 618-619 (b) Faller, J. W.; Thomsen, M. E.; Mattina, M. J. *J. Am. Chem. Soc.* **1971**, *93*, 2642-2653 (c) Bosnich, B.; Mackenzie, P. B. *Pure Appl. Chem.* **1982**, *54*, 189-195 (d) Akermark, B.; Vitagliano, A. *Organometallics* **1985**, *4*, 1275-1283 (e) Albinati, A.; Ammann, C.; Pregosin, P. S.; Rüegger, H. *Organometallics* **1990**, *9*, 1826-1833 (f) Breutel, C.; Pregosin, P. S.; Salzmann,

R.; Togni, A. *J. Am. Chem. Soc.* **1994**, *116*, 4067-4068 (g) Pregosin, P. S.; Salzmann, R. *Coord. Chem. Rev.* **1996**, *155*, 35-68.

(106) (a) Vrieze, K.; van Leeuwen, P. W. N. M. In *Progress in Inorganic Chemistry*; Lippard, S. L., Ed.; John Wiley and Sons: New York, 1971; Vol. 14 (b) Tatsumi, K.; Hoffman, R.; Yamamoto, A.; Stille, J. K. *Bull. Chem. Soc. Jpn.* **1981**, *54*, 1857-1867.

(107) (a) Hansson, S.; Norrby, P.; Sjögren, M.; Akermark, B. *Organometallics* **1993**, *12*, 4940-4948 (b) Burckhardt, U.; Baumann, M.; Trabesinger, G.; Gramlich, V.; Togni, A. *Organometallics* **1997**, *16*, 5252-5259 (c) Burckhardt, U.; Baumann, M.; Togni, A. *Tetrahedron: Asymmetry* **1997**, *8*, 155-159.

(108) (a) Vrieze, K.; Maclean, C.; Cossee, P.; Hilbers, C. *Recl. Trav. Chim. Pays-Bas* **1966**, *85*, 1077-1098 (b) Gogoll, A.; Örnebro, J.; Grennberg, H.; Bäckvall, J. E. *J. Am. Chem. Soc.* **1994**, *116*, 3631-3632.

(109) Powell, J.; Robinson, S. D.; Shaw, B. L. *Chem. Commun. (London)* **1965**, 78-79.

(110) Grabulosa, A.; Muller, G.; Ordinas, J. I.; Mezzetti, A.; Maestro, M. A.; Font-Bardia, M.; Solans, X. *Organometallics* **2005**, *24*, 4961-4973.

(111) (a) Tsuji, J. *Palladium Reagents and Catalysts*; Wiley: New York, 1995 (b) Baltzer, N.; Macko, L.; Schaffner, S.; Zehnder, M. *Helv. Chim. Acta* **1996**, *79*, 803-812.

(112) Grabulosa, A.; Muller, G.; Ceder, R.; Maestro, M. A. *Eur. J. Inorg. Chem.* **2010**, 3372-3383.

(113) (a) van Leeuwen, P. W. N. M.; Ed. *Supramolecular Catalysis*; Wiley-VCH: Weinheim, 2008 (b) Blaser, H.-U.; Federsel, H.-J.; Ed. *Asymmetric Catalysis on Industrial Scale: Challenges, Approaches and Solutions*; 2 ed.; Wiley, 2010 (c) Grabulosa, A. *P-Stereogenic Ligands in Enantioselective Catalysis*; Royal Society of Chemistry: Cambridge, 2011 (d) Behr, A. *Applied Homogeneous Catalysis*; Wiley-VCH: Weinheim, 2012.

(114) (a) Pye, J. P.; Rossen, K.; Reamer, R. A.; Tsou, N. N.; Volante, R. P.; Reider, P. J. *J. Am. Chem. Soc.* **1997**, *119*, 6207-6208 (b) Wada, Y.; Imamoto, T.; Tsuruta, H.; Yamaguchi, K.; Gridnev, I. D. *Adv. Synth. Catal.* **2004**, *346*, 777-788 (c) Cui, X.; Burgess, K. *Chem. Rev.* **2005**, *105*, 3272-3296 (d) Zhang, X.; Huang, K.; Hou, G.; Cao, B.; Zhang, X. *Angew. Chem. Int. Ed.* **2010**, *49*, 6421-6424 (e) Vidal-Ferran, A.; Mon, I.; Bauzá, A.; Frontera, A.; Rovira, L. *Chem. Eur. J.* **2015**, *21*, 11417-11426 (f) Fernández-Pérez, H.; Mon, I.; Frontera, A.; Vidal-Ferran, A. *Tetrahedron* **2015**, *71*, 4490-4494 (g) Fernández-Pérez, H.; Balakrishna, B.; Vidal-Ferran, A. *Eur. J. Org. Chem.* **2018**, 1525-1532.

(115) (a) Imamoto, T.; Tsuruta, H.; Wada, Y.; Masuda, H.; Yamaguchi, K. *Tetrahedron Lett.* **1995**, *36*, 8271-8274 (b) Imamoto, T.; Watanabe, J.; Wada, Y.; Masuda, H.; Yamada, H.; Tsuruta, H.; Matsukawa, S.; Yamaguchi, K. *J. Am. Chem. Soc.* **1998**, *120*, 1635-1636 (c) Yamanoi, Y.; Imamoto, T. *Rev. Heteroatom Chem.* **1999**, *20*, 227-248 (d) Tsuruta, H.; Imamoto, T. *Tetrahedron: Asymmetry* **1999**, *10*, 877-882 (e) Nagata, K.; Matsukawa, S.; Imamoto, T. *J. Org. Chem.* **2000**, *65*, 4185-4188 (f) Gridnev, I. D.; Higashi, N.; Asakura, K.; Imamoto, T. *J. Am. Chem. Soc.* **2000**, *122*, 7183-7194 (g) Imamoto, T. *Pure Appl. Chem.* **2001**, *73*, 373-376 (h) Gridnev, I. D.; Yamamoi, Y.; Higashi, N.; Tsuruta, H.; Yasutake, M.; Imamoto, T. *Adv. Synth. Catal.* **2001**, *343*, 118-136 (i) Ohashi, A.; Imamoto, T. *Org. Lett.* **2001**, *3*, 373-375 (j) Crépy, K. V. L.; Imamoto, T. *Tetrahedron Lett.* **2002**, *43*, 7735-7737 (k) Ohashi, A.; Kikuchi, S.; Yasutake, M.; Imamoto, T. *Eur. J. Org. Chem.* **2002**, 2535-2546 (l) Crépy, K. V. L.; Imamoto, T.; Seidel, G.; Fürstner, A. *Org. Synth.* **2005**, *82*, 22 (m) Gridnev, I. D.; Imamoto, T. *ACS Catal.* **2015**, *5*, 2911-2915 (n) Yang, Z.; Xia, C.; Liu, D.; Liu, Y.; Sugiya, M.; Imamoto, T.; Zhang, W. *Org. Biomol. Chem.* **2015**, *13*, 2694-2702.

(116) (a) Gridnev, I. D.; Yasutake, M.; Higashi, N.; Imamoto, T. *J. Am. Chem. Soc.* **2001**, *123*, 5268-5276 (b) Gridnev, I. D.; Yasutake, M.; Imamoto, T.; Beletskaya, I. P. *Proc. Natl. Acad. Sci.* **2004**, *101*, 5385-5390.

(117) Gridnev, I. D.; Imamoto, T. *Organometallics* **2001**, *20*, 545-549.

(118) (a) Hoge, G.; Wu, H.; Kissel, W. S.; Pflum, D. A.; Greene, D. J.; Bao, J. *J. Am. Chem. Soc.* **2004**, *126*, 5966-5967 (b) Wu, H.; Hoge, G. *Org. Lett.* **2004**, *6*, 3645-3647.

(119) (a) Imamoto, T.; Nishimura, M.; Koide, A.; Yoshida, K. *J. Org. Chem.* **2007**, *72*, 7413-7416 (b) Yanagisawa, A.; Takeshita, S.; Izumi, Y.; Yoshida, K. *J. Am. Chem. Soc.* **2010**, *132*, 5328-5329 (c) Garçon, M.; Cabré, A.; Verdaguer, X.; Riera, A. *Organometallics* **2017**, *36*, 1056-1065.

(120) Imamoto, T.; Tamura, K.; Zhang, Z.; Horiuchi, Y.; Sugiya, M.; Yoshida, K.; Yanagisawa, A.; Gridnev, I. D. *J. Am. Chem. Soc.* **2012**, *134*, 1754-1769.

(121) Grabulosa, A.; Doran, S.; Brandariz, G.; Muller, G.; Benet-Buchholz, J.; Riera, A.; Verdaguer, X. *Organometallics* **2014**, *33*, 692-701.

(122) (a) Williams, B. S.; Dani, P.; Lutz, M.; Spek, A. L.; Koten, G. *Helv. Chim. Acta* **2001**, *84*, 3519-3530 (b) Ding, B.; Zhang, Z.; Xu, Y.; Liu, Y.; Sugiya, M.; Imamoto, T.; Zhang, W. *Org. Lett.* **2013**, *15*, 5476-5479 (c) Yang, Z.; Wei, X.; Liu, D.; Liu, Y.; Sugiya, M.; Imamoto, T.; Zhang, W. *J. Organomet. Chem.* **2015**, *791*, 41-45.

(123) (a) van Leeuwen, P. W. N. M.; Kamer, P. C. J.; Reek, J. N. H.; Dierkes, P. *Chem. Rev.* **2000**, *100*, 2741-2769 (b) Goudriaan, P. E.; Jang, X.; Kuil, M.; Lemmens, R.; van Leeuwen, P. W. N. M.; Reek, J. N. H. *Eur. J. Org. Chem.* **2008**, 6079-6092 (c) Patureau, F. W.; Siegler, M. A.; Spek, A. L.; Sandee, A. J.; Jugé, S.; Aziz, S.; Berkessel, A.; Reek, J. N. H. *Eur. J. Inorg. Chem.* **2012**, 496-503 (d) Nurttila, S. S.; Linnebank, P. R.; Krachko, T.; Reek, J. N. H. *ACS Catal.* **2018**, *8*, 3469-3488.

(124) van Leeuwen, P. W. N. M.; Roobeek, C. F.; Wife, R. L.; Frijns, J. H. G. *J. Chem. Soc. Chem. Commun.* **1986**, 31-33.

(125) Tang, W.; Zhang, X. *Chem. Rev.* **2003**, *103*, 3029-3069.

(126) Siutkowski, M.; Mercier, F.; Ricard, L.; Mathey, F. *Organometallics* **2006**, *25*, 2585-2589.

(127) Li, W.; Hou, G.; Chang, M.; Zhang, X. *Adv. Synth. Catal.* **2009**, *351*, 3123-3127.

(128) Vargas, S.; Rubio, M.; Suárez, A.; del Río, D.; Álvarez, E.; Pizzano, A. *Organometallics* **2006**, *25*, 961-973.

(129) Imamoto, T.; Iwadate, N.; Yoshida, K. *Org. Lett.* **2006**, *8*, 2289-2292.

(130) (a) Verdaguer, X.; Lange, U. E. W.; Reding, M. T.; Buchwald, S. L. *J. Am. Chem. Soc.* **1996**, *118*, 6784-6785 (b) Schnider, P.; Koch, G.; Prétôt, R.; Wang, G.; Bohnen, F. M.; Krüger, C.; Pfaltz, A. *Chem. Eur. J.* **1997**, *3*, 887-892 (c) Liu, Y.; Du, H. *J. Am. Chem. Soc.* **2013**, *135*, 6810-6813.

(131) (a) Padevet, J.; Schrems, M. G.; Scheil, R.; Pfaltz, A. *Beilstein J. Org. Chem.* **2016**, *12*, 1185-1195 (b) Pfaltz, A.; Müller, M.-A.; Gruber, S. *Adv. Synth. Catal.* **2018**, *360*, 1340-1345.

(132) Yamanoi, Y.; Imamoto, T. *J. Org. Chem.* **1999**, *64*, 2988-2989.

(133) Gridnev, I. D.; Imamoto, T.; Hoge, G.; Kouchi, M.; Takahashi, H. *J. Am. Chem. Soc.* **2008**, *130*, 2560-2572.

(134) *Handbook of Homogeneous Hydrogenation*; de Vries, J. G.; Elsevier, C. J., Eds.; Wiley-VCH: Weinheim, 2007.

(135) (a) Crépy, K. V. L.; Imamoto, T. *Adv. Synth. Catal.* **2003**, *345*, 79-101 (b) Gridnev, I. D.; Imamoto, T. *Acc. Chem. Res.* **2004**, *37*, 633-644 (c) Preetz, A.; Baumann, W.; Drexler, H.; Fischer, C.; Sun, J.; Spannenberg, A.; Zimmer, O.; Hell, W.; Heller, D. *Chem. Asian J.* **2008**, *3*, 1979-1982 (d) Schmidt, T.; Dai, Z.;

Drexler, H.; Hapke, M.; Preetz, A.; Heller, D. *Chem. Asian J.* **2008**, *3*, 1170-1180 (e) Schmidt, T.; Drexler, H.; Sun, J.; Dai, Z.; Baumann, W.; Preetz, A.; Heller, D. *Adv. Synth. Catal.* **2009**, *351*, 750-754.

(136) Rossen, K. *Angew. Chem. Int. Ed.* **2001**, *40*, 4611-4613.

(137) (a) Halpern, J.; Riley, D. P.; Chan, A. S. C.; Pluth, J. J. *J. Am. Chem. Soc.* **1977**, *99*, 8055-8057 (b) Brown, J. M.; Chaloner, P. A. *J. Chem. Soc. Chem. Commun.* **1980**, 344-346 (c) Brown, J. M.; Chaloner, P. A. *J. Am. Chem. Soc.* **1980**, *102*, 3040-3048 (d) Brown, J. M.; Chaloner, P. A.; Morris, G. A. *J. Chem. Soc. Chem. Commun.* **1983**, 664-666 (e) Preetz, A.; Drexler, H.; Fischer, C.; Dai, Z.; Börner, A.; Baumann, W.; Spannenberg, A.; Thede, R.; Heller, D. *Chem. Eur. J.* **2008**, *14*, 1445-1451 (f) Preetz, A.; Baumann, W.; Fischer, C.; Drexler, H.; Schmidt, T.; Thede, R.; Heller, D. *Organometallics* **2009**, *28*, 3673-3677.

(138) (a) Drexler, H.; Baumann, W.; Schmidt, T.; Zhang, S.; Sun, A.; Spannenberg, A.; Fischer, C.; Bushcmann, H.; Heller, D. *Angew. Chem. Int. Ed.* **2005**, *44*, 1184-1188 (b) Alberico, E.; Baumann, W.; de Vries, J. G.; Drexler, H.-J.; Gladiali, S.; Heller, D.; Henderickx, H. J. W.; Lefort, L. *Chem. Eur. J.* **2011**, *17*, 12683-12695.

(139) (a) Chan, A. S. C.; Pluth, J. J.; Halpern, J. *J. Am. Chem. Soc.* **1980**, *102*, 5952-5954 (b) Chan, A. S. C.; Halpern, J. *J. Am. Chem. Soc.* **1980**, *102*, 838-840.

(140) (a) Buergler, J. F.; Togni, A. *Chem. Commun.* **2011**, *47*, 1896-1898 (b) Buergler, J. F.; Niedermann, K.; Togni, A. *Chem. Eur. J.* **2012**, *18*, 632-640 (c) Schwenk, R.; Togni, A. *Dalton Trans.* **2015**, *44*, 19566-19575.

(141) (a) Zassinovich, G.; Mestroni, G.; Gladiali, S. *Chem. Rev.* **1992**, *92*, 1051-1089 (b) Noyori, R.; Hashiguchi, S. *Acc. Chem. Res.* **1997**, *30*, 97-102 (c) Noyori, R.; Yamakawa, M.; Hashiguchi, S. *J. Org. Chem.* **2001**, *66*, 7931-7944 (d) Bäckvall, J. E. *J. Organomet. Chem.* **2002**, *652*, 105-111 (e) Clapham, S. E.; Hadzovic, A.; Morris, R. H. *Coord. Chem. Rev.* **2004**, *248*, 2201-2237 (f) Gladiali, S.; Alberico, E. *Chem. Soc. Rev.* **2006**, *35*, 226-236 (g) Samec, J. S. M.; Bäckvall, J. E.; Andersson, P. G.; Brandt, P. *Chem. Soc. Rev.* **2006**, *35*, 237-248.

(142) (a) Grabulosa, A., Universitat de Barcelona, 2005 (b) Clavero, P.; Grabulosa, A.; Rocamora, M.; Muller, G.; Font-Bardia, M. *Dalton Trans.* **2016**, *45*, 8513-8531.

(143) Yang, H.; Alvarez-Gressier, M.; Lugan, N.; Mathieu, R. *Organometallics* **1997**, *16*, 1401-1409.

(144) Medici, S.; Gagliardo, M.; Williams, S. B.; Chase, P. A.; Gladiali, S.; Lutz, M.; Spek, A. L.; van Klink, G. P. M.; van Koten, G. *Helv. Chim. Acta* **2005**, *88*, 694-705.

(145) (a) Maj, A. M.; Pietrusiewicz, K. M.; Suisse, I.; Agbossou, F.; Mortreux, A. *J. Organomet. Chem.* **2001**, *626*, 157-160 (b) Cheng, X.; Horton, P. N.; Hursthouse, M.; Hii, K. K. *Tetrahedron: Asymmetry* **2004**, *15*, 2241-2246.

(146) Yamakawa, M.; Ito, H.; Noyori, R. *J. Am. Chem. Soc.* **2000**, *122*, 1466-1478.

(147) (a) Gamez, P.; Fache, F.; Lemaire, M. *Tetrahedron: Asymmetry* **1995**, *6*, 705-718 (b) Hayes, A. M.; Morris, D. J.; Clarkson, G. J.; Wills, M. *J. Am. Chem. Soc.* **2005**, *127*, 7318-7319 (c) Blacker, A. J. In *Handbook of Homogeneous Hydrogenation*; de Vries, J. G., Elsevier, C. J., Eds.; Wiley-VCH: Weinheim, 2007; Vol. 3.

(148) Fujii, A.; Hashiguchi, S.; Uematsu, N.; Ikariya, T.; Noyori, R. *J. Am. Chem. Soc.* **1996**, *118*, 2521-2522.

(149) Johansson Seechurn, C. C. C.; Kitching, M. O.; Colacot, T. J.; Snieckus, V. *Angew. Chem. Int. Ed.* **2012**, *51*, 5062-5085.

(150) Oestreich, M.; Ed. *The Mizoroki-Heck Reaction*; Wiley: Chichester, 2009.

(151)   (a) Dounay, A. B.; Overman, L. E. *Chem. Rev.* **2003**, *103*, 2945-2963 (b) Shibasaki, M.; Vogl, E. M.; Ohshima, T. *Adv. Synth. Catal.* **2004**, *346*, 1533-1552.

(152)   (a) von Matt, P.; Pfaltz, A. *Angew. Chem. Int. Ed. Engl.* **1993**, *32*, 566568 (b) Gilberston, S. R.; Genov, D. G.; Rheingold, A. L. *Org. Lett.* **2000**, *2*, 2885-2888 (c) Hashimoto, Y.; Horie, Y.; Hayashi, M.; Saigo, K. *Tetrahedron: Asymmetry* **2000**, *11*, 2205-2210.

(153)   (a) Andersen, N. G.; Ramsden, P. D.; Che, D.; Parvez, M.; Keay, B. A. *Org. Lett.* **1999**, *1*, 2009-2011 (b) Benoit, W. L.; Parvez, M.; Keay, B. A. *Tetrahedron: Asymmetry* **2009**, *20*, 69-77.

(154)   Xu, H.; Ekoue-Kovi, K.; Wolf, C. *J. Org. Chem.* **2008**, *73*, 7638-7650.

(155)   Fitton, P.; Rick, E. A. *J. Organomet. Chem.* **1971**, *28*, 287-291.

(156)   (a) Ito, H.; Ito, S.; Sasaki, Y.; Matsuura, K.; Sawamura, M. *J. Am. Chem. Soc.* **2007**, *129*, 14856-14857 (b) Kimura, M.; Uozumi, Y. *J. Org. Chem.* **2007**, *72*, 707-714 (c) Lu, Z.; Ma, S. *Angew. Chem. Int. Ed.* **2008**, *47*, 258-297.

(157)   (a) Frost, C. G.; Howarth, J.; Williams, J. M. J. *Tetrahedron: Asymmetry* **1992**, *3*, 1089-1122 (b) Trost, B. M.; van Vranken, D. L. *Chem. Rev.* **1996**, *96*, 395-422.

(158)   Trost, B. M.; Crawley, M. L. *Chem. Rev.* **2003**, *103*, 2921-2943.

(159)   Fiaud, J.; Legros, J. *J. Org. Chem.* **1987**, *52*, 1907-1911.

(160)   Castaño, A. M.; Aranyos, A.; Szabó, K. J.; Bäckvall, J. E. *Angew. Chem. Int. Ed. Engl.* **1995**, *34*, 2551-2553.

(161)   Trost, B. M.; Dietsche, T. J. *J. Am. Chem. Soc.* **1973**, *95*, 8200-8201.

(162)   Weiss, T. D.; Helmchen, G.; Kazmaier, U. *Chem. Commun.* **2002**, 1270-1271.

(163)   Pregosin, P. S.; Ruegger, H.; Salzmann, R.; Albinati, A.; Lianza, F.; Kunz, R. W. *Organometallics* **1994**, *13*, 83-90.

(164)   (a) Trost, B. M.; Strege, P. E. *J. Am. Chem. Soc.* **1977**, *99*, 1649-1651 (b) Trost, B. M.; Weber, L.; Strege, P. E.; Fullerton, T. J.; Dietsche, T. J. *J. Am. Chem. Soc.* **1978**, *100*, 3416-3426.

(165)   Auburn, P. R.; Mackenzie, P. B.; Bosnich, B. *J. Am. Chem. Soc.* **1985**, *107*, 2033-2046.

(166)   (a) Togni, A.; Breutel, C.; Schnyder, A.; Spindler, F.; Landert, H.; Tijani, A. *J. Am. Chem. Soc.* **1994**, *116*, 4062-4066 (b) Diéguez, M.; Jansat, S.; Gómez, M.; Ruiz, A.; Muller, G.; Claver, C. *Chem. Commun.* **2001**, 1132-1133 (c) Oohara, N.; Katagiri, K.; Imamoto, T. *Tetrahedron: Asymmetry* **2003**, *14*, 2171-2175 (d) Gladiali, S.; Taras, R.; Ceder, R. M.; Rocamora, M.; Muller, G.; Solans, X.; Font-Bardia, M. *Tetrahedron: Asymmetry* **2004**, *15*, 1477-1485.

(167)   (a) Togni, A.; Burckhardt, U.; Gramlich, V.; Pregosin, P. S.; Salzmann, R. *J. Am. Chem. Soc.* **1996**, *118*, 1031-1037 (b) Zhang, W.; Yoneda, Y.-I.; Kida, T.; Nakatsuji, Y.; Ikeda, I. *Tetrahedron: Asymmetry* **1998**, *9*, 3371-3380 (c) Imai, Y.; Zhang, A.; Kida, T.; Nakatsuji, Y.; Ikeda, I. *Tetrahedron Lett.* **1998**, *39*, 4343-4346 (d) Helmchen, G.; Pfaltz, A. *Acc. Chem. Res.* **2000**, *33*, 336-345 (e) Danjo, H.; Higuchi, M.; Yada, M.; Imamoto, T. *Tetrahedron Lett.* **2004**, *45*, 603-606.

(168)   (a) Hamada, Y.; Seto, N.; Takayanagi, Y.; Nakano, T.; Hara, O. *Tetrahedron Lett.* **1999**, *40*, 7791-7794 (b) Hayashi, T. *J. Organomet. Chem.* **1999**, *576*, 195-202 (c) Hayashi, T. *Acc. Chem. Res.* **2000**, *33*, 354-362 (d) Tsuruta, H.; Imamoto, T. *Synlett* **2001**, 999-1002 (e) Boele, M. D. K.; Kamer, P. C. J.; Lutz, F.; Spek, A. L.; de Vries, J. G.; van Leeuwen, P. W. N. M.; van Strijdonck, G. P. F. *Chem. Eur. J.* **2004**, *10*, 6232-6246.

(169)   (a) Nemoto, T.; Masuda, T.; Akimoto, Y.; Fukuyama, T.; Hamada, Y. *Org. Lett.* **2005**, *7*, 4447-4450 (b) Nemoto, T.; Fukuyama, T.; Yamamoto, E.; Tamura, S.;

Fukuda, T.; Matsumoto, T.; Akimoto, Y.; Hamada, Y. *Org. Lett.* **2007**, *9*, 927-930.

(170)   (a) Jin, L.; Nemoto, T.; Nakamura, H.; Hamada, Y. *Tetrahedron: Asymmetry* **2008**, *19*, 1106-1113 (b) Nemoto, T.; Kanematsu, M.; Tamura, S.; Hamada, Y. *Adv. Synth. Catal.* **2009**, *351*, 1773-1778.

(171)   Trost, B. M.; Murphy, D. J. *Organometallics* **1985**, *4*, 1143-1145.

(172)   Bravo, M. J.; Ceder, R. M.; Grabulosa, A.; Muller, G.; Rocamora, M.; Bayón, J. C.; Peral, D. *Organometallics* **2015**, *34*, 3799-3808.

Chapter IV. Half-sandwich complexes of Ir(III), Rh(III) and Ru(II) with the MaxPhos ligand

4. Half-sandwich complexes of Ir(III), Rh(III) and Ru(II) with the MaxPhos ligand

4.1. *Introduction. Chiral-at-metal complexes*

The study of chiral metal complexes is one of the most intense research areas of current organometallic chemistry.[1] This research is mainly driven by the potential application of chiral metal complexes for the catalytic synthesis of non-racemic chiral compounds.[2]

Typically, a chiral environment is generated around the metal by coordination of enantiopure organic ligands having atom-centred, axial or planar chirality.[3] Taking into account that metal coordination is the most common way to activate the substrates for chemical transformations, it seems reasonable to think that catalysts based on stereogenic metal centres would offer the most promising approach for achieving efficient transfer of chirality during an asymmetric process.[4]

Reactions mediated by Lewis acid metal complexes involve the formation and cleavage of chemical bonds in which the metal is implicated, with the potential loss of metal enantiopurity. Moreover, a major requirement for metallic catalyst precursors is the existence of coordination positions available for the substrates, which are usually occupied by solvent molecules. Therefore, a good candidate for a catalyst containing a metal centre as a source of chirality has to be susceptible to substitution but stereochemically stable.[5] Building up metallic complexes fulfilling both requirements at once is not an easy task.

Al literature survey shows that there are many organic transformations that are still underdeveloped, for which no metal complex with chiral ligands has been found to yield products with useful levels of *ee*.[1,6] Consequently, research efforts have been directed towards the exploration of other organometallic architectures, where the chiral information is not located at the ligand, but at the metal centre.[1c,7]

Chiral-at-metal or *M*-stereogenic complexes are defined as compounds bearing a stereogenic metal centre. Their chirality parallels, to a certain extend, the classic stereogenic carbon atoms of organic chemistry. In the same way that organic molecules featuring tetrahedral carbon atoms with four different substituents are chiral, tetrahedral metal complexes with four different ligands are chiral as well (Figure 1).

Tetrahedral

6 different ligands

Octahedral

3 and 4 different ligands

15 pairs of enantiomers

fac–[MABCL$_3$]

C_1 Chiral

mer–[MABCL$_3$]

(one of the three possible)

C_s Achiral

cis,cis–[MA$_2$B$_2$C$_2$]
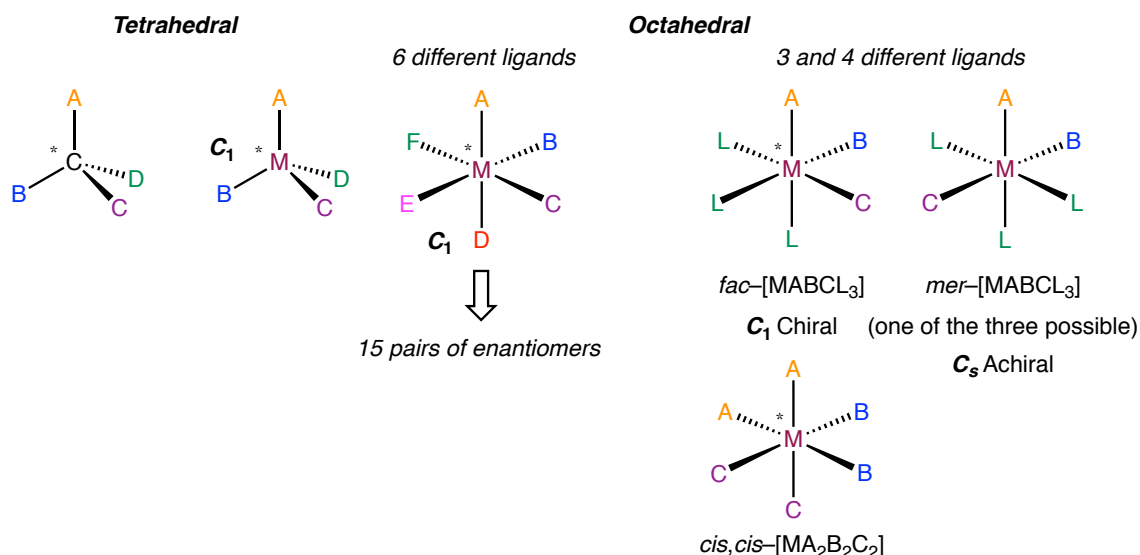
Figure 1. Coordination geometries of some typical *M*-stereogenic complexes.

Many *M*-stereogenic complexes are either tetrahedral or octahedral. Tetrahedral complexes, have the same origin of chirality as its tetrahedral carbon analogues, even though sometimes they are not configurationally stable, such as [NiBrClFI]$^{2-}$.[6] Octahedral complexes are usually somewhat more stable but have the complication that a large number of isomers are in theory possible.[8] For instance, octahedral complexes with 6 different monodentate ligands can form 15 pairs of enantiomers. In the case of octahedral complexes with four different monodentate ligands, as in octahedral [MABCL$_3$], the complexes are chiral if they take a *fac* arrangement whereas the *mer* geometry is achiral (Figure 1).

There are two main types of chiral-at-metal complexes: those having different monodentate ligands and those with one or more bidentate ligands (Figure 2).[1c]
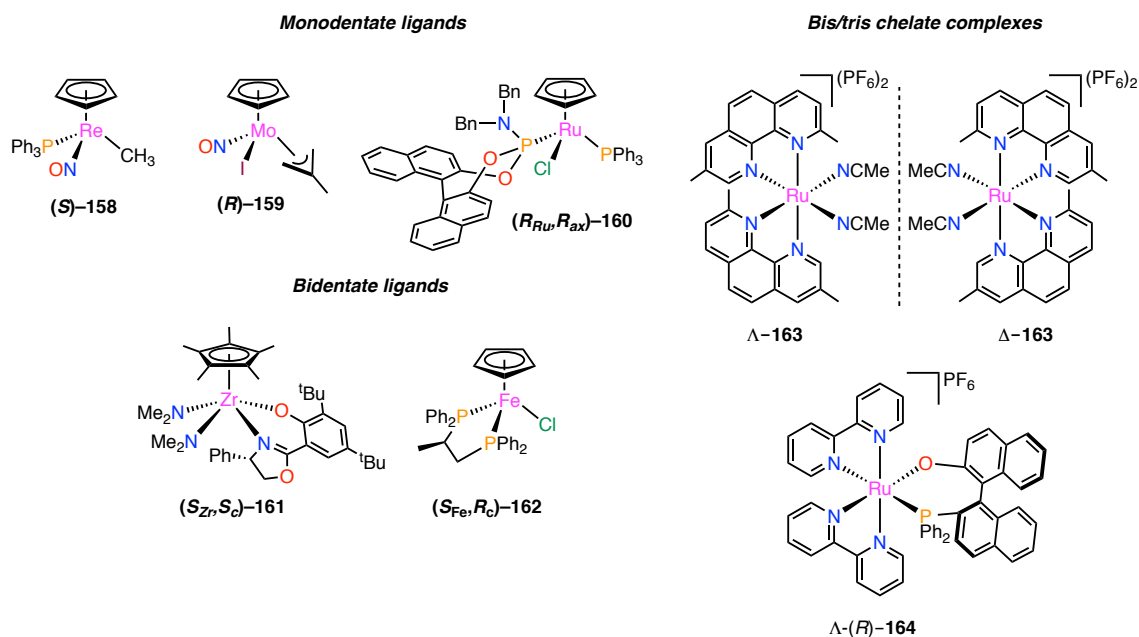
Figure 2. Selected examples of chiral-at-metal complexes.

As it is depicted in Figure 2, among the chiral-at-metal half-sandwich complexes, usually three- or four-legged, there are those with monodentate ligands and others with bidentate ligands displaying a C_1-symmetry. Besides, *bis*- or *tris*-chelate octahedral complexes with achiral ligands, such as phenanthrolines also lead to chiral-at-metal complexes.[9]

Regarding the complexes depicted in Figure 2 it is sometimes not evident to see if a coordination compound would exhibit optical activity. By definition, a molecule is chiral if it is non-superimposable on its mirror image and in terms of symmetry a chiral molecule lacks an improper (S_n) axis of symmetry.

Hence, molecules belonging to point group C_1, such as complexes **158-162** are chiral. The same property is observed for dissymmetric molecules, as it is the case for well-known *tris*-chelate complexes, such as [Co(en)]Cl$_3$ or the *cis*-(*bis*)-chelate complexes **163** (only the *cis*-isomer can possess a pair of enantiomers; the *trans*-isomer is achiral), depicted in Figure 2 where enantiomers are distinguished by using the labels Δ and Λ.

4.1.1. *R/S Nomenclature*

The absolute configuration of a stereogenic metal centre is specified in a similar way to chiral organic compounds having a stereogenic carbon atom, following the well-known Cahn-Ingold-Prelog (CIP) priority rules.[10] The problem of assigning priorities to polyhapto ligands or, in other words, organic groups where more than one carbon atom is interacting with the metal centre, such as the η^5- cyclopentadienyl ligand, was first addressed by Tirouflet and co-workers.[11] They suggested that the sum of the atomic number of all atoms of a polyhapto ligand connected to the metal should be considered. Stanley and Baird[12] later suggested a similar modification of the CIP priority rules to determine the absolute configuration of a stereogenic metal complex based on the sum of the atomic weights of the atoms in polyhapto ligands coordinated to a metal centre.

For example, the η^5-cyclopentadienyl ligand would be considered a pseudo-atom of molecular weight 60 (five carbon atoms linked to the metal), and the η^6-benzene ligand of molecular weight 72 (six carbon atoms bonded to the metal centre). Therefore, the priority sequence can be drawn as follows:

$I^- > Br^- > \eta^6\text{-}C_6H_6 > \eta^5\text{-}C_5H_5 > \eta^3\text{-}C_3H_3 > Cl^- > PR_3$ *(e.g. phosphines) > OR_1R_2 (e.g. alkoxydes) > NR_1R_2 (e.g. amines or oxazolines) > η^1-C (such as in –CH₃)*

The determination of *R* or *S* descriptor for the absolute configuration can then be performed in the same way as for stereogenic carbon atoms applying the CIP priority rules as it can be seen in the examples depicted in Figure 2.

4.1.2. *Configurational stability of chiral-at-metal complexes*

Coordination compounds that are chiral only due the presence of a stereogenic centre at the metal form a pair of enantiomers with identical physical properties. As with organic compounds, different enantiomers can be identified by polarimetry, and a pair of enantiomers will give opposite optical rotation.[6,13] Circular dichroism (CD) spectroscopy is also commonly applied, and the spectra of two enantiomers are mirror images of each other with opposite sign.[14]

Often, the same absolute configuration is assigned to structurally related compounds with similar CD spectra, and similar compounds with mirror image of CD spectra can exhibit opposite absolute configuration.[1c] Chiral-at-metal complexes are often intensely coloured, and in such cases the optical rotation cannot be easily determined. Nevertheless, in the solid state the absolute configuration of an

enantiopure metal complex can be univocally assigned by X-ray diffraction, when it is possible to grow suitable crystals for its determination.[15] Needless to say, the presence of a metal is very useful to determine the absolute configuration.

Diastereomeric complexes with a stereogenic metal centre do have different physical properties and can be analysed by NMR spectroscopy. When an optically pure ligand is employed in synthesis, two diastereomers form that differ only in the configuration at the metal centre. The diastereomeric ratio can be calculated from the intensities of corresponding diastereomeric signals in ^{1}H or ^{31}P{^{1}H} NMR spectra, albeit some care has sometimes to be taken when analysing spectra at low temperatures, particularly in those complexes which display dynamic exchange processes.[14a]

In the solid state, chiral-at-metal complexes are configurationally stable. However, the more labile nature of the metal-ligand bonds, along with the fluxional processes present in some coordination geometries, sometimes derives in optical erosion.[6,16] Examples of this behaviour are depicted in Figure 3.
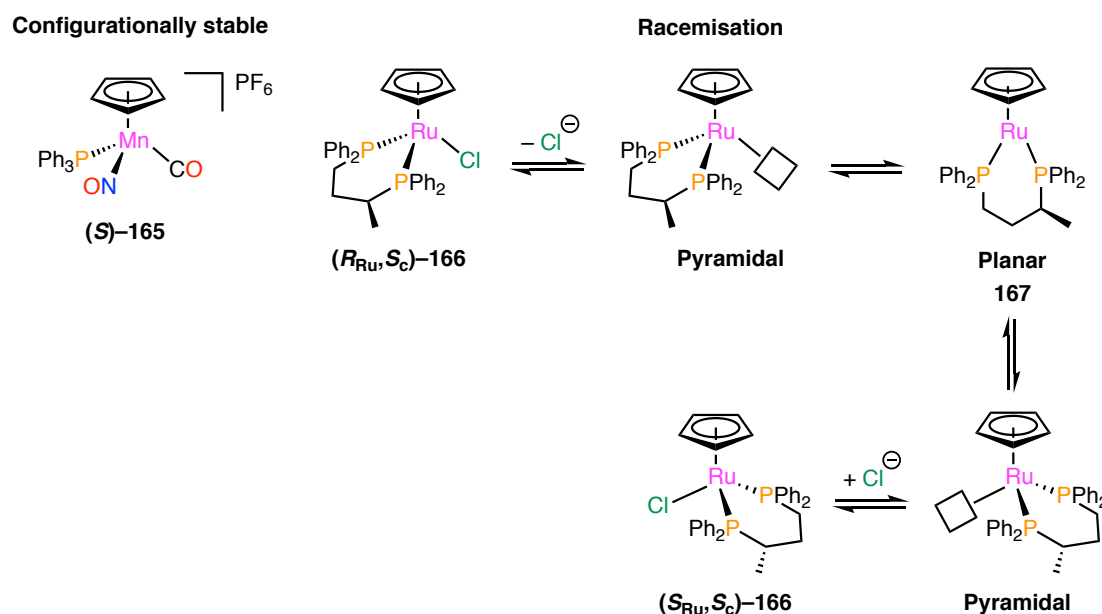
Figure 3. Configurationally stable **165** and proposed mechanism of epimerisation of complex **166**. The square denotes a vacant coordination position.

While complex **165** is configurationally stable in solution, probably due to the stabilising effect of the carbonyl and nitrosyl π-acidic ligands, **166** epimerises leading to the formation of a 77:23 ratio mixture of diastereomers where the kinetics of the reaction can be easily studied by ^{31}P{^{1}H} NMR.[16c]

These dynamic exchanges have been detected in other systems with C_1-symmetric *P,N* ligands, being intermediates with a coordination number of 5 the most

prone to suffer such processes, where trigonal bipyramidal geometries quickly isomerise in square-planar pyramids (Berry's pseudorotation).

(S_P, S_M, S_C)–168 (S_P, R_M, S_C)–168

M = Rh, Ir
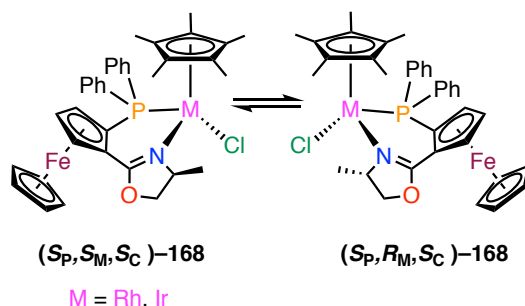
Figure 4. Epimerization at Rh and Ir in half sandwich complexes.

As it is showed in Figure 4, Carmona and co-workers[17] reported the synthesis of **168**, where fractional crystallization allowed the obtention of distereomerically pure complexes (S_P, S_M, S_C)-**168** and (S_P, R_M, S_C)-**168** (98%). Unexpectedly, after 20 days at room temperature in CDCl$_3$ the diastereomeric excess decreased for the Rh complex to 42%.

Racemisation is usually unwanted and constitutes, indeed, an important problem, as a partial or fully racemised metal complex will give lower or no enantiomeric excess when employed as a catalyst in enantioselective reactions.[17]

4.2. *Precedents on the synthesis of optically pure M-stereogenic half-sandwich complexes*

In octahedral half-sandwich complexes, one of the ligands is an arene ring system, mainly benzene or cyclopentadienyl (η^5-C$_5$H$_5$, Cp) and their derivatives (Figure 5).

Three-legged   *Four-legged*
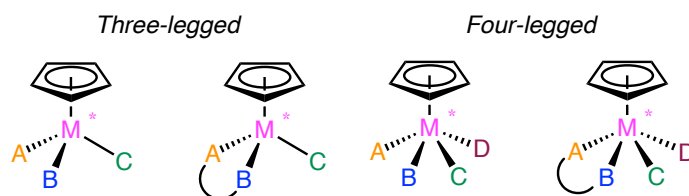
Figure 5. Common coordination geometries in *M*-stereogenic half-sandwich complexes. A–B represents a chiral bidentate ligand.

These arene ligands occupy three of six possible coordination positions of an octahedral metal complex, or in other words, a face of the geometrical octahedron, whereas the other three sites can be occupied by other ancillary ligands. These

complexes have also been named "pseudotetrahedral" or "piano stool complexes" since its shape reminds more a tetrahedron rather than its formal octahedral geometry.

Interestingly, when these three ancillary ligands are all different or if a coordinated C_1-symmetric bidentate ligand is present, the resulting complexes become chiral and stereogenic at the metal (Figure 5).[1a,b]

In this section a summary of the main synthetic procedures to prepare chiral-at-metal half-sandwich complexes is presented.

4.2.1. *Resolution of racemic mixtures*

Enantiopure chiral-at-metal complexes can be accessed by resolution of racemic mixtures using chiral auxiliaries.[1b,c,6] In this approach, the racemic mixture of the metal complex is treated with a chiral, optically pure agent that is capable of forming a covalent bond to one of the ligands. Hence, a mixture of two diastereomers, which differ only in the configuration at the metal, is formed and sometimes they can be separated by fractional crystallization or by column chromatography. The chiral auxiliary can be subsequently removed, affording the chiral-at-metal complex in enantiopure form.

In the late sixties, Brunner and co-workers,[6,18] reported for the first time, a textbook example of application of such methodology (Scheme 1).
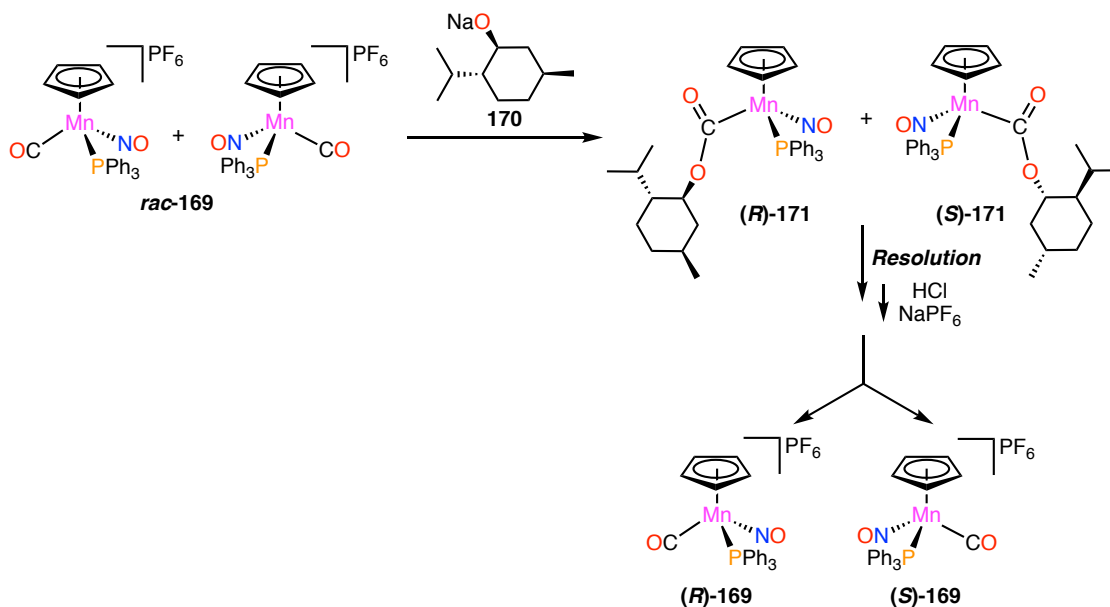
Scheme 1. Resolution of *rac*-169.

The racemic mixture of cationic complex *rac*-**169** was treated with enantiopure sodium menthoxide giving the diastereomeric acyl complexes **171** that could be separated by fractional crystallisation. After cleaving off the menthoxide by treatment with gaseous HCl, the pure enantiomers of **169** were obtained and its optical purity was confirmed by CD measurements. Interestingly, the configurational stability was high and no *ee* erosion was observed for solutions in dichloromethane over a period of several days. Other authors have also make use of resolution of racemic mixtures with chiral agents for the preparation of enantiomerically enriched *M*-stereogenic complexes achieving excellent results.[19]

4.2.2. *Preparation of diastereopure M-stereogenic half sandwich complexes with chiral monodentate ligands*

The complexes described in the previous section contained achiral ligands, but are chiral because of the presence of a stereogenic metal centre. If such complexes bear a chiral ligand, they exhibit stereogenic centres both at the metal and at the ligand, giving rise to the formation of a mixture of two diastereomers. These can be separated to afford single diastereomers, and as opposed to enantiomers they typically do not form in a 1:1 ratio and their stereochemical purity can be quickly assessed by NMR spectroscopy, because diastereomers typically give distinguishable signals in their spectra. For instance, if they contain phosphorus ligands, $^{31}P\{^{1}H\}$ NMR spectroscopy have proven to be especially useful.[20]

Bauer and co-workers[1c,20c] reported the isolation of a diastereopure ruthenium complex with a coordinated chiral phosphoramidite by substitution of a triphenylphosphine in the starting complex (Scheme 2).
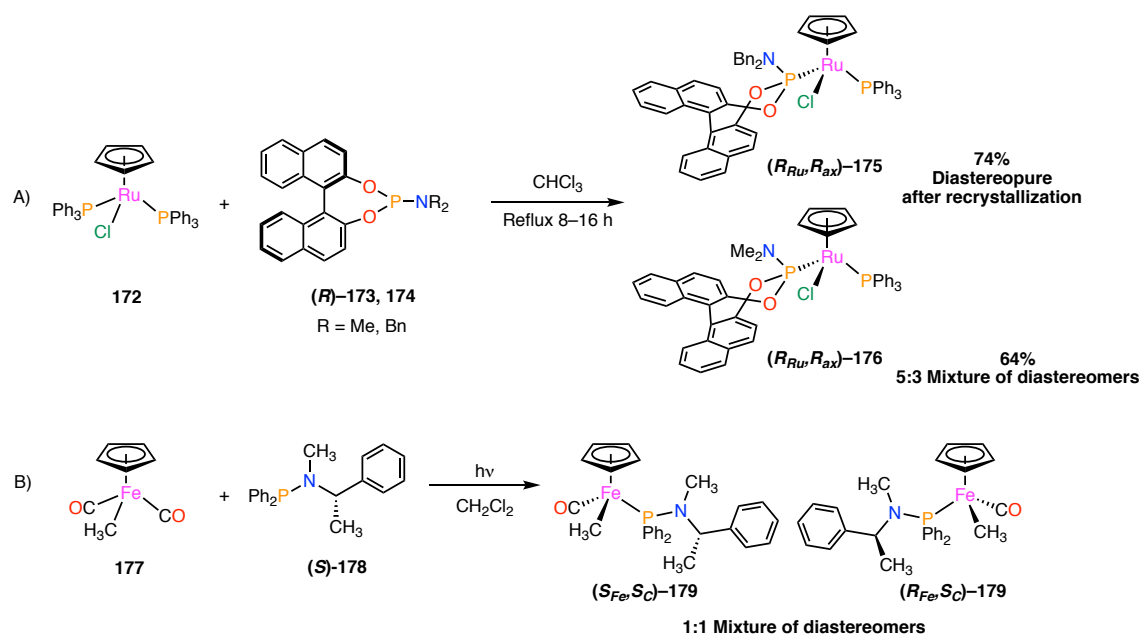
Scheme 2. Synthesis of diastereomeric ruthenium complexes with monodentate chiral ligands.

Interestingly, the phosphoramidite ligand **173** with NMe$_2$ substituents afforded complex **176** as a 5:3 mixture of inseparable diastereomers, while ligand **174** yielded a 1:8 diastereomeric ratio, which was successfully separated by fractional crystallization. Apparently the bulkier ligand **174**, triggers the formation of mainly one diastereoisomer.

Brunner and co-workers[20a,b] also studied a related ligand exchange reaction, releasing one carbonyl ligand in **177** and coordinating the chiral aminophosphine **178** generating a 1:1 mixture of diastereoisomers. Although the reaction is not regioselective, the products appeared to be configurationally stable which allowed their purification and separation by means of column chromatography.

4.2.3. *Preparation of diastereopure M-stereogenic half sandwich complexes with chiral C$_1$-bidentate ligands*

The preparation of *M*-stereogenic complexes with monodentate ligands often leads to mixtures of diastereomeric products. In contrast, the use of bidentate ligands, especially those having a *C$_1$*-symmetry, can increase the rigidity of a metal complex, and therefore difficult or supress the epimerisation processes. This fact represents a massive advantage since the reactions appeared to be much more stereoselective allowing the formation of mainly one optically pure species (Scheme 3).
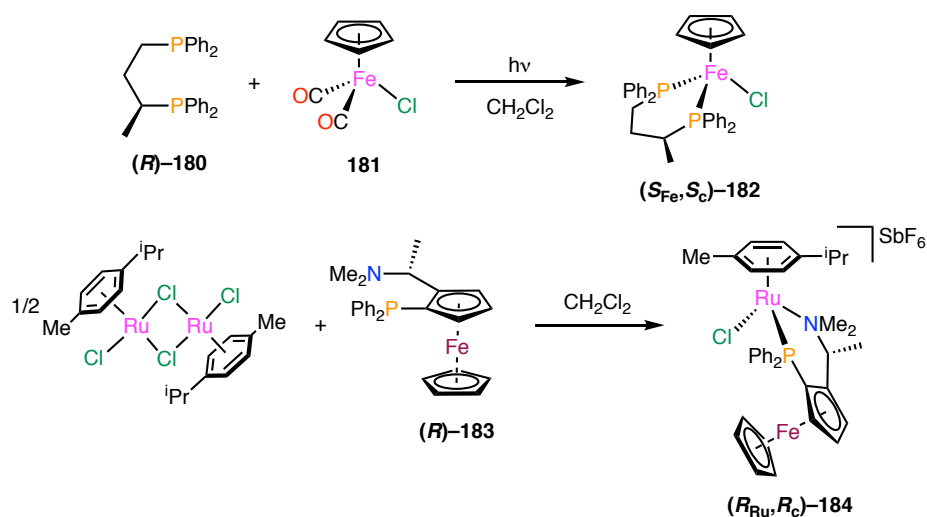
Scheme 3. Synthesis of *M*-stereogenic complexes using C_1-symmetric bidentate ligands.

When **181** was reacted in the presence of UV-light with the chiral diphosphine (***R***)-**180**, the reaction gave only one product (***S*_{Fe},*S*_c)–182** as pure diastereomer. Unfortunately, **182** isomerises in solution at room temperature to a 95:5 equilibrium of diastereomers as it was confirmed by NMR.[21]

Coordination of (***R***)-**183** to [Ru(μ-Cl)(p-cymene)]$_2$ also affords the formation of one diastereomer, being in this case a stable orange solid that does not isomerise in solution.[22] The bulkiness of the aminophosphine ligand probably accounts for the higher configurational stability of the metal.

C_1-symmetric ligands are often applied to avoid the erosion of the stereochemical information of a metal complex through racemization or epimerization. Therefore, modulating the steric and electronic properties of such ligands would be an efficient way to build up new optically pure *M*-stereogenic complexes for its future application to asymmetric transformations.

4.3. *Precedents on C₁-symmetric ligands and metal centred chirality*

Chapter 3 described the formation of *P*-stereogenic hydrogen-bridged-supramolecular assemblies with the optically pure Secondary Phosphine Oxide ^tBuMeP(O)H. If we consider the *pseudobidentate* unit itself, it possesses a C_2-symmetry in which the electronic environment of both phosphorus atoms is the same. In the literature, there are many examples of C_2-symmetric diphosphorus ligands with diphosphines being the most studied systems.[23]

One of the reasons that spurred the use of such ligands with a C_2-symmetry was the reduced number of intermediates and transition states during the catalytic cycles, what simplifies their study. In fact, the excellent catalytic results in asymmetric hydrogenation obtained with C_2-diphosphines, created the general impression that these ligands were able to promote much more high enantioselectivities than other less symmetric analogues.[23a,24] More recently, it has been demonstrated that this idea is not always true.[25] What is more, the use of diphosphorus ligands with C_1-symmetry offers a wider range of possibilities, since each phosphorus atom can be modified independently in a sequential manner, allowing the preparation of modular ligands, that can be used, as it has been explained in the previous section, to synthesise *M*-stereogenic complexes.

Nevertheless, the number of C_1-diphosphorate ligands, containing a single stereogenic phosphorus atom is surprisingly scarce (Figure 6).
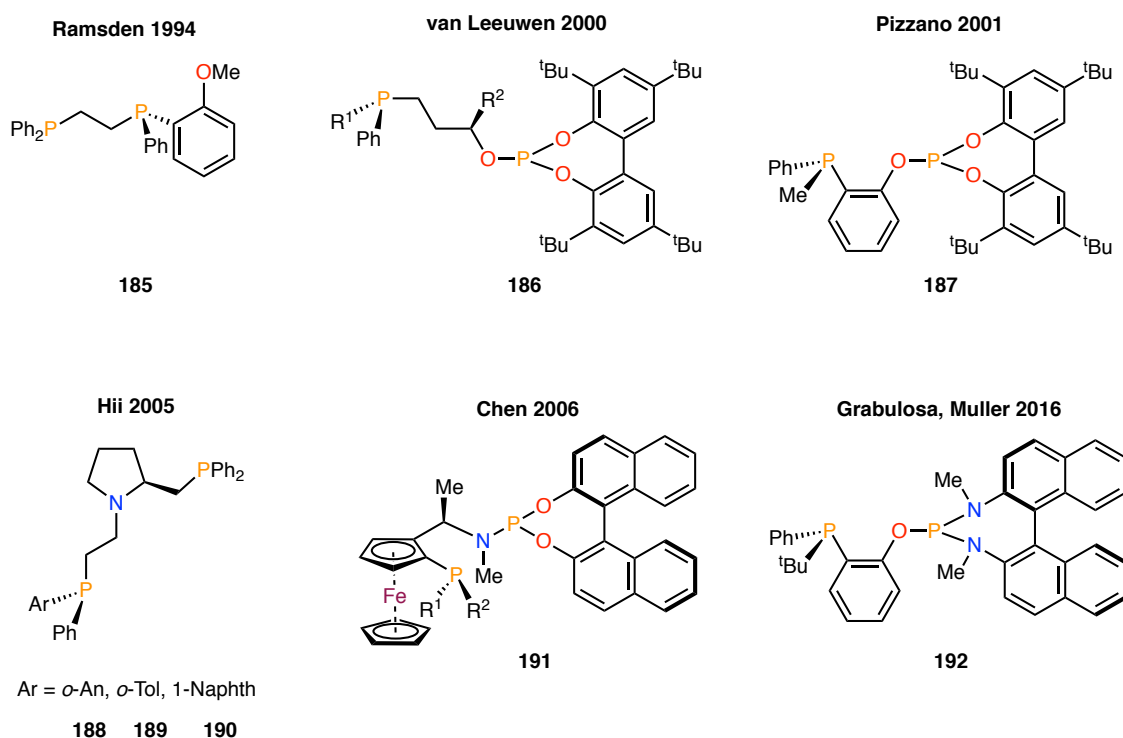
Figure 6. C_1-symmetric ligands containing, at least, one stereogenic phosphorus atom.

In 1994 Ramsden and co-workers[26] described the synthesis of a diphosphine in which the stereogenic phosphorus came from a precursor prepared using the Jugé-Stephan method. Some years later, van Leeuwen and co-workers[27] reported a family of phosphine-phosphite compounds that were applied in the Rh-catalysed hydroformylation of styrene with enantioselectivities up to 63%. It is interesting to

remark the papers of Pizzano and co-workers,[28] who also prepared, a year later, a family of phosphine-phosphite ligands by condensation of *P*-stereogenic *o*-phosphinophenols, generally obtained by the Jugé-Stephan method, and a chlorophosphine derivative in the presence of a base. Recently, Grabulosa, Muller and co-workers[29] have successfully applied the same methodology in the synthesis of phosphine-phosphoramidite derivatives with a C_1-symmetry, leading to a family of Pd catalysts for allylic substitution reactions.

Other interesting ligands are the aminodiphosphines described by Hii and co-workers[30] by reaction of diarylphosphinocarboxylic acids with (–)-2-(diphenylphosphino)methylpyrrolidines furnishing amidodiphosphines which can be in turn easily reduced to afford the corresponding *P,N* ligands. Finally, the ferrocenyl-diphosphines of Chen and co-workers[31] are also noticeable to mention, which have displayed 99% *ee* in Rh-catalysed asymmetric hydrogenations.

All the systems shown in Figure 6 are ligands containing mainly aryl substituents on the phosphorus atom. In contrast, when it comes to design alkyl- C_1-symmetric diphosphines, one of the synthetic approaches is the Evans-Imamoto method[32] consisting on the asymmetric deprotonation of a prochiral substrate mediated by the adduct *sec*-BuLi/(–)-sparteine, as it was explained in Chapter 2.

This method has allowed the obtention of many diphosphines with a very small bite angle, especially with C_2-symmetry, such as MiniPhos[33] or the BisP* family.[33b,34]

An important exception is the C_1-symmetric trichickenfootphos (TCFP) described by Hoge and co-workers[35] prepared by means of preparative HPLC instead.

Hoge 2004
TrichickenfootPhos
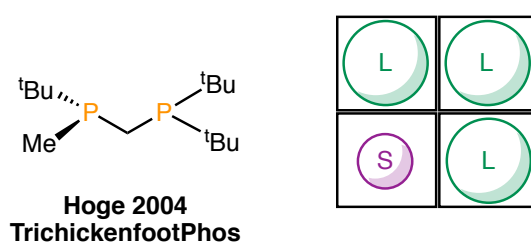
Figure 7. Trichickenfootphos ligand and quadrant model for its steric biasing, where "S" denotes small and "L" large.

However, limitations on the availability of (–)-sparteine as chiral auxiliary has led to several authors to find other strategies to prepare *P*-stereogenic diphosphines containing alkyl groups. In this line, Danjo, Imamoto and co-workers[36] persisted, after some unsuccessful attempts, in the preparation of 1,2-diphosphinobenzenes, meeting success with a clever use of *bis*(phosphine)boronium salts. In these compounds, two

secondary phosphines are connected through a BH_2 bridge displaying a bite angle similar to that reported for the TCFP[35] (Scheme 4).
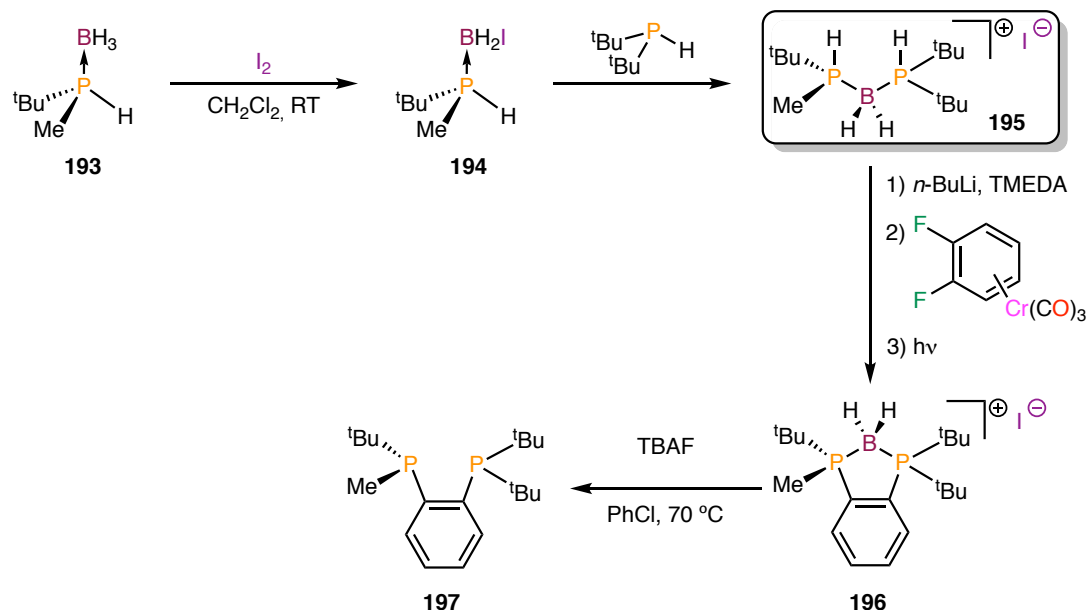
Scheme 4. Preparation of *P*-stereogenic *bis*(phosphine)boronium iodide and 1,2-diphosphinobenzene.

Monoiodination of **193** with 0.5 equivalents of iodine furnished **194**, which was reacted with di-*tert*-butyl phosphine to afford enantiomerically pure (*S*)-**195** in 62% yield. (Scheme 4) Furthermore, deprotonation of (*S*)-**195** with two equivalents of *n*-BuLi and double S_NAr on the activated difluorobenzene afforded the optically pure diphosphinobenzeneboronium salt **196** after photochemical dechromination in 78% yield. The BH_2 bridge can be cleaved using TBAF at relatively high temperature, to release the free diphopshine without loss of optical purity.

This synthesis have two important implications, one of them is the preparation of C_1-symmetric phosphines using air stable boronium salts achieving ligands with high grades of optical purity. On the other hand, we can see a new role of the borane group, since it typically acts but "only" as a protecting group that has to be removed when the free phosphorus compound is required. However, in the presented synthesis, the BH_2 plays a more active role in the chemistry involved, enabling the preparation of crowded diphosphines difficult to obtain by other ways.

4.3.1. *Synthesis and coordination chemistry of the MaxPhos ligand*

Inspired in TrichickenfootPhos ligand,[35] our research group envisaged in 2010 the preparation of a nitrogenated analogue that was named MaxPhos (Scheme 5), which is a rare example of *P*-stereogenic, C_1-symmetric ligand with a short bridge between the phosphorus atoms.[37]
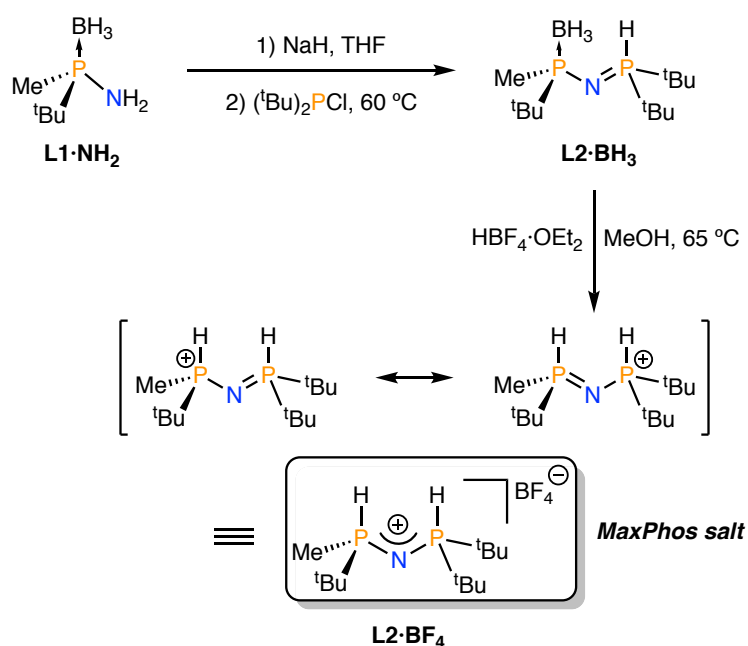
Scheme 5. Synthesis of **L2·BF₄**.

As it has been explained, reductive cleavage of a chiral aminophosphine, prepared after condensation of *cis*-1-amino-2-indanol with $^{t}BuPCl_2$ and subsequent nucleophilic ring-opening with the Grignard reagent, affords synthon **L1·NH₂**, amenable to further transformations. It has to be recalled that since both enantiomers *cis*-1-amino-2-indanol are commercially available, multigram quantities of any enantiomer of **L1·NH₂** can be prepared.

L1·NH₂ can be deprotonated by sodium hydride and reacted with ($^{t}Bu)_2$PCl yielding the intermediate iminophosphorane **L2·BH₃** which was found to exist exclusively as its P–H tautomer.

It is important to remark at this point that, in a similar manner as SPOs does, *P*-stereogenic secondary iminophopshoranes (SIPs) have also a tautomeric equilibrium between the pentavalent iminophosphorane and the corresponding aminophosphorane (Scheme 6).
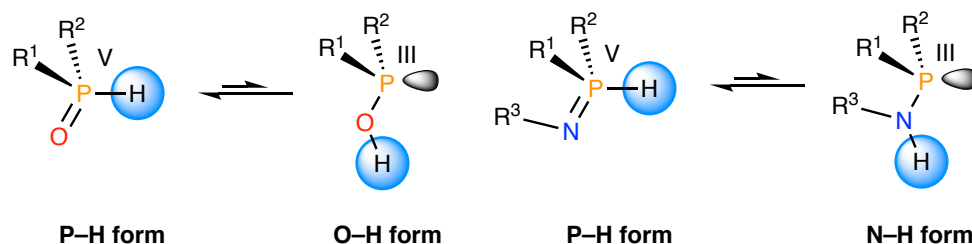
Scheme 6. Phosphinous acid/SPO tautomerism (*left*) and aminophosphine/SIP tautomerism (*right*).

The tautomerism of SIPs has exactly the same features as the SPOs equilibrium: P(V) air-stable species are normally the predominant tautomers, but in the presence of a metal source, coordination to the metal efficiently shifts the equilibrium towards the P(III) form. Furthermore, SIPs are configurationally stable, since the PH/NH tautomerism does not affect its optical purity.

In addition, thanks to this tautomeric equilibrium involving the P atoms and the NH bridge, after treatment of **L2·BH₃** with tetrafluoroboric acid, it was obtained as its bench-stable crystalline tetrafluoroborate salt, in contrast to many of the new generation highly basic and air-sensitive *P*-stereogenic ligands with alkyl substituents.[38]

The MaxPhos ligand can be seen as a nitrogen-containing analogue of the trichickenfootphos (TCFP) reported by Hoge and co-workers having a wider P-N-P angle of 103.04º than the P-C-P angle in TCFP according to X-ray measurements. This is translated, due to the shorter P-N bonds compared to P-C bonds in a slightly shorter bite angle of 70.0º than that of TCFP (72.6º).[37a,39] Both P-N bonds have almost identical distances suggesting that the resonance-hybrid **L2·BH₃** depicted in Scheme 5 is the most accurate descriptor for the [MaxPhos·H]⁺ cation and that the positive charge is evenly distributed between the two P atoms.

It has to be noted that, in contrast with TCFP, MaxPhos is extremely stable and can be prepared in large scale without the use of chromatographic methods for its purification.

In solution, NMR of MaxPhos·HBF₄ is consistent with the presence of a single compound. In the $^{31}P\{^1H\}$, two distinct resonances for the non-equivalent PH groups were visible at 6.57 and 6.83 ppm with $J_{H,P}$ values of 458 and 477 Hz, respectively, proving that the tautomeric equilibrium is fully displaced towards the PH form.[39]

The free MaxPhos ligand can be obtained by deprotonation of **L2·BF₄** with *n*-BuLi at –78 ºC and treatment of the resulting mixture with deoxygenated ⁱPrOH to ensure the neutrality of the resulting aminophosphine product (Scheme 7).[39-40]
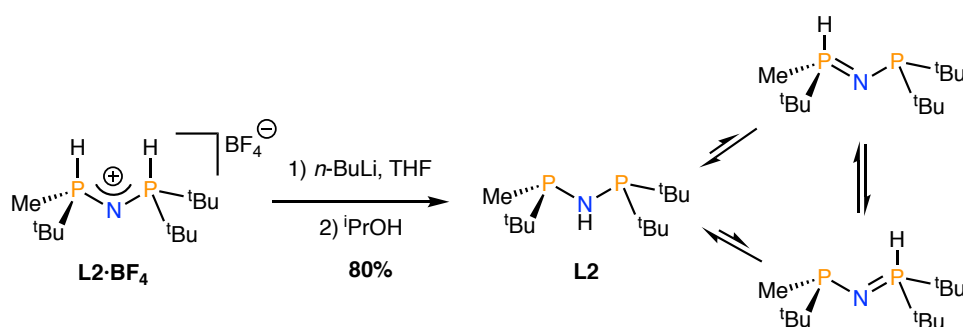
Scheme 7. Preparation of the free neutral MaxPhos ligand and its three tautomeric forms.

This method allowed the isolation of the air-sensitive oil with $^{31}P\{^1H\}$ NMR (C_6D_6) resonances at 79.5 and 52.8 ppm and a ^1H NMR (C_6D_6) spectrum that did not show evidences of H–P resonances, indicating that the only species in solution for the neutral ligand is the NH tautomer.

The coordination chemistry of this ligand was initially explored with Rh(I) diene complexes,[37a] which were found to be excellent precursors for the asymmetric hydrogenation of functionalised olefins[39] and later for intramolecular Pauson-Khand reactions.[41] These studies were followed by the synthesis of several Ni(II) and Pd(II) complexes some of which were used in asymmetric allylic substitutions (Figure 8).[40]
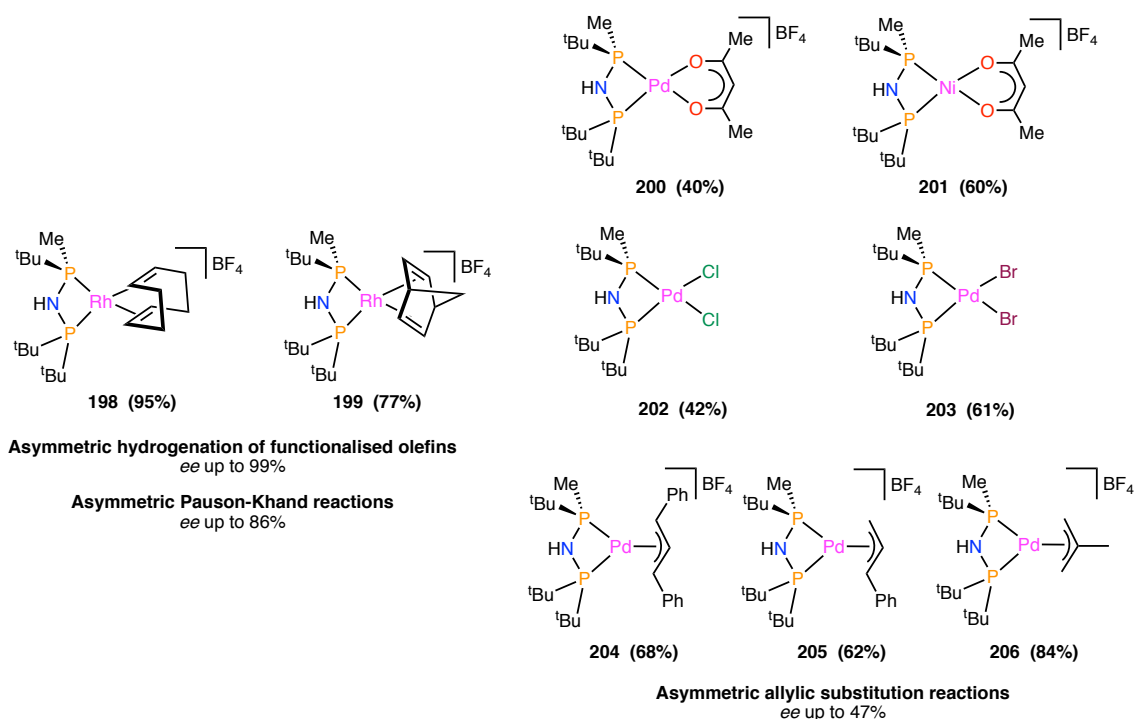
Figure 8. Several d^8-MaxPhos complexes with Rh(I), Pd(II) and Ni(II) centres.

The synthesis of many of these complexes was carried out using directly the phosphonium salt **L2·BF$_4$** in the presence of the metallic source. This process often requires a base, which can be present in the precursor (as it happens with the acetylacetonate complexes[40]) or external, for instance, sodium carbonate.[37a]

In all the reported cases, the MaxPhos ligand was coordinated to d^8 metals with square-planar geometry. With the aim of expanding the range of metals coordinated to MaxPhos, in this THESIS we present the studies concerning the preparation of pseudotetrahedral half-sandwich complexes of Rh(III), Ir(III) and Ru(II) containing the [(η^n-ring)M(MaxPhos)L] cations. We chose this type of complexes because the C_1-symmetric nature of MaxPhos results in a stereogenic metal atom upon coordination.[1a,b] Although the preparation of optically pure, metal-stereogenic complexes is a classic topic of coordination chemistry,[6] it is receiving renewed interest[8,42] due to the expectations of the application of chiral-at-metal complexes in asymmetric catalysis.[1c,7c,42] Having a complex with a resolved metallic atom reacting with the substrates during the catalytic cycle may lead to very enantioselective systems, as it has been demonstrated recently in a few reactions by Meggers and coworkers.[7d,9c,e,43]

This field, however, is severely underdeveloped due to the scarcity of methods to prepare optically pure, chiral-at-metal systems. In this THESIS, we show that the MaxPhos ligand leads to the exclusive formation of a single isomer of the complexes. In addition, we found that in the case of Ir(III), a cyclometallated compound is obtained with high diastereoselectivity.

4.4. *Half-sandwich complexes of Ir(III), Rh(III) and Ru(II) with the MaxPhos ligand*

4.4.1. *Rhodium and Iridium M-stereogenic complexes with the MaxPhos ligand*

Reaction of the acetylacetonate complexes $[(\eta^5\text{-}C_5Me_5)M(acac)Cl]$ (M = Rh, Ir)[44] with (S_P)-**L2·BF$_4$**[37,39] in refluxing dichloromethane gave cationic complexes with the formula $[(\eta^5\text{-}C_5Me_5)MCl(MaxPhos)][BF_4]$ (M = Rh (**L2Rh1**), Ir (**L2Ir1**)). Formally, the acetylacetonate is protonated by the cationic diphosphane and the generated acetylacetone is displaced from the coordination sphere of the metal by the phosphorus atoms of the resulting neutral diphosphane (Scheme 8).
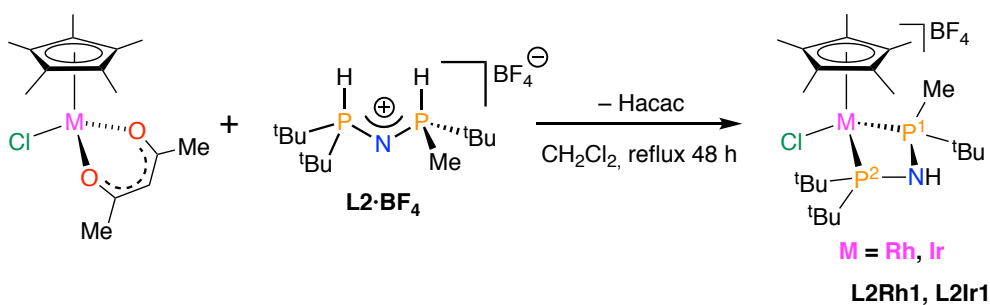
Scheme 8. Reaction of **L2·BF$_4$** with Rh- and Ir-acac precursors.

Complexes **L2Rh1** and **L2Ir1** were characterised by analytical and spectroscopic means and by the determination of their crystal structure by X-ray diffraction. The assignment of the NMR signals was verified by performing selective decoupling experiments and by two-dimensional homonuclear and heteronuclear (COSY, NOESY, HSQC, HMQC and HMBC) correlations as it is detailed in the Experimental Section (Chapter 6).

The IR spectra showed a broad and weak N–H absorption in the 3260-3270 cm^{-1} range as well as a strong band centred at around 1040 cm^{-1} attributed to the BF$_4$ anion.

NMR data are consistent with the presence of the C$_5$Me$_5$ and MaxPhos ligands in 1:1 molar ratio, in both cases (Figure 9).
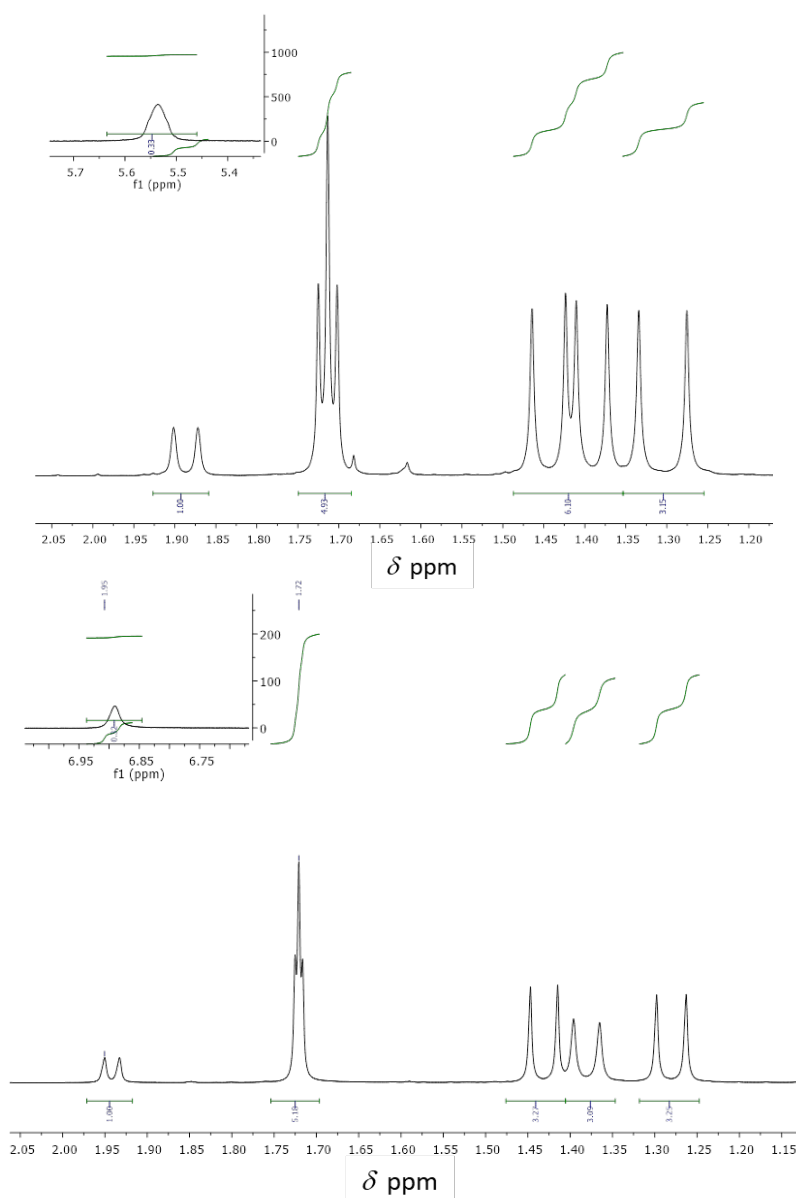
Figure 9. ^{1}H NMR spectra (400 MHz, CDCl$_3$, 25 ºC) of complexes **L2Rh1** (*top*) and **L2Ir1** (*bottom*).

The ^{31}P{^{1}H} NMR spectrum of the rhodium complex **L2Rh1** consists of two doublets of doublets centred at 51.1 (P^{1}) and 88.3 (P^{2}) ppm, with $^{1}J_{RhP}$ and $^{2}J_{PP}$ coupling constants of around 116 and 89 Hz, respectively (Figure 10).
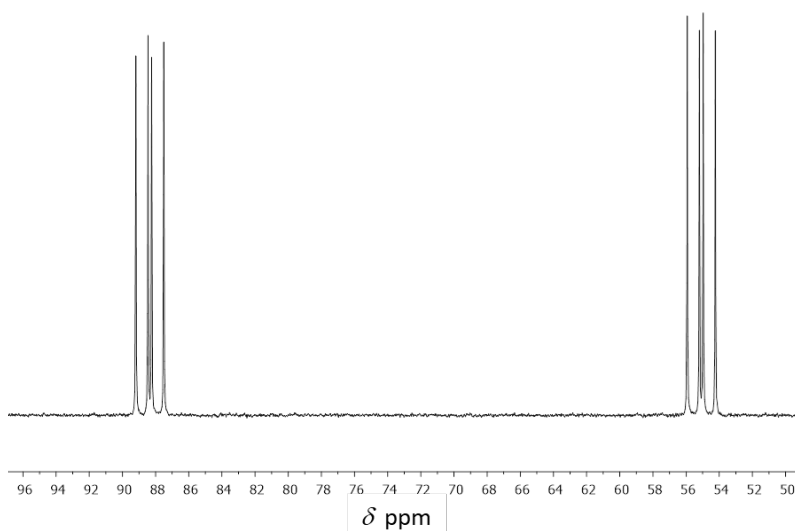
Figure 10. ^{31}P{^{1}H} NMR spectrum (400 MHz, CDCl$_3$, 25 ºC) of the Rh complex **L2Rh1**.

The iridium complex **L2Ir1** shows two doublets at 19.2 (P^1) and 55.3 (P^2) ppm, with a $^2J_{PP}$ coupling constant of 56.2 Hz.

It is important to note that, in some preparations of the iridium complex **L2Ir1**, two additional doublets (less than 1% abundance) centred at 29.70 and 53.96 ppm with a coupling constant of 52.5 Hz were also detected. These signals can be tentatively assigned to the R_{Ir},R_P epimer.

The phosphorus nuclei and ^{t}Bu substituents have been assigned by two-dimensional ^{31}P–^{1}H and ^{13}C–^{1}H correlation spectra, respectively (Figure 11).
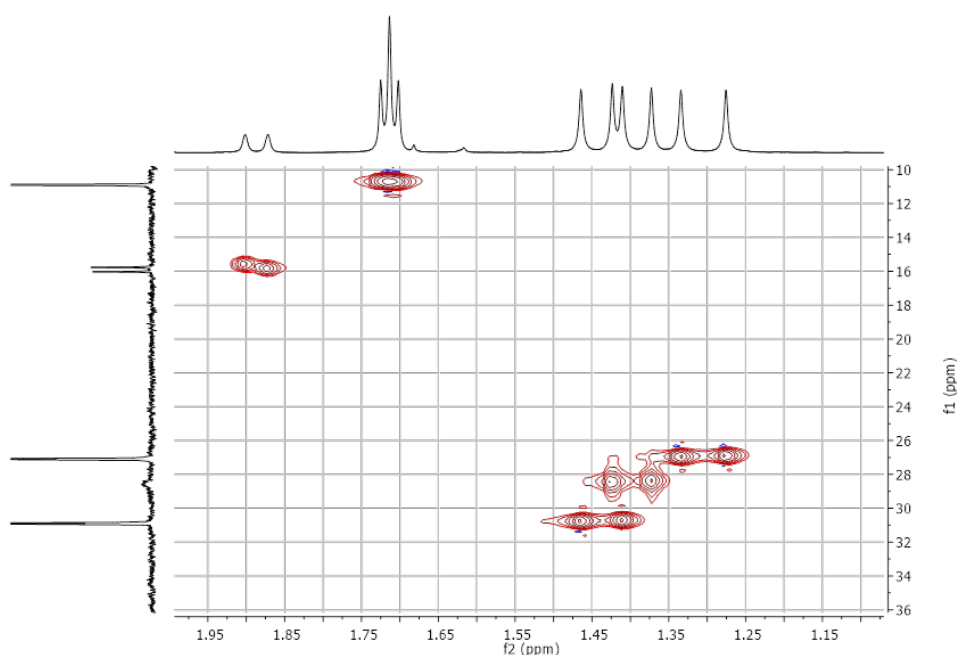
Figure 11. ^{1}H–^{13}C HSQC (CDCl$_3$, 25 ºC) of complex **L2Rh1**.

184

The diastereotopic ^{t}Bu groups linked to the P^2 phosphorus atom create asynchronous resonances for each pair of related nuclei. Interestingly, in complex **L2Rh1** one of the *tert*-butyl groups of P^2 appeared very broad in the $^{13}C\{^1H\}$ NMR spectrum, but its chemical shift could be unequivocally ascertained, thanks to the ^{13}C–^1H correlation spectrum (Figure 11).

In the case of Ir complex **L2Ir1**, ^1H–^{31}P HMBC experiments verified the connectivity of the coordinated MaxPhos ligand, where the ^1H–^{31}P couplings at 2 and 3 bonds of distance permits univocally confirm its structure (Figure 12).
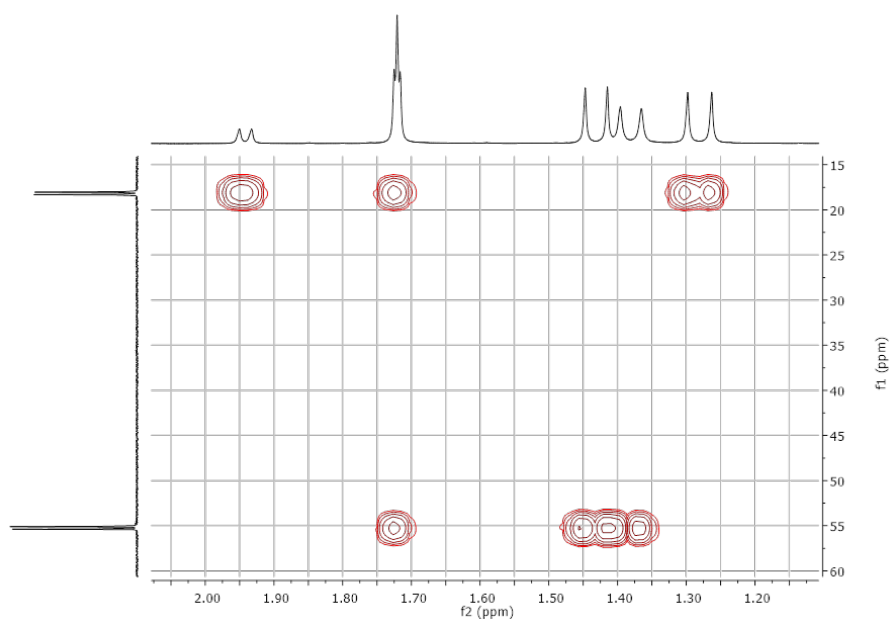
Figure 12. ^1H–^{31}P HMBC (CDCl$_3$, 25 ºC) of **L2Ir1**.

During the formation of the new complexes, the metal becomes a stereogenic centre and therefore two stereoisomers with different configuration at the metal can be obtained. Since from 213 to 298 K only one set of signals was observed in the NMR spectra of both complexes, the preparative route employed is completely diastereoselective. It may be anticipated that, within the four-membered metallacycle M–P–N–P, the epimer at the metal in which the bulkiest C$_5$Me$_5$ group is *anti* to two ^{t}Bu substituents would be preferred on steric grounds to the isomer in which this group is *syn* to both ^{t}Bu groups (Figure 13).
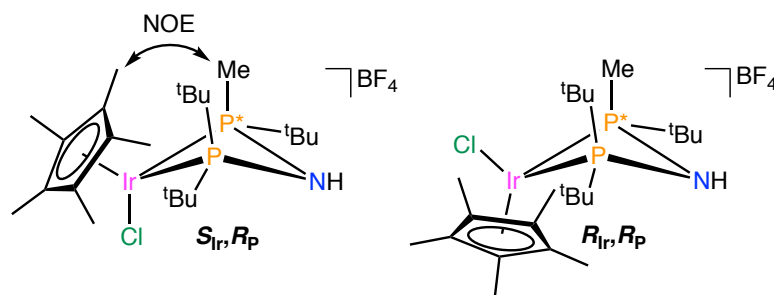
Figure 13. Epimers of complex **L2Ir1**, being $(\mathbf{\textit{S}_{Ir}, \textit{R}_P})$**-L2Ir1** the major diastereomer observed in solution.

A NOE contact between the methyl bonded to P^1 and the C_5Me_5 protons confirmed this hypothesis (Figure 13).

Therefore, the configuration at the metal in compounds **L2Rh1** and **L2Ir1** is *S*.[10-11,45]

X-ray diffraction analyses were carried out to establish the molecular structure of complexes **L2Rh1** and **L2Ir1** and confirm the absolute configuration of the metallic atom.

It should be noted that, due to the nomenclature rules,[10-11,45] the descriptor of the configuration at phosphorus changes from *S* (free ligand) to *R*, when the MaxPhos ligand coordinates to the metal.

Molecular representations of the cations are displayed in Figure 14 and Table 1 collects the main geometrical parameters of the metal coordination sphere. From a crystallographic point of view, both crystal structures are isostructural as similar asymmetric units are packed in the same space group, with comparable unit cell parameters. At a molecular level, both structures exhibit also similar characteristics. Both cations are formally pseudo-tetrahedral, with the metal coordinated to a pentamethylcyclopentadienyl fragment, to the two phosphorus atoms of the MaxPhos ligand and to a chlorine atom.
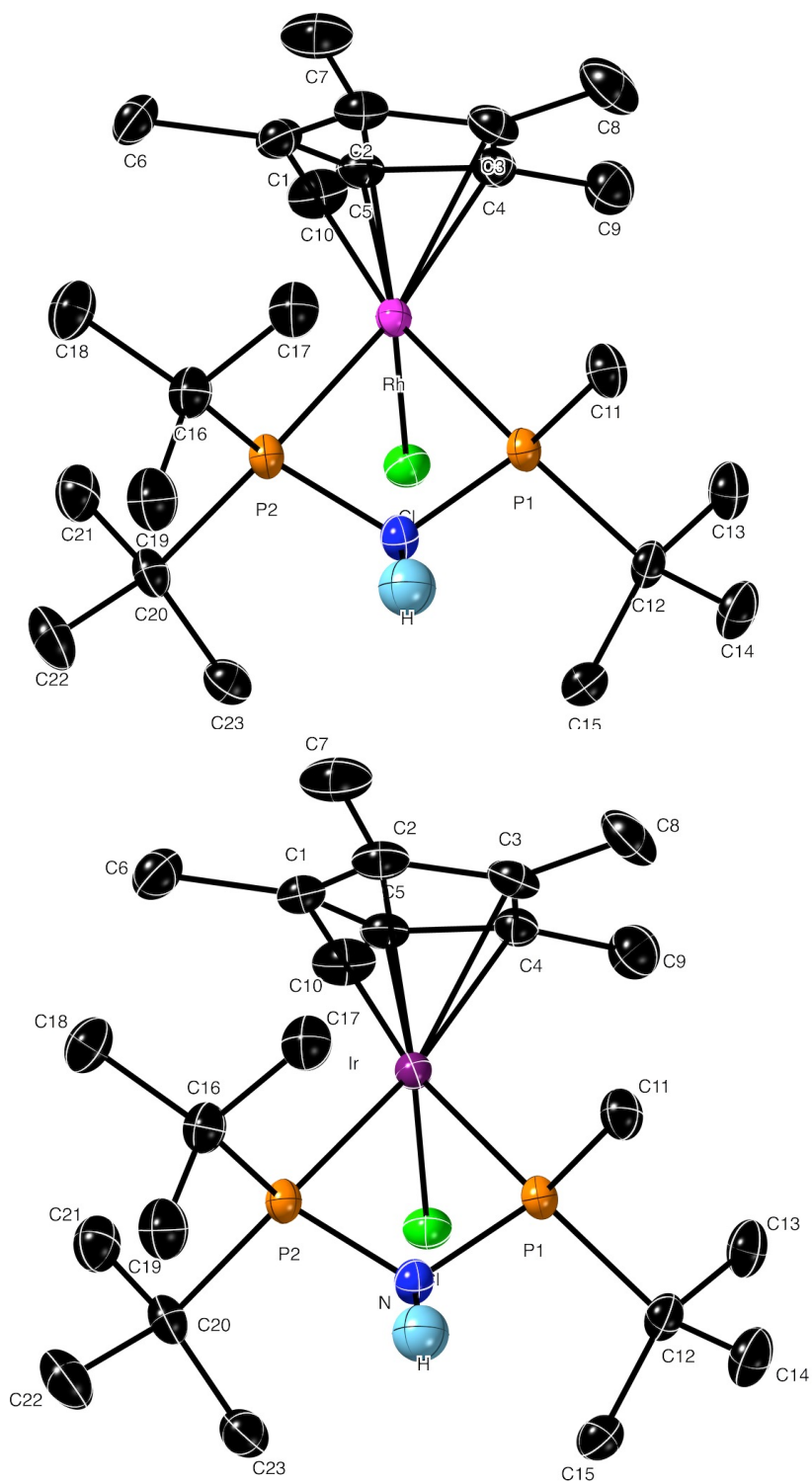
Figure 14. Molecular structure of the cation of complexes **L2Rh1** and **L2Ir1** (thermal ellipsoids drawn at a 50% probability level). Hydrogen atoms (except those of N-H fragments) have been omitted for clarity

Table 1. Selected bond lengths (Å) and angles (°) for complexes **L2Rh1** (M = Rh) and **L2Ir1** (M = Ir).

Bond	L2Rh1	L2Ir1	Angle	L2Rh1	L2Ir1
M-Cl	2.3908(8)	2.3961(10)	Cl-M-P(2)	95.46(3)	94.96(4)
M-P(1)	2.3119(8)	2.3054(10)	Cl-M-Ct[a]	113.14(5)	112.81(7)
M-P(2)	2.3905(8)	2.3683(11)	P(1)-M-P(2)	68.85(3)	68.85(4)
M-Ct[a]	1.8845(15)	1.8900(19)	P(1)-M-Ct[a]	135.45(5)	135.92(7)
Cl-M-P(1)	91.20(3)	91.12(4)	P(2)-M-Ct[a]	138.70(5)	139.02(7)

[a]Ct is the centroid of the ring of the η^5-C_5Me_5 fragment.

The structural parameters describing the coordination of P(1) and P(2) atoms to the metal centre differ significantly. Longer M–P bond lengths and larger (C_5Me_5)-M-P bond angle values are associated to P(2), carrying two ^{t}Bu substituents, to minimize the steric repulsion between the bulkiest fragments, the ^{t}Bu substituent and the C_5Me_5 ligand. In contrast, related chelate complexes with C_2-symmetric diphosphorus ligands exhibit similar Rh-P bond lengths, as for example in [(η^5-C_5Me_5)RhCl{κ^2P,P-$(PPh_2)_2NMe$}] (2.297(2) and 2.303(2) Å).[46] The absolute configuration of the metal is S, in accordance with the atom priority sequence η^5-C_5Me_5 > Cl > P(2) > P(1).[10-11,45]

The chelating coordination of the MaxPhos ligand in complexes **L2Rh1** and **L2Ir1** leads to the formation of a four-membered M-P(1)-N-P(2) ring, with a small P-M-P bite-angle (**L2Rh1**: 68.85(3) and **L2Ir1**: 68.85(4)°). These values are smaller than those in previously reported complexes with the MaxPhos ligand with d^8 metals having a square-planar geometry.[37a,39-41] Indeed, they lie on the inferior limit of those reported in M–P–N–P four membered metallacycles.[37a,39,41,46-47] Both P–N bond lengths are statistically identical (P(1)-N: 1.688(3) and 1.688(4) Å; P(2)-N: 1.691(3) and 1.694(4) Å in **L2Rh1** and **L2Ir1**, respectively). These values are similar than previously reported complexes with the MaxPhos ligand.[37a,39-41] The M–Cl and M–C_5Me_5 bond lengths are consistent with those reported for related (η^5-C_5Me_5)MCl(diphosphane) rhodium or iridium complexes.[48]

4.4.2. *Ruthenium M-stereogenic complexes with the MaxPhos ligand*

The salt (S_P)-[HMaxPhos][BF_4] was mixed with the Ru precursor [(η^6-*p*-MeC$_6$H$_4$^{i}Pr)Ru(acac)Cl][49] under the conditions described above to prepare the Rh and Ir complexes **L2Rh1** and **L2Ir1** but only traces of the desired complex **L2Ru1** (Scheme 9) were obtained according to ^{31}P{^{1}H} NMR. The modification of reaction conditions (temperature, time, solvent, addition of bases) led to the recovery of the unreacted starting materials. Only the use of microwave heating resulted into some conversion but as it remained below 10%, the strategy of using the MaxPhos salt was abandoned. However, when a solution of the free MaxPhos ligand obtained by the deprotonation of the salt with *n*-BuLi, as previously reported,[39] was reacted with the well-known Ru dimer [RuCl(μ-Cl)(η^6-*p*-MeC$_6$H$_4$^{i}Pr)]$_2$ in the presence of NH$_4$BF$_4$, the cationic complex [(η^6-*p*-MeC$_6$H$_4$^{i}Pr)RuCl(MaxPhos)][BF$_4$] (**L2Ru1**) was obtained in 85% of isolated yield (Scheme 9).
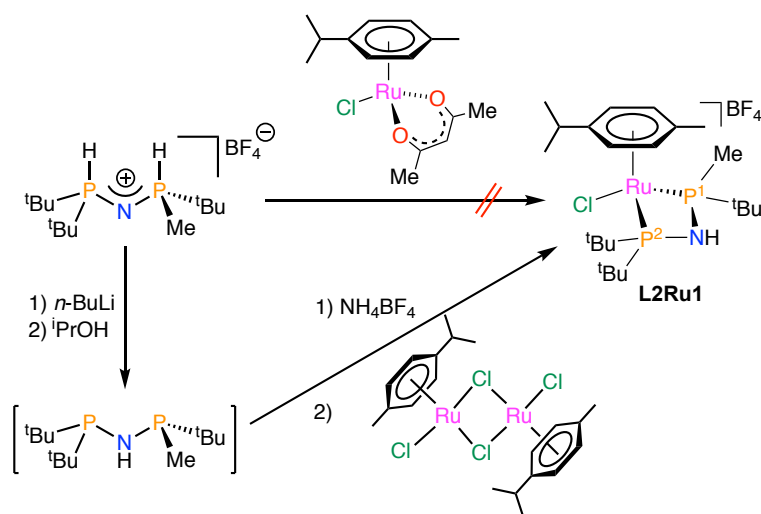
Scheme 9. Preparation of the ruthenium complex **L2Ru1**.

The complex was characterized by analytical and spectroscopic techniques, as detailed in the Experimental Section in Chapter 6. The IR spectrum, as expected, showed a broad N–H absorption band centred at 3287 cm^{-1} and an intense band of the BF$_4$ anion at 1065 cm^{-1}.

In the ^{31}P{^{1}H} NMR spectrum two doublets were found at 63.1 and 90.3 ppm, with a $^2J_{PP}$ coupling constant of 89.3 Hz (Figure 15).
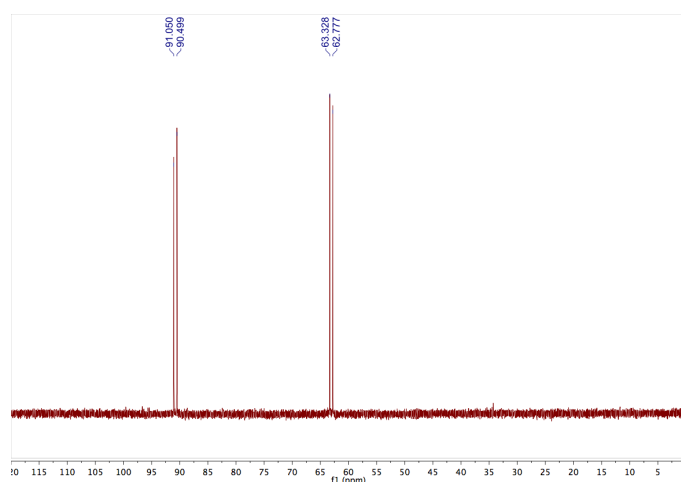
Figure 15. $^{31}P\{^1H\}$ NMR (162 MHz, CDCl$_3$, 25 °C) of **L2Ru1**.

The monodimensional ^1H and $^{13}C\{^1H\}$ NMR spectra as well as the $^{13}C–^1H$ correlation spectrum demonstrated the presence of the *p*-cymene and the MaxPhos ligands. Thus, four ^1H and six ^{13}C resonance signals appeared in the region of coordinated arene rings along with a triplet centred at 5.28 ppm in the ^1H NMR spectrum that can be assigned to the NH group of the MaxPhos ligand (Figure 16).
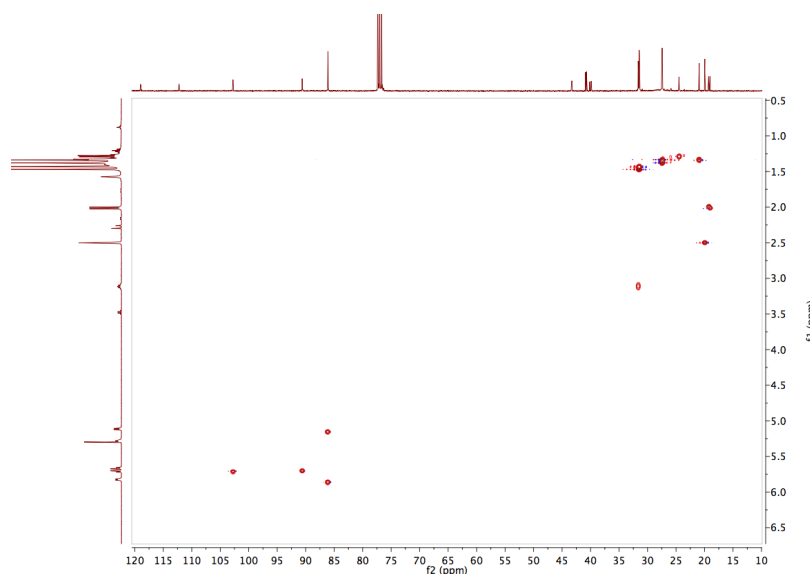
Figure 16. $^1H–^{13}C$ HSQC (CDCl$_3$, 25 °C) of **L2Ru1**.

In the aliphatic region, the expected doublets for the methyl and *tert*-butyl groups of the ligand were present but, interestingly, one of the *tert*-butyl groups of the ligand did not appear in the ^1H NMR spectrum at room temperature while it was also missing in the $^{13}C\{^1H\}$ NMR spectrum. The missing doublet of the *tert*-butyl group emerged in the ^1H NMR spectrum upon heating at 50 °C (Figure 17).

190
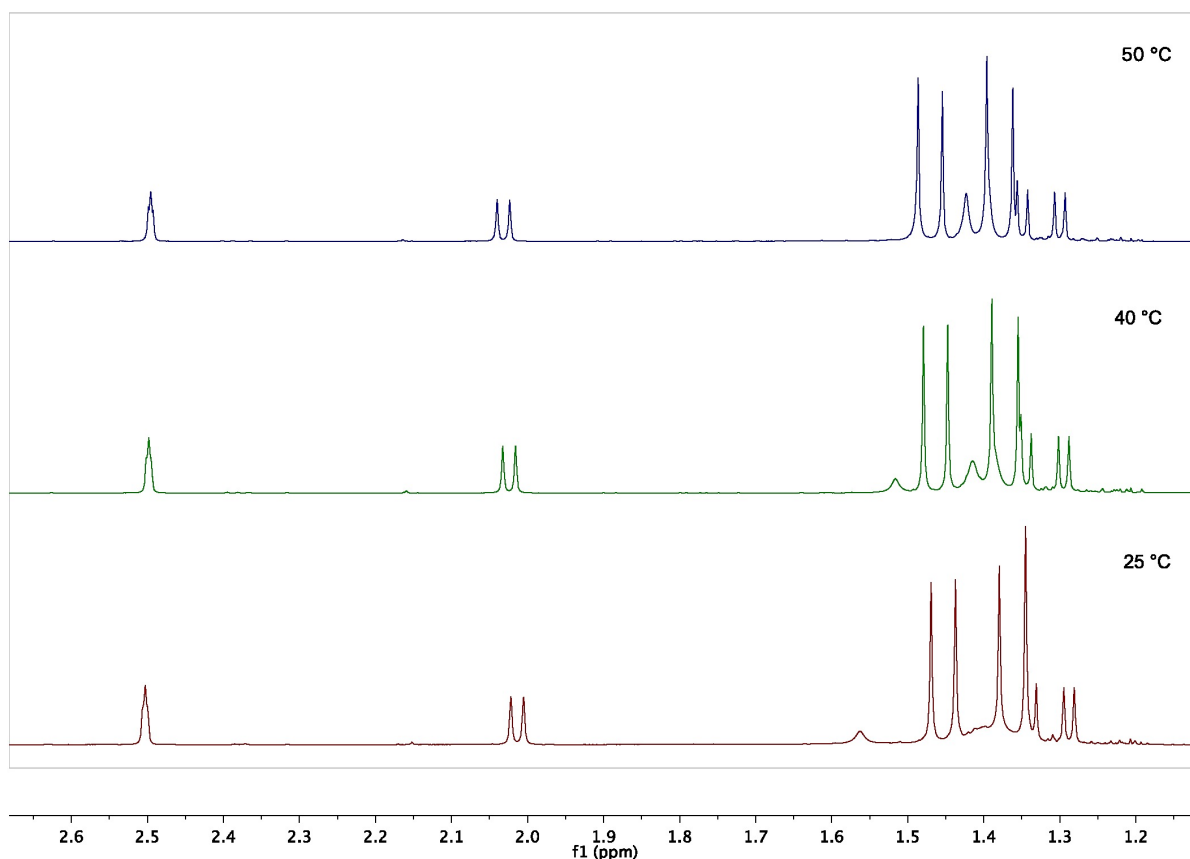
Figure 17. ^{1}H NMR Variable temperature measurements (400 MHz, CDCl$_3$).

Complex **L2Ru1** also contains a stereogenic Ru atom. Since a single set of signals was observed by NMR, it can be deduced that the reaction was again completely diastereoselective.

Despite many attempts, single crystals of **L2Ru1** could not be obtained. However, single crystals, suitable for X-ray studies, of the related hexafluorophosphate salt **L2Ru1·PF$_6$** were obtained instead.

Complex **L2Ru1·PF$_6$** was prepared following the same reaction conditions described for its analogous compound **L2Ru1** (Scheme 9) but using NH$_4$PF$_6$, once the free MaxPhos ligand was formed "*in situ*", in order to drive the reaction to the formation of the monocationic complex **L2Ru1·PF$_6$**.

L2Ru1·PF$_6$ was characterised by NMR means and the presence of the hexafluorophosphate counterion was easily assessed by IR measurements were a broad band at 839 cm^{-1} confirms the expected ν(PF$_6$) (see Figure 18).
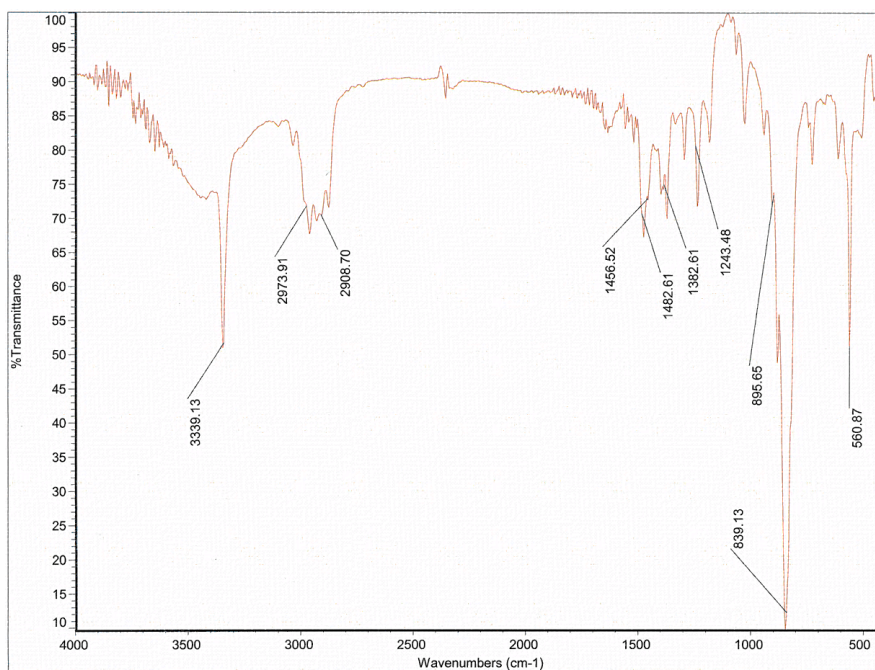
Figure 18. IR spectrum (KBr dispersion) of complex **L2Ru1·PF₆**.

A view of the cation **L2Ru1·PF₆** is displayed in Figure 19 whereas Table 2 collects the main geometrical parameters of the coordination sphere of the Ru atom.
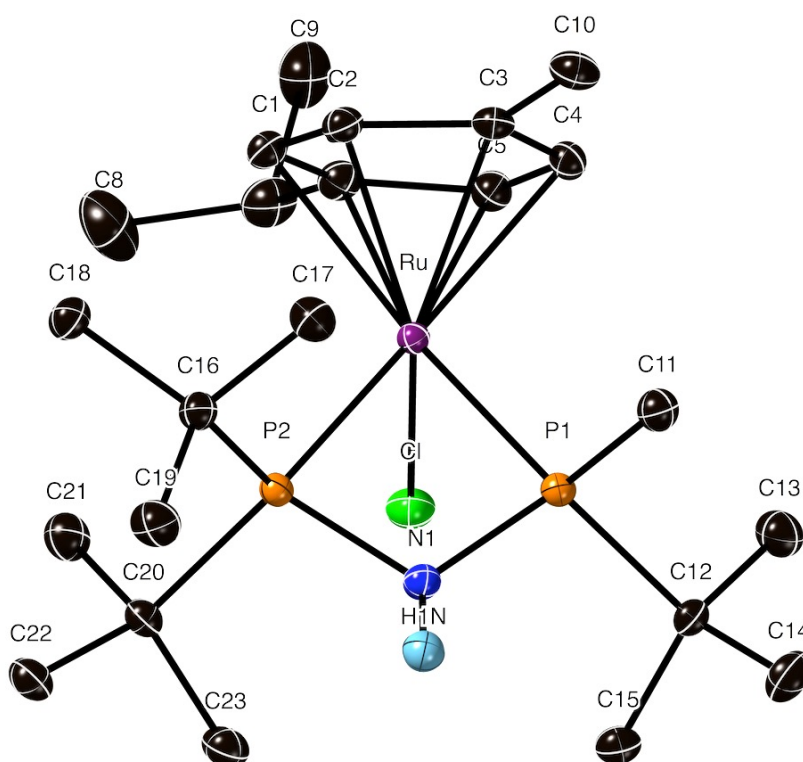
Figure 19. Molecular structure of the cation of complex **L2Ru1·PF₆** (thermal ellipsoids drawn at a 50% probability level). Hydrogen atoms (except that of the N-H fragment) have been omitted for clarity.

192

Table 2. Selected bond lengths (Å) and angles (°) for complex **L2Ru1·PF6**.

Bond	Length (Å)	Angle	(°)
Ru-Cl	2.3918(3)	Cl-Ru-P(2)	92.280(12)
Ru-P(1)	2.3292(3)	Cl-Ru-Ct^a	117.29(3)
Ru-P(2)	2.3930(3)	P(1)-Ru-P(2)	68.356(13)
Ru-Ct^a	1.7755(6)	P(1)-Ru-Ct^a	135.71(3)
Cl-Ru-P(1)	89.717(12)	P(2)-Ru-Ct^a	137.47(3)

^{a}Ct is the centroid of the ring of the η^6-p-MeC$_6$H$_4{}^i$Pr fragment.

The structure of **L2Ru1·PF6** is similar to those of **L2Rh1** and **L2Ir1**, showing a pseudotetrahedral Ru atom coordinated to the *p*-cymene phenyl ring, the two phosphorus atoms of the MaxPhos ligand and a chloride atom. The absolute configuration of the Ru atom is again *S*. The same comments on the distances and angles made in the description of the structures of **L2Rh1** and **L2Ir1** hold here, with **L2Ru1·PF6** having an even smaller P-Ru-P bite-angle of 68.356(13)°.

4.4.3. *C–H activation on (S$_{Ir}$,R$_P$)-[(η^5-C$_5$Me$_5$)IrCl(MaxPhos)][BF$_4$]*

The reaction of the iridium complex **L2Ir1** with AgBF$_4$ in CH$_2$Cl$_2$ provided a mixture of complexes [(η^5-C$_5$Me$_5$)Ir(MaxPhos)][BF$_4$] (**L2Ir2**) in which the cyclometallation of the diphosphane ligand occurs through one of the methyl groups of one of the *tert*-butyl substituents. Intramolecular C(sp^3)-H activation on (η^5-C$_5$Me$_5$)Ir^{III} complexes is not unprecedented.[50] Attempts to detect the plausible 16 electron intermediate (η^5-C$_5$Me$_5$)Ir(MaxPhos)$^{2+}$ were unsuccessful. The cyclometallated complexes **L2Ir2** and **L2Ir2'** (Scheme 10) were the only observed products even when the reaction was carried out at 253 K indicating that the metallation is a highly favoured process.
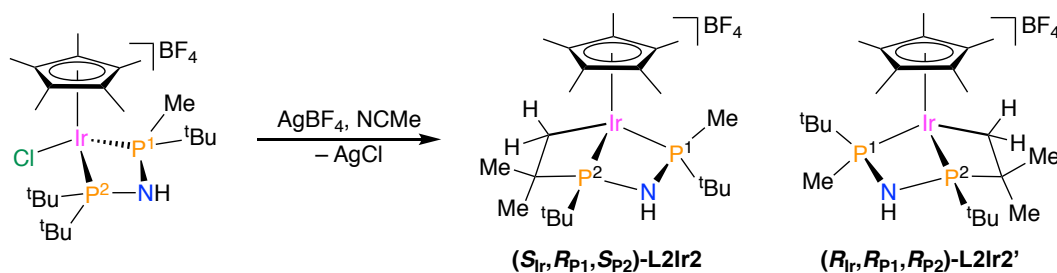
Scheme 10. Synthesis of the two isolated diastereoisomers of complex **L2Ir2**.

According to NMR spectroscopic data, complex **L2Ir2** was obtained as a mixture of two isomers in an 82/18 molar ratio. The non-equivalent geminal protons of the metallated CH$_2$ group resonate as a doublet of pseudotriplets at 2.13 and 1.39 ppm for the major isomer.

Similarly, two distinct carbon and proton resonances were recorded for the methyl groups of the P^{2}CMe$_2$ moiety. The metallated methylene carbon is strongly shielded by the neighbour metal and appears at –7.43 (major isomer) and –2.61 (minor) ppm, shifted by about 30 ppm toward higher field frequencies with respect to non-metallated phosphane methyl groups. The ^{31}P–^{1}H-correlation spectrum reveals that, for the two isomers, the metallated methylene belongs to ^{t}Bu groups bonded to the P^2 phosphorus (Figure 20).
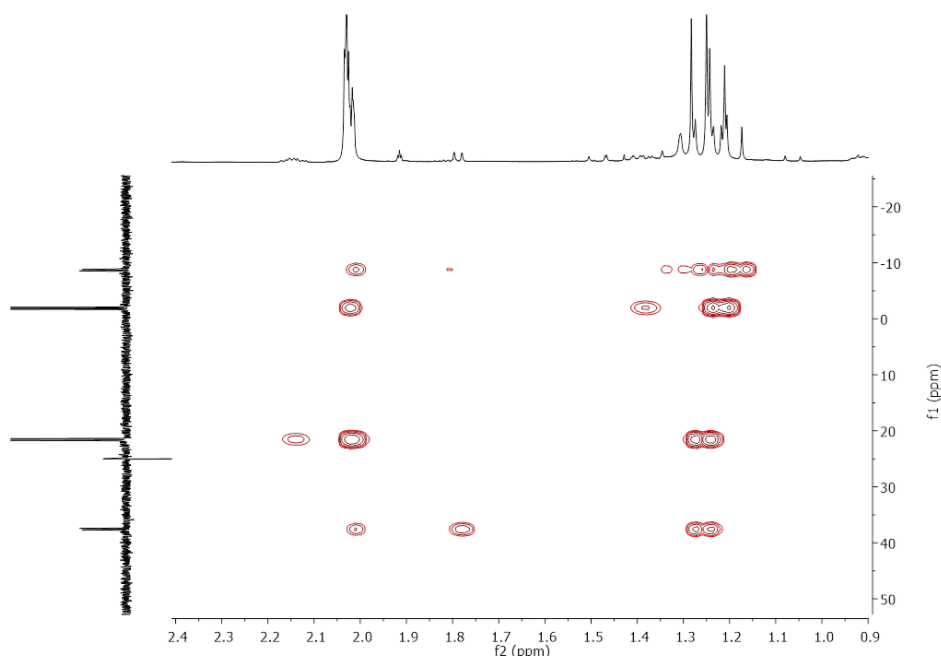
Figure 20. ^{1}H–^{31}P HSQC (CD$_2$Cl$_2$, 25 °C) of complexes **L2Ir2**.

Consistently, the chemical shift of the P^2 nucleus is shifted by about 60 ppm upfield for both isomers of **L2Ir2**. The irradiation of the *pro-S* proton of the metallated methylene of the major isomer enhances the resonance of the ^{t}Bu, but not that of the Me, bonded to the P^1 atom. These data strongly suggests that the absolute configuration of the major (**L2Ir2**) and minor (**L2Ir2'**) isomers is S_{Ir},R_{P1},S_{P2} and R_{Ir},R_{P1},R_{P2}, respectively.

A plausible pathway for the cyclometallation reaction (Scheme 11) starts with the abstraction of the chloride ligand on complex **L2Ir2** by the silver salt.
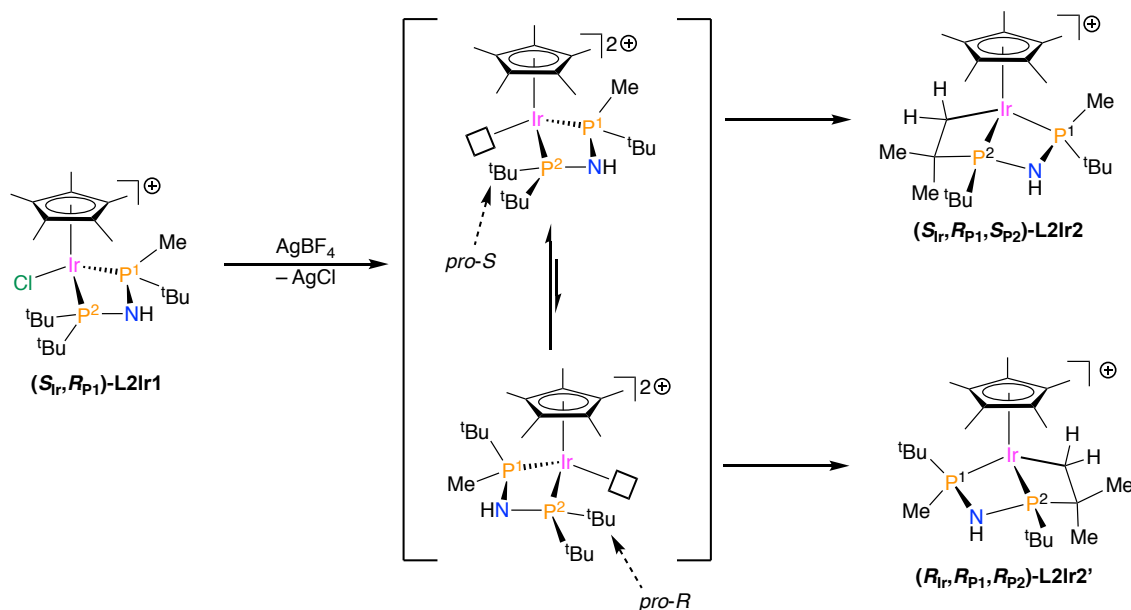
Scheme 11. Plausible pathway for the metallation reaction of **L2Ir2**.

The two epimers at iridium of the resulting 16 electron species would be in equilibrium. Most probably, due to both steric (two bulky ^{t}Bu groups) and electronic (^{t}Bu being a better electron donor than Me) factors, the ^{t}Bu groups of the P^2 atom, but not that of the P^1 phosphorus, undergo metallation.

Furthermore, only the methyl groups of the *pro-S* ^{t}Bu group could take part in the process in one epimer and only the methyl groups of the *pro-R* ^{t}Bu group in the other epimer (Scheme 11). Taking into account that metallation makes the P^2 atom stereogenic, this stereochemical feature forces the P^2 and the iridium centres to adopt the same configuration affording access to only the S_{Ir},R_{P1},S_{P2} and R_{Ir},R_{P1},R_{P2} diastereomers. The former isomer, according to NMR data, is more abundant than the latter. In this isomer, within the Ir–P–N–P four-membered metallacycle, the bulkiest C_5Me_5 ligand is *syn* to a methyl and to a ^{t}Bu group, on the P^1 and P^2 atoms, respectively. However, in the minor isomer, the bulky ring group is *syn* to two ^{t}Bu groups, one on each of the two phosphorus atoms.

4.4.4. *Reaction of (S_{Rh},R_P)-[(η^5-C$_5$Me$_5$)RhCl(MaxPhos)][BF$_4$] and (S_{Ru},R_P)-[(η^6-p-MeC$_6$H$_4$^{i}Pr)RuCl(MaxPhos)][BF$_4$] with AgBF$_4$*

A similar metallation product was not observed when slight excess of AgBF$_4$ was added to complex **L2Rh1** in CH$_2$Cl$_2$ at room temperature or in acetone at reflux. The reaction resulted in decomposition to a number of unidentified compounds. However, when acetonitrile was used as the solvent, the dicationic complex [(η^5-C$_5$Me$_5$)Rh(MaxPhos)(NCMe)][BF$_4$]$_2$ (**L2Rh2**) was isolated from the reaction medium in 72% yield (Scheme 12).
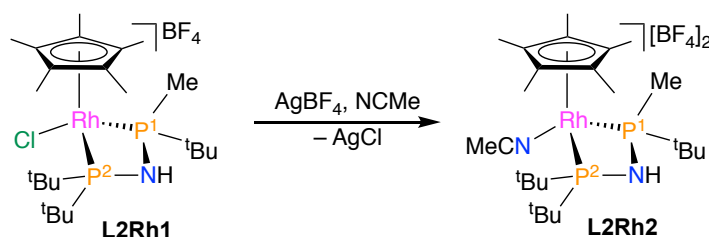
Scheme 12. Formation of dicationic complex **L2Rh2**.

The NMR spectra of **L2Rh2** indicated that only one of the two possible epimers at the metal was present. In the ^{31}P{^{1}H} NMR spectrum it gave a pair of doublets of doublets centred at 56.0 (P^1) and 90.7 (P^2), with a $^2J_{PP}$ coupling of 77.4 Hz and an average $^1J_{PRh}$ coupling of 110 Hz (Figure 21).
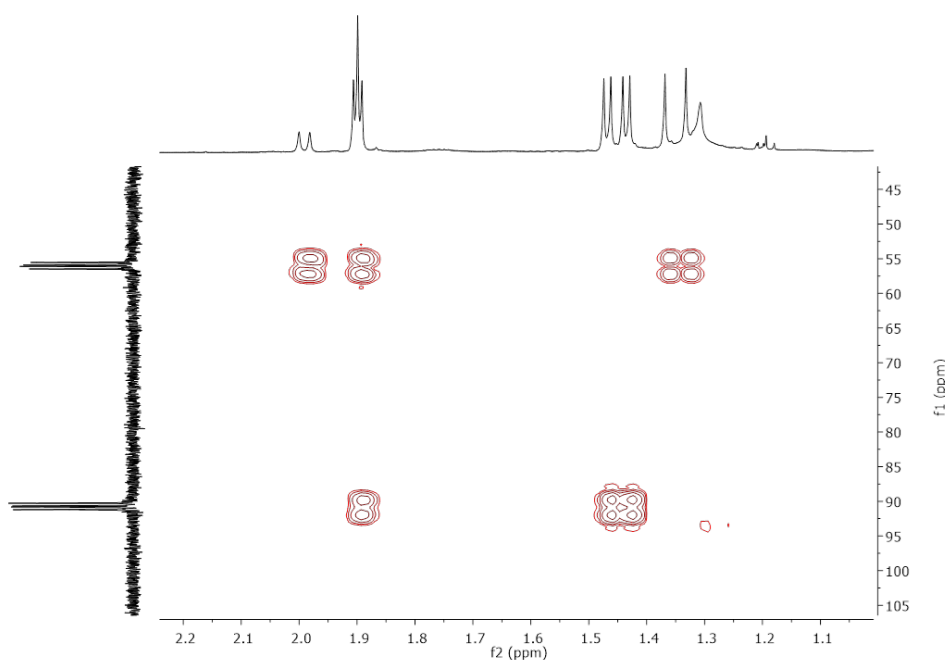
Figure 21. ^{1}H–^{31}P HSQC (CD$_2$Cl$_2$, 25 ºC) of **L2Rh2**.

NOE contacts between the P^1 methyl protons and those of the *pro-R* ^{t}Bu group bonded to the P^2 atom and between the latter and the C_5Me_5 protons indicated that the absolute configuration of **L2Rh2** is S_{Rh},R_{P1}. Again, in the preferred isomer, the methyl substituent on the P^1 phosphorus is located *syn* to the bulkiest η^5-C_5Me_5 ligand within the Rh-P-N-P four-membered metallacycle.

As happened with Rh complex **L2Rh1**, no metallation was observed when the Ru complex **L2Ru1** was treated with slight excess of AgBF$_4$ in CH$_2$Cl$_2$ at room temperature. Unlike **L2Rh1**, however, no decomposition took place and only a broadening of the ^{31}P{^{1}H} and ^{1}H NMR peaks of **L2Ru1** could be observed. This behaviour suggests the formation of a poorly stabilised unsaturated Ru species upon Cl abstraction. The addition of acetonitrile allowed for the isolation of the dicationic complex **L2Ru2** (Scheme 13).
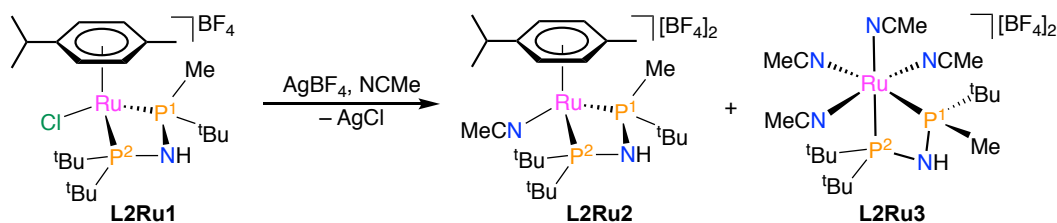
Scheme 13. Preparation of ruthenium complex **L2Ru2** and formation of complex **L2Ru3**.

NMR data indicated that **L2Ru2** was also formed as a single isomer. In the ^{31}P{^{1}H} NMR spectrum, it gave a pair of doublets centred at 67.7 (P^1) and 94.8 (P^2), with a $^2J_{PP}$ coupling of 73.9 Hz (Figure 22).
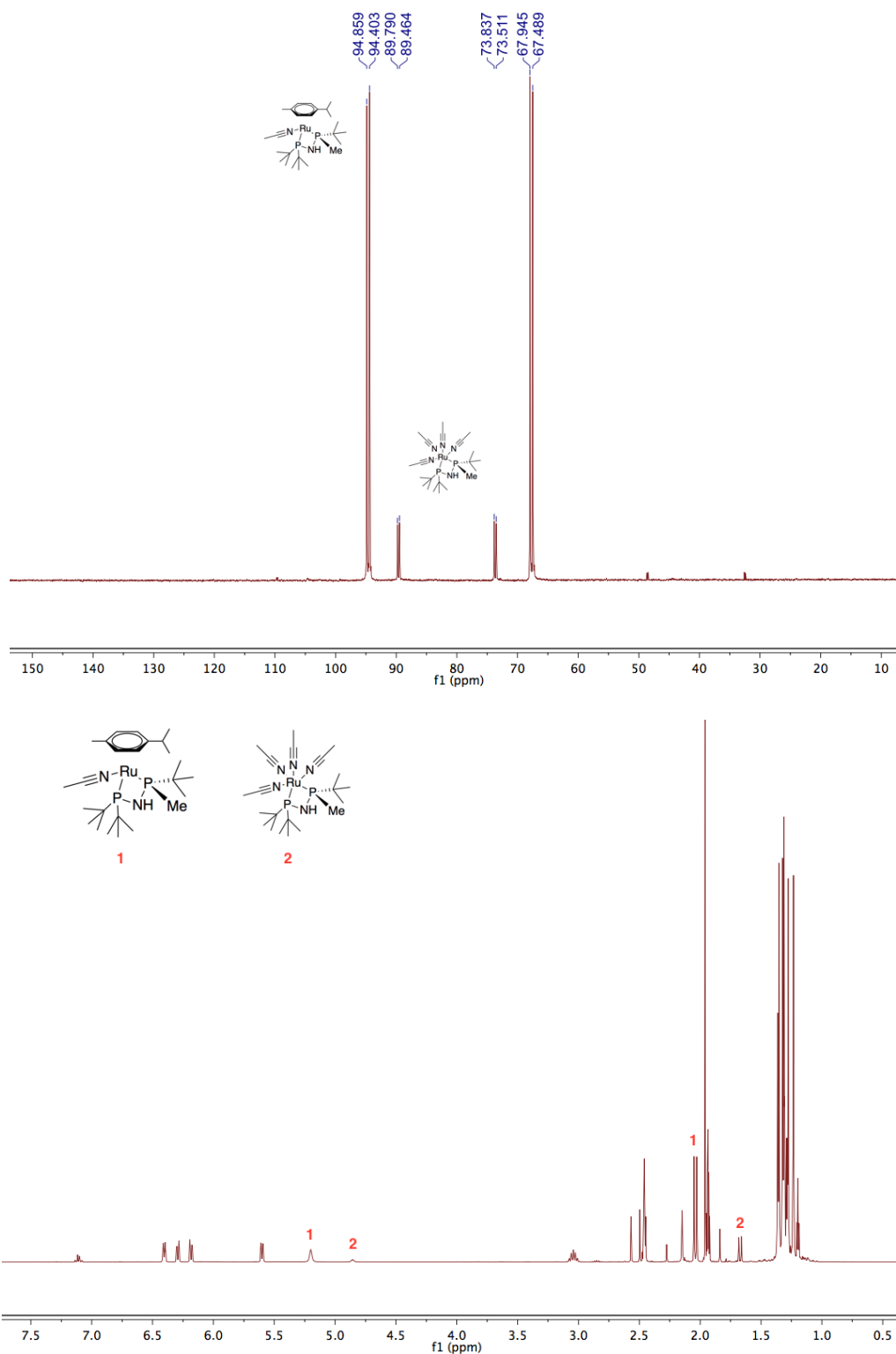
Figure 22. $^{31}P\{^1H\}$ NMR (162 MHz, CH$_3$CN, 25 ºC) (up) and ^1H NMR (400 MHz, CH$_3$CN, 25 ºC) (down) of complexes **L2Ru2** and **L2Ru3**.

In the ^1H and $^{13}C\{^1H\}$ NMR spectra a single set of resonances was found, with the peaks of the aromatic CH groups of the coordinated *p*-cymene ring shifted downfield compared to **L2Ru1**, due to the more electron-poor nature of **L2Ru2**. At longer

198

reaction times or when the reaction was carried out in acetonitrile as solvent, complex **L2Ru2** was found to be contaminated with free *p*-cymene and another species that could be identified as **L2Ru3** by mass spectrometry (Figure 23).
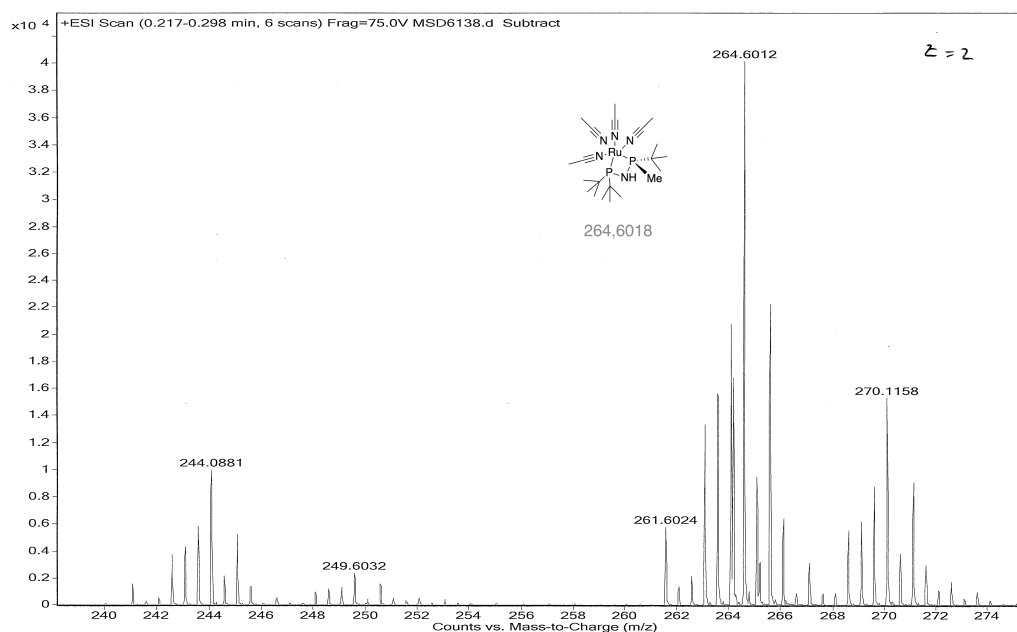
Figure 23. ESI–(+) mass spectrum of complex **L2Ru3** in acetone.

This coordination compound, which was not isolated, displays two doublets at 73.6 (P^1) and 89.6 ppm (P^2), with a $^2J_{PP}$ of 52.8 Hz in the ^{31}P{^{1}H} NMR spectrum (Figure 22).

The octahedral complex **L2Ru3** arises from the substitution of the *p*-cymene ring in **L2Ru2** by three acetonitrile molecules.

4.5. *Ru- and Ir-catalysed transfer hydrogenation*

Except for the metallation, the reactions in this Chapter proceeded in a very stereoselective manner, allowing the preparation of diastereomerically pure *M*-stereogenic MaxPhos complexes. As it has been described, the major diastereomers posses an *S* configuration on the metal centre, since this conformation minimises the steric hindrance; the Cp* or the arene are *cis* to the methyl, which have been confirmed by NOESY experiments (Figure 24).
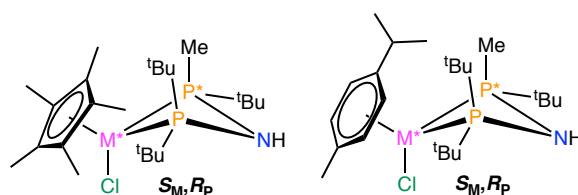
Figure 24. Stereochemistry of the $[(\eta^n\text{-arene})MCl(MaxPhos)][BF_4]$ complexes.

With this in mind we studied the catalytic activity of these complexes in asymmetric transfer hydrogenation of the model substrate acetophenone.

As it has been mentioned in Chapter 3, the model substrate, used to test the efficiency of the catalysts, for hydrogen transfer of ketones is acetophenone with isopropanol as hydrogen source and potassium *tert*-butoxide or KOH as base (Scheme 14).

As it is detailed in the Experimental Section (Chapter 6) all the reactions were carried out activating the catalytic precursor, in order to form the hydride active species, over 15 min in the presence of ^{t}BuOK as base. Then, aliquots of the reaction mixture were taken off and analysed by chiral GC.

The results obtained for the transfer hydrogenation reaction at 82 ºC with $[(\eta^6\text{-}p\text{-}MeC_6H_4{}^i Pr)RuCl(MaxPhos)][BF_4]$ (**L2Ru1**) and $[(\eta^5\text{-}C_5Me_5)IrCl(MaxPhos)][BF_4]$ (**L2Ir1**) as catalytic precursors are given in Table 3.
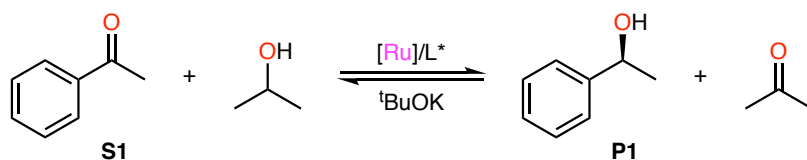
Scheme 14. Asymmetric hydrogen transfer of acetophenone as model substrate.

Table 3. Results for the hydrogen transfer of acetophenone with $[(\eta^6\text{-}p\text{-}MeC_6H_4{}^iPr)RuCl(MaxPhos)][BF_4]$ (**L2Ru1**) and $[(\eta^5\text{-}C_5Me_5)IrCl(MaxPhos)][BF_4]$ (**L2Ir1**) as catalytic precursors (0.5%).

Entry	L2Ru1 (mmol)	^{t}BuOH (mmol)	Reaction time (min)	GC Conv. [%]
1	0.02	0.1	60	60
2	0.02	0.1	120	75
3	0.02	0.1	190	82
	L2Ir1 (mmol)	^{t}BuOH (mmol)	Reaction time (min)	GC Conv. [%]
4	0.02	0.1	60	100

As it can be seen, full conversion was achieved after 3 h using a 0.5% of precursor **L2Ru1**, but no enantioselectivity was observed. In order to induce some chiral discrimination, the reaction was also carried out, under the same conditions, but in a lower temperature (40 ºC). Unfortunately, only a 6% of conversion was detected after 24 h of reaction.

In the case of Ir complex **L2Ir1**, full conversion was achieved in a much less time, proving that the metal has a clear influence on the activity of the reaction. Moreover a 16% of *ee* was detected displaying some chiral induction, compared to its analogous complex with Ru.

4.6. *Conclusions*

The cationic diphosphane (S_P)-[HMaxPhos][BF$_4$] is able to protonate the half-sandwich rhodium and iridium acetylacetonates [(η^5-C$_5$Me$_5$)M(acac)Cl] rendering chiral-at-metal complexes of the formula [(η^5-C$_5$Me$_5$)MCl(MaxPhos)][BF$_4$] (**L2Rh1**, **L2Ir1**).

   In contrast, the preparation of the related Ru complexes [(η^6-*p*-MeC$_6$H$_4$^{i}Pr)RuCl(MaxPhos)][X] (**L2Ru1**, **L2Ru1·PF$_6$**) required the use of free MaxPhos.

   The bulkiness of the MaxPhos ligand when coordinated to an octahedral metal is revealed by NOE contacts between the methyl group of P^1 and one of the *tert*-butyl groups of P^2 with the η^n-ring. This suggests steric clashing between the MaxPhos ligand and the η^n-ring, resulting in a broadening in ^{1}H and ^{13}C{^{1}H} NMR shifts of one of the *tert*-butyl groups of P^2.

   The iridium complex **L2Ir1** undergoes the facile intramolecular aliphatic activation of one of the ^{t}Bu groups affording the cyclometallated complex [(η^5-C$_5$Me$_5$)Ir(MaxPhos)][BF$_4$] (**L2Ir2**).

   The distinct steric and electronic features of the Me and ^{t}Bu substituents on the stereogenic phosphorus atom of the MaxPhos ligand determine the reactivity of its metallic derivatives that ultimately results in high regio- and diastereoselectivities.

   Thus, the S_M,R_{P1} diastereomers of the complexes **L2Rh1**-**L2Ru1**, **L2Rh2** and **L2Ru2** were selectively obtained in high yield and the metallation of complex **L2Ir1** takes place with perfect regioselectivity and high diastereoselectivity affording exclusively the diastereomers (S_{Ir},R_{P1},S_{P2})- **L2Ir2** and (R_{Ir},R_{P1},R_{P2})- **L2Ir2'**.

   Square planar, Rh(I)-MaxPhos complexes (d^8 configuration) have displayed good to excellent enantioselectivities in asymmetric hydrogenation of alkenes and Pauson-Khand reactions. Unfortunately, this is not the case in the transfer hydrogenation of acetophenone presented in this Chapter, in which no enantioselectivity has been observed so far. It seems that the MaxPhos ligand is not a good choice to prepare useful octahedral precatalysts for this reaction. Furthermore the higher temperatures used in this process may also play a detrimental role in the enantioselection.

   The results obtained in the present chapter have been recently published as a full paper: Tellez, J.; Gallen, A.; Ferrer, J.; Lahoz, F. J.; Garcia-Orduna, P.; Riera, A.; Verdaguer, X.; Carmona, D.; Grabulosa, A. *Dalton Trans.* **2017**, *46*, 15865-15874.

4.7. *References*

(1)   (a) Halterman, R. L. *Chem. Rev.* **1992**, *92*, 965-994 (b) Ganter, C. *Chem. Soc. Rev.* **2003**, *32*, 130-138 (c) Bauer, E. B. *Chem. Soc. Rev.* **2012**, *41*, 3153-3167.

(2)   (a) Trost, B. M.; Verhoeven, T. R. In *Comprehensive Organometallic Chemistry*; Wilkinson, G., Stone, F. G. A., Abel, E. W., Eds.; Pergamon: Oxford, 1982; Vol. 8 (b) Noyori, R. *Science* **1990**, *248*, 1194-1199 (c) Ojima, I.; Ed. *Catalytic Asymmetric Synthesis*; 3 ed.; Wiley, 2010.

(3)   (a) Noyori, R. *Asymmetric Catalysis in Organic Synthesis*; Wiley and Sons, Inc.: New York, 1994 (b) *Comprehensive asymmetric catalysis*; Jacobsen, E. N.; Pfaltz, A.; Yamamoto, A., Eds.; Springer: Berlin, 1999.

(4)   Fontecave, M.; Hamelin, O.; Ménage, S. *Top. Organomet. Chem.* **2005**, *15*, 271-288.

(5)   (a) Pardo, P.; Carmona, D.; Lamata, P.; Rodríguez, R.; Lahoz, F. J.; García-Orduña, P.; Oro, L. A. *Organometallics* **2014**, *33*, 6927-6936 (b) Carmona, D.; Carmona, M.; Rodriguez, R.; Mendez, I.; Passarelli, V.; Lahoz, F. J.; Garcia-Orduna, P. *Dalton Trans.* **2017**, *46*, 7332-7350 (c) Carmona, D.; Carmona, M.; Tejedor, L.; Rodríguez, R.; Passarelli, V.; Lahoz, F. J.; García-Orduña, P. *Chem. Eur. J.* **2017**, *23*, 14532-14546 (d) Carmona, M.; Rodríguez, R.; Passarelli, V.; Lahoz, F. J.; García-Orduña, P.; Carmona, D. *J. Am. Chem. Soc.* **2018**, *140*, 912-915.

(6)   Brunner, H. *Angew. Chem. Int. Ed.* **1999**, *38*, 1194-1208.

(7)   (a) Gong, L.; Lin, Z.; Harms, K.; Meggers, E. *Angew. Chem. Int. Ed.* **2010**, *49*, 7955-7957 (b) Tian, C.; Gong, L.; Meggers, E. *Chem. Commun.* **2016**, *52*, 4207-4210 (c) Zhang, L.; Meggers, E. *Acc. Chem. Res.* **2017**, *50*, 320-330 (d) Zhang, L.; Meggers, E. *Chem. Asian J.* **2017**, *12*, 2335-2342.

(8)   Meggers, E. *Eur. J. Inorg. Chem.* **2011**, 2911-2926.

(9)   (a) Chen, L. A.; Tang, X.; Xi, J.; Xu, W.; Gong, L.; Meggers, E. *Angew. Chem. Int. Ed.* **2013**, *52*, 14021-14025 (b) Chen, L.-A.; Xu, W.; Huang, B.; Ma, J.; Wang, L.; Xi, J.; Harms, K.; Gong, L.; Meggers, E. *J. Am. Chem. Soc.* **2013**, *135*, 10598-10601 (c) Huo, H.; Fu, C.; Harms, K.; Meggers, E. *J. Am. Chem. Soc.* **2014**, *136*, 2990-2993 (d) Meggers, E. *Angew. Chem. Int. Ed.* **2017**, *56*, 5668-5675 (e) Zheng, Y.; Tan, Y.; Harms, K.; Marsch, M.; Riedel, R.; Zhang, L.; Meggers, E. *J. Am. Chem. Soc.* **2017**, *139*, 4322-4325 (f) Ma, J.; Zhang, X.; Huang, X.; Luo, S.; Meggers, E. *Nat. Protoc.* **2018**, *13*, 605.

(10)   Cahn, R. S.; Ingold, C.; Prelog, V. *Angew. Chem. Int. Ed. Engl.* **1966**, *5*, 385-415.

(11)   Lecomte, C.; Dusausoy, Y.; Protas, J.; Tirouflet, J.; Dormond, A. *J. Organomet. Chem.* **1974**, *73*, 67-76.

(12)   Stanley, K.; Baird, M. C. *J. Am. Chem. Soc.* **1975**, *97*, 6598-6599.

(13)   Brunner, H.; Zwack, T. *Organometallics* **2000**, *19*, 2423-2426.

(14)   (a) Amouri, H.; Thouvenot, R.; Gruselle, M. *C. R. Chimie* **2002**, *5*, 257-262 (b) Carmona, D.; Lahoz, F. J.; Elipe, S.; Oro, L. A.; Lamata, M. P.; Viguri, F.; Sánchez, F.; Martínez, S.; Cativiela, C.; López-Ram de Víu, M. P. *Organometallics* **2002**, *21*, 5100-5114.

(15)   (a) Brunner, H.; Schindler, H. D. *J. Organomet. Chem.* **1970**, *24*, C7-C10 (b) Brunner, H.; Oeschey, R.; Nuber, B. *Inorg. Chem.* **1995**, *34*, 3349-3351.

(16)   (a) Brunner, H.; Aclasis, J.; Langer, M.; Steger, W. *Angew. Chem. Int. Ed.* **1974**, *13*, 810-811 (b) Brunner, H.; Nuber, B.; Prommesberger, M.

203

Tetrahedron: Asymmetry **1998**, *9*, 3223-3229 (c) Brunner, H.; Muschiol, M.; Tsuno, T.; Takahashi, T.; Zabel, M. *Organometallics* **2010**, *29*, 428-435.

(17)   Carmona, D.; Medrano, R.; Dobrinovich, I. T.; Lahoz, F. J.; Ferrer, J.; Oro, L. A. *J. Organomet. Chem.* **2006**, *691*, 5560-5566.

(18)   (a) Brunner, H. *Angew. Chem. Int. Ed.* **1969**, *8*, 382-383 (b) Brunner, H. *Z. Anorg. Allg. Chem.* **1969**, *368*, 120-126.

(19)   (a) Merrifield, J. H.; Strouse, C. E.; Gladysz, J. A. *Organometallics* **1982**, *1*, 1204-1211 (b) Gladysz, J. A.; Boone, B. J. *Angew. Chem. Int. Ed. Engl.* **1997**, *36*, 550-583 (c) Kromm, K.; Osburn, P. L.; Gladysz, J. A. *Organometallics* **2002**, *21*, 4275-4280.

(20)   (a) Brunner, H.; Fisch, K.; Jones, P. G.; Salbeck, J. *Angew. Chem. Int. Ed. Engl.* **1989**, *28*, 1521-1523 (b) Brunner, H.; Faustmann, P.; Dietl, A.; Nuber, B. *J. Organomet. Chem.* **1997**, *542*, 255-263 (c) Costin, S.; Rath, N. P.; Bauer, E. B. *Inorg. Chim. Acta* **2009**, *362*, 1935-1942.

(21)   Brunner, H.; Ike, H.; Muschiol, M.; Tsuno, T.; Umegaki, N.; Zabel, M. *Organometallics* **2011**, *30*, 414-421.

(22)   Standfest-Hauser, C.; Slugovc, C.; Mereiter, K.; Schmid, R.; Kirchner, K.; Xiao, L.; Weissensteiner, W. *J. Chem. Soc. Dalton Trans.* **2001**, 2989-2995.

(23)   (a) Vineyard, B. D.; Knowles, W. S.; Sabacky, M. J.; Bachman, G. L.; Weinkauff, D. J. *J. Am. Chem. Soc.* **1977**, *99*, 5946-5952 (b) Whitesell, J. K. *Chem. Rev.* **1989**, *89*, 1581-1590.

(24)   (a) Knowles, W. S. *Acc. Chem. Res.* **1983**, *16*, 106-112 (b) Knowles, W. S. *Adv. Synth. Catal.* **2003**, *345*, 3-13.

(25)   (a) Agbossou-Niedecorn, F.; Suisse, I. *Coord. Chem. Rev.* **2003**, *242*, 145-158 (b) Grushin, V. V. *Chem. Rev.* **2004**, *104*, 1629-1662 (c) Chikkali, S. H.; Vlugt, J. I. v. d.; Reek, J. N. H. *Coord. Chem. Rev.* **2014**, *262*, 1-15.

(26)   Ramsden, J. A.; Brown, J. M.; Hursthouse, M. B.; Karalulov, A. I. *Tetrahedron: Asymmetry* **1994**, *5*, 2033-2044.

(27)   (a) Deerenberg, S.; Kamer, P. C. J.; van Leeuwen, P. W. N. M. *Organometallics* **2000**, *19*, 2065-2072 (b) Diéguez, M.; Deerenberg, S.; Pàmies, O.; Claver, C.; van Leeuwen, P. W. N. M.; Kamer, P. C. J. *Tetrahedron: Asymmetry* **2000**, *11*, 3161-3166 (c) Deerenberg, S.; Schrekker, H. S.; van Strijdonck, G. P. F.; Kamer, P. C. J.; van Leeuwen, P. W. N. M.; Fraange, J.; Goubitz, K. *J. Org. Chem.* **2000**, *65*, 4810-4817 (d) Deerenberg, S.; Pàmies, O.; Diéguez, M.; Claver, C.; Kamer, P. C. J.; van Leeuwen, P. W. N. M. *J. Org. Chem.* **2001**, *66*, 7626-7631.

(28)   (a) Vargas, S.; Rubio, M.; Suárez, A.; del Río, D.; Álvarez, E.; Pizzano, A. *Organometallics* **2006**, *25*, 961-973 (b) Rubio, M.; Suarez, A.; Alvarez, E.; Bianchini, C.; Oberhauser, W.; Peruzzini, M.; Pizzano, A. *Organometallics* **2007**, *26*, 6428-6436.

(29)   Clavero, P.; Grabulosa, A.; Rocamora, M.; Muller, G.; Font-Bardia, M. *Eur. J. Inorg. Chem.* **2016**, 4054-4065.

(30)   Lam, H.; Horton, P. N.; Hursthouse, M. B.; Aldous, D. J.; Hii, K. K. *Tetrahedron Lett.* **2005**, *46*, 8145-8148.

(31)   Chen, W.; Mbafor, W.; Roberts, S. M.; Whittall, J. *J. Am. Chem. Soc.* **2006**, *128*, 3922-3923.

(32)   Muci, A. R.; Campos, K. R.; Evans, D. A. *J. Am. Chem. Soc.* **1995**, *117*, 9075-9076.

(33)   (a) Gridnev, I. D.; Yamamoi, Y.; Higashi, N.; Tsuruta, H.; Yasutake, M.; Imamoto, T. *Adv. Synth. Catal.* **2001**, *343*, 118-136 (b) Gridnev, I. D.; Yasutake, M.; Higashi, N.; Imamoto, T. *J. Am. Chem. Soc.* **2001**, *123*, 5268-5276 (c) Gridnev, I. D.; Imamoto, T. *Organometallics* **2001**, *20*, 545-549.

(34)   (a) Gridnev, I. D.; Yasutake, M.; Imamoto, T.; Beletskaya, I. P. *Proc. Natl. Acad. Sci.* **2004**, *101*, 5385-5390 (b) Crépy, K. V. L.; Imamoto, T.; Seidel, G.; Fürstner, A. *Org. Synth.* **2005**, *82*, 22.

(35)   (a) Hoge, G.; Wu, H.; Kissel, W. S.; Pflum, D. A.; Greene, D. J.; Bao, J. *J. Am. Chem. Soc.* **2004**, *126*, 5966-5967 (b) Gridnev, I. D.; Imamoto, T.; Hoge, G.; Kouchi, M.; Takahashi, H. *J. Am. Chem. Soc.* **2008**, *130*, 2560-2572.

(36)   (a) Imamoto, T.; Watanabe, J.; Wada, Y.; Masuda, H.; Yamada, H.; Tsuruta, H.; Matsukawa, S.; Yamaguchi, K. *J. Am. Chem. Soc.* **1998**, *120*, 1635-1636 (b) Yamamoto, Y.; Koizumi, T.; Katagiri, K.; Furuya, Y.; Danjo, H.; Imamoto, T.; Yamaguchi, K. *Org. Lett.* **2006**, *8*, 6103-6106 (c) Yamamoto, Y.; Danjo, H.; Yamaguchi, K.; Imamoto, T. *J. Organomet. Chem.* **2008**, *693*, 3546-3552.

(37)   (a) Revés, M.; Ferrer, C.; León, T.; Doran, S.; Etayo, P.; Vidal-Ferran, A.; Riera, A.; Verdaguer, X. *Angew. Chem. Int. Ed.* **2010**, *49*, 9452-9455 (b) León, T.; Riera, A.; Verdaguer, X. *J. Am. Chem. Soc.* **2011**, *133*, 5740-5743.

(38)   Imamoto, T. *Chem. Rec.* **2016**, *16*, 2655-2669.

(39)   Cristóbal-Lecina, E.; Etayo, P.; Doran, S.; Revés, M.; Martín-Gago, P.; Grabulosa, A.; Constantino, A. R.; Vidal-Ferran, A.; Riera, A.; Verdaguer, X. *Adv. Synth. Catal.* **2014**, *356*, 795-804.

(40)   Grabulosa, A.; Doran, S.; Brandariz, G.; Muller, G.; Benet-Buchholz, J.; Riera, A.; Verdaguer, X. *Organometallics* **2014**, *33*, 692-701.

(41)   Cristóbal-Lecina, E.; Costantino, A. R.; Grabulosa, A.; Riera, A.; Verdaguer, X. *Organometallics* **2015**, *34*, 4989-4993.

(42)   Meggers, E. *Chem. Eur. J.* **2010**, *16*, 752-758.

(43)   (a) Shen, X.; Huo, H.; Wang, C.; Zhang, B.; Harms, K.; Meggers, E. *Chem. Eur. J.* **2015**, *21*, 9720-9726 (b) Wang, C.; Chen, L.-A.; Huo, H.; Shen, X.; Harms, K.; Gong, L.; Meggers, E. *Chem. Sci.* **2015**, *6*, 1094-1100 (c) Zheng, Y.; Harms, K.; Zhang, L.; Meggers, E. *Chem. Eur. J.* **2016**, *22*, 11977-11981 (d) Luo, S.; Zhang, X.; Zheng, Y.; Harms, K.; Zhang, L.; Meggers, E. *J. Org. Chem.* **2017**, *82*, 8995-9005.

(44)   Rigby, W.; Lee, H.-B.; Bailey, P. M.; McCleverty, J. A.; Maitlis, P. M. *J. Chem. Soc. Dalton Trans.* **1979**, 387-394.

(45)   Prelog, V.; Helmchen, G. *Angew. Chem. Int. Ed. Engl.* **1982**, *21*, 567-583.

(46)   Valderrama, M.; Contreras, R.; Boys, D. *J. Organomet. Chem.* **2003**, *665*, 7-12.

(47)   (a) Mague, J. T.; Lloyd, C. L. *Organometallics* **1988**, *7*, 983-993 (b) Simón-Manso, E.; Valderrama, M. *J. Organomet. Chem.* **2006**, *691*, 380-386 (c) Ganesamoorthy, C.; Mague, J. T.; Balakrishna, M. S. *J. Organomet. Chem.* **2007**, *692*, 3400-3408 (d) Pernik, I.; Hooper, J. F.; Chaplin, A. B.; Weller, A. S.; Willis, M. C. *ACS Catal.* **2012**, *2*, 2779-2786 (e) Naicker, D.; Friedrich, H. B.; Pansuriya, P. B. *RSC Adv.* **2016**, *6*, 31005-31013.

(48)   Groom, C. R.; Bruno, I. J.; Lightfoot, M. P.; Ward, S. C. *Acta Cryst.* **2016**, *B72*, 171-179.

(49)   Carmona, D.; Ferrer, J.; Oro, L. A.; Apreda, M. C.; Foces-Foces, C.; Cano, F. H.; Elguero, J.; Jimeno, M. L. *J. Chem. Soc. Dalton Trans.* **1990**, 1463-1476.

(50)   (a) Prinz, M.; Grosche, M.; Herdtweck, E.; Herrmann, W. A. *Organometallics* **2000**, *19*, 1692-1694 (b) Hanasaka, F.; Tanabe, Y.; Fujita, K.-i.; Yamaguchi, R. *Organometallics* **2006**, *25*, 826-831.

Chapter V. MaxPHOX iridacycles on the asymmetric hydrogenation of N-alkyl imines

5. MaxPHOX iridacycles for the asymmetric hydrogenation of *N*-alkyl imines

5.1. *Introduction. Ir-catalysed asymmetric hydrogenation*

Asymmetric hydrogenation has proved to be a powerful tool for the transformation of prochiral substrates into optically pure compounds and has been extensively studied since the pioneering studies of Knowles and Noyori during 1970's.[1]

The design of the phosphorus ligands has always been entwined to asymmetric hydrogenation. The starting point was the Wilkinson's catalyst,[2] [RhCl(PPh$_3$)$_2$], which was transformed into a chiral catalyst by replacing triphenylphosphine by a monodentate *P*-stereogenic phosphine. Although the enantioselectivities in the asymmetric hydrogenation with such complexes were low, these initial studies constituted an important proof of principle that opened the area of asymmetric catalysis.[1a]

A few years later Kagan's seminal work[3] shifted the focus to bidentate chelating diphosphines, which in most cases proved to be superior to monophosphines. With DIOP he also introduced some ligand design principles that strongly influenced the development of asymmetric catalysis.[3]

He noted that bidentate ligands offer some advantages over monodentate ligands: their conformationally more rigid ligand backbones allowed a better control of the metal-substrate binding modes resulting in a more efficient discrimination of enantiotopic faces of the prochiral substrate. DIOP was also an example of C_2-symmetric diphosphine, simplifying the latter mechanistic studies of Rh-DIOP complexes in asymmetric hydrogenation reactions. An apparent advantage of C_2-symmetric ligands (Figure 1) is that the number of putative transition states is halved compared to ligands devoid of any symmetry element.
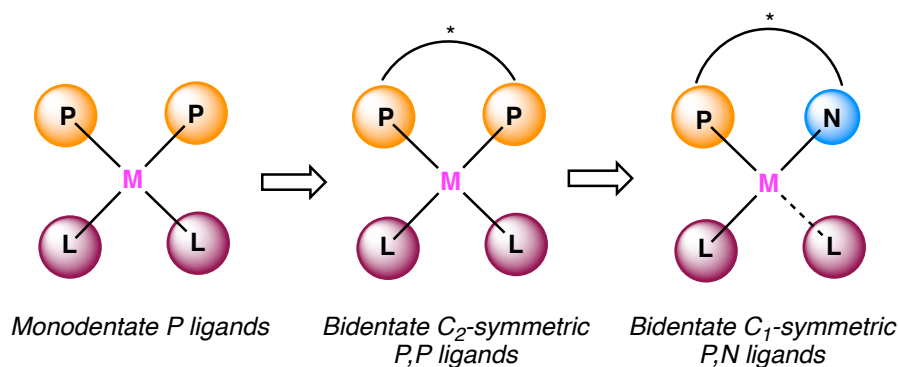
Figure 1. Evolution from monodentate over C_2-symmetric bidentate diphosphorus ligands to unsymmetrical *P*,*N* ligands.

Moreover from a synthetic point of view, this symmetry often makes the characterisation of the different reaction intermediates easier. Although C_2-symmetric diphosphines dominated the asymmetric catalysis field for a long time, there is no fundamental reason that makes such ligands especially good. Indeed, many C_1-symmetric ligands have been found that induce higher enantioselectivities in asymmetric hydrogenations. This has been rationalised by Achiwa and co-workers[4] since the intermediates in the catalytic cycle are non-symmetric, the metal-substrate complex interacts differently with the two phosphorus atoms, hence the electronic properties of both phosphorus atoms should be optimised independently. Obviously other types of bidentate, C_1-symmetric ligands are those with different donor atoms. In this regard, nitrogen donors seem especially promising as they display electronic properties as rather *hard* σ donors that differ significantly from the behaviour as *soft* π acceptors attributed to phosphorus (Figure 2).[5]

P atom

Electronically soft

π-acceptor,
σ-donor

R^1, R^2 tune the P atom both sterically and electronically

N atom

Electronically hard

σ-donor

sp^2 hybridization on N, decreases basicity

Incorporation of N atom into a ring, increases chelate rigidity
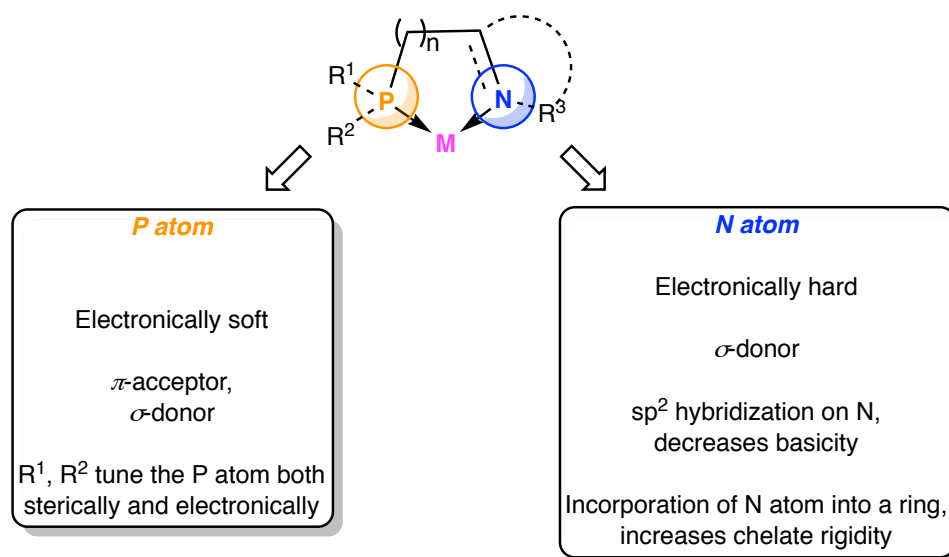
Figure 2. General features of a *P,N* ligand.

Following this rationale, phosphinooxazoline ligands (PHOX) were developed independently by Pfaltz[6] and Helmchen.[7] The earliest applications of such ligands were in Pd-catalysed allylic substitution reactions,[8] proving that, due to the well-known *trans*-labilising effect, the incoming nucleophile attacks preferentially the carbon atom located *trans* to the phosphorus atom, allowing the rationalisation of the stereochemical course of the reaction.[5]

The area of enantioselective homogeneous hydrogenation has been clearly dominated by Rh(I) and Ru(II) complexes with *P,P* diphosphine ligands as chiral inductors and more recently with *P,N* ligands, followed at a certain distance by Ir(I) systems, whose potential is being intensively explored at present.[9] Ir complexes with chiral phosphines have been found to be particularly good ligands for hydrogenation of unfunctionalised alkenes and imines.[10]

In fact, a wide variety of rhodium and ruthenium complexes are able to selectively hydrogenate a huge number of olefins.[11] However, most of these substrates require of a coordinating functional group adjacent to the double bond, such as amides, carboxylic acids or esters. The success of functionalised olefins as model substrates to test the effectiveness of the transition-metal complexes, can be traced back to the reaction mechanism: the coordinating functional group of the olefin coordinates the metal centre during the catalytic cycle forming chelates that are effectively hydrogenated.[12]

5.2. *Precedents on the synthesis of P,N-based iridium catalysts*

5.2.1. *Crabtree's and Pfaltz's catalysts*

In contrast to the reactions with functionalised olefins rhodium and ruthenium catalysts display a poor reactivity with non-functionalised olefins, lacking a second coordinating group. In 1977 Crabtree and co-workers[13] described for the first time the use of Ir-based catalysts for the hydrogenation of double bonds.[13-14] Until that time, little attention had been paid to such complexes as catalytic precursors. Crabtree reported that non-chiral Ir complexes of type [Ir(COD)(PR$_3$)$_2$]PF$_6$ and [Ir(COD)(PR$_3$)(py)]PF$_6$ were able to fully hydrogenate non-functionalised alkenes in non-coordinating solvents such as chloroform or dichloromethane (Figure 3).
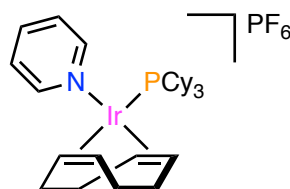
Crabtree's catalyst 1977

Figure 3. The Crabtree's catalyst, [Ir(COD)(PCy$_3$)(py)]PF$_6$.

Even more importantly, the authors reported for the first time the hydrogenation of tetrasubstituted olefins, although with these substrates incomplete conversions were regularly found.[13,15] The best results were achieved with the so-called Crabtree's catalyst. The higher activity of this particular system was attributed to the *cis* conformation of the pyridine and the PCy$_3$ moiety. Despite its activity, the formation of inactive polymetallic Ir species was detected when the substrates were to weakly coordinated and that is serious limitation of the system, which required higher loadings to achieve full conversions.[16]

Inspired by these promising results, two decades later Pfaltz and co-workers[17] disclosed a family of iridium complexes giving a higher activity in the asymmetric hydrogenation of both functionalised and non-functionalised olefins[18] but also of *N*-aryl imines.[17a] These complexes contained a *P,N* chiral ligand known as phosphinooxazoline (PHOX), as shown in Figure 4.

208
Pfaltz-type catalysts 1997
[Ir(PHOX)]BArF
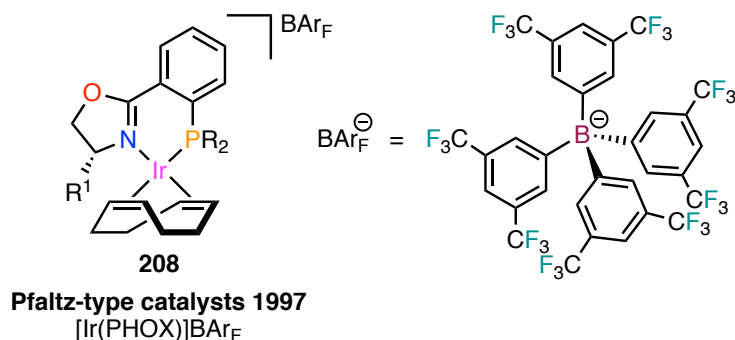
Figure 4. The Pfaltz-type Ir(PHOX) catalysts with BArF as counterion.

Apart from the PHOX ligands, Pfaltz and co-workers also introduced the use of counterions with extremely low coordinating ability. Initially, they employed the PF_6^- but they soon realised that, as it was firstly noted by Crabtree and co-workers,[13,15] there was an important problem of catalyst deactivation.[17e] In their studies of the counterions' effect, the group of Pfaltz found that the use of poorly coordinating anions prevented the deactivation, being the tetrakis[3,5-bis(trifluoromethyl)phenyl] borate (BArF⁻) the most efficient. The BArF⁻ anion is bulky and non-polar and also serves as halide extractor.[19] Besides, the Ir complexes prepared with BArF⁻ as counterion proved to be particularly air- and moisture-stable. Interestingly, even though the complexes are cationic, its purification could be carried out by means of column chromatography instead of the usual recrystallizations normally used in these cases.

5.2.2. *Oxazoline-based P,N-catalysts*

After the works published by Pfaltz[6] and Helmchen[7], many systems based on oxazolines as *N*-donor groups have been thoroughly studied, especially phosphinooxazolines. Apart from their relatively easy synthesis, their main advantage is modularity since both the phosphine or the oxazolines groups can be installed at the last step and therefore series of ligands can be easily obtained.[20]

For example, a typical synthetic approach for the preparation of PHOX ligands **215** involves the conversion of 2-bromobenzonitrile (**209**) into phosphine (**210**) by halogen-metal exchange and subsequent nucleophilic substitution reaction upon treatment with chlorodiphenylphosphine (Scheme 1).[20]
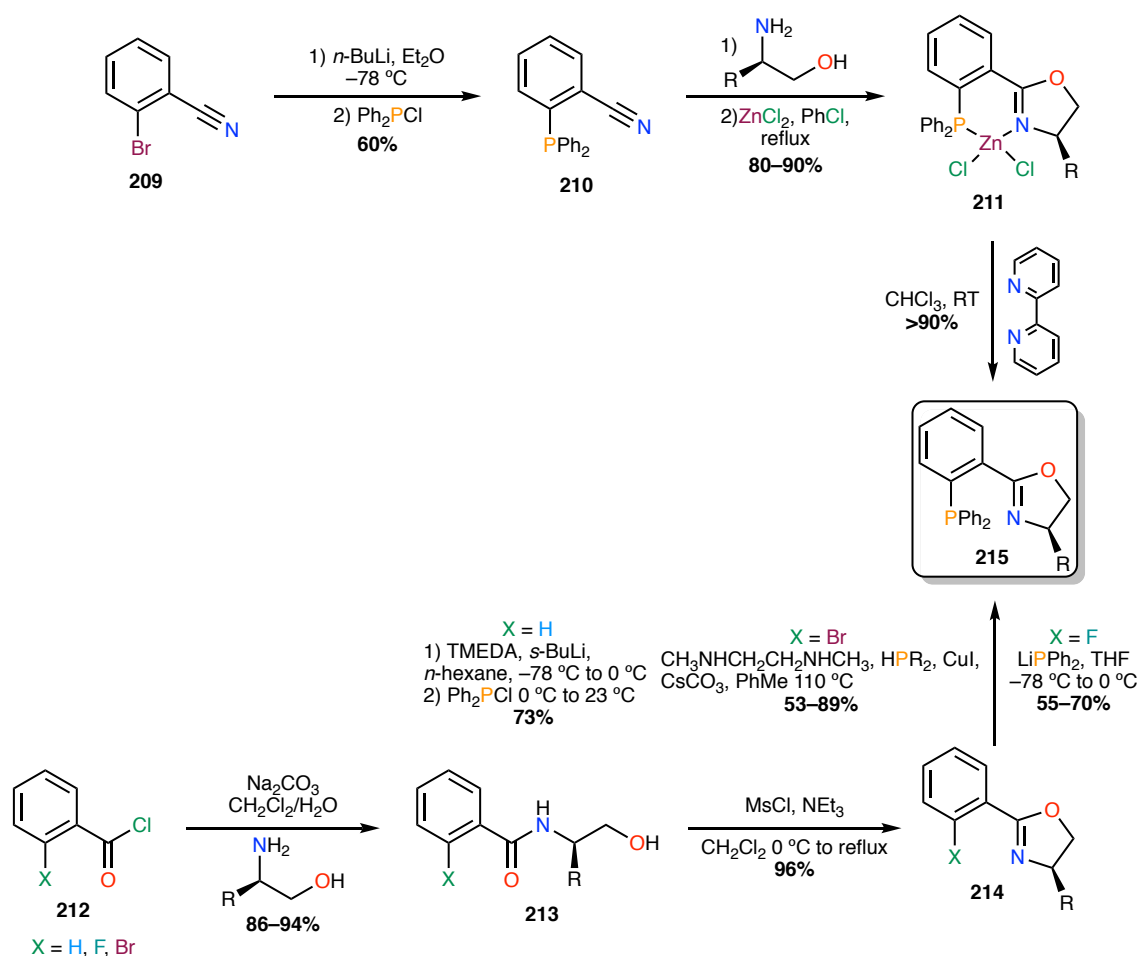
Scheme 1. Synthetic approaches to PHOX ligands bearing an aryl backbone.

Oxazoline formation with amino alcohols in the presence of the metallic salt, such as zinc chloride, followed by decoordination of the resulting Zn-PHOX complex **211** affords the desired ligands **215** differing on the substitution pattern of the oxazoline.[21]

Another approach that facilitates variation of the phosphine moiety involves the amide coupling of an acid chloride **212** followed by intramolecular condensation of the resulting *β*-hydroxy amide upon activation with mesyl chloride. Unfunctionalised arenes **213** can be converted into the corresponding PHOX ligands (**214**) by a sequence of *ortho*-lithiation and subsequent nucleophilic quenching with a chlorodiarylphosphine. Other arene substitution patterns allow milder conditions of functionalization: fluoroarenes can be transformed into the desired phosphines by means of nucleophilic aromatic substitutions.[22] Alternatively, the C–P bond can be formed by an Ullman-type coupling of a secondary phosphine with bromoarenes.[23]

Using this already mentioned synthetic strategies a large family of PHOX derivatives containing an aromatic backbone have been prepared and tested for their performance in transition metal catalysis (Figure 5).
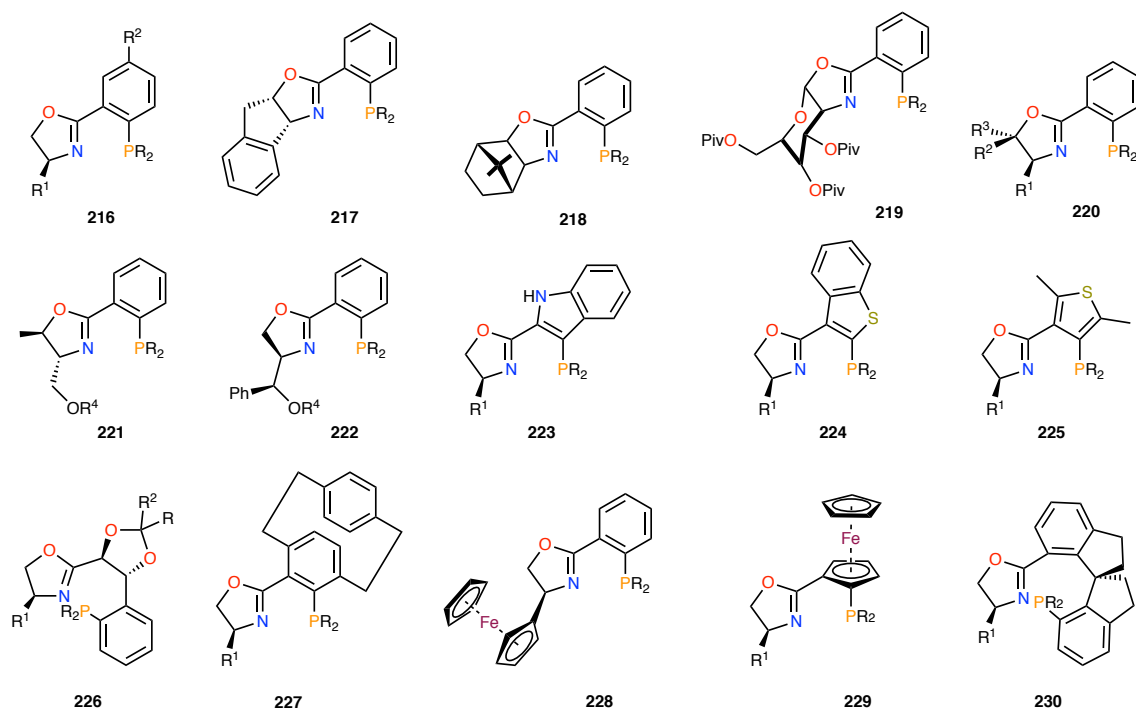
Figure 5. Representative family of PHOX ligands with (hetero)aryl backbone.

Their preparation includes variation of the amino alcohol part derived from commercially available bulky α-amino acids such as valine, phenylalanine or phenylglycine.[20b] Most of the phosphinooxazolines contain aromatic phosphines, but occasionally alkyl phosphines were also employed when very electron-rich phosphines were required. The introduction of ligands **216**, bearing electronically modified in the aromatic ligand backbone was realised by Stoltz and co-workers,[24] Saigo[25] and Helmchen[17b,26] reported on ligands **217** bearing tricyclic oxazolines that were derived from indan-1,2-diol and tetralin-1,2-diol, respectively. Additionally, the synthesis of **218** from (2*S*,3*R*)-3-hydroxy-bornylamine was described by Helmchen.[26b] The use of glucosamine-derived ligands **219** was described by Kunz and co-workers,[27] and Pfaltz[28] proved the utility of ligands **220** introducing two additional geminal alkyl or aryl groups. Moberg[29] showed that ligands **221** and **222** carrying an additional free hydroxyl or methyl ether group in the oxazoline part could be accessed by reduction and subsequent derivatisation of serine. The groups of Tietze[30] and Guiry[5,31] reported the synthesis of heteroaryl ligands **224**-**225**, which were named HETPHOX.

Zhou[32] reported the four-step synthesis of SIPHOX ligands **230** using 1,1'-spirobiindan-7,7'-diol (SPINOL) as starting material. The Morken group[33] contributed a family of ketal-containing ligands (**226**), named StePHOX, accessed by ring opening of coumarin followed by Sharpless asymmetric dihydroxylation, ketalization, and

oxazoline formation. In parallel, paracyclophane-based ligands **227** displaying a "*pseudo-ortho*" substitution were described by Bolm and co-workers.[34]

Oxazoline-based *P,N* ligands with planar chirality have also been described in the literature. Among these ligands there are a number of phosphinooxazolines that carry a ferrocene unit. Patti and co-workers[35] reported the preparation of PHOX ligands **228** with a ferrocenyl side chain on the oxazoline. Later on, Uemura[36] and Richards[37] independently described the synthesis of *ortho*-substituted ferrocene-PHOX ligands **229** prepared by directed *ortho*-lithiathion of ferrocenyloxazoline and subsequent treatment with clorophosphines.

Among all the presented ligands it is particularly interesting to mention Zhou's SIPHOX ligand.[32a] This phosphinooxazoline ligand contains a rigid and bulky spirobiindane backbone. Once coordinated to iridium, with BAr_F as counterion, the complex (Figure 6) is very efficient for the asymmetric hydrogenation of *N*-aryl imines.

231
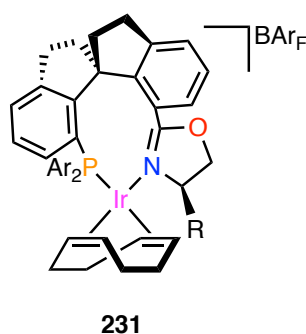
Figure 6. The Zhou's catalyst.

Apart from the mentioned aromatic backbones, many oxazoline-based ligands that carry alkyl backbones have been also described in the literature (Figure 7).
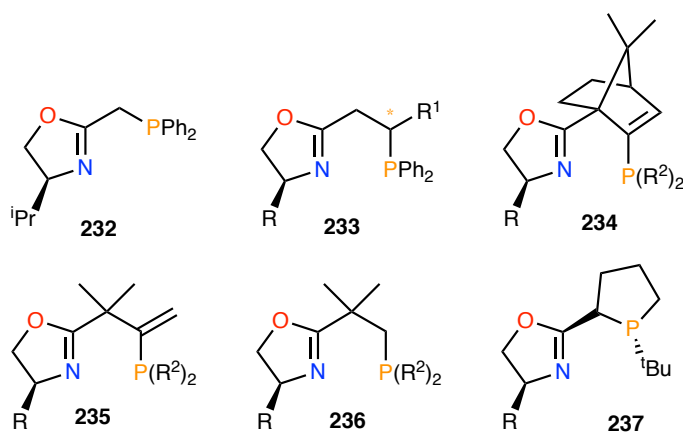
Figure 7. Selected examples of oxazoline-based *P,N*-ligands with alkyl backbones.

In 1993, Sprinz and Helmchen[7] described the synthesis of **232**, the first phosphinooxazoline with an alkyl group tethering the two donor atoms. Later the Gilbertson group[38] introduced vinyl phosphinooxazoline ligands **234** and **235**, in which the norbornyl derivatives could be accessed in four steps from ketopinic acid. In 2009, Schrems and Pfaltz[39] described the synthesis of structurally related ligands called NeoPHOX **236**. More recently the Zhang group[9a,40] has described the use of *P*-stereogenic phospholane-oxazoline ligands bearing the *tert*-butyl moiety (**237**).

As it can be seen, many PHOX-like ligands have been studied since the first examples reported by Pfaltz in 1997. However, in pursue of exploring new catalytic applications, especially asymmetric hydrogenations and allylic substitutions[6,8,17b,41]), the development of oxazoline-based ligands consisting of trivalent *P*-donor moieties different than phosphines have been also reported.

5.2.3. *Oxazoline-phosphinite and -phosphite-based catalysts*

With all the described methodologies in hand, Pfaltz and co-workers[17d] studied in 2001 the preparation of a new class of iridium complexes with phosphinite-oxazoline ligands: the SerPHOX and the ThrePHOX.[17d,42]

In comparison to the "classic" Ir-PHOX complexes, the phosphorus unit is linked to an oxygen atom and it is also attached closer to the stereogenic centre of the oxazoline ring (Scheme 2).
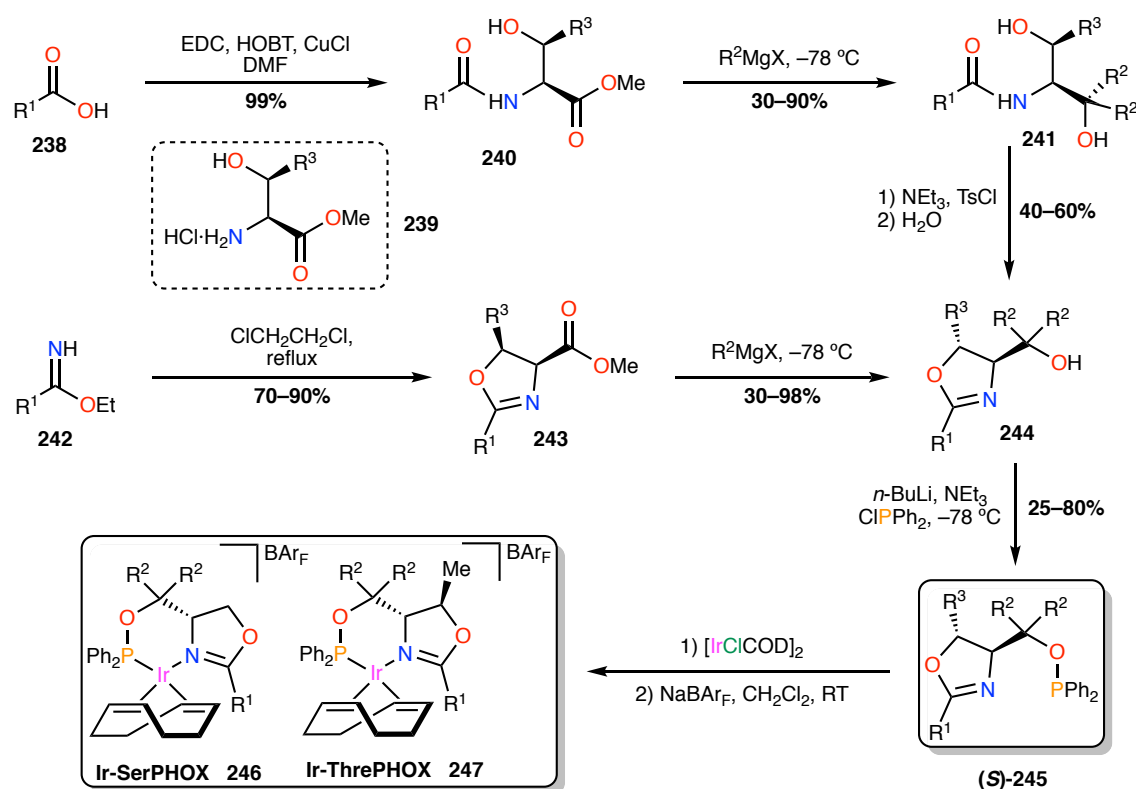
Scheme 2. Synthesis of the SerPHOX and ThrePHOX iridium complexes.

In these syntheses, both enantiomers of the phosphinite-oxazoline ligands **245** are readily prepared in three or four steps, starting from imidates (**242**) or carboxylic acids (**238**) and L-serine (Ser) or threonine (Thre) methyl ester hydrochloride (**239**) or the corresponding D isomers.[43]

Another interesting ligand, developed in 2004, is SimplePHOX, whose synthesis is based on the reaction between a chiral amino alcohol (obtained from an amino acid) and 2-hydroxy-2-methylpropionic acid, which affords the corresponding oxazonyl alcohol. Later deprotonation and treatment with clorophosphine derivatives yields the desired ligands, as it is detailed in Scheme 3.

216
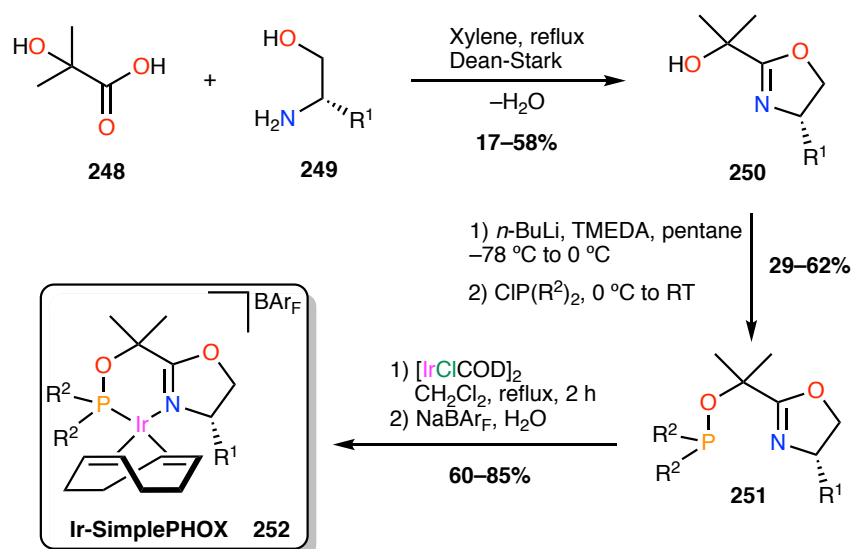
Scheme 3. Preparation of Ir-SimplePHOX catalysts.

Excellent results have been obtained in the Ir-catalysed asymmetric hydrogenation of unfunctionalised alkenes, both with the PHOX and the phosphinite-oxazoline ligands (Figure 8).
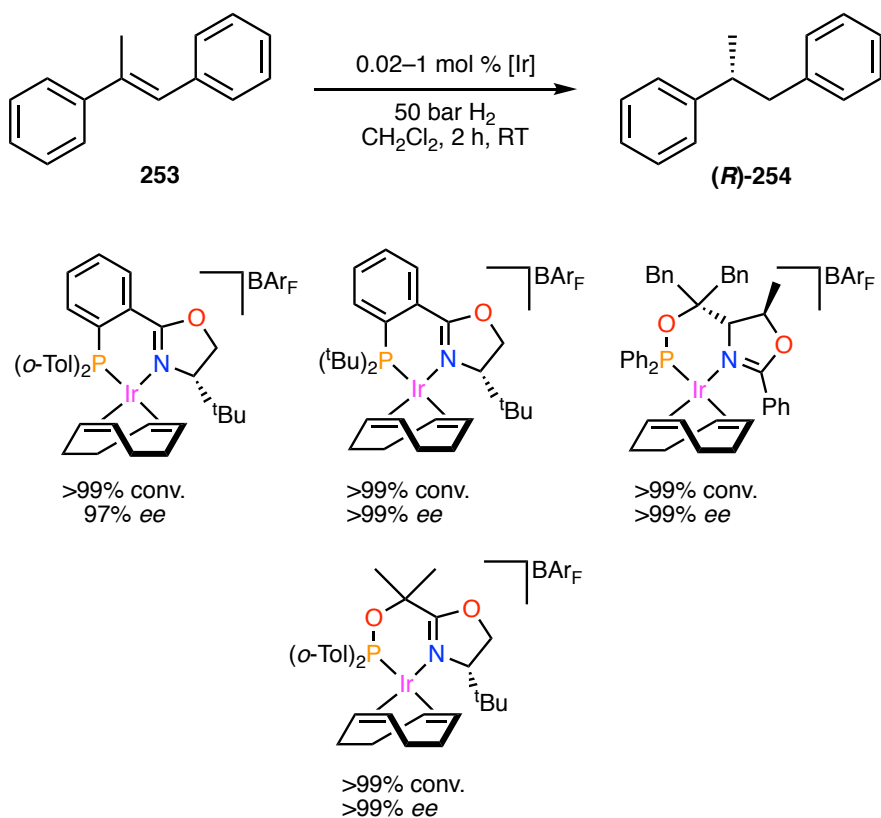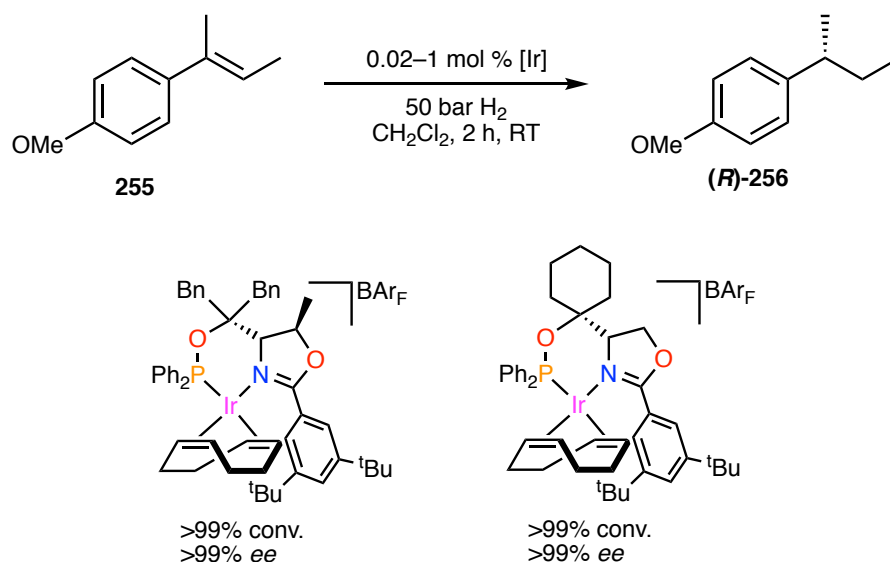
Figure 8. Catalytic results in the asymmetric hydrogenation of alkenes using PHOX, SerPHOX, ThrePHOX and SimplePHOX iridium complexes.

Figure 8, shows some selected examples of the application of Ir-based catalysts of this type to the asymmetric hydrogenation of (*E*)-1,2-diphenyl-1-propene and (*E*)-2-(4-methoxyphenyl)-2-butene achieving full conversions and enantioselectivities up to 99%.[17e,44]

In 2009, Diéguez, Andersson, Börner and co-workers[45] developed a library of up to 96 biaryl phosphite-oxazoline ligands. These ligands are formed out of a SerPHOX or ThrePHOX derived backbone and chiral biarylphosphinites. The corresponding iridium complexes, having BAr$_F$ as counterion (Figure 9) have displayed excellent results in the asymmetric hydrogenation of substituted terminal aryl and alkyl olefins.
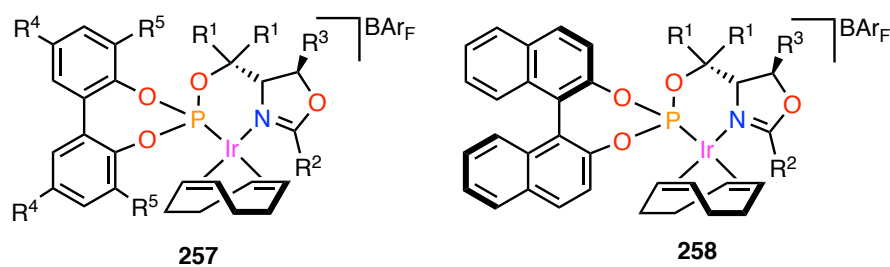
Figure 9. Diéguez-Andersson-Börner phosphite-oxazoline catalysts.[45]

It is interesting to mention that these phosphite-oxazoline catalysts, unlike others presented, contain more than one stereogenic element on the backbone. The confluence of axial chirality with the stereogenic carbon centres does not create a strong match/mismatch effect on the catalytic hydrogenation of olefins.[46] Apparently,

the induction of chirality is mainly driven by the biaryl moieties rather than the other stereogenic elements.

5.2.4. *Pyridine-based P,N-catalysts*

A large number of bidentate *P,N*-ligands contain pyridine as the *N*-donor fragment[47]. Since complexes of the formula [Ir(py)(COD)PR₃], which were firstly studied by Crabtree and co-workers[13,14b,48] had shown high catalytic activity in the hydrogenation of tri- and tetrasubstituted olefins,[16] the interest of chiral analogues of Cratree's precatalyst has prompted many research groups to investigate metal complexes that bear pyridine-based chiral bidentate *P,N*-ligands.[14b]

With the idea of reproducing the coordination sphere to the Crabtree's catalyst, Pfaltz and co-workers[49] and Knochel and co-workers[50] developed another remarkable family of catalysts derived from pyridine and quinoline (Figure 10). These complexes have been very active in the asymmetric hydrogenation of alkyl-substituted olefins and furanes.
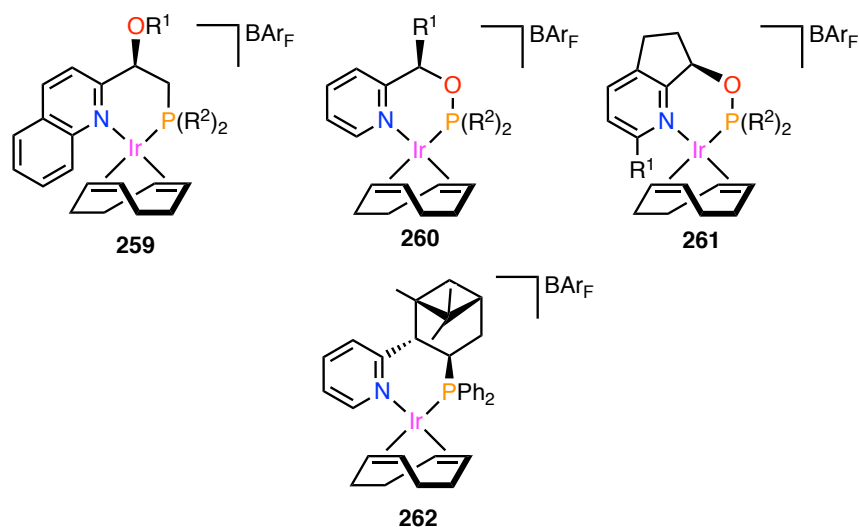
Figure 10. Ir complexes reported by Pfaltz[49] (top) and Knochel[50] (bottom).

It is noteworthy to mention the catalyst developed, in 2003, by Knochel and co-workers[50] containing terpene-pyridine derived ligands, which displayed enantioselectivities up to 97% in the asymmetric hydrogenation of *α*-acetamidocinnamates.

5.2.5. *Oxazole-, thiazole-, and imidazole-based P,N-catalysts*

In 2004, Andersson and co-workers[51] reported on a first generation of bicyclic oxazole-based ligands describing the phosphinites **263**-**265** (Figure 11).
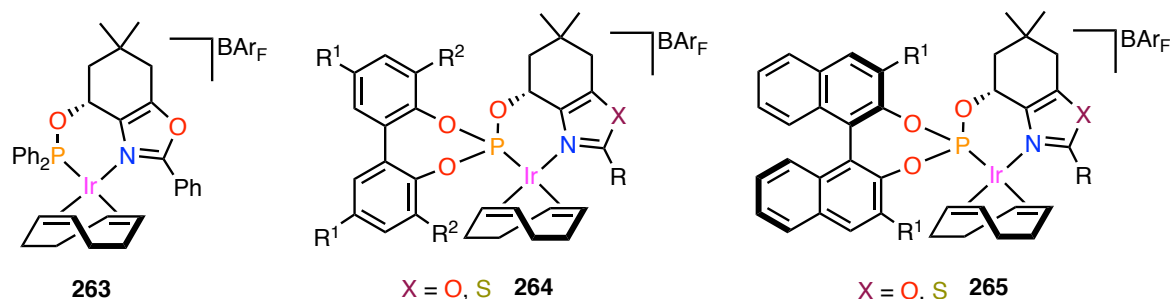
Figure 11. Andersson and Diéguez's[51] oxazole-based phosphinite and phosphite iridium complexes.

More recently, the Andersson group, in collaboration with Diéguez and co-workers[52], described the construction of a biarylphosphite ligand library (**266**-**268**) where the *N*-donor moiety consists on an oxazole or thiazole group.

Andersson and co-workers[51b,c] also reported on phosphinotiazoles, phosphinoimidazoles and aminophosphinooxazolines as highly efficient ligands for asymmetric Ir-catalysed hydrogenations (Figure 12).
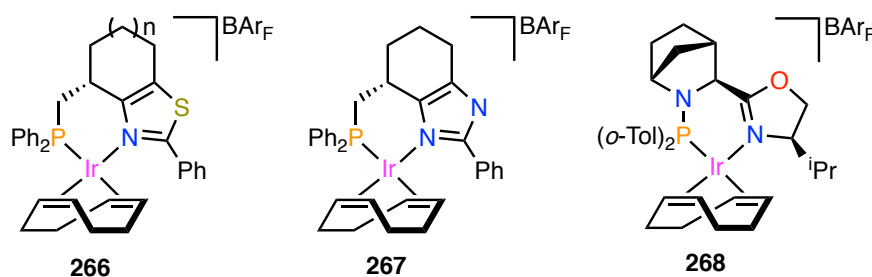
Figure 12. Bidentate thiazole-, imidazole- and aminophosphino-oxazoline-based *P,N*-Ir catalysts.

It is noteworthy to mention that these ligands containing a bicyclic backbone and an oxazole or thiazole moiety, once coordinated to Ir centres, have displayed enantioselectivities in asymmetric hydrogenation of unfunctionalised alkenes comparable or even superior in some cases[53] to the best phosphinooxazoline ligands reported.

5.2.6. *Synthesis and coordination chemistry of the MaxPHOX ligands*

Chapter 2 described that the reaction between optically pure, mesylated *tert*-butylmethyl phosphinous acid-borane synthon and chiral amino oxazoline allows for the selective synthesis of a new type of phosphinooxazoline ligands, known as MaxPHOX.[54] These MaxPHOX ligands are built from three independent chiral fragments: an aminoalcohol, an aminoacid and a *P*-stereogenic phosphinous acid (Figure 13).
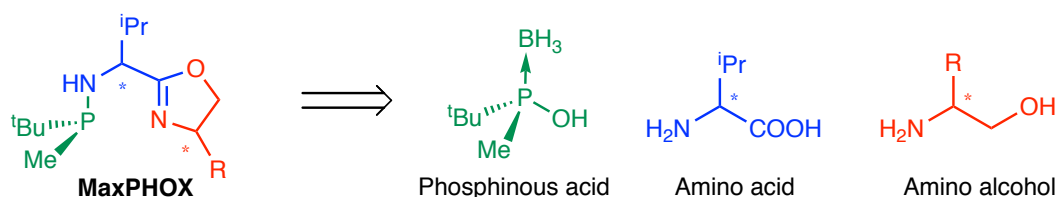
Figure 13. General structure of the MaxPHOX ligands.

One of the key advantages of this MaxPHOX system is the structural diversity arising from its possible configurations and substitution patterns, which can be adapted to a specific reaction. In this line, our group envisaged the preparation of a small library of PHOX-type ligands that could adapt to the requirements of each specific substrate in some transition-metal catalysed enantioselective reactions.

5.2.6.1. *Synthesis of the MaxPHOX ligands*

The first MaxPHOX ligand (**273**, Scheme 4) was synthesised in our group using the methodology depicted in Scheme 4 by means of a $S_N2@P$ reaction between the amino oxazoline **272** and the optically pure phosphinous acid-borane (*R*)-**L1·OH**.
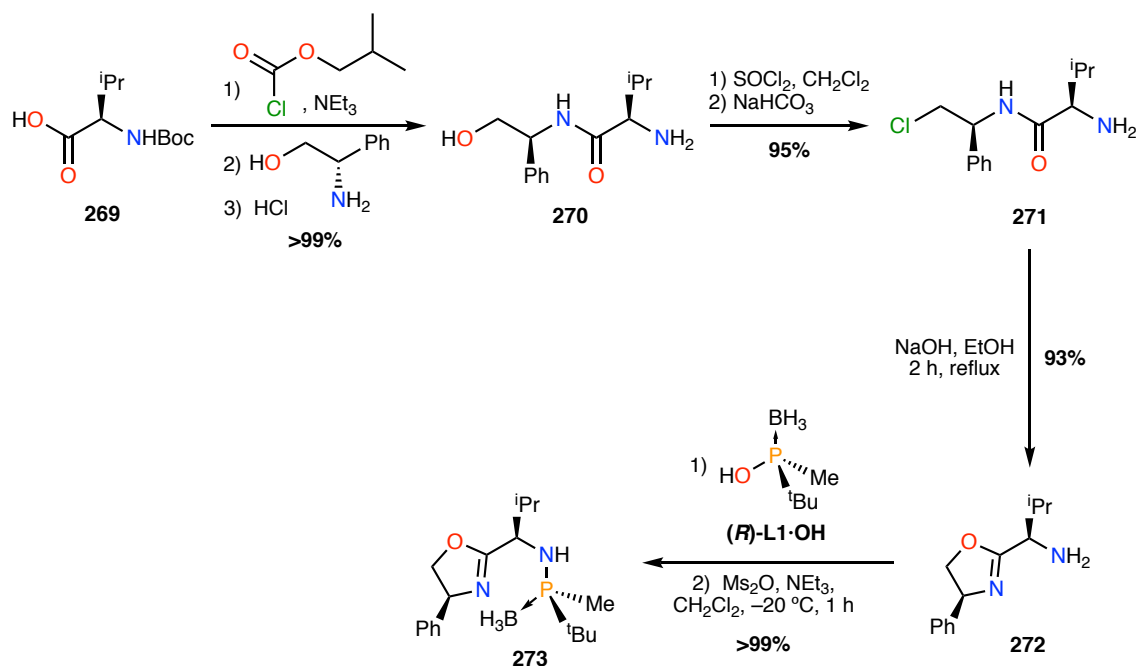
Scheme 4. Synthesis of the amino oxazoline **272** and reaction with (*R*)-**L1·OH** to afford the MaxPHOX ligand **273**.

As it can be seen, the synthetic route for the preparation of the amino oxazoline **272** starts with the coupling of the *N*-Boc amino acid and L-valinol derivative. Then, after cleavage under acidic conditions of the Boc protecting group, the aminoalcohol is reacted with thionyl chloride to afford the chloro derivative. Finally, compound **271** undergoes a cyclization, in the presence of base, to yield the oxazoline ring. Once obtained, **272** is reacted as a nucleophile in a $S_N2@P$ reaction with chiral synthon (*R*)-**L1·OH**.

However, our group soon realised that this methodology did not work when bulky substituents were introduced in the oxazoline moiety, due to the instability of the amino oxazoline units. Therefore, a new route was designed consisting on the reaction of a chiral amino alcohol (Scheme 5) with the mesylated phosphinous acid-borane (*R*)-**L1·OH**.
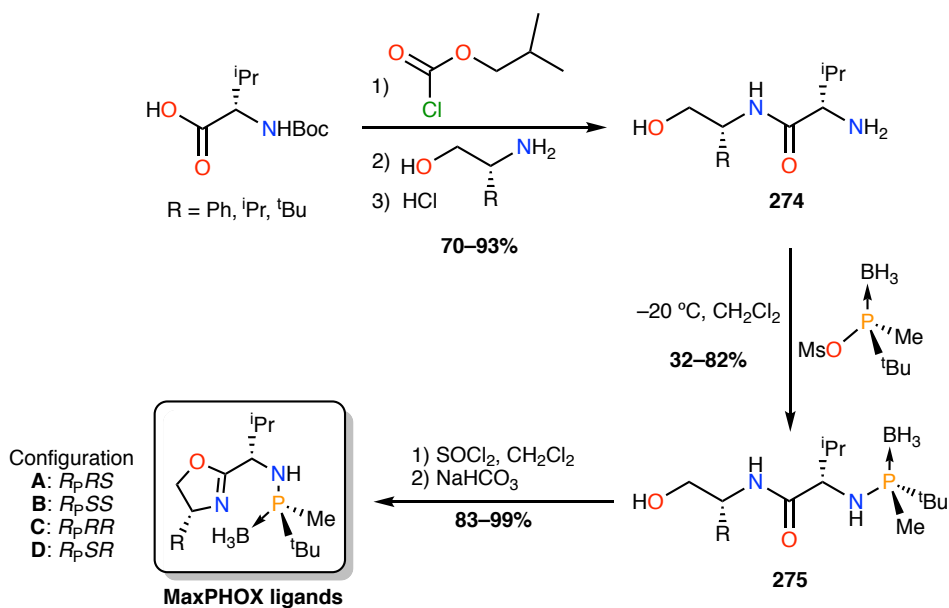
Scheme 5. Synthetic route for the MaxPHOX ligands.

The already formed aminophosphine-borane could then be activated with SOCl₂ to suffer a cyclisation under basic conditions to yield the desired aminophosphine-oxazoline-borane.[55]

This new synthetic route has accessed a family of MaxPHOX ligands with different functionalisations in excellent yields. Moreover, in those cases where further purification was required; the aminophosphine-oxazoline ligands could be easily purified by column chromatography.

5.2.6.2. *Synthesis of iridium MaxPHOX complexes*

Our group has also developed a method to deprotect and successfully coordinate the MaxPHOX ligands to Ir(I). The synthesis of the Ir(I)-MaxPHOX complexes can be done in three steps, (Scheme 6) starting from the deprotection of the boronated MaxPHOX ligand with pyrrolidine.
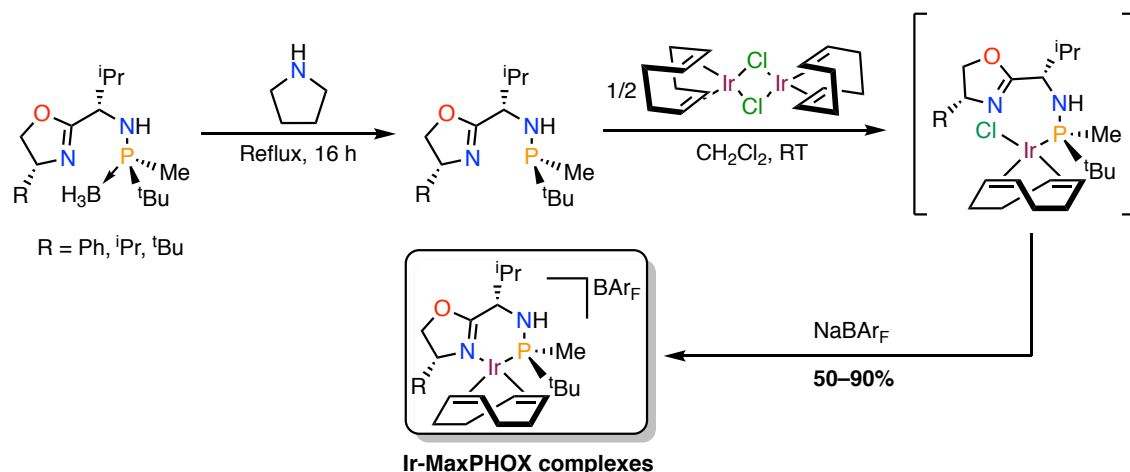
Scheme 6. Preparation of the Ir(I)-MaxPHOX complexes.

Interestingly, this secondary amine proved to be a better deboronation reagent than the more commonly used DABCO, because the pyrrolidine-borane adduct formed does not interfere in the subsequent reaction steps. Once the phosphine moiety is deprotected, the remaining pyrrolidine can be removed by heating the solution under high vacuum, a process that do not cause erosion on the optical purity of the ligand. At this point, the ligand is reacted in dichloromethane with [IrCl(COD)]₂ in the presence of NaBAr_F, which acts as a halogen abstractor and allows the formation of the cationic complex. Finally the crude is purified with flash column chromatography in order to remove the pyrrolidine-borane adduct.

After the optimisation of all these strategies, our group managed to synthesise a library of Ir-MaxPHOX catalysts[54-55] (Figure 14).

The 4 Ir-MaxPHOX diastereoisomers
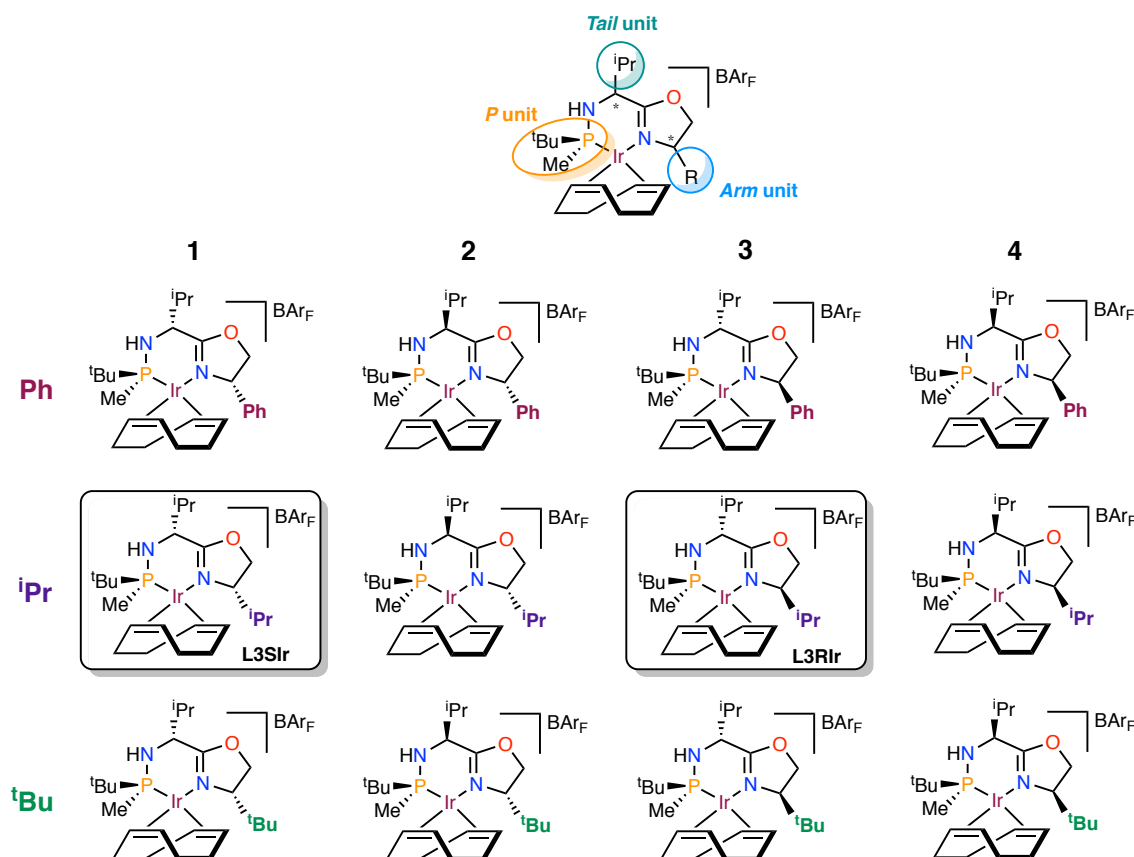
Figure 14. Library of the 12 Ir-MaxPHOX catalysts. Each column contains catalysts with the same configuration while each row those with the same substituents in the oxazoline ring. For the sake of simplicity, since only catalysts **1iPr** and **3iPr** have been used in the present THESIS, they are referred as **L3IrS** and **L3IrR**, where R/S indicates the stereochemistry of the oxazoline's chiral centre.

As it can be seen, they all have three independent chiral centres that can be substituted and functionalised with specific bulky groups. This means that for a given catalyst, 8 stereoisomers could be synthesised as 4 pairs of enantiomers.

The three chiral units present in the catalyst structure can be named as P unit, and located in the backbone the "tail" and the "arm" (Figure 14), belonging to the stereocentre on the bridge and on the oxazoline, respectively.

It has been found that the more significant chiral discrimination during the catalytic cycles, more precisely, in the Ir-catalysed asymmetric hydrogenation of *N*-aryl imines and cyclic enamides,[54-55] is mainly performed by the P unit and the arm. Despite this fact, a non-negligible influence is also played by the tail unit, which allows a better adjust of the enantioselectivity in some catalytic systems.

5.2.7. *Synthesis of phosphinooxazoline iridacycles*

While the mechanism for Rh-catalysed asymmetric hydrogenation of olefins is very well-established, with a cycle that takes place through Rh(I)/Rh(III) species,[56] the mechanism for Ir-catalysed reactions is much more speculative.

Crabtree demonstrated that the reactivity of iridium complexes is strikingly different from that of analogous rhodium complexes.[13,16,57] Therefore it is not possible to draw conclusions on the mechanism of iridium-catalysed asymmetric based on rhodium-catalysed reactions.[48a,58] The electrophilic nature of the cationic iridium species seems to be essential for the observed high reactivity toward tri- and tetrasubstituted alkenes. Thus, for high catalytic activity, coordinating solvents or anions must be avoided. That led to Pfaltz and co-workers in 2004[19b] to study the reaction's mechanism in a non-coordinating media: dichloromethane and BAr$_F$ as a bulky, very weakly coordinating anion.

Cyclooctadiene Ir-complexes, which are used as precatalysts, are air- and moisture-stable compounds, whose structures are known in detail from X-ray and NMR data. However, the catalytically active complexes, formed after dissociation of COD upon treatment with hydrogen, are highly reactive, short-lived species that have not been able to be characterised so far. Only in rare cases, stable hydrido complexes with additional strong ligands such as [(PHOX)Ir(H)$_2$(PPh$_3$)Cl] or [(PHOX)Ir(H)$_2$(TMEDA)] have been detected.[59]

Crabtree[14a] was able to identify iridium dihydride complexes by ^{1}H and ^{31}P{^{1}H} NMR spectroscopy, after treating [(PR$_3$)(pyridine)Ir(COD)]PF$_6$ with H$_2$.[14a] He also presented evidence that these dihydrides are intermediates in the catalytic hydrogenation of cyclooctadiene. However, no experimental information about the catalytic cycle in the hydrogenation of simple alkenes is available. Therefore, the mechanism of Ir-catalysed asymmetric hydrogenation and the nature of the enantioselective step remain elusive. In spite of that, there are two proposed mechanisms mainly based on computational studies.[60] Although there is still some controversy, Dietiker and Chen[61] suggested an Ir(I)/Ir(III) cycle on the basis of mass spectrometry studies on the Ir-PHOX-mediated hydrogenation of styrene (Scheme 7).
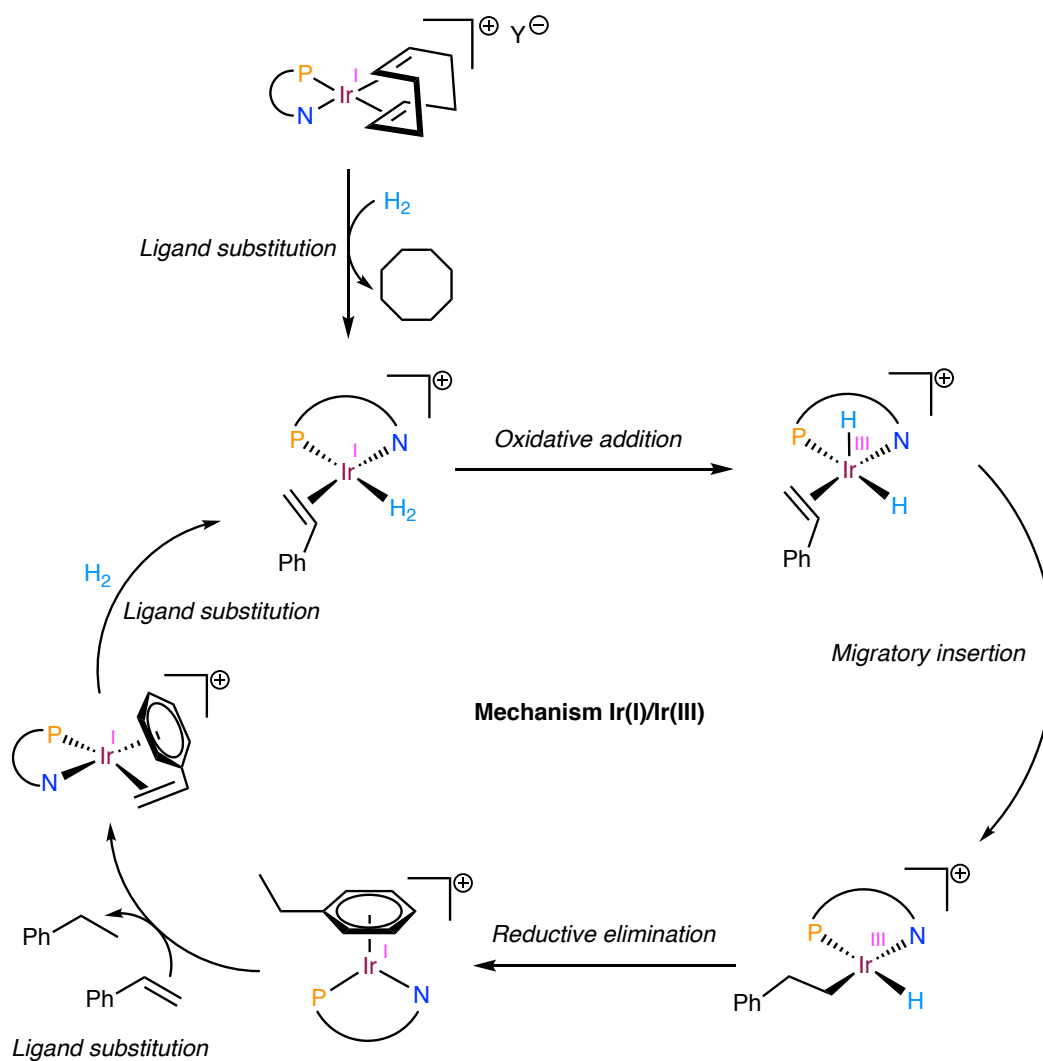
Scheme 7. Ir(I)/Ir(III) proposed mechanism for the catalytic hydrogenation of olefins.

The catalytic species is a dihydride-Ir(III) complex formed after oxidative addition of H_2. Migratory insertion of the substrate into a metal-hydride bond is followed by reductive elimination of the product and regeneration of Ir(I).[61-62]

In contrast, DFT studies carried out by Brand and co-workers[60a] indicated that an Ir(I)/Ir(III) is energetically unlikely, and instead, an Ir(III)/Ir(V) cycle was proposed. (Scheme 8)
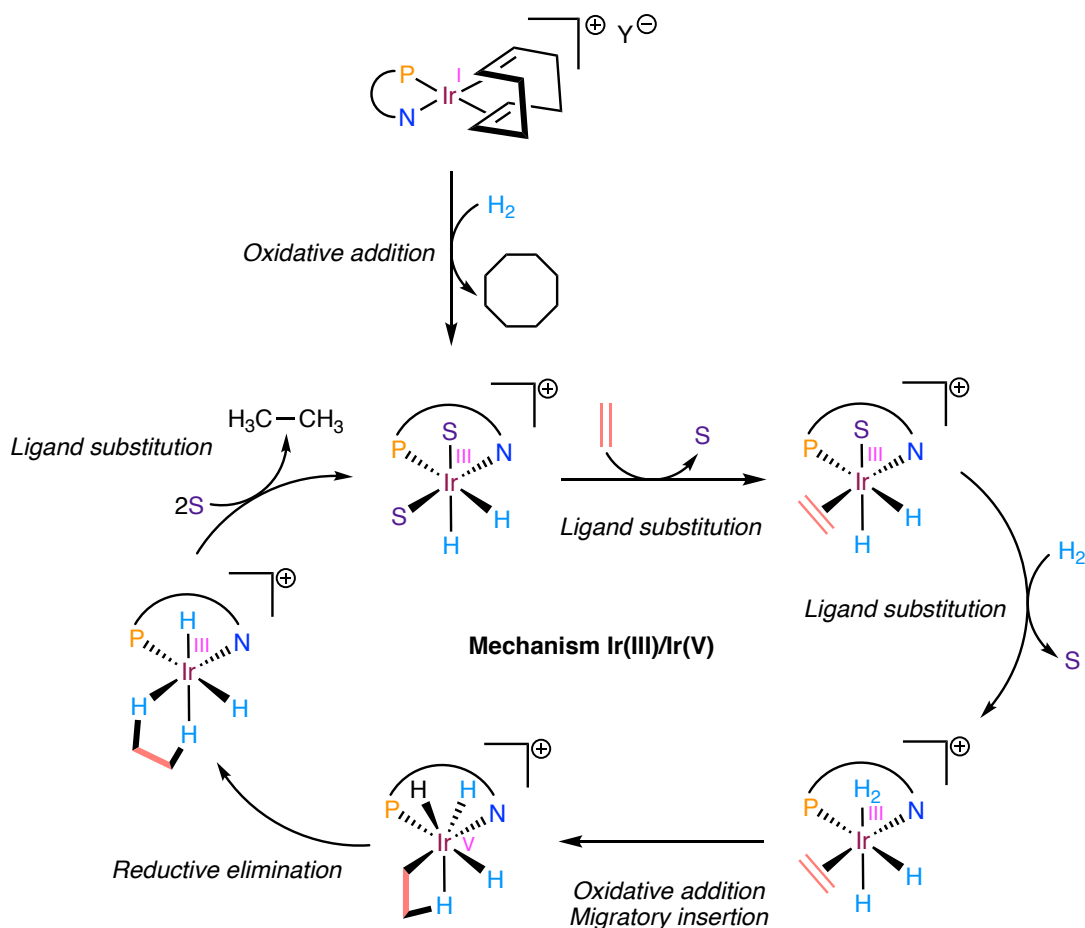
Scheme 8. Ir(III)/Ir(V) proposed mechanism for the catalytic hydrogenation of olefins.

Migratory insertion of the substrate occurs simultaneously with oxidative addition of a second H_2 molecule, resulting in an Ir(V) intermediate. Proton transfer to the substrate is accompanied with regeneration of Ir(III).

Several DFT studies carried out by Andersson and co-workers[60b] based on a full model of a thiazole derivative of Ir-PHOX, supports that the mechanism involving Ir(III)/Ir(V) intermediates is the preferred pathway for alkene hydrogenation.[60b] They extended those calculations for the Ir-catalysed asymmetric hydrogenation of prochiral olefins, considering all the possible diastereomeric pathways, where four plausible mechanisms were found: two involving Ir(I)/Ir(III) species and two with Ir(III)/Ir(V), respectively. Among all of them, the preferred route was found for the Ir(III)/Ir(V) catalytic cycles (Scheme 9).
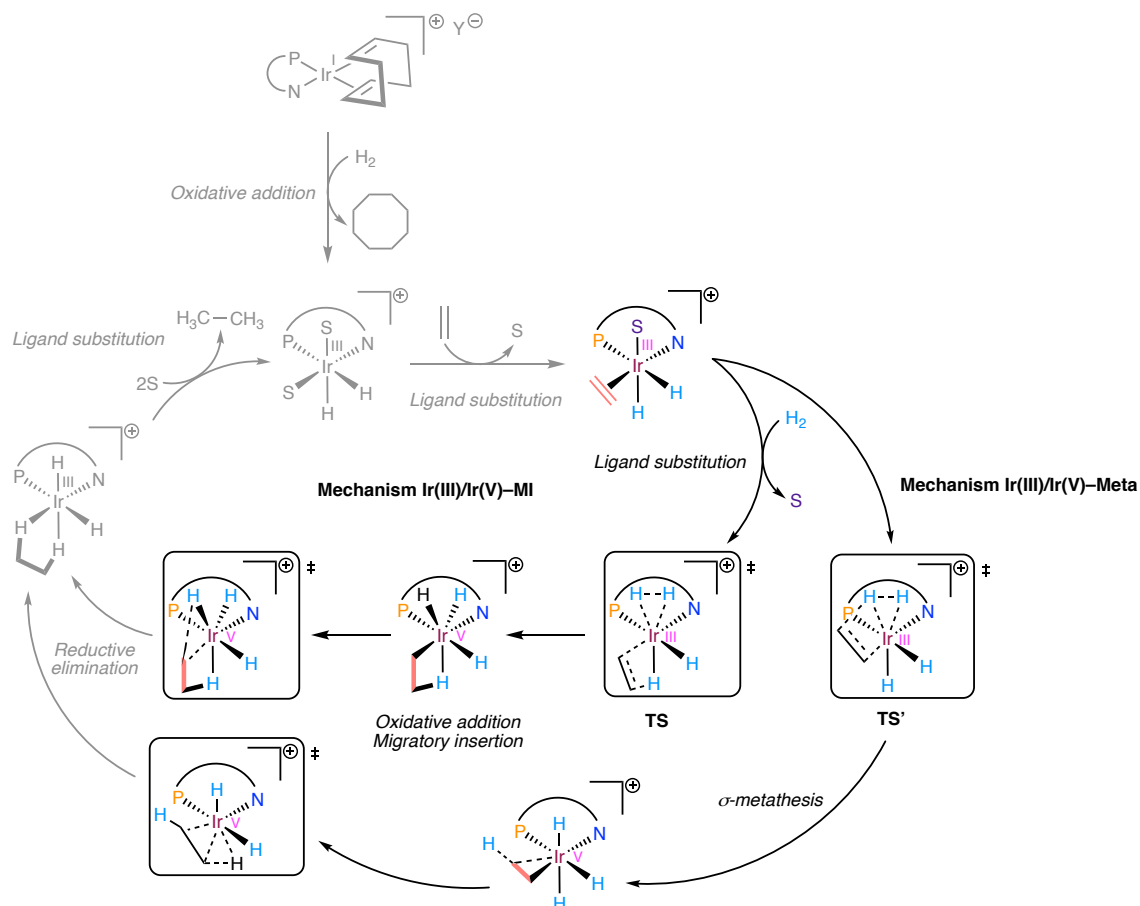
Scheme 9. Two reaction pathways for the Ir-catalysed asymmetric hydrogenation of prochiral alkenes. Ir(III)/Ir(V)–MI proceeds in a migratory insertion/reductive elimination sequence, whereas Ir(III)/Ir(V)–Meta proceeds through a metathesis/reductive elimination route.

As it is depicted in Scheme 9, the first mechanism (MI) involves migratory insertion and reductive elimination while the second pathway (Meta) takes place through a σ-metathesis followed by reductive elimination. **TS** and **TS'** are thought to be the transition states that determine the enantioselectivity of the reaction.

Diéguez, Andersson and co-workers[14b,45,52] have also studied by computational tools the Ir-catalysed hydrogenation mechanism of trisubstituted and disubstituted alkenes with PHOX-derived ligands, concluding that the most plausible cycle involves Ir(III)/Ir(V) intermediates with an hydride migratory insertion step (MI).

Unfortunately, in spite of many efforts, no experimental evidences of Ir(V) intermediates have been found so far. Pfaltz and co-workers[19b] have devoted many efforts in the characterisation of some of the species involved in the catalytic cycle. Nonetheless, NMR studies at low temperatures allowed the identification of Ir(III) dihydrides of the type [Ir(PHOX)(H)$_2$(THF)$_2$]BAr$_F$. On the other hand, the effect of the counterion on the enantioselectivity is dramatic: the less coordinating the counterion

the higher the *ee*. Unfortunately, experiments in non-coordinating solvents led to highly reactive intermediatesdue to the lack of a stabilizing effect of a coordinating ligand. Several experiments have shown that in the absence of such stabilizing solvents, bimetallic species were detected instead.[63]

Pfaltz and co-workers[63] were able to isolate two diastereomeric Ir(III) complexes **276a** and **276b** in which the alkene is coordinated to the Ir centre *via* opposite enantiotopic faces (Figure 15).

276a   *dr* 11:1   **276b**
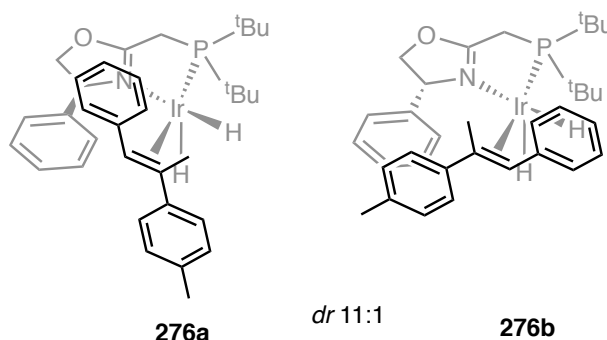
Figure 15. Ir(III)-olefin coordinated complexes characterised by Pfaltz and co-workers.[63]

Those species were unreactive in the absence of molecular hydrogen, but once they were treated with H_2, the corresponding (*R*) and (*S*) alkane was formed, in agreement with the theoretical calculations for an Ir(III)/Ir(V) mechanism.

On the other hand, a completely different portrait is drawn for the mechanistic insights of the Ir-catalysed asymmetric hydrogenation of imines.

Since no experimental mechanistic studies of imine hydrogenation with Ir-PHOX type complexes had been reported, Hopmann and Bayer[60c] carried out DFT calculations with catalyst **277** (Scheme 10) on nine different catalytic cycles based on proposed mechanisms for imine hydrogenations with other types of iridium complexes.
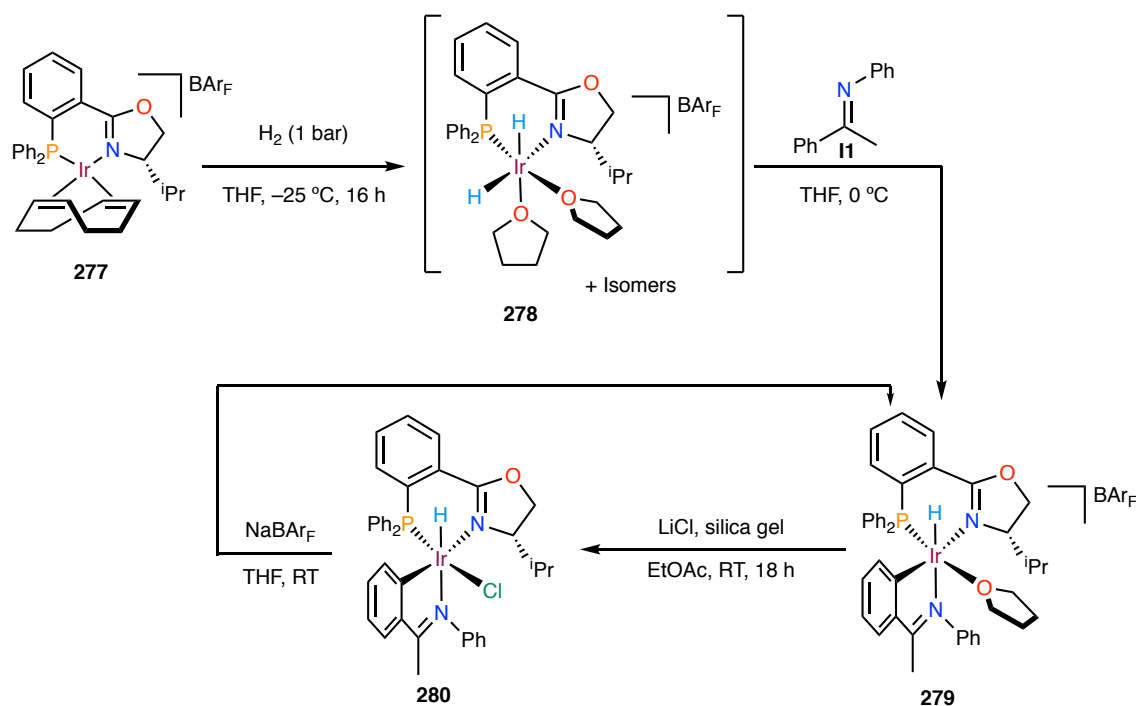
Scheme 10. Formation of cyclometallated imines complexes reported by Pfaltz and co-workers.[64]

The computed energies of the turnover-limiting transition states indicated a pathway involving proton transfer from an Ir-hydride complex to a free, uncoordinated imine, followed by hydride transfer to the resulting iminium ion. As all proposed mechanisms included Ir-dihydride complexes as intermediates, Pfaltz and co-workers[64] decided to prepare a dihydride complex from the Ir(PHOX) precursor **277** following the procedure developed by Mazet and co-workers[19b] and to study its reactivity with acetophenone *N*-phenyl imine as typical substrate (Scheme 10).

They observed that the dihydride complex, generated by reaction of **277** with H_2 in THF at low temperature, once treated with **I1**, yields the cyclometallated Ir(III) complex **279**. The reaction can be understood in two steps: first the hydrogenation and release of COD followed by the oxidative addition of the imine, which undergoes the C–H activation that leads to the iridacycle.

This iridacycle proved to very sensitive and rapidly decomposed upon exposure to air.[64] The authors were unable to obtain suitable crystals for X-ray determination of **279** with BAr$_F$ as counterion, which often precludes crystallisation, but they succeeded with hexafluorophosphate. Finally, the neutral chloride complex **280** was readily obtained by treatment with LiCl and silica (Scheme 10).

An analogous cyclometallation reaction of $[Ir(H)_2(PPh_3)_2(acetone)_2]PF_6$ with benzaldehyde *N*-benzylimine has been reported by James[65] and by Oro and co-

workers[66], but the resulting iridacycles showed no catalytic activity in the hydrogenation of *N*-aryl imines.

Interestingly, Pfaltz[64] found that iridacycle **280** having the chloride ligand, did not display any catalytic activity in the hydrogenation of *N*-aryl imines either. However, when the chloride was replaced with the non-coordinating anion BAr$_F$ by addition of an equimolar amount of NaBAr$_F$, an active catalyst was generated that furnished the same enantiomer of amine **A1** with identical enantioselectivity as the reduction catalysed by the non-cyclometallated complex **277** (Scheme 11).
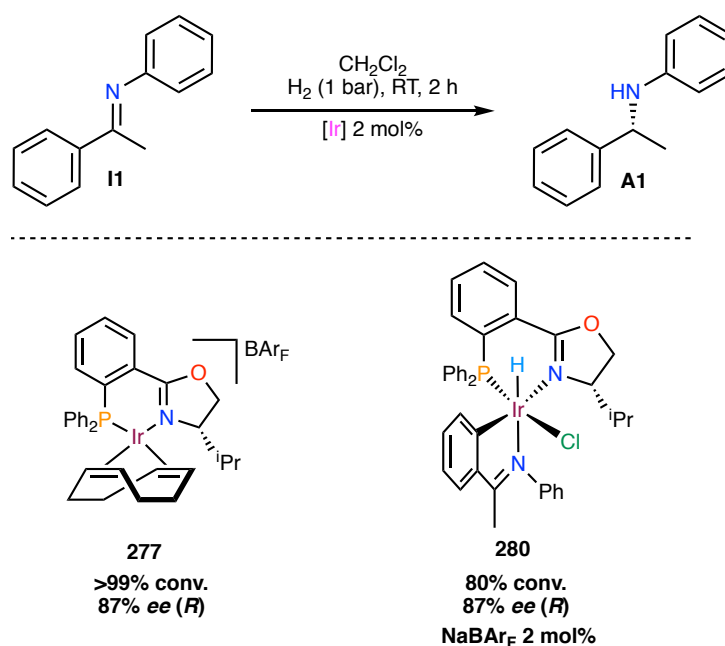
Scheme 11. Comparison of complexes **277** and **280** as precatalysts for the hydrogenation of **I1**.

In the view of these results, Pfaltz wondered whether this iridacycle could actually act as a key intermediate of the hydrogenation mechanism or just an off-cycle inactive species in equilibrium with those really involved in the process. Hence, they hypothesised that the imine would be part of the catalyst, remaining attached to it during the whole catalytic cycle. In order to prove it, as it has been mentioned, they were able to isolate the chloride-substituted iridacycle **280**.
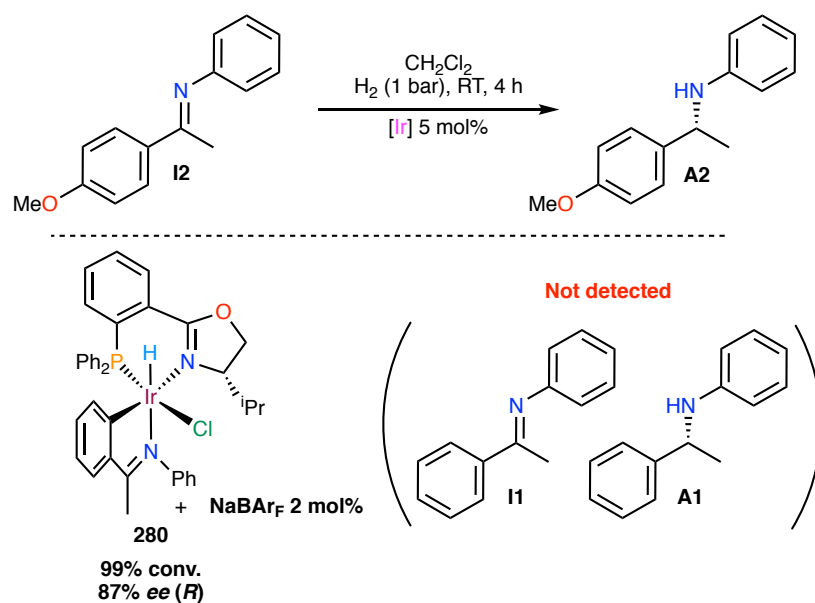
Scheme 12. Hydrogenation of imine **I2** with iridacycle **280** in the presence of NaBAr$_F$.

Furthermore, no trace of imine **I1** used as cyclometallating agent, or the corresponding reduced amine **A1** were detected by chiral GC, proving that the metal-chelated imine is not labile and does not dissociate from the metal centre during the catalytic cycle.

Pfaltz and co-workers[64] also pointed out that the difficulties to hydrogenate *N*-aryl imines of dialkyl ketones with Crabtree-type catalysts is due to the less tendency of such species to undergo a C–H activation and form the corresponding cyclometallated species, since the hybridization of the carbon atom is sp^3 instead of sp^2. Surprisingly, cyclometallating with **I1**, a significant increase of both conversions and enantioselectivities were observed.[64]

The Ir-MaxPHOX complexes presented in the previous section, have shown an outstanding selectivity in the hydrogenation of cyclic enamides[55] and more recently in the hydrogenation of *N*-aryl imines.[54]

In our group, two new cyclometallated Ir(III) hydrido complexes have been recently prepared[54] by reaction of Ir(I) MaxPHOX complexes **L3RIr** and **L3SIr** with **I1** under the same reaction conditions reported by Pfaltz and co-workers[64] (Scheme 13).
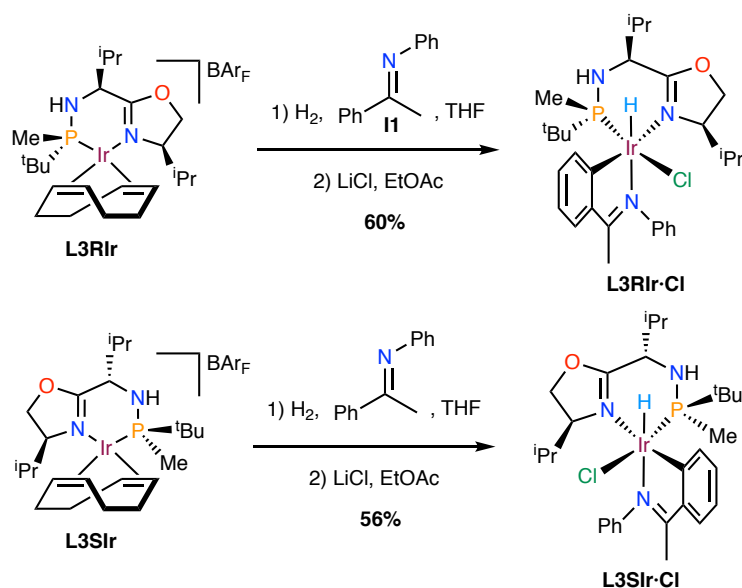
Scheme 13. Synthesis of iridacicles **L3RIr·Cl** and **L3SIr·Cl**.

These complexes were isolated as air-stable pale yellow solids by filtration on silica gel. ^{1}H and ^{31}P{^{1}H} NMR confirmed that **L3RIr·Cl** and **L3SIr·Cl** were diatereomerically pure compounds, since a single resonance for the Ir–H was observed at −19.76 ppm (d, J_P = 26 Hz) and −19.62 ppm (d, J_P = 23 Hz) for **L3RIr·Cl** and **L3SIr·Cl**, respectively. It should be noted, as it was described in Chapter 4, that heteroleptic octahedral complexes such as these iridacycles can provide various diastereomers. It is therefore remarkable that in this case only one of them was generated.

Both complexes were successfully crystallised, and the resulting X-ray structures confirmed the octahedral Ir(III)-d^6 coordination. The phosphinooxazoline ligand and the cyclometallated imine ligands are perpendicular to each other, with the oxazoline nitrogen atom in *trans* to the phenyl ring. In both complexes, the C=N–Ph group is located away from the isopropyl substituent of the oxazoline ring. Finally, the hydride and chloride ligands are *cis* to each other and *trans* to the imine nitrogen and phosphine ligands respectively.

In order to verify whether the isolated imine iridacycles can be used as precatalysts, compound **L3RIr·Cl** was tested in the hydrogenation of imines. Thus, 1 mol% of **L3RIr·Cl** was treated with 2 equivalents of NaBAr$_F$ in order to produce the active catalyst by counter ion exchange (Scheme 14).

234
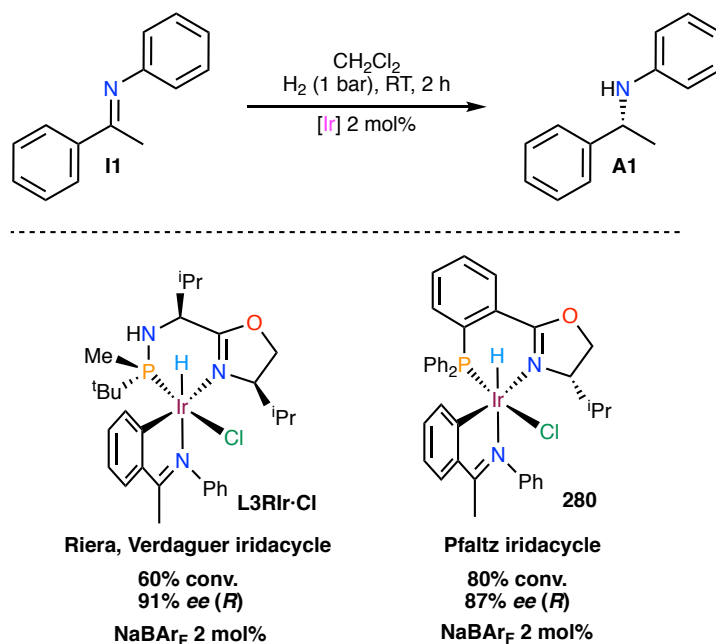
Scheme 14. The use of iridacycles as precatalysts in the hydrogenation of imines.

The use of this mixture as catalyst afforded the reduced product with 60% conversion and 91% *ee*. Despite the lower conversion observed, in comparison to the results obtained by Pfaltz and co-workers,[64] this can be justified by an inefficient chloride abstraction reaction. Nevertheless, these results strongly suggest that the cationic cyclometallated complex arising from chloride abstraction of **L3RIr·Cl** is an active species in the catalytic cycle.

5.2.7.1. *Mechanistic studies on Ir(III)-cyclometallated complexes*

For quite a long time, the mechanism of imine reduction by iridium catalysts has been the subject of debate.[60c,66-67]

Andersson and co-workers[60a] published in 2003 a computational study in which they proposed a catalytic cycle via Ir(III) and Ir(V) intermediates generated by addition of two molecules of H_2 to the Ir(I) centre. Their conclusion was based on density functional theory (DFT) calculations of various potential reaction pathways, using $Me_2PCH=CHCH=NMe$ as a truncated achiral model for the PHOX ligand and ethylene as substrate.[60a] However, it appeared that the lowest energetic pathway was the one involving the Ir(V) species, a hypothesis that was not confirmed by experimental results. Further experimental as well as computational work was necessary to establish a reasonable mechanism that explained the observed enantioselectivities.

As it has been explained, in 2004, Pfaltz and co-workers used NMR and DFT studies of Ir(phosphine-oxazoline)dihydride complexes to show that these species

preferred a configuration with the hydrides *cis* to each other and one of them *trans* to the coordinating nitrogen in the oxazoline ring.[19b] These studies also emphasised the importance of calculating the complete chiral ligand, rather than smaller model complexes, as the structure of the ligand controls the outcome of the enantiomeric product by both steric and electronic factors. They actually found that there are many factors that control the enantioselectivity of the reaction.[17a] While no clear trends in enantioselectivity have been elucidated for the substituents on the phosphine, substitution on the oxazoline has been shown to control both enantioselectivity and reactivity. A PHOX ligand bearing an isopropyl group was found to be more selective than isobutyl or phenyl substituents, giving both lower conversions and enantioselectivities. Besides, the selectivity is also dependent on the imine substrate: those bearing bulky and flexible substituents often lead to lower chiral induction.

Furthermore, it is interesting to note that, for a given ligand, similarly substituted olefins and imines can form products of opposite absolute configurations.[68] This indicates that even if there could be similarities between the mechanisms, the stereodetermining step for the two substrates must differ.

The influence of the solvent and the presence of additives have also been found to affect the enantioselectivity, with non-coordinating solvents such as dichloromethane and benzene being the best choice for acyclic imines.[60c,69] Strongly coordinating solvents or additives can reduce significantly the *ee* values, probably because they block a contact point between substrate and metal centre.[70]

In contrast, the potential *E/Z* isomerization of the substrate does not have an important effect on the enantioselection process. Even though *E-* and *Z-* isomers should interact differently with the catalyst, and hence have an influence on the *ee*, high enantioselectivities have still been achieved when isomer mixtures of imines were used.[70-71] Due to these different observations, several authors have concluded that the mechanism for the iridium catalysed imine hydrogenation must be different from the Ir(III)/Ir(V) cycle, which is widely accepted for the alkene hydrogenation with *P,N*-ligands.[60b]

In order to shed light on this topic, very recently Norrby, Wiest, Andersson and co-workers[72] have revisited the mechanism of the iridium-catalysed asymmetric hydrogenation of prochiral imines for an Ir(I)-PHOX complex **281** (Figure 16).
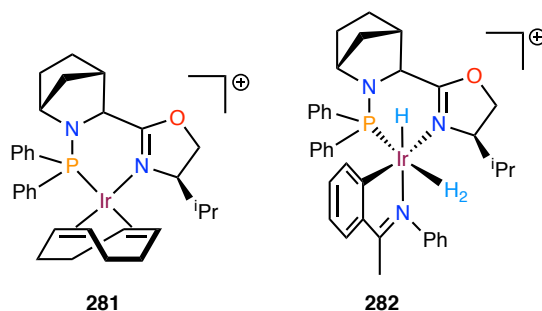
Figure 16. Ir precatalyst and iridacycle with phosphine-oxazoline ligand studied by Norrby, Wiest and Andersson in the asymmetric reduction of diphenylimine **I1**.

Since the discovery in 2013 by Pfaltz and co-workers[64] that the Ir(III) cyclometallated complex was active in the hydrogenation of acetophenone-derived imines, computational studies have settled this iridacycle as a key species for the correct elucidation of the reaction mechanism.

With all this in hand, Norrby, Wiest and Andersson[72] considered four potential mechanisms involving an iridacycle as the active catalyst (Figure 16). These mechanisms were (*i*) an outer sphere Ir(III) pathway, (*ii*) an inner pathway through an heptacoordinated Ir complex, (*iii*) an inner sphere *C*-migration pathway and (*iv*) an inner sphere *N*-migration pathway. All of them involve iridacycle **282** as the active catalyst (Scheme 15).
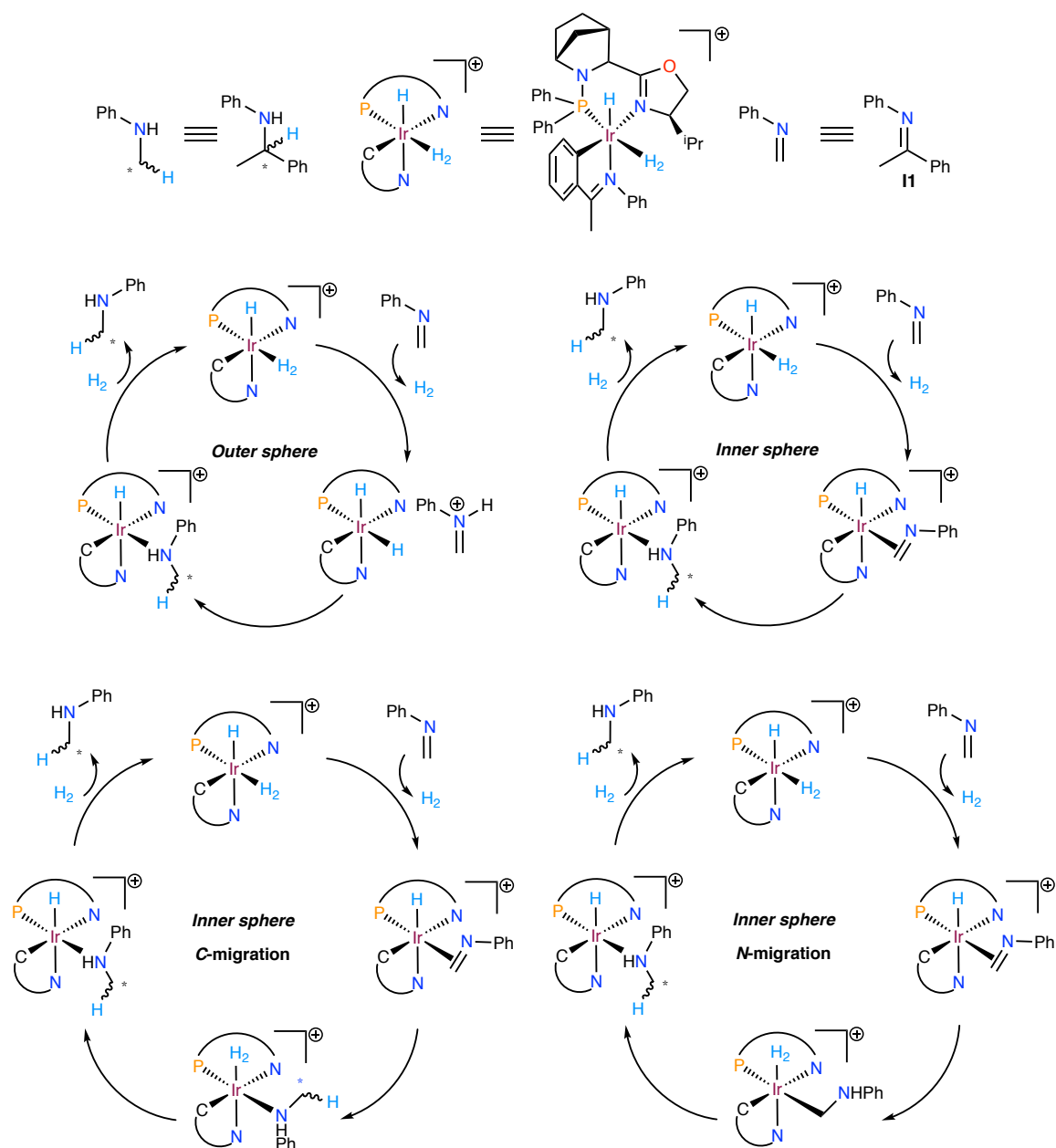
Scheme 15. Different mechanisms proposed by Andersson and co-workers[72] for the enantioselective hydrogenation of **I1** as substrate.

They concluded that the mechanism that fits the best with the experimental enantioselectivities and has the lower energy barriers was surprisingly the outer-sphere mechanism; predicting a 90% *ee* of *R* amine **A1** in excellent agreement with experiment for catalyst **282**. The proposed outer sphere mechanism is depicted in Scheme 16.
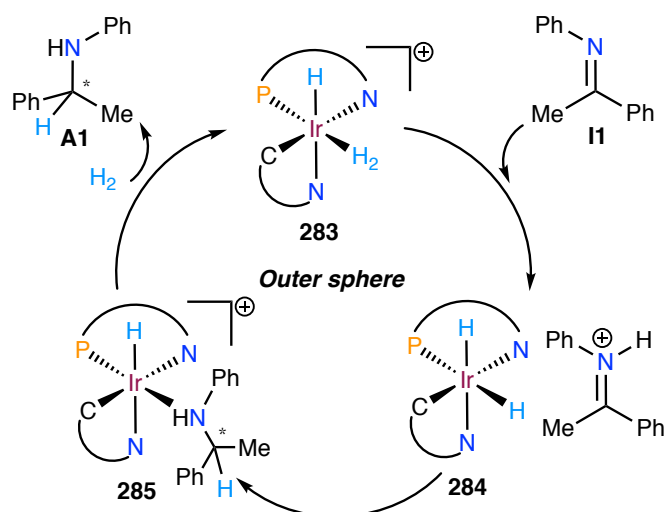
Scheme 16. Norrby-Wiest-Andersson's proposed outer sphere mechanism for the iridium-catalysed hydrogenation of *N*-aryl imines.

As it can bee seen, the outer sphere mechanism begins with the binding of H_2 to an open coordination site of the catalyst. Proton transfer to the unbound imine substrate occurs, followed by hydride transfer and release of the product, completing the catalytic cycle. According to this proposal, the active species in the catalytic cycle would be the cationic hydride-dihydrogen complex **283**, which, upon proton transfer, activates the imine to form the neutral dihydride complex **284**. The stereodetermining step is the hydride transfer *trans* to phosphorus to the activated imine to yield complex **285**.

In the case of the MaxPHOX iridacyles, presented in the previous section and described in our research group, this model is in agreement with the experimental catalytic results observed. In the Ir(III)-MaxPHOX system, the imine ligand and the oxazoline isopropyl substituent are the fragments that surround the hydride transferred to the protonated imine in the stereodetermining step.[54] Analysing the selectivity observed with the four stereoisomers of the MaxPHOX ligands, they concluded that the configuration of the phosphorus atom and the carbon at the tail are highly relevant.

Two effects could explain this behaviour. First, small conformational differences on the reacting site may provide a selectivity bias (Figure 17).
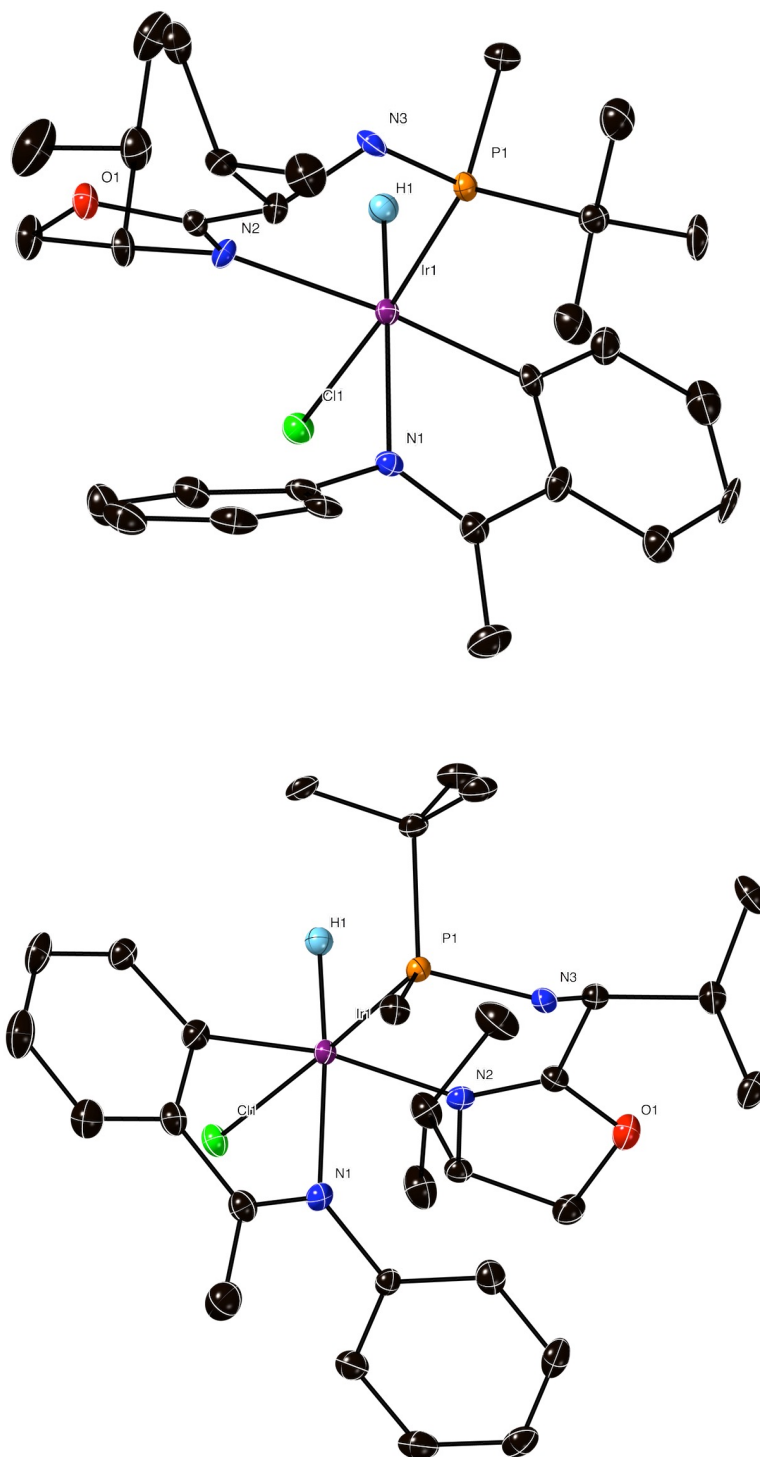
Figure 17. X-ray structures of **L3RIr·Cl** and **L3SIr·Cl**. Ortep diagram showing 50% probability ellipsoids. Counter ion and hydrogen atoms have been omitted for clarity.[54]

More precisely they found by examining the *pseudo*-enantiomeric reacting sites that while the *N*-phenyl of the cyclometallated imine is titled upwards, the other diastereomer of the *P*,*N* ligand forces the *N*-phenyl ring to be almost perpendicular to the Ir-imine metallacycle.

These conformational differences of the *N*-phenyl group are strongly influenced by the configuration of the phosphine and tail positions and should lead to differences in selectivity between **L3RIr·Cl** and **L3SIr·Cl**.[73]

A second effect would be the relative stability of complexes **286a/286b** with a vacant coordination site (Scheme 17).

286a   **286b**
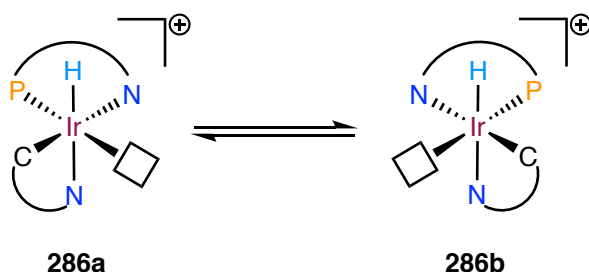
Scheme 17. Equillibrium between complexes **286a** and **286b** with a vacant coordination site.

It can be concluded that the coordination of H_2 to either complex **286a** or **286b** would provide a different selectivity outcome. Therefore, the stereochemical stability of the iridium complexes appears to be essential to guarantee high selectivity during hydrogenation. This notion is in agreement with the fact that in the present case **L3RIr** and **L3SIr·Cl** have the stereochemistry of **286a**, whereas Pfaltz and co-workers,[64] reported the X-ray structure of an [IrH(THF)(PHOX)(imine)]⁺ complex, in which the cyclometallated phenyl group is *trans* to phosphine and that upon removal of the solvent molecule provides a complex with the same stereochemistry as **286b**. In the parent system, it seems that the chirality on phosphorus and the tail positions in the MaxPHOX ligand are important for stabilising the arrangement of the ligands around the metal centre in the true catalytic species.[54]

5.3. *Synthesis and coordination chemistry of Ir(III) MaxPHOX cyclometallated complexes*

5.3.1. *Synthesis of the Ir(III) MaxPHOX iridacycles*

Following the previous coordination studies reported by our group, we decided to study the cyclometallation process of **I1** with the [IrCODMaxPHOX]BAr$_F$ diastereomers **L3RIr** and **L3SIr** (Scheme 18).
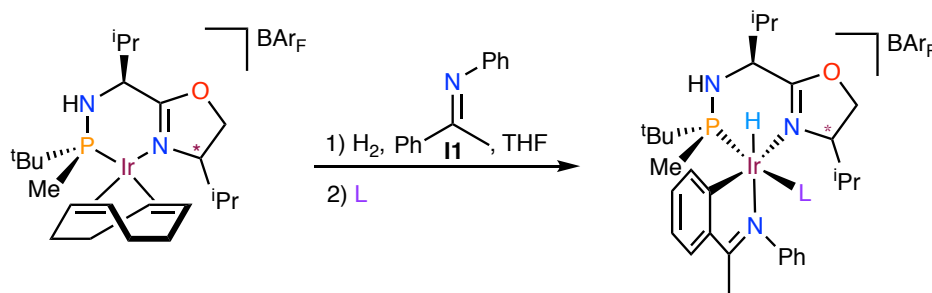
Scheme 18. Cyclometallation reaction of Ir(I) MaxPHOX precursors with imine **I1** and a monodentate ligand.

As it is depicted in Scheme 18, reaction of square-planar Ir(I) d^8-precursors with imine **I1** in the presence of H$_2$ yields, by means of an oxidative addition, the corresponding octahedral Ir(III) d^6-iridacycle. Interestingly, the Csp^2–H activation does not take place by simply stirring the square-planar Ir(I) complex with the cyclometallating agent but has to be carried out under hydrogen atmosphere. Hence, the molecular H$_2$ hydrogenates the COD in a first step and, once released, allows the coordination of the iminic nitrogen and the subsequent cyclometallation. As it can be seen, this process leads to a vacant coordination site, which can be later filled by a stabilising ligand, L.

Using this methodology we have been able to prepare and fully characterise two families of iridacycles with the **L3SIr** and **L3RIr** diastereomers of the *P,N* ligand, respectively and several stabilising ligands: CO, PPh$_3$, PMe$_3$, PMe^{t}Bu(O)H, CH$_3$CN and THF (Figure 18).
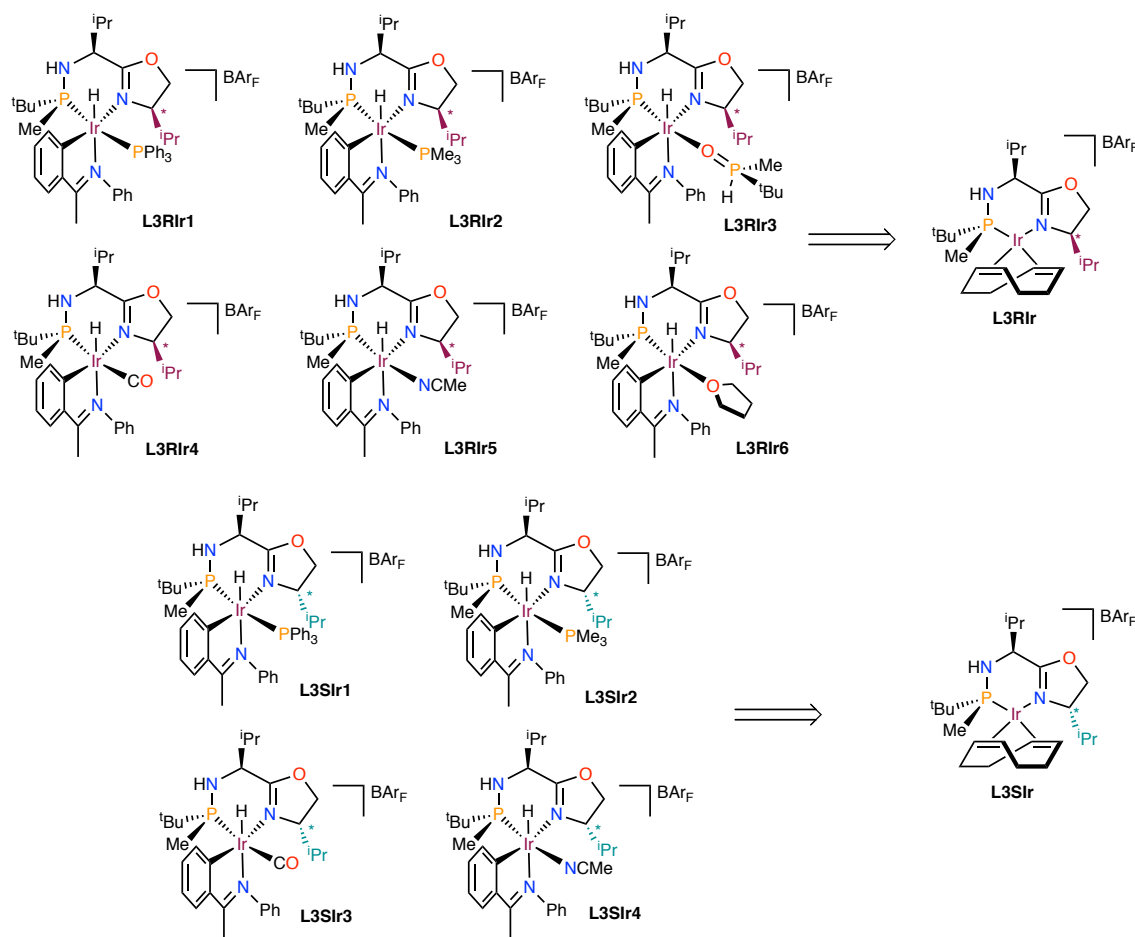
Figure 18. Ir(III) cyclometallated complexes with the **L3SIr** and **L3RIr** diastereomers of the MaxPHOX ligand.

As it can be seen, among the different stabilising ligands we can find some that are π-acidic like the CO and phosphines (PPh$_3$, PMe$_3$, PMe^{t}Bu(O)H) and others which are basically σ-donors such as THF. Interestingly, the electronic and steric nature of these ligands has a strong effect on the diastereoselectivity of the cyclometallation process, as described in the next section.

5.3.2. *Influence of the stabilising ligand on the cyclometallation*

As it has mentioned, the nature of the incoming ligand has a significant effect on the diastereoselectivity of the reaction, which can be easily determined by ^{1}H and ^{31}P{^{1}H} NMR. Furthermore, all this type of complexes has one common feature: the presence of the hydride ligand. Hydrides are extremely shielded and appear at negative chemical shifts in the ^{1}H NMR spectrum, which make them easy to identify.

In this section the spectroscopic characterisation of the different prepared iridacycles is discussed.

5.3.2.1. *Iridacycles with the CO ligand*
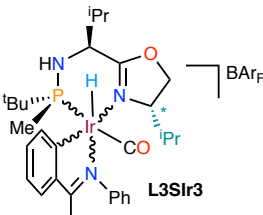
Reaction of Ir **L3SIr** diastereomer and Ir **L3RIr** with one equivalent of **I1** in a hydrogen atmosphere followed by pressurization with carbon monoxide affords a mixture of two *diastereomeric* iridacycles (Scheme 19).
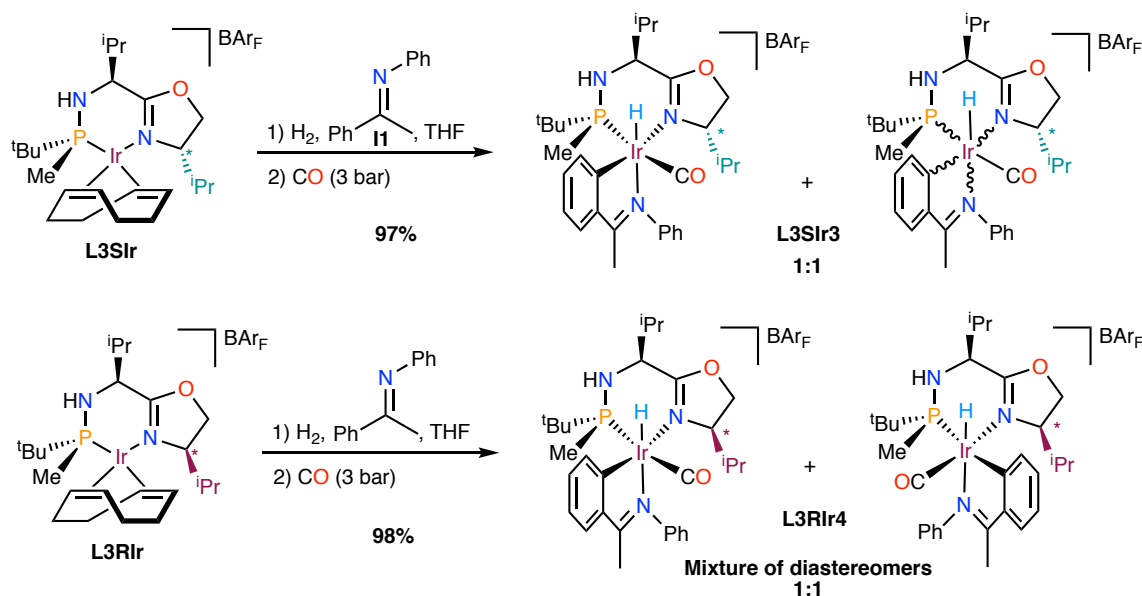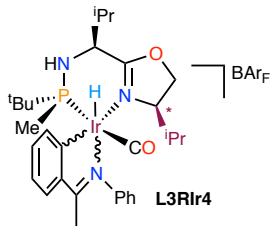
Scheme 19. Preparation of iridacycles **L3SIr3** and **L3RIr4** containing the CO ligand.

According to ¹H NMR, two doublets in the hydride region of the spectrum appear with a J_{HP} of 17.8 Hz for the **L3SIr3** diastereomer and 22 Hz for the **L3RIr4** diastereomer, respectively (Table 1).

Table 1. Selected NMR data of complexes **L3RIr4** and **L3RIr3**

Iridacycle	¹H NMR (400 MHz, C₆D₆, 25 °C) δ(ppm)	J_{HP} (Hz)	³¹P{¹H} NMR (162 MHz, C₆D₆, 25 °C) δ(ppm)
	−6.8 (d, 1H) −16.7 (d, 1H)	17.8	+44.7 (s) +51.1 (s)

	−17.4 (d, 1H) −17.5 (d, 1H)	22.0	+36.5 (s) +36.7 (s)

The large differences regarding the chemical shifts of the two hydride species of complex **L3RIr3** may suggest the formation of two stereoisomers, in which the connectivity of the ligands in the coordination sphere is not the same. Arguably, in one of the species the N of the imine could be located *trans* to the hydride, while in the other, displaying a hydride resonance near to −6.8 ppm, the less electron-rich environment might indicate the formation of a different complex. However, the presence of a very similar H–P coupling constant indicates a *cis* disposition of the P unit and the hydride ligand.

On the other hand, for complex **L3RIr4**, two very close doublets were observed, suggesting in this case, the presence of two diastereomeric hydrides.

These observations are in agreement with the chemical shifts assigned to the phosphorus atoms of the phosphinooxazoline ligand, in which in the first case the differences of chemical shifts are much higher ($\Delta\delta$ = 6.40 ppm) than those of the **L3RIr4** system ($\Delta\delta$ = 0.20 ppm).

When a freshly prepared solutions of **L3RIr3** and **L3RIr4** were left to stir for 48 h under inert atmosphere, no significant changes were observed in the ^{1}H NMR spectra proving that no isomerisation between the complexes occur.

Mass spectrometry data gives the same intense monocationic peak for both complexes supporting that they are isomers. In addition, a peak corresponding to the loss of CO is also observed. There was no clue of dimeric species, since isotopic distributions corresponding to two Ir atoms could not be detected.

In agreement with the presence of a coordinated CO molecule, a sharp band at 2052 cm^{-1} could be clearly seen at IR.

5.3.2.2. *Iridacycles with phosphine ligands*

Precursors **L3RIr** and **L3SIr** were reacted, after treatment with **I1** in the presence of H_2, with triphenylphosphine and trimethylphosphine as stabilising ligands (Scheme 20).
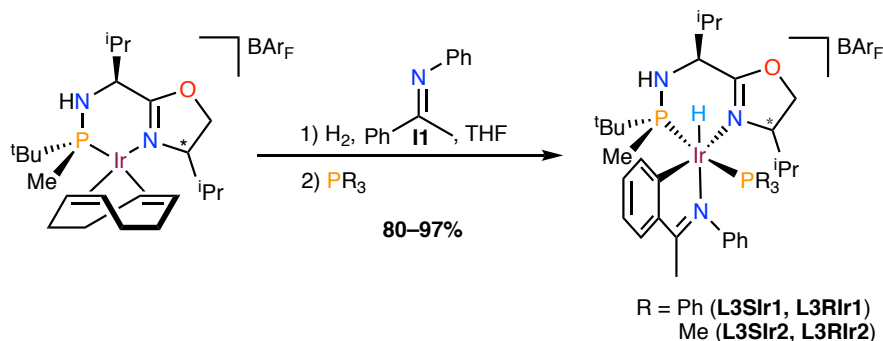
Scheme 20. Reaction of Ir(I) complexes **L3RIr** and **L3SIr**, after cyclometallation with **I1**, with PPh_3 and PMe_3.

After precipitation with hexanes, all four complexes were isolated in moderate to good yields as air-stable pale yellow solids.

In the case of triphenylphosphine complex **L3SIr1** two isomers were obtained as it can be clearly seen in the ^1H NMR spectrum (Figure 19).
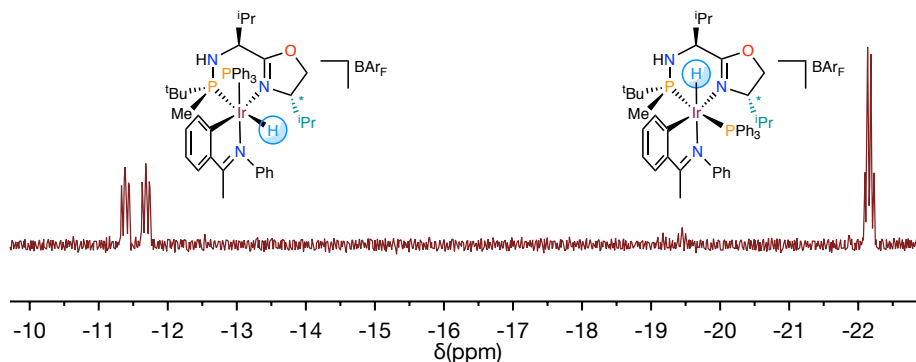
Figure 19. ^1H NMR (400 MHz, C_6D_6, 25 °C) of the hydride region of complex **L3SIr1**.

The marked differences in chemical shifts ($\Delta\delta$ = 10.8 ppm) and the integration suggests the formation of two different complexes in equimolar amounts. In addition, the doublet of multiplets belonging to the first signal at −11.5 ppm with a J_{HP} of 119.4 Hz would indicate that the hydrido ligand is located *trans* to the phosphorus atom of the MaxPHOX moiety. The multiplicity of the multiplets resembles a quadruplet and can be attributed to the coupling of the hydride with the protons of the methyl group of the phosphine. In contrast, the quadruplet of doublets at −22.3 ppm could be assigned to a species in which the arrangement of the hydride is *cis* to both phosphorus atoms of the

ligands. All this data was in agreement with the $^{31}P\{^{1}H\}$ NMR spectrum in which two distinct resonances appeared as singlets at 60.0 and 58.1 ppm, respectively.

Interestingly, the other isomer of the *P,N* ligand, **L3RIr1**, yielded only one single diastereomer as it was confirmed by ^{1}H NMR, displaying a triplet at –19.77 with a J_{HP} = 16.4 Hz. The multiplicity of the signal can be attributed to the coupling of the hydride with the two phosphorus atoms located in *cis*. Hence, instead of being a doublet of doublets it collapses in a perfect triplet located at –19.8 ppm displaying a coupling constant J_{HP} of 16.4 Hz (Figure 20).
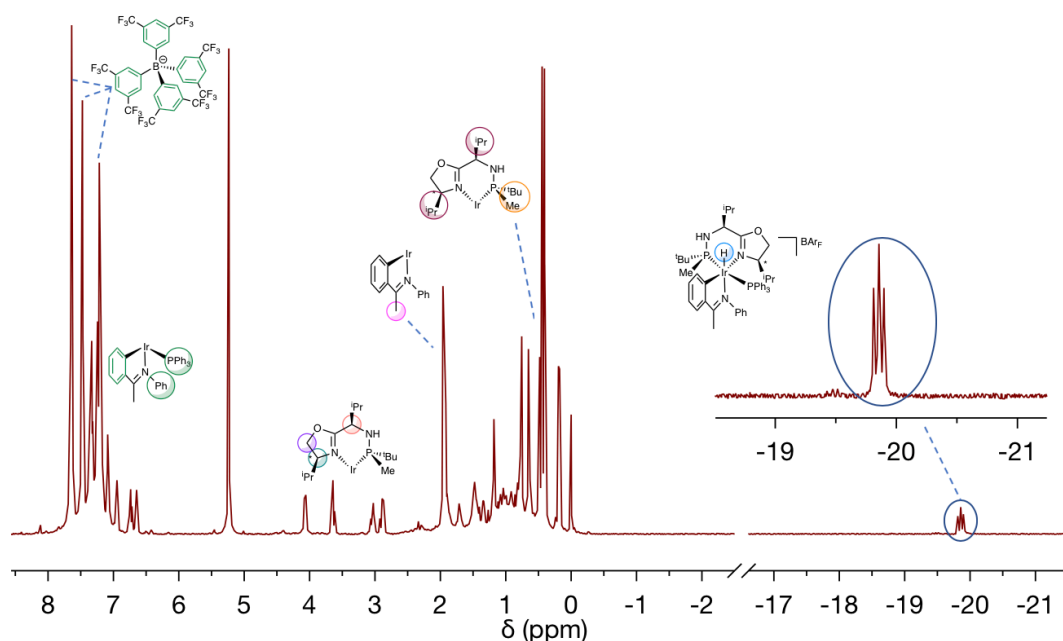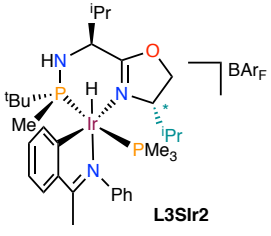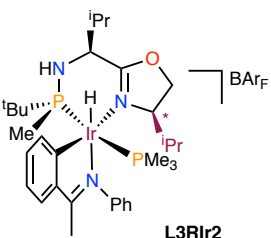
Figure 20. ^{1}H NMR **(400 MHz, CD₂Cl₂, 25 °C)** spectrum of **L3RIr1**.

Besides, the pattern in the $^{31}P\{^{1}H\}$ NMR spectrum of **L3RIr1** was also rather different than **L3SIr1**. Instead of having singlets, two sets of doublets at +38.5 and +8.5 ppm, showing the very same J_{PP} of 346.7 Hz, were found instead.

In both **L3RIr1** and **L3SIr1**, the same molecular peak was found in mass spectrometry analysis, indicating the same constitution, even though the distribution of the ligands around the octahedral Ir(III) centre is clearly different.

Another behaviour was observed when using PMe₃ as stabilising ligand. After treatment with a slight excess of trimethylphosphine of the already activated Ir(I)-MaxPHOX (**L3SIr**) with **I1**, only one stereoisomer of the iridacycle was isolated. As it was observed for the PPh₃ systems, the ^{1}H NMR displayed only one triplet in the hydride region as it is depicted in Table 2.

Table 2. NMR selected data for complexes **L3SIr2** and **L3RIr2**.

Iridacycle	^{1}H NMR (400 MHz, C$_6$D$_6$, 25 °C) δ(ppm)	J_{HP} (Hz)	^{31}P{^{1}H} NMR (162 MHz, C$_6$D$_6$, 25 °C) δ(ppm)	J_{PP} (Hz)
L3SIr2	−19.95 (t, 1H)	19.4	+38.9 (d, *P*N) −45.1 (d, *P*Me$_3$)	349.3
L3RIr2	−19.98 (t, 1H)	19.6	+39.0 (d, *P*N) −45.2 (d, *P*Me$_3$)	349.4

Interestingly, reaction of the other Ir(I)-MaxPHOX complex **L3RIr** with PMe$_3$ yielded in a very stereoselective manner the analogous complex **L3RIr2**, which displayed a very similar spectroscopic data compared to **L3SIr2**. Indeed, the hydrido ligand resonates in the ^{1}H NMR at the very same chemical shift and with the same coupling constant as **L3SIr2**, being this behaviour also present in the ^{31}P{^{1}H} NMR as it is depicted in Table 2.

Furthermore, we were able to grow suitable crystals for X-ray determination of complex **L3RIr2** by slow diffusion in pentane (Figure 21 and Table 3).
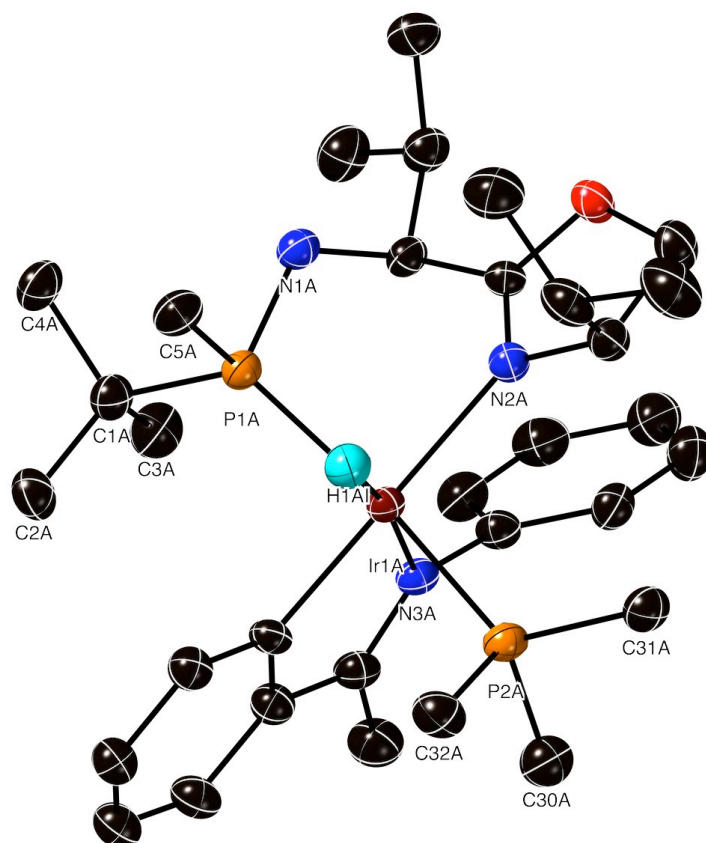
Figure 21. X-ray structure of **L3RIr2**. Ortep diagram showing 50% probability ellipsoids. Counter ion and hydrogen atoms have been omitted for clarity.

Table 3. Selected bond distances (Å) and angles (º) of **L3RIr2**.

Bond	Length (Å)	Angle	(°)
P1A–Ir1A	2.322	C1A–P1A–N1A	101.539
P2A–Ir1A	2.332	C1A–P1A–C5A	102.626
N2A–Ir1A	2.177	P1A–Ir1A–N2A	87.342
N3A–Ir1A	2.187	C16A–Ir1A–N3A	78.274
C16A–Ir1A	2.026	Ir1A–C16A–C21A	115.154
H1A–Ir1A	1.456	Ir1A–N3A–C22A	113.953

As expected, the Ir(III) hydride displays an octahedral coordination with the PMe$_3$ ligand *trans* with respect to the ^{t}BuMeP moiety, and the cyclometallated imine *N* trans with respect to the metal hydride. Interestingly, the two phosphorus units, the *P,N* ligand and the PMe$_3$, are coordinated to the Ir centre with almost the same bond

249

distance of 2.3 Å. This suggests similar electronic properties for both phosphine ligands. A similar statement can be made regarding the coordinated iminium and *N*-oxazoline donor atoms with Ir.

On the other hand, the cyclometallated imine forms a plane five-membered ring in which the angles range between 113 to 115° as it is found for this type of complexes.[64]

Besides, as it can be seen in the molecular structure (Figure 21) coordination of the phosphinooxazoline ligand preserves the absolute configuration of the phosphorus atom.

Inspired by the work of Pfaltz and co-workers[74], who merged the coordination chemistry of phosphinooxazoline ligands to Ir with a secondary phosphine oxide unit in a bidentate fashion, we decided to study the coordination chemistry of our optically pure (*S*)-L1 SPO, described in Chapter 3 with irydacycle **L3RIr** (Scheme 21).
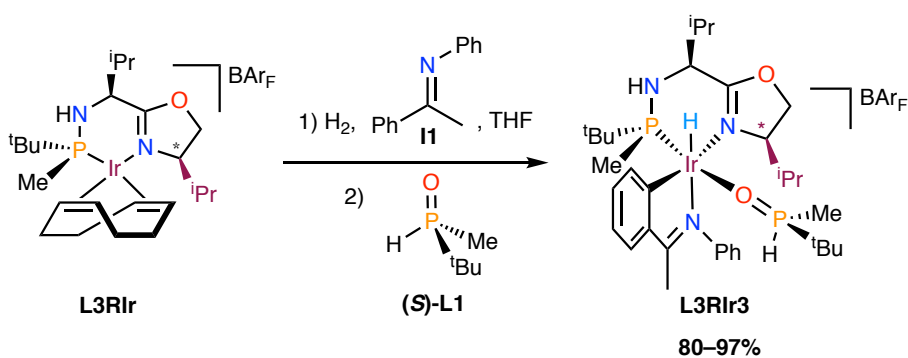
Scheme 21. Synthesis of iridacycle **L3RIr3**.

Interestingly, the reaction proceeds in a complete stereoselective pathway, affording one single diastereomer as it can be seen in the ^{1}H NMR, where only one doublet centred at −19.7 ppm (*J* = 26.9 Hz) is observed (Figure 22).
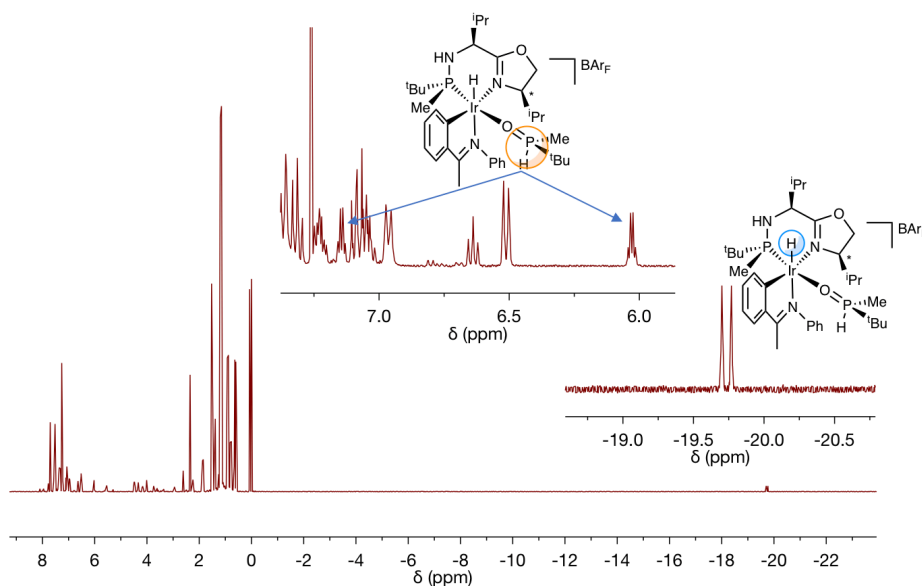
Figure 22. ^{1}H NMR(400 MHz, CDCl$_3$, 25 °C) spectrum of **L3RIr3**.

A more detailed analysis of the ^{1}H NMR indicates the presence of a P–H bond, by means of a doublet of quadruplets at 7.14–6.03 ppm with a J_{HP} of 442 Hz and J_{HH} = 3.8 Hz. The smaller coupling is due to the H-H coupling of the hydrogen attached to phosphorus with the Me group. This fact proves that **(*S*)-L1** is bounded to the metal through the oxygen, a fact also supported by ^{31}P{^{1}H} NMR, since the presence of a broad singlet at +60.9 ppm is typically found for complexes having this *O*-coordinated mode.

When the isolated complex was re-dissolved in THF and its ^{31}P{^{1}H} NMR spectrum was collected again after 48 h, a significant amount of uncoordinated **(*S*)-L1** ligand was found, showing a singlet around 45.5 ppm. This behaviour suggests that the sterically hindered *O*-coordinated alkyl **(*S*)-L1** is not strongly bounded to the Ir centre, being easily exchanged by polar solvent molecules such as THF.

5.3.2.3. *Iridacycles with a solvent molecule*

At this point, in the view of the high stability showed by these Ir(III) systems and that we envisaged to develop an iridacycle that could be conveniently used in imine hydrogenation. To be catalytically active, the ligand should be able to stabilise the resulting complex, but at the same time, be labile enough to be easily replaced by the substrate.

Hence we performed the cyclometallation reaction of both diastereomers of the *P*,*N* ligand with **I1** and H$_2$, followed by later addition of one drop of acetonitrile (Scheme 22).
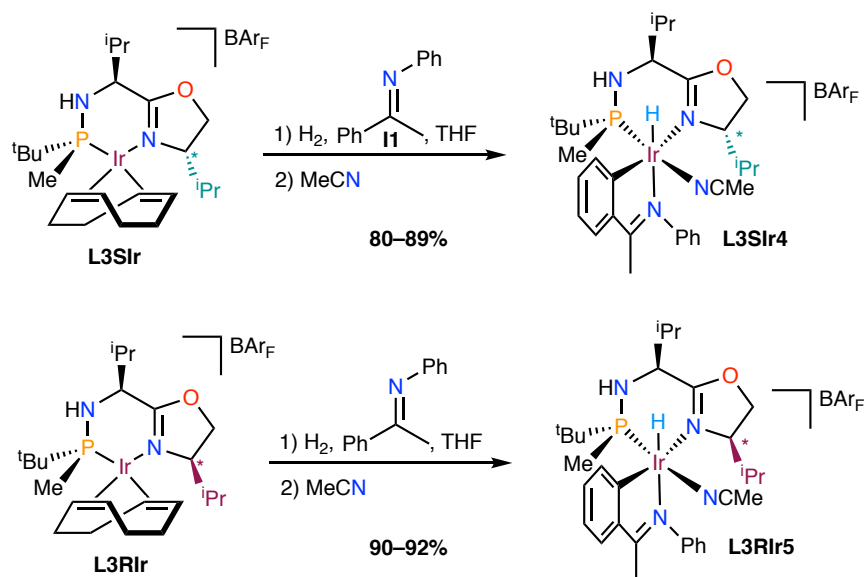
Scheme 22. Preparation of complexes **L3SIr4** and **L3SIr5**.

In both cases, the reaction was completely diastereoselective affording only one isomer of the octahedral iridacycle as easily seen by ^{1}H NMR (Figure 23).
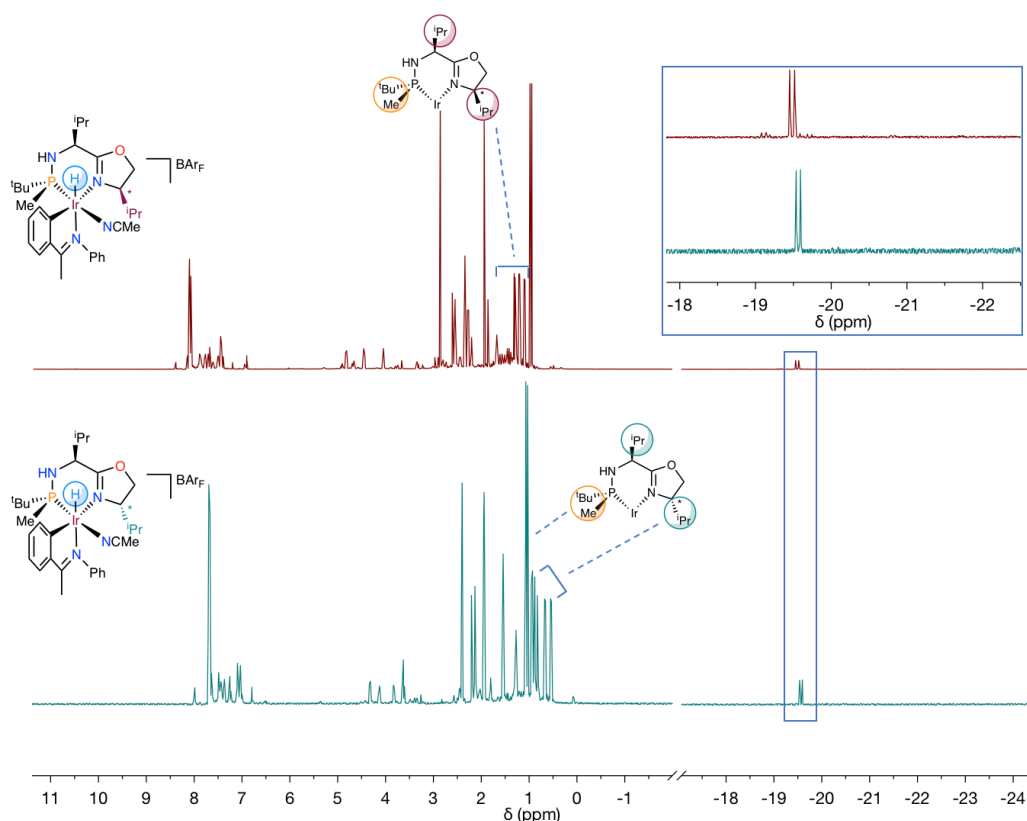
Figure 23. ^{1}H NMR (400 MHz, CD₃CN, 25 °C) spectra of **L3SIr4** (bottom) and **L3RIr5** (top).

252

There is only one hydride peak around –19.5 ppm with a J_{HP} of 22.7 Hz for **L3SIr4** and 26 Hz for **L3RIr5**, indicating the presence of only one isomer. As expected due to their diastereomeric nature, the complexes present similar spectra, even though there are small differences especially in the oxazoline system and the iPr and tBu groups of the phosphine unit.

We then decided to perform the same reaction with **L3RIr**, with THF-d_8 as solvent to see if THF was capable of stabilising the complex (Scheme 23).
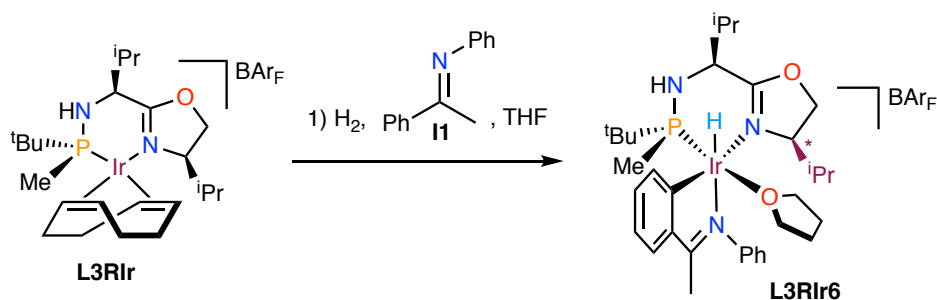
Scheme 23. Cyclometallation of **L3RIr** with **I1** without any ligand.

When the reaction crude in THF was concentrated and analysed by ^{1}H NMR spectroscopy (Figure 24).
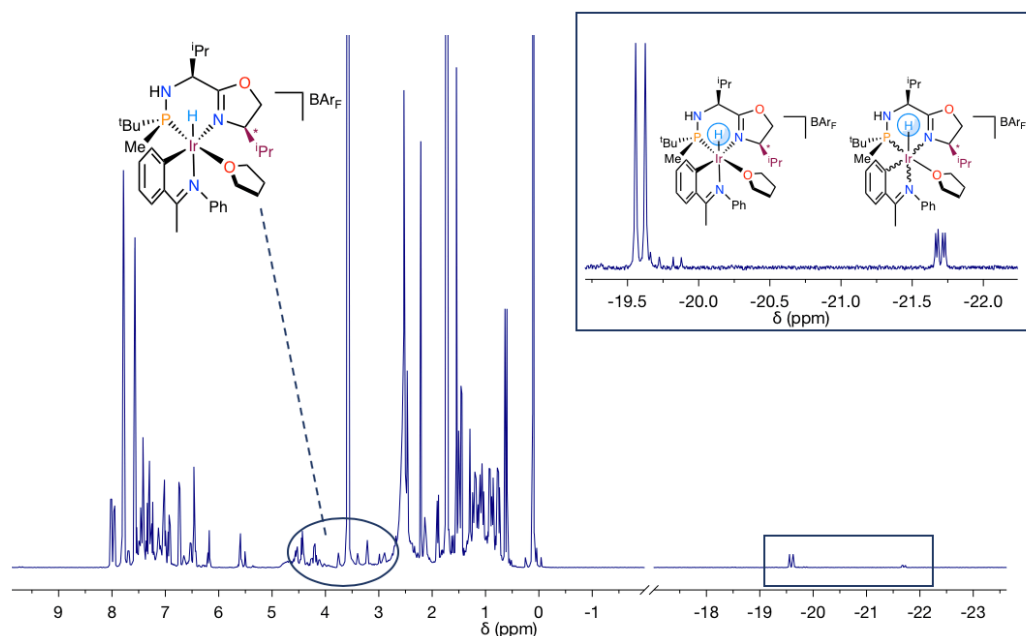
Figure 24. ^{1}H NMR (400 MHz, THF-d_8, 25 ºC) of the **L3RIr6** reaction crude.

As it is shown, in the absence of a stabilising ligand before the isolation of the complex, more than one hydride is formed, possibly because the formation of the iridacycle occurs via pentacoordinated species, which are known to be fluxional.[19b,63]

Typically, pentacoordinated transition metal complexes can isomerise by exchanging the axial and equatorial positions through the well-known Berry pseudorotation.[19b,63]

As it has been described, the use of CH_3CN, Ph_3P and Me_3P as ligands provided a single stereoisomer of the corresponding cationic octahedral Ir(III) complexes, as shown by ^1H and $^{31}P\{^1H\}$ NMR spectra. We finally envisaged the coordination of an olefin. Since coordinated alkenes are easily hydrogenated and released under the presence of H_2, ethylene would represent a highly desirable ligand.

Hence, a solution containing the freshly prepared iridacycle in THF-d_8 was pressurised with ethylene (3 bar) and ^1H NMR of the isolated crude was recoded (Figure 25).
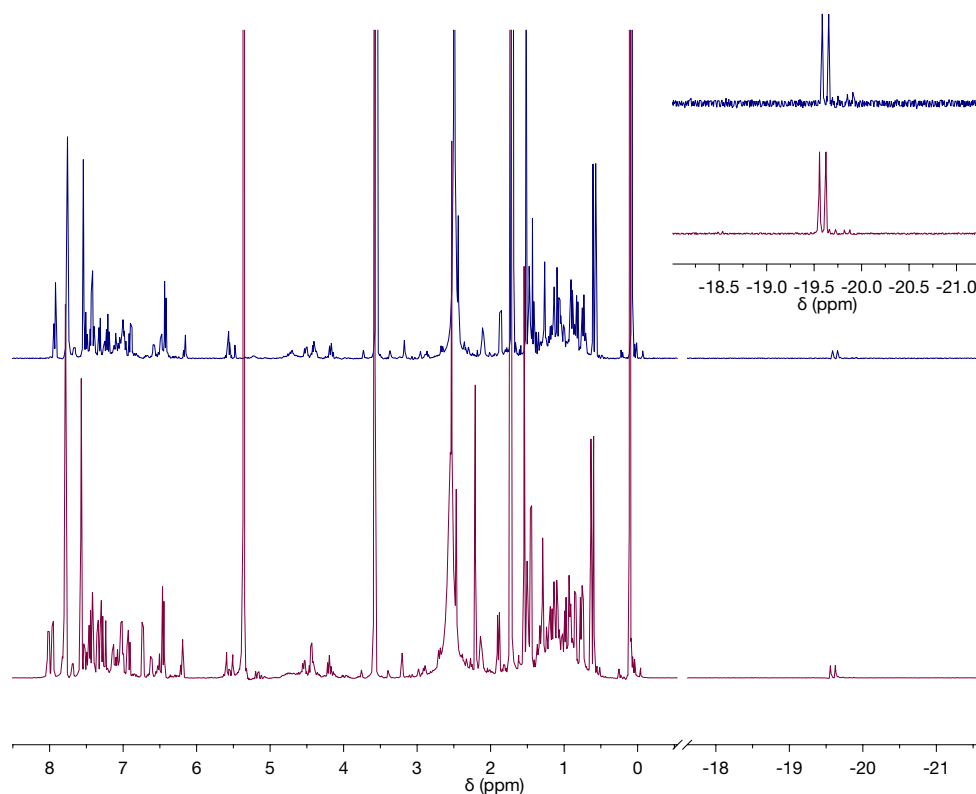
Figure 25. ^1H NMR (400 MHz, THF-d_8, 25 ºC) of the reaction crude obtained after pressurization with ethylene (top) and ^1H NMR (400 MHz, CD_2Cl_2, 25 ºC) of the recrystallized isolated THF complex (bottom) **L3RIr6**.

It can be clearly seen that the resonance of the hydride ligand appears at the same shift than in the THF isolated complex **L3RIr6** and, indeed, both spectra looked almost identical proving that the formed complex did not contain coordinated ethylene but a THF molecule instead.

Not satisfied with these results, we decided to study the formation of the olefin-coordinated complex by pressurization with ethylene at 3 bar of a solution containing the already activated Ir(I) MaxPHOX precursor **L3RIr** with **I1** but using CD$_2$Cl$_2$ as solvent instead of THF-d_8 (Scheme 24).
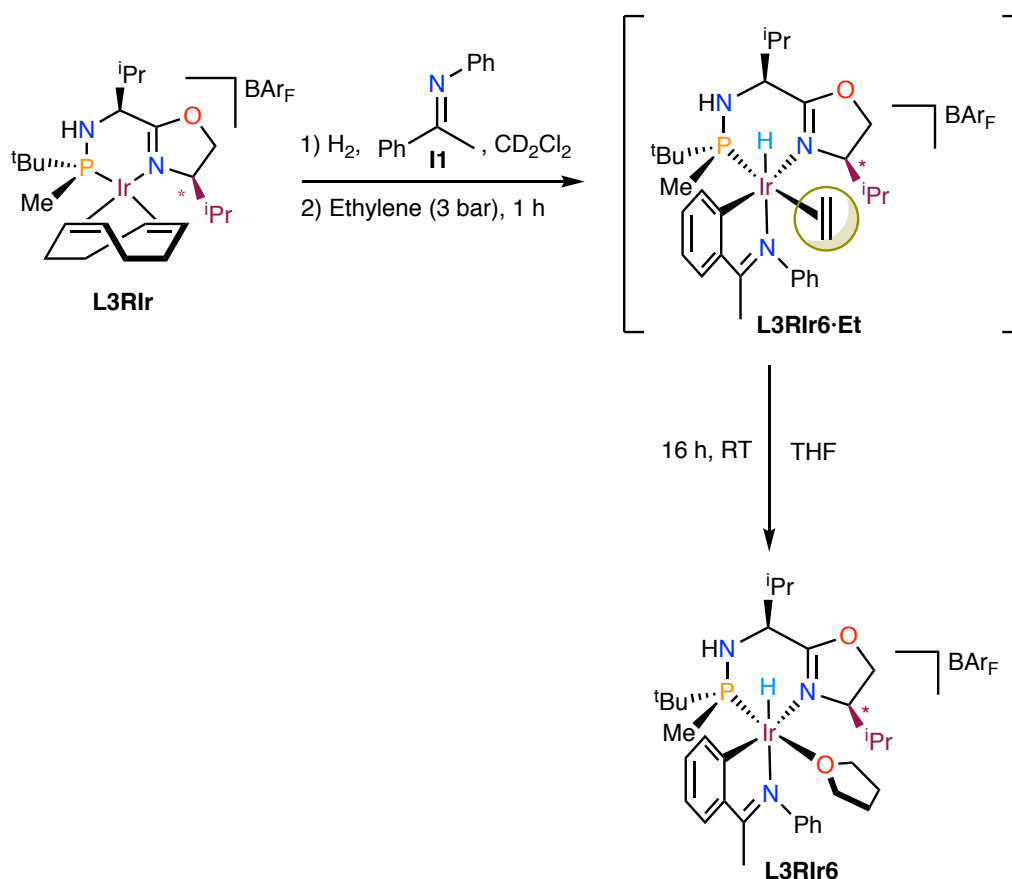
Scheme 24. Reactivity of the ethylene iridacycle **L3RIr6·Et**.

Under ethylene-saturated solution, we were able to detect the iridacycle **L3RIr6·Et** containing the coordinated olefin, whose ^{1}H NMR spectrum is depicted in Figure 26.
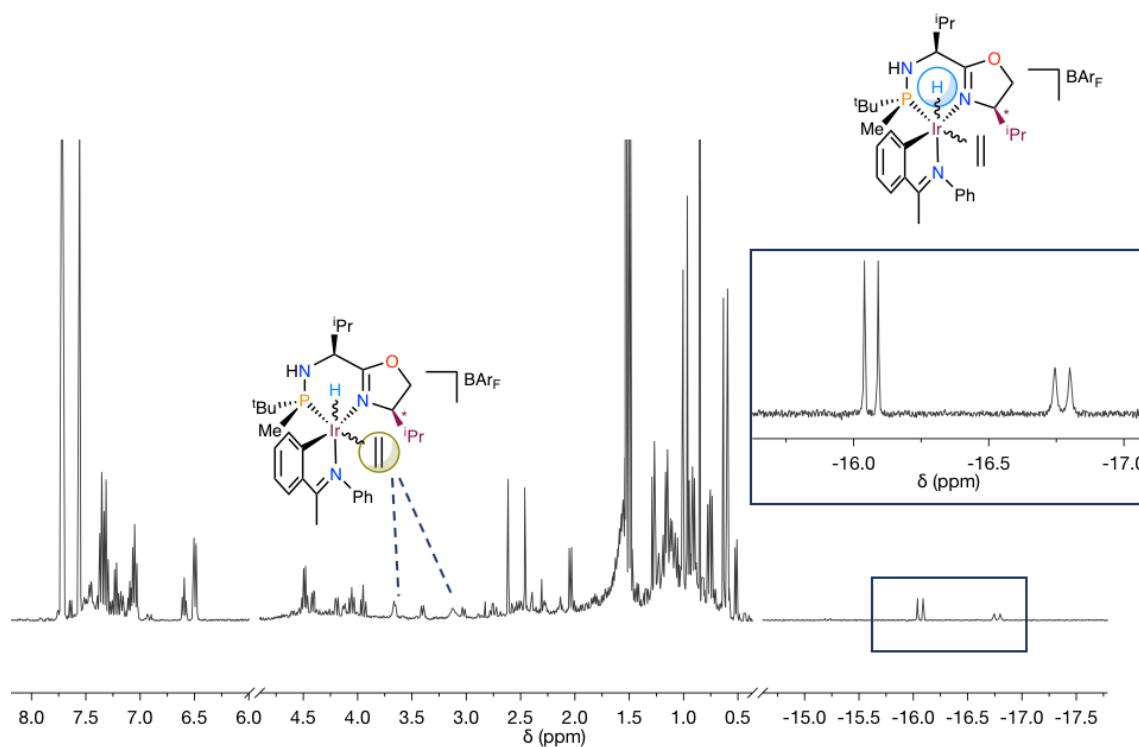
Figure 26. ^{1}H NMR (400 MHz, THF-d_8, 25 ºC) of **L3RIr6·Et** containing the coordinated olefin.

It can be seen that under these conditions complex **L3RIr6·Et** is formed as mixture of two diastereomers in an almost equimolar amounts both displaying doublets with the same coupling constant of 23.4 Hz.

The formation of the iridacycle was also confirmed by mass spectrometry, even though the molecular peak belonging to the whole cationic fragment appears as a very minor product. This fact can be explained due to the coordination of the acetonitrile molecules present in the source, which can quickly substitute the ethylene ligand.

It is interesting to note that when ethylene-saturated solution was slowly degassed under a nitrogen stream after addition of one drop of THF, we isolated the corresponding THF-Ir(III) complex (**L3RIr6**) with higher purity than just running the reaction in THF. The ethylene/THF exchange was monitored by ^{1}H NMR (Figure 27), which showed that after 16 h, the substitution had completely taken place.
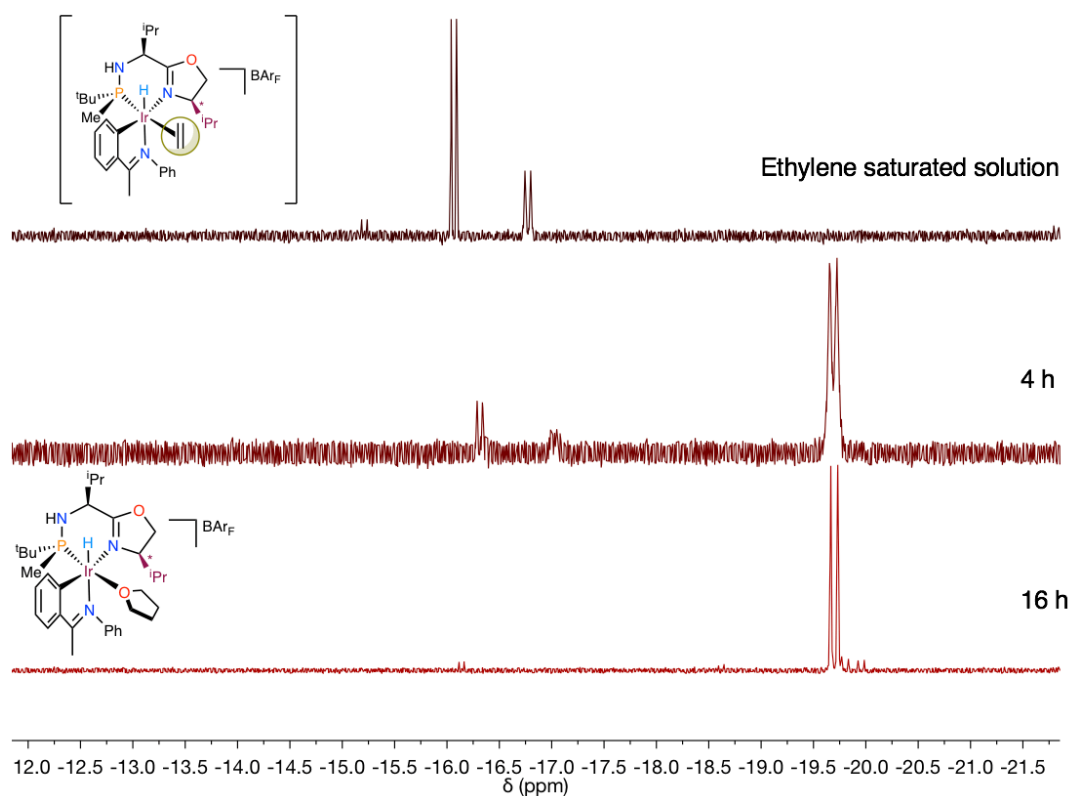
Figure 27. ^{1}H NMR (400 MHz, CD$_2$Cl$_2$, 25 ºC) spectra of the substitution of ethylene by THF (only the hydride region is shown).

Unfortunately, all attempts to isolate the olefin-coordinated complex **L3RIr6·Et**, before the addition of THF did not yield any definite product. Apparently, formation of these iridacycles in non-coordinating solvents triggers the formation of polymetallic species, since multiple hydride peaks were detected. Besides, mass spectrometry analyses indicate the presence of compounds containing more than one iridium atom in the structure.

When the above-mentioned reaction is carried out pressurizing with ethylene in THF as solvent, after precipitation with pentane, the THF complex **L3RIr6** is obtained in excellent yield and purity. Actually this synthetic route represents, at present, the best way to prepare **L3RIr6**, which has been fully characterised as detailed in the Experimental Section (Chapter 6).

It is still unclear which is the actual role of ethylene that allows obtaining complex **L3RIr6** in better purity and yield, a plausible hypothesis is that the alkene assists in the isomerization of intermediate unsaturated species to yield the final compound.

Complex **L3RIr6** is a perfectly air-stable compound but despite many attempts it was not possible to obtain suitable crystals for X-ray diffraction. Sometimes the BAr$_F$ counterion prevents crystallisation and therefore analogous cationic complexes with

257

BF$_4$ and PF$_6$ as counterions were prepared. The synthetic procedure for these analogues is shown in Scheme 25.
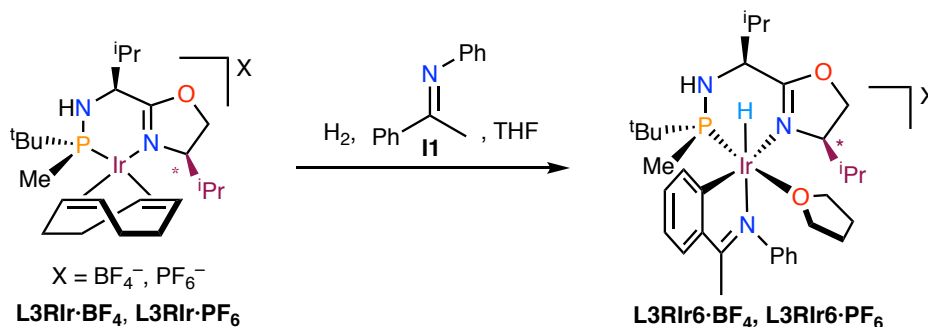
Scheme 25. Preparation of **L3RIr6·BF$_4$** and **L3RIr6·PF$_6$**.

As it can be seen, cyclometallation takes place following the same procedure as before, but employing the Ir(I)-MaxPHOX cationic precursor with the desired counterion as it is detailed in the Experimental Section (Chapter 6).

The presence of the proper anion can be easily seen by IR, displaying a sharp band at 1051 cm^{-1} for the ν(BF$_4$) and 846 cm^{-1} for the ν(PF$_6$) as well as by NMR means (see Experimental Section).

While, the BF$_4$ complex has not yielded suitable crystals yet, the PF$_6$ analogue crystallised in such a way that the vacant coordination site, normally filled by the so-called stabilising ligand, contained a coordinated PO$_2$F$_2^-$ unit, from the hydrolysis of the PF$_6$ anion.

Complex **L3RIr6** has proven to be an excellent catalyst for the hydrogenation of *N*-methyl and *N*-alkyl imines as it will be described in Section 5.4.3.

5.3.3. *Influence of the cyclometallating agent in the diastereoselectivity*

As it has been discussed, there is a significant effect on the diastereoselectivity of the reaction depending on the diastereomer of the *P,N* ligand used. In general, the Ir(I)-MaxPHOX **L3RIr** proved to be more selective than **L3SIr** in combination with the size/electronic properties of the stabilising ligand.

However, the role of the cyclometallating species in the stereoselectivity could also be important. In order to evaluate such contribution, we carried out the C–H activation of three aromatic compounds bearing one nitrogen atom, strategically located, in order to be able to form a five-membered Ir-cyclometallated ring. Hence, we
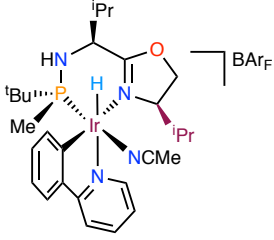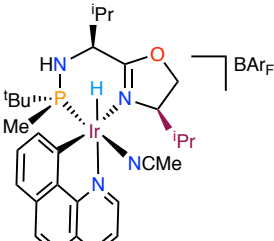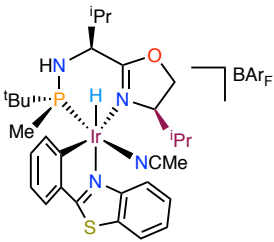
selected complex Ir(I)-MaxPHOX **L3RIr**, since it has displayed the best diastereoselectivities along with acetonitrile as a ligand. The three reactions have been conducted cyclometallating the Ir(I) complex under the presence of 2-phenylpyridine, 7,8-benzoquinoline and 2-phenylbenzothiazole, respectively, and pressurizing with 3 bar of hydrogen. Then, one drop of acetonitrile was added and the complexes were isolated by precipitation with pentane as yellow solids (Scheme 26).
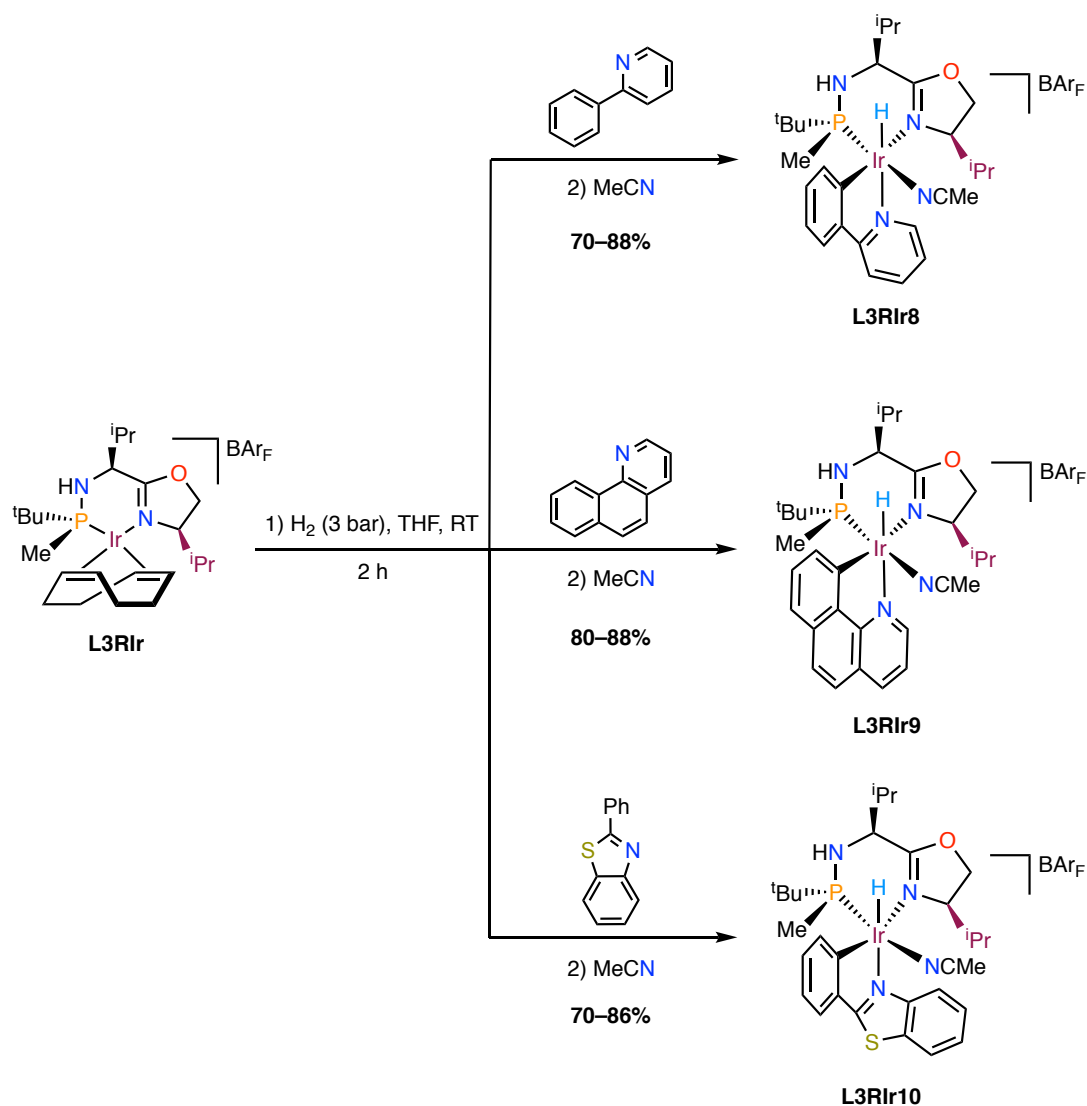
Scheme 26. Synthesis of complexes **L3RIr8**, **L3RIr9** and **L3RIr10**.

The complexes were characterised by the habitual spectroscopic techniques. Interestingly the ^{1}H NMR of the three complexes showed the presence of two diastereomers in all of the cases as it is depicted in Table 4.

Table 4. Selected ^{1}H NMR data of complexes **L3RIr8**, **L3RIr9** and **L3RIr10**.

Iridacycle	^{1}H NMR (400 MHz, CD$_3$CN, 25 °C) δ(ppm)	J_{HP} (Hz)
L3RIr8	−18.5 (d, 1H) −18.9 (d, 1H)	20.9 25.6
L3RIr9	−18.8 (d, 1H) −19.2 (d, 1H)	21.0 25.0
L3RIr10	−20.1 (d, 1H) −21.0 (d, 1H)	20.5 25.2

As it is depicted in Table 4, the presence of two distinct resonances in the hydride region for the three cyclometallated complexes indicates the formation of two stereoisomers for each one. Both the chemical shifts and the coupling constants are almost identical between isomers having the same cyclometallating agent.

Furthermore the neutral complex **L3RIr7** bearing a chloride was also prepared using the conditions reported by Pfaltz and co-workers[64] (Scheme 27).
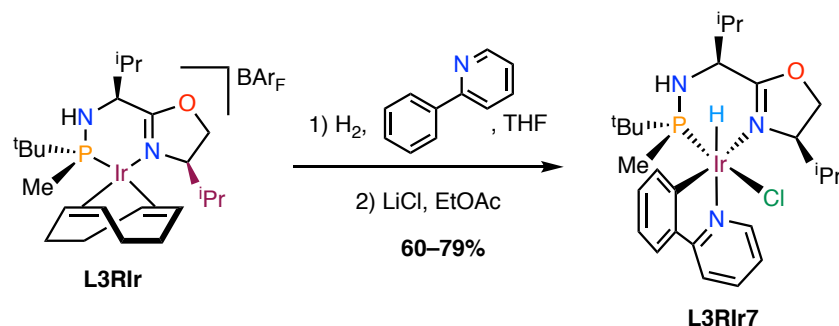
Scheme 27. Preparation of complex **L3RIr7**.

The cyclometallation occurs under the usual conditions of 3 bar of hydrogen in the presence of 2-phenylpyridine as cyclometallating ligand. Treatment with LiCl in a SiO$_2$ suspension affords the chloride complex **L3RIr7**, which can be purified by flash column chromatography eluting with pentane/TBME (1:1).

This complex showed clear differences with its acetonitrile analogue according to ^{1}H NMR spectroscopy. While the acetonitrile complex **L3RIr8** displayed two doublets, belonging to the hydride ligands, with similar coupling constants; complex **L3RIr7** presented mainly one at –18.5 ppm with a much larger J_{HP} of 43 Hz.

It is clear that the stabilising ligand has a strong effect on the diastereoselectivity of the cyclometallation process but the influence of the cyclometallating ligand proves to be even more important. Hence, in this last experiment, the use of a chloride as the sixth ligand forms a 1:7 diastereomeric mixture, whereas the same reaction with **I1** proceeds in a complete stereoselective manner.[54]

The basicity of the cyclometallating imine also plays a key role in the formation of the Ir(III) complex. To this end, the reaction of **L3RIr** and acetophenone *N*-methyl imine (**I8**) as cyclometallating ligand was studied (Scheme 28).
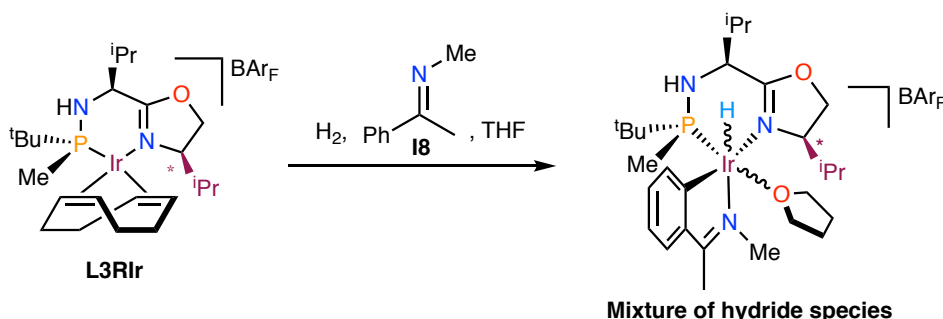
Scheme 28. Attempts to cyclometallate **I8**.

Surprisingly, analysis of the reaction crude by ^{1}H NMR means showed a mixture of hydrido complexes (Figure 28).
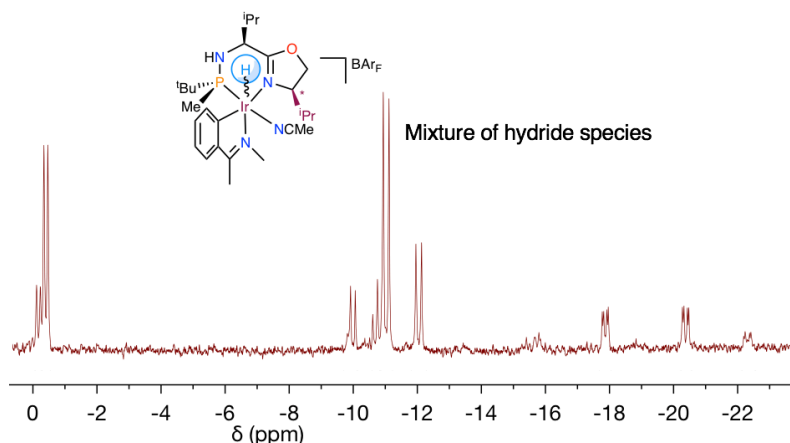
Figure 28. ^{1}H NMR (400 MHz, CD$_2$Cl$_2$, 25 ºC) spectrum of **L3RIr** treated with **I8** under 3 bar of H$_2$.

The enhanced basicity of the **I8** compared to the *N*-aryl imines can undergo secondary reactions that compete with the expected cyclometallation process, leading to the formation of a number of uncharacterised species.

Nevertheless, with all these coordination studies in hand, we decided to test our Ir(III)-cyclometallated systems, both "*in situ*" and as preformed complexes, as potential catalysts for the enantioselective hydrogenation of *N*-methyl and *N*-alkyl imines.

5.4. *Asymmetric hydrogenation of N-Alkyl Imines*

Chiral amines play an important role as building blocks for the synthesis of pharmaceuticals and agrochemicals.[75] They are also of considerable importance as chiral auxiliaries, catalysts and resolving agents.[32a,68,76]

Therefore, asymmetric hydrogenation of ketimines has received much attention as an attractive, very direct route to enantiomerically enriched amines.[77] High yields, perfect atom economy and mild conditions make this approach ideal for industrial applications. This is impressively demonstrated by the multi-ton scale production of the herbicide metolachlor, based on an extremely active and productive Ir-diphosphine catalyst.[78] During the last two decades a wide range of chiral Ti, Rh, Ir, Pd, Ru[75] and most recently Fe[75,79] complexes have been developed that catalyse the hydrogenation of various imines with high enantioselectivity. However, the scope of most catalysts is rather narrow and there are still important classes of imines that give unsatisfactory results with the available catalysts. Especially the hydrogenation of imines derived from dialkyl ketones remains a stubbornly challenging problem. With the exception of the dual catalyst system reported by Xiao and co-workers,[80] consisting of a chiral Ir(Cp*)–

diamine complex and an elaborate chiral binaphthol-derived phosphoric acid (TRIP), most catalysts give very low enantioselectivities with these substrates.

Although imines derived from dialkyl ketones are challenging substrates, its range of application is quite limited. In contrast, optically pure *N*-alkyl amines, especially *N*-methyl amines, are particularly interesting, since they are known to be frequent pharmacophores in biologically active compounds (Figure 29).

Figure 29. Selected chiral *N*-alkyl amine pharmaceuticals.
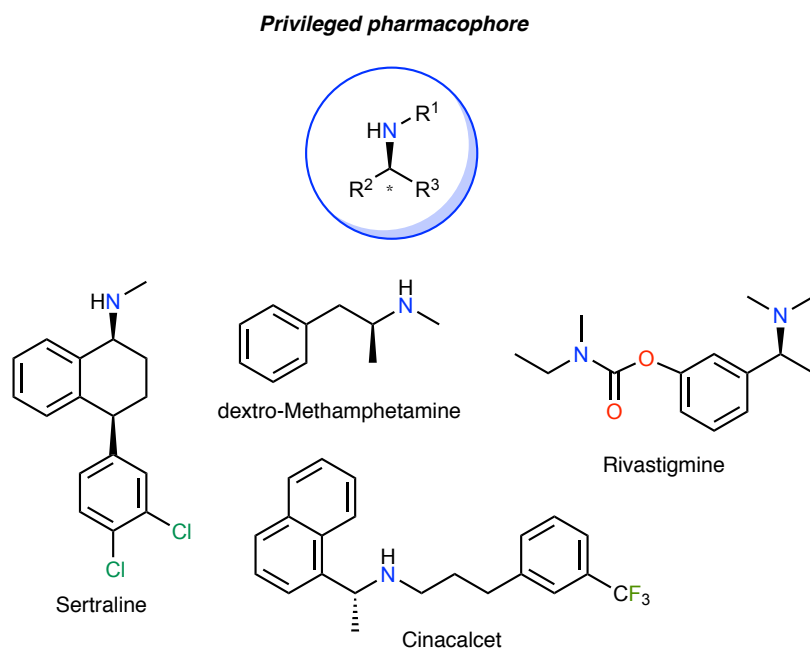
Examples include sertraline (to treat depression),[81] dextro-methamphetamine (to treat ADHD and narcolepsy),[82] rivastigmine (to treat Alzheimer's and Parkinson's diseases)[83] and cinacalcet (to treat hyperparathyroidism).[84]

Due to the importance of this moiety, much effort has been devoted to the asymmetric synthesis of optically pure *N*-methyl amines.[85]

An ideal methodology to obtain this class of compounds is the catalytic reduction of the corresponding imines. However, the high basicity and nucleophilicity of *N*-methyl amines often results in catalyst deactivation. The most successful approaches for the asymmetric reduction of *N*-methyl imines up to date are Ti-catalysed hydrosilylation, reported by Buchwald, and Brönsted acid-catalysed reduction using Hantzsch ester in the presence of Boc$_2$O, reported by List.[86]

In the first case, in 1996, Buchwald and co-workers[86a] reported a very efficient enantioselective imine hydrosilylation using a Ti-difluoride catalyst (Scheme 29).
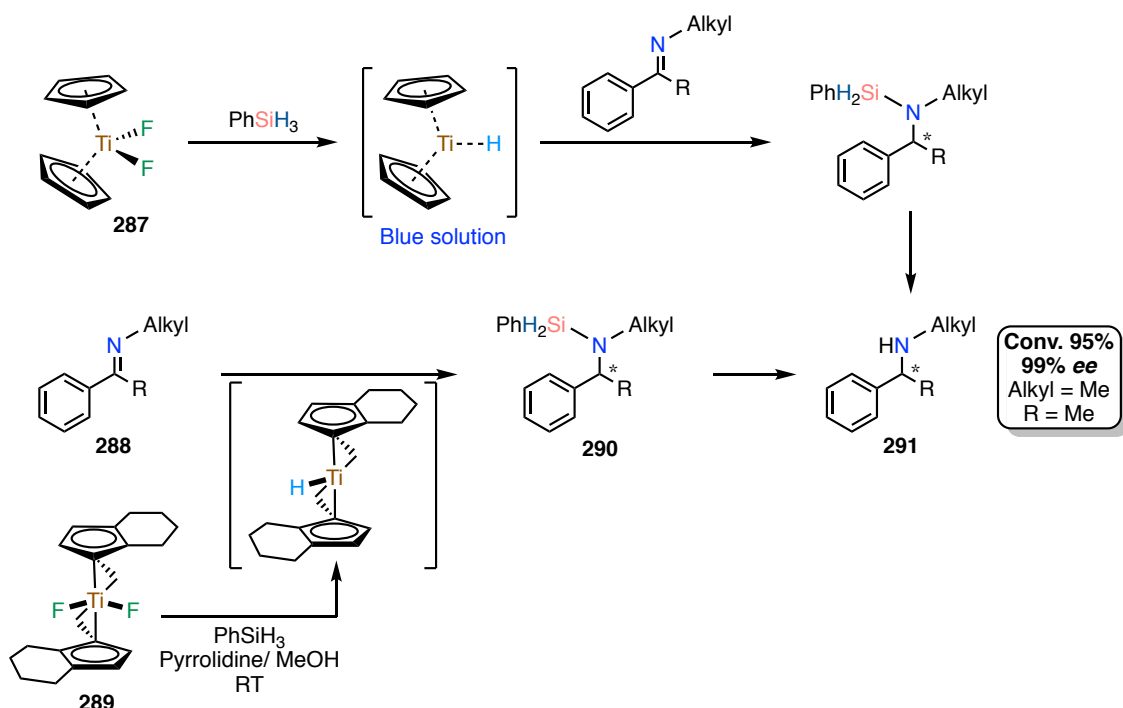
Scheme 29. Buchwald's asymmetric reduction of **I8** by Ti-catalysed hydrosilylation.

As it is depicted in Scheme 29, for the model substrate **I8**, the enantioselectivities reached 99% *ee*, being the only methodology to date that is able to have a complete control over the chiral discrimination of the prochiral imine. Unfortunately, this system has severe drawbacks of poor atom economy and the difficulties to handle the unstable Ti-hydrides. Furthermore, the parent approach did not perform well with sterically hindered imines, even though Buchwald and co-workers[87] were able to overcome this difficulty by using different amines as additives.

A second approach to prepare chiral *N*-methyl and *N*-alkyl imines has been recently developed by List and co-workers[86b] and it is based on the use of binaphthyl-derived sulphonamides as organic catalysts. The hydrogenation of **I8** as model substrate in the presence of the Hantzsch ester (acting as an hydride donor) and posterior addition of Boc$_2$O is depicted in Scheme 30 and affords really good results.
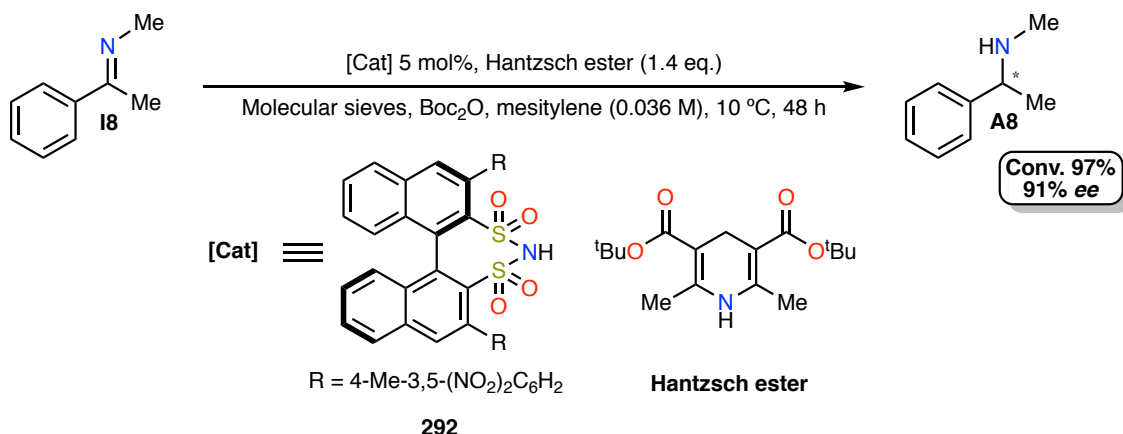
Scheme 30. List's organocatalytic enantioselective reduction of **I8**.

By means of this organocatalytic approach the group was able to hydrogenate **I8** with enantioselectivities up to 91%. As it has been mention, the reaction must be conducted in the presence of Boc$_2$O, otherwise the freshly formed amine deactivates the catalytic system.

A final example was reported by Abdur-Rashid and co-workers[88] and consists of the Ru-catalysed asymmetric hydrogenation of **I8** using a Ru-BINAP-DPEN catalyst in the presence of potassium *tert*-butoxide (Scheme 31).
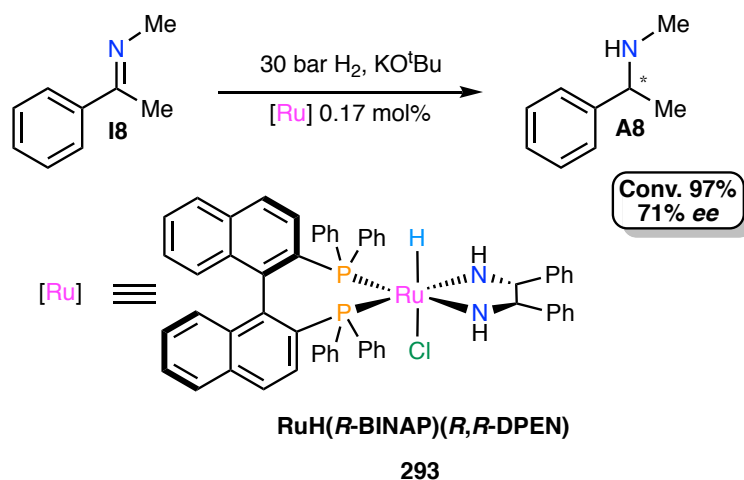
Scheme 31. Ru-catalysed asymmetric hydrogenation of **I8**.

In spite of the high enantioselectivities obtained with this Ru-based system, "direct" metal-catalysed asymmetric hydrogenations of this kind of substrates are rare in the literature due to problems of catalyst deactivation. As it has been presented, in the last examples, the final amine product is protected with either a SiR$_3$ or Boc group, thus circumventing the basicity issue associated with the free amine.

On the other hand, organocatalytic asymmetric imine reduction and reductive amination has also been developed to afford chiral aliphatic amines with high enantioselectivities.[89] However, these reactions generally suffer from lower yields and very long reaction times compared to transition metal catalysed hydrogenations. Furthermore, they require hydride donors such as dihydropyridines that generate stoichiometric amounts of waste products. To sum up, it can be said that a readily accessible catalyst for the asymmetric direct hydrogenation of *N*-alkyl and *N*-methyl imines remains elusive.

From an industrial perspective,[85b] the direct hydrogenation of imines is a much more desirable process; however, in contrast to the good results obtained with *N*-aryl ketimines,[69,75,90] the hydrogenation of *N*-methyl ketimines has not yet been achieved with useful levels of enantioselectivity.

Pfaltz and co-workers[17a] reported the hydrogenation **I8** with Ir-PHOX catalysts, achieving only 58% *ee* (Scheme 32).
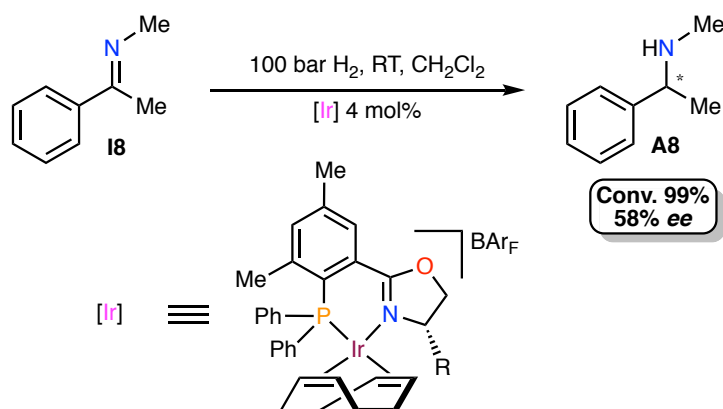
Scheme 32. Pfaltz's attempts for the Ir-catalysed asymmetric hydrogenation of **I8**.

The conversion was complete, but harsh pressures of hydrogen (100 bar) and high catalyst loadings (4 mol%) were required. It is likely that this difference between *N*-aryl and *N*-alkyl ketimines is due to the aforementioned basicity of this class of compounds.

With all this background in hand we envisaged that the Ir-MaxPHOX systems presented in the previous section would be good candidates as catalysts for the asymmetric hydrogenation of alkyl imines. Hence, our work started with the preparation of the substrates, as it will be presented in the following section.

5.4.1. *Synthesis of the N-alkyl imines*

There are several methods to prepare *N*-alkyl imines, mostly based on the reaction between a ketone and a primary amine under the presence of a desiccant agent (Scheme 33).
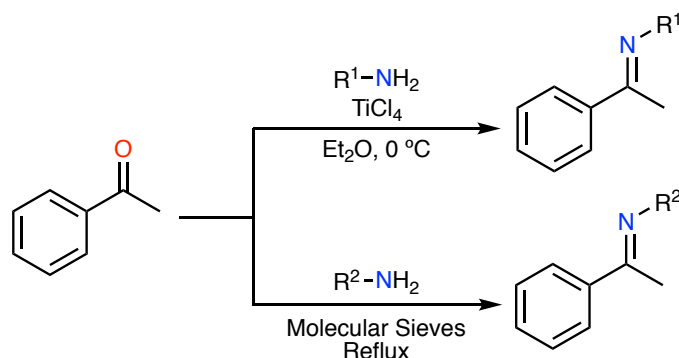
Scheme 33. Synthetic routes used to prepare *N*-alkyl imines.

In the case of small and highly nucleophilic amines, such as methyl or ethylamine, the reaction affords the desired products by just employing molecular sieves as dehydrating agent. In contrast, for more hindered amines the presence of a stronger desiccant is required, with $TiCl_4$ being the most used in these cases.[86b] Imines obtained using molecular sieves do not usually need of further purification, but in contrast, the $TiCl_4$ method often requires distillation or recrystallization of the imines obtained.

Although *N*-alkyl imines are easier to prepare than *N*-aryl imines, they are more prone to decompose in the presence of water, making them less easy-to-handle and store. The imines prepared in the present THESIS using these methods are described in the Experimental Section (Chapter 6).

5.4.2. *Hydrogenation of N-alkyl imines with Ir(I)-MaxPHOX*

Our group has very recently reported that cationic Ir(I)-MaxPHOX complexes are highly active and selective in the hydrogenation of *N*-aryl imines.[54] Thereafter, we decided to assess whether these catalysts were also effective for the asymmetric reduction of *N*-alkyl imines. These studies were carried out in collaboration with Dr. E. Salomó, who provided the methodology for the hydrogenation reactions.

Among the different available imines, we selected acetophenone *N*-methyl imine (**I8**) as a model substrate to test the efficiency of the Ir(I)-MaxPHOX catalysts. In spite

of its simplicity, this imine has proven to be a very tricky substrate, since the corresponding amine is very basic and nucleophilic. Besides, this imine can be easily prepared by condensation of methylamine and acetophenone by stirring the mixture at room temperature under molecular sieves, which makes it a cheap and good option to start with.

Four Ir-MaxPHOX catalysts bearing an *iso*-propyl group on the "arm" and on the "tail" were tested in the Ir-catalysed asymmetric hydrogenation of *N*-methyl imine, **I8** since this combination of substituents displayed the best results in the hydrogenation of *N*-aryl imines[54] (Scheme 34).
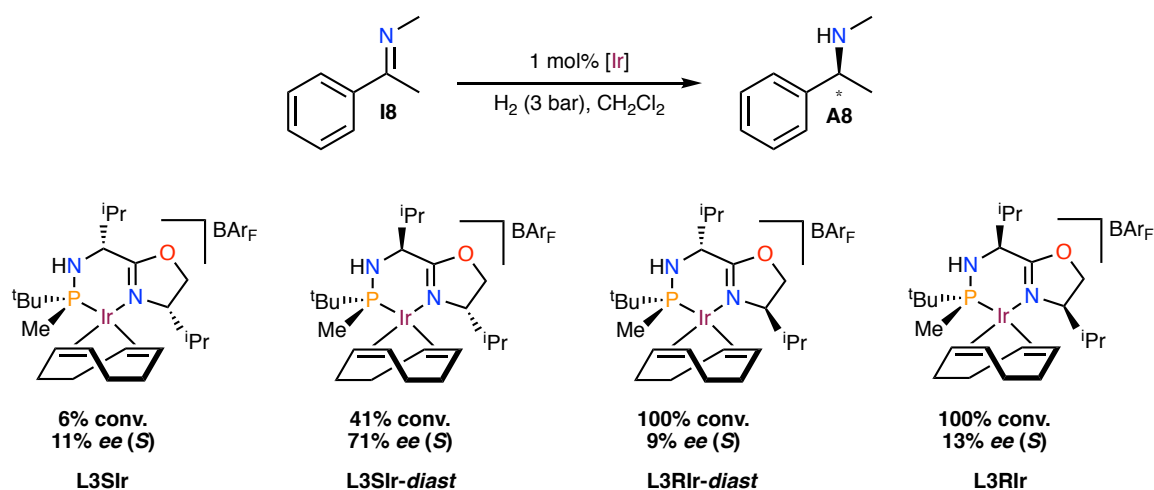
Scheme 34. Asymmetric hydrogenation of **I8** with the selected Ir-MaxPHOX catalysts. Conversions were determined by ^{1}H NMR analysis of the crude reaction mixture, while the *ee* value was determined by HPLC (*in collaboration with Dr. E. Salomó*).

The experiments were carried out using 1% of the Ir-MaxPHOX catalyst in dichloromethane at 3 bar of H$_2$ at room temperature. As it can be seen, conversions ranged from full to very low values and did not follow any clear trend. The enantioselectivities were also rather low, even reducing the hydrogen pressure from 3 bar to 1 bar.

As it was discussed in Section 5.2.7, Pfaltz and co-workers[64] found in 2013 that the actual active species in the Ir-catalysed asymmetric hydrogenation of *N*-aryl imines was an octahedral Ir(III) iridacycle, formed by cyclometallation of a *N*-phenyl imine.[64] Therefore we decided to investigate if such cyclometallation process would take place in our systems during the activation in hope of improving the obtained catalytic results.

The following section describes the preliminary screening carried out in order to find the most suitable cyclometallating additive that would improve the enantioselectivity of the hydrogenation **I8**.

5.4.2.1. *Influence of the cyclometallating agent*

Taking into account that the *N*-phenyl imine with Ir(I)-PHOX complexes in the presence of hydrogen tend to react by activation of the Csp^2–H bond to produce the corresponding cyclometallated iridacycles[64] we studied the asymmetric reduction of *N*-methyl imine as model substrate with each four Ir(I)-MaxPHOX catalysts of Scheme 35.
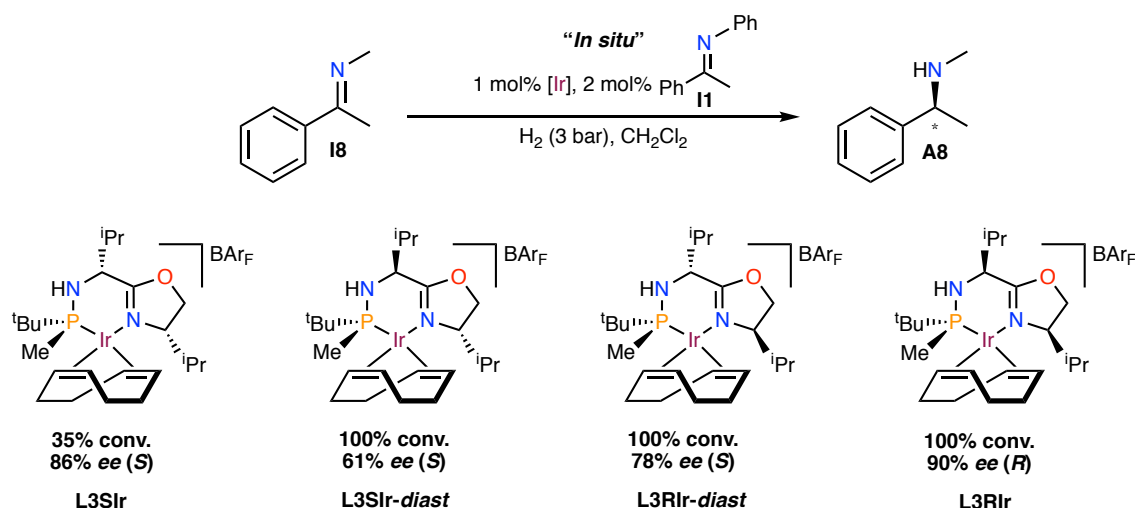
Scheme 35. Hydrogenation of **I8** with Ir-MaxPHOX catalysts using **I1** as additive (*in collaboration with Dr. E. Salomó*).

All these experiments were carried out activating the catalysts before the addition of the substrate, in order to form the catalytically active species, namely the iridacycle. Ir(I)-MaxPHOX precursor was reacted with the additive **I1** under 3 bar of H_2 at room temperature over thirty minutes. Then, the substrate **I8** was added into the reactor as it is detailed in the Experimental Section (Chapter 6).

Under these conditions, as it can be seen in Scheme 35, a significant enhancement of both conversion and enantioselectivity was observed. Particularly active and selective was complex **L3RIr**, hence after this preliminary screening; all the later experiments would have been conducted employing this Ir-MaxPHOX diastereomer. This is in agreement with the coordination studies carried out for this system, since it has yielded only one diastereomerically pure iridacycle (see Section 5.3).

Interestingly, when the catalytic reaction was performed by *directly* mixing all the reagents (substrate, additive and precursor without any prior activation) the results dramatically changed, with an important erosion of the *ee* (Scheme 36), resembling the results observed when no additive was employed in the catalytic essays.
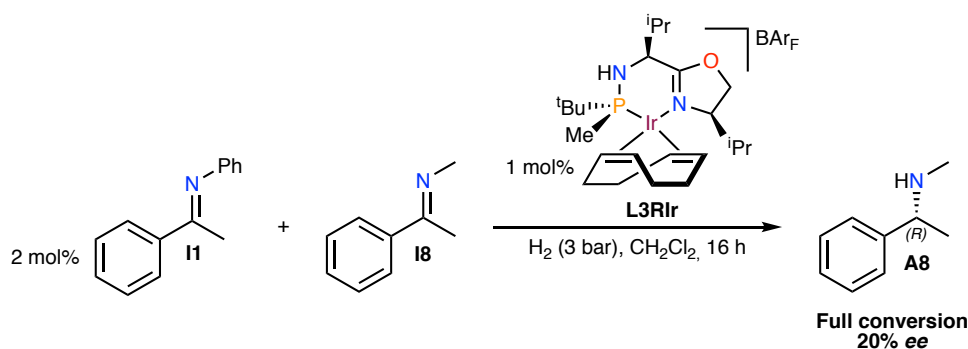
Scheme 36. Asymmetric hydrogenation of **I8** without activation of the catalyst (*in collaboration with Dr. E. Salomó*).

As it can be seen, the enantioselectivities for Ir-MaxPHOX complex **L3RIr** decreased from 90% to 20%, proving that the already hydrogenated amine or the *N*-alkyl imine have an interaction with the Ir(I) precursor that hinders the chiral discrimination of the substrate. In contrast when there was a delay time of activation, the high *ee* values obtained proved that the Ir(III) catalyst, once formed, is robust enough to prevent deactivation.

It can be concluded that the presence of the additive is crucial in order to prevent catalytic deactivation decrease of the enantioselectivity. Therefore, other cyclometallating additives were employed in order to study the effect on the *ee* values. In principle, another cyclometallated species, would lead to a different catalyst and modify the outcome of the reaction. Scheme 37 and Table 5 summarise these experiments.
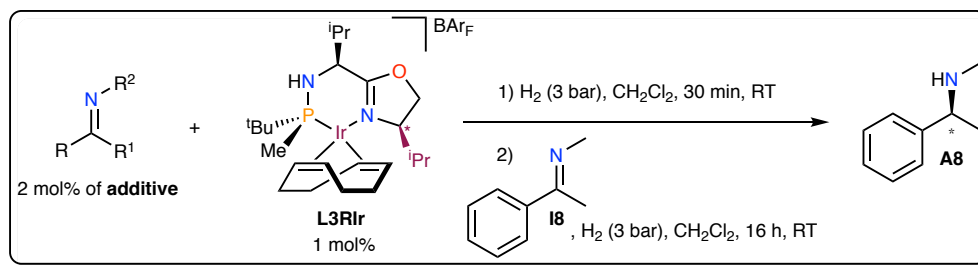
Additives
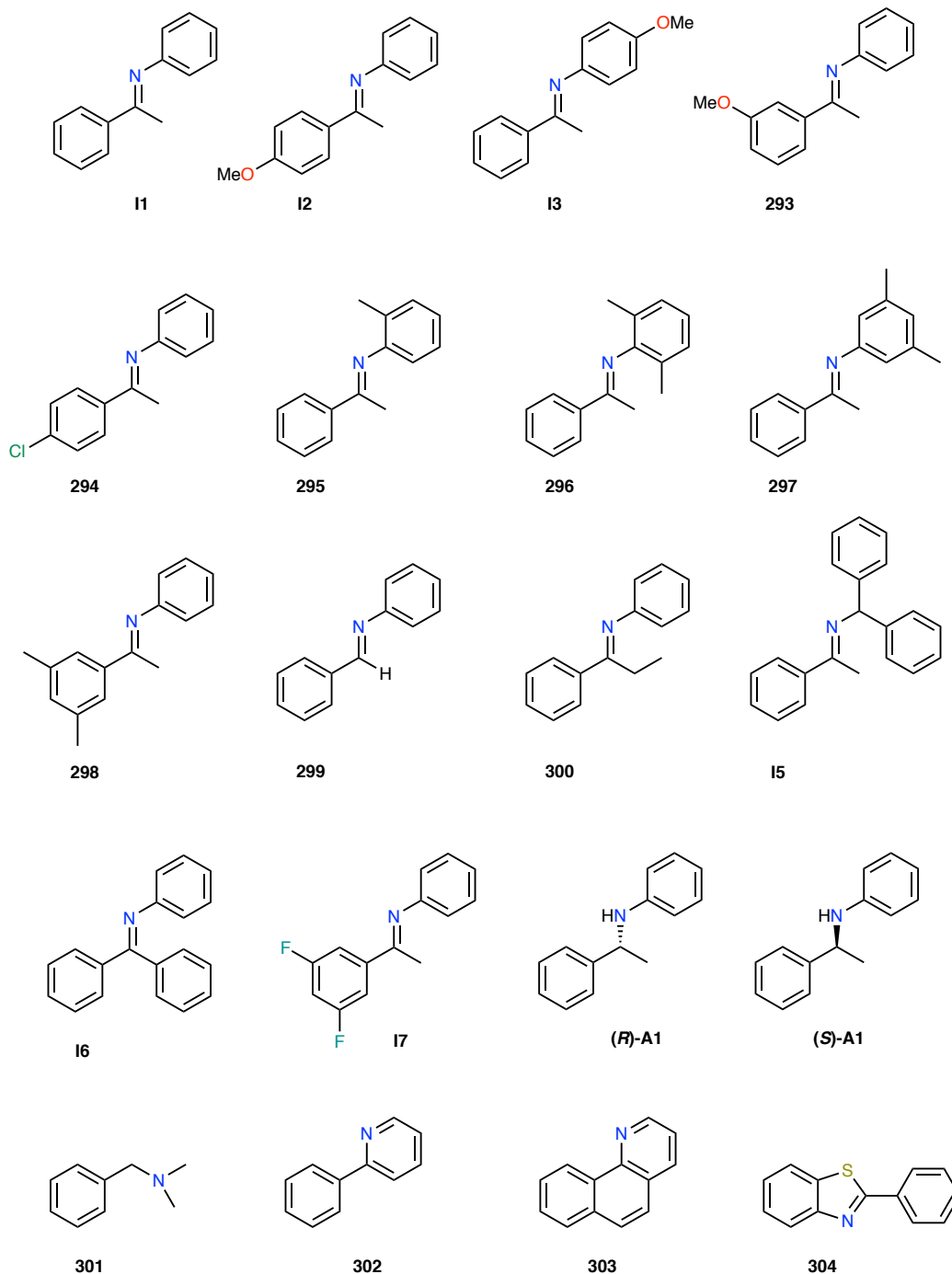
Scheme 37. Reaction screening for some additives in the asymmetric hydrogenation of **I8** (*in collaboration with Dr. E. Salomó*).

271

Table 5. Influence of the different additives on the asymmetric Ir-catalysed reduction of **I8**. a) Conversions were determined by ^{1}H NMR of the crude reaction mixture. b) *ee* value was determined by HPLC.

Entry	Additive	Conversion (%)[a]	*ee* (%)[b]
1	**I1**	100	90
2	**I2**	100	88
3	**I3**	100	87
4	**293**	100	83
5	**294**	49	60
6	**295**	100	82
7	**296**	36	40
8	**297**	100	87
9	**298**	100	62
10	**299**	16	–
11	**300**	100	85
12	**I5**	50	49
13	**I6**	100	72
14	**I7**	100	69
15	(*R*)-**A1**	100	75
16	(*S*)-**A1**	100	5
17	**301**	100	22
18	**302**	33	24
19	**303**	52	57
20	**304**	43	46

Taking *N*-phenyl imine **I1** as a starting point, additives **I1** to **294** contain electro-donating and electro-withdrawing substituents on the aromatic moieties. As it is shown, whereas **I1** led to full conversion and 90% *ee*, electro-donating methoxy substituents slightly decreased the enantioselectivity (**I1**-**293**). Interestingly, when a more electro-withdrawing group such as Cl, is attached on the arene, a significant decrease in both conversion and *ee* is obtained. In the same line, two fluorine substituents located on *meta* positions (**I7**) give better enantioselectivities but still lower than the observed for **I1**.

Imines **295** to **298**, which contain methyl substituents on the aromatic positions, did not improve the enantioselectivity either, with the *ee* ranging from 40 to 87%. Apparently, the enhancement of the steric hindrance in the phenyl rings does not play a favourable role on the chiral discrimination process. Additives, **299** and **300**, having different substituents at the iminic carbon atom, but preserving the unfunctionalised aromatic rings, did not lead to any improvement on the enantioselectivity. A similar behaviour was observed when we tried to expand the aromatic system, both in the ketone part (**I6**) or attaching two phenyl groups on the part coming from the amine (**I5**).

Furthermore, some secondary amines were also studied as cyclometallating ligands. Particularly interesting is the pair of optically pure amines (*R*)-**A1** and (*S*)-**A1**, displaying a clear *match-mismatch* effect on the enantioselectivities, where (*R*)-**A1** in combination with the iridium precursor **L3RIr** afforded the best *ee* values.

Finally, additives **302** to **304** in spite of having a structure prone to cyclometallate, they did not furnish better results than that with **I1**, probably because their cyclometallation reactions with **L3RIr** did not afford one single diastereomer. Hence, in the view of these results, the originally tested additive **I1** was chosen as the selected additive to perform a small reaction scope.

5.4.2.2. *Reaction scope*

With the catalyst and the additive selected, we proceeded to explore the scope of the hydrogenation with various *N*-alkyl imines (Scheme 38).

I8
0 °C
100% conv.
92% *ee*

I9
0 °C
100% conv.
95% *ee*

I10
−10 °C
100% conv.
94% *ee*

I11
RT
100% conv.
89% *ee*

I12
RT
100% conv.
91% *ee*

I13
−10 °C
100% conv.
93% *ee*

I14
−10 °C
100% conv.
90% *ee*

I15
0 °C
100% conv.
93% *ee*

I16
−10 °C
100% conv.
94% *ee*

I17
−10 °C
100% conv.
93% *ee*

I18
5 bar of H_2, RT
49% conv.
<5% *ee*

I19
RT
100% conv.
85% *ee*

I20
RT
38% conv.
--% *ee*

I21
RT
0% conv.
--% *ee*

I22
RT
26% conv.
--% *ee*

I23
RT
10% conv.
--% *ee*

I24
RT
100% conv.
--% *ee*

I4
RT
100% conv.
86% *ee*
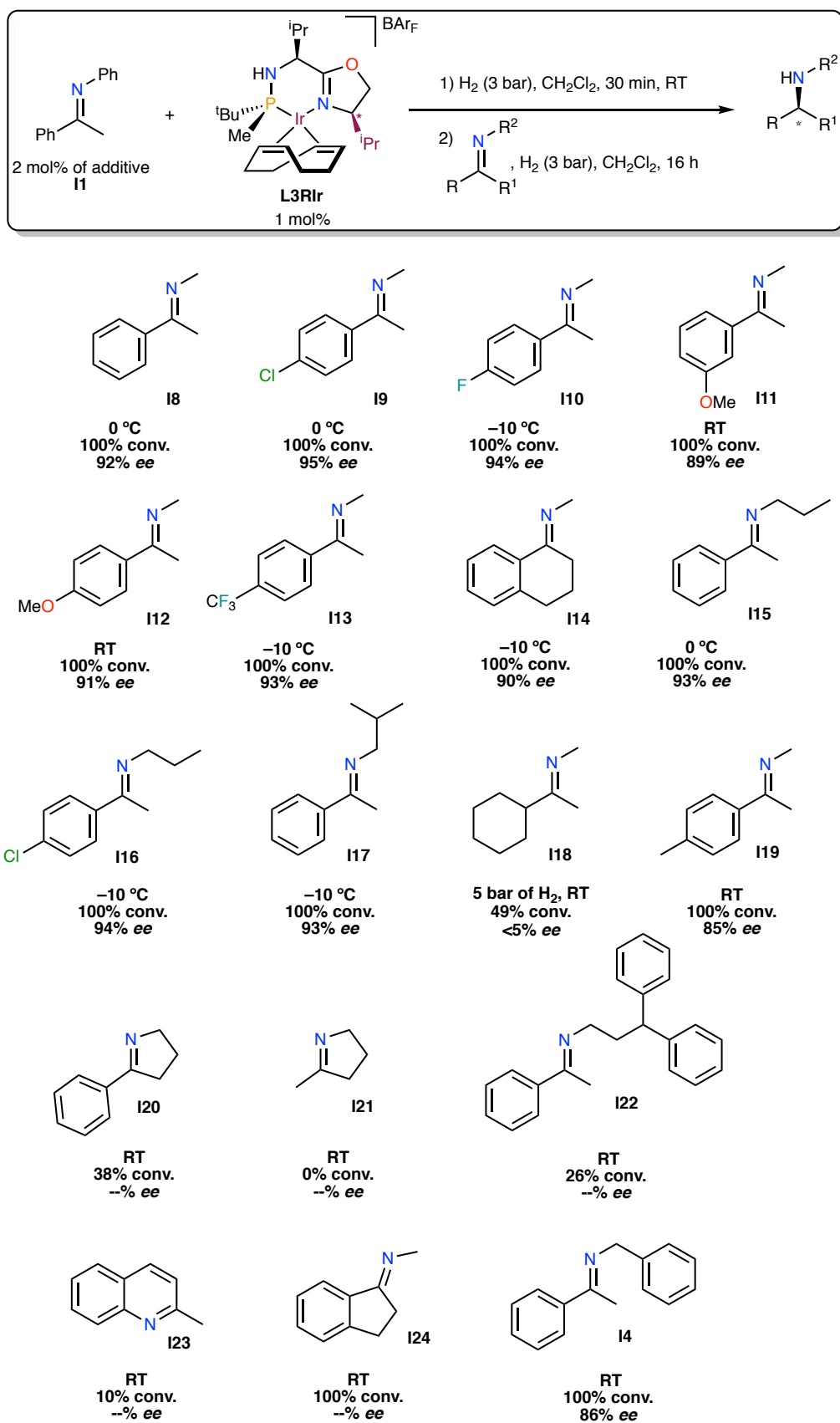
Scheme 38. Scope for the hydrogenation of *N*-alkyl imines with MaxPHOX **L3RIr** using additive **I1**. Catalyst **L3RIr** with additive **I1** afforded the amines as the (*R*) enantiomer as it was determined by optical rotation and HPLC (*in collaboration with Dr. E. Salomó*).

As expected, an improvement of the chiral discrimination was often observed when the reactions were performed at lower temperatures. Consequently, the suitable temperature was optimised for each substrate. Imine **I8** was reduced with a 92% *ee*, whereas imines **I11** and **I12** bearing electro-donating groups appeared to be less reactive. The reaction for these had to be conducted at room temperature and the *ee*'s for the corresponding amines were 89 and 91%, respectively. Substrates **I9**, **I10** and **I13** contain electron-withdrawing groups and in these cases, the temperature could be decreased to -10 ℃ to afford 95, 94 and 93% of *ee* for the reduction of each imine, respectively. Hence, the presence of such electron-withdrawing groups facilitates the reaction by further activation of the substrate, as it was also observed in the hydrogenation of *N*-aryl imines.[54]

Cyclic imine **I14** was also successfully hydrogenated with an *ee* of 89% at -10 ℃. The good results obtained with imines **I15**, **I16** and **I17** indicate that substrates with different *N*-alkyl groups from methyl can also be reduced with excellent *ee* values, proving the robustness and versatility of the catalytic system.

Although substrate **I19** displayed enantioselectivities lower than expected at room temperature, the enantioselectivities are not that different compared the model **A0** substrate.

A more challenging substrate was **I18** since it does not contain any aromatic sp^2 carbon atom prone to cyclometallate. Actually, the reaction proceeds to a 50% of conversion but without any enantioselection, a behaviour that is attributed to the unfavoured formation of the iridacycle.

Nevertheless, the enantioselectivities obtained are clearly better than those without using imine **I1** as additive, showing that the iridacycle intermediate is key for the hydrogenation of imines. The lack of reactivity observed in this case can be attributed to the fact that **I18** cannot form an iridacycle as the cyclohexane ring does not contain any Csp^2 atoms. The low enantioselectivity fits with the proposed mechanism, as it will be explained in Section 5.5.

Substrates **I20** and **I21** were even more difficult to hydrogenate and we only achieved a 38% *ee* for **I20**, while after struggling with **I21** varying the reaction conditions we were only able to get conversions up to 5%. On the other hand, the low conversion of imine **I22**, was attributed to solubility issues.

The hydrogenation of **I23** employing the MaxPHOX system at 55 bar of H_2 did not afford any conversion. Alternatively, when imine **I1** was used as additive, the conversion increased to 10% with only 3 bars of H_2.

Further studies will be carried on with this class of substrates since they are especially difficult to hydrogenate at low pressures.

For **I24** we could not find a method to evaluate the enantioselectivity of the process so the *ee* remains unknown.

Hydrogenation of **I4**, without adding any additive, leads to a 77% *ee* of the *S* enantiomer, whereas in the presence of **I1** the *R* enantiomer is preferentially obtained in 86% *ee*. Although the use of the additive improves only slightly the enantioselectivity, it furnishes the opposite enantiomer, suggesting a different reaction pathway when the iridacycle acts as a catalyst.

5.4.2.3. *Influence of amines in the reaction media*

The results obtained with **I21** presented in the previous section, suggested that the nucleophilicity or basicity of the substrates/products could interfere with the catalytic system. In this line, hydrogenation of **I8** was carried out in the presence of a 20% mol of different amines. The results obtained are given in Table 6.

Table 6. Study of the effect of different amines on the catalytic system. a) Conversions were determined by ^{1}H NMR analysis of the crude reaction mixture. b) *ee* value was determined by HPLC analyses (*in collaboration with Dr. E. Salomó*).

Entry	Base	Conv. (%)	*ee* (%)
1	B1	100	89
2	B2	100	90
3	B3	0	--
4	B4	0	--

In these experiments, the amines (**B1** to **B4**) were added along with the substrate after performing "*in situ*" the iridacycle. Interestingly, the addition of a tertiary amine (**B1**) or secondary (**B2**) does not affect the enantioselectivity of the reaction. In contrast, more nucleophilic amines such as propylamine (**B3**) or benzylamine (**B4**) decrease dramatically the conversion of the process. Apparently, iridacycles can tolerate the presence of bases to some extend, with the exception of primary amines, which probably, due to its high nucleophilic character, coordinate and deactivate the catalytic system.

Further experiments had been carried out also with **I21**, which is more nucleophilic than any of the *N*-aryl and *N*-methyl imines studied. In this sense, when a small amount (20 mol%) of **I21** was added to a solution of *N*-phenyl imine as substrate, no trace of hydrogenated product was detected (Scheme 39).
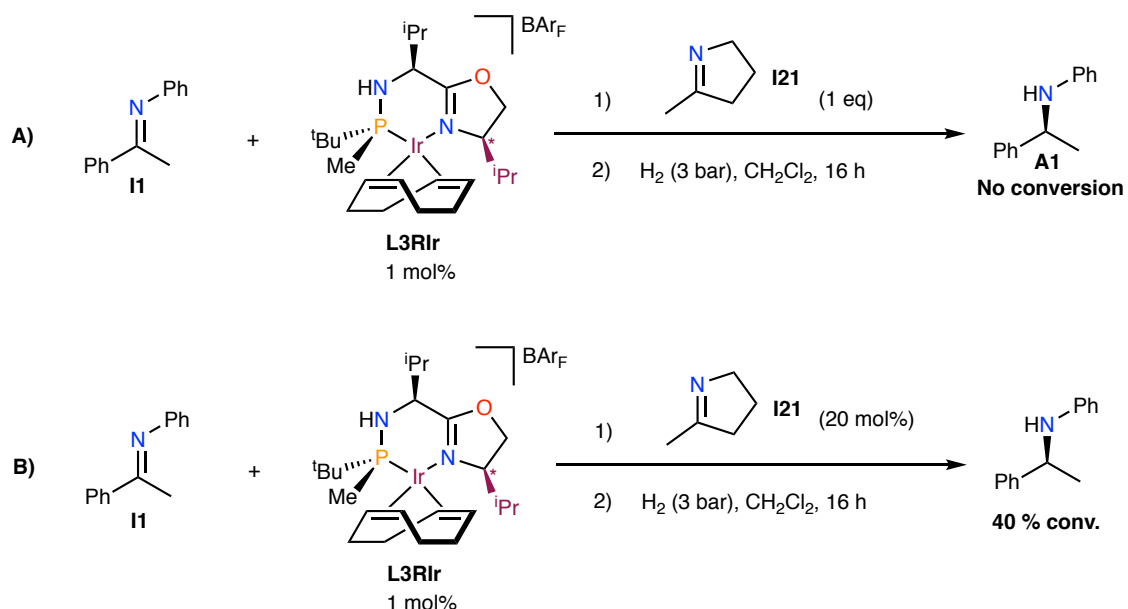
Scheme 39. Study of the effect of **I21** on the catalytic system (*in collaboration with Dr. E. Salomó*).

What is more, the addition of the same amount of imine after formation of the iridacycle, allows the detection of a 40% conversion of the *N*-aryl hydrogenated amine. The addition of **I21** did not stop completely the catalytic cycle, once the iridacycle had been already formed, a data that is in agreement with the results obtained for the previously presented screening of amines.

5.4.3. *Catalysis with preformed Ir(III)-MaxPHOX cyclometallated complexes*

The "*in situ*" formation of the iridacycle by means of the Ir(I) MaxPHOX precursor and **I1** as additive, followed by posterior addition of the desired *N*-alkyl imine as substrate, has proven to be an effective methodology.

Nevertheless, with the idea to find a better understanding of the nature of the catalytic species involved in the cycle and to look for a more reliable and robust procedure that could be applied at a larger scale, we envisaged the preparation of a family of Ir(III) cyclometallated complexes with **I1** as cyclometallating agent (Figure 30).
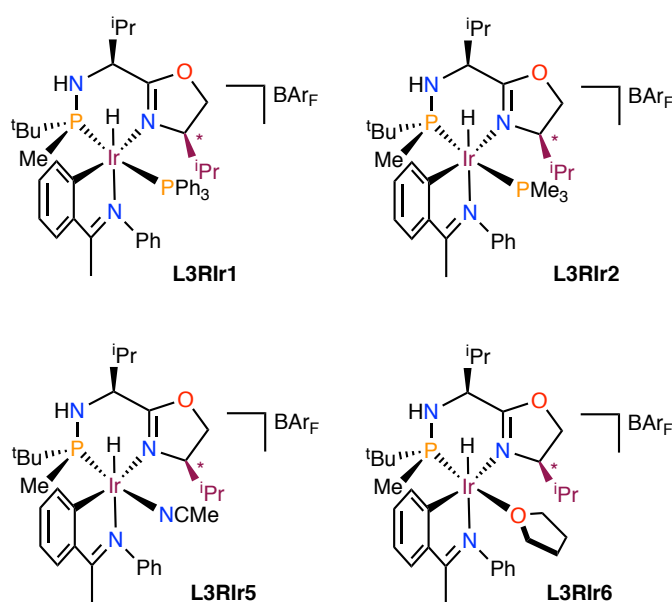
Figure 30. Preformed iridacycles with **I1** as cyclometallating agent and several ligands.

As it has shown it Section 5.3, Ir(I)-MaxPHOX precursor **L3RIr** afforded one single diastereoisomer of the corresponding iridacycle with several ligands, albeit not all of them were catalytically active. In Figure 30 are depicted those iridacycles with potential application as catalysts for the asymmetric hydrogenation of *N*-alkyl imines. The presented iridacycles are air-stable and can be directly used in the catalytic runs.

On the other hand, as it was explained in Section 5.2.7, our group recently reported the use of neutral iridacycles, containing a chloride ligand, as catalysts for the asymmetric hydrogenation of *N*-aryl imines.[54] These iridacycles proved to be stable solids, but when they were directly applied as catalysts, very low conversions were obtained. In fact, these compounds had to be treated with NaBAr_F in order to abstract the coordinated chloride and generate a vacant coordination site.

Consequently, we aimed for a family of cationic catalysts containing BArF as counteranion, and having a stabilising ligand (L) that occupies the sixth coordination position of the iridacycle. The nature of this ligand must be labile enough to be released in solution and allow the approximation of the substrate (Scheme 40).
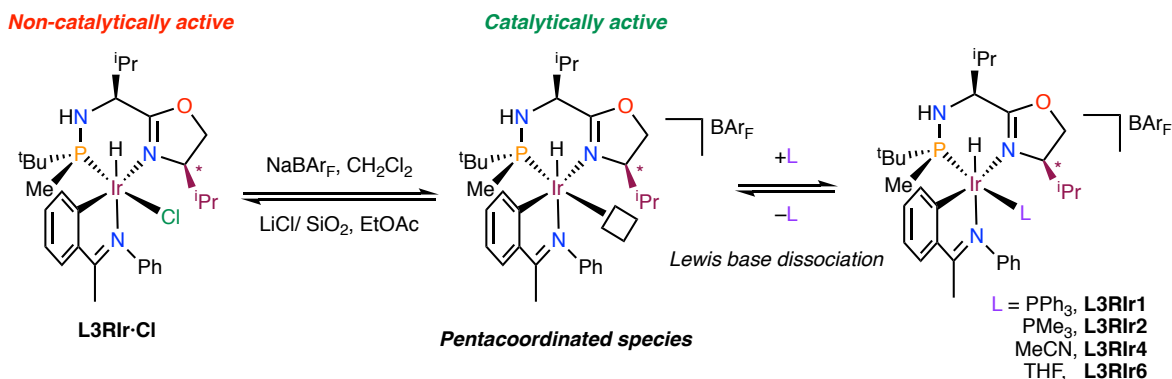
Scheme 40. Catalytically and non-catalytically active Ir(III) cyclometallated complexes.

Complexes **L3RIr1** to **L3RIr6** were tested as catalysts for the enantioselective hydrogenation of the model substrate **I8** at 3 bar of H_2 using dichloromethane as solvent. The obtained results are given in Table 7.

Table 7. Catalytic results for the asymmetric hydrogenation of **I8** with the four isolated iridacycles **L3RIr1** to **L3RIr6**. a) Conversions were determined by ^{1}H NMR of the reaction crude. b) *ee* values were determined by HPLC.

Entry	Catalyst	Temp. (°C)	Conv. (%)[a]	*ee* (%)[b]
1	"*In situ*"	RT	100	90
2	**L3RIr4**	RT	100	85
3	**L3RIr1**	RT	0	-
4	**L3RIr2**	RT	100	90
5	**L3RIr6**	RT	100	91
6	**L3RIr2**	0 °C	0	--
7	**L3RIr6**	0 °C	100	91

Iridacycle **L3RIr4** gave full conversion but the *ee* was slightly lower compared with the "*in situ*" analogous experiment. It seems that even traces of strong coordinating solvents such as acetonitrile can have some influence on the catalytic results, hindering the reproducibility of the system. In contrast, complex **L3RIr1** gave no conversion at all even at room temperature. This can be rationalised by the fact that the ligand is too strongly bound to the metal and did not allow for the catalysis to happen.

On the other hand, catalysts **L3RIr2** and **L3RIr6** afforded full conversions and the enantioselectivities were comparable to that of the "*in situ*" experiments. In particular, as **L3RIr2** and **L3RIr6** offered the best results at room temperature, we attempted to run the catalysis at lower temperatures, in order to increase the enantioselectivities. We observed that **L3RIr6** was much more active than **L3RIr2**, since hydrogenation at 0 ºC with **L3RIr2** did not afford any reduced product whereas **L3RIr6** achieved full conversion (entries 6 and 7).

In order to test the activity at low temperatures of the trimethylphosphine complex **L3RIr2**, we ran the catalytic hydrogenation of a more easy-to-reduce *N*-methyl imine, containing the CF$_3$ group on the aromatic ring (Scheme 41).
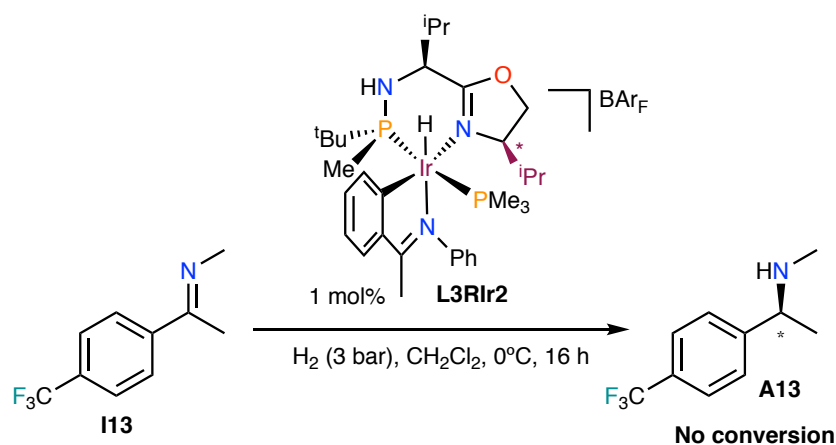
Scheme 41. Assessment of the activity of complex **L3RIr2** towards substrate **I13**.

Unfortunately, we did not observed any conversion when the reaction of imine **I13** was carried out at 0 ºC with complex **L3RIr2**. This fact can be attributed to the less labile nature of the phosphine compared to other ligands.

It seems reasonable to think that the THF ligand, since it is not strongly bonded, confers to iridacycle **L3RIr6** the nature of more a pentacoordinated compound rather than a true octahedral (saturated) system. Consequently, it allows the catalytic cycle to occur even at low temperatures due to the free vacant coordination position in solution.

5.4.3.1. *Reaction scope*

In order to be useful from a practical point of view, the new isolated catalyst **L3RIr6** had to offer at least the same results obtained with the "*in situ*" hydrogenation experiments. Fortunately, we were able to reproduce the asymmetric reduction of some of the best results obtained in the hydrogenation of *N*-alkyl imines with our Ir-MaxPHOX preformed catalyst **L3RIr6**.

The results obtained running the catalytic essays with the isolated iridacycle **L3RIr6** are depicted in Table 8 and compared with all those obtained using the "*in situ*" methodology. All experiments were conducted at 3 bar of H_2 using 1 mol% of catalyst in dichloromethane, under the usual conditions.

Table 8. Reaction scope of iridacycle **L3RIr6** compared to the "*in situ*" experiments. *ee* values were determined by HPLC.

Entry	Imine	Temp. (°C)	"*In situ*" *ee*(%)	Cat. L3RIr1 *ee*(%)
1	I8	0	92	91
2	I12	RT	91	91
3	I11	RT	89	89
4	I9	0	95	94
5	I10	−10	94	93
6	I13	−10	93	93
7	I14	−10	90	89
8	I15	0	93	92
9	I16	−10	94	93
10	I17	−10	93	94
11	I19	−10	85	85
12	I18	RT	5	5
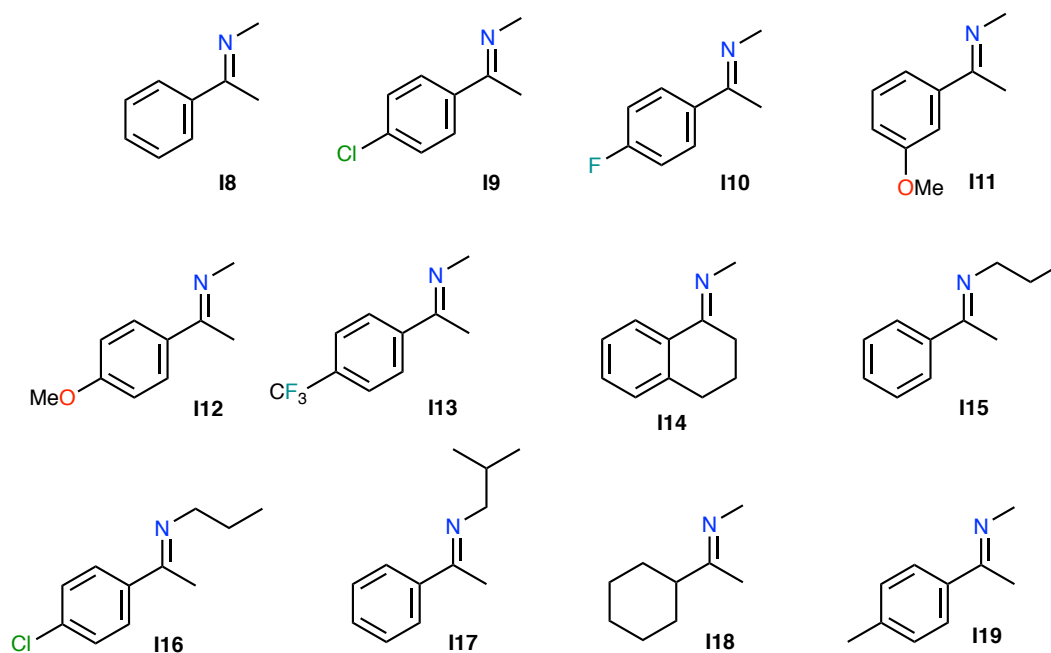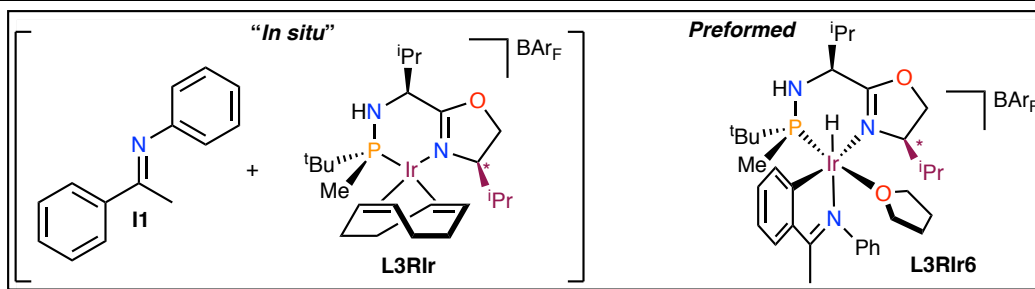
As shown in Table 8 the results are practically the same. This proves that **L3RIr6** is a viable and reproducible option as an iridacycle-catalyst for the hydrogenation of *N*-alkyl imines. Unfortunately, as it is shown in Table 8, no enantioselection was observed when using **I18** as substrate so far, even employing the preformed catalyst, proving that the presence of an sp^2 carbon atom is required for the reaction to take place.

Besides, these results also highlight the fact that the Ir(III) cyclometallated species are the "true" catalysts for these reactions. Therefore, a better-understanding of the reaction mechanism and the stereodetermining step would allow the design of more versatile *P,N* optically pure ligands, which might lead to improve the catalytic results and open the door for the hydrogenation of even more challenging substrates such as aliphatic imines.

Notably, it is important to mention that catalyst **L3RIr6** has been recently tested in the hydrogenation of styrene (Scheme 42).
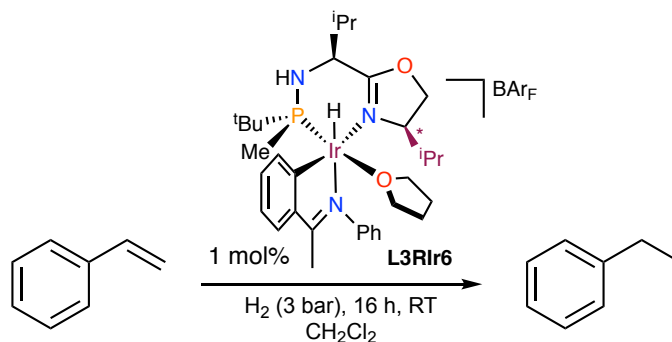
Scheme 42. Hydrogenation of styrene using complex **L3RIr6**.

The reaction was conducted pressurizing at 3 bar of H_2 a solution of styrene with 1 mol% of the catalyst **L3RIr6**. We were pleased to see that our system displayed full conversions at 16 h, as it was determined by GC analyses. This promising result could set our complex as a potential catalyst for the hydrogenation of unfunctionalised alkenes, whose asymmetric version is currently being studied.

5.4.3.2. *Mechanistic insights of the Ir-catalysed asymmetric hydrogenation of acetophenone N-methyl imine*

In the view of the catalytic results, we decided to investigate if the cyclometallated *N*-phenyl imine was decoordinated and reduced during the catalysis in order to shed some light on the mechanistic insights of the reaction.

Therefore, a mixture of the cyclometallating *N*-phenyl imine, its corresponding amine and the acetophenone *N*-methyl imine used as substrate first analysed by GC (Figure 31).
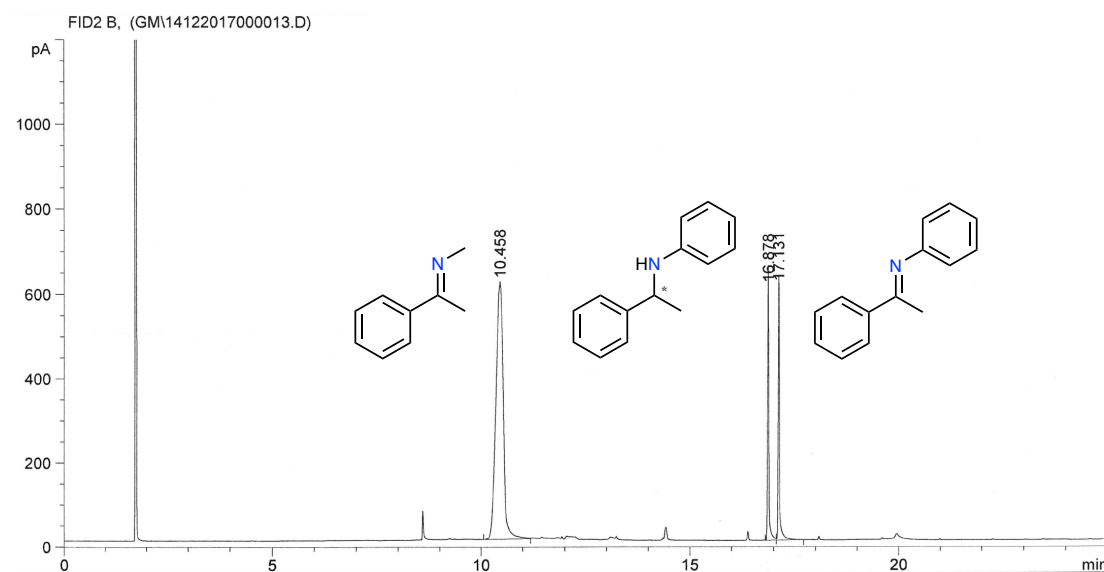
Figure 31. GC trace of a mixture of acetophenone *N*-phenyl imine (**I8**) (10 mol%), acetophenone *N*-phenyl amine (**A1**) (10 mol%) and acetophenone *N*-methyl imine (**I1**) (100 mol%) in dichloromethane.

As it can be seen, they have different enough retention times to allow the unambiguous identification of the three compounds.

Furthermore we performed the catalytic reaction of **I8** under the usual conditions (3 bar of H$_2$ at room temperature over 16 h) but using a 10% mol of catalyst **L3RIr6**, hence resembling the conditions of the aforementioned chromatogram (Scheme 43).
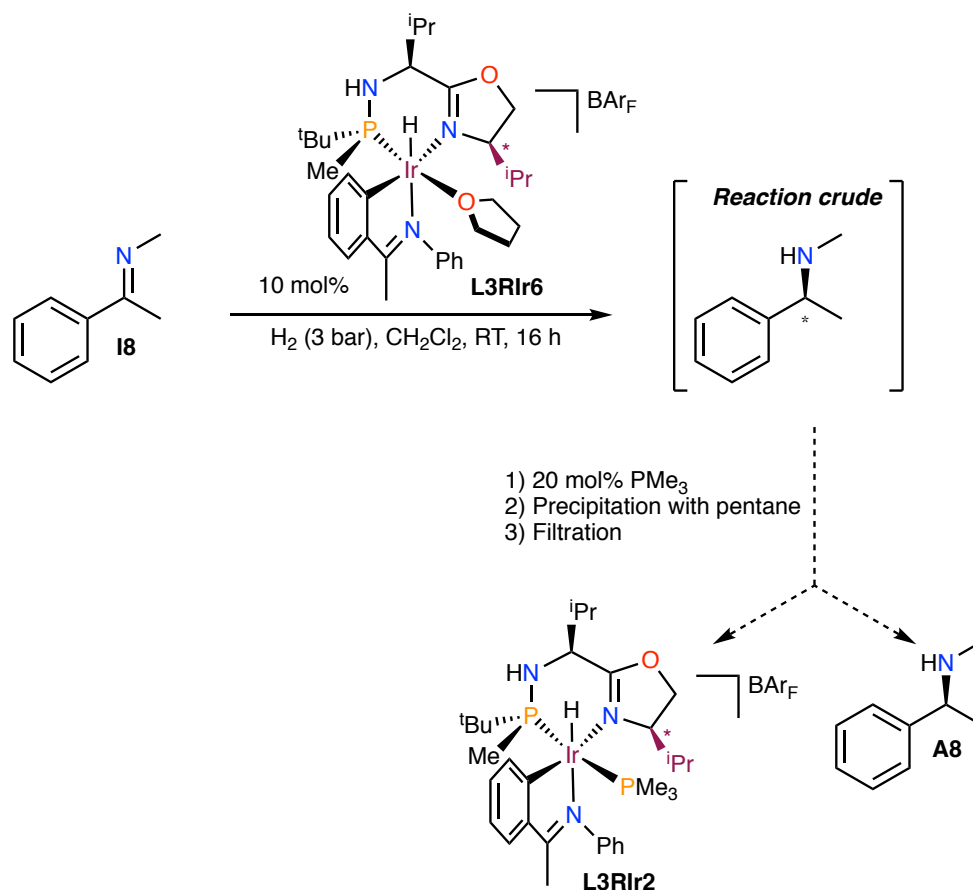
Scheme 43. Reaction of **I8** using 10 mol% catalyst **L3RIr6** and isolation of complex **L3RIr2**.

After 16 h a 20 % mol of PMe$_3$ was added to the reaction crude, which was concentrated and precipitated with pentane, to afford complex **L3RIr2** in a 45% yield. The recovered complex was analysed by NMR and by mass spectrometry, proving that the complex obtained is the same as prepared by cyclometallation of *N*-phenyl imine with hydrogen and later addition of PMe$_3$ (Figure 32).
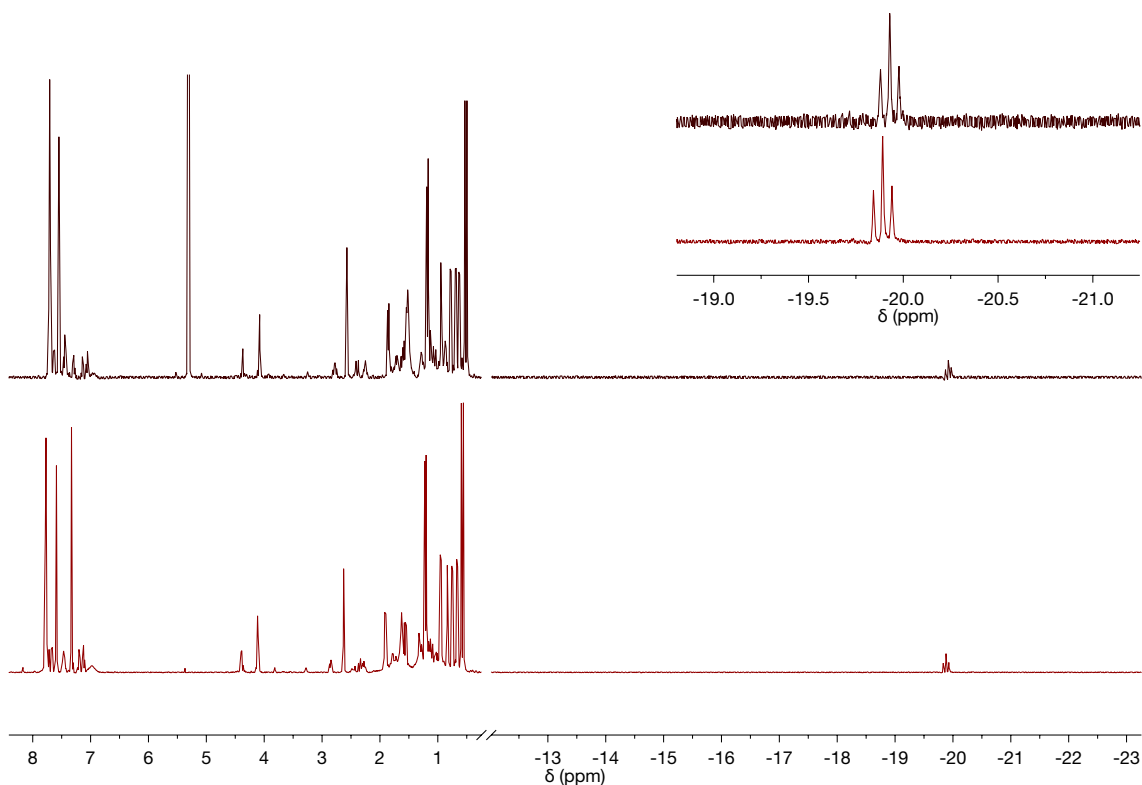
Figure 32. ^{1}H NMR (400 MHz, CD$_2$Cl$_2$, 25 °C) spectra of the isolated complex after the catalytic run (top) and spectrum of the preformed complex **L3RIr2** (bottom).

As it shown in Figure 32 both spectra are identical proving that the structure of the catalyst does not change during the catalytic cycles. In parallel, the mother liquors of the filtrate were analysed by GC, showing only one signal, belonging to the hydrogenated *N*-methyl amine (**A8**) (Figure 33).
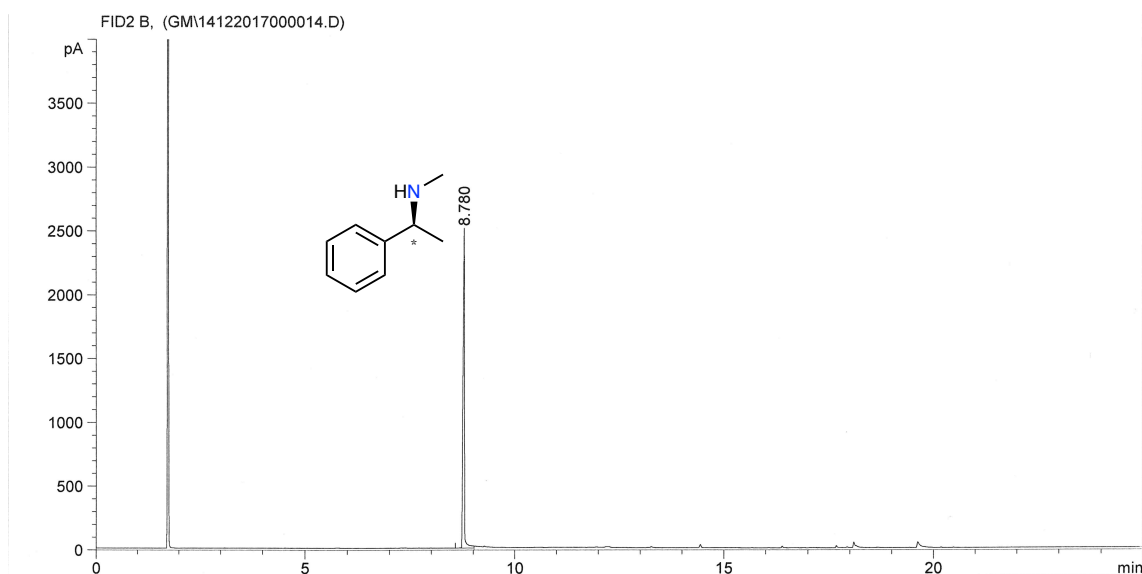
Figure 33. GC trace of the filtered reaction crude after precipitation of the catalyst.

286

As it can be seen in Figure 33 there is no trace of *N*-phenyl imine or its corresponding amine on the chromatogram, which indicates that no release of the cyclometallating ligand occurs so far and that the structure of the catalyst is preserved during the catalytic cycles. This is also in agreement with the fact that when a strong-bond ligand occupies the reactive position of the iridacycle, the reaction is blocked and lower or even no conversions were obtained.

5.5. *Model for the hydride transfer*

The hydrogenation of *N*–phenyl imines has been proposed to proceed through an outer sphere mechanism.[72] As it was commented in Section 5.2.7, recently Norrby, Wiest, Andersson and co–workers[72] reported theoretical calculations for the transition state in which the hydride is transferred to the iminium cation, determining the stereochemistry of the reduced amine. The authors highlighted some interactions between the iminium cation and the iridacycle that allow the rationalisation of the experimental results.[72]

Taking into account the similarities between the catalytic systems described by Norrby *et al*[72] and the Ir–MaxPHOX catalysts, we decided to apply the same model to our Ir catalysts in order to predict the stereochemical outcome for the reduction of *N*–alkyl imines.

To this end, a DFT mechanistic study, carried out in collaboration with Prof. Agustí Lledós from the *Universitat Autònoma de Barcelona*, (B_3LYP–D_3 functional, including solvent effects) has been performed in dichloromethane using the computed structure of complex **L3RIr6** and **I8** as substrate. The iridium complex **L3RIr6** is activated by the substitution of the labile THF ligand by a dihydrogen molecule, leading to the catalytically active species **L3RIr6–H_2** with a ΔG of 4.8 kcal mol^{-1}. The catalytic cycle, depicted in Figure 34 and Scheme 44, starts with the approximation of the imine to the η^2–H_2 complex **L3RIr6–H_2** generating intermediate **I** (–0.6 kcal mol^{-1}).
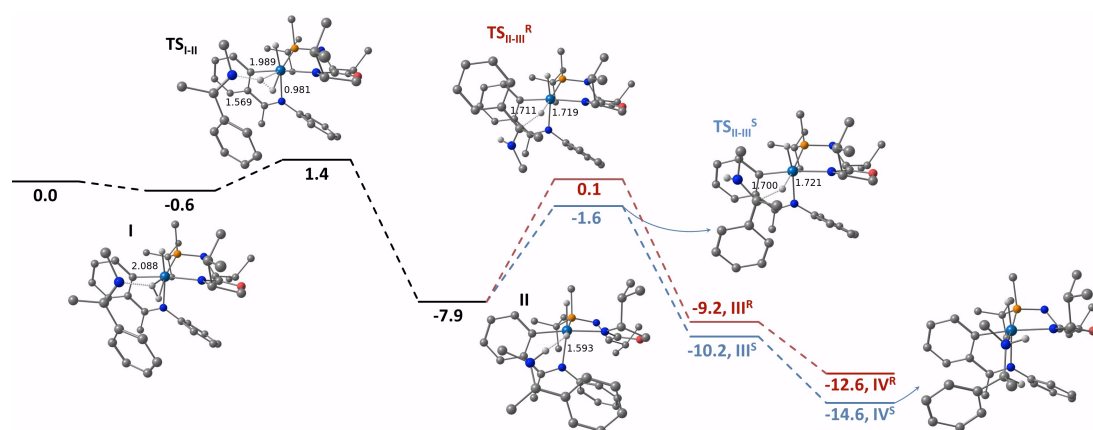
Figure 34. DFT computed reaction profile (B3LYP–D3/BS2 in CH_2Cl_2). Relative Gibbs energies in kcal mol^{-1} taking the separated catalyst **L3RIr6–H$_2$** and **I8** as reference. The discussed structures and TSs are shown highlighting the most important distances in Å.
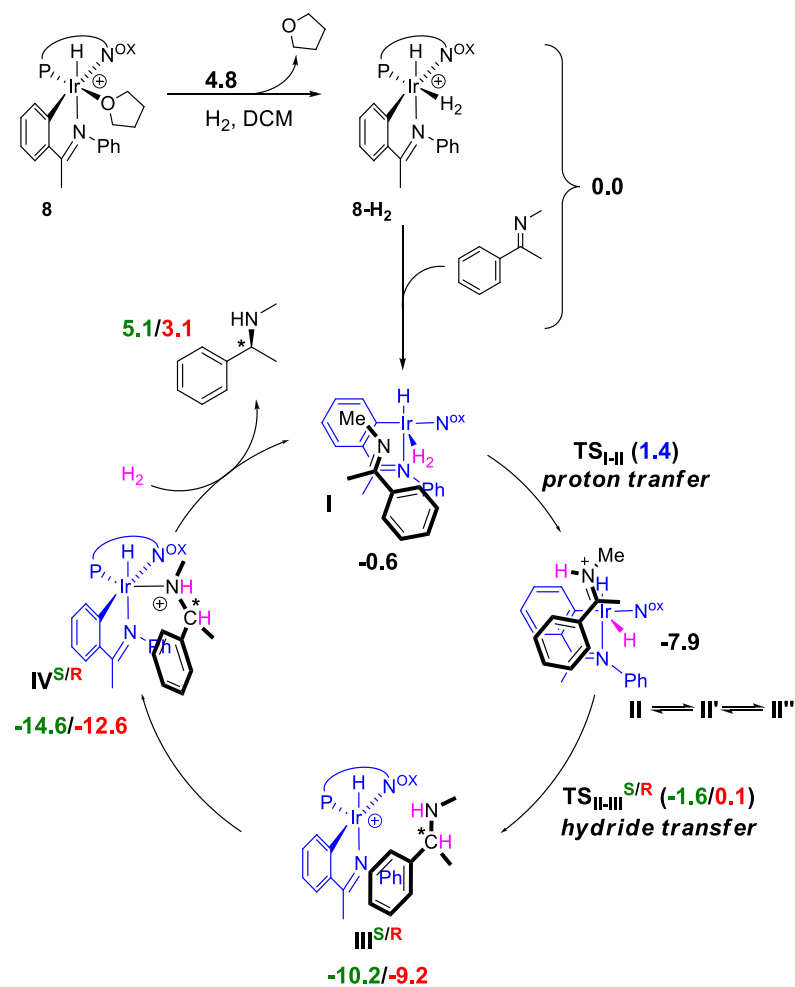
Scheme 44. DFT computed mechanism (B3LYP–D3/BS2 in CH_2Cl_2) for the asymmetric hydrogenation of *N*–methyl imines to amines; the numbers are relative Gibbs energies in kcal mol^{-1} (in green for the *S* formation and red for the *R* formation), taking as zero–energy the separated catalytically active species **L3RIr6**–H$_2$ and **I8**. Relative energies of transition states are indicated in parenthesis.

In **I**, in addition to the π–stacking between the aromatic portions of the cyclometallated ligand and the substrate, a dihydrogen bond, involving the iminic nitrogen and the coordinated dihydrogen molecule (H–H···N = 2.09 Å), stabilises the structure.

From **I,** a subsequent proton transfer entailing heterolytic splitting of the dihydrogen ligand leads to the protonated imine and the dihydridoiridium(III) catalyst (intermediate **II**), falling at -7.9 kcal mol^{-1}. Transition state of this step (**TS$_{I–II}$**) requires an energy barrier of 2.0 kcal mol^{-1}. Intermediate **II** is characterised by a high flexibility and a low ΔG for the dissociation of the iminium cation (-1.0, 3.5 and -1.0 kcal mol^{-1} for intermediates **II**, **II'** and **II''**, respectively), implying an easy rearrangement of the relative orientation of the substrate. For this reason only the lower conformation was reported on the energy profile and taken as a reference for the subsequent energy barrier.

Transition state **TS$_{II–III}$**, corresponding to the hydride transfer to the protonated imine has the higher energy barrier of the catalytic cycle and governs the rate and the enantioselectivity of the reaction. The prochiral protonated imine can, in principle, approach the catalyst offering the two sides of the plane defined by the C–N double bond, leading to the amine with *R* or *S* configuration.

This represents a lose transition state in which multiple orientations of the substrate are possible. A quadrant model that accounts for the possible orientations of the iminium ion is depicted in Figure 35a.
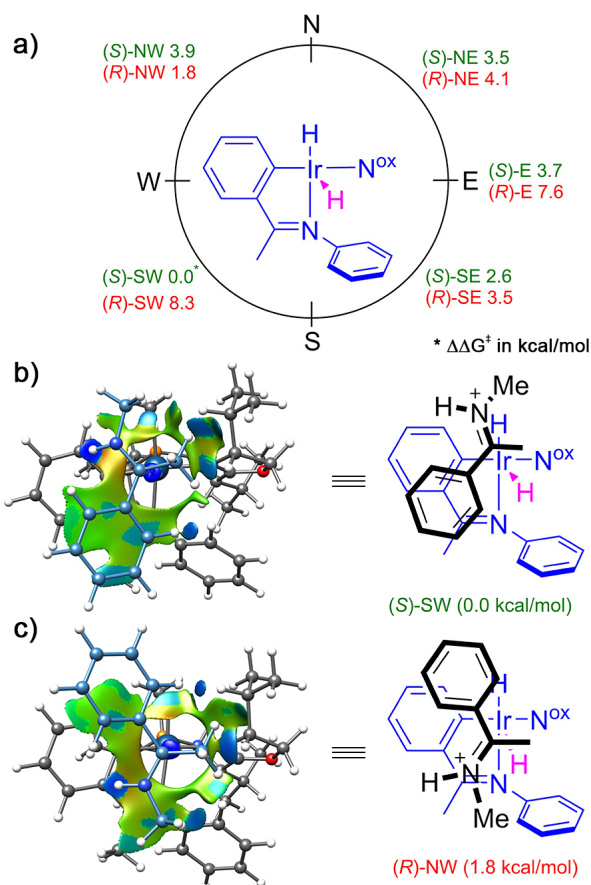
Figure 35. a) DFT computed quadrant model for the hydride transfer stereodetermining step. Transition state relative $\Delta\Delta G^{\ddagger}$ values for different orientations of the substrate phenyl group (in green: TSs leading to *S* isomer; in red: TSs leading to *R* isomer). The hydride transferred to the substrate is highlighted in magenta. b) Most favourable TS leading to *S* isomer, $\Delta\Delta G^{\ddagger}$ = 0.0 kcal mol^{-1} ($\Delta G^{\ddagger}$ = 6.3 kcal mol^{-1} with respect to the iminium intermediate). c) Most favourable TS leading to *R* isomer, $\Delta\Delta G^{\ddagger}$ = 1.8 kcal mol^{-1}. Color code for NCI analysis: red: repulsive, blue: attractive.

The most favourable TS is that in which the phenyl ring of the substrate is placed in the SW quadrant (Figure 35b) and leads to the *S* enantiomer, as observed experimentally. The most favourable TS leading to the *R* isomer is 1.8 kcal mol^{-1} above with the phenyl group in the NW quadrant (Figure 35c). From these values the calculated enantiomeric excess is 90%, which is in close agreement with the experimental findings. Non–covalent interaction analysis (NCI) shows that in the (*S*)–SW TS the phenyl group of the iminium ion generates a larger π-π interaction surface than the (*R*)–NW TS (Figure 35b, c), thus leading to a more favourable transition sate.

Later on, intermediate **III**$^{S/R}$ can evolve to intermediate **IV**$^{S/R}$ in which the amine is *N*–coordinated to the Ir. Finally, the replacement of the amine product in intermediate **IV**$^{S/R}$ (−14.6 and −12.6 kcal mol–1) by a dihydrogen molecule restore catalyst

L3RIr6–H₂ and closes the cycle (ΔG = 3.1 and 5.1 kcal mol^{-1} for the *R* and *S* products, respectively).

In support of this notion is the fact that the reduction of an aliphatic substrate like cyclohexylmethylketone *N*–methyl imine provided a racemate. Actually, as it has been explained in Section 5.4.3, hydrogenation of cyclohexylmethylketone *N*–methylimine with 1 mol% of **L3RIr6** provided a racemate with 50% conversion. Similar calculations to those reported in Figure 35(quadrant model) for this substrate give a ΔΔG‡ difference of only 0.1 kcal mol^{-1} between the most favourable TSs leading to opposite enantiomers. This behaviour can be also highlighted by a non-covalent interactions plot (Figure 36).
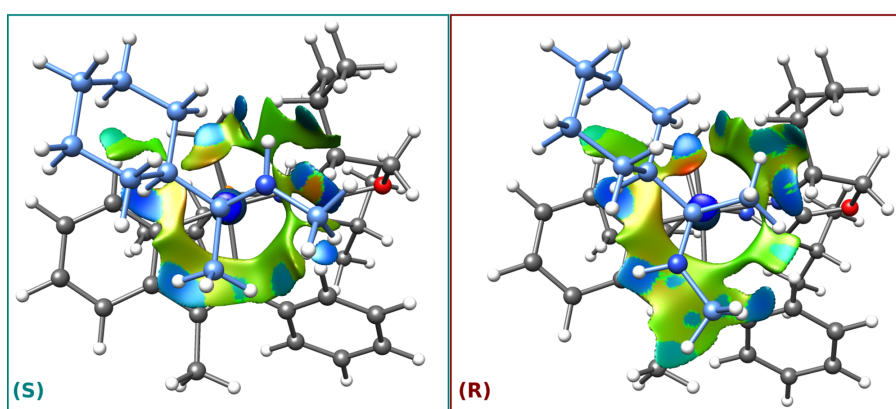
Figure 36. Comparison of the NCI plots the two lowest transition states of the hydride transfer step for the hydrogenation of cyclohexylmethylketone *N*-methyl imine leading to the formation of the *S*- and *R*-products. Non-covalent interactions are represented as blue (strong), green (weak) and red (repulsive) blobs.

Representation of the two lowest TSs for the hydrogenation of cyclohexylmethylketone *N*–methylamine displays that the free rotation of the Cy ring achieves the same stabilisation interactions for both prochiral approachings confirming the experimental data reporting a 4.4% *ee* for the *R* configuration.

5.6. *Conclusions*

Cyclometallation of Ir(I) MaxPHOX complexes with acetophenone *N*-phenyl imine in the presence of molecular hydrogen has led to the formation of a family of optically pure iridacycles.

It has been found that the stereoselectivity of the formation of these iridacycles is highly dependent on the nature of the cyclometallating ligand, the stereochemistry of the *P,N* moiety (especially the oxazoline group) and the ligand, later introduced in order to fill the sixth coordination position of the octahedron and stabilise the resulting complex.

We have successfully hydrogenated with full conversions and excellent enantioselectivities different challenging *N*-alkyl imines. To do so, it was crucial to take into consideration the importance of the imine-iridacycles as key intermediates for the asymmetric hydrogenation of imines. By using **I1** as an additive, we were able to form a proper iridacycle "*in situ*" that could catalyse the reduction of *N*-alkyl imines and overcome the catalyst deactivation issue.

In parallel, in order to obtain a more robust and practical methodology, we assessed the catalytic hydrogenation of these *N*-alkyl imines with our preformed catalysts. We found that the presence of strongly coordinating solvents such as acetonitrile, or stabilising groups like phosphines as ligands did not reproduce the conversions and enantioselectivities obtained by using "*in situ*" methodologies.

We managed to isolate an air-stable iridacycle containing a coordinated THF molecule and studied its scope in the hydrogenation of different *N*-alkyl ketimines, which gave catalytic results comparable or even better to those obtained generating the iridacycle "*in situ*".

To the best of our knowledge, the results obtained in terms of conversion and *ee* are, up to date, the best in the asymmetric catalytic hydrogenation of *N*-alkyl imines so far. We believe this new kind of iridacycle-catalyst holds a great potential and expect them to be useful in the hydrogenation of many others challenging imines and possibly ketones and even unfunctionalised alkenes.

Mechanistic studies of the catalytic hydrogenation reaction catalysed by our THF-iridacycle have demonstrated that there is no decoordination or exchange of the cyclometallated imine during the catalytic cycles. DFT theoretical studies supports these observations suggesting an outer-sphere reaction mechanism in agreement with the models recently described in the literature for these systems.

The results obtained in the present chapter have been recently published as a communication: Salomo, E.; Gallen, A.; Sciortino, G.; Ujaque, G.; Grabulosa, A.; Lledos, A.; Riera, A. and Verdaguer, X. *J. Am. Chem. Soc.*; doi 10.1021/jacs.8b11547.

5.7. *References*

(1)   (a) Knowles, W. S.; Sabacky, M. J. *Chem. Commun.* **1968**, 1445-1446 (b) Knowles, W. S.; Sabacky, M. J.; Vineyard, B. D. *J. Chem. Soc., Chem. Commun.* **1972**, 10-11 (c) Knowles, W. S.; Sabacky, M. J.; Vineyard, B. D.; Weinkauff, D. J. *J. Am. Chem. Soc.* **1975**, *97*, 2567-2568 (d) Vineyard, B. D.; Knowles, W. S.; Sabacky, M. J.; Bachman, G. L.; Weinkauff, D. J. *J. Am. Chem. Soc.* **1977**, *99*, 5946-5952 (e) Abbott, S. J.; Jones, S. R.; Weinman, S. A.; Knowles, J. R. *J. Am. Chem. Soc.* **1978**, *100*, 2558-2560 (f) Miyashita, A.; Yasuda, A.; Takaya, H.; Toriumi, K.; Ito, T.; Souchi, T.; Noyori, R. *J. Am. Chem. Soc.* **1980**, *102*, 7932-7934.

(2)   Osborn, J. A.; Jardine, F. H.; Young, J. F.; Wilkinson, G. J. *J. Chem. Soc. (A)* **1966**, 1711-1732.

(3)   Kagan, H. B.; Dang, T. *J. Am. Chem. Soc.* **1972**, *94*, 6429-6433.

(4)   Inoguchi, K.; Sakuraba, S.; Achiwa, K. *Synlett* **1992**, 169-178.

(5)   Carroll, M. P.; Guiry, P. J. *Chem. Soc. Rev.* **2014**, *43*, 819-833.

(6)   von Matt, P.; Pfaltz, A. *Angew. Chem. Int. Ed. Engl.* **1993**, *32*, 566568.

(7)   Sprinz, J.; Helmchen, G. *Tetrahedron Lett.* **1993**, *34*, 1769-1772.

(8)   (a) von Matt, P.; Loiseleur, O.; Koch, G.; Pfaltz, A. *Tetrahedron: Asymmetry* **1994**, *5*, 573-584 (b) von Matt, P.; Lloyd-Jones, G. C.; Minidis, A. B. F.; Pfaltz, A.; Macko, L.; Neuburger, M.; Zehnder, M.; Ruegger, H.; Pregosin, P. S. *Helv. Chim. Acta* **1995**, *78*, 265-284.

(9)   (a) Tang, W.; Wang, W.; Zhang, X. *Angew. Chem. Int. Ed.* **2003**, *42*, 943-946 (b) Hilgraf, R.; Pfaltz, A. *Adv. Synth. Catal.* **2005**, *347*, 61-77.

(10)   (a) Jiang, X.; van den Berg, M.; Minnaard, A. J.; Feringa, B. L.; de Vries, J. G. *Tetrahedron: Asymmetry* **2004**, *15*, 2223-2229 (b) Grabulosa, A. *P-Stereogenic Ligands in Enantioselective Catalysis*; Royal Society of Chemistry: Cambridge, 2011.

(11)   Tang, W.; Zhang, X. *Chem. Rev.* **2003**, *103*, 3029-3069.

(12)   (a) Rossen, K. *Angew. Chem. Int. Ed.* **2001**, *40*, 4611-4613 (b) Crépy, K. V. L.; Imamoto, T. *Adv. Synth. Catal.* **2003**, *345*, 79-101 (c) Gridnev, I. D.; Imamoto, T. *Acc. Chem. Res.* **2004**, *37*, 633-644 (d) Preetz, A.; Baumann, W.; Drexler, H.; Fischer, C.; Sun, J.; Spannenberg, A.; Zimmer, O.; Hell, W.; Heller, D. *Chem. Asian J.* **2008**, *3*, 1979-1982 (e) Schmidt, T.; Dai, Z.; Drexler, H.; Hapke, M.; Preetz, A.; Heller, D. *Chem. Asian J.* **2008**, *3*, 1170-1180 (f) Schmidt, T.; Drexler, H.; Sun, J.; Dai, Z.; Baumann, W.; Preetz, A.; Heller, D. *Adv. Synth. Catal.* **2009**, *351*, 750-754 (g) Gridnev, I. D.; Imamoto, T. *Chem. Commun.* **2009**, 7447-7464.

(13)   Crabtree, R. H.; Felkin, H.; Morris, G. E. *J. Organomet. Chem.* **1977**, *141*, 205-215.

(14)   (a) Crabtree, R. H.; Felkin, H.; Fillebeen-Khan, T.; Morris, G. E. *J. Organomet. Chem.* **1979**, *168*, 183-195 (b) Verendel, J. J.; Pàmies, O.; Diéguez, M.; Andersson, P. G. *Chem. Rev.* **2014**, *114*, 2130-2169.

(15)   Crabtree, R. H.; Gautier, A.; Giordano, G.; Khan, T. *J. Organomet. Chem.* **1977**, *141*, 113-121.

(16)   Crabtree, R. *Acc. Chem. Res.* **1979**, *12*, 331-337.

(17)   (a) Schnider, P.; Koch, G.; Prétôt, R.; Wang, G.; Bohnen, F. M.; Krüger, C.; Pfaltz, A. *Chem. Eur. J.* **1997**, *3*, 887-892 (b) Helmchen, G.; Pfaltz, A. *Acc. Chem. Res.* **2000**, *33*, 336-345 (c) Blackmond, D. G.; Lightfoot, A.; Pfaltz, A.; Rosner, T.; Schnider, P.; Zimmermann, N. *Chirality* **2000**, *12*, 442-449 (d) Blankenstein, J.; Pfaltz, A. *Angew. Chem. Int. Ed.* **2001**, *40*, 4445-4446 (e)

Pfaltz, A.; Blankenstein, J.; Hilgraf, R.; Hörmann, E.; McIntyre, S.; Menges, F.; Schönleber, M.; Smidt, S. P.; Wüstenberg, B.; Zimmermann, N. *Adv. Synth. Catal.* **2003**, *345*, 33-43.

(18) Lightfoot, A.; Schnider, P.; Pfaltz, A. *Angew. Chem. Int. Ed.* **1998**, *37*, 2897-2899.

(19) (a) Smidt, S. P.; Zimmermann, N.; Studer, M.; Pfaltz, A. *Chem. Eur. J.* **2004**, *10*, 4685-4693 (b) Mazet, C.; Smidt, S. P.; Meuwly, M.; Pfaltz, A. *J. Am. Chem. Soc.* **2004**, *126*, 14176-14181.

(20) (a) *Comprehensive asymmetric catalysis*; Jacobsen, E. N.; Pfaltz, A.; Yamamoto, A., Eds.; Springer: Berlin, 1999 (b) Kamer, P. C. J.; van Leeuwen, P. W. N. M.; Ed. *Phosphorus(III) Ligands in Homogeneous Catalysis: Design and Synthesis*; Wiley, 2012.

(21) (a) Witte, H.; Seeliger, W. *Liebigs Ann. Chem.* **1974**, *1974*, 996-1009 (b) Witte, P.; Lal, T. K.; Waymouth, R. M. *Organometallics* **1999**, *18*, 4147-4155.

(22) Peer, M.; de Jong, J. C.; Kiefer, M.; Langer, T.; Rieck, H.; Shell, H.; Sennhenn, P.; Sprinz, J.; Steinhagen, H.; Wiese, B.; Helmchen, G. *Tetrahedron* **1996**, *52*, 7547-7583.

(23) Krout, M., R.; Mohr, J. T.; Stoltz, B. M. *Org. Synth.* **2009**, *86*, 181-193.

(24) (a) Tani, K.; Behenna, D. C.; McFadden, R. M.; Stoltz, B. M. *Org. Lett.* **2007**, *9*, 2529-2531 (b) McDougal, N. T.; Streuff, J.; Mukherjee, H.; Virgil, S. C.; Stoltz, B. M. *Tetrahedron Lett.* **2010**, *51*, 5550-5554 (c) Hethcox, J. C.; Shockley, S. E.; Stoltz, B. M. *ACS Catal.* **2016**, *6*, 6207-6213 (d) Hethcox, J. C.; Shockley, S. E.; Stoltz, B. M. *Angew. Chem. Int. Ed.* **2016**, *55*, 16092-16095.

(25) (a) Sudo, A.; Saigo, K. *J. Org. Chem.* **1997**, *62*, 5508-5513 (b) Hashimoto, Y.; Horie, Y.; Hayashi, M.; Saigo, K. *Tetrahedron: Asymmetry* **2000**, *11*, 2205-2210 (c) Oka, N.; Wada, T.; Saigo, K. *J. Am. Chem. Soc.* **2003**, *125*, 8307-8317.

(26) (a) Langer, T.; Janssen, J.; Helmchen, G. *Tetrahedron: Asymmetry* **1996**, *7*, 1599-1602 (b) Wiese, B.; Helmchen, G. *Tetrahedron Lett.* **1998**, *39*, 5727-5730.

(27) Gläser, B.; Kunz, H. *Synlett* **1998**, 53-54.

(28) Stohler, R.; Wahl, F.; Pfaltz, A. *Synthesis* **2005**, 1431-1436.

(29) (a) Frölander, A.; Lutsenko, S.; Privalov, T.; Moberg, C. *J. Org. Chem.* **2005**, *70*, 9882-9891 (b) Frölander, A.; Moberg, C. *Org. Lett.* **2007**, *9*, 1371-1374.

(30) Tietze, L. F.; Lohmann, J. K. *Synlett* **2002**, 2083-2085.

(31) (a) Kilroy, T. G.; Cozzi, P. G.; End, N.; Guiry, P. J. *Synlett* **2004**, 106-110 (b) Kilroy, T. G.; Cozzi, P. G.; End, N.; Guiry, P. J. *Synthesis* **2004**, 1879-1888 (c) Guiry, P. J.; Sauders, C. P. *Adv. Synth. Catal.* **2004**, *346*, 497-537 (d) McCartney, D.; Nottingham, C.; Müller-Bunz, H.; Guiry, P. J. *J. Org. Chem.* **2015**, *80*, 10151-10162 (e) Rokade, B. V.; Guiry, P. J. *ACS Catal.* **2018**, *8*, 624-643.

(32) (a) Zhu, S.-F.; Xie, J.-B.; Zhang, Y.-Z.; Li, S.; Zhou, Q.-L. *J. Am. Chem. Soc.* **2006**, *128*, 12886-12891 (b) Zhu, S.-F.; Zhou, Q.-L. *Acc. Chem. Res.* **2017**, *50*, 988-1001.

(33) (a) Trudeau, S.; Morken, J. P. *Tetrahedron* **2006**, *62*, 11470-11476 (b) Schuster, C. H.; Li, B.; Morken, J. P. *Angew. Chem. Int. Ed.* **2011**, *50*, 7906-7909.

(34) Whelligan, D. K.; Bolm, C. *J. Org. Chem.* **2006**, *71*, 4609-4618.

(35) Patti, A.; Lotz, M.; Knochel, P. *Tetrahedron: Asymmetry* **2002**, *12*, 3375-3380.

(36) (a) Nishibayashi, Y.; Uemura, S. *Synlett* **1995**, 79-81 (b) Yonehara, K.; Mori, K.; Hashizume, T.; Chung, K.-G.; Ohe, K.; Uemura, S. *J. Organomet. Chem.* **2000**, *603*, 40-49.

(37) Richards, C. J.; Damalidis, T.; Hibbs, D. E.; Hursthouse, M. B. *Synlett* **1995**, 74-76.

(38) (a) R. Gilbertson, S.; T. Chang, C.-W. *Chem. Commun.* **1997**, 975-976 (b) Gilbertson, S. R.; Chang, C.-W. T. *J. Org. Chem.* **1998**, *63*, 8424-8431.

(39) Schrems, M. G.; Pfaltz, A. *Chem. Commun.* **2009**, 6210-6212.

(40) Dai, Q.; Li, W.; Zhang, X. *Tetrahedron* **2008**, *64*, 6943-6948.

(41) (a) Prétôt, R.; Pfaltz, A. *Angew. Chem. Int. Ed. Engl.* **1998**, *37*, 323-325 (b) Cozzi, P. G.; Zimmermann, N.; Hilgraf, R.; Schaffner, S.; Pfaltz, A. *Adv. Synth. Catal.* **2001**, *343*, 450-454.

(42) Menges, F.; Pfaltz, A. *Adv. Synth. Catal.* **2002**, *344*, 40-44.

(43) Miyazawa, T.; Otomatsu, T.; Fukui, Y.; Yamada, T.; Kuwata, S. *J. Chem. Soc. Chem. Commun.* **1988**, 419-420.

(44) Roseblade, S. J.; Pfaltz, A. *Acc. Chem. Res.* **2007**, *40*, 1402-1411.

(45) Mazuela, J.; Verendel, J. J.; Coll, M.; Schäffner, B.; Börner, A.; Andersson, P. G.; Pàmies, O.; Diéguez, M. *J. Am. Chem. Soc.* **2009**, *131*, 12344-12353.

(46) (a) Pamies, O.; Dieguez, M.; Net, G.; Ruiz, A.; Claver, C. *Chem. Commun.* **2000**, 2383-2384 (b) Pàmies, O.; van Strijdonck, G. P. F.; Diéguez, M.; Deerenberg, S.; Net, G.; Ruiz, A.; Claver, C.; Kamer, P. C. J.; van Leeuwen, P. W. N. M. *J. Org. Chem.* **2001**, *66*, 8867-8871 (c) Pàmies, O.; Diéguez, M.; Claver, C. *J. Am. Chem. Soc.* **2005**, *127*, 3646-3647 (d) Bellini, R.; Magre, M.; Biosca, M.; Norrby, P.-O.; Pàmies, O.; Diéguez, M.; Moberg, C. *ACS Catal.* **2016**, *6*, 1701-1712 (e) Magre, M.; Pàmies, O.; Diéguez, M. *ACS Catal.* **2016**, *6*, 5186-5190.

(47) (a) Newkome, G. R. *Chem. Rev.* **1993**, *93*, 2067-2089 (b) Espinet, P.; Soulantica, K. *Coord. Chem. Rev.* **1999**, *193-195*, 499-556 (c) Chelucci, G.; Orrù, G.; Pinna, G. A. *Tetrahedron* **2003**, *59*, 9471-9515.

(48) (a) Xu, Y.; Mingos, D. M. P.; Brown, J. M. *Chem. Commun.* **2008**, 199-201 (b) Yang, S.; Che, W.; Wu, H.-L.; Zhu, S.-F.; Zhou, Q.-L. *Chem. Sci.* **2017**, *8*, 1977-1980.

(49) (a) Drury, W. J.; Zimmermann, N.; Keenan, M.; Hayashi, M.; Kaiser, S.; Goddard, R.; Pfaltz, A. *Angew. Chem. Int. Ed.* **2003**, *43*, 70-74 (b) Kaiser, S.; Smidt, S. P.; Pfaltz, A. *Angew. Chem. Int. Ed.* **2006**, *45*, 5194-5197.

(50) Bunlaksananusorn, T.; Polborn, K.; Knochel, P. *Angew. Chem. Int. Ed.* **2003**, *42*, 3941-3943.

(51) (a) Källström, K.; Hedberg, C.; Brandt, P.; Bayer, A.; Andersson, P. G. *J. Am. Chem. Soc.* **2004**, *126*, 14308-14309 (b) Hedberg, C.; Källström, K.; Brandt, P.; Hansen, L. K.; Andersson, P. G. *J. Am. Chem. Soc.* **2006**, *128*, 2995-3001 (c) Kaukoranta, P.; Engman, M.; Hedberg, C.; Bergquist, J.; Andersson, P. G. *Adv. Synth. Catal.* **2008**, *350*, 1168-1176.

(52) (a) Mazuela, J.; Paptchikhine, A.; Tolstoy, P.; Pàmies, O.; Diéguez, M.; Andersson, P. G. *Chem. Eur. J.* **2010**, *16*, 620-638 (b) Biosca, M.; Paptchikhine, A.; Pàmies, O.; Andersson, P. G.; Diéguez, M. *Chem. Eur. J.* **2015**, *21*, 3455-3464.

(53) Trifonova, A.; Diesen, J. S.; Chapman, C. J.; Andersson, P. G. *Org. Lett.* **2004**, *6*, 3825-3827.

(54) Salomo, E.; Rojo, P.; Hernández-Lladó, P.; Riera, A.; Verdaguer, X. *J. Org. Chem.* **2018**, *83*, 4618-4627.

(55) Salomó, E.; Orgué, S.; Riera, A.; Verdaguer, X. *Angew. Chem. Int. Ed.* **2016**, *55*, 7988-7992.

(56) Feldgus, S.; Landis, C. R. *J. Am. Chem. Soc.* **2000**, *122*, 12714-12727.

(57) Crabtree, R. H.; Felkin, H.; Morris, G. E. *J. Chem. Soc. Chem. Commun.* **1976**, 716-717.

(58)   (a) Brown, J. M.; Chaloner, P. A. *J. Chem. Soc. Chem. Commun.* **1980**, 344-346 (b) Brown, J. M.; Chaloner, P. A. *J. Am. Chem. Soc.* **1980**, *102*, 3040-3048 (c) Brown, J. M.; Parker, D. *J. Org. Chem.* **1982**, *47*, 2722-2730 (d) Alcock, N. W.; Brown, J. M.; Derome, A. E.; Lucy, A. R. *J. Chem. Soc. Chem. Commun.* **1985**, 575-578 (e) Alcock, N. W.; Brown, J. M.; Maddox, P. J. *J. Chem. Soc. Chem. Commun.* **1986**, 1532-1534 (f) Brown, J. M.; Maddox, P. J. *J. Chem. Soc. Chem. Commun.* **1987**, 1276-1278 (g) Brown, J. M.; Maddox, P. J. *J. Chem. Soc. Chem. Commun.* **1987**, 1278-1280 (h) Ramsden, J. A.; Claridge, T. D. W.; Brown, J. M. *J. Chem. Soc., Chem. Commun.* **1995**, 2469-2471 (i) Brown, J. M. In *Handbook of Homogeneous Hydrogenation*; de Vries, J. G., Elsevier, C. J., Eds.; Wiley-VCH: Weinheim, 2007; Vol. 3 (j) Xu, Y.; Celik, M. A.; Thompson, A. L.; Cai, H.; Yurtsever, M.; Odell, B.; Green, J. C.; Mingos, D. M. P.; Brown, J. M. *Angew. Chem. Int. Ed.* **2009**, *48*, 582-585.

(59)   (a) Carmona, D.; Ferrer, J.; Lorenzo, M.; Santander, M.; Ponz, S.; Lahoz, F. J.; López, J. A.; Oro, L. A. *Chem. Commun.* **2002**, 870-871 (b) Drago, D.; Pregosin, P. S.; Pfaltz, A. *Chem. Commun.* **2002**, 286-287.

(60)   (a) Brandt, P.; Hedberg, C.; Andersson, P. G. *Chem. Eur. J.* **2003**, *9*, 339-347 (b) Church, T. L.; Rasmussen, T.; Andersson, P. G. *Organometallics* **2010**, *29*, 6769-6781 (c) Hopmann, K. H.; Bayer, A. *Organometallics* **2011**, *30*, 2483-2497.

(61)   Dietiker, R.; Chen, P. *Angew. Chem. Int. Ed.* **2004**, *43*, 5513-5516.

(62)   Fan, Y.; Cui, X.; Burgess, K.; Hall, M. B. *J. Am. Chem. Soc.* **2004**, *126*, 16688-16689.

(63)   Gruber, S.; Neuburger, M.; Pfaltz, A. *Organometallics* **2013**, *32*, 4702-4711.

(64)   Schramm, Y.; Barrios-Landeros, F.; Pfaltz, A. *Chem. Sci.* **2013**, *4*, 2760-2766.

(65)   Marcazzan, P.; Patrick, B. O.; James, B. R. *Russ. Chem. Bull.* **2003**, *52*, 2715-2721.

(66)   Martín, M.; Sola, E.; Tejero, S.; Andrés, J. L.; Oro, L. A. *Chem. Eur. J.* **2006**, *12*, 4043-4056.

(67)   (a) Landaeta, V. R.; Muñoz, B. K.; Peruzzini, M.; Herrera, V.; Bianchini, C.; Sánchez-Delgado, R. A. *Organometallics* **2006**, *25*, 403-409 (b) Balcells, D.; Nova, A.; Clot, E.; Gnanamgari, D.; Crabtree, R. H.; Eisenstein, O. *Organometallics* **2008**, *27*, 2529-2535 (c) Chen, H.-Y. T.; Wang, C.; Wu, X.; Jiang, X.; Catlow, C. R. A.; Xiao, J. *Chem. Eur. J.* **2015**, *21*, 16564-16577.

(68)   Trifonova, A.; Diesen, J. S.; Andersson, P. G. *Chem. Eur. J.* **2006**, *12*, 2318-2328.

(69)   Hopmann, K. H.; Bayer, A. *Coord. Chem. Rev.* **2014**, *268*, 59-82.

(70)   Baeza, A.; Pfaltz, A. *Chem. Eur. J.* **2010**, *16*, 4003-4009.

(71)   Tani, K.; Onouchi, J.-i.; Yamagata, T.; Kataoka, Y. *Chem. Lett.* **1995**, *24*, 955-956.

(72)   Tutkowski, B.; Kerdphon, S.; Lime, E.; Helquist, P.; Andersson, P. G.; Norrby, P.-O.; Wiest, O. *ACS Catal.* **2018**, *8*, 615-623.

(73)   Kumaran, E.; Leong, W. K. *Organometallics* **2012**, *31*, 1068-1072.

(74)   Liniger, M.; Gschwend, B.; Neuburger, M.; Schaffner, S.; Pfaltz, A. *Organometallics* **2010**, *29*, 5953-5958.

(75)   Xie, J.; Zhu, S.; Zhou, Q. *Chem. Rev.* **2011**, *111*, 1713-1760.

(76)   (a) Moessner, C.; Bolm, C. *Angew. Chem. Int. Ed.* **2005**, *44*, 7564-7567 (b) Mršić, N.; Minnaard, A. J.; Feringa, B. L.; Vries, J. G. d. *J. Am. Chem. Soc.* **2009**, *131*, 8358-8359.

(77)   (a) Willoughby, C. A.; Buchwald, S. L. *J. Am. Chem. Soc.* **1992**, *114*, 7562-7564 (b) Willoughby, C. A.; Buchwald, S. L. *J. Am. Chem. Soc.* **1994**, *116*, 8952-8965.

(78)   Blaser, H.-U. *Adv. Synth. Catal.* **2002**, *344*, 17-31.

(79)   Zhou, S.; Fleischer, S.; Junge, K.; Beller, M. *Angew. Chem. Int. Ed.* **2011**, *50*, 5120-5124.

(80)   Li, C.; Wang, C.; Villa-Marcos, B.; Xiao, J. *J. Am. Chem. Soc.* **2008**, *130*, 14450-14451.

(81)   Doogan, D. P.; Caillard, V. *J. Clin. Psychiatry* **1988**, *49 Suppl*, 46-51.

(82)   Parkes, J. D.; Fenton, G. W. *J. Neurol., Neurosurg. Psychiatry* **1973**, *36*, 1076-1081.

(83)   Finkel, S. I. *Clin. Ther.* **2004**, *26*, 980-990.

(84)   Torres, P. U. *J. Renal Nutr.* **2006**, *16*, 253-258.

(85)   (a) Noyori, R. *Asymmetric Catalysis in Organic Synthesis*; Wiley and Sons, Inc.: New York, 1994 (b) Blaser, H.-U.; Federsel, H.-J.; Ed. *Asymmetric Catalysis on Industrial Scale: Challenges, Approaches and Solutions*; 2 ed.; Wiley, 2010 (c) Andersson, P. G.; Munslow, I. J. In *Modern Reduction Methods*; Wiley-VCH: Weinheim, 2008.

(86)   (a) Verdaguer, X.; Lange, U. E. W.; Reding, M. T.; Buchwald, S. L. *J. Am. Chem. Soc.* **1996**, *118*, 6784-6785 (b) Wakchaure Vijay, N.; Kaib Philip, S. J.; Leutzsch, M.; List, B. *Angew. Chem. Int. Ed.* **2015**, *54*, 11852-11856.

(87)   Verdaguer, X.; Lange Udo, E. W.; Buchwald Stephen, L. *Angew. Chem. Int. Ed.* **1998**, *37*, 1103-1107.

(88)   (a) Abdur-Rashid, K.; Lough, A. J.; Morris, R. H. *Organometallics* **2001**, *20*, 1047-1049 (b) Rautenstrauch, V.; Hoang-Cong, X.; Churlaud, R.; Abdur-Rashid, K.; Morris, R. H. *Chem. Eur. J.* **2003**, *9*, 4954-4967.

(89)   (a) Rueping, M.; Sugiono, E.; Azap, C.; Theissmann, T.; Bolte, M. *Org. Lett.* **2005**, *7*, 3781-3783 (b) Hoffmann, S.; Seayad, A. M.; List, B. *Angew. Chem. Int. Ed.* **2005**, *44*, 7424-7427 (c) Storer, R. I.; Carrera, D. E.; Ni, Y.; MacMillan, D. W. C. *J. Am. Chem. Soc.* **2006**, *128*, 84-86 (d) Saito, K.; Akiyama, T. *Chem. Commun.* **2012**, *48*, 4573-4575.

(90)   Fleury-Brégeot, N.; de la Fuente, V.; Castillón, S.; Claver, C. *ChemCatChem* **2010**, *2*, 1346-1371.

Chapter VI. Experimental section

6.   Experimental Section

6.1. *General remarks*

All air- and moisture-sensitive compounds such as Grignard reagents, organolithiums, free phosphines and their precursors were prepared under a purified nitrogen atmosphere using standard *Schlenk* and vacuum-line techniques. All solvents were obtained from a solvent purification system (PURESOLV™) or purified by standard procedures and distilled under nitrogen atmosphere.[1] All reagents were used as received from commercial suppliers: Aldrich, TCI, Strem and Across without further purification, unless otherwise stated. Et_3N was distilled from CaH_2 and collected over 4 Å molecular sieves before use. Some reactions were monitored by Thin Layer Chromatography (TLC) using aluminium sheets of Merck silica gel 60 F_{254}, being UV light (λ = 254 nm) the most used revelator. Silica gel chromatography was performed by using 35-70 mm of SiO_2. Molecular sieves were activated in an oven heating at 350 ºC during 7-10 hours. The, the activated molecular sieves were stored at 110 ºC.

For low temperature baths, cryogenic mixtures of CO_2(s)/acetone have been used for –78 ºC and ice-water for 0 ºC. For long reactions (more than 5 hours) Cryocool CC-100 system and 2-propanol as solvent were employed instead.

6.2. *Instrumentation*

All the compounds were characterized by means of habitual spectroscopic techniques: Nuclear Magnetic Resonance (NMR), and infrared spectroscopy (IR). Non-spectroscopic techniques were also used: Elemental Analysis (EA), Gas Chromatography (GC), High Performance Liquid Chromatography (HPLC), Mass Spectrometry (MS), polarimetry, Circular Dichroism (CD), and Melting Point (MP). X-Ray Diffraction (XRD) was performed in order to determine solid-state structures.

6.2.1. *Nuclear Magnetic Resonance (NMR)*

Nuclear Magnetic Resonance (NMR) spectra were recorded at the *Unitat d'RMN* of the *Universitat de Barcelona*.

^{1}H, ^{13}C{^{1}H}, ^{31}P{^{1}H}, ^{19}F and HSQC ^{1}H–^{13}C NMR spectra were recorded on Bruker 400 and Varian Mercury 400 spectrometers at room temperature using CDCl$_3$ as solvent unless otherwise specified. The fields are 400 MHz (^{1}H), 101 MHz (^{13}C{^{1}H}), 162 MHz (^{31}P{^{1}H}) and 376 MHz (^{19}F). Deuterated solvents (CDCl$_3$, CD$_2$Cl$_2$, C$_6$D$_6$, CD$_3$OD, CD$_3$COCD$_3$, D$_2$O, DMSO-d_6, toluene-d_8, THF-d_8) have a deuteration percentage of at least 99%.

Chemical shifts are reported downfield in units of δ (ppm) from the following standards: tetramethylsilane (TMS) for ^{1}H NMR and ^{13}C{^{1}H} NMR spectra; orthophosphoric acid (85% H$_3$PO$_4$) for ^{31}P{^{1}H} NMR and trichlorofluoromethane (CFCl$_3$) for ^{19}F NMR spectra. A 1% solution of trimethylphosphite (TMP) in deuterated benzene was also used as external reference (140.1 ppm) for ^{31}P{^{1}H} NMR.

Coupling constants (J) are expressed in Hertz (Hz). The following abbreviations are used for multiplicities: *s*, singlet; *d*, doublet; *t*, triplet; *q*, quadruplet; *dd*, doublet of doublets; *dt*, doublet of triplets; *td*, triplet of doublets; *tt*, triplet of triplets *qd*, quadruplet of doublets; *ddd*, doublet of doublets of doublets; *m*, multiplet; *bs*, broad signal; *bq*, broad quadruplet; and *p*, pseudo.

In the case of ^{1}H NMR, and ^{31}P{^{1}H} NMR spectra of phosphine-boranes the quadrupolar moment of boron produces broadening of the signals coupled with boron. Estimation of J_{BP} and J_{BH} has been made selecting the two central signals that are usually better resolved.

6.2.2. *Infrared spectroscopy (IR)*

Infrared spectra were carried out in a solid suspension of KBr using a FTIR Nicolet Nexus 5700 and Nicolet Avatar 300 FT-IR spectrophotometers at the *Departament de Química Inorgànica i Orgànica, Secció de Química Inorgànica*, of the *Universitat de Barcelona*. Regarding the spectra description, only the bands corresponding to C–H, B–H, P–F and B–F are assigned, because they are characteristic and easy to identify. Other bands are not assigned even though the most intense absorption bands are registered by their wave number, ν, and expressed in cm^{-1} among the spectral range of 4000-400 cm^{-1}.

6.2.3. *Elemental Analysis (EA)*

Elemental analyses (C, H, N) were performed in an EA-1108 CE Instruments (Thermo Fisher) apparatus at the *Servei d'Anàlisi Elemental dels Centres Científics i Tecnològics* of the *Universitat de Barcelona*. Organometallic compounds were analysed using WO_3 or SeO as combustion catalysts.

6.2.4. *Mass spectrometry (MS)*

Electrospray ionisation (ESI) mass spectra were performed at the *Servei d'Espectrometria de Masses* of the *Universitat de Barcelona*. They were acquired on a ZQ mass spectrometer (Micromass, UK) by direct introduction of the sample with a Rheodyne injector and using as eluent a $H_2O{:}CH_3CN$ (1:1) mixture under a flow of 100 μL/min. High-resolution mass analyses (HRMS) were carried out in a LC/MSD-TOF mass spectrometer using electrospray ionisation. The sample was introduced through an HPLC Agilent 1100 pumping system and using as eluent a $H_2O{:}CH_3CN$ (1:1) mixture under a flow of 200 μL/min, and purine (121.0509 g/mol) and HP-0921 (922.0098 g/mol) as internal reference masses. Unstable samples were dissolved in acetone (0.1 mM) and introduced via a syringe pump with a flow rate of 200 mL/h. Nitrogen was used as nebulizing and drying gas. Drying gas temperature was held at RT. Nebulizing and drying gas flows, capillary exit, and skimmer voltages and hexapol accumulation times were readjusted for each sample to obtain very soft ionization conditions and minimize fragmentation during the ESI process. For each measurement, 16–500 scans were averaged to improve the signal-to-noise ratio.

6.2.5. *Polarimetry*

Optical rotations were measured with a Perkin-Elmer 241MC polarimeter at 23 °C using a sodium lamp at the sodium D-line wavelength (589.592 nm). The solvent and the concentration (g/100 mL) for each compound are indicated in parentheses.

6.2.6. *Circular dichroism (CD)*

CD spectra of some compounds were determined in acetone ($\sim$5 × 10^{-4} mol/L solutions) in a 1 cm path length cell by using a JASCO J-810 spectropolarimeter. All measurements have been carried out in collaboration with Dr. Daniel Carmona in the *Instituto de Síntesis Química y Catálisis Homogénea (ISQCH), CSIC - Universidad de Zaragoza.*
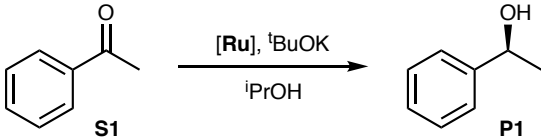
6.2.7. *X-ray diffraction analyses (XRD)*

All the X-ray analyses have been carried out in the X-ray diffraction unit of the ICIQ (*Institut Català d'Investigació Química*) in Tarragona by Dr. Eduardo C. Escudero-Adán, using a Bruker D8 venture diffractometer.

6.2.8. *Gas Chromatography (GC)*

In this section a detailed description of the conditions of the gas chromatography analyses for those substrates and products studied in the different catalytic processes is presented.

6.2.8.1. *Asymmetric transfer hydrogenation of acetophenone*

Chromatograph	HP 5890 detector FID
Capillary chiral column	Chiraldex DM
Column head pressure	100 kPa (He)
Length	30 m x 0.25 mm
Temperature programme	120 ºC isothermal, 30 min
t_R, **S1**	7.4 min
t_R, (*R*)-**P1**	12.3 min
t_R, (*S*)-**P2**	12.8 min

6.2.8.2. *Asymmetric Mizoroki-Heck reaction of cyclopentene*

Chromatograph	HP 5890 detector FID
Capillary chiral column	Chiraldex DM
Column head pressure	100 kPa (He)
Length	30 m x 0.25 mm
Temperature programme	150 ºC isothermal, 70 min
t_R, **S2'**	40.2 min
t_R, **(*R*)-P2**	37.6 min
t_R, **(*S*)-P2**	38.3 min

6.2.8.3. *Asymmetric Mizoroki-Heck reaction of dihydrofuran*

Chromatograph	HP 5890 detector FID
Capillary chiral column	Chiraldex DM
Column head pressure	100 kPa (He)
Length	30 m x 0.25 mm
Temperature programme	150 ºC isothermal, 70 min
t_R, **S2'**	44.5 min
t_R, **(*R*)-P3**	38.6 min
t_R, **(*S*)-P3**	40.1 min
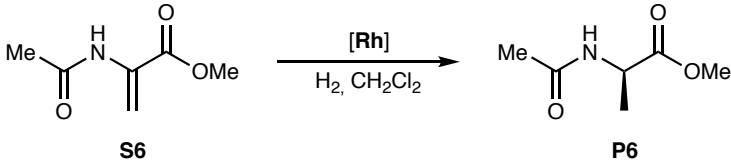
6.2.8.4. *Allylic alkylation of cinnamyl acetate*

Chromatograph	Agilent 6890N detector FID
Capillary chiral column	HP-5% PhMeSiloxane
Column head pressure	100 kPa (He)
Length	30 m x 0.32 mm
Temperature programme	80 ºC, 2 min → 280 ºC, 40 min
t_R, **S4**	7.4 min
t_R, **P4'**	8.7 min
t_R, **P4**	9.9 min
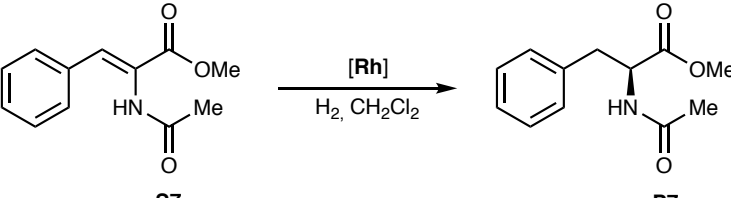
6.2.8.5. *Asymmetric hydrogenation of dimethyl itaconate (DMI)*

Chromatograph	HP 5890 detector FID
Capillary chiral column	Chiraldex DM
Column head pressure	100 kPa (He)
Length	30 m x 0.25 mm
Temperature programme	80 ºC isothermal, 30 min
t_R, **S5**	29.7 min
t_R, (*R*)-**P5**	21.7 min
t_R, (*S*)-**P5**	22.2 min

6.2.8.6. *Asymmetric hydrogenation of methyl α-acetamidoacrylate (MAA)*

Chromatograph	HP 5890 detector FID
Capillary chiral column	Chirasil-L-Val
Column head pressure	100 kPa (He)
Length	25 m x 0.25 mm
Temperature programme	180 ºC isothermal, 30 min
t_R, **S6**	1.99 min
t_R, (*R*)-**P6**	2.15 min
t_R, (*S*)-**P6**	2.18 min

6.2.8.7. *Asymmetric hydrogenation of methyl (Z)-α-acetamidocinnamate (MAC)*

Chromatograph	HP 5890 detector FID
Capillary chiral column	Chirasil-L-Val
Column head pressure	150 kPa (He)
Length	25 m x 0.25 mm
Temperature programme	180 ºC isothermal, 30 min
t_R, **S7**	10.9 min
t_R, (*R*)-**P7**	4.82 min
t_R, (*S*)-**P7**	5.12 min

6.2.8.8. *Asymmetric hydrogenation reaction of geraniol*

Chromatograph	HP 5890 detector FID
Capillary chiral column	β-Dex 225
Column head pressure	100 kPa (He)
Length	25 m x 0.25 mm
Temperature programme	95 ºC isothermal, 70 min
t_R, **S8**	60 min
t_R, (**R**)-**P8**	53.0 min
t_R, (**S**)-**P8**	52.0 min

6.2.8.9. *Hydrogenation of styrene*

Chromatograph	Agilent 6890N detector FID
Capillary chiral column	HP-5% PhMeSiloxane
Column head pressure	100 kPa (He)
Length	30 m x 0.32 mm
Temperature programme	40 ºC, 2 min → 250 ºC, 20 min
t_R, **S9**	5.1 min
t_R, **P9**	5.9 min

6.2.9. *High Performance Liquid Chromatography (HPLC)*
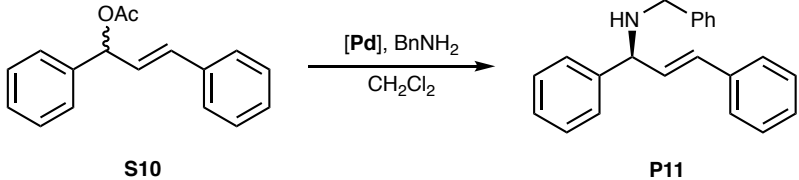
6.2.9.1. *Asymmetric allylic substitution reactions*

HPLC analyses of the allylic substitution products were carried out in a Waters 717 Plus autosampler chromatograph with a Waters 996 multidiode array detector, fitted with a Chiracel OD-H chiral column. The eluent was a mixture of *n*-hexane and ^{i}PrOH (95:5) in all the determinations. In all cases, 10 mg of product were dissolved in 20 mL of the eluent and subsequently filtered before the injection of the sample. The specific conditions are depicted below.

6.2.9.2. *Asymmetric allylic alkylation of rac-(E)-3-acetoxy-1,3-diphenyl-1-propene*

Eluent	95:5 *n*-hexane/^{i}PrOH
Flux	0.5 mL/min
Column head pressure	300-350 psi
Temperature programme	25 ºC, 30 min
t_R, (*S*)-**S10**	11.8 min
t_R, (*R*)-**S10**	12.7 min
t_R, (*R*)-**P10**	13.8 min
t_R, (*S*)-**P10**	14.5 min

6.2.9.3. *Asymmetric allylic amination of rac-(E)-3-acetoxy-1,3-diphenyl-1-propene*

Eluent	99:1 *n*-hexane/PrOH
Flux	0.3 mL/min
Column head pressure	210-240 psi
Temperature programme	25 ºC, 50 min
t_R, (*S*)-**S10**	25.1 min
t_R, (*R*)-**S10**	27.4 min
t_R, (*R*)-**P11**	28.8 min
t_R, (*S*)-**P11**	29.9 min

6.2.9.4. *Asymmetric hydrogenation of imines*
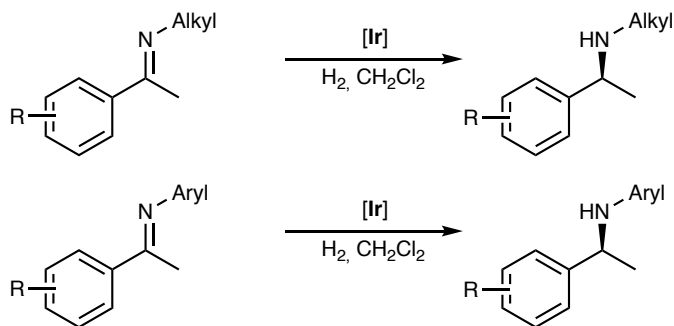
HPLC analyses of the chiral amines have been done using a Hewlett-Packard 1050 equipment by Enantia S.L. Conditions of each analysis are specified in section 6.4.3 of this chapter.

6.3. *Catalytic procedures*

6.3.1. *Transfer hydrogenation reactions*

A 50 mL *Schlenk* flask was charged with the ruthenium precursor (0.02 mmol) and potassium *tert*-butoxide (11.2 mg, 0.1 mmol) and was purged with three vacuum/argon cycles. Under a gentle flow of argon, 25 mL of 2-propanol were added and the flask was heated to reflux (85 ºC) for 15 min. After this time, acetophenone, (**S1**, 0.468 mL, 4.0 mmol) was rapidly added to start the catalytic run. The reaction was monitored at the allotted times by taking aliquots of around 0.1 mL and analysing them by GC.[2]

6.3.2. *Mizoroki-Heck reactions*

A 10 mL microwave vial containing a non-oriented edge spinner was charged with the Pd precursor (0.02 mmol), the substrate olefin (**S2**, **S3**) (1.2 mmol), 4-iodoacetophenone (0.4 mmol), diisopropylethylamine (1.2 mmol) and dodecane (0.4 mmol) in 6 mL of DMF. The vial was then introduced into an Anton Paar Monowave 300 microwave synthesis reactor. The vial was heated up to 100 ºC in two minutes and then maintained during 6 hours with continuous stirring (600 rpm) at this temperature. After this time the vial was cooled to 50 ºC and the reaction crude was filtered through a small plug of silica eluting with DMF. Conversion and enantioselectivity was determined by GC.

For the *in situ* experiments, the 10 mL microwave vial was charged with a solution of Pd(OAc)$_2$ or PdCl$_2$ (0.02 mmol) and ligand **L1** (0.08 mmol) in 3 mL of DMF. After stirring 15 min, a solution of the substrate olefin (**S2** or **S3**) (1.2 mmol), 4-iodoacetophenone (0.4 mmol), diisopropylethylamine (1.2 mmol) and dodecane (0.4 mmol) in 4 mL of DMF was added. Then, the vial was introduced in the microwave synthesis reactor, and heated up to in two minutes and then maintained during 6 hours with continuous stirring (600 rpm) at this temperature. After this time the vial was cooled to 50 ºC and the reaction crude was filtered through a small plug of silica eluting with DMF. Conversion and enantioselectivity was determined by GC.

6.3.3. *Allylic alkylation reactions of cinnamyl acetate*

A 25 mL *Schlenk* tube under nitrogen at room temperature was charged with the Pd precursor (0.01 mmol) and then 1 mL of CH_2Cl_2 was added. Once the Pd complex was dissolved, cinnamyl acetate, (**S4**, 1 mmol) was added. After 5 min stirring dimethyl malonate (3 mmol), BSA (3 mmol) and KOAc (1 mg) were dissolved, in this precise order, in 5 mL of CH_2Cl_2 and added to the previous solution. The reaction mixture was allowed to stir at room temperature for the desired time. Then, the solution was diluted with diethyl ether (20 mL) and washed with a saturated ammonium chloride solution (3 x 10 mL) and water (3 x 10 mL). The organic phase was dried over anhydrous Na_2SO_4 and filtered off, and the solvent was removed under reduced pressure. Conversion was determined by ^{1}H NMR spectroscopy. Purification of the product was performed by column chromatography using SiO_2 and ethyl acetate as eluent. Conversion and the regioisomeric ratio (linear/branched) were determined by GC.[3]

6.3.4. *Allylic alkylation reactions with dimethyl malonate*

Under a nitrogen atmosphere, the appropriate Pd complex (0.01 mmol), precursor *rac*-(*E*)-3-acetoxy-1,3-diphenyl-1-propene, **S10**, (1 mmol), dimethyl malonate (3 mmol), BSA (3 mmol) and KOAc (1 mg) were dissolved in dichloromethane (5 mL) in this precise order. The flask was covered with aluminium foil, and the mixture was stirred for the allotted time. To quench the reaction, diethyl ether (20 mL) and aqueous 10% ammonium chloride solution (20 mL) were added. After extraction, the organic phase was dried with anhydrous sodium sulfate, filtered and the solvent was removed *in vacuo*. The crude product was analysed by ^{1}H NMR spectroscopy to estimate the conversion. The crude product was dissolved in ethyl acetate, and the solution was purified through a column of silica to remove the metallic impurities. The eluent was then removed *in vacuo* and the residue was analysed by NMR spectroscopy and HPLC.[4]

6.3.5. *Allylic amination reactions with benzylamine*

Under a nitrogen atmosphere, the Pd precursor (0.01 mmol), substrate *rac*-(*E*)-3-acetoxy-1,3-diphenyl-1-propene, **S10**, (1 mmol) and benzylamine (3 mmol) were dissolved, in this precise order, in 5 mL of dichloromethane. The flask was covered with aluminium foil, and left stirring for the allotted time. In order to quench the reaction, diethyl ether (20 mL) and aqueous 10% ammonium chloride solution (20 mL) were added. After extraction, the organic phase was dried with anhydrous sodium sulphate, filtered and the solvent was removed *in vacuo*. The crude product was analysed by ^{1}H NMR spectroscopy to estimate the conversion. The crude product was dissolved in ethyl acetate and the solution was purified through a column of silica to remove the metallic impurities. The eluent was then removed *in vacuo*, and the residue was analysed by NMR spectroscopy and HPLC.[4]

6.3.6. *Asymmetric olefin hydrogenation reactions*

Hydrogenation reactions at 50 bar of hydrogen pressure were carried out in a 50 mL stainless steel autoclave, while experiments until 3 bar of hydrogen pressure were carried out in a Fischer–Porter glass tube. In both cases the reactor was carefully dried in the oven and purged with H_2 prior to use.

When the reaction was carried out with the preformed precursor, a mixture of 0.01 mmol of [Rh] and 1.0 mmol of substrate **S5**, **S6**, **S7** or **S8** were dissolved in 20 mL of CH_2Cl_2 in a *Schlenk* tube under nitrogen. The solution was stirred at room temperature for 10 min and was then transferred into the reactor. For the *in situ* experiments a solution of the ligand **L1** (0.022 mmol) and [Rh(COD)$_2$]BF$_4$ (0.01 mmol) in CH_2Cl_2 (5 mL) was stirred under nitrogen for 15 min at room temperature. Then, a solution of substrate **S5**, **S6**, **S7** or **S8** (1.0 mmol) in 15 mL of CH_2Cl_2 was added and the resulting mixture was transferred into the reactor. For both cases the reactor was pressurized with 3 bar of H_2 and stirred at 800 rpm. After the desired time, the hydrogen pressure was carefully released. The reaction mixture was filtered through a short pad of silica, eluted with dichloromethane, and subjected to conversion and *ee* determination by chiral GC or HPLC analyses.[5]

311

6.3.7. *Styrene hydrogenation reactions*

A 10 mL *Schlenk* flask was charged with the Ir precursor **L3RIr6** (0.001 mmol) and a solution of styrene, **S9**, (0.1 mmol) in 5 mL of CH_2Cl_2. After stirring the resulting solution for 10 min, it was transferred into the reactor. Then, the reactor was filled with 3 bar of H_2 and stirred at 800 rpm. After the desired time, the hydrogen pressure was carefully released. The reaction mixture was filtered through a short pad of silica, eluted with dichloromethane, and subjected to conversion and *ee* determination by GC.

6.3.8. *Asymmetric hydrogenation of imines*

6.3.8.1. *General procedure for the asymmetric hydrogenation of N-aryl imines*

In a 10 mL glass vial containing a magnetic stirrer, a mixture of [Ir(COD)Cl]$_2$ (0.005 mmol), the SPO ligand **L1** (0.02 mmol) and the substrate (0.5 mmol) were dissolved in toluene (3 mL). The vial was placed in an autoclave and purged 3 times with N_2 and 3 times with H_2. The autoclave was pressurized with hydrogen to 20–25 bar and the reaction was stirred at room temperature unless otherwise stated. After the allotted time, the autoclave was carefully opened and the hydrogen pressure slowly released. The solution of the vial was transferred to a 10 mL round bottle flask and the solvent was evaporated to dryness under reduced pressure. Both conversion and selectivity were determined by ^{1}H NMR. For the *ee* determination, the amines were derivatised to the corresponding *N*-acetylated amines with trifluoroacetic anhydride (3 eq) and pyridine (6 eq). After filtration through a short silica pad and eluting with dichloromethane, the filtrate was analysed by HPLC.[6]

6.3.8.2. *General procedure for the asymmetric hydrogenation of N-alkyl imines*

The appropriate Ir(III) complex ($3.13 \cdot 10^{-3}$ mmol, 0.01 eq) was placed in a glass pressure tube, purged with vacuum-nitrogen cycles and 2 mL of CH_2Cl_2 were added. The tube was then purged with vacuum-hydrogen cycles and charged with 3 bar of H_2. When required, the tube was cooled down to the desired temperature. The corresponding *N*-alkyl imine (0.313 mmol, 1.00 eq) was dissolved in 1 mL of CH_2Cl_2 and added using a pressure syringe. The mixture was left stirring overnight at the desired temperature. The tube was depressurized and the solvent removed under vacuum to afford the corresponding hydrogenated compound as a dark yellow oil or

solid. The *ee* value was determined by HPLC/GC analysis of the corresponding trifluoroacetamide derivative on a chiral stationary phase.

For the *in situ* experiments, 5 mg of catalyst **L3RIr** ($3.45 \cdot 10^{-3}$ mmol, 0.01 eq) and the corresponding additive **I1** (0.345 mmol, 0.02 eq) were placed in glass pressure tube. The tube was purged with vacuum-nitrogen cycles and then 2 mL of CH_2Cl_2 were added. The tube was the purged with vacuum-hydrogen cycles and charged with 3 bar of H_2. The mixture was left to stir for 30 min at room temperature to form the iridacycle. *N*-methyl-1-phenylethanimine (1 eq) was dissolved in 1 mL of CH_2Cl_2 and added using a pressure syringe. The mixture was left stirring overnight. The tube was depressurized and the solvent removed under vacuum to afford the hydrogenated compounds as dark yellow oils.

6.4. *Preparation of the ligands*

6.4.1. *Synthesis of the enantiomerically enriched precursors*

(2*R*,3*aS*,8*aR*)-2-*tert*-butyl-3,3*a*,8,8*a*-tetrahydro-2*H*-indeno[1,2-*d*][1,3,2]oxazaphosphole-borane, O1[7]
To a solution of (1*S*,2*R*)-(–)-*cis*-1-amino-2-indanol (5.00 g, 33.6 mmol) in THF (50 mL) was added ^{t}BuPCl$_2$ (35.3 mmol).
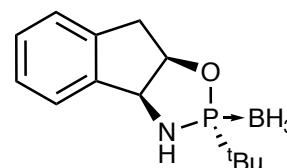
After 30 min at room temperature, the mixture was refluxed for 8 hours. Then, the crude was cooled to 0 °C, borane-dimethylsulfide adduct (4.80 mL, 50.40 mmol) was added and the reaction was let to stir for 30 min. The reaction was quenched with saturated NH$_4$Cl at room temperature and extracted with EtOAc (4 x 20 mL) and the combined organic layer was dried with anhydrous magnesium sulfate, filtered, and concentrated under vacuum. The resulting crude was crystallized with *n*-hexane yielding 4.51 g of diastereomerically pure white crystals. From the mother liquors, a second crop was obtained after purification by column chromatography (SiO$_2$, *n*-hexane:EtOAc gradient), giving an overall yield of 6.51 g (78%).
^{1}H NMR: 7.37–7.33 (m, 1H), 7.25–7.32 (m, 2H), 7.19–7.24 (m, 1H), 5.38 (ddd, *J* = 10.0, *J* = 7.0, *J* = 4.0, 1H), 4.85 (m, 1H), 3.39 (dd, *J* = 18.0, *J* = 7.0, 1H), 3.27 (dd, *J* = 18.0, *J* = 4.0, 1H), 2.61 (m, NH), 1.17 (d, *J* = 15.0, 3xCH3), 0.90–0.03 (m, BH3).
^{31}P{^{1}H} NMR: +167.9 (m).

(1*S*,2*R*)-1-(*tert*-butyl(methyl)phosphinoamino)-2,3-dihydro-1*H*-inden-2-ol-borane, O2[7]

To a solution of **O1** (1.00 g, 4.01 mmol) in toluene at 100 °C, methylmagnesium chloride in Et_2O 3 M (3.00 mL, 8.82 mmol) was added in three portions of 1 equivalent each. Each portion was added every 30 minutes.
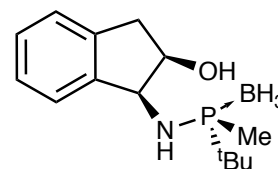
The reaction flask was cooled to 0 °C, a saturated solution of NH_4Cl was then added, and after stirring a few minutes; the solution was extracted with EtOAc. The combined organic layers were dried with anhydrous magnesium sulfate, filtered, and concentrated under vacuum. Column chromatography on silica gel (*n*-hexane:EtOAc gradient) yielded 964 mg (91%) of the product as a white solid.

^{1}H NMR: 7.41–7.35 (m, 1H), 7.32–7.24 (m, 3H), 4.78 (td, *J* = 10.0, *J* = 5.0, 1H), 4.51 (td, *J* = 5.0, *J* = 1.0, 1H), 3.11 (dd, *J* = 17.0, *J* = 5.0, 1H), 2.91 (dd, *J* = 17.0, *J* = 1, 1H), 2.30–2.11 (m, 2H), 1.47 (d, *J* = 9.0, 3H), 1.29 (d, *J* = 14.0, 3xCH3), 1.08–0.20 (m, BH3).

^{31}P{^{1}H} NMR: +71.1 (m). HPLC analysis: CHIRALPAK IA, 10% EtOH, 90% heptane, 0.5 mL/min, λ = 254 nm, $t_R(S)$ = 16.7 min, $t_R(R)$ = 20.3 min.

(*S*)-*tert*-butyl(methyl)phosphanamine-borane, (*S*)-L1·NH₂[8]

Ammonia (180 mL) was condensed in a two-neck flask at –78 °C. Small portions of Li (183 mg, 28.26 mmol) were then added. The mixture was stirred for 10 min and the solution turned blue.
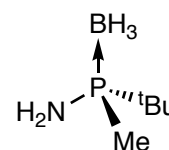
A solution of **O2** (1.88 g, 7.06 mmol) in THF (20 mL) and [t]BuOH (1.3 mL) was then added dropwise. After 10 min solid NH_4Cl was added and the flask was left open in the hood to evacuate the ammonia. At this point, 10 mL of water were added and the aqueous layer was washed twice with 10 mL of EtOAc. The combined organic extracts were dried with anhydrous $MgSO_4$, filtered, and concentrated under reduced pressure. Column chromatography on silica gel (*n*-hexane:EtOAc gradient) yielded 730 mg (78%) of the product as a white solid.

^{1}H NMR: 1.76 (s, 2H), 1.35 (d, J_P = 9.0, 3H), 1.14 (d, J_P = 14.0, 9H), 0.86–0.08 (m, 3H, BH3) **^{13}C{^{1}H} NMR**: 29.9 (d, J_P = 40.0, C), 24.3 (d, J_P = 3.0, 3xCH3), 11.0 (d, J_P = 38.0, CH3). **^{31}P{^{1}H} NMR**: +64.3 (q, J_P = 69.0, P-BH3). **HRMS**: calcd. for $C_5H_{18}BNP$ [M–H][+]; 132.1113, found 132.1108.

(*R*)-*tert*-butyl(methyl) phosphinous acid-borane, (*R*)-L1·OH[9]
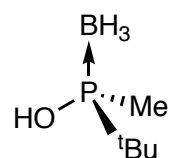
A) From (1*S*,2*R*)-1-(*tert*-butyl(methyl)phosphinoamino)-2,3-dihydro-1*H*-inden-2-ol-borane, O2[7]

Aminophosphine-borane O2 (1.00 g, 7.5 mmol) was dissolved in a mixture of methanol (40 mL) and water (2 mL). Sulfuric acid (96 wt. % in H_2O) (4 eq, 1.7 mL, 30.0 mmol) was slowly added dropwise and the solution was warmed up to 50 °C and stirred for 2 h. Most of the methanol was removed *in vacuo* and the aqueous crude was extracted with Et_2O (5 x 5 mL). The combined organic phases were washed with brine and dried over anhydrous $MgSO_4$. The solution was then evaporated to dryness under a nitrogen stream, yielding 0.98 g (98%) of (*R*)-L1·OH as a colourless oil.

B) From (*S*)-*tert*-butyl(methyl)phosphanamine-borane, (*S*)-L1·NH₂[8]

Aminophosphine-borane (*S*)-L1·NH₂ (2.00 g, 7.5 mmol), was dissolved in a mixture of methanol (40 mL) and water (2 mL). Sulfuric acid (96 wt. % in H_2O) (4 eq, 1.7 mL, 30.0 mmol) was slowly added dropwise and the solution was warmed up to 80 °C and stirred for 16 h. Most of the methanol was removed *in vacuo* and the aqueous crude was extracted with Et_2O (5 x 5 mL). The combined organic phases were washed with brine and dried over anhydrous $MgSO_4$. The solution was then evaporated to dryness under a nitrogen stream, yielding 0.97 g (97%) of (*R*)-L1·OH as a colourless oil.

^{1}H NMR: 1.45 (d, J_P = 9.0, 3H), 1.17 (d, J_P = 14.0, 9H), 0.60 (qd, J_P = 94.0, J_P = 15.0, 3H, BH₃). **^{13}C{^{1}H} NMR**: 30.9 (d, J_P = 41.0, C), 24.1 (d, J_P = 4.0, 3xCH₃), 11.0 (d, J_P = 38, CH₃). **^{31}P{^{1}H} NMR**: +121.1 (q, J_P = 69.0, P-BH₃). **HRMS**: calcd. for $C_5H_{16}BOP$ [M–H–BH₃]⁺, 121.0777; found 121.0777.

Diisopropylammonium   **(*R*)-*tert-***

butyl(methyl)phosphinite-borane, (*R*)-L1·O[10]

Phosphinous acid-borane, (*R*)-L1·OH (50 mg, 0.37 mmol)
was placed in a vial and dissolved in 0.5 mL of pentane at 0 °C.
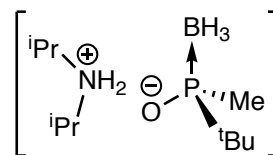
Then, diisopropylamine (1 eq, 0.37 mmol) was added dropwise via a syringe, and the
resulting white suspension was kept in the fridge overnight. The resulting crystalline
precipitate was filtered and dried under a stream of nitrogen (83 mg, 96%).

^{1}H NMR: 7.43 (s, 1H), 3.27–3.16 (m, 2H), 1.29 (d, J = 6.0, 12H), 1.22 (d, J_P = 9.0, 3H),
1.09 (d, J_P = 13.0, 9H), 0.79–0.01 (m, 3H, BH$_3$). **^{13}C{^{1}H} NMR**: 46.6 (s, 2xCH), 30.9
(d, J_P = 43.0, C), 24.6 (s, 3xCH$_3$), 21.0 (d, J_P = 11.0, 4xCH$_3$), 13.3 (d, J_P = 35.0, CH$_3$).
^{31}P{^{1}H} NMR: +92.3 (m). **HRMS**: calcd. For C$_5$H$_{15}$OBP, [M]$^+$, 133.0959; found
133.0959. **IR**: 3439, 2923, 2860, 2388 and 2342. **[α]$_D$** = −6.1° (c 1.0, CHCl$_3$).

6.4.2. *Synthesis of the optically pure ligands*

(*R*)-*tert*-butyl(methyl)phosphine oxide tetrafluoroborate,
(*R*)-L1·BF$_3$

(*R*)-*tert*-butyl(methyl)phosphinous acid-borane (*R*)-L1·OH (123
mg, 0.92 mmol) was dissolved in CH$_2$Cl$_2$ (4 mL) and HBF$_4$·OEt$_2$ (0.14 mL, 1.01 mmol)
was added dropwise at 0 °C. The solution was stirred at this temperature for 40 min.
Aqueous solution of HBF$_4$ (10%) (2 mL) was added and the two phases were
separated, the aqueous phase was extracted with CH$_2$Cl$_2$ (2 x 5 mL) and the combined
organic layers were dried with Na$_2$SO$_4$ and concentrated *in vacuo*. Et$_2$O was added and
the formation of a white solid was observed. Filtration yielded 50 mg (29%) of the
product as a white solid. (*R*)-L1·BF$_3$ was prepared analogously starting from (*R*)-L1.
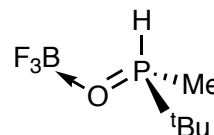
^{1}H NMR: 6.72 (dq, J_{HP} = 497.0, J_{HH} = 4.0, 1H), 1.86 (dd, J_{HP} = 13.0, J_{HH} = 4.0, 3H),
1.31 (d, J_{HP} = 19.0, 9H). **^{13}C{^{1}H} NMR**: 29.9 (d, J_{CP} = 70.0, C), 23.0 (d, J_{CP} = 3.0,
3CH$_3$), 6.1 (d, J_{CP} = 60.0, CH$_3$). **^{31}P{^{1}H} NMR**: +62.9 (d, br, J_{PF} = 9.0). **^{19}F NMR**: −
147.80 (d, J_{FP} = 9.0). **HRMS**: calcd. for C$_{10}$H$_{27}$O$_2$P$_2$ 2([M] − BF$_3$)$^+$, 241.1481; found,
241.1478. **EA**: Anal. calcd. for C$_5$H$_{13}$BF$_3$OP, %: C, 31.95; H, 6.97. Found, %: C, 32.39;
H, 7.33. **IR**: 2969, 2932, 1476, 1308, 1086, 901, 826. **[α]$_D$** = +12.3° (c 1.0, CHCl$_3$).

(*R*)-*tert*-butyl(methyl)phosphine oxide, (*R*)-L1
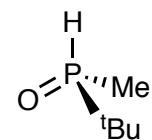
Method 1: (*R*)-*tert*-butyl(methyl)phosphinous acid-borane (*R*)-L1·OH (700 mg, 5.22 mmol) was dissolved in CH_2Cl_2 (15 mL) and HBF_4·OEt_2 (0.78 mL, 5.74 mmol) was added dropwise at 0 ºC. The solution was stirred at this temperature for 30 min, saturated aqueous solution of $NaHCO_3$ (7 mL) was added dropwise and the solution was stirred a further 10 min at room temperature. The two phases were separated, the aqueous phase was extracted with CH_2Cl_2 (10 x 3 mL) and the combined organic layers were washed with brine (10 mL). The organic layer was dried over Na_2SO_4, filtered and concentrated *in vacuo* to yield 500 mg (80%) of the desired product as oil.

Method 2: Diisopropylammonium (*R*)-*tert*-butyl(methyl)phosphinite-borane (*R*)-L1·O (500 mg, 2.13 mmol) was dissolved in CH_2Cl_2 (15 mL), cooled to 0 ºC and HBF_4·OEt_2 (0.32 mL, 2.34 mmol) was added dropwise. After 30 min, saturated aqueous solution of $NaHCO_3$ (10 mL) was carefully added and the solution was stirred a further 10 min at room temperature. After this time, the solution was neutralised with diluted HCl (2%) until a slightly acidic pH. The two phases were separated, the aqueous phase was extracted with CH_2Cl_2 (10 x 3 mL) and the combined organic phases were washed with brine (10 mL). The final organic fraction was dried with Na_2SO_4, filtered and concentrated *in vacuo* to yield 200 mg (78%) of the desired product as oil.

To determine the enantiomeric purity of the product a small sample was treated with BH_3·SMe_2 (1 eq) in THF. After 1 h at 0 ºC, (*R*)-L1·OH was isolated (*ee* of the methylated product = 99.5% (GC)).

¹H NMR: 6.59 (dq, J_{HP} = 446.0, J_{HH} = 4.0, 1H), 1.48 (dd, J_{HP} = 12.8, J_{HH} = 4.0, 3H), 1.17 (d, J_{HP} = 16.4, 9H). **¹³C{¹H} NMR**: 30.8 (d, J_{CP} = 70.0, C), 23.4 (d, J_{CP} = 2.0, 3CH₃), 9.7 (d, J_{CP} = 62.0, CH₃). **³¹P{¹H} NMR**: +45.5 (s). **HRMS**: calcd. for $C_5H_{13}OP$ ([M] + H)⁺, 121.0777; found, 121.0778. **IR**: 2951, 2296, 1477, 1298, 1174, 968. $[\alpha]_D$ = +12.5º (c 1.5, CHCl₃).

(*S*)-(*tert*-butylmethylphosphino)(di-*tert*-butylphosphino)amine tetrafluoroborate, (*S*)-[HMaxPhos]BF$_4$, L2[8],[11]
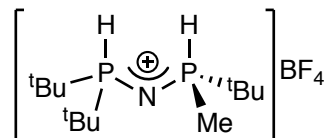
^{1}H NMR: 6.83 (dd, *J* = 477.0, *J* = 4.0, 1H), 6.57 (dd, *J* = 458.0, *J* = 6.0, 1H), 1.77 (dd, *J* = 13.0, *J* = 4.0, 3H), 1.33 (d, *J* = 17.0, 9H), 1.30 (d, *J* = 17.0, 9H), 1.24 (d, *J* = 18.0, 9H). ^{31}**P{^{1}H} NMR**: +47.6 (d, J_P = 32.0), +34.6 (d, J_P = 32.0).

(*R*)-1-*tert*-butyl-N-((*S*)-1-((*S*)-4-(iso-propyl)-4,5-dihydrooxazol-2-yl)-2-methylpropyl)-1-methylphosphanamine-borane, L3R[12]
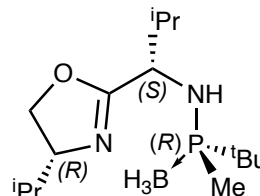
^{1}H NMR: 4.27 (dd, *J* = 10.0, *J* = 8.0, 1H), 3.99 (t, *J* = 8.0, 1H), 3.91 (td, *J* = 10.0, *J* = 5.0, 1H), 3.83 (dt, *J* = 10.0, *J* = 8.0, 1H), 2.31 (br d, *J* = 10.0, 1H), 2.04–1.87 (m, 1H), 1.74–1.58 (m, 1H), 1.33 (d, J_P = 9.0, 3H), 1.13 (d, J_P = 14.0, 9H), 0.99 (d, *J* = 7.0, 3H), 0.94 (d, *J* = 8.0, 3H), 0.90 (d, *J* = 7.0, 3H), 0.89 (d, *J* = 7.0, 3H), 0.81–0.06 (m, 3H, BH$_3$). ^{31}**P{^{1}H} NMR**: +73.7–71.5 (m, P-BH$_3$).

(*R*)-1-*tert*-butyl-N-((*S*)-1-((*R*)-4-(iso-propyl)-4,5-dihydrooxazol-2-yl)-2-methylpropyl)-1-methylphosphanamine-borane, L3S[12]
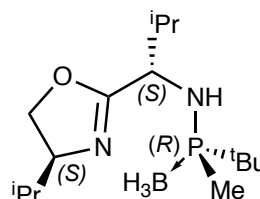
^{1}H NMR: 4.28 (dd, *J* = 9.0, *J* = 8.0, 1H), 3.96–3.91 (m, 1H), 3.90–3.82 (m, 2H), 2.25 (br d, *J* = 11.0, 1H), 2.00–1.85 (m, 1H), 1.79–1.64 (m, 1H), 1.33 (d, J_P = 9.0, 3H), 1.11 (d, J_P = 9.0, 9H), 0.97 (d, *J* = 7.0, 3H), 0.95–0.91 (m, 6H), 0.88 (d, *J* = 7.0, 3H), 0.81–0.06 (m, 3H, BH$_3$). ^{31}**P{^{1}H} NMR**: +74.6–71.4 (m, P-BH$_3$).

(*R*)-1-*tert*-butyl-N-((*S*)-1-((*R*)-4-(*tert*-butyl)-4,5-dihydrooxazol-2-yl)-2-methylpropyl)-1-methylphosphanamine-borane, L4R[12]
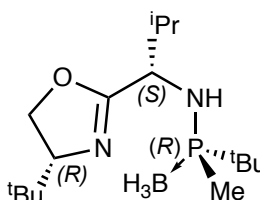
^{1}H NMR: 4.23 (dd, *J* = 10.0, *J* = 9, 1H), 3.98 (dd, *J* = 10.0, *J* = 9.0, 1H), 3.92–3.77 (m, 2H), 2.41–2.22 (m, 1H), 2.00–1.86 (m, 1H), 1.32 (d, J_P = 9.0, 3H), 1.10 (d, J_P = 14.0, 9H), 0.94 (d, *J* = 7.0, 6H), 0.91–0.86 (m, 9H), 0.84–0.06 (m, 3H, BH$_3$). ^{31}**P{^{1}H} NMR**: +75.0–71.3 (m, P-BH$_3$).

6.4.3. *Synthesis of the substrates and additives for the asymmetric hydrogenations*

6.4.3.1. *Preparation of N-aryl imines*

Method A: In a dry round bottom flask, the corresponding ketone (1 eq) and the amine (3 eq) were dissolved in Et_2O. The mixture was cooled to 0 ºC and $TiCl_4$ (0.5 eq) was carefully added dropwise. Once the addition was completed, the white suspension was left stirring overnight at room temperature. The white residues were filtered-off through celite and the solution was concentrated under reduced pressure. The oil obtained can be purified (if needed) by crystallization or by vacuum distillation.

Method B: In a dry round bottom flask, the corresponding ketone (1 eq) and the amine (3 eq) were dissolved with freshly distilled Et_2O. Activated molecular sieves (4 Å, 1 g per mmol of ketone) were added and the mixture was left stirring for 48 h at room temperature. The suspension was filtered through celite and the filtrate solution was concentrated under reduced pressure. The resulting oil can be purified, if needed, by crystallization or by vacuum distillation.

Acetophenone *N*-phenyl imine, **I1**[13]
Compound **I1** was prepared following methodology A.
¹H NMR: 8.02–7.91 (m, 2H), 7.55–7.40 (m, 3H), 7.41–7.30 (m, 2H), 7.13–7.04 (m, 1H), 6.84–6.76 (m, 2H), 2.23 (s, 3H).
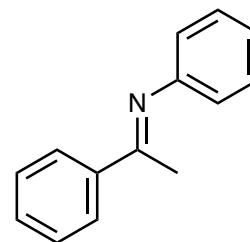
4-methoxyacetophenone *N*-phenyl imine, **I2**[13]
Compound **I2** was prepared following methodology A.
¹H NMR: 8.04–7.91 (m, 2H), 7.40–7.30 (m, 2H), 7.10–7.04 (m, 1H), 6.98–6.94 (m, 2H), 6.84–6.76 (m, 3H), 3.87 (s, 3H), 2.21 (s, 3H).
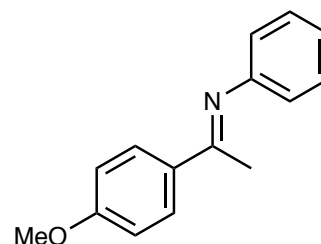
Acetophenone *N*-(4-methoxyphenyl) imine, I3[13]

Compound **I3** was prepared following methodology A.

^{1}**H NMR**: 8.03–7.88 (m, 2H), 7.48–7.38 (m, 3H), 6.93–6.87 (m, 2H), 6.80–6.70 (m, 2H), 3.82 (s, 3H), 2.25 (s, 3H).
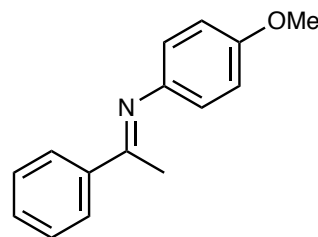
N-benzyl-1-phenylimine, I4[14]

Compound **I4** was prepared following methodology B.

^{1}**H NMR**: 7.92–7.90 (m, 2H), 7.49–7.46 (m, 3H), 7.43–7.27 (m, 5H), 4.76 (s, 2H), 2.35 (s, 3H).
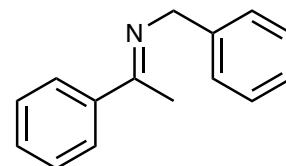
N-benzhydryl-1-phenylimine, I5[15]

Compound **I5** was prepared following methodology B.

^{1}**H NMR**: 7.91–7.89 (m, 2H), 7.44–7.41 (m, 3H), 7.36–7.14 (m, 10H), 5.82 (s, 1H), 2.27 (s, 3H).
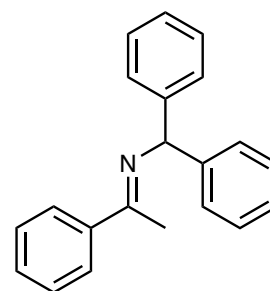
N,1,1-triphenylmethanimine, I6[16]

Compound **I6** was prepared following methodology B.

^{1}**H NMR**: 7.76–7.73 (m, 2H), 7.48–7.38 (m, 5H), 7.26–7.10 (m, 5H), 6.93–6.89 (m, 1H), 6.73–6.71 (m, 2H). **HRMS**: calcd. for $C_{19}H_{16}N$ [M+H]$^+$; 258.1277, found 258.1284.
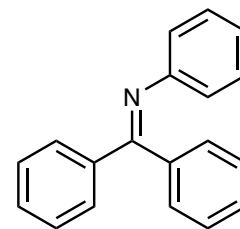
3,5-difluorophenyl-*N*-phenylimine, I7

Compound **I7** can be prepared using both methodologies A and B.

^{1}**H NMR**: 7.50–7.49 (dd, J = 6.4, J = 2.3, 2H), 7.37 (t, J = 7.5, 2H), 7.12 (br t, J = 2.4, 2H), 6.79–6.77 (dd, J = 8.5, J = 1.2, 1H), 2.21 (s, 3H). ^{19}**F NMR**: –109.5 (t, J = 8.7). **HRMS**: calcd. for $C_{14}H_{12}F_2N$ [M+H]$^+$; 232.0932, found 232.0931. **EA**: Anal. calcd. for $C_{14}H_{11}F_2N$, %: C, 72.72; H, 4.79; N, 6.06. Found, %: C, 72.49; H, 4.80; N, 6.16. **IR**: 3439, 3078, 1626, 1600, 1430, 1326, 1230, 1117, 1078, 978, 865, 757, 513.
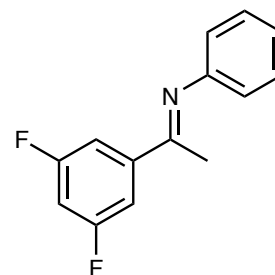
6.4.3.2. *Preparation of enantiomerically enriched aryl amines via asymmetric hydrogenation reactions*

The procedure for the preparation of optically enriched aryl amines is a general catalytic method, which has been described in section 6.2.9.4.

(−)-(*R*)-*N*-(1-phenylethyl)aniline, A1

^{1}**H NMR**: 7.41–7.25 (m, 4H), 7.28–7.18 (m, 1H), 7.18–7.03 (m, 2H), 6.68–6.59 (m, 1H), 6.55–6.46 (m, 2H), 4.48 (q, *J* = 7.0, 1H), 4.02 (br s, 1H), 1.51 (dd, *J* = 7.0, *J* = 1, 3H). **HPLC**: CHIRALCEL OD-H. Heptane/^{i}PrOH 90:10, 1 mL/min, λ = 220 nm, t_R(+) = 15.4 min,

t_R(−) = 17 min.
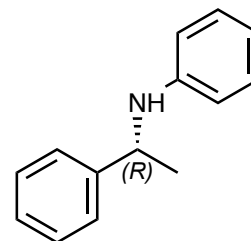
(−)-(*R*)-*N*-(1-(4-methoxyphenyl)ethyl)aniline, A2

^{1}**H NMR**: 7.30–7.26 (m, 2H), 7.11–7.06 (m, 2H), 6.87–6.84 (m, 2H), 6.53–6.47 (m, 2H), 4.44 (q, *J* = 6.7, 1H), 3.78 (s, 3H), 1.49 (d, *J* = 6.6, 3H). **HPLC**: CHIRALPAK IA. Heptane/^{i}PrOH 96:4, 0.5 mL/min, λ = 210 nm, t_R(+) = 16.1 min, t_R(−) = 17.6 min.
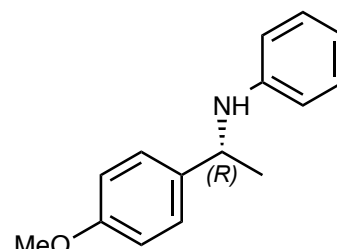
(−)-(*R*)-4-methoxy-*N*-(1-phenylethyl)aniline, A3

^{1}**H NMR**: 7.39–7.28 (m, 4H), 7.24–7.19 (m, 1H), 6.74–6.61 (m, 2H), 6.47 (d, *J* = 9, 2H), 4.41 (q, *J* = 7, 1H), 3.69 (s, 3H), 1.50 (d, *J* = 7.2, 3H). **HPLC**: CHIRALPAK IA. Heptane/^{i}PrOH 96:4, 0.5 mL/min, λ = 210 nm, t_R(+) = 17.3 min, t_R(−) = 18.4 min.
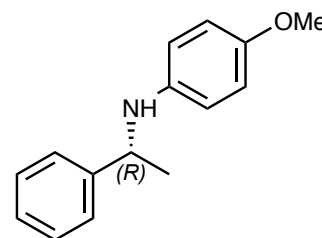
(+)-(*R*)-*N*-benzyl-1-phenylethylamine, A4

^{1}**H NMR**: 7.23–7.35 (m, 10H), 3.80 (q, *J* = 6.7, 1H), 3.66 (d, *J* = 13, 1H), 3.59 (d, *J* = 13, 1H), 1.36 (d, *J* = 6.6, 3H). **HPLC**: CHIRALCEL OJ. Heptane/^{i}PrOH 9:1, 0.5 mL/min, λ = 210 nm, t_R(+) = 14.4 min, t_R(−) = 15.3 min.
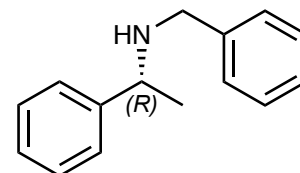
(+)-(*R*)-*N*-benzhydryl-1-phenylethylamine, A5

¹H NMR: 7.35–7.16 (m, 15H), 4.63 (s, 1H), 3.67 (q, *J* = 6.7, 1H), 1.90 (s, 1H), 1.36 (d, *J* = 6.7, 3H). **HPLC**: CHIRALCEL OJ. Heptane/ⁱPrOH 96:4, 0.5 mL/min, λ = 210 nm, t_R(+) = 17.3 min, t_R(–) = 18.4 min.
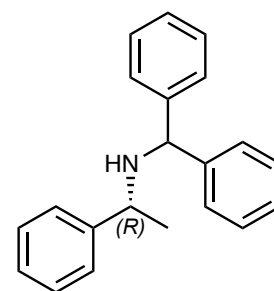
N-benzhydrylaniline, A6

¹H NMR: 7.40–7.30 (m, 10H), 7.20–7.10 (m, 2H), 6.83–6.82 (m, 2H), 6.70–6.67 (m, 1H), 5.20 (s, 1H).
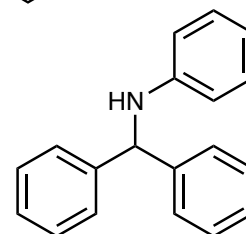
(–)-(*S*)-*N*-(1-(3,5-difluorophenyl)ethyl)aniline, A7

¹H NMR: 7.11 (t, *J* = 7.3, 2H), 6.90 (d, *J* = 6.4, 2H), 6.70–6.63 (m, 2H), 6.47 (d, *J* = 5.6, 2H) 4.43 (q, *J* = 6.7, 1H), 1.5 (d, *J* = 6.7, 3H). **¹⁹F NMR**: –109.5 (t, *J* = 8.1). **HPLC**: CHIRALCEL OJ. Heptane/ⁱPrOH 9:1, 0.5 mL/min, λ = 210 nm, t_R(+) = 15.8 min, t_R(–) = 19.9 min.
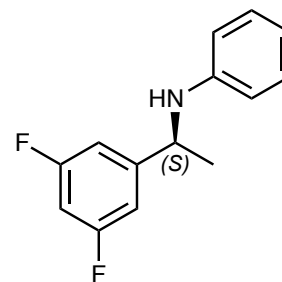
6.4.3.3. *Preparation of N-methyl and N-alkyl imines*

In a dry round bottom *Schlenk* flask, the corresponding ketone (1 eq) was purged with N₂ over activated molecular sieves (4 Å, 1 g per mmol of ketone) and then a solution of methylamine in EtOH (33 wt.%, 6 eq) was added. The mixture was stirred for 48 h at room temperature. The suspension was filtered through celite and the filtrate solution was concentrated under reduced pressure. The resulting oil can be purified by crystallization or by vacuum distillation if required.

(*E*)-*N*-methyl-1-phenylethylimine, I8[17]

¹H NMR: 7.84–7.60 (m, 2H), 7.48–7.30 (m, 3H), 3.35 (q, *J* = 1.2, 3H), 2.24 (q, *J* = 1.2, 3H).
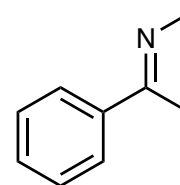
(*E*)-1-(4-chlorophenyl)-*N*-methylethan-1-imine, I9[17]

¹H NMR: 7.74–7.65 (m, 2H), 7.42–7.29 (m, 2H), 3.34 (q, *J* = 1.0, 3H), 2.21 (q, *J* = 1.0, 3H).
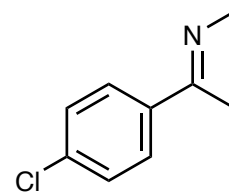
(*E*)-1-(4-fluorophenyl)-*N*-methylethan-1-imine, I10[17]

¹H NMR: 7.78–7.71 (m, 2H), 7.07–7.00 (m, 2H), 3.34–3.32 (m, 3H), 2.22 (q, *J* = 1.0, 3H).
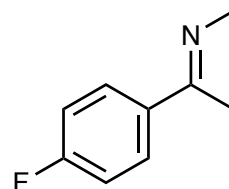
(*E*)-1-(3-methoxyphenyl)-*N*-phenylethan-1-imine, I11[17]

¹H NMR: 7.36–7.33 (m, 1H), 7.33–7.26 (m, 2H), 6.93 (ddd, *J* = 7.0, *J* = 3, *J* = 2.0, 1H), 3.84 (s, 3H), 3.35 (q, *J* = 1.0, 3H), 2.23 (q, *J* = 1.0, 3H).
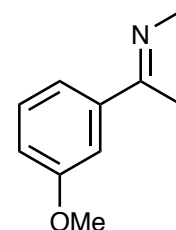
(*E*)-1-(4-methoxyphenyl)-*N*-methylethan-1-imine, I12[17]

¹H NMR: 7.76–7.64 (m, 2H), 6.90–6.82 (m, 2H), 3.81 (s, 3H), 3.30 (q, *J* = 1, 3H), 2.19 (q, *J* = 1, 3H).
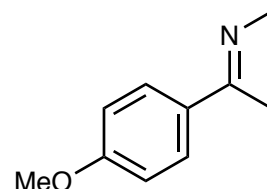
(*E*)-*N*-methyl-1-(4-(trifluoromethyl)phenyl)ethan-1-imine, I13[17]

¹H NMR: 7.88–7.83 (m, 2H), 7.65–7.60 (m, 2H), 3.41–3.31 (m, 3H), 2.26 (q, *J* = 1.0, 3H).
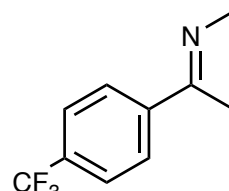
(*E*)-*N*-methyl-3,4-dihydronaphthalen-1-imine, I14[17]

¹H NMR: 8.03 (dd, *J* = 8.0, *J* = 2.0, 1H), 7.26–7.13 (m, 2H), 7.09–7.04 (m, 1H), 3.28–3.18 (m, 3H), 2.83–2.68 (m, 2H), 2.57–2.42 (m, 2H), 1.95–1.83 (m, 2H).
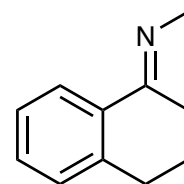
(*E*)-1-phenyl-*N*-propylethan-1-imine, I15[17]

¹H NMR: 7.81–7.71 (m, 2H), 7.44–7.31 (m, 3H), 3.49–3.40 (m, 2H), 1.77 (t, *J* = 7.0, 2H), 1.02 (t, *J* = 7.0, 3H).
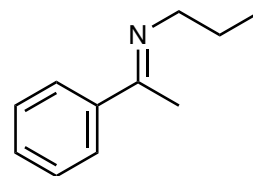
(*E*)-1-(4-chlorophenyl)-*N*-phenylethan-1-imine, I16[18]

¹H NMR: 7.74–7.68 (m, 2H), 7.35–7.30 (m, 2H), 3.50–3.35 (m, 2H), 2.21 (t, *J* = 1.0, 3H), 1.83–1.70 (m, 2H), 1.01 (t, *J* = 7.0, 3H).
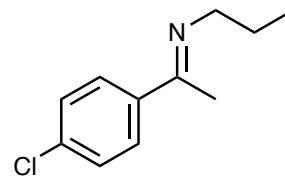
(*E*)-*N*-isobutyl-1-phenylethan-1-imine, I17[19]

¹H NMR: 7.82–7.70 (m, 2H), 7.41–7.31 (m, 3H), 3.27 (dt, *J* = 7.0, *J* = 1, 2H), 2.22 (t, *J* = 1.0, 3H), 2.07 (dp, *J* = 13.0, *J* = 7.0, 1H), 1.01 (d, *J* = 7.0, 6H).
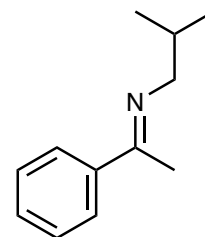
(*E*)-1-cyclohexyl-*N*-methylethan-1-imine, I18[17]

13/1 mixture of *E*/*Z* isomers.

¹H NMR: (major isomer) 3.07 (s, 3H), 2.16–2.10 (m, 1H), 1.87–1.66 (m, 8H), 1.33–1.18 (m, 5H).
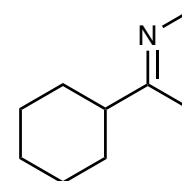
6.4.3.4. *Preparation of enantiomerically enriched N-alkyl amines via asymmetric hydrogenation reactions*

Catalyst **L3RIr6** (3.13·10^{-3} mmol, 0.01 eq) was placed in a glass pressure tube, purged with vacuum-nitrogen cycles and 2 mL of CH_2Cl_2 were added. The tube was the purged with vacuum-hydrogen cycles and charged with 3 bar of H_2. When required, the tube was cooled down to the desired temperature. The corresponding *N*-alkyl imine (0.313 mmol, 1.00 eq) was dissolved in 1 mL of CH_2Cl_2 and added using a pressure syringe. The mixture was left stirring overnight at the desired temperature. The tube was depressurized and the solvent removed under vacuum to afford the corresponding hydrogenated compound as a dark yellow oil or solid. The *ee* value was determined by HPLC/GC analysis of the corresponding trifluoroacetamide derivative on a chiral stationary phase.

(*S*)-*N*-methyl-1-phenylethan-1-amine, **A8**[20]

^{1}**H NMR**: 7.36–7.26 (m, 4H), 3.65 (q, *J* = 7.0, 1H), 2.31 (s, 3H), 1.37 (d, *J* = 7.0, 3H). **HPLC**: CHIRALCEL OD-H. Heptane/iPrOH 98:02, 0.5 mL/min, λ = 210 nm. t_S(−)= 13.4 min, t_R(+)= 14.7 min. (*ee* = 91%).
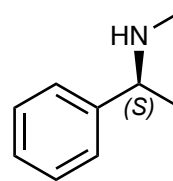
(*S*)-1-(4-chlorophenyl)-*N*-methylethan-1-amine, **A9**[20]

^{1}**H NMR**: 7.40–7.19 (m, 4H), 3.62 (q, *J* = 7.0, 1H), 2.29 (s, 3H), 1.32 (d, *J* = 7.0, 3H). **GC**: β-DEX (30 m). 140 ºC (50 min). T_{det} = 300 ºC. T_{inj} = 220 ºC. Split 50:1, Flux: 1 mL/ min; He. t_S(−) = 38.7 min, t_R(+) = 39.1 min. (*ee* = 94%).
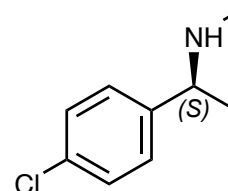
(*S*)-1-(4-fluorophenyl)-*N*-methylethan-1-amine, **A10**

^{1}**H NMR**: 7.29–7.22 (m, 2H), 7.04–6.95 (m, 2H), 3.63 (q, *J* = 7.0, 1H), 2.29 (s, 3H), 1.33 (d, *J* = 7.0, 3H). **GC**: β-DEX (30 m). 120 ºC---5 ºC/min---130 ºC (40 min)---30 ºC/min---210 ºC (5 min). T_{det} = 300 ºC. T_{inj} = 220 ºC. Split 50:1, Flux: 1 mL/ min; He. t_S(−) = 22.4 min, t_R(+) = 22.7 min. (*ee* = 93%).
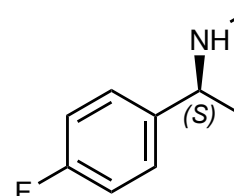
(*S*)-1-(3-methoxyphenyl)-*N*-methylethan-1-amine, A11

^{1}**H NMR**: 7.27–7.22 (m, 1H), 6.90–6.86 (m, 2H), 6.78 (ddd, *J* = 8.0, *J* = 3, *J* = 1.0, 1H), 3.81 (s, 3H), 3.62 (q, *J* = 7.0, 1H), 2.31 (s, 3H), 1.35 (d, *J* = 7.0, 3H) ppm. **GC**: *β*-DEX (30 m). 120 ºC (10 min)---2 ºC/min---140 ºC (60 min)---20 ºC/min---210 ºC (5 min). T_{det} = 300 ºC. T_{inj} = 220 ºC. Split 50:1, Flux: 1 mL/ min; He. t_S(–) = 51.8 min, *t*(+) = 52.2 min. (*ee* = 89%).
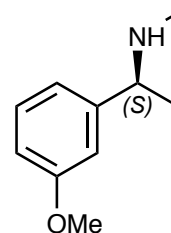
(*S*)-1-(4-methoxyphenyl)-*N*-methylethan-1-amine, A12[21]

^{1}**H NMR**: 7.24–7.17 (m, 2H), 6.92–6.81 (m, 2H), 3.80 (s, 3H), 3.60 (q, *J* = 7.0, 1H), 2.30 (s, 3H), 1.34 (d, *J* = 7.0, 3H) ppm. **HPLC**: CHIRALCEL OJ. Heptane/EtOH 95:05, 0.5 mL/min, λ = 210 nm. t_R(+) = 15.1 min, t_S(–) = 16.7 min. (*ee* = 91%).
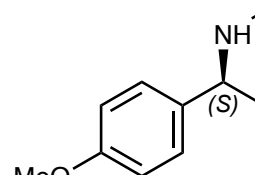
(*S*)-*N*-methyl-1-(4-(trifluoromethyl)phenyl)ethan-1-amine, A13

^{1}**H NMR**: 7.58 (dtd, *J* = 9.0, *J* = 2.0, *J* = 1.0, 2H), 7.47–7.37 (m, 2H), 3.71 (q, *J* = 7.0, 1H), 2.30 (s, 3H), 1.35 (d, *J* = 7.0, 3H). **HPLC**: CHIRALPAK AS. Heptane/iPrOH 98:02, 0.5 mL/min, λ = 210 nm. t_R(+) = 10.2 min, t_S(–) = 11.9 min. (*ee* = 93%).
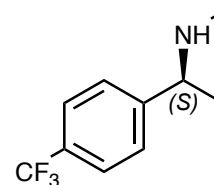
(*S*)-*N*-methyl-1,2,3,4-tetrahydronaphthalen-1-amine, A14[20]

^{1}**H NMR**: 7.37–7.29 (m, 1H), 7.19–7.11 (m, 2H), 7.11–6.99 (m, 1H), 3.66 (t, *J* = 5, 1H), 2.89–2.62 (m, 2H), 2.50 (s, 3H), 2.04–1.81 (m, 3H), 1.81–1.67 (m, 1H). **GC**: *β*-DEX (30 m). 160 ºC (30 min). T_{det} = 300 ºC. T_{inj} = 220 ºC. Split 50:1, Flux: 1 mL/ min; He. t_S (+) = 25.7 min, t_R (–) = 26.3 min. (*ee* = 89%).
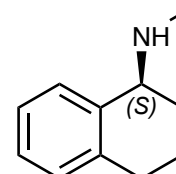
(*S*)-*N*-(1-phenylethyl)propan-1-amine, A15[22]

¹H NMR: 7.28–7.21 (m, 4H), 7.19–7.14 (m, 1H), 3.68 (q, J = 7.0, 1H), 2.40 (ddd, J = 11.0, J = 8.0, J = 6.0, 1H), 2.31 (ddd, J = 11.0, J = 8.0, J = 7.0, 1H), 1.44–1.33 (m, 2H), 1.28 (d, J = 7.0, 3H), 0.80 (t, J = 7.0, 3H). **HPLC**: CHIRALPAK ADH. Heptane/iPrOH 98:02, 0.5 mL/min, λ = 210 nm. t_R(+) = 8.9 min, t_S(−) = 9.9 min. (*ee* = 92%).
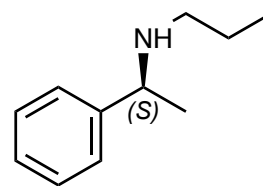
(*S*)-*N*-(1-(4-chlorophenyl)ethyl)propan-1-amine, A16[19]

¹H NMR: 7.32–7.23 (m, 4H), 3.74 (q, J = 6.0, 1H), 2.45 (ddd, J = 11.0, J = 8.0, J = 6.0 Hz, 1H), 2.35 (ddd, J = 11.0, J = 8.0, J = 7.0, 1H), 1.51–1.41 (m, 2H), 1.32 (d, J = 6.0, 3H), 0.87 (t, J = 7.0, 3H). **HPLC**: CHIRALCEL OJ. Heptane/iPrOH 98:02, 0.4 mL/min, λ = 210 nm. t_S(−)= 17.1 min, t_R(+)= 19.2 min. (*ee* = 94%).
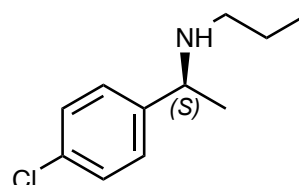
(*S*)-2-methyl-*N*-(1-phenylethyl)propan-1-amine, A17[18]

¹H NMR: 7.34–7.29 (m, 4H), 7.25–7.21 (m, 1H), 3.74 (q, J = 7.0, 1H), 2.34 (dd, J = 11.0, J = 6.0, 1H), 2.21 (dd, J = 11.0, J = 7.0, 1H), 1.71 (dt, J = 13.0, J = 7.0, 1H), 1.35 (d, J = 7.0, 3H), 0.87 (dd, J = 7.0, J = 2.0, 6H). **HPLC**: CHIRALCEL OD-H. Heptane/iPrOH 98:02, 0.5 mL/min, λ = 210 nm. t_R(+)= 10.4 min, t_S(−)= 12.1 min. (*ee* = 93%).
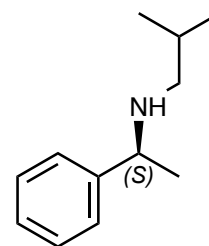
rac-1-cyclohexyl-*N*-methylethan-1-amine, A18

¹H NMR: 3.27 (s, 3H), 2.54–2.47 (m, 1H), 1.78–1.66 (m, 11H), 1.03 (d, 3H). GC: β-DEX (30 m). 90 ºC (10 min)---20 ºC/min---140ºC (20 min)---20 ºC/min---210 ºC (5 min). T_{det} = 300 ºC. T_{inj} = 220 ºC. Split 50:1, Flux: 1 mL/ min; He.
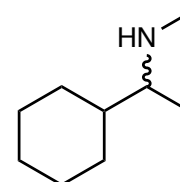
6.4.3.5. *Trifluoroacylation of amines*
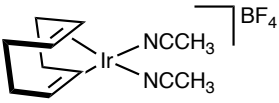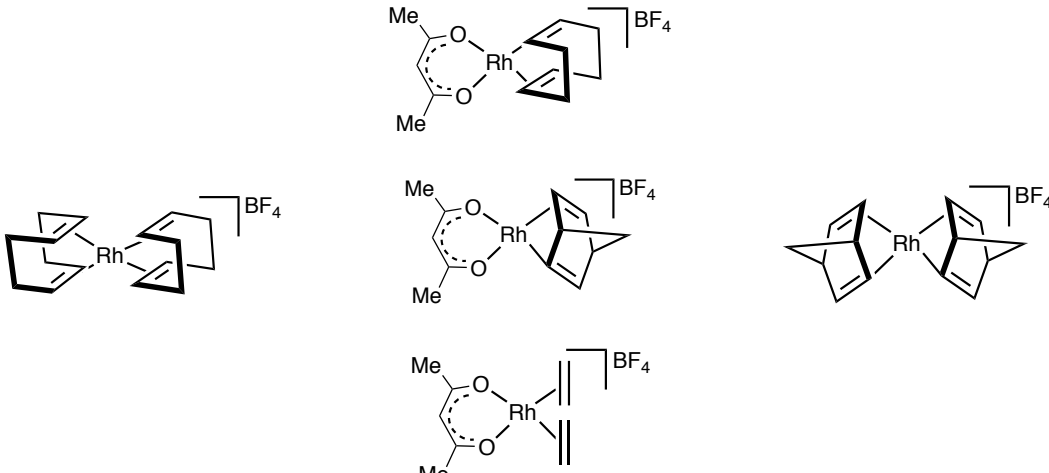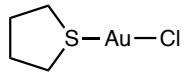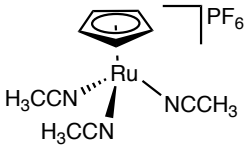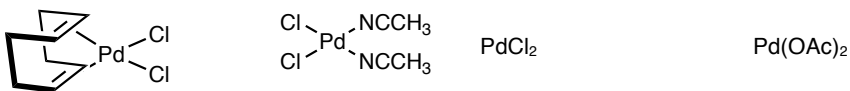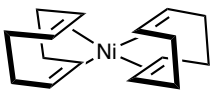
The corresponding amine (0.35 mmol, 1 eq) was placed in a round bottom flask and dissolved in 2 mL of CH_2Cl_2. At this point, 213 μL of pyridine (2.1 mmol, 6 eq) and 143 μL of trifluoroacetic anhydride (1.0 mmol, 3 eq) were added and the mixture was left stirring for 2 h. The reaction was concentrated under reduced pressure and the crude was purified with a short silica column to afford the products as colourless oils.

6.5. *Preparation of the catalytic precursors*
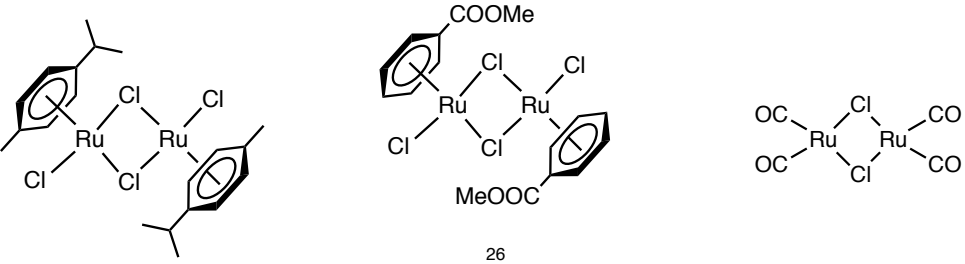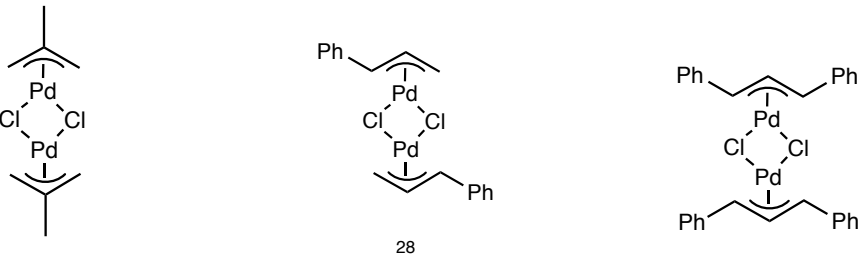
6.5.1. *Metallic precursors*

Taking into account the variety of metals used in this thesis, a summary of all the metallic precursors is presented here. Among all of them, some have been prepared according to the methods described in the literature. Those that do not contain any specifications have been achieved from commercial suppliers.

6.5.1.1. *Monomeric precursors*

[Ir]	 23
[Rh]	
[Au]	 24 H[AuCl$_4$]
[Ru]	 25 RuCl$_3$·xH$_2$O
[Pd]	PdCl$_2$ Pd(OAc)$_2$
[Ni]	

6.5.1.2. *Dimeric precursors*

[Ir]	
[Rh]	
[Ru]	
[Pd]	

6.5.2. *Synthesis of the complexes*

6.5.2.1. *Complexes with the SPO ligand*

trans-[RhCl(CO)(κP-(S)-L1)$_2$], L1Rh1

To a solution of (*S*)-**L1** (70 mg, 0.58 mmol) in CH_2Cl_2 (5 mL) [Rh(CO)$_2$Cl]$_2$ (57 mg, 0.15 mmol) was added. The orange reaction mixture was stirred at rt for 1 h, concentrated to dryness under vacuum and the residue was recrystallized in CH_2Cl_2/hexane. The title complex was obtained as a yellow solid (100 mg, 82%).
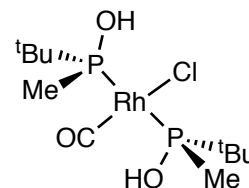
^{1}H NMR (C$_6$D$_6$): 5.98 (s, br, 2H), 1.32 (m, 6H), 1.08 (t, $J_{virtual}$ = 7.6, 18H). **^{13}C{^{1}H} NMR**: 188.1 (dt, J_{CRh} = 77.2, J_{CP} = 17.3, C), 35.4 (t, $J_{virtual}$ = 17.1, C), 25.1 (t, $J_{virtual}$ = 3.5, CH$_3$), 14.9 (td, $J_{virtual}$ = 14.4, J_{CRh} = 3.4, CH$_3$). **^{31}P{^{1}H} NMR (C$_6$D$_6$)**: +129.6 (d, J_{RhP} = 117.5). **HRMS**: calcd. for $C_{10}H_{26}O_2P_2Rh$ [M − Cl − CO]$^+$, 343.0458; found, 343.0465; $C_{11}H_{26}O_3P_2Rh$ [M − Cl]$^+$, 371.0411; found, 371.0407. **EA**: Anal. calcd for $C_{11}H_{26}ClO_3P_2Rh$, %: C, 32.49; H, 6.45. Found, %: C, 31.65; H, 5.93. **IR**: 3400, 2961, 2057, 1983, 1635, 1465, 1104, 1017, 874, 809, 722. **[α]$_D$** = −369.0° (c 1, CH_2Cl_2).

[AuCl(κP-(S)-L1)], L1Au1

To a solution of (*S*)-**L1** (98 mg, 0.82 mmol) in CH_2Cl_2 (5 mL) [Au(tht)Cl] (190 mg, 0.59 mmol) was added and it was stirred at rt for 1 h. The solution was concentrated to dryness under vacuum and the residue was recrystallized in CH_2Cl_2/Et$_2$O. The desired complex was obtained as a pale grey solid (180 mg, 87%). **^{1}H NMR**: 1.71 (d, J_{HP} = 9.9, 3H), 1.22 (d, J_{HP} = 16.5, 9H). **^{13}C{^{1}H} NMR**: 34.7 (d, J_{CP} = 47.3, C), 24.5 (d, J_{CP} = 6.7, 3CH$_3$), 15.3 (d, J_{CP} = 40.1, CH$_3$). **^{31}P{^{1}H} NMR**: +113.6 (s). **HRMS**: calcd. for $C_5H_{13}AuOP$ ([M] − Cl)$^+$, 317.0364; found, 317.0360. **IR**: 3148, 2965, 2865, 1635, 1470, 1313, 1291, 1113, 913, 883, 857, 809, 613, 465. **[α]$_D$** = −20.8° (c 1, CH_2Cl_2).
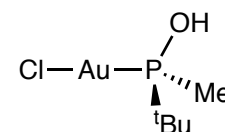
[RuCl$_2$(η^6-p-cymene)(κP-(S)-L1)], L1Ru1

A suspension of [RuCl$_2$(p-cymene)]$_2$ (60 mg, 98 mmol) and (*S*)-**L1** (29 mg, 245 mmol, 2.5 eq) in *n*-hexane (20 mL) was heated at 75 °C for 16 h. After this time, the orange precipitate was filtered off and washed with pentane. The title product was obtained as an orange solid that did not require any further purification (75 mg, 90%).
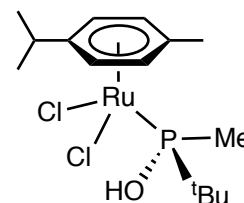
¹H NMR: 5.71 (d, J_{HH} = 6.0, 1H), 5.63 (d, J_{HH} = 6.0, 1H), 5.57 (d, J_{HH} = 6.4, 2H), 5.16 (br s, 1H), 2.83 (sept, J_{HH} = 6.8, 1H), 2.09 (s, 3H), 1.81 (d, J_{HP} = 8.0, 3H), 1.30 (d, J_{HP} = 14.8, 9H), 1.26 (d, J_{HH} = 7.2, 3H), 1.24 (d, J_{HH} = 6.8, 3H). **¹³C{¹H} NMR**: 107.1 (s, C^{Ar}), 93.8 (s, C^{Ar}), 89.5 (d, J_{CP} = 4.7, 2CH^{Ar}), 85.7 (d, J_{CP} = 5.2, CH^{Ar}), 83.2 (d, J_{CP} = 6.5, CH^{Ar}), 38.0 (d, J_{CP} = 32.1, P-C(CH$_3$)$_3$), 30.7 (s, CH(CH$_3$)$_2$), 25.8 (s, CH(CH$_3$)$_2$), 25.7 (s, CH(CH$_3$)$_2$), 22.1 (d, J_{CP} = 13.4, P-C(CH$_3$)$_3$), 18.2 (s, C^{Ar}-CH$_3$), 15.1 (d, J_{CP} = 31.6, CH$_3$). **³¹P{¹H} NMR**: +131.9 (s). **HRMS**: calcd for C$_{15}$H$_{27}$ClOPRu ([M] − Cl)$^+$, 391.0525; found 391.0527. **EA**: Anal. calcd for C$_{15}$H$_{27}$Cl$_2$OPRu, %: C, 42.26; H, 6.38. Found, %: C, 39.81; H, 6.43. **IR**: 3408, 3074, 2961, 2874, 1648, 1465, 1126, 887, 839, 743, 604. $[\alpha]_D$ = +40.1° (c 1, CH$_2$Cl$_2$).

[RuCl₂(CO)₃(κO-(S)-L1)], L1Ru2

Complex [RuCl$_2$(CO)$_3$]$_2$ (40 mg, 78 mmol) was added to a solution of (**S**)-**L1** (20 mg, 166 mmol, 2.1 eq) in THF (3 mL). The reaction mixture was stirred for 2 h at room temperature protected from light. After that time, the solvent was removed under vacuum. The oil obtained was washed with *n*-hexane and dried under vacuum to give the desired product (25 mg, 43%).
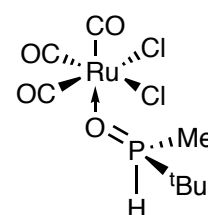
¹H NMR: 7.01 (dq, J_{HP} = 495.2, J_{HH} = 4.0, 1H), 1.69 (dd, J_{HP} = 13.2, J_{HH} = 4.0, 3H), 1.19 (d, J_{HP} = 17.2, 9H). **¹³C{¹H} NMR**: 187.0 (s, CO), 183.71 (s, CO), 29.9 (d, J_{CP} = 73.6, C), 23.6 (s, (CH$_3$)$_3$), 9.7 (s, J_{CP} = 62.1, CH$_3$). **³¹P{¹H} NMR**: +60.3 (s). **HRMS**: calcd for C$_8$H$_{17}$NO$_4$PCl$_2$Ru: 393.9310 ([M] + NH$_4$)$^+$; found 393.9319. **IR**: 2968, 2131, 2042, 1468, 1294, 1094, 961, 805, 622. $[\alpha]_D$ = −9.4° (c 1, CH$_2$Cl$_2$).

trans-[RuCl₂(CO)₂(κP-(S)-L1)₂], L1Ru3

Complex [RuCl$_2$(CO)$_3$]$_2$ (72 mg, 0.14 mmol) was dissolved into a solution of ligand (**S**)-**L1** (75 mg, 0.63 mmol) in toluene (3 mL). The reaction mixture was heated for 8 h at 110 °C using a microwave oven. After that time, the solvent was removed under vacuum. The oil obtained was washed with *n*-pentane and dried under vacuum to give the desired product (100 mg, 76%).
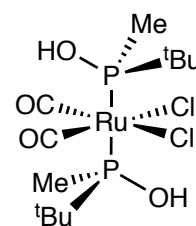
^{1}H NMR (C$_6$D$_6$): 1.69 (pseudotriplet, $J_{virtual}$ = 2.8, 6H), 0.96 (t, $J_{virtual}$ = 8.0, 18H). **^{13}C{^{1}H} NMR**: 195.4 (t, J_{CP} = 11.1, 2CO), 35.5 (t, $J_{virtual}$ = 17.4, C), 24.3 (t, $J_{virtual}$ = 2.8, CH$_3$), 13.0 (t, $J_{virtual}$ = 16.9, CH$_3$). **^{31}P{^{1}H} NMR**: +124.9 (s). **HRMS**: calcd for C$_{12}$H$_{30}$NO$_4$P$_2$Cl$_2$Ru ([M] + NH$_4$)$^+$, 486.0063; found 486.0071. **EA**: Anal. calcd for C$_{12}$H$_{26}$Cl$_2$O$_4$P$_2$Ru, %: C, 30.78; H, 5.60. Found, %: C, 31.51; H, 5.72. **IR**: 3439, 2961, 2870, 2126, 2048, 2000, 1643, 1469, 1300, 1152, 883, 583. **[α]$_D$** = −35.4° (c 1, CH$_2$Cl$_2$).

trans-[PdCl$_2$(κP-(*S*)-L1)$_2$], *trans*-L1Pd1

[Pd(COD)Cl$_2$] (89 mg, 0.31 mmol) was dissolved into a solution of ligand (*S*)-L1 (76 mg, 0.63 mmol) in CH$_2$Cl$_2$ (3 mL). The reaction mixture was allowed to stir at room temperature over 1 h. After that time, the solution was concentrated *in vacuo* and the product was recrystallized with CH$_2$Cl$_2$/hexane yielding the title product as a pale yellow solid (124 mg, 96%).
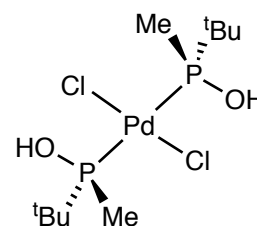
^{1}H NMR: 1.63 (br d, *J* = 2.8, 6H), 1.23 (pseudotriplet, $J_{virtual}$ = 8.0, 18H). **^{13}C{^{1}H} NMR**: 36.2 (br s, C), 25.5 (br s, CH$_3$), 10.7 (br s, CH$_3$). **^{31}P{^{1}H} NMR**: +117.3 (s). **HRMS**: calcd for C$_{10}$H$_{25}$O$_2$P$_2$Pd ([M] − 2Cl − H)$^+$, 345.0364; found 345.0364. **EA**: Anal. calcd for C$_{10}$H$_{26}$Cl$_2$O$_2$P$_2$Pd, %: C, 28.76; H, 6.28. Found, %: C, 31.02; H, 6.09. **IR**: 3439, 2957, 2870, 1630, 1457, 1291, 1104, 1043, 900, 835, 739, 600, 500. **[α]$_D$** = +60.0° (c 1, CH$_2$Cl$_2$).

[Pd(μ-Cl)(κP-(*S*)-L1)$_2$]$_2$, L1Pd2

PdCl$_2$ (143 mg, 0.81 mmol) was dissolved into a solution of ligand (*S*)-L1 (200 mg, 1.66 mmol) in THF (20 mL) and the reaction mixture was refluxed for 16 h in air. Solvent was eliminated under reduced pressure and the crude was purified by flash chromatography (SiO$_2$, CH$_2$Cl$_2$:Et$_2$O, 8:2) to yield 210 mg (68%) of L1Pd2 as a pale yellow solid.
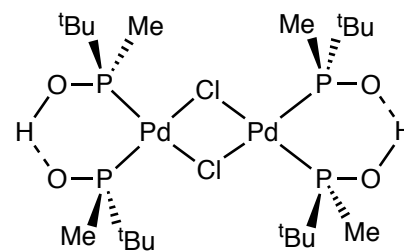
^{1}H NMR: 1.66 (d, J_{HP} = 10.4, 12H), 1.25 (d, J_{HP} = 16.0, 36H). **^{13}C{^{1}H} NMR**: 39.0–38.5 (m, 4C), 26.5 (m, 12CH$_3$), 14.8–14.3 (m, 4CH$_3$). **^{31}P{^{1}H} NMR**: +109.0 (s). **HRMS**: calcd for C$_{20}$H$_{50}$Cl$_2$O$_4$P$_4$Pd$_2$ ([M] + H)$^+$, 763.0182; found 763.0202. **IR**: 2945, 1462, 1280, 1033, 868, 812, 734. **[α]$_D$** = +272° (c 0.5, CHCl$_3$).

[Pd(μ-Cl)(κP-(S)-L1)$_2$]$_2$, L1Pd5

A solution of **L1Pd2** (260 mg, 0.34 mmol) in CH$_2$Cl$_2$ (5 mL) was treated with HBF$_4$·OEt$_2$ (0.9 mL, 6.6 mmol) and the reaction mixture was stirred over 1 h. The solution was extracted with
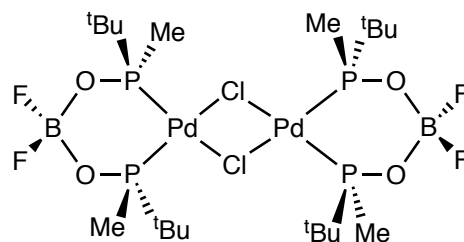
water (3 x 20 mL) and the organic layer was dried with Na$_2$SO$_4$, filtered and concentrated *in vacuo* to yield 270 mg (93%) of product as a pale yellow solid.

^{1}**H NMR**: 1.79 (d, J_{HP} = 10.0, 12H), 1.35 (d, J_{HP} = 17.2, 36H). ^{13}**C{^{1}H} NMR**: 39.7 (d, J_{CP} = 40.6, 4C), 26.1 (s, 12CH$_3$), 15.1 (d, J_{CP} = 45.8, 4CH$_3$). ^{31}**P{^{1}H} NMR**: +124.1 (s). ^{19}**F NMR**: −138.85 (t, J_{FP} = 6.8, ^{10}BF$_2$), −138.90 (t, J_{FP} = 6.8, ^{11}BF$_2$). **HRMS**: calcd for C$_{20}$H$_{47}$B$_2$Cl$_2$F$_3$O$_4$P$_4$Pd$_2$ ([M] − HF)$^+$, 838.0026; found 838.0087. **EA**: Anal. calcd for C$_{20}$H$_{48}$B$_2$Cl$_2$F$_4$O$_4$P$_4$Pd$_2$, %: C, 28.00; H, 5.64. Found, %: C, 29.06; H, 5.78. **IR**: 2970, 1465, 1083, 1026, 930, 896, 861, 752, 739. [α]$_D$ = +280° (c 0.5, CH$_2$Cl$_2$).

[Pd(μ-OAc)(κP-(S)-L1)$_2$]$_2$, L1Pd3, L1Pd4

Pd(OAc)$_2$ (112 mg, 0.5 mmol) was added to a solution of (S)-**L1** (120 mg, 1.0 mmol)
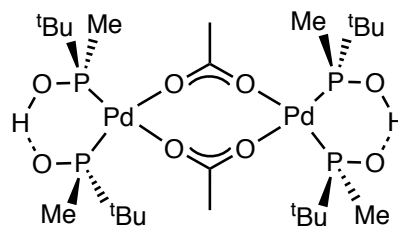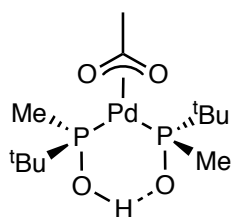
in toluene (10 mL) and the reaction mixture was refluxed for 16 h. The solution was cooled at room temperature and the solvent was evaporated under reduced pressure. The remaining oil was purified by flash chromatography (SiO$_2$, CH$_2$Cl$_2$:Et$_2$O, 8:2) to afford 250 mg (62%) of the acetate complex as a pale yellow solid.

^{1}**H NMR (C$_6$D$_6$)**: 2.25 (s, 3H, mono), 1.87 (s, 6H, dim), 1.62 (d, J_{HP} = 8.8, 6H, mono), 1.40 (d, J_{HP} = 11.2, 18H, dim), 1.11 (d, J_{HP} = 11.6, 36H, mono + dim), 1.07 (d, J_{HP} = 11.6, 36H, mono + dim). ^{13}**C{^{1}H} NMR (C$_6$D$_6$)**: 183.1 (s, 2CO, dim), 181.6 (s, CO, mono), 38.3 (d, J_{CP} = 13.8, C, mono), 37.7 (d, J_{CP} = 13.1, C, dim), 26.2 (d, J_{CP} = 33.7, CH$_3$), 17.2 (dd, J_{CP} = 28.3, 4.0, PCH$_3$), 12.6 (d, J = 32.3, CH$_3$), 12.2 (s, CH$_3$), 11.9 (s, CH$_3$). ^{31}**P{^{1}H} NMR (C$_6$D$_6$)**: +110.6 (s), +106.9 (s). **HRMS**: calcd for C$_{10}$H$_{25}$O$_2$P$_2$Pd ([M] − AcO)$^+$, 345.0365; found 345.0364. **IR**: 3426, 2939, 2896, 2865, 1591, 1409, 1361, 1278, 1187, 1009, 874, 813, 730, 683, 604. [α]$_D$ = +201° (c 0.5, CH$_2$Cl$_2$).

[Pd(μ-OAc)(κP-(S)-L1)₂]₂, L1Pd6, L1Pd7

A solution of **L1Pd3**, **L1Pd4** (765 mg, 1 mmol) in CH_2Cl_2 (5 mL) was treated with Ag(OAc) (334 mg, 2 mmol) and the reaction mixture was stirred over 1 h protected from light. The grey suspension was filtered-off and the solution was concentrated *in vacuo* to yield 700 mg (77%) of product as a pale yellow solid.
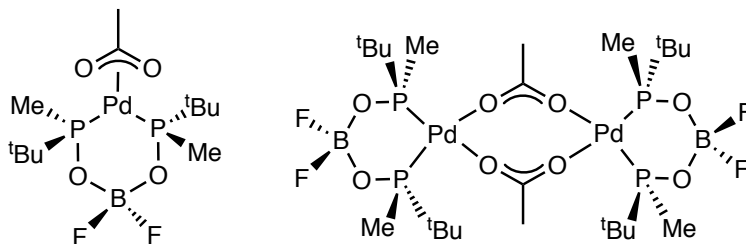
^1H NMR (C_6D_6): 2.01 (s, 3H, mono), 1.93 (s, 6H, dim), 1.77 (d, J_{HP} = 8.5, 6H, mono), 1.62 (d, J_{HP} = 13, 18H, dim), 1.30 (d, J_{HP} = 12, 36H, mono + dim), 1.27 (d, J_{HP} = 11.9, 36H, mono + dim). **$^{13}C\{^1H\}$ NMR (C_6D_6)**: 188.1 (s, 2CO, dim), 182.3 (s, CO, mono), 38.0 (d, J_{CP} = 15, C, mono), 37.6 (d, J_{CP} = 14, C, dim), 29.7 (m, CH_3), 26.5 (m, PCH_3), 25.3 (m, CH_3), 14.5 (m, CH_3), 14.1 (m, CH_3). **$^{31}P\{^1H\}$ NMR**: +121.3 (s). **^{19}F NMR**: −138.2 (t, J_{FP} = 7, $^{10}BF_2$), −138.3 (t, J_{FP} = 7, $^{11}BF_2$). **HRMS**: calcd for $C_{10}H_{24}BF_2O_2P_2Pd$ (1/2[M] − 2AcO)⁺, 393.0347; found 393.0349; calcd for $C_{12}H_{27}NBF_2O_2P_2Pd$ (1/2[M] − 2AcO + CH_3CN)⁺, 434.0615; found 434.0611. **IR**: 3417, 2948, 2352, 1621, 1457, 1387, 1087, 1013, 882, 743. **[α]$_D$** = +220° (c 0.5, CH_2Cl_2).

[Pd(η³-Ph₂C₃H₃)Cl(κP-(S)-L1)], L1Pd8

Dimer [Pd(η³-C₃H₃Ph₂)Cl]₂ (201 mg, 0.30 mmol) was dissolved into a solution of (**S**)-**L1** (75 mg, 0.63 mmol) in CH_2Cl_2 (10 mL). The suspension was stirred for 3 h at room temperature producing a clear yellowish solution. The solvent was evaporated *in vacuo* and the product was recrystallized with CH_2Cl_2/hexane yielding a yellow solid (200 mg, 73%).
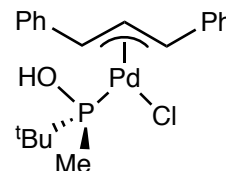
^1H NMR: 7.54-7.24 (m, 2Ph, M + m), 6.61 (dd, J_{HH} = 16.0, J_{HH} = 8.4, 1H$_{central}$, m), 6.32 (dd, J_{HH} = 13.6, J_{HH} = 10.8, 1H$_{central}$, M), 5.51 (d, J = 7.2, m), 5.35 (dd, J = 13.6, J = 10.0, M), 4.53 (d, J = 11.6, m), 4.42 (d, J = 10.8, M), 1.59 (d, J_{HP} = 10.0, 3H, m), 1.03 (d, J_{HP} = 15.6, 9H, M), 0.73 (d, J_{HP} = 15.6, 9H, m), 0.44 (d, J_{HP} = 8.0, 3H, M). **$^{13}C\{^1H\}$ NMR**: 129.1–126.1 (m, C, CH Ar), 38.7 (d, J_{CP} = 43.4, C), 26.4 (s, CH_3), 14.6 (d, J_{CP} = 38.4, CH_3). **$^{31}P\{^1H\}$ NMR**: +131.2 (s, M), +125.1 (s, m). **HRMS**: calcd for $C_{20}H_{26}OPPd$ ([M] − Cl)⁺, 419.0750; found 419.0764. **IR**: 3443, 2952, 2861, 1648, 1604, 1470, 1287, 1026, 865, 735, 696. **[α]$_D$** = +50° (c 1, CH_2Cl_2).

[Pd(η^3-Ph$_2$C$_3$H$_3$)(κP-(S)-L1)$_2$], L1Pd9

Dimer [Pd(η^3-C$_3$H$_3$Ph$_2$)Cl]$_2$ (100 mg, 0.15 mmol) was dissolved into a solution of (*S*)-L1 (75 mg, 0.63 mmol) in THF (10 mL). The suspension was stirred for 1 h at room temperature, NEt$_3$ (0.1 mL, 0.72 mmol) was added and the deep yellow solution was allowed to stir for further 30 min at room temperature. The solvent was evaporated *in vacuo* and the product was recrystallized with CH$_2$Cl$_2$/hexane yielding a yellow solid (159 mg, 98%).
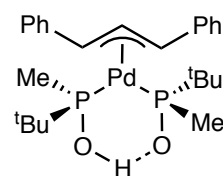
^{1}H NMR: 7.17–6.95 (m, 2Ph), 6.06 (ddd, J = 14.0, J = 10.8, J = 1.2, 1H, M), 5.52 (dd, J = 14.0, J = 5.6, 1H, m), 5.29 (dd, J = 13.6, J = 9.2, 1H, m), 4.98 (dd, J = 13.6, J = 10.4, 1H, m), 4.46 (ddd, J = 14.4, J = 8.4, J = 2.0, 1H, M), 3.97 (td, J = 10.8, J = 1.2, 1H, M), 1.31 (d, J_{HP} = 8.4, 3H, M), 1.14 (d, J_{HP} = 15.2, 9H, M), 0.82 (d, J_{HP} = 15.2, 9H, M), 0.76 (d, J_{HP} = 8.8, 3H, M). **^{13}C{^{1}H} NMR**: 128.9–127.1 (m, 2Ph), 113.4 (s, C$_{central}$, M), 113.4 (s, C$_{central}$, m), 91.2 (dd, J_{CP} = 27.3, J = 5.1, C$_{allyl}$, M), 78.6 (m, C$_{allyl}$, m), 77.6 (m, C$_{allyl}$, m), 69.4 (d, J_{CP} = 33.3, C$_{allyl}$, M), 39.1 (d, J_{CP} = 20.2, 2C), 25.8 (d, J_{CP} = 5.1, 3CH$_3$), 25.4 (d, J_{CP} = 6.1, 3CH$_3$), 8.9 (s, 2CH$_3$). **^{31}P{^{1}H} NMR**: +109.2 (d, J_{PP} = 68.0, M), +108.9 (d, J_{PP} = 61.6, m), +106.4 (d, J_{PP} = 61.6, m), +105.6 (d, J_{PP} = 68.0, M). **HRMS**: calcd for C$_{25}$H$_{39}$O$_2$P$_2$Pd ([M] + H)$^+$, 539.1454; found 539.1459. **EA**: Anal. calcd for C$_{25}$H$_{38}$O$_2$P$_2$Pd, %: C, 55.72; H, 7.11. Found, %: C, 53.59; H, 8.10. **IR**: 3417, 2935, 2739, 2670, 2487, 1648, 1483, 1400, 1183, 1017, 874, 687. [α]$_D$ = +893° (c 1, CH$_2$Cl$_2$).

[Pd(η^3-Ph$_2$C$_3$H$_3$)(κP-(S)-L1)$_2$], L1Pd10

A solution of **L1Pd9** (200 mg, 0.37 mmol) in CH$_2$Cl$_2$ (5 mL) was treated with HBF$_4$·OEt$_2$ (0.9 mL, 6.6 mmol). The reaction mixture was stirred for 30 min at room temperature and then it was extracted with water (3 x 10 mL). The organic layer was dried over Na$_2$SO$_4$, filtered and the solvent was evaporated *in vacuo*. The product was obtained as a pale yellow solid (199 mg, 92%).
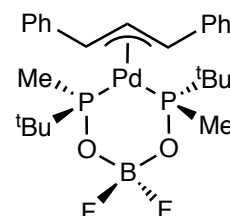
^{1}H NMR: 7.51–7.19 (m, 2Ph), 6.34 (ddd, J = 14.4, J = 10.8, J = 1.2, 1H, M), 6.08 (dt, J = 9.2, J = 2.8, 1H, m), 5.61 (dd, J = 13.6, J = 9.2, 1H, m), 5.19–5.12 (m, 1H, m), 4.92 (ddd, J = 14.0, J = 9.2, J = 1.6, 1H, M), 4.35 (t, J = 12.0, 1H, M), 1.38 (d, J_{HP} = 8.0, 3H, M), 1.16 (d, J_{HP} = 16.0, 9H, M), 0.81 (d, J_{HP} = 16.0, 9H, M), 0.75 (d, J_{HP} = 8.8, 3H, M).

^{13}C{^{1}H} NMR: 140.1–126.6 (m, 2Ph), 113.4 (t, J_{CP} = 7.1, C_{allyl}, M), 109.1 (t, J_{CP} = 6.1, C_{allyl}, m), 93.9 (dd, J_{CP} = 27.3, J = 6.1, C_{allyl}, M), 80.3 (t, J_{CP} = 15.2, C_{allyl}, m), 79.5 (t, J_{CP} = 18.2, C_{allyl}, m), 71.1 (dd, J_{CP} = 33.3, J = 5.1, C_{allyl}, M), 39.3 (ddd, J = 28.3, J = 14.1, J = 2, 2C, M), 37.4 (dd, J = 33.3, J = 16.2, 2C, m), 25.7 (d, J_{CP} = 4.0, 3CH$_3$), 25.3 (d, J_{CP} = 6.1, 3CH$_3$), 13.1 (d, J_{CP} = 27.2, CH$_3$), 12.2 (d, J_{CP} = 30.3, CH$_3$). ^{31}P{^{1}H} NMR: +125.9 (d, J_{PP} = 81.0), +118.3 (d, J_{PP} = 81.0). ^{19}F NMR: −136.1 - −136.4 (m, ^{11}BF$_2$), −137.3 - −138.0 (m, ^{10}BF$_2$). HRMS: calcd for C$_{25}$H$_{37}$BO$_2$F$_2$NaP$_2$Pd ([M] + Na)$^+$, 609.1256; found 609.1263. IR: 2941, 2860, 1462, 1365, 1288, 1199, 1063, 1020, 995, 940, 889, 757, 736, 698, 591. $[\alpha]_D$ = +851° (c 1, CH$_2$Cl$_2$).

6.5.2.2. *Complexes with the MaxPhos ligand*

[(η^5-C$_5$Me$_5$)MCl(MaxPhos)][BF$_4$] (M = Rh (L2Rh1), Ir (L2Ir1))

At room temperature, to a solution of the corresponding complex [(η^5-C$_5$Me$_5$)M(acac)Cl] (1.2 mmol) in 5 mL of CH$_2$Cl$_2$, (S_P)-[HMaxPhos][BF$_4$] (636.3 mg, 1.2 mmol) was added. The resulting orange (Rh) or yellow (Ir) solution was heated at reflux for 48 h and then was filtered to remove any insoluble material. The solution was concentrated under reduced pressure to ~1 mL. The slow addition of *n*-hexane led to the precipitation of a red-brown (Rh) or yellow (Ir) solid, which was washed with *n*-hexane (3 × 5 mL) and vacuum-dried.

[(η^5-C$_5$Me$_5$)RhCl(MaxPhos)][BF$_4$] (L2Rh1). Yield: 93%.

^{1}H NMR (300.13 MHz): 5.56 (brs, NH), 1.91 (d, J = 8.9, 3H, P^{1}Me), 1.74 (pt, J = 3.1, 15H, C$_5$Me$_5$), 1.46 (d, J = 16.2, 9H, P^2 ^{t}Bu), 1.42 (d, J = 15.3, 9H, P^2 ^{t}Bu) and 1.33 (d, J = 17.6, 9H, P^1 ^{t}Bu). ^{13}C{^{1}H} NMR (75.48 MHz): 103.7 (dt, J = 5.0, J = 2.7, C$_5$Me$_5$), 43.7 (dd, J = 5.4, J = 2.9, 15H, P^{2}CMe$_3$), 40.7 (dd, J = 16.9, J = 4.1, P^{1}CMe$_3$), 40.1 (dd, J = 11.8, J = 1.6, P^{2}CMe$_3$), 30.8 (d, J = 4.7, P^{2}CMe$_3$), 28.6 (br, P^{2}CMe$_3$), 27.0 d, J = 3.7, P^{1}CMe$_3$), 15.8 (d, J = 19.6, P^{1}Me) and 10.8 (brs, C$_5$Me$_5$). ^{31}P{^{1}H} NMR (121.42 MHz): +88.3 (dd, J_{RhP} = 115.6, J_{P1P2} = 89.0, P^2) and +55.1 (dd, J_{RhP} = 117.0, P^1).

EA: Anal. calcd for C$_{23}$H$_{46}$BClF$_4$NNP$_2$Rh, %: C, 44.28; H, 7.38; N, 2.24. Found, %: C, 44.11; H, 7.90; N, 2.05. IR: ν(NH) 3262, ν(BF$_4$) 1040. CD (acetone, 5.1 × 10^{-4} M, RT): λ, nm, ($\Delta\varepsilon$): 427 (+3.55); 341 (−11.99); 305 (+5.20).
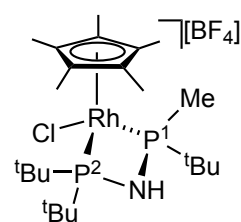
[(η^5-C$_5$Me$_5$)IrCl(MaxPhos)][BF$_4$] (L2Ir1). Yield: 89%.
^{1}H NMR (500.13 MHz): 6.89 (brs, NH), 1.94 (d, J = 8.8, 3H, P^{1}Me), 1.72 (pt, J = 2.2, 15H, C$_5$Me$_5$), 1.43 (d, J = 16.1, 9H, pro$R$-^{t}Bu P^2), 1.38 (d, J = 15.4, 9H, pro$S$-^{t}Bu P^2) and 1.28 (d, J = 17.5, 9H, P^1 ^{t}Bu). **^{13}C{^{1}H} NMR (125.77 MHz)**: 98.3 (dt, J = 1.3, C$_5$Me$_5$), 42.5 (dd, J = 12.2, J = 4.9, 15H, P^{2}CMe$_3$), 39.5 (dd, J = 32.9, J = 5.3, P^{2}CMe$_3$), 39.2 (d, J = 20.2, P^{1}CMe$_3$), 30.9 (d, J = 4.3, P^{2}CMe$_3$), 28.4 (br), 27.1 (d, J = 3.4, P^{1}CMe$_3$), 16.0 (d, J = 29.1, P^{1}Me) and 10.2, (s, C$_5$Me$_5$). **^{31}P{^{1}H} NMR (202.46 MHz)**: +55.2 (d, J_{P1P2} = 56.2, P^2) and +19.2 (d, P^1). **EA**: Anal. calcd for C$_{23}$H$_{46}$BClF$_4$IrNP$_2$, %: C, 38.74; H, 6.50; N, 1.96. Found, %: C, 38.25; H, 6.12; N, 2.14. **IR**: ν(NH) 3268, ν(BF$_4$) 1040. **CD (acetone, 5.2 × 10^{-4} M, RT)**: λ, nm, ($\Delta\varepsilon$): 368 (+2.54); 297 (−9.15).
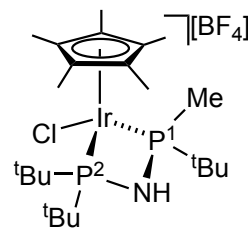
[(η^6-p-MeC$_6$H$_4$^{i}Pr)RuCl(MaxPhos)][X] (X = BF$_4$ (L2Ru1), PF$_6$ (L2Ru1'))

A solution of (S)-[HMaxPhos][BF$_4$] (200 mg, 0.56 mmol) in 10 mL of THF was cooled to −78 °C and n-BuLi (0.5 mL of a 1.6 M solution in hexanes, 0.8 mmol) was added slowly. The reaction mixture was stirred for 30 min and then it was warmed to room temperature. At this point methanol (1 mL), ammonium tetrafluoroborate or hexafluorophosphate (1.9 mmol) and the Ru dimer [RuCl(μ-Cl)(η^6-p-MeC$_6$H$_4$^{i}Pr)]$_2$ (171 mg, 0.28 mmol) were added. The resulting mixture was stirred at room temperature for 48 h protected from light and after this time was evaporated to dryness. The crude was extracted with water (10 mL) and dichloromethane (3 × 20 mL) and the organic layers were combined and dried with anhydrous sodium sulphate. The resulting solution was brought to dryness under vacuum. The crude was further recrystallized from CH$_2$Cl$_2$/Et$_2$O to yield the title product as a pale brown solid.

[(η^6-p-MeC$_6$H$_4$^{i}Pr)RuCl(MaxPhos)][BF$_4$] (L2Ru1). Yield: 85%.
^{1}H NMR (400.13 MHz): 5.83 (dt, J = 6.0, J = 1.6, 1H, p-Me^{i}PrC$_6$H$_4$), 5.71 (dd, J = 6.4, J = 1.6, 1H, p-MeC$_6$H$_4$^{i}Pr), 5.66 (d, J = 6.4, 1H, p-Me^{i}PrC$_6$H$_4$), 5.28 (pt, 1H, NH), 5.11 (d, J = 6.0, 1H, p-Me^{i}PrC$_6$H$_4$), 3.11 (sept, J = 6.4, 1H, p-Me^{i}PrC$_6$H$_4$), 2.50 (brs, t, J = 1.6, 3H, p-Me^{i}PrC$_6$H$_4$), 2.01 (d, J = 8.4, 3H, P^{1}Me), 1.46 (d, J = 16.0, 9H, P^2 ^{t}Bu), 1.36 (d, J = 17.2, 9H, P^2 ^{t}Bu), 1.33 (d, J = 6.3, 3H, p-Me^{i}PrC$_6$H$_4$), 1.28 (d, J = 6.8, 3H, p-Me^{i}PrC$_6$H$_4$).
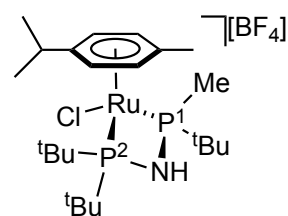
^{13}C{^{1}H} NMR (101.01 MHz): 118.9 (dd, J = 8.6, J = 2.0, p-Me^{i}PrC$_6$H$_4$), 112.2 (dd, J = 4.7, J = 3.3, p-Me^{i}PrC$_6$H$_4$), 102.7 (s, p-Me^{i}PrC$_6$H$_4$), 90.6 (d, J = 7.6, p-Me^{i}PrC$_6$H$_4$), 86.1 (s, 2C, p-Me^{i}PrC$_6$H$_4$), 43.3 (dd, J = 8.0, J = 2.9, P^{2}CMe$_3$), 40.8 (d, J = 16.6, P^{1}CMe$_3$), 40.0 (dd, J = 28.8, J = 3.6, P^{2}CMe$_3$), 31.6 (s, p-Me^{i}PrC$_6$H$_4$), 31.4 (d, J = 4.7, P^{2}CMe$_3$), 27.4 (d, J = 3.7, P^{2}CMe$_3$), 24.4 (d, J = 2.2, p-Me^{i}PrC$_6$H$_4$), 20.9 (s, p-Me^{i}PrC$_6$H$_4$), 19.9 (s, p-Me^{i}PrC$_6$H$_4$), 19.1 (d, J = 23.3, P^{1}Me). ^{31}P{^{1}H} NMR (162.01 MHz): +90.8 (d, J_{P1P2} = 89.3, P^2), +63.1 (d, P^1). EA: Anal. calcd. for C$_{23}$H$_{45}$BClF$_4$NP$_2$Ru, %: C, 44.49; H, 7.31; N, 2.26. Found, %: C, 44.52; H, 7.43; N, 2.50. IR: v(NH) 3287, v(BF$_4$) 1065.

[(η^6-p-MeC$_6$H$_4$^{i}Pr)RuCl(MaxPhos)][PF$_6$] (L2Ru1·PF$_6$).

Yield: 68%.

^{1}H NMR (400.13 MHz): 5.83 (dt, J = 6.0, J = 2.0, 1H, p-Me^{i}PrC$_6$H$_4$), 5.72 (dd, J = 6.4, J = 1.2, 1H, p-Me^{i}PrC$_6$H$_4$), 5.68 (d, J = 6.4, 1H, p-Me^{i}PrC$_6$H$_4$), 5.09 (d, J = 6.0, 1H, p-Me^{i}PrC$_6$H$_4$), 4.62 (pt, 1H, NH), 3.10 (sept, J = 6.4, 1H, p-Me^{i}PrC$_6$H$_4$), 2.49 (brs, t, J = 1.2, 3H, p-Me^{i}PrC$_6$H$_4$), 1.97 (d, J = 8.4, 3H, P^{1}Me), 1.44 (d, J = 16.0, 9H, P^{2t}Bu), 1.37 (brs, 9H, P^2 ^{t}Bu), 1.35 (d, J = 17.6, 9H, P^2 ^{t}Bu), 1.33 (d, J = 5.6, 3H, p-Me^{i}PrC$_6$H$_4$), 1.29 (d, J = 6.8, 3H, p-Me^{i}PrC$_6$H$_4$). ^{13}C{^{1}H} NMR (101.01 MHz): 119.2 (dd, J = 8.7, J = 2.1, p-Me^{i}PrC$_6$H$_4$), 112.4 (dd, J = 4.5, J = 3.4, p-Me^{i}PrC$_6$H$_4$), 102.8 (d, J = 3.4, p-Me^{i}PrC$_6$H$_4$), 90.6 (d, J = 7.6, p-Me^{i}PrC$_6$H$_4$), 86.3 (s, p-Me^{i}PrC$_6$H$_4$), 86.2 (s, p-Me^{i}PrC$_6$H$_4$), 43.4 (dd, J = 7.5, J = 2.9, P^{2}CMe$_3$), 40.8 (d, J = 16.3, P^{1}CMe$_3$), 40.0 (dd, J = 28.4, J = 3.5, P^{2}CMe$_3$), 31.7 (s, p-Me^{i}PrC$_6$H$_4$), 31.5 (d, J = 4.7, P^{2}CMe$_3$), 27.4 (d, J = 3.7, P^{2}CMe$_3$), 24.5 (d, J = 2.6, p-Me^{i}PrC$_6$H$_4$), 20.9 (s, p-Me^{i}PrC$_6$H$_4$), 19.9 (s, p-Me^{i}PrC$_6$H$_4$), 19.2 (d, J = 23.2, P^{1}Me). ^{31}P{^{1}H} NMR (121.01 MHz): +92.3 (d, J_{P1P2} = 88.0, P^2), +64.8 (d, P^1). EA: Anal. calcd. for C$_{23}$H$_{45}$ClF$_6$NP$_3$Ru, %: C, 40.68; H, 6.68; N, 2.06. Found, %: C, 40.42; H, 6.84; N, 2.20. IR: v(NH) 3343, v(PF$_6$) 845.
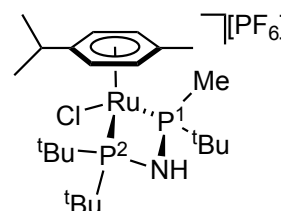
[(η^5-C$_5$Me$_5$)Ir(MaxPhos)][BF$_4$] (L2Ir2)

At 253 K, to a solution of the complex [(η^5-C$_5$Me$_5$)IrCl(MaxPhos)][BF$_4$] (150.0 mg, 0.21 mmol) in 5 mL of CH$_2$Cl$_2$ AgBF$_4$ (45.0 mg, 0.23 mmol) was added. The resulting solution was stirred for 4 h and then was filtered to remove the AgCl formed. The pale yellow solution was concentrated under reduced pressure to ~1 mL. The slow addition of Et$_2$O led to the formation of an oily residue that was broken up by stirring the suspension in Et$_2$O.

Yield: 120.0 mg, 84%. Diastereomeric ratio: 82/18. **EA**: Anal. calcd for $C_{23}H_{45}BF_4IrNP_2$, %: C, 40.83; H, 6.70; N, 2.07. Found, %: C, 40.35; H, 6.39; N, 2.04. **IR**: ν(NH) 3298, ν(BF$_4$) 1051.

S_{Ir},R_{P1},S_{P2}-L2Ir2.Yield: 82%.

^{1}H NMR (500.13 MHz, CD$_2$Cl$_2$): 5.85 (brs, NH), 2.13 (dpt, $J_{P2H} \approx J_{HH}$ = 8.9, J_{P1H} = 5.0, 1H, pro$S$-Ir-CHH), 2.03 (pt, J = 2.2, 15H, C$_5$Me$_5$), 2.02 (P^{1}Me overlapped), 1.39 (dpt, $J_{P2H} \approx J_{HH}$ = 9.5, J_{P1H} = 3.5, 1H, pro$R$-Ir-CHH), 1.27 (d, J = 16.5, 9H, P^1 ^{t}Bu), 1.26 (3H, P^{2}CMe, overlapped), 1.24 (d, J = 16.0, 3H, P^{2}CMe) and 1.23 (d, J = 16.1, 9H, P^2 ^{t}Bu). **^{13}C{^{1}H} NMR (125.77 MHz, CD$_2$Cl$_2$)**: 95.3 (pt, J = 2.7 Hz, C_5Me$_5$), 59.5 (dd, J = 30.1, J = 4.2, P^2CMe$_2$), 38.1 (dd, J = 29.6, J = 8.8, P^1CMe$_3$), 36.7 (pt, J = 2.5, P^2CMe$_3$), 28.6 (d, J = 4.0, P^{2}CMe), 26.3 (d, J = 4.3, P^{1}CMe_3), 25.9 (d, J = 4.3, P^{2}CMe_3), 23.8 (d, J = 7.0, P^{2}CMe), 18.4 (d, J = 30.7, P^{1}Me$_3$), 10.4 (s, C$_5$$Me_5$) and −7.4 (dd, J = 40.3, J = 15.0, Ir-C). **^{31}P{^{1}H} NMR (202.46 MHz, CD$_2$Cl$_2$)**: +21.5 (d, J_{P1P2} = 60.2, P^1) and −1.9 (d, P^2).

R_{Ir},R_{P1},R_{P2}-L2Ir2. Yield: 18%.

^{1}H NMR (500.13 MHz, CD$_2$Cl$_2$): 5.74 (brs, NH), 2.02 (pt, J = 2.2, 15H, C$_5$Me$_5$), 1.82, (dpt, $J_{P2H} \approx J_{HH}$ = 9.2, J_{P1H} = 4.7, 1H, Ir-CHH), 1.79 (d, J = 8.4, P^{1}Me), 1.33 (3H, P^{2}CMe, overlapped) and 1.19 (d, J = 16.2, 9H, P^2 ^{t}Bu). **^{13}C{^{1}H} NMR (125.77 MHz, CD$_2$Cl$_2$)**: 95.4 (pt, J = 2.9, C_5Me$_5$), 58.9 (dd, J = 31.4, J = 1.9, P^2CMe$_2$), 37.1 (pt, J = 4.5, PCMe$_3$), 29.6 (d, J = 3.9, P^{2}CMe), 25.1 (d, J = 5.4, P^{2}CMe_3), 24.8 (d, J = 5.8, P^{2}CMe_3), 10.6 (s, C$_5$$Me_5$), 8.6 (dd, J = 27.4, J = 5.1, P^{1}Me$_3$) and −2.6 (dd, J = 64.0, J = 5.5, Ir-C). **^{31}P{^{1}H} NMR (202.46 MHz, CD$_2$Cl$_2$)**: +37.5 (d, J_{P1P2} = 51.9, P^1) and −8.7 (d, P^2).
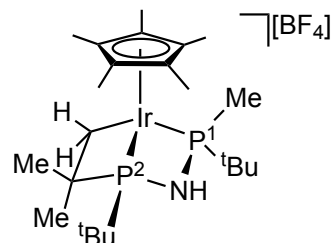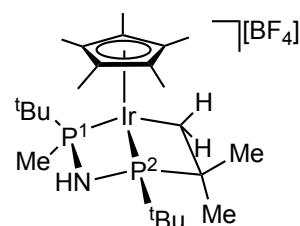
[(η^5-C$_5$Me$_5$)Rh(MaxPhos)(NCMe)][BF$_4$]$_2$ (L2Rh2)

To a solution of complex **L2Rh1** (75.0 mg, 0.12 mmol) in 10 mL of MeCN, AgBF$_4$ (26.0 mg, 0.13 mmol) was added. The resulting solution was stirred for 6 h at RT and then was filtered to remove the AgCl formed. The yellow solution was concentrated under reduced pressure to ~1 mL. The slow addition of Et$_2$O led to the formation of a yellow solid, which was washed with Et$_2$O (3 × 5 mL) and vacuum-dried. **Yield**: 62.0 mg, 72%.
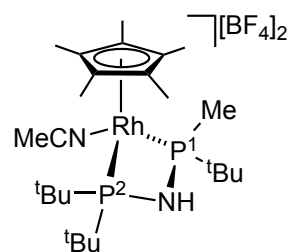
^{1}H NMR (500.13 MHz, CD$_2$Cl$_2$): 5.97 (brs, NH), 1.99 (d, J = 9.2, 3H, P^{1}Me), 1.90 (pt, J = 3.7, 15H, C$_5$Me$_5$), 1.46 (d, J = 16.5, 9H, P^2 ^{t}Bu), 1.44 (d, J = 16.4, 9H, P^2 ^{t}Bu), 1.35 (d, J = 18.1, 9H, P^1 ^{t}Bu) and 1.31 (brs, CNMe). **^{31}P{^{1}H} NMR (202.46 MHz, CD$_2$Cl$_2$)**: +90.7 (dd, J_{RhP} = 108.5, J_{P1P2} = 77.4, P^2) and +56.0 (dd, J_{RhP} = 112.2, P^1). **HRMS**: calcd for C$_{23}$H$_{45}$NP$_2$Rh [M–NCMe–H]$^+$, 500.2077; found 500.2129; calcd for C$_{23}$H$_{46}$NP$_2$Rh [M–NCMe]$^{2+}$, 250.6078; found 250.6028. **IR**: ν(NH) 3261, ν(BF$_4$) 1040. **CD (acetone, 4.9 × 10^{-4} M, RT)**: λ, nm, ($\Delta\varepsilon$): 394 (+3.30); 327 (–7.31); 299 (–6.99).

[(η^6-p-MeC$_6$H$_4$^{i}Pr)Ru(MaxPhos)(NCMe)][BF$_4$]$_2$ (L2Ru2)
To a solution of complex **L2Ru1** (60.0 mg, 0.097 mmol) in 10 mL of CH$_2$Cl$_2$ AgBF$_4$ (20 mg, 0.13 mmol) was added. After 1 h, acetonitrile (1 mL) was added and the resulting solution was stirred for 1 h at RT shielded from light and then it was filtered to remove the AgCl formed. The clear solution was brought to dryness yielding the title product as a yellowish oil. **Yield**: 60.0 mg, 88%.
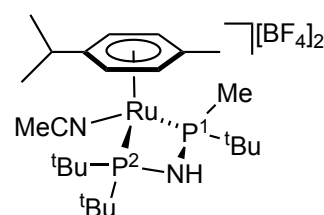
^{1}H NMR (400.13 MHz, CD$_3$CN): 6.43 (dt, J = 6.4, J = 1.6, 1H, p-Me^{i}PrC$_6$H$_4$), 6.32 (d, J = 6.4, 1H, p-Me^{i}PrC$_6$H$_4$), 6.21 (dd, J = 6.8, J = 1.6, 1H, p-Me^{i}PrC$_6$H$_4$), 5.60 (d, J = 6.4, 1H, p-Me^{i}PrC$_6$H$_4$), 5.20 (brs, 1H, NH), 3.07 (sept, J = 6.8, 1H, p-Me^{i}PrC$_6$H$_4$), 2.49 (brs, t, J = 2.0, 3H, p-Me^{i}PrC$_6$H$_4$), 2.04 (d, J = 8.8, 3H, P^{1}Me), 1.35 (d, J = 16.0, 9H, P^2 ^{t}Bu), 1.34 (d, J = 16.0, 9H, P^2 ^{t}Bu), 1.26 (d, J = 16.0, 9H, P^1 ^{t}Bu), 1.30 (d, J = 6.0, 3H, p-Me^{i}PrC$_6$H$_4$). **^{13}C{^{1}H} NMR (101.01 MHz, CD$_3$CN)**: 124.1 (dd, J = 6.7, J = 1.7, p-Me^{i}PrC_6H$_4$), 117.6 (pt, J = 3.6, p-Me^{i}PrC_6H$_4$), 100.9 (s, p-Me^{i}PrC_6H$_4$), 93.0 (d, J = 5.4, p-Me^{i}PrC_6H$_4$), 91.7 (s, p-Me^{i}PrC_6H$_4$), 91.0 (s, p-Me^{i}PrC_6H$_4$), 43.4 (dd, J = 9.8, J = 2.8, P^2CMe$_3$), 42.1 (d, J = 17.0, P^1CMe$_3$), 41.2 (dd, J = 28.9, J = 3.5, P^2CMe$_3$), 32.5 (s, p-Me^{i}PrC_6H$_4$), 29.6 (d, J = 4.5, P^{2}CMe_3), 26.7 (d, J = 4.0, P^{2}CMe_3), 26.3 (d, J = 3.5, P^{1}CMe_3), 24.0 (d, J = 2.2, p-Me^{i}PrC_6H$_4$), 21.8 (s, p-Me^{i}PrC$_6$H$_4$), 20.2 (s, p-Me^{i}PrC$_6$H$_4$), 19.5 (d, J = 26.0, P^1Me). **^{31}P{^{1}H} NMR (162.01 MHz, CD$_3$CN)**: +94.8 (d, J_{P1P2} = 73.9, P^2), +67.7 (d, P^1). **HRMS**: calcd for C$_{25}$H$_{48}$N$_2$P$_2$Ru [M]$^{2+}$, 270.1162; found 270.1158. **IR**: ν(NH) 3469, ν(BF$_4$) 1022.

6.5.2.3. *Complexes with MaxPHOX ligands*

General procedure for the preparation of [Ir(P,N)(COD)]BArF complexes (**L3S**, **L3R**, **L4R**).[12]

The corresponding borane protected ligand **L3S**, **L3R**, **L4R** (1 eq) was dissolved in pyrrolidine (0.06 M) and stirred for 16 h at 90 °C. Afterwards, pyrrolidine was removed 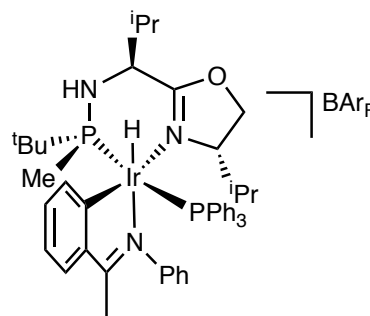*in vacuo* at room temperature over 1 h. When no pyrrolidine remained, the crude was further dried under vacuum for 30 min at 50 °C. A solution of [Ir(COD)(Cl)]$_2$ (0.5 eq) in CH$_2$Cl$_2$ (0.06 M) was then added to the free ligand via cannula and the resulting solution was stirred for 40 min at room temperature. NaBArF (1 eq) was added to the previous deep orange solution and the mixture was stirred 1 h more at room temperature. The crude was evaporated *in vacuo* until 1 mL and then was filtered through a small plug of silica gel, washing first with *n*-hexane and then eluting with *n*-hexane:CH$_2$Cl$_2$ (1:1). The reddish fraction was collected and concentrated to yield the corresponding iridium complexes as deep orange solids.

[Ir(L3S)(COD)]BArF, L3SIr

^{1}H NMR: 7.75–7.67 (m, 8H), 7.53 (br s, 4H), 4.96–4.86 (m, 1H), 4.67–4.58 (m, 1H), 4.50 (dd, J = 10.0, J = 4.0, 1H), 4.28 (t, J = 10.0, 1H), 4.22 (br s, 1H), 3.98 (dt, J = 10.0, J = 4, 1H), 3.86–3.73 (m, 1H), 3.42 (ddd, J = 18.0, J = 10.0, J = 7, 1H), 2.37–2.24 (m, 1H), 2.23–2.00 (m, 6H), 1.97–1.92 (m, 1H), 1.91–1.84 (m, 1H), 1.77–1.66 (m, 2H), 1.41 (d, J_P = 7, 3H), 1.10 (d, J_P = 15.0, 9H), 1.08 (d, J = 7.0, 3H), 0.98 (d, J = 7.0, 3H), 0.91 (d, J = 7.0, 3H), 0.80 (d, J = 7.0, 3H). **^{31}P{^{1}H} NMR**: +59.7 (s). **^{19}F NMR**: –62.4 (s).
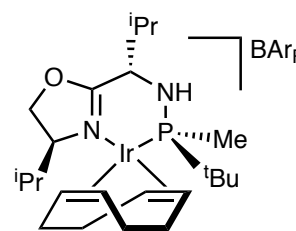
[Ir(L3R)(COD)]BArF, L3RIr

^{1}H NMR: 7.72–7.68 (m, 8H), 7.53 (br s, 4H), 4.92–4.84 (m, 1H), 4.68–4.60 (m, 1H), 4.57 (dd, J = 10.0, J = 4.0, 1H), 4.35 (t, J = 10.0, 1H), 3.97–3.85 (m, 2H), 3.65–3.52 (m, 2H), 2.49–2.38 (m, 1H), 2.38–2.28 (m, 1H), 2.26–2.02 (m, 5H), 1.84–1.69 (m, 3H), 1.47–1.44 (m, 1H), 1.32 (d, J_P = 7.0, 3H), 1.18 (d, J_P = 15.0, 9H), 1.01 (d, J = 7.0, 3H), 0.95 (d, J = 7.0, 3H), 0.93 (d, J = 7.0, 3H), 0.75 (d, J = 7.0, 3H). **^{31}P{^{1}H} NMR**: +62.1 (s). **^{19}F NMR**: –62.4 (s).
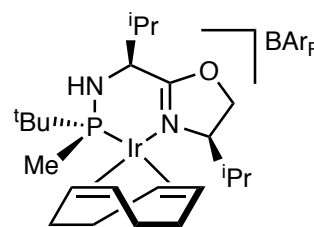
[Ir(L4R)(COD)]BArF, L4RIr

^{1}**H NMR**: 7.70 (br m, 8H), 7.53 (br s, 4H), 4.88–4.71 (m, 2H), 4.67 (dd, J = 10.0, J = 3.0, 1H), 4.34 (t, J = 10.0, 1H), 3.98 (dt, J = 12.0, J = 3, 1H), 3.97–3.87 (m, 1H), 3.76 (dd, J = 9.0, J = 3.0, 1H), 3.48–3.33 (m, 1H), 2.56–2.44 (m, 1H), 2.43–2.35 (m, 2H), 2.31–2.18 (m, 1H), 2.18–2.08 (m, 1H), 2.08–1.91 (m, 2H), 1.66–1.47 (m, 2H), 1.38 (d, J_P = 8.0, 3H), 1.20 (d, J_P = 15.0, 9H), 1.01 (d, J = 7.0, 3H), 0.94 (s, 9H), 0.89 (d, J = 7.0, 3H). ^{31}**P{^{1}H} NMR**: +62.9 (s). ^{19}**F NMR**: –62.4 (s).
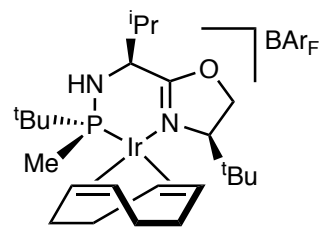
[Ir(L3R)(COD)]BF₄, L3RIr·BF₄

The corresponding borane protected ligand **L3R** (1 eq) was dissolved in freshly distilled pyrrolidine (0.06 M) and stirred for 16 h at 90 °C. Afterwards, pyrrolidine was removed *in vacuo* at room temperature over 1 h. When no pyrrolidine remained, the crude was further dried under vacuum for 30 min at 50 °C. A solution of [Ir(COD)(Cl)]₂ (0.5 eq) in CH₂Cl₂ (0.06 M) was then added to the free ligand via cannula and the resulting solution was stirred for 40 min at room temperature. NaBF₄ (1 eq) was added and the mixture was stirred 1 h more at room temperature. The crude was evaporated *in vacuo* until 1 mL and then was filtered through a small plug of silica gel, washing first with *n*-hexane and then eluting with *n*-hexane:MeOH (1:0.5). The reddish fraction was collected and evaporated to dryness. The crude was washed twice with pentane and concentrated *in vacuo* to yield the product as an orange solid.
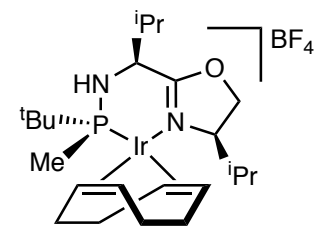
^{1}**H NMR**: 5.01–4.92 (m, 1H), 4.75–4.70 (m, 1H), 4.45 (dd, J = 9.5, J = 3.9, 1H), 4.06–4.02 (m, 1H), 3.86 (d, J = 7.4, 1H), 3.67 (m, 1H), 2.27–2.11 (m, 5H), 2.03–1.96 (m, 3H), 1.81 (m, 1H), 1.79–1.71 (m, 4H), 1.38 (d, J = 8.0, 3H), 1.12 (d, J = 15.0, 9H), 1.05 (d, J = 6.6, 3H), 0.95 (d, J = 6.9, 3H), 0.91 (d, J = 6.9, 3H), 0.86 (d, J = 6.6, 3H). ^{31}**P{^{1}H} NMR**: +60.0 (s). ^{19}**F NMR**: –152.1 (s).

343

L3SIr1

A *Schlenk* flask was charged with 50 mg of complex **L3SIr** (0.035 mmol, 1 eq) and 13.5 mg (0.035 mmol, 1 eq) of acetophenone *N*-phenyl imine, **I1**. The flask was purged with three vacuum/N_2 cycles and the solids were 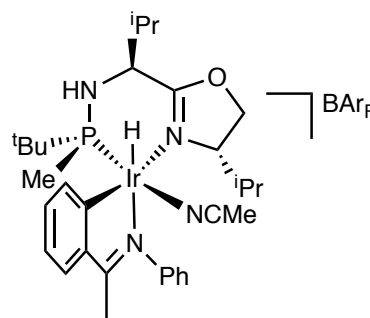dissolved in 3 mL of TH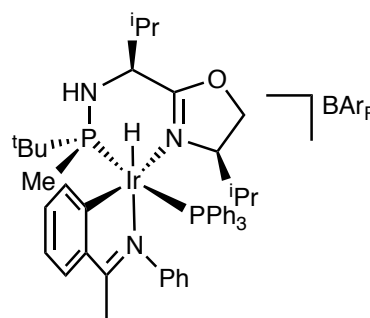F. The solution was transferred into a Fisher-Porter tube and stirred for 2 h under 2 bar of H_2. During this period, the initially orange solution turned yellow. At the due time, the hydrogen was vented and 9.2 mg of PPh_3 (0.035 mmol, 1 eq) were added and the resulting solution was stirred at room temperature for 30 min. The solvent was evacuated and the crude was recrystallized in CH_2Cl_2/pentane.

Yellow solid. **Yield**: 93% (57 mg). **^{1}H NMR (400 MHz, C_6D_6)**: 8.42 (br s, 8H), 7.98–7.96 (m, 2H), 7.69 (br s, 4H), 7.41–7.37 (m, 10H), 7.06–7.04 (m, 20H), 6.95–6.91 (m, 14H), 6.79–6.77 (d, *J* = 8.4, 2H), 4.21 (q, *J* = 6.4, 1H), 3.81–3.78 (m, 1H), 3.69 (t, *J* = 9.3, 1H), 3.61–3.58 (m, 1H), 3.24–3.22 (m, 1H), 1.99–1.93 (m, 1H), 1.11 (d, *J* = 6.7, 3H), 0.94 (d, *J* = 6.4, 3H), 0.88 (d, *J* = 6.3, 3H), 0.54 (d, *J* = 15, 9H), 0.02 (d, *J* = 6.4, 3H), −0.1 (d, *J* = 6.3, 3H), −11.5 (dm, *J* = 119.4, 1H), −22.3 (qd, *J* = 19, *J* = 5, 1H). **^{31}P{^{1}H} NMR (162 MHz, C_6D_6)**: +60.0 (s), +58.1 (s). **HRMS**: calcd for $C_{47}H_{60}N_3OP_2Ir$ [M + H]$^{2+}$, 468.6915; found 468.6915; calcd for $C_{29}H_{44}N_3OPIr$ [M − PPh_3]$^+$, 674.2845; found 674.2848; calcd for $C_{47}H_{59}N_3OP_2Ir$ [M]$^+$, 936.3757; found 936.3753; calcd. for $C_{32}H_{12}BF_{24}$ [M]$^-$, 863.0654; found 863.0662.

L3SIr2

A *Schlenk* flask was charged with 50 mg of complex **L3SIr** (0.035 mmol, 1 eq) and 13.5 mg (0.035 mmol, 1 eq) of acetophenone *N*-phenyl imine, **I1**. The flask was purged with three vacuum/N_2 cycles and the solids were dissolved in 3 mL of THF.
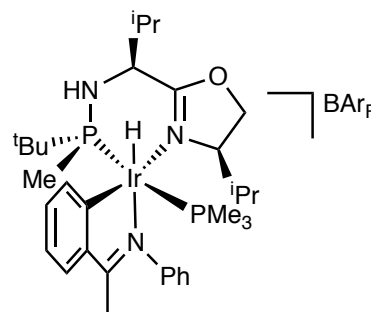
The solution was transferred into a Fisher-Porter tube and stirred for 2 h under 2 bar of H_2. During this period, the initially orange solution turned yellow. At the due time, the flask was vented and 35 mL of a 1 M THF solution of PMe_3 (0.035 mmol, 1 eq) were added and the resulting solution was stirred at room temperature for 30 min. The solvent was evacuated and the crude was recrystallized in CH_2Cl_2/pentane.

Pale-yellow solid. **Yield**: 97% (54 mg). **^{1}H NMR**: 7.75 (br s, 8H), 7.67 (d, J = 7.6, 1H), 7.64 (dd, J = 8.0, J = 1.2, 1H), 7.52 (br s, 4H), 7.42–7.38 (m, 2H), 7.28–7.22 (m, 2H), 7.15 (t, J = 7.6, 1H), 7.01 (td, J = 7.2, J = 1.2, 1H), 6.9 (s, 1H), 4.30 (dd, J = 14.4, J = 5.2, 1H), 4.09–4.00 (m, 2H), 2.82–2.77 (m, 1H), 2.50 (d, J = 1.2, 3H), 2.30–2.18 (m, 1H), 1.87 (d, J = 9.2, 3H), 1.54–1.45 (m, 1H), 1.17 (dd, J = 8.8, J = 2.0, 9H), 0.90 (d, J = 7.2, 3H), 0.77 (d, J = 6.8, 3H), 0.69 (d, J = 6.8, 3H), 0.61 (d, J = 6.8, 3H), 0.51 (d, J = 14.0, 9H), −19.95 (t, J = 19.6, 1H). **^{31}P{^{1}H} NMR**: +38.9 (d, J = 349.3, PN), −45.1 (d, J = 349.3, PMe$_3$). **HRMS**: calcd for $C_{32}H_{53}N_3OP_2Ir$ [M]$^+$, 750.3287; found 750.3284; calcd for $C_{29}H_{44}N_3OPIr$ [M − PMe$_3$]$^+$, 674.2845; found 674.2833; calcd. for $C_{32}H_{12}BF_{24}$ [M]$^-$, 863.0654; found 863.0663.

L3SIr3

A *Schlenk* flask was charged with 50 mg of complex **L3SIr** (0.035 mmol, 1 eq) and 13.5 mg (0.035 mmol, 1 eq) of acetophenone *N*-phenyl imine, **I1**. The flask was purged with three vacuum/N$_2$ cycles and the so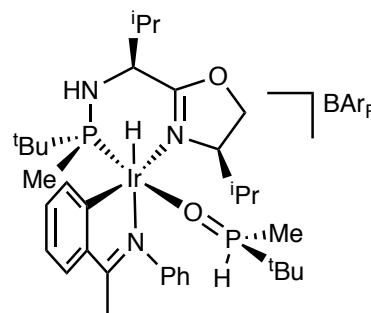lids were dissolved in 3 mL of THF. The solution was transferred into a Fisher-Porter tube and stirred for 2 h under 2 bar
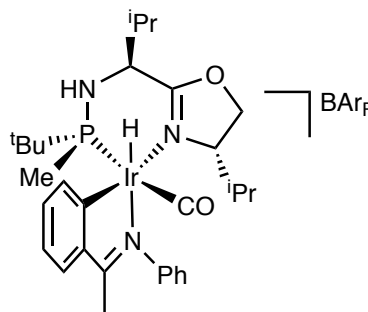
of H$_2$. During this period, the initially orange solution turned yellow. At the due time, the flask was vented and repressurised with 2 bar of CO and the resulting solution was stirred at room temperature for 40 min. The solvent was evacuated and the crude was recrystallized in CH$_2$Cl$_2$/pentane.

Pale-yellow solid. **Yield**: 97% (53 mg). **^{1}H NMR (400 MHz, CD$_2$Cl$_2$)**: 7.97 (dd, J = 7.6, J = 1.6, 1H), 7.72 (br s, 8H), 7.57 (br s, 6H), 7.44–7.43 (m, 3H), 7.37–7.34 (br t, J = 6.7, 2H), 7.08 (t, J = 7.4, 1H), 6.78 (dd, J = 8.4, J = 1.2, 2H), 4.49 (q, J = 6.8, 1H), 4.23 (dd, J = 9.1, J = 3.0, 1H), 4.15 (dd, J = 9.3, J = 2.8, 1H), 4.08 (d, J = 10.0, 1H), 3.88–3.85 (m, 1H), 3.47 (dd, J = 9.0, J = 3.1, 1H), 2.43 (br d, J = 11.0, 1H), 1.51 (d, J = 6.7, 3H), 1.16 (d, J = 10.0, 9H), 0.73 (d, J = 3.1, 3H), 0.64 (d, J = 3.0, 3H), 0.59 (d, J = 3.1, 3H), 0.52 (d, J = 3.0, 3H), −6.8 (d, J = 17.8, 1H), −16.7 (d, J = 17.8, 1H). **^{31}P{^{1}H} NMR (162 MHz, CD$_2$Cl$_2$)**: +51.1 (s), +44.7 (s).

HRMS: calcd for $C_{29}H_{44}N_3OPIr$ [M − CO]$^+$, 674.2845; found 674.2834; calcd for $C_{30}H_{44}N_3O_2PIr$ [M]$^+$, 702.2795; found 702.2793; calcd. for $C_{32}H_{12}BF_{24}$ [M]$^-$, 863.0654; found 863.0662. **IR**: 3443, 2965, 2926, 2052, 1609, 1383, 1361, 1274, 1126, 1026 and 809.

L3SIr4

A *Schlenk* flask was charged with 50 mg of complex **L3SIr** (0.035 mmol, 1 eq) and 13.5 mg (0.035 mmol, 1 eq) of acetophenone *N*-phenyl imine, **I1**. The flask was purged with three vacuum/N_2 cycles and the solids were dissolved in 3 mL of THF. The solution was transferred into a Fisher-Porter tube and stirred for 2 h under 2 bar of H_2. During this period, the initially orange solution turned yellow. At the due time, the flask was vented and one drop of acetonitrile was added and the resulting solution was stirred at room temperature for 30 min. The solvent was evacuated and the crude was recrystallized in CH_2Cl_2/pentane.

Pale-yellow solid. **Yield**: 89% (49 mg). **^{1}H NMR (400 MHz, CD$_3$CN)**: 7.99 (dd, J = 7.2, J = 1.6, 1H), 7.67 (br s, 12H), 7.48–7.42 (m, 3H), 7.31 (dt, J = 45.0, J = 7.5, 2H), 7.09 (br d, J = 7.4, 2H), 7.04 (t, J = 6.8, 1H), 4.33 (dd, J = 9.1, J = 2.7, 1H), 4.13 (br d, J = 9.2, 1H), 3.84–3.81 (m, 1H), 3.64–3.61 (m, 1H), 2.47–2.43 (m, 1H), 2.40 (s, 3H), 2.05–2.01 (m, 1H), 1.05 (d, J = 14.9, 9H), 0.94 (d, J = 9.4, 3H), 0.89 (d, J = 7.2, 3H), 0.82 (d, J = 7.1, 3H), 0.66 (d, J = 7.2, 3H), 0.54 (d, J = 7.1, 3H), −19.57 (d, J = 22.7). **^{31}P{^{1}H} NMR (162 MHz, CD$_3$CN)**: +42.9 (d, J = 20.3). **HRMS**: calcd for $C_{29}H_{44}N_3OPIr$ [M − CH$_3$CN]$^+$, 674.2845; found 674.2843; calcd. for $C_{32}H_{12}BF_{24}$ [M]$^-$, 863.0654; found 863.0661. **IR**: 3461, 2965, 1652, 1352, 1283, 1270, 1091, 1022, 800 and 683.

L3RIr1

A *Schlenk* flask was charged with 50 mg of complex **L3RIr** (0.035 mmol, 1 eq) and 13.5 mg (0.035 mmol, 1 eq) of acetophenone *N*-phenyl imine, **I1**. The flask was purged with three vacuum/N_2 cycles and the solids were 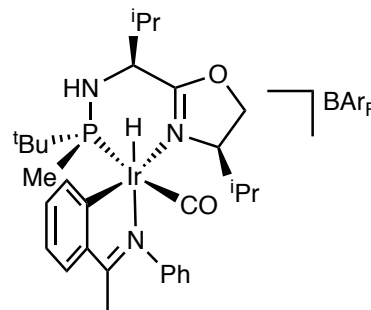dissolved in 3 mL of THF. The solution was transferred into a Fisher-Porter tube and stirred for 2 h under 2 bar of H_2. During this period, the initially orange solution turned yellow. At the due time, the hydrogen was vented and 9.2 mg of PPh$_3$ (0.035 mmol, 1 eq) were added and the resulting solution was stirred at room temperature for 30 min. The solvent was evacuated and the crude was recrystallized in CH_2Cl_2/pentane.

Yellow solid. **Yield**: 94% (59 mg). **^{1}H NMR (400 MHz, CD$_2$Cl$_2$)**: 7.72 (br s, 8H), 7.56 (br s, 6H), 7.46–7.39 (m, 6H), 7.35–7.26 (m, 11H), 7.16 (d, J = 7.6, 2H), 7.04 (d, J = 7.6, 1H), 6.82 (t, J = 7.6, 1H), 6.73 (td, J = 7.6, J = 1.6 Hz, 1H), 4.15 (dd, J = 9.6, J = 2.4, 1H), 3.73 (t, J = 8.8, 1H), 3.12 (dd, J = 14.4, J = 8.8, 1H), 2.96 (d, J = 8.8, 1H), 2.05 (s, 3H), 2.01 (d, J = 8.4, 3H), 1.97 (m, 1H), 1.81–1.77 (m, 1H), 0.85 (d, J = 6.4, 3H), 0.73 (d, J = 6.8, 3H), 0.57 (d, J = 6.8, 3H), 0.51 (d, J = 14.4, 9H), 0.27 (d, J = 6.8, 3H), −19.77 (t, J = 16.4, 1H) ppm. **^{13}C{^{1}H} NMR (101 MHz, CD$_2$Cl$_2$)**: 183.7 (C), 174.1 (C), 163.0–161.4 (m, C), 149.4 (C), 148.7 (C), 142.8 (CH), 135.2 (CH), 134.6 (m, CH), 132.1–128.7 (m, CH), 127.5 (CH), 126.4 (CH), 124.9 (CH), 123.7 (CH), 122.1 (CH), 117.9 (CH), 71.9 (CH), 68.7 (CH$_2$), 58.6 (CH), 38.8 (dd, J = 30.3, J = 6.1, C), 28.9 (d, J = 8.1, CH), 28.7 (CH), 25.9 (3xCH$_3$), 20.8 (d, J = 42.2, CH$_3$), 20.2 (CH$_3$), 19.2 (CH$_3$), 18.1 (CH$_3$), 18.0 (CH$_3$), 14.8 (CH$_3$). **^{31}P{^{1}H} NMR (162 MHz, CD$_2$Cl$_2$)**: +38.5 (d, J = 346.7, PN), +8.5 (d, J = 346.7, PPh$_3$). **HRMS**: calcd for C$_{47}$H$_{60}$N$_3$OP$_2$Ir [M + H]$^{2+}$, 468.6915; found 468.6915; calcd for C$_{29}$H$_{44}$N$_3$OPIr [M − PPh$_3$]$^+$, 674.2845; found 674.2848; calcd for C$_{47}$H$_{59}$N$_3$OP$_2$Ir [M]$^+$, 936.3757; found 936.3753; calcd. for C$_{32}$H$_{12}$BF$_{24}$ [M]$^−$, 863.0654; found 863.0662. **IR**: 3452, 1617, 1352, 1287, 1130, 887 and 691.

L3RIr2

A *Schlenk* flask was charged with 50 mg of complex **L3RIr** (0.035 mmol, 1 eq) and 13.5 mg (0.035 mmol, 1 eq) of acetophenone *N*-phenyl imine, **I1**. The flask was purged with three vacuum/N$_2$ cycles and the solids were dissolved in 3 mL of THF.

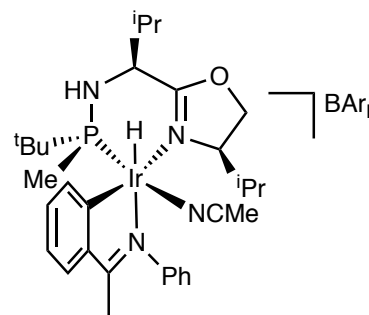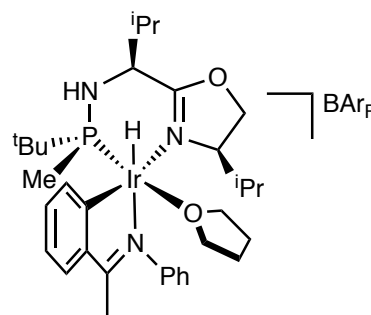The solution was transferred into a Fisher-Porter tube and stirred for 2 h under 2 bar of H$_2$. During this period, the initially orange solution turned yellow. At the due time, the flask was vented and 35 mL of a 1 M THF solution of PMe$_3$ (0.035 mmol, 1 eq) were added and the resulting solution was stirred at room temperature for 30 min. The solvent was evacuated and the crude was recrystallized in CH$_2$Cl$_2$/pentane.

Pale-yellow solid. **Yield**: 96% (54 mg). **¹H NMR**: 7.70 (br s, 8H), 7.66 (d, J = 7.6, 1H), 7.60 (dd, J = 8.0, J = 1.2, 1H), 7.53 (br s, 4H), 7.41–7.38 (m, 2H), 7.28–7.22 (m, 2H), 7.13 (t, J = 7.6, 1H), 7.05 (td, J = 7.2, J = 1.2, 1H), 6.9 (s, 1H), 4.32 (dd, J = 14.4, J = 5.2, 1H), 4.07–4.01 (m, 2H), 2.81–2.75 (m, 1H), 2.56 (d, J = 1.2, 3H), 2.30–2.18 (m, 1H), 1.84 (d, J = 9.2, 3H), 1.56–1.47 (m, 1H), 1.14 (dd, J = 8.8, J = 2.0, 9H), 0.88 (d, J = 7.2, 3H), 0.76 (d, J = 6.8, 3H), 0.68 (d, J = 6.8, 3H), 0.59 (d, J = 6.8, 3H), 0.51 (d, J = 14.0, 9H), −19.95 (t, J = 19.6, 1H). **¹³C{¹H} NMR (101 MHz, CD$_2$Cl$_2$)**: 182.3 (C), 172.5 (C), 162.9–161.4 (m, C), 148.9–147 (C), 143.7 (CH), 135.2 (CH), 132.9 (CH), 130.8 (CH), 129.4–128.9 (m, CH), 127.6 (CH), 126.4 (CH), 123.8–122.6 (CH), 117.9 (CH), 73.1 (CH), 68.4 (CH$_2$), 58.5 (d, J = 2.2, CH), 39.1 (d, J = 6.6, C), 29.3 (CH), 28.8 (d, J = 7.7, CH), 25.5 (3xCH$_3$), 20.5 (d, J = 43.2, CH$_3$), 20.4 (CH$_3$), 18.6 (CH$_3$), 18.3 (CH$_3$), 17.7 (CH$_3$), 16.6 (d, J = 34.1, 3xCH$_3$), 13.8 (CH$_3$). **³¹P{¹H} NMR**: +38.9 (d, J = 349.3, PN), −45.1 (d, J = 349.3, PMe$_3$). **HRMS**: calcd for C$_{32}$H$_{53}$N$_3$OP$_2$Ir [M]$^+$, 750.3287; found 750.3284; calcd for C$_{29}$H$_{44}$N$_3$OPIr [M − PMe$_3$]$^+$, 674.2845; found 674.2833; calcd. for C$_{32}$H$_{12}$BF$_{24}$ [M]$^−$, 863.0654; found 863.0663. **IR**: 3457, 2965, 1635, 1352, 1278, 1165, 1130, 891, 717 and 683.

L3RIr3

A *Schlenk* flask was charged with 50 mg of complex **L3RIr** (0.035 mmol, 1 eq) and 13.5 mg (0.035 mmol, 1 eq) of acetophenone *N*-phenyl imine, **I1**. The flask was purged with three vacuum/N$_2$ 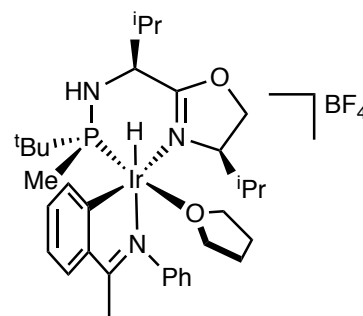cycles and the solids were dissolved in 3 mL of THF. The solution was transferred into a Fisher-Porter tube and stirred for 2 h under 2 bar of H$_2$. Then, the initially orange solution turned yellow. The hydrogen was vented and 5 mg of (*S*)-**L1** (0.042 mmol, 1.2 eq) were added and the resulting solution was stirred at room temperature for 30 min. The solvent was evacuated and the crude was recrystallized in CH$_2$Cl$_2$/pentane.

Yellow solid. **Yield**: 97% (57 mg). **¹H NMR**: 7.79–7.77 (m, 1H), 7.70 (br s, 8H), 7.59–7.57 (m, 1H), 7.52 (br s, 4H), 7.37–7.31 (m, 2H), 7.14 (q, J_P = 442, J = 3.8, 0.5H), 7.08–7.05 (m, 3H), 6.63 (br t, J = 7.3, 1H), 6.51 (d, J = 9.8, 2H), 6.03 (q, J_P = 442, J = 3.8, 0.5H), 4.49 (q, J = 1.1, 1H), 4.36–4.31 (m, 2H), 4.19–4.15 (m, 1H), 4.03–3.98 (t, J = 9.3, 1H), 2.96–2.92 (m, 1H), 2.35 (s, 3H), 1.86 (d, J = 9.7, 3H), 1.52 (br d, J = 11.2, 1H), 1.42 (d, J = 9.7, 9H), 1.19 (d, J = 11.4, 9H), 1.17 (d, J = 16, 3H), 0.82 (d, J = 10.7, 3H), 0.79 (d, J = 10.7, 3H), 0.75 (d, J = 10.7, 3H), 0.66 (d, J = 10.7, 3H), −19.7 (d, J = 26.9, 1H).

^{31}P{^{1}H} NMR: +60.9 (br s, P_{SPO}), +35.5 (d, J = 15.6, PN). HRMS: calcd for $C_{29}H_{44}N_3OPIr$ [M − SPO]$^+$, 674.2845; found 674.2848; calcd for $C_{34}H_{57}N_3O_2P_2Ir$ [M]$^+$, 794.3549; found 794.3526; calcd. for $C_{32}H_{12}BF_{24}$ [M]$^-$, 863.0654; found 863.0661.

L3RIr4

A *Schlenk* flask was charged with 50 mg of complex **L3RIr** (0.035 mmol, 1 eq) and 13.5 mg (0.035 mmol, 1 eq) of acetophenone *N*-phenyl imine, **I1**. The flask was purged with three vacuum/N_2 cycles and the solids were dissolved in 3 mL of THF. The solution was transferred into a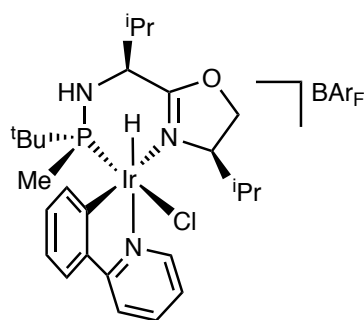 Fisher-Porter tube and stirred for 2 h under 2 bar of H_2. During this period, the initially orange solution turned yellow. At the due time, the flask was vented and repressurised with 2 bar of CO and the resulting solution was stirred at room temperature for 40 min. The solvent was evacuated and the crude was recrystallized in CH_2Cl_2/pentane.

Pale-yellow solid. **Yield**: 98% (55 mg). ^{1}H NMR (400 MHz, C_6D_6): 8.38 (br s, 4H), 8.15 (br s, 1H), 7.70 (br s, 2H), 7.54 (br s, 2H), 7.75 (d, J = 7.0, 1H), 7.13–7.11 (m, 3H), 7.09–7.05 (m, 2H), 6.67 (t, J = 7.3, 1H), 6.42 (dd, J = 7.6, J = 1.1, 2H), 3.27–3.24 (m, 2H), 3.21–3.11 (m, 2H), 2.73 (d, J = 11.0, 1H), 2.66–2.55 (m, 2H), 2.08 (s, 3H), 1.26 (d, J = 8.8, 3H), 1.11 (d, J = 7, 9H), 0.53 (d, J = 6.7, 3H), 0.48 (d, J = 6.7, 3H), 0.47 (d, J = 6.7, 3H), 0.44 (d, J = 6.7, 3H), −17.4 (d, J = 22.0, 1H), −17.5 (d, J = 22.0, 1H). ^{31}P{^{1}H} NMR (162 MHz, C_6D_6): +36.7 (s), +36.5 (s). HRMS: calcd for $C_{29}H_{44}N_3OPIr$ [M − CO]$^+$, 674.2845; found 674.2834; calcd for $C_{30}H_{44}N_3O_2PIr$ [M]$^+$, 702.2795; found 702.2793; calcd. for $C_{32}H_{12}BF_{24}$ [M]$^-$, 863.0654; found 863.0662. IR: 3443, 2965, 2926, 2052, 1609, 1383, 1361, 1274, 1126, 1026 and 809.

L3RIr5

A *Schlenk* flask was charged with 50 mg of complex **L3RIr** (0.035 mmol, 1 eq) and 13.5 mg (0.035 mmol, 1 eq) of acetophenone *N*-phenyl imine, **I1**. The flask was purged with three vacuum/N_2 cycles and the solids were dissolved in 3 mL of THF. The solution was transferred into a Fisher-Porter tube and stirred for 2 h under 2 bar of H_2. During this period, the initially orange solution turned yellow. At the due time, the flask was vented and one drop of acetonitrile was added and the resulting solution was stirred at room temperature for 30 min. The solvent was evacuated and the crude was recrystallized in CH_2Cl_2/pentane.

Pale-yellow solid. **Yield**: 92% (51 mg). **^{1}H NMR (400 MHz, CD$_3$CN)**: 7.74 (dd, J = 6.8, J = 2.0, 1H), 7.70 (br s, 8H), 7.66 (br s, 4H), 7.50–7.41 (m, 2H), 7.38–7.36 (m, 1H), 7.32–7.25 (m, 1H), 7.10–7.06 (br s, 1H), 7.06–7.03 (m, 2H), 6.51–6.48 (m, 1H), 4.42 (dd, J = 9.2, J = 4.8, 1H), 4.29–4.25 (m, 1H), 4.05 (t, J = 10.0, 1H), 2.96–2.91 (m, 1H), 2.45 (s, 3H), 2.04 (d, J = 9.2, 1H), 1.87 (dd, J = 9.6, J = 1.2, 3H), 1.53 (s, 3H), 1.44 (d, J = 6.8, 1H), 0.90 (d, J = 7.2, 3H), 0.80 (d, J = 6.8, 3H), 0.78 (d, J = 7.2, 3H), 0.69 (d, J = 6.8, 3H), 0.56 (d, J = 14.8, 9H), −19.81 (d, J = 26.0, 1H). **^{13}C{^{1}H} NMR (101 MHz, CD$_2$Cl$_2$)**: 183.9 (C), 170.8 (C), 163.0–161.6 (m, C), 148.8–148.3 (m, C), 143.4 (CH), 135.3 (CH), 132.9 (CH), 130.7 (CH), 129.9–128.9 (m, CH), 127.4 (CH), 126.5 (CH), 123.8 (CH), 122.6 (CH), 121.1 (CH), 118.0 (m, CH$_2$), 71.4 (CH), 69.5 (CH$_2$), 58.2 (m, CH), 37.6 (d, J = 38.4, C), 28.8 (d, J = 7.1, CH), 26.2 (d, J = 3.0, 3xCH$_3$), 21.5 (d, J = 52.5, CH$_3$), 20.6 (CH$_3$), 18.9 (CH$_3$), 18.4 (CH$_3$), 17.2 (CH$_3$), 13.7 (CH$_3$) ppm. **^{31}P{^{1}H} NMR (162 MHz, CD$_3$CN)**: +33.8 (s).

HRMS: calcd for C$_{29}$H$_{44}$N$_3$OPIr [M − CH$_3$CN]$^+$, 674.2845; found 674.2843; calcd. for C$_{32}$H$_{12}$BF$_{24}$ [M]$^-$, 863.0654; found 863.0661. **IR**: 3461, 2965, 1652, 1352, 1283, 1270, 1091, 1022, 800 and 683.

L3RIr6

A *Schlenk* flask was charged with 50 mg of complex **L3RIr** (0.035 mmol, 1 eq) and 13.5 mg (0.035 mmol, 1 eq) of acetophenone *N*-phenyl imine, **I1**. The flask was purged with three vacuum/N_2 cycles and the solids were dissolved in 3 mL of THF.

The solution was transferred into a Fisher-Porter tube and stirred for 2 h under 2 bar of H$_2$. During this period, the initially orange solution turned yellow. At the due time, the flask was vented, repressurized with 3 bar of ethylene and the resulting solution was stirred at room temperature for 30 min. The solvent was evacuated and the crude was recrystallized in CH$_2$Cl$_2$/pentane.

Olive-green solid. **Yield**: 98% (54 mg). **^{1}H NMR (400 MHz, CD$_2$Cl$_2$)**: 7.72 (br s, 8H), 7.56 (br s, 4H), 7.49–7.45 (m, 2H), 7.35–7.31 (m, 2H), 7.17–6.99 (m, 2H), 7.14 (t, J = 3.6, 1H), 6.88–6.72 (m, 2H), 4.41 (s, 1H), 4.02 (s, 1H), 4.04 (br s, 1H), 3.67 (m, 4H), 2.45 (s, 3H), 2.34 (br s, 1H), 1.94 (d, J = 10.0, 2H), 1.80 (br s, 4H), 0.91 (d, J = 6.0, 3H), 0.85 (d, J = 6.4, 3H), 0.80 (d, J = 6.8, 3H), 0.72 (d, J = 6.8, 3H), 0.65 (d, J = 15.6, 9H), −19.49 (d, J = 28.0, 1H). **^{13}C{^{1}H} NMR (101 MHz, CD$_2$Cl$_2$)**: 184.2 (C), 182.2 (C), 164.9–163.4 (m, C), 152.2 (C), 151.3 (C), 150.8 (C), 145.8 (CH), 137.2 (CH), 132.6–130.5 (CH), 128.4 (CH), 125.6 (CH), 119.6 (CH), 71.7 (s, CH$_2$), 69.6 (CH$_2$), 59.9 (d, J = 31.1, CH), 30.9 (CH$_3$), 30.3 (CH$_3$), 28.3 (3xCH$_3$), 21.7 (CH$_2$), 22.3 (CH$_3$), 20.2 (CH$_3$), 20.1 (CH$_3$), 19.1 (CH$_3$), 16.3 (CH$_3$). **^{31}P{^{1}H} NMR (162 MHz, CD$_2$Cl$_2$)**: +37.6 (s). **HRMS**: calcd for C$_{29}$H$_{44}$N$_3$OPIr [M − THF]$^+$, 674.2845; found 674.2850; calcd for C$_{31}$H$_{47}$N$_4$OPIr [M − THF + CH$_3$CN]$^+$, 715.3111; found 715.3114; calcd. for C$_{32}$H$_{12}$BF$_{24}$ [M]$^-$, 863.0654; found 863.0682. **IR**: 3417, 2970, 1643, 1348, 1287, 1130, 891, 713 and 678.

L3RIr6·BF$_4$

A *Schlenk* flask was charged with 50 mg of complex **L3RIr·BF$_4$** (0.035 mmol, 1 eq) and 13.5 mg (0.035 mmol, 1 eq) of acetophenone *N*-phenyl imine, **I1**. The flask was purged with three vacuum/N$_2$ cycles and the solids were dissolved in 3 mL of THF. The solution was transferred into a Fisher-Porter tube and stirred for 2 h under 2 bar of H$_2$. During this period, the initially orange solution turned yellow. At the due time, the flask was vented, repressurised with 3 bar of ethylene and the resulting solution was stirred at room temperature for 30 min. The solvent was evacuated and the crude was recrystallized in CH$_2$Cl$_2$/pentane.

Olive-green solid. **Yield**: 86% (26.3 mg). **^{1}H NMR (400 MHz, CD$_2$Cl$_2$)**: 7.48–7.47 (m, 2H), 7.38–7.34 (m, 2H), 7.20–6.99 (m, 2H), 7.23 (t, J = 3.6, 1H), 6.85–6.73 (m, 2H), 4.43 (s, 1H), 4.02 (s, 1H), 4.04 (br s, 1H), 3.70 (m, 4H), 2.49 (s, 3H), 2.38 (br s, 1H), 1.98 (d, J = 10, 2H), 1.87 (br s, 4H), 0.91 (d, J = 6.0, 3H), 0.87 (d, J = 6.4, 3H), 0.80 (d, J = 6.8, 3H), 0.75 (d, J = 6.8, 3H), 0.63 (d, J = 15.6, 9H), −19.49 (d, J = 28.0, 1H). **^{31}P{^{1}H} NMR (162 MHz, CD$_2$Cl$_2$)**: +37.3 (s). **HRMS**: calcd for C$_{29}$H$_{44}$N$_3$OPIr [M − THF]$^+$, 674.2845; found 674.2850; calcd for C$_{31}$H$_{47}$N$_4$OPIr [M − THF + CH$_3$CN]$^+$, 715.3111; found 715.3114; calcd. for C$_{32}$H$_{12}$BF$_{24}$ [M]$^-$, 87.0029; found 87.0030. **IR**: 3413, 2957, 2926, 2873, 1626, 1470, 1387, ν(BF$_4$) 1126, 878 and 748.

L3RIr7

A *Schlenk* flask was charged with 50 mg of complex **L3RIr** (0.035 mmol, 1 eq) and 5.4 mg (0.035 mmol, 1 eq) of 2-phenylpyridine. The flask was purged with three vacuum/N$_2$ cycles and the solids were dissolved in 3 mL of THF. The solution was transferred into a Fisher-Porter tube and stirred for 2 h under 2 bar of H$_2$. During this period, the initially orange solution turned yellow. At the due time, the flask was vented and the reaction mixture was stirred at room temperature for 4 h. The solvent was removed with a N$_2$ flow, and LiCl (50 mg), SiO$_2$ (50 mg), and EtOAc (2 mL) were added. The reaction was left to stir overnight. The solvent was again removed with a N$_2$ flow. The crude was suspended in pentane/TBME (1:1) and eluted through SiO$_2$. Only the yellow-coloured band was collected, affording the desired product.

Yellow-green solid. **Yield**: 79% (18.5 mg). **^{1}H NMR**: 8.45 (d, J = 5.5, 1H), 8.27 (d, J = 4.8, 1H), 7.95 (d, J = 8.2, 1H), 7.52–7.38 (m, 3H), 6.54 (br t, J = 7.5, 1H), 6.42 (br t, J = 7.3, 1H), 4.84–4.83 (m, 1H), 4.50 (dd, J = 9.4, J = 4.1, 2H), 3.92–3.86 (m, 1H), 3.78–3.74 (m, 1H), 3.70–3.69 (m, 1H), 3.45–3.42 (m, 1H), 1.84 (br d, J = 11.0, 1H), 1.39 (d, J = 7.3, 3H), 1.04 (d, J = 7.0, 3H), 0.94 (d, J = 5.0, 3H), 0.86 (d, J = 4.0, 3H), 0.78 (d, J = 4.0, 3H), 0.73 (d, J = 5.0, 3H), −18.5 (d, J = 42.3, 1H), −18.8 (d, J = 26.1, 1H). **^{31}P{^{1}H} NMR**: +47.4 (s), +36.1 (s). **HRMS**: calcd for C$_{26}$H$_{40}$N$_3$OPIr [M − Cl]$^+$, 634.2532; found 634.2532.

L3RIr8

A *Schlenk* flask was charged with 50 mg of complex **L3RIr** (0.035 mmol, 1 eq) and 5.4 mg (0.035 mmol, 1 eq) of 2-phenylpyridine. The flask was purged with three vacuum/N_2 cycles and the solids were dissolved in 3 mL of THF. The solution was transferred into a Fisher-Porter tube and stirred for 2 h under 2 bar of H_2. During this period, the initially orange solution turned yellow. At the due time, the flask was vented and one drop of acetonitrile was added and the resulting solution was stirred at room temperature for 30 min. The solvent was evacuated and the crude was recrystallized in CH_2Cl_2/pentane.
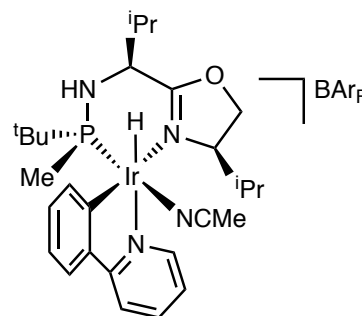
Pale-yellow solid. **Yield**: 88% (20.6 mg). **^{1}H NMR (400 MHz, CD$_3$CN)**: 8.69 (d, J = 4.7, 1H), 8.36 (d, J = 5.4, 1H), 8.19 (d, J = 6.0, 1H), 7.99–7.92 (m, 3H), 7.6 (d, J = 5.3, 1H), 7.2 (m, 1H), 4.52–4.46 (m, 1H), 4.18–4.15 (m, 1H), 4.10–4.01 (m, 1H), 3.83–3.79 (m, 1H), 2.59–2.42 (m, 2H), 2.26 (d, J = 11, 1H), 1.09 (d, J = 7.1, 3H), 1.04 (d, J = 14.0, 3H), 0.85 (d, J = 7.3, 3H), 0.77 (d, J = 7.0, 3H), 0.38 (d, J = 7.3, 3H), 0.33 (d, J = 7.2, 3H), −18.5 (d, J = 20.9, 1H), −18.9 (d, J = 25.6, 1H). **^{31}P{^{1}H} NMR (162 MHz, CD$_3$CN)**: +47.7 (br s), +33.9 (br s). **HRMS**: calcd for $C_{26}H_{40}N_3OPIr$ [M − CH$_3$CN]$^+$, 634.2532; found 634.2532; calcd for $C_{28}H_{43}N_4OPIr$ [M]$^+$, 675.2798; found 675.2799; calcd. for $C_{32}H_{12}BF_{24}$ [M]$^−$, 863.0654; found 863.0667.

L3RIr9

A *Schlenk* flask was charged with 50 mg of complex **L3RIr** (0.035 mmol, 1 eq) and 6.3 mg (0.035 mmol, 1 eq) of 7,8-benzoquinoline. The flask was purged with three vacuum/N_2 cycles and the solids were dissolved in 3 mL of THF. The solution was transferred into a Fisher-Porter tube and stirred for 2 h under 2 bar of H_2. During this period, the initially orange solution turned yellow. At the due time, the flask was vented and one drop of acetonitrile was added and the resulting solution was stirred at room temperature for 30 min. The solvent was evacuated and the crude was recrystallized in CH_2Cl_2/pentane.
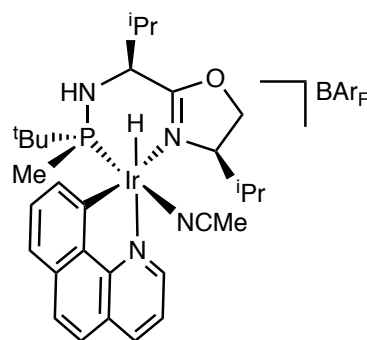
Pale-yellow solid. **Yield**: 88% (48 mg). **^{1}H NMR (400 MHz, CD$_3$CN): 9.3 (d,** $J =$ 7.6, 1H), 9.01 (d, J = 7.6, 1H), 8.65 (d, J = 4.1, 1H), 8.50 (d, J = 4.1, 1H), 8.26–8.18 (m, 3H), 7.88–7.81 (m, 3H), 7.63–7.57 (m, 3H), 7.43–7.38 (m, 3H), 4.57–4.51 (m, 2H), 4.39–4.38 (m, 2H), 4.16 (m, 2H), 3.90–3.88 (m, 2H), 2.61–2.51 (m, 4H), 2.01 (d, J = 12, 1H), 1.95 (d, J = 7.0, 6H), 1.85 (d, J = 14.0, 18H), 1.08–0.81 (m, 24H), −18.8 (d, J = 21.0, 1H), −19.2 (d, J = 25.0, 1H). **^{31}P{^{1}H} NMR (162 MHz, CD$_3$CN)**: +47.1 (br s), +33.7 (br s). **HRMS**: calcd for C$_{28}$H$_{40}$N$_3$OPIr [M − CH$_3$CN]$^+$, 658.2532; found 658.2528; calcd for C$_{30}$H$_{43}$N$_4$OPIr [M]$^+$, 699.2798; found 699.2796; calcd. for C$_{32}$H$_{12}$BF$_{24}$ [M]$^-$, 863.0654; found 863.0656.

L3RIr10

A *Schlenk* flask was charged with 50 mg of complex **L3RIr** (0.035 mmol, 1 eq) and 7.4 mg (0.035 mmol, 1 eq) of 2-phenylbenzothiazole. The flask was purged with three vacuum/N$_2$ cycles and the solids were dissolved in 3 mL of THF. The solution was transferred
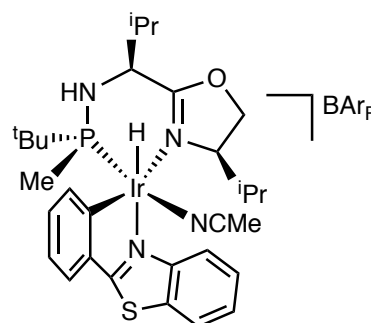
into a Fisher-Porter tube and stirred for 2 h under 2 bar of H$_2$. During this period, the initially orange solution turned yellow. At the due time, the flask was vented and one drop of acetonitrile was added and the resulting solution was stirred at room temperature for 30 min. The solvent was evacuated and the crude was recrystallized in CH$_2$Cl$_2$/pentane.

Pale-yellow solid. **Yield**: 86% (48.5 mg). **^{1}H NMR (400 MHz, CD$_3$CN): 7.93 (dd,** J = 8.0, J = 2.5, 2H), 7.84 (br d, J = 7.5, 2H), 7.64 (br d, J = 7.5, 2H), 7.43–7.37 (m, 6H), 7.11–7.03 (m, 4H), 4.54 (br d, J = 5.1, 2H), 4.12–4.09 (m, 2H), 4.05–4.00 (m, 4H), 2.63–2.55 (m, 4H), 1.91 (d, J = 12.0, 2H), 1.09–0.78 (m, 48H), −20.1 (d, J = 20.5, 1H), −21.0 (d, J = 25.2, 1H). **^{31}P{^{1}H} NMR (162 MHz, CD$_3$CN)**: +48.9 (br s), +35.7 (br s). **HRMS**: calcd for C$_{28}$H$_{40}$N$_3$OPSIr [M − CH$_3$CN]$^+$, 690.2250; found 690.2249; calcd for C$_{30}$H$_{43}$N$_4$OPSIr [M]$^+$, 731.2519; found 731.2518; calcd. for C$_{32}$H$_{12}$BF$_{24}$ [M]$^-$, 863.0654; found 863.0659.

6.6. *References*

(1)   Armarego, W. L. F. *Purification of Laboratory Chemicals*; Eight ed.; Butterworth Heinemann: Oxford, 2017.

(2)   Clavero, P.; Grabulosa, A.; Rocamora, M.; Muller, G.; Font-Bardia, M. *Dalton Trans.* **2016**, *45*, 8513-8531.

(3)   Clavero, P.; Grabulosa, A.; Rocamora, M.; Muller, G.; Font-Bardia, M. *Eur. J. Inorg. Chem.* **2016**, 4054-4065.

(4)   Bravo, M. J.; Ceder, R. M.; Grabulosa, A.; Muller, G.; Rocamora, M.; Font-Bardia, M. *J. Organomet. Chem.* **2017**, *830*, 42-55.

(5)   Bravo, M. J.; Ceder, R. M.; Muller, G.; Rocamora, M. *Organometallics* **2013**, *32*, 2632-2642.

(6)   Jiang, X.; Minnaard, A. J.; Hessen, B.; Feringa, B. L.; Duchateau, A. L. L.; Andrien, J. G. O.; Boogers, J. A. F.; de Vries, J. G. *Org. Lett.* **2003**, *5*, 1503-1506.

(7)   León, T.; Riera, A.; Verdaguer, X. *J. Am. Chem. Soc.* **2011**, *133*, 5740-5743.

(8)   Revés, M.; Ferrer, C.; León, T.; Doran, S.; Etayo, P.; Vidal-Ferran, A.; Riera, A.; Verdaguer, X. *Angew. Chem. Int. Ed.* **2010**, *49*, 9452-9455.

(9)   Orgué, S.; Flores-Gaspar, A.; Biosca, M.; Pàmies, O.; Diéguez, M.; Riera, A.; Verdaguer, X. *Chem. Commun.* **2015**, *51*, 17548-17551.

(10)   Salomó, E.; Prades, A.; Riera, A.; Verdaguer, X. *J. Org. Chem.* **2017**, *82*, 7065-7069.

(11)   Cristóbal-Lecina, E.; Etayo, P.; Doran, S.; Revés, M.; Martín-Gago, P.; Grabulosa, A.; Constantino, A. R.; Vidal-Ferran, A.; Riera, A.; Verdaguer, X. *Adv. Synth. Catal.* **2014**, *356*, 795-804.

(12)   Salomó, E.; Orgué, S.; Riera, A.; Verdaguer, X. *Angew. Chem. Int. Ed.* **2016**, *55*, 7988-7992.

(13)   Baeza, A.; Pfaltz, A. *Chem. Eur. J.* **2010**, *16*, 4003-4009.

(14)   Schnider, P.; Koch, G.; Prétôt, R.; Wang, G.; Bohnen, F. M.; Krüger, C.; Pfaltz, A. *Chem. Eur. J.* **1997**, *3*, 887-892.

(15)   Capra, J.; Le Gall, T. *Synlett* **2010**, 441-444.

(16)   Renzi, P.; Hioe, J.; Gschwind, R. M. *J. Am. Chem. Soc.* **2017**, *139*, 6752-6760.

(17)   Wakchaure Vijay, N.; Kaib Philip, S. J.; Leutzsch, M.; List, B. *Angew. Chem. Int. Ed.* **2015**, *54*, 11852-11856.

(18)   Verdaguer, X.; Lange Udo, E. W.; Buchwald Stephen, L. *Angew. Chem. Int. Ed.* **1998**, *37*, 1103-1107.

(19)   Wang, C.; Wu, X.; Zhou, L.; Sun, J. *Chem. Eur. J.* **2008**, *14*, 8789-8792.

(20)   Verdaguer, X.; Lange, U. E. W.; Reding, M. T.; Buchwald, S. L. *J. Am. Chem. Soc.* **1996**, *118*, 6784-6785.

(21)   Marcseková, K.; Wegener, B.; Doye, S. *Eur. J. Org. Chem.* **2005**, 4843-4851.

(22)   Saidi, O.; Blacker, A. J.; Farah, M. M.; Marsden, S. P.; Williams, J. M. J. *Chem. Commun.* **2010**, *46*, 1541-1543.

(23)   (a) Klemperer, W. G.; Main, D. J. *Inorg. Chem.* **1990**, *29*, 2355-2360 (b) Passarelli, V.; Pérez-Torrente, J. J.; Oro, L. A. *Inorg. Chem.* **2014**, *53*, 972-980.

(24)   Uson, R.; Laguna, A.; Laguna, M. *Inorg. Synth.* **1989**, *26*, 85-86.

(25)   Kündig, E. P.; Monnier, F. R. *Adv. Synth. Catal.* **2004**, *346*, 901-904.

(26)   Pinto, P.; Marconi, G.; Heinemann, F. W.; Zenneck, U. *Organometallics* **2004**, *23*, 374-380.

(27)   Dent, W. T.; Long, R.; Wilkinson, A. J. *J. Chem. Soc.* **1964**, 1585-1588.

(28)   Auburn, P. R.; Mackenzie, P. B.; Bosnich, B. *J. Am. Chem. Soc.* **1985**, *107*, 2033-2046.

(29)   von Matt, P.; Lloyd-Jones, G. C.; Minidis, A. B. F.; Pfaltz, A.; Macko, L.; Neuburger, M.; Zehnder, M.; Ruegger, H.; Pregosin, P. S. *Helv. Chim. Acta* **1995**, *78*, 265-284.

Appendix

Abbreviations

acac	acetylacetonate
AcO	acetate group
Ac$_2$O	acetic anhydride
ACN	acetonitrile
AcOEt	ethyl acetate
Ad	adamantyl group
Alk	alkyl group
o-An	*o*-anisyl group (2-methoxyphenyl)
Ar	aryl group
Anal.	analysis
BAr$_F$	3,5-*bis*(trifluoromethyl)phenyl borate anion
BINAP	2,2'-*bis*(diphenylphosphino)1,1'-binaphthyl
Bn	benzyl group
BOC	*tert*-butoxycarbonyl
BSA	*N*,*O*-bis(trimethylsilyl)acetamide
sec-Bu	*sec*-butyl (2-butyl) group
tert-Bu	*tert*-butyl (1,1-dimethylethyl) group
CAMP	cyclohexylmethyl(2-methoxyphenyl)phosphine
Cat.	catalyst
CHIRAPHOS	2,3-*bis*(diphenylphosphino)butane
COD	1,4-cyclooctadiene
Conv.	conversion
COSY	*Correlation Spectroscopy*
DABCO	1,4-diazabicyclo[2.2.2]octane
cy	cyclohexyl
dba	dibenzylideneacetone
DEPT	*Distortionless Enhancement by Polarization Transfer*
DFT	*Density Functional Theory*
DIOP	*O*-isopropylidene-2,3-dihydroxy-1,4-*bis*(diphenylphosphino)butane
DIPAMP	*bis*[(2-methoxyphenyl)phenylphosphino]ethane
DMM	dimethyl malonate
L-DOPA	(2*S*)-2-amino-3-(3,4-dihydroxyphenyl)propanoic acid
DRX	*X-ray diffraction*

DuPHOS	2,5-diethylphospholan-1-yl-phenyl-2,5-diethylphospholane
EA	Elemental Analysis
EDC	*N*-(3-dimethylaminopropyl)-*N'*-ethylcarbodiimide hydrochloride
Et-FerroTANE	1,1'-*bis*(2,4-diethylphosphotane)ferrocene
ee	enantiomeric excess
eq.	equivalents
GC	*Gas Chromatography*
HSQC	*Heteronuclear Single Quantum Correlation*
HMDS	hexamethyldisilazane
HOBT	1-hydroxybenzotriazole
IPA	isopropyl alcohol
IR	*Infrared Spectroscopy*
JOSIPHOS	1-dicyclohexylphosphino-1-[2-diphenylphosphinoferrocenyl]etane
Mes	mesityl group (2,4,6-trimethylphenyl)
NOE	*Nuclear Overhauser Effect*
NOESY	*Nuclear Overhauser Effect Spectroscopy*
Nu	nucleophile
NMR	*Nuclear Magnetic Resonance*
OMen	menthoxyde group
PAMP	phenyl(2-methoxyphenyl)phosphine
py	pyridine
Ph	phenyl
RT	*room temperature*
TOF	*Turnover Frequency*
TON	*Turnover Number*
THF	tetrahydrofurane
SPINOL	1,1'-spirobiindan-7,7'-diol

Appendix I. Selected NMR Spectra

NMR ^{13}C 100.6 MHz

C$_6$D$_6$

NMR ^{31}P 161.9 MHz

CDCl$_3$

L1Au1

NMR ^{1}H 400 MHz

CDCl$_3$

7.260

1.719
1.695
1.247
1.203

δ (ppm)

NMR ^{13}C 100.6 MHz

CDCl$_3$

77.318
77.000
76.682

34.395
33.928

24.518
24.452

15.482
15.085

34.395
33.928

24.518
24.452

15.482
15.085

δ (ppm)

δ (ppm)

NMR ^{31}P 161.9 MHz

C$_6$D$_6$

—124.951

L1Ru3

NMR ^{1}H 400 MHz

C$_6$D$_6$

1.699
1.692
1.685
0.981
0.961
0.941

1.08

3.00

9.60

NMR ^{13}C 100.6 MHz

C$_6$D$_6$

gHSQC 400 MHz

C$_6$D$_6$

NMR ^{31}P 202.4 MHz

CDCl$_3$

—109.084

L1Pd2

NMR ^{1}H 400 MHz

CDCl$_3$

1.658
1.632
1.261
1.220

3.00
8.78

NMR ^{13}C 100.6 MHz

CDCl$_3$

77.318
77.000
76.683
38.935
38.522
26.381
14.845
14.781
14.401

NMR ^{31}P 161.9 MHz

CDCl$_3$

−124.046

L1Pd5

NMR ^{1}H 400 MHz

CDCl$_3$

7.260

5.299

1.798
1.773
1.371
1.328

1.00

2.81

δ (ppm)

NMR ^{19}F 376.3 MHz

CDCl$_3$

−138.822
−138.839
−138.857
−138.884
−138.901
−138.918

0.95

3.10

δ (ppm)

NMR ^{13}C 100.6 MHz

CDCl$_3$

39.918
39.516
29.692
26.134
15.284
14.830

gHSQC 400 MHz

CDCl$_3$

NMR ^{31}P 161.9 MHz

CDCl$_3$

−110.636
106.937

L1Pd3

L1Pd4

1.00
1.30

δ (ppm)

NMR ^{1}H 400 MHz

CDCl$_3$

−7.260

2.353
2.351
1.974
1.727
1.705
1.513
1.485
1.221
1.192
1.181
1.152

1.727
1.705
1.513
1.485
1.221
1.192
1.181
1.152

f1 (ppm)

0.26
0.55
1.00
1.19
7.56

δ (ppm)

NMR ^{13}C 100.6 MHz

C$_6$D$_6$

δ (ppm)

NMR ^{31}P 161.9 MHz

CDCl$_3$

L1Pd8

δ (ppm)

NMR ^{1}H 400 MHz

CDCl$_3$

7.537
7.533
7.521
7.517
7.360
7.355
7.341
7.255
7.250
7.243
7.238
6.643
6.622
6.603
6.581
6.322
6.315
5.515
5.497
5.381
5.356
5.347
5.323
4.541
4.512
4.435
4.408
1.598
1.573
1.200
1.051
1.012
0.812
0.751
0.712
0.446
0.426

1.85
6.15
1.00
0.99
0.81
0.70
3.52
5.54
1.20
1.61

δ (ppm)

NMR ^{13}C 100.6 MHz

CDCl$_3$

129.104
128.491
128.078
127.438
126.127
38.975
38.760
38.551
26.405
14.810
14.429

δ (ppm)

370

NMR ^{31}P 161.9 MHz

C$_6$D$_6$

109.441
109.116
109.016
108.736
106.643
106.257
105.772
105.348

L1Pd9

1.08
0.12
0.37
1.00

125   120   115   110   105   100   95   90   85   8

δ (ppm)

NMR ^{1}H 400 MHz

C$_6$D$_6$

7.159
7.110
7.099
7.037
7.008

2.374
2.356
1.320
1.299
1.160
1.122
1.089
1.084
1.061
1.039
0.836
0.798
0.766
0.744

6.090
6.087
6.063
6.060
6.055
6.052
6.027
6.024
5.322
5.288
4.495
4.490
4.474
4.467
4.459
4.454
4.438
4.433
4.004
4.001
3.997
3.974
3.971
3.949
3.946
3.943

6.0   5.5   5.0   4.5   4.0

f1 (ppm)

7.34

0.95

0.73
0.67
0.61

1.00

0.98

1.51

1.93
6.00
1.56
0.95
5.13
3.20

0   9.5   9.0   8.5   8.0   7.5   7.0   6.5   6.0   5.5   5.0   4.5   4.0   3.5   3.0   2.5   2.0   1.5   1.0   0.5   0.

δ (ppm)

NMR ^{13}C 100.6 MHz

CDCl$_3$

128.747
128.586
126.976
113.427
109.143
91.397
91.348
91.129
91.085
77.317
69.589
69.263
45.779
39.157
38.961
25.832
25.783
25.427
25.369
8.846

δ (ppm)

gHSQC 400 MHz

f1 (ppm)

f2 (ppm)

NMR ^{31}P 161.9 MHz
CDCl$_3$

NMR ^{1}H 400 MHz

CDCl$_3$

L1Pd10

Appendix II. Crystallographic Data

X-ray structure of compound (*S*)-L1·BF₃

Ortep plot with the ellipsoids at 50% probability level. Some H atoms have been omitted for clarity.
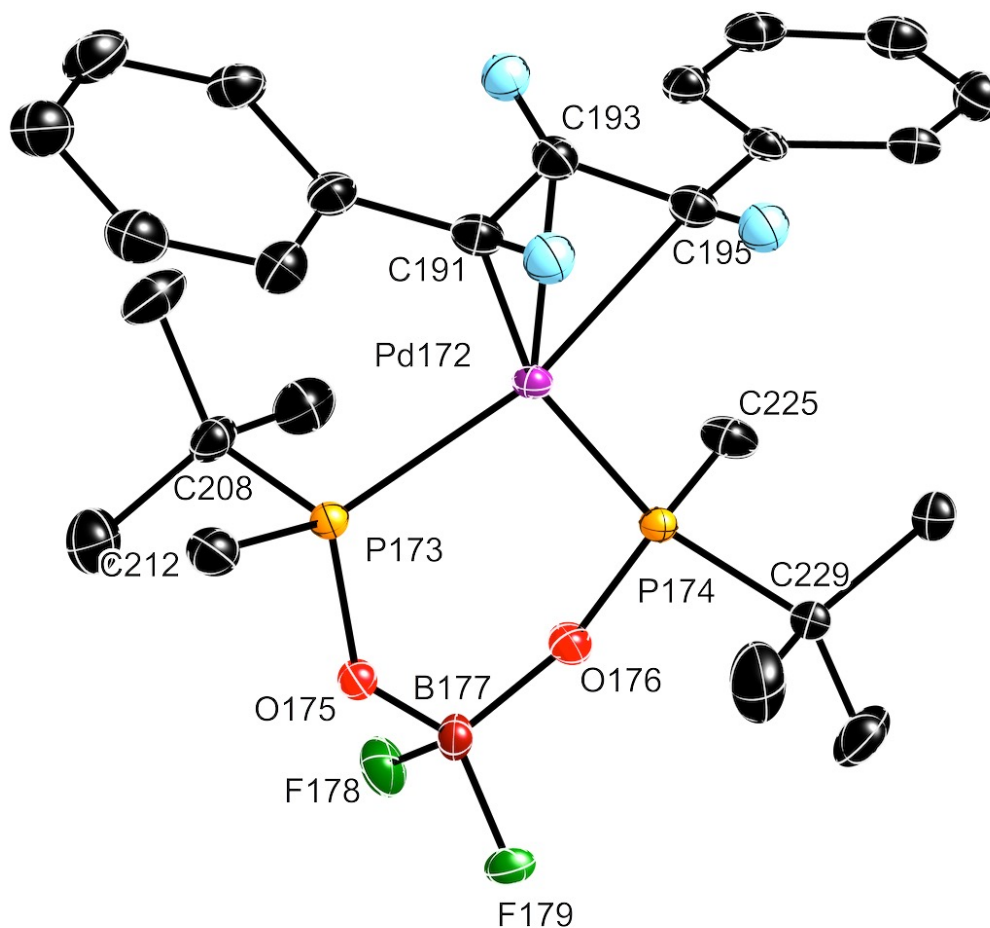

Crystal preparation

Approximately 10 mg of compound **(*S*)-L1·BF₃** were dissolved in 1 mL of dichloromethane in a vial and placed in a fridge at 4 ºC. Slow evaporation of the solvent produced a few monocrystals of the compound.

Crystal data and structure refinement for (*S*)-L1·BF₃

Empirical formula	$C_5H_{13}BF_3OP$
Formula weight	187.93
Temperature	100(2) K
Wavelength	0.71073 Å
Crystal system	Monoclinic
Space group	P2(1)
Unit cell dimensions	a = 5.930(2) Å α = 90º
	b = 11.012(5) Å β = 108.874(15)º
	c = 7.395(4) Å γ = 90º
Volume	457.0(3) Å³
Z	2
Density (calculated)	1.366 Mg/m³
Absorption coefficient	0.293 mm⁻¹
F(000)	196
Crystal size	0.30 x 0.30 x 0.10 mm³
Theta range for data collection	2.911 to 30.554º
Index ranges	−8 ≤ h ≤ 5, −15 ≤ k ≤ 15, −7 ≤ l ≤ 10
Reflections collected	4041
Independent reflections	2322 [R(int) = 0.0238]
Completeness to theta = 30.554º	93.4%
Absorption correction	Empirical
Max. and min. transmission	0.971 and 0.917
Refinement method	Full-matrix least-squares on F^2
Data/restraints/parameters	2322/1/108
Goodness-of-fit on F^2	1.070
Final R indices [I>2sigma(I)]	R1 = 0.0296, wR2 = 0.0736
R indices (all data)	R1 = 0.0318, wR2 = 0.0750
Flack parameter	x = −0.06(8)
Largest diff. peak and hole	0.266 and −0.293 e Å⁻³

X-ray structure of complex (*S*)-L1Au1

Ortep plot with the ellipsoids at 50% probability level. H atoms have been omitted for clarity.
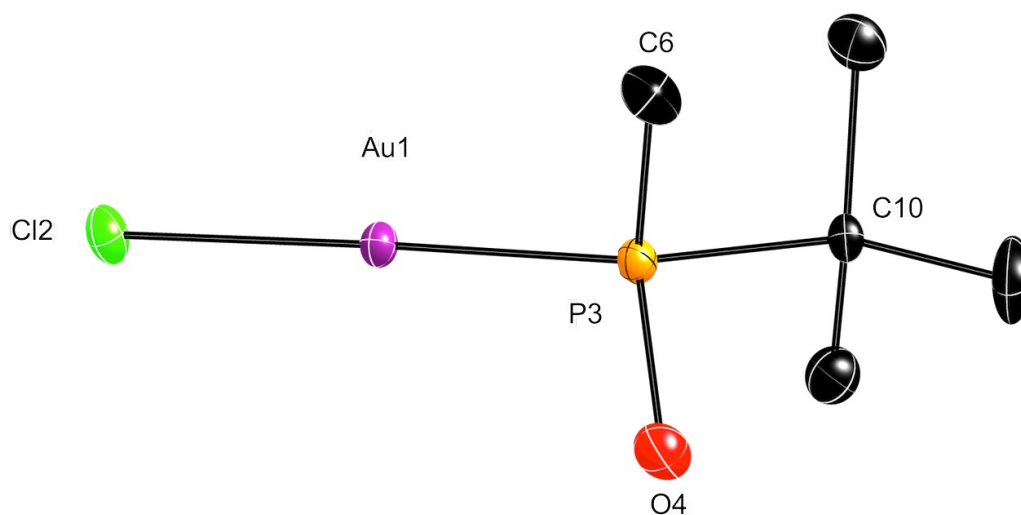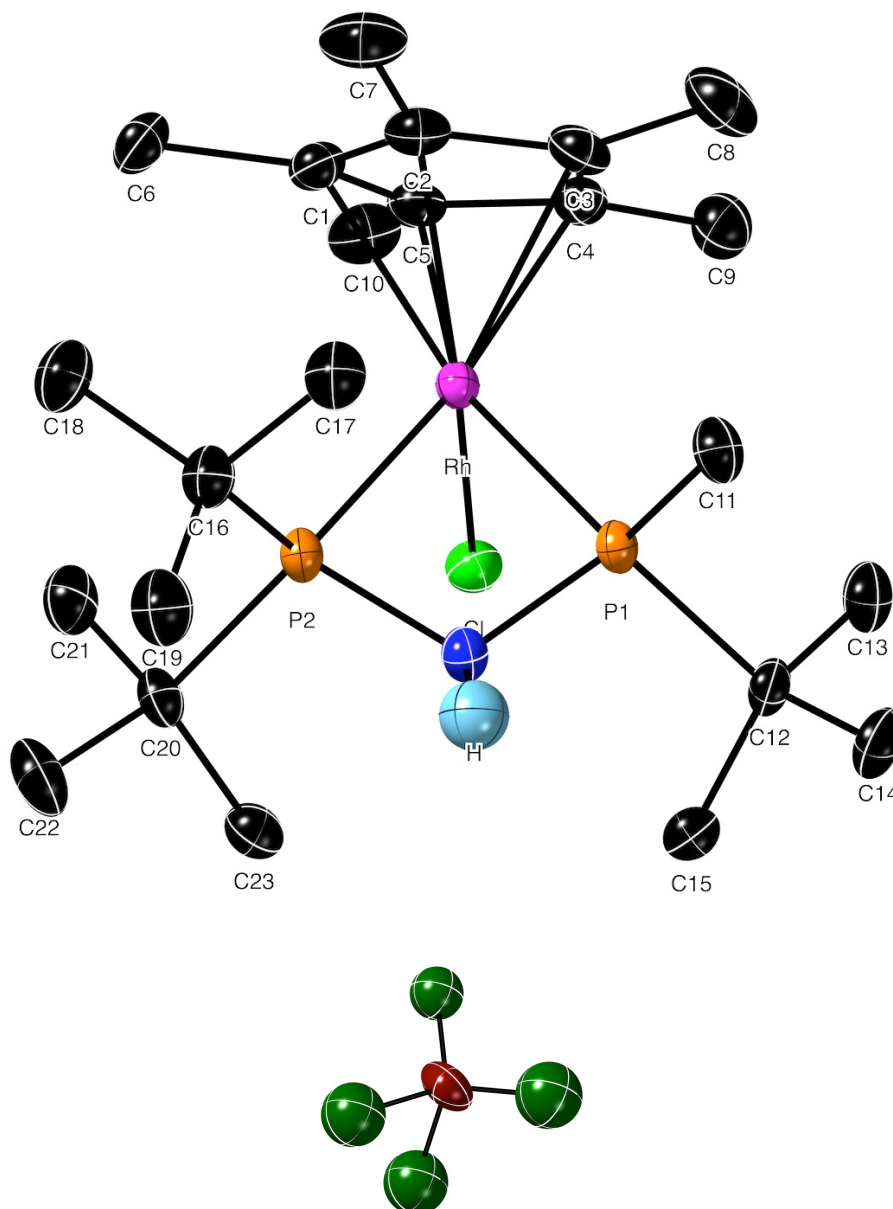

Crystal preparation

Approximately 10 mg of complex (*S*)-**L1Au1** were dissolved in 1 mL of dichloromethane in a vial and frozen in liquid nitrogen. Layering with *n*-hexane yielded monocrystals of the complex.

APPENDIX

Crystal data and structure refinement for (*S*)-L1Au1

Empirical formula	$C_5H_{13}AuClOP$
Formula weight	352.54
Temperature	100(2) K
Wavelength	0.71073 Å
Crystal system	Trigonal
Space group	P3(1)
Unit cell dimensions	a = 15.7761(2) Å α = 90º
	b = 15.7761(2) Å β = 90º
	c = 9.66840(10) Å γ = 120º
Volume	2083.94(6) Å^3
Z	9
Density (calculated)	2.528 Mg/m^3
Absorption coefficient	16.276 mm^{-1}
F(000)	1458
Crystal size	0.30 x 0.05 x 0.05 mm^3
Theta range for data collection	2.0790 to 33.0870º
Index ranges	$-23 \leq h \leq 24, -23 \leq k \leq 24, -14 \leq l \leq 14$
Reflections collected	31856
Independent reflections	9762 [R(int) = 0.0269]
Completeness to theta = 33.0870º	96.1%
Absorption correction	Multi-scan
Max. and min. transmission	0.497 and 0.382
Refinement method	Full-matrix least-squares on F^2
Data/restraints/parameters	9762/1/259
Goodness-of-fit on F^2	1.106
Final R indices [I>2sigma(I)]	R1 = 0.0508, wR2 = 0.1279
R indices (all data)	R1 = 0.0513, wR2 = 0.1282
Flack parameter	x = 0.027(14)
Largest diff. peak and hole	2.554 and -3.519 e Å^{-3}

X-ray structure of complex (*R*)-L1Ru1

Ortep plot with the ellipsoids at 50% probability level. H atoms have been omitted for clarity.
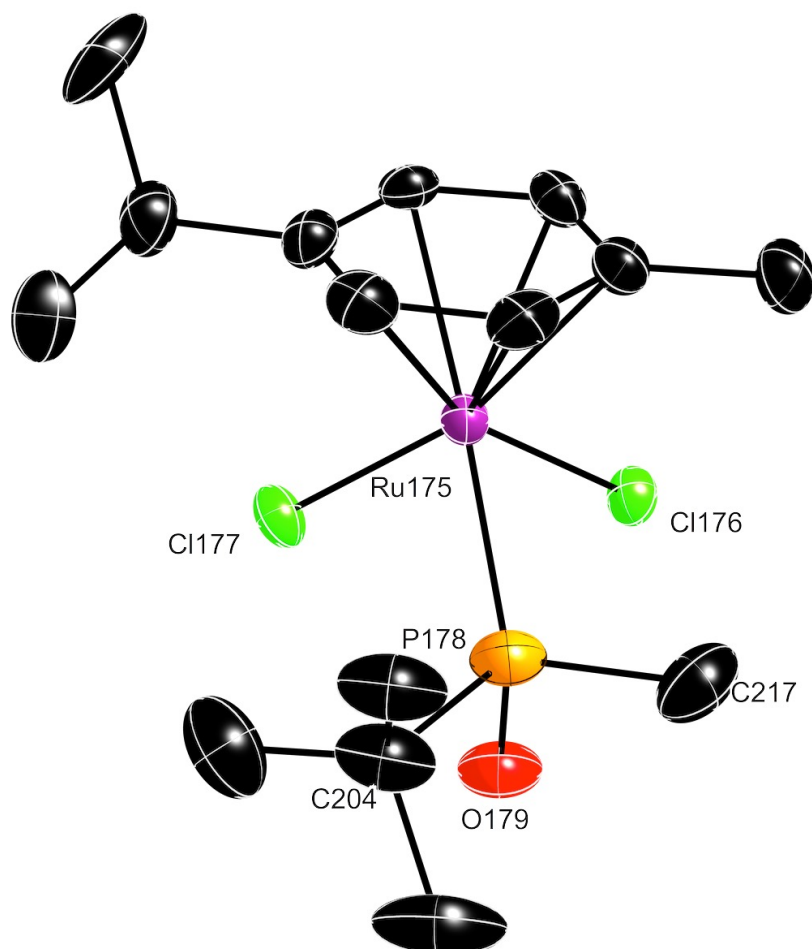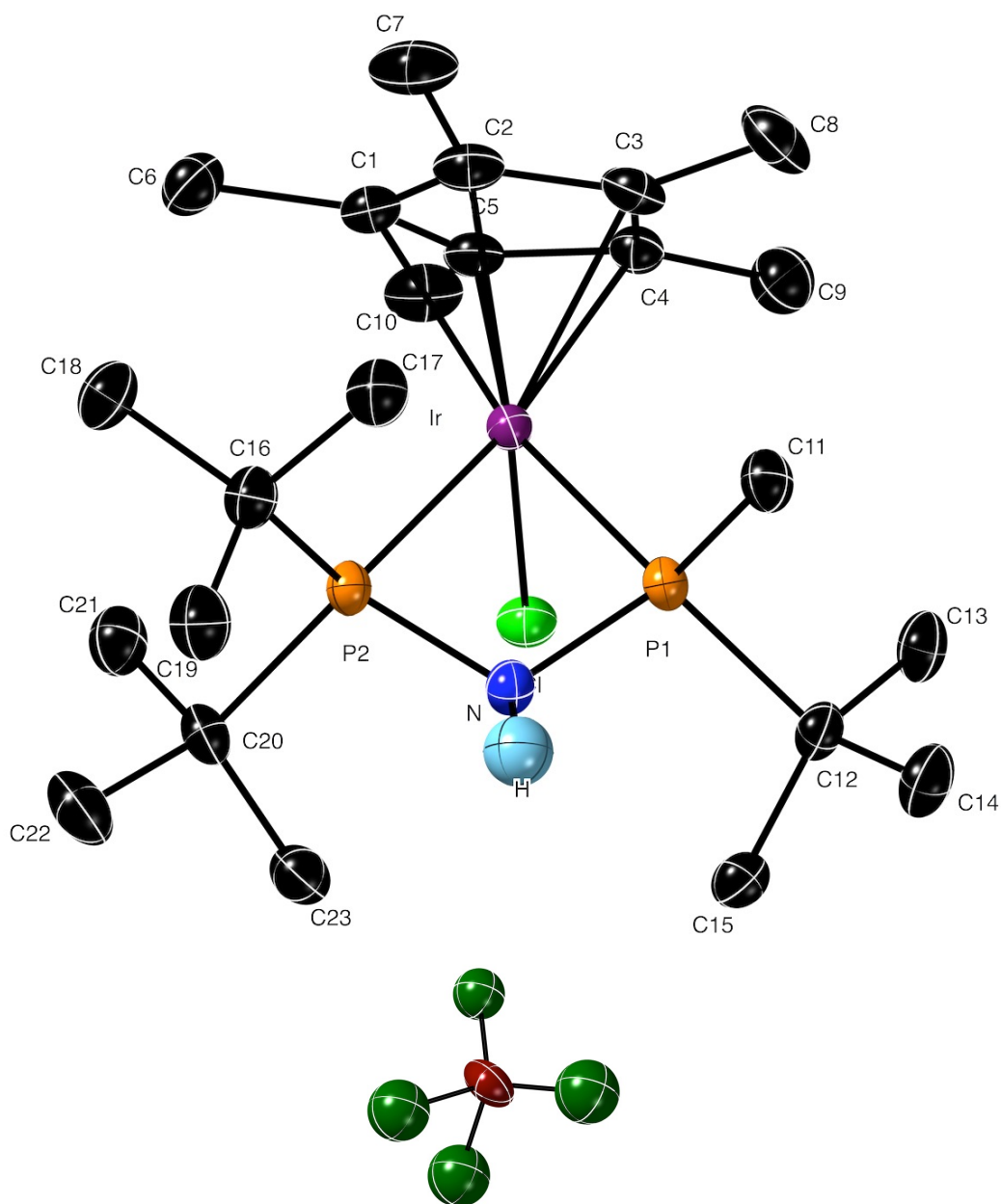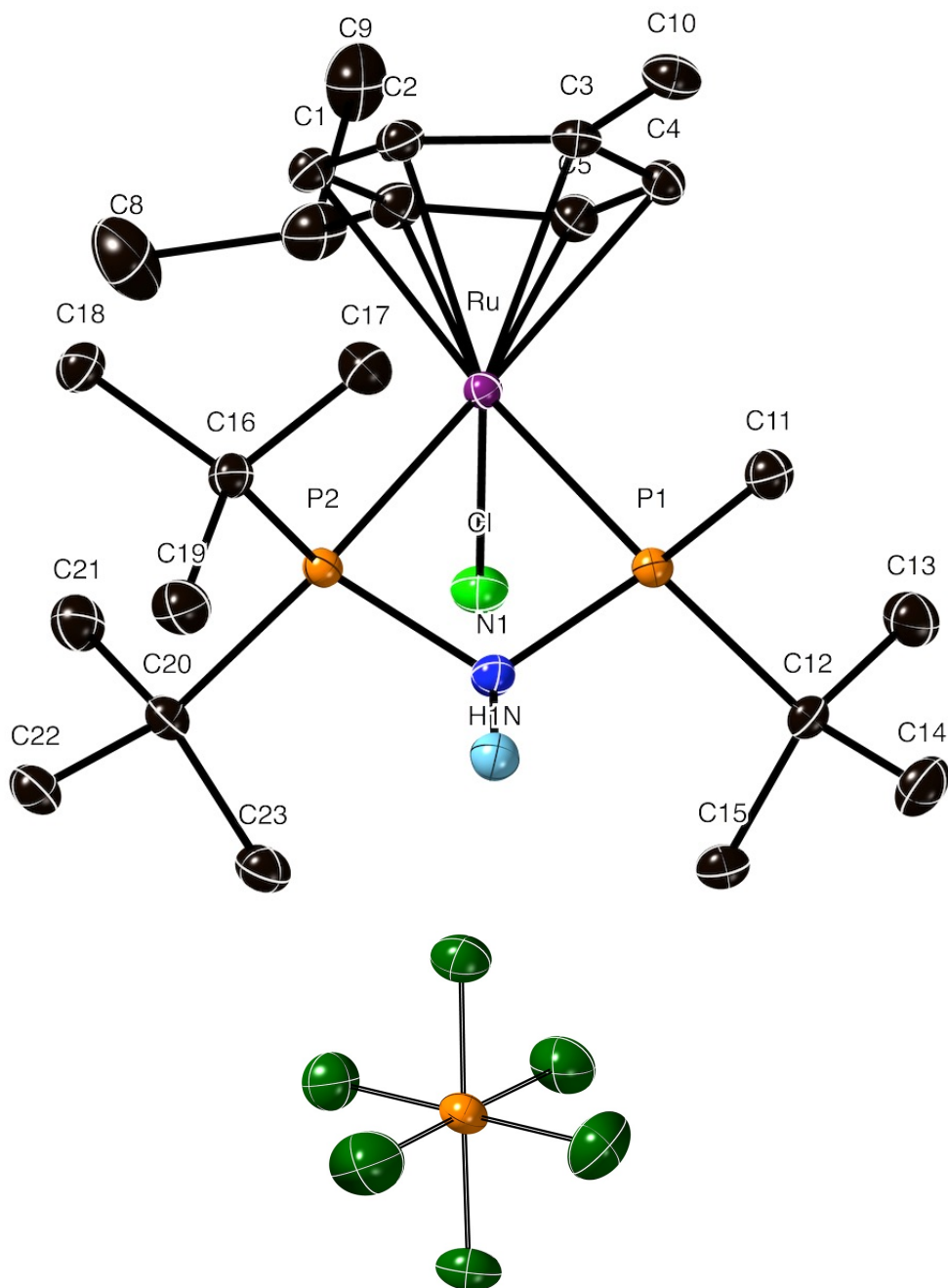

Crystal preparation

Approximately 10 mg of complex **(*R*)-L1Ru1** were dissolved in 1 mL of dichloromethane in a vial and frozen in liquid nitrogen. Layering with *n*-hexane yielded monocrystals of the complex.

Crystal data and structure refinement for (*R*)-L1Ru1

Empirical formula	$C_{15}H_{26}Cl_{12}OPRu$
Formula weight	425.30
Temperature	100(2) K
Wavelength	0.71073 Å
Crystal system	Triclinic
Space group	P1
Unit cell dimensions	a = 10.3177(4) Å α = 85.9475(12)°
	b = 12.7035(4) Å β = 81.7449(12)°
	c = 15.0982(6) Å γ = 71.2831(10)°
Volume	1854.22(12) Å^3
Z	4
Density (calculated)	1.523 Mg/m^3
Absorption coefficient	1.214 mm^{-1}
F(000)	868
Crystal size	0.20 x 0.20 x 0.08 mm^3
Theta range for data collection	2.25 to 31.08°
Index ranges	$-11 \leq h \leq 15, -15 \leq k \leq 19, -20 \leq l \leq 22$
Reflections collected	35696
Independent reflections	16631 [R(int) = 0.0304]
Completeness to theta = 31.08°	91.6%
Absorption correction	Multi-scan
Max. and min. transmission	0.909 and 0.793
Refinement method	Full-matrix least-squares on F^2
Data/restraints/parameters	16631/1647/1298
Goodness-of-fit on F^2	1.042
Final R indices [I>2sigma(I)]	R1 = 0.0375, wR2 = 0.0891
R indices (all data)	R1 = 0.0492, wR2 = 0.0984
Flack parameter	x = 0.00(2)
Largest diff. peak and hole	1.062 and -0.795 e Å^{-3}

X-ray structure of complex (*S*)-L1Pd2

Ortep plot with the ellipsoids at 50% probability level. Some H atoms have been omitted for clarity.
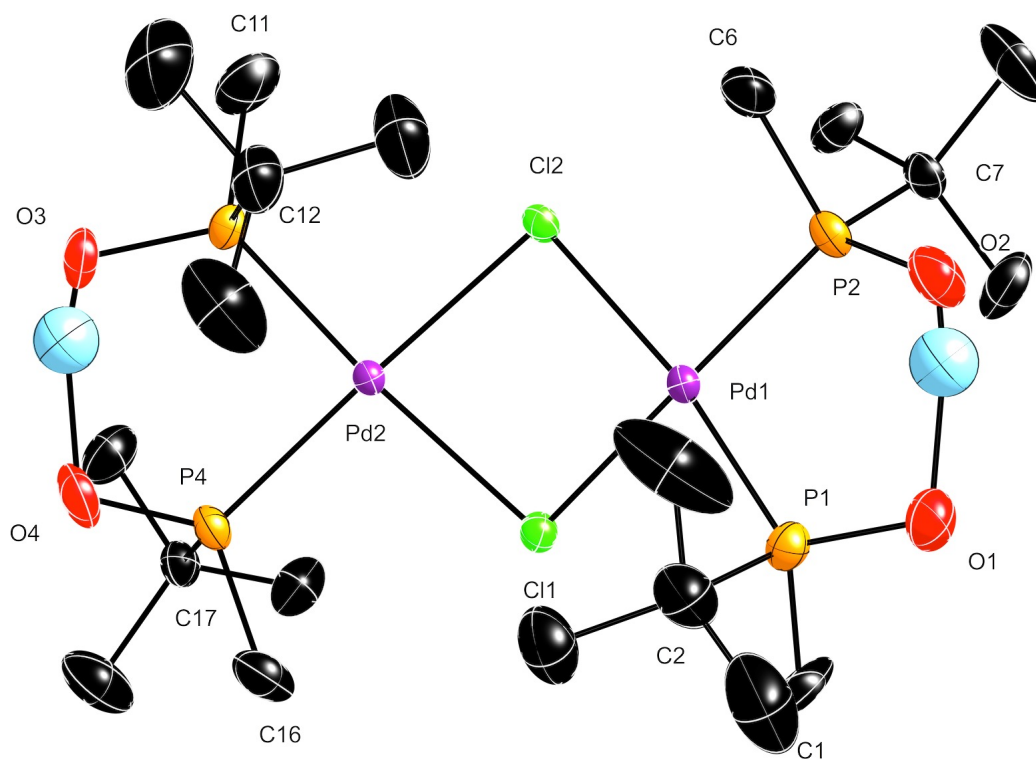
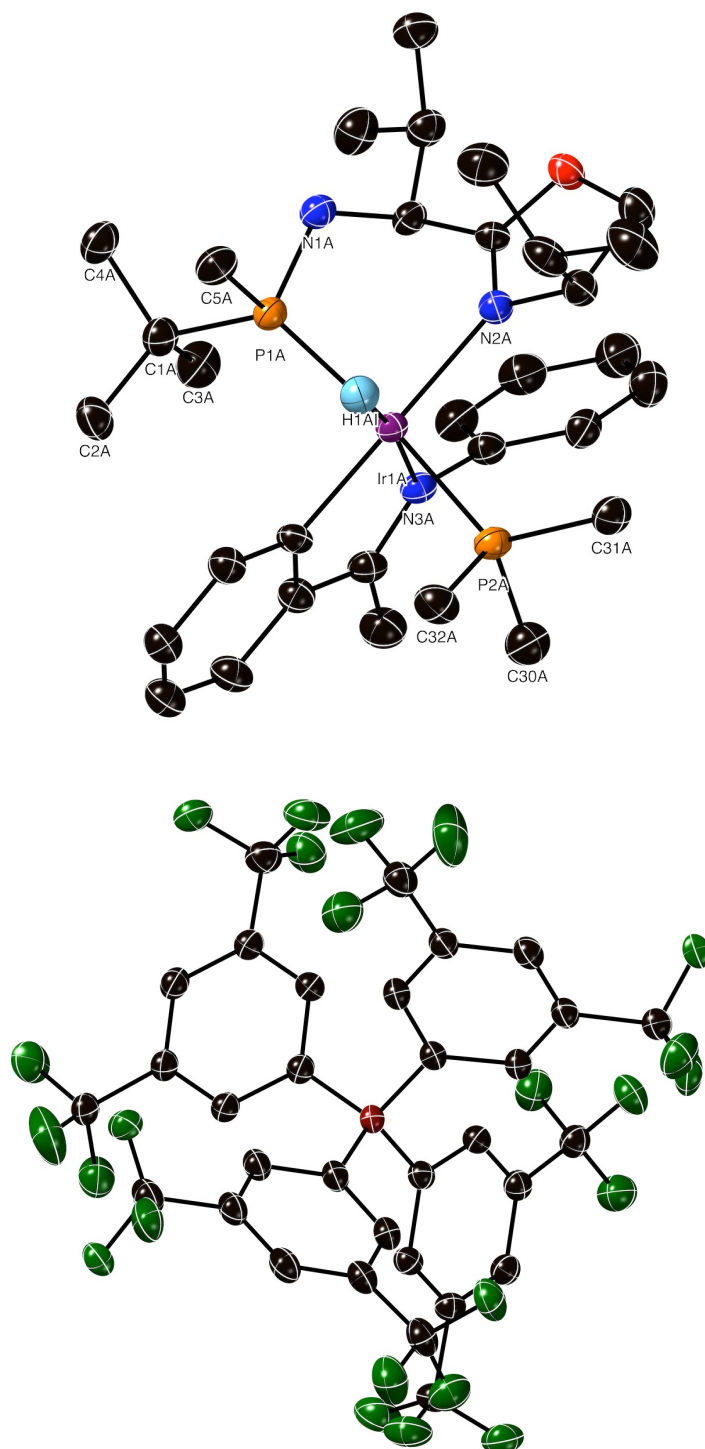## Crystal preparation

Approximately 10 mg of complex **(*S*)-L1Pd2** were dissolved in 1 mL of dichloromethane in a vial and placed in a fridge at 4 ºC. Slow evaporation of the solvent produced a few monocrystals of the complex.

Crystal data and structure refinement for (*S*)-L1Pd2

Empirical formula	$C_{20}H_{50}Cl_2O_4P_4Pd_2$
Formula weight	762.18
Temperature	100(2) K
Wavelength	0.71073 Å
Crystal system	Monoclinic
Space group	P2(1)
Unit cell dimensions	a = 7.4353(5) Å α = 90º
	b = 17.0371(10) Å β = 90.4112(19)º
	c = 12.4919(8) Å γ = 90º
Volume	1582.38(17) Å^3
Z	2
Density (calculated)	1.600 Mg/m^3
Absorption coefficient	1.530 mm^{-1}
F(000)	776
Crystal size	0.30 x 0.20 x 0.05 mm^3
Theta range for data collection	1.630 to 30.575º
Index ranges	$-10 \leq h \leq 8, -24 \leq k \leq 18, -16 \leq l \leq 17$
Reflections collected	22738
Independent reflections	8728 [R(int) = 0.0286]
Completeness to theta = 31.08º	99.3%
Absorption correction	Empirical
Max. and min. transmission	0.927 and 0.762
Refinement method	Full-matrix least-squares on F^2
Data/restraints/parameters	8728/4/308
Goodness-of-fit on F^2	1.169
Final R indices [I>2sigma(I)]	R1 = 0.0457, wR2 = 0.1060
R indices (all data)	R1 = 0.0470, wR2 = 0.1066
Flack parameter	x = 0.02(5)
Largest diff. peak and hole	1.854 and -1.981 e Å^{-3}

X-ray structure of complex (*S*)-L1Pd10

Ortep plot with the ellipsoids at 50% probability level. Some H atoms have been omitted for clarity.


Crystal preparation

Approximately 10 mg of complex (*S*)-**L1Pd10** were dissolved in 1 mL of dichloromethane in a vial and placed in a fridge at 4 ºC. Slow evaporation of the solvent produced a few monocrystals of the complex.

Crystal data and structure refinement for (*S*)-L1Pd10

Empirical formula	$C_{25}H_{37}BF_2O_2P_2Pd$
Formula weight	600.85
Temperature	100(2) K
Wavelength	0.71073 Å
Crystal system	Monoclinic
Space group	C2
Unit cell dimensions	$a = 25.6108(12)$ Å $\alpha = 90°$
	$b = 13.8705(6)$ Å $\beta = 101.3847(13)°$
	$c = 23.6977(10)$ Å $\gamma = 90°$
Volume	8252.6(6) Å^3
Z	12
Density (calculated)	1.451 Mg/m^3
Absorption coefficient	0.857 mm^{-1}
F(000)	3708
Crystal size	0.30 x 0.25 x 0.10 mm^3
Theta range for data collection	2.31 to 31.98°
Index ranges	$-38 \leq h \leq 38, -20 \leq k \leq 19, -17 \leq l \leq 35$
Reflections collected	52238
Independent reflections	25775 [R(int) = 0.0339]
Completeness to theta = 31.98°	90.7%
Absorption correction	Multi-scan
Max. and min. transmission	0.919 and 0.783
Refinement method	Full-matrix least-squares on F^2
Data/restraints/parameters	25775/615/1081
Goodness-of-fit on F^2	1.099
Final R indices [I>2sigma(I)]	R1 = 0.0487, wR2 = 0.1043
R indices (all data)	R1 = 0.0545, wR2 = 0.1071
Flack parameter	x = 0.000(8)
Largest diff. peak and hole	0.858 and −1.076 e Å^{-3}

APPENDIX

X-ray structure of complex L2Rh1

Ortep plot with the ellipsoids at 50% probability level. Some H atoms have been omitted for clarity.

Crystal preparation

Approximately 10 mg of complex **L2Rh1** were dissolved in 1 mL of dichloromethane in a vial and frozen in liquid nitrogen. Layering with diethyl ether yielded monocrystals of the complex.

Crystal data and structure refinement for L2Rh1

Empirical formula	$C_{23}H_{46}BClF_4NP_2Rh$
Formula weight	623.74
Temperature	100(2) K
Wavelength	0.71073 Å
Crystal system	Orthorhombic
Space group	P21
Unit cell dimensions	a = 9.7378(4) Å α = 90º
	b = 16.4348(7) Å β = 90º
	c = 18.1370(8) Å γ = 90º
Volume	2902.6(2) Å^3
Z	4
Density (calculated)	1.427 Mg/m^3
Absorption coefficient	0.829 mm^{-1}
F(000)	1296
Crystal size	0.198 x 0.174 x 0.116 mm^3
Theta range for data collection	2.246 to 29.301º
Index ranges	$-13 \leq h \leq 13, -22 \leq k \leq 21, -24 \leq l \leq 24$
Reflections collected	46914
Independent reflections	7739 [R(int) = 0.0341]
Completeness to theta = 29.301º	96.4%
Absorption correction	Multi-scan
Max. and min. transmission	0.9045 and 0.8078
Refinement method	Full-matrix least-squares on F^2
Data/restraints/parameters	7739/0/314
Goodness-of-fit on F^2	1.053
Final R indices [I>2sigma(I)]	R1 = 0.0267, wR2 = 0.0658
R indices (all data)	R1 = 0.0285, wR2 = 0.0672
Flack parameter	x = −0.037(9)
Largest diff. peak and hole	1.041 and −0.581 e Å^{-3}

X-ray structure of complex L2Ir1

Ortep plot with the ellipsoids at 50% probability level. Some H atoms have been omitted for clarity.

Crystal preparation

Approximately 10 mg of complex **L2Ir1** were dissolved in 1 mL of dichloromethane in a vial and frozen in liquid nitrogen. Layering with diethyl ether yielded monocrystals of the complex.

Crystal data and structure refinement for L2Ir1

Empirical formula	$C_{23}H_{46}BClF_4NP_2Ir$
Formula weight	713.01
Temperature	100(2) K
Wavelength	0.71073 Å
Crystal system	Orthorhombic
Space group	P21
Unit cell dimensions	a = 9.7215(4) Å $\alpha = 90°$
	b = 16.4551(7) Å $\beta = 90°$
	c = 18.1397(8) Å $\gamma = 90°$
Volume	2901.8(2) Å^3
Z	4
Density (calculated)	1.632 Mg/m^3
Absorption coefficient	4.842 mm^{-1}
F(000)	1424
Crystal size	0.366 x 0.103 x 0.091 mm^3
Theta range for data collection	2.377 to 29.351°
Index ranges	$-12 \leq h \leq 13, -21 \leq k \leq 22, -24 \leq l \leq 24$
Reflections collected	24563
Independent reflections	7497 [R(int) = 0.0265]
Completeness to theta = 29.351°	93.4%
Absorption correction	Multi-scan
Max. and min. transmission	0.5257 and 0.3260
Refinement method	Full-matrix least-squares on F^2
Data/restraints/parameters	7497/0/317
Goodness-of-fit on F^2	1.034
Final R indices [I>2sigma(I)]	R1 = 0.0218, wR2 = 0.0512
R indices (all data)	R1 = 0.0232, wR2 = 0.0517
Flack parameter	x = −0.014(4)
Largest diff. peak and hole	0.096 and −0.485 e Å^{-3}

X-ray structure of complex L2Ru1·PF$_6$

Ortep plot with the ellipsoids at 50% probability level. Some H atoms have been omitted for clarity.

Crystal preparation

Approximately 10 mg of complex **L2Ru1·PF$_6$** were dissolved in 1 mL of dichloromethane in a vial and frozen in liquid nitrogen. Layering with diethyl ether yielded monocrystals of the complex.

Crystal data and structure refinement for L2Ru1·PF$_6$

Empirical formula	$C_{23}H_{45}ClF_6NP_3Ru$
Formula weight	679.03
Temperature	100(2) K
Wavelength	0.71073 Å
Crystal system	Orthorhombic
Space group	P21
Unit cell dimensions	a = 10.8826(6) Å α = 90º
	b = 16.1242(8) Å β = 90º
	c = 17.1538(8) Å γ = 90º
Volume	3010.0(3) Å^3
Z	4
Density (calculated)	1.498 Mg/m^3
Absorption coefficient	0.820 mm^{-1}
F(000)	1400
Crystal size	0.40 x 0.40 x 0.20 mm^3
Theta range for data collection	3.28 to 39.44º
Index ranges	$-12 \leq h \leq 17, -28 \leq k \leq 21, -14 \leq l \leq 30$
Reflections collected	31150
Independent reflections	14925 [R(int) = 0.0183]
Completeness to theta = 39.44º	93.3%
Absorption correction	Multi-scan
Max. and min. transmission	0.853 and 0.735
Refinement method	Full-matrix least-squares on F^2
Data/restraints/parameters	14925/0/333
Goodness-of-fit on F^2	1.034
Final R indices [I>2sigma(I)]	R1 = 0.0213, wR2 = 0.0508
R indices (all data)	R1 = 0.0231, wR2 = 0.0518
Flack parameter	x = −0.029(7)
Largest diff. peak and hole	0.065 and −0.440 e Å^{-3}

APPENDIX

X-ray structure of compound L3RIr2

Ortep plot with the ellipsoids at 50% probability level. Some H atoms have been omitted for clarity.

Crystal preparation

Approximately 10 mg of complex **L3RIr2** were dissolved in 1 mL of dichloromethane in a vial and placed in a fridge at 4 ºC. Slow evaporation of the solvent produced a few monocrystals of the complex.

Crystal data and structure refinement for L3RIr2

Empirical formula	$C_{64}H_{65}BF_{24}IrN_3OP_2$
Formula weight	1613.14
Temperature	100(2) K
Wavelength	0.71073 Å
Crystal system	Triclinic
Space group	P1
Unit cell dimensions	a = 13.14495(15)Å α = 76.3410(8)°
	b = 13.47863(12) Å β = 78.4708(9)°
	c = 22.0101(2) Å γ = 62.6282(10)°
Volume	3346.24(7) Å^3
Z	2
Density (calculated)	1.601 Mg/m^3
Absorption coefficient	2.153 mm^{-1}
F(000)	1612
Crystal size	0.15 x 0.15 x 0.20 mm^3
Theta range for data collection	1.725 to 34.747°
Index ranges	$-20 \leq h \leq 20, -21 \leq k \leq 21, -35 \leq l \leq 34$
Reflections collected	83414
Independent reflections	83414 [R(int) = ?]
Completeness to theta = 34.747°	96.9%
Absorption correction	Multi-scan
Max. and min. transmission	0.738 and 0.568
Refinement method	Full-matrix least-squares on F^2
Data/restraints/parameters	83414/260/1838
Goodness-of-fit on F^2	1.092
Final R indices [I>2sigma(I)]	R1 = 0.0540, wR2 = 0.1650
R indices (all data)	R1 = 0.0741, wR2 = 0.1878
Flack parameter	x = 0.0215(16)
Largest diff. peak and hole	4.850 and -5.292 e Å^{-3}

Appendix III. Index of selected structures

t-BuMeP(O)H ligand and derivatives
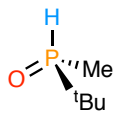
L1

t-BuMeP(O)H complexes
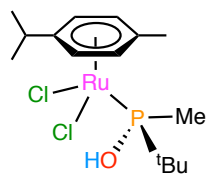
L1Ru1
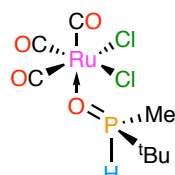
L1Ru2
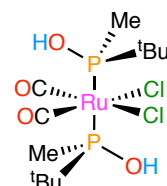
L1Ru3
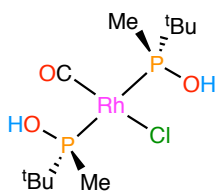
L1Rh1
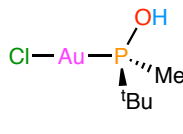
L1Au1
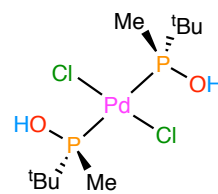
L1Pd1
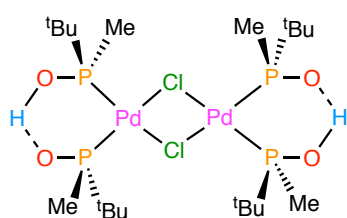
L1Pd2
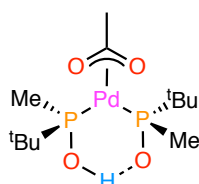
L1Pd3
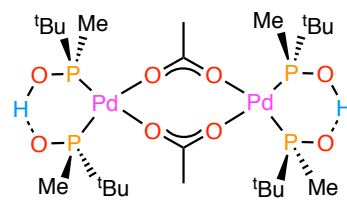
L1Pd4
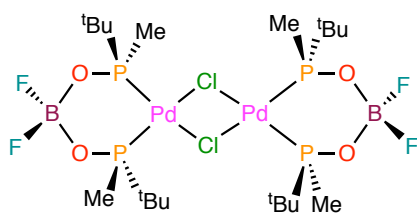
L1Pd5
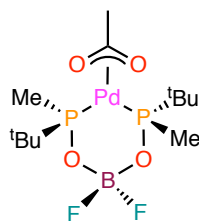
L1Pd6
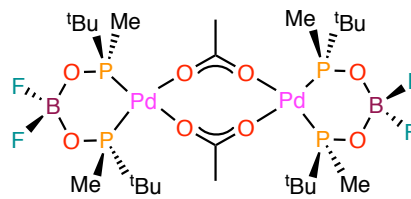
L1Pd7
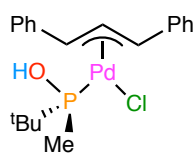
L1Pd8
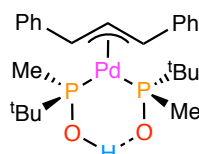
L1Pd9
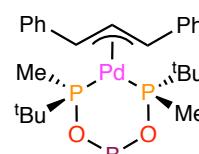
L1Pd10

MaxPhos ligand

L2

MaxPhos complexes

L2Rh1

L2Ir1

L2Ru1

L2Rh2

L2Ir2

L2Ru2

MaxPHOX ligands

L3R **L3S**

MaxPHOX iridacycles

L3RIr1 **L3RIr2** **L3RIr3**

L3RIr4 **L3RIr5** **L3RIr6**

L3SIr1 **L3SIr2**

L3SIr3 **L3SIr4**
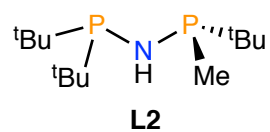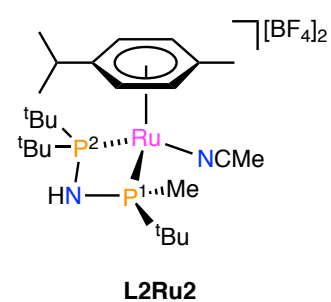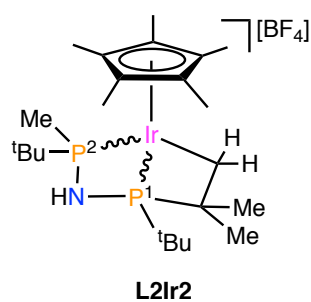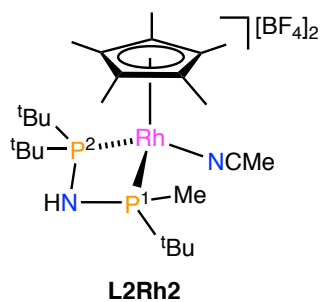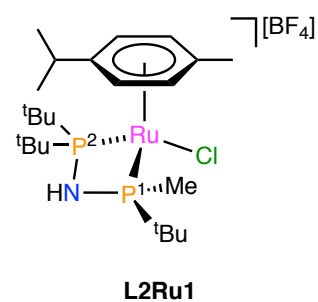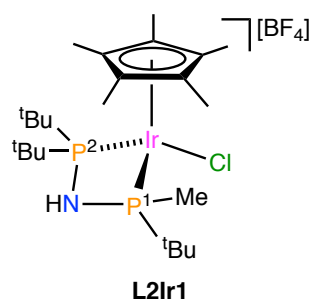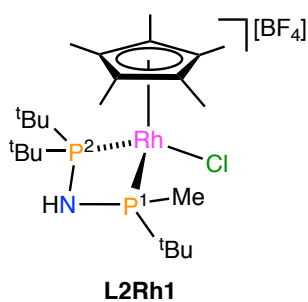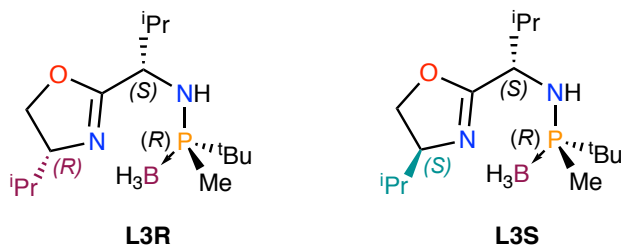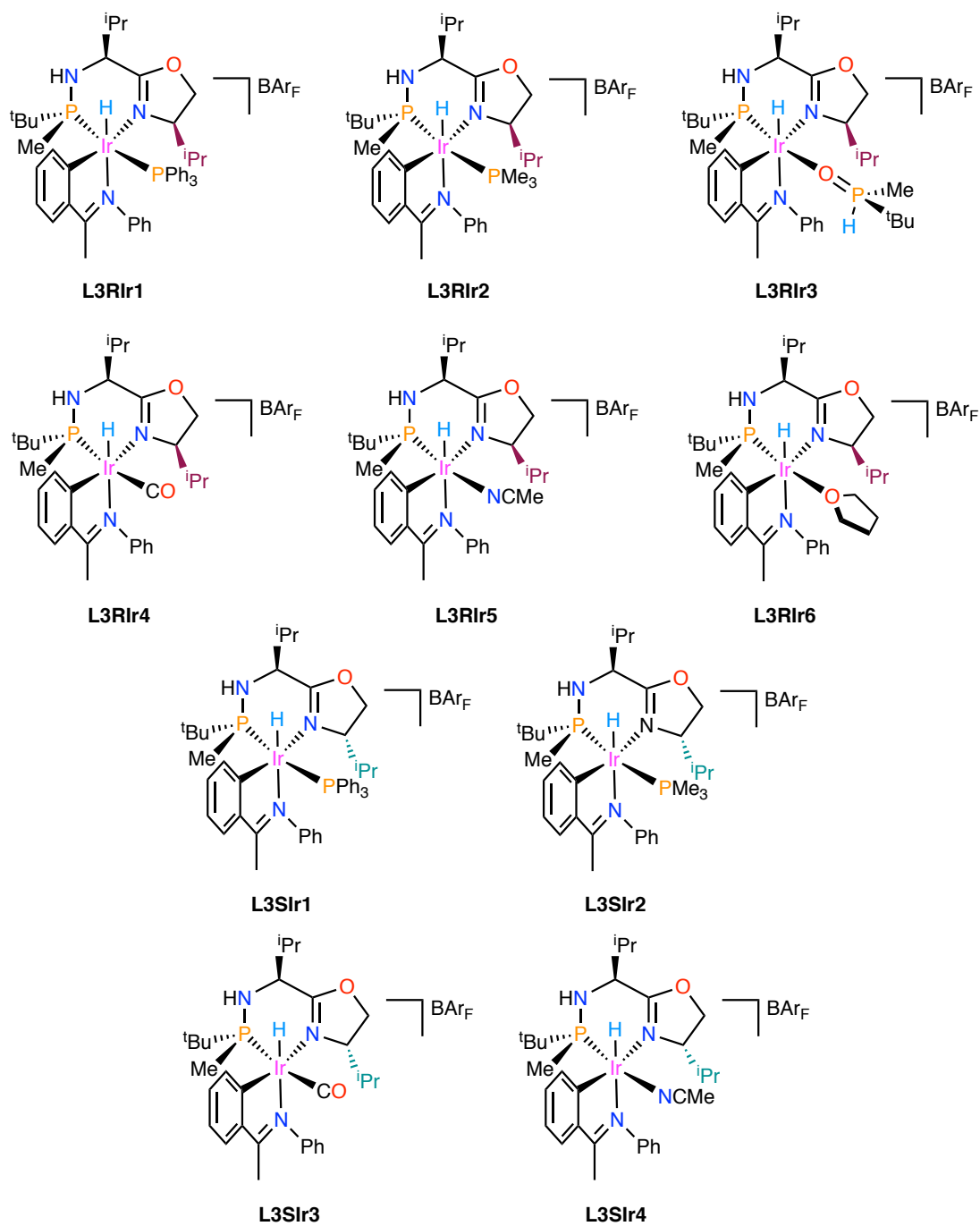
Alkyl imine substrates
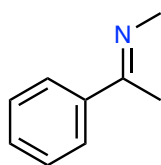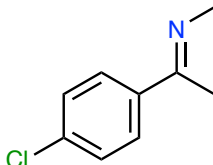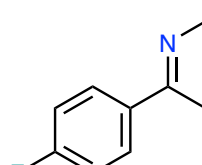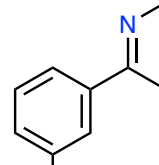
I8 **I9** **I10** **I11**
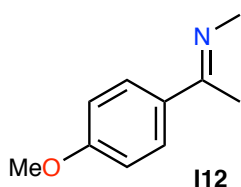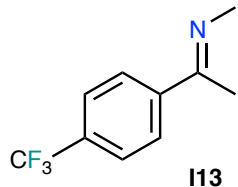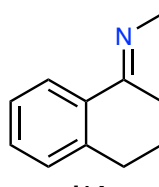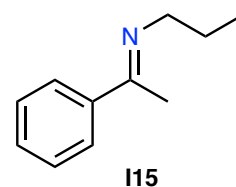
I12 **I13** **I14** **I15**
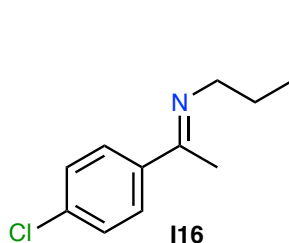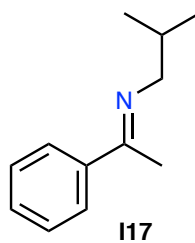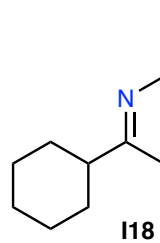
I16 **I17** **I18**
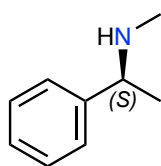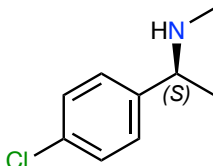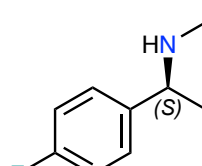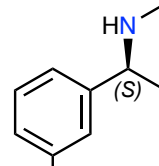
A8 **A9** **A10** **A11**
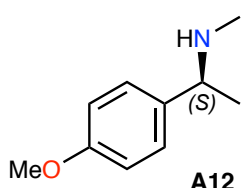
A12 **A13** **A14** **A15**

A16 **A17** **A18**